

THE DEVELOPMENT OF A SYNTHETIC STRATEGY TOWARD
DIHYDROOXEPINE-CONTAINING EPIPOLYTHIODIKETOPIPERAZINES:
ENANTIOSELECTIVE TOTAL SYNTHESIS OF (–)-ACETYLARANOTIN AND
RELATED INVESTIGATIONS

Thesis by

Julian Andrew Codelli

In Partial Fulfillment of the Requirements

for the Degree of

Doctor of Philosophy

CALIFORNIA INSTITUTE OF TECHNOLOGY

Pasadena, California

2014

(Defended September 12, 2013)

© 2014

Julian Andrew Codelli

All Rights Reserved

To Megan

ACKNOWLEDGEMENTS

First and foremost, I would like to thank my research advisor, Professor Sarah Reisman, for the privilege of conducting my doctoral research under her mentorship at Caltech. As one of her first students, I've received a tremendous amount of support and guidance from Sarah over the years, as we've shared the frustrations and successes of a nascent research program. The opportunity to work with such an intelligent and passionate yet accessible advisor has been truly rewarding.

I'm also grateful to the rest of my thesis committee members, Professors John Bercaw and David Tirrell, and chairman, Professor Brian Stoltz. Their input has been invaluable in helping me plan out both my graduate research and my career trajectory. The CCE Division at Caltech is truly a unique place. The collaborative atmosphere fostered among groups makes conducting research here an enjoyable and enriching experience, and the staff have done a terrific job keeping things running smoothly. In particular, I'm indebted to Larry Henling, Dr. David van der Velde, and the late Dr. Michael Day, for their assistance with structural determination, and Dr. Scott Virgil for sharing his wealth of knowledge on a variety of topics, from instrumentation to lab technique.

I must thank the members of the Reisman lab, past and present. The lab has grown over the years, but remains a stimulating and fun environment in which to do research. In particular, I'd like to thank Raul Navarro, Dr. Lindsay Repka, John Yeoman, and Dr. Roger Nani, who have been great friends and colleagues the past five years, as well as Kangway Chuang, Maddi Kieffer, Dr. Jake Cha, Jani Ni, Haoxuan Wang, and Lauren Chapman. For better or worse, they have made it easy to survive graduate school without having to make many friends outside of the lab. Likewise, the Stoltz lab has been a great

source of friends, chemicals, and advice, and was particularly instrumental in getting our research program up and running.

I've had the pleasure of working closely with several talented scientists during my time at Caltech. I owe many thanks to Dr. Angela Puchlopek, who in addition to being a great friend assumed the frustrating task of optimizing the early stages of our synthetic route toward acetylaranotin. Angela also explored alternative protecting group strategies and approaches toward the dihydrooxepine-containing monomer, and conducted preliminary experiments pertaining to the synthesis of MPC1001B. Andy Lim, another good friend, took ownership of our investigation into the double cycloaddition process for the preparation of highly substituted pyrrolizidines. Though I have only recently begun to work with Amy McCarthy and Dr. Geanna Min, I am confident that they will soon expand our program to include a more diverse array of ETP natural products. The opportunity to work with graduate students and postdoctoral researchers from various backgrounds and with various communication styles has greatly strengthened my ability to work as part of a team, in addition to contributing to my development as an individual scientist.

Of course, I would never have made it this far into my academic career without having been mentored by outstanding scientists as an undergraduate. In combination with the introductory organic chemistry courses taught by Profs. Jean Fréchet and John Ellman at UC Berkeley, my summer research experience with Dr. Monique Cosman at the Lawrence Livermore National Lab inspired me to gravitate towards organic chemistry and its application to the study of biological systems. My subsequent experience in the Bertozzi Lab not only gave me a chance to learn from one of the most brilliant minds in

chemical biology (Prof. Carolyn Bertozzi), but also inspired me to pursue graduate studies with a focus on synthetic chemistry. During this time, I benefitted from the mentorship of an amazing scientist, Jeremy Baskin, who taught me much of what I know about lab technique and greatly contributed to my success as a researcher, both at the undergraduate and graduate levels.

Though visits with my family have become less and less frequent over the years, my siblings (Alex and Erin) and grandparents (Heinrich, Abbie, Donald, and Jane) have remained a constant source of support and love. The same can be said of Rhine Ramirez and Brandon Willer, my two best friends from high school. In my childhood, my parents (Chris and Carol) provided such a loving and nurturing environment in which to cultivate my scientific curiosity, whether that meant keeping the bookshelves stocked with do-it-yourself science books, or allowing me to “grow” penicillin in the garage. Words can’t express my gratitude for this, and for the support they have continued to give throughout my graduate studies.

Finally, I must thank my wife (and best friend for the past 10 years), Megan. Though the frustrations of experimental science often kept me in lab late into the evening (much to her chagrin), she was always there for me when I got home. I couldn’t have done any of this without her unwavering support, love, understanding, and sacrifice, and I can’t wait to see what the future has in store for us in Seattle.

ABSTRACT

To the chemist, the epipolythiodiketopiperazine (ETP) fungal metabolites represent a fascinating family of natural products, not only for their unique structural elements, but also for the unusual modes by which they are hypothesized to exert their biological activities. Though efforts at the total synthesis of these molecules have led to an evolution of innovative synthetic methodologies and strategies, challenges remain—particularly with respect to acid-sensitive and highly oxygenated ETP structures, such as those containing one or more dihydrooxepine ring. As part of a broad research program targeting ETP natural products, we have developed a synthetic strategy towards dihydrooxepine-containing ETPs.

Herein, the enantioselective total synthesis of (–)-acetylaranotin is described. This represents the first total synthesis of any dihydrooxepine-containing ETP natural product. The key steps of the synthesis include an enantioselective azomethine ylide (1,3)-dipolar cycloaddition reaction to set the absolute and relative stereochemistry, a rhodium-catalyzed cycloisomerization/chloride elimination sequence to generate the dihydrooxepine moiety, and a stereoretentive diketopiperazine sulfenylation to install the epidisulfide.

Our strategy was extended to the synthesis of a small panel of epitetrathiodiketopiperazines, including the natural products SCH64877 and emethallicin C as well as analogs, which are currently being evaluated for biological activity. Furthermore, preliminary investigations into the synthesis of dihydrooxepine-containing macrocycles have been conducted, with a particular focus on the preparation of bis(*ortho*-methoxyaryl) ethers.

Finally, as part of our efforts to further explore interesting side reactions observed during synthetic studies toward acetylalaranotin, a catalytic asymmetric double (1,3)-dipolar cycloaddition reaction was developed. This reaction provides access to highly substituted, enantioenriched pyrrolidazines from inexpensive, commercially available starting materials. Furthermore, the reactivity of diketopiperazine intermediates prepared *en route* to acetylalaranotin toward aerobic oxidation was briefly explored.

TABLE OF CONTENTS

CHAPTER 1	1
Epipolythiodiketopiperazine Natural Products	
1.1 INTRODUCTION.....	1
1.2 OVERVIEW OF EPIPOLYTHIODIKETOPIPERAZINE	
NATURAL PRODUCTS	2
1.2.1 Biosynthesis	4
1.2.2 Biological Activity	7
1.3 PREVIOUS/CONCURRENT SYNTHETIC EFFORTS	11
1.3.1 Early Strategies for Installing the ETP Core	12
1.3.2 The Thioacetal Protecting Group Strategy	14
1.3.3 Recent Advances: Late Stage Oxidation/Displacement	14
1.3.4 Recent Advances: Direct Diketopiperazine Sulfenylation	17
1.4 CONCLUSIONS	20
1.5 NOTES AND REFERENCES	21
CHAPTER 2	28
Enantioselective Total Synthesis of (–)-Acetylaranotin	
2.1 INTRODUCTION.....	28
2.1.1 Biological Activity	29
2.1.2 Previous Synthetic Approaches.....	30

2.1.3 Concurrent Synthetic Approaches	32
2.1.4 Retrosynthetic Analysis	34
2.2 FORWARD SYNTHETIC EFFORTS	38
2.3 CONCLUDING REMARKS	55
2.4 EXPERIMENTAL SECTION	56
2.4.1 Materials and Methods	56
2.4.2 Preparative Procedures and Spectroscopic Data	57
2.5 NOTES AND REFERENCES	113
APPENDIX 1	118
Spectra Relevant to Chapter 2	
APPENDIX 2	213
X-Ray Crystallography Reports Relevant to Chapter 2	
CHAPTER 3	245
C ₂ -Symmetric Dihydrooxepine-Containing ETPs and MPC1001B	
3.1 INTRODUCTION	245
3.2 C ₂ -SYMMETRIC DIHYDROOXEPINE-CONTAINING EPIPOLYTHIODIKETOPIPERAZINE NATURAL PRODUCTS	246
3.3 MACROCYCLIC DIHYDROOXEPINE-CONTAINING EPIPOLYTHIODIKETOPIPERAZINE NATURAL PRODUCTS	253
3.4 CONCLUDING REMARKS	257
3.5 EXPERIMENTAL SECTION	259
3.5.1 Materials and Methods	259
3.5.2 Preparative Procedures and Spectroscopic Data	260

3.6 NOTES AND REFERENCES	281
--------------------------------	-----

APPENDIX 3	284
-------------------	------------

Spectra Relevant to Chapter 3	
-------------------------------	--

CHAPTER 4	323
------------------	------------

Further Investigation of Side Reactions	
---	--

4.1 INTRODUCTION.....	323
-----------------------	-----

4.2 AN ENANTIOSELECTIVE CASCADE CYCLOADDITION	
---	--

PROCESS TO FORM HIGHLY SUBSTITUTED PYRROLIZIDINES	324
---	-----

4.3 DIKETOPIPERAZINE OXIDATION AND STEREOCHEMISTRY	331
--	-----

4.4 CONCLUDING REMARKS	334
------------------------------	-----

4.5 EXPERIMENTAL SECTION	335
--------------------------------	-----

4.5.1 Materials and Methods	335
-----------------------------------	-----

4.5.2 Preparative Procedures and Spectroscopic Data	336
---	-----

4.6 NOTES AND REFERENCES	371
--------------------------------	-----

APPENDIX 4	375
-------------------	------------

Spectra Relevant to Chapter 4	
-------------------------------	--

APPENDIX 5	448
-------------------	------------

X-Ray Crystallography Reports Relevant to Chapter 4	
---	--

ABOUT THE AUTHOR	459
-------------------------	------------

LIST OF ABBREVIATIONS

$[\alpha]_D$	angle of optical rotation of plane-polarized light
Å	angstrom(s)
<i>p</i> -ABSA	<i>para</i> -acetamidobenzenesulfonyl azide
Ac	acetyl
APCI	atmospheric pressure chemical ionization
app	apparent
aq	aqueous
Ar	aryl group
At	benztriazolyl
atm	atmosphere(s)
BHT	2,6-di- <i>tert</i> -butyl-4-methylphenol (“butylated hydroxytoluene”)
Bn	benzyl
Boc	<i>tert</i> -butoxycarbonyl
BOP-Cl	bis(2-oxo-3-oxazolidinyl)phosphinic chloride
bp	boiling point
br	broad
Bu	butyl
<i>i</i> -Bu	<i>iso</i> -butyl
<i>n</i> -Bu	butyl or <i>norm</i> -butyl
<i>t</i> -Bu	<i>tert</i> -butyl
Bz	benzoyl
C	cytosine

<i>c</i>	concentration of sample for measurement of optical rotation
¹³ C	carbon-13 isotope
¹⁴ C	carbon-14 isotope
/C	supported on activated carbon charcoal
°C	degrees Celcius
calc'd	calculated
CAN	ceric ammonium nitrate
Cbz	benzyloxycarbonyl
CCDC	Cambridge Crystallographic Data Centre
CDI	1,1'-carbonyldiimidazole
cf.	consult or compare to (Latin: <i>confer</i>)
cm ⁻¹	wavenumber(s)
cod	1,5-cyclooctadiene
comp	complex
conc.	concentrated
Cy	cyclohexyl
Cys	cysteine
CSA	camphor sulfonic acid
d	doublet
<i>d</i>	dextrorotatory
D	deuterium
dba	dibenzylideneacetone
DBU	1,8-diazabicyclo[5.4.0]undec-7-ene

DCE	1,2-dichloroethane
<i>de</i>	diastereomeric excess
DIAD	diisopropyl azodicarboxylate
DIPEA	<i>N,N</i> -diisopropylethylamine
DMAD	dimethyl acetylenedicarboxylate
DMAP	4-dimethylaminopyridine
DME	1,2-dimethoxyethane
DMF	<i>N,N</i> -dimethylformamide
DMSO	dimethylsulfoxide
DMTS	dimethylhexylsilyl
DNA	deoxyribonucleic acid
DPPA	diphenylphosphorylazide
dPPP	1,3-bis(diphenylphosphino)propane
dr	diastereomeric ratio
DTT	dithiothreitol
<i>ee</i>	enantiomeric excess
E	methyl carboxylate (CO_2CH_3)
E^+	electrophile
<i>E</i>	trans (entgegen) olefin geometry
EC_{50}	median effective concentration (50%)
EDC	<i>N</i> -ethyl- <i>N'</i> -(3-dimethylaminopropyl)carbodiimide
e.g.	for example (Latin: <i>exempli gratia</i>)
EI	electron impact

eq	equation
ESI	electrospray ionization
Et	ethyl
<i>et al.</i>	and others (Latin: <i>et alii</i>)
ETP	epipolythiodiketopiperazine
FAB	fast atom bombardment
Fmoc	fluorenylmethyloxycarbonyl
g	gram(s)
G	guanine
h	hour(s)
¹ H	proton
² H	deuterium
³ H	tritium
[H]	reduction
HATU	2-(7-aza-1 <i>H</i> -benzotriazol-1-yl)-1,1,3,3-tetramethyluronium hexafluorophosphate
HMDS	hexamethyldisilamide or hexamethyldisilazide
HMPT	hexamethylphosphoramide
<i>hν</i>	light
HPLC	high performance liquid chromatography
HRMS	high resolution mass spectrometry
Hz	hertz
IC ₅₀	half maximal inhibitory concentration (50%)
i.e.	that is (Latin: <i>id est</i>)

IR	infrared spectroscopy
<i>J</i>	coupling constant
<i>k</i>	rate constant
kcal	kilocalorie(s)
kg	kilogram(s)
L	liter or neutral ligand
<i>l</i>	levorotatory
LA	Lewis acid
LD ₅₀	median lethal dose (50%)
LDA	lithium diisopropylamide
LTMP	lithium 2,2,6,6-tetramethylpiperidide
m	multiplet or meter(s)
M	molar or molecular ion
<i>m</i>	meta
μ	micro
<i>m</i> -CPBA	<i>meta</i> -chloroperbenzoic acid
Me	methyl
mg	milligram(s)
MHz	megahertz
MIC	minimum inhibitory concentration
min	minute(s)
mL	milliliter(s)
MM	mixed method

mol	mole(s)
MOM	methoxymethyl
mp	melting point
Ms	methanesulfonyl (mesyl)
MS	molecular sieves
<i>m/z</i>	mass-to-charge ratio
N	normal or molar
NBS	<i>N</i> -bromosuccinimide
NCS	<i>N</i> -chlorosuccinimide
nm	nanometer(s)
NMR	nuclear magnetic resonance
NOE	nuclear Overhauser effect
NOESY	nuclear Overhauser enhancement spectroscopy
Nu^-	nucleophile
<i>o</i>	ortho
[O]	oxidation
<i>t</i> -Oct	<i>tert</i> -octyl (1,1,3,3-tetramethylbutyl)
<i>p</i>	para
PCC	pyridinium chlorochromate
PDC	pyridinium dichromate
Ph	phenyl
pH	hydrogen ion concentration in aqueous solution
$\text{p}K_a$	acid dissociation constant

PMB	<i>para</i> -methoxybenzyl
ppm	parts per million
PPTS	pyridinium <i>para</i> -toluenesulfonate
Pr	propyl
<i>i</i> -Pr	isopropyl
<i>n</i> -Pr	propyl or <i>norm</i> -propyl
Pro	proline
psi	pounds per square inch
py	pyridine
pyr	pyridine
q	quartet
R	alkyl group
<i>R</i>	rectus
REDAL	sodium bis(2-methoxyethoxy)aluminum hydride
ref	reference
<i>R_f</i>	retention factor
RNA	ribonucleic acid
s	singlet or seconds
<i>s</i>	selectivity factor = $k_{\text{rel(fast/slow)}} = \ln[(1 - C)(1 - ee)]/\ln[(1 - C)(1 + ee)]$, where C = conversion
<i>S</i>	sinister
sat.	saturated
SEM	2-(trimethylsilyl)ethoxymethyl
SOD	superoxide dismutase

Su	succinimide
t	triplet
T	thymine
TBAF	tetra- <i>n</i> -butylammonium fluoride
TBAT	tetra- <i>n</i> -butylammonium difluorotriphenylsilicate
TBDPS	<i>tert</i> -butyldiphenylsilyl
TBS	<i>tert</i> -butyldimethylsilyl
TCA	trichloroacetic acid
temp	temperature
Teoc	trimethylsilylethoxycarbonyl
TES	triethylsilyl
Tf	trifluoromethanesulfonyl
TFA	trifluoroacetic acid
TFE	2,2,2-trifluoroethanol
THF	tetrahydrofuran
THIQ	tetrahydroisoquinoline
TIPS	triisopropylsilyl
TLC	thin layer chromatography
TMEDA	<i>N,N,N',N'</i> -tetramethylethylenediamine
TMS	trimethylsilyl
TOF	time-of-flight
tol	tolyl
Troc	2,2,2-trichloroethoxycarbonyl

Ts	<i>para</i> -toluenesulfonyl (tosyl)
UV	ultraviolet
w/v	weight per volume
v/v	volume per volume
X	anionic ligand or halide
Z	cis (zusammen) olefin geometry

Chapter 1

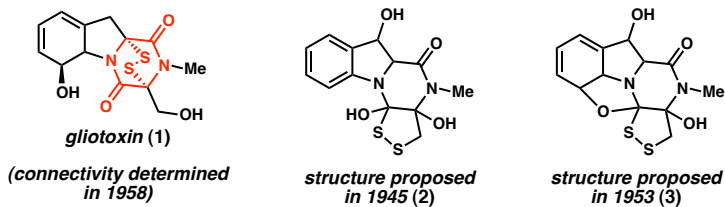
Epipolythiodiketopiperazine Natural Products

1.1 INTRODUCTION

To the chemist, the epipolythiodiketopiperazine (ETP) fungal metabolites represent a fascinating family of natural products, not only for their unique structural elements, but also for the unusual modes by which they are hypothesized to exert their biological activities.¹ Gliotoxin (**1**, see Figure 1.1) was the first of these molecules to be isolated,² and has been the most extensively studied: numerous manuscripts document gliotoxin's biological activities, and efforts to elucidate the details of its biosynthesis are ongoing. At the time of its isolation, the structure of gliotoxin was completely unprecedented; efforts to determine its connectivity via degradation studies and spectroscopy required collaboration between multiple research groups, and were presented over the course of thirteen separate reports.^{3,4} With the subsequent discovery of a multitude of ETP subfamilies, each possessing unique structural elements peripheral to

the ETP core, the story of ETP chemistry and biology has come to beautifully exemplify the interplay between molecular structure and function.

Figure 1.1. Gliotoxin (**1**) and previously proposed structures (**2** and **3**)

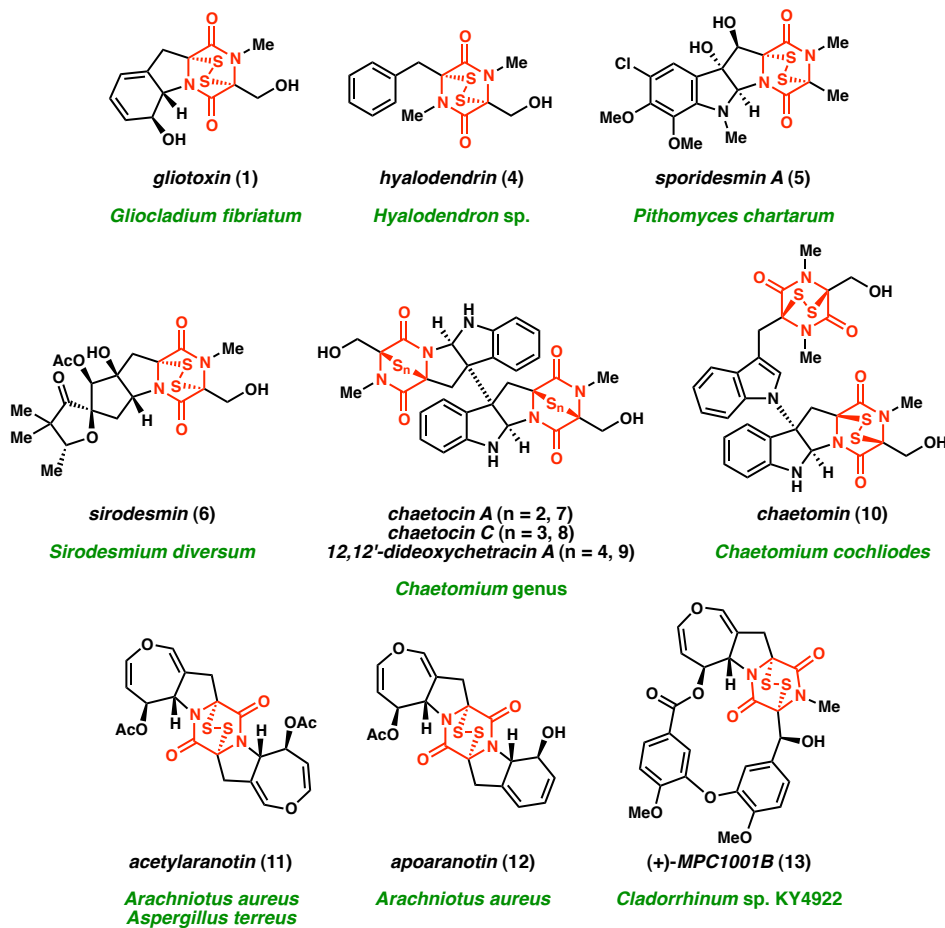


1.2 OVERVIEW OF EPIPOLYTHIODIKETOPIPERAZINE NATURAL PRODUCTS

The structural element at the core of each ETP natural product is the namesake epipolythiodiketopiperazine bicyclic (Figure 1.2), comprising a diketopiperazine ring and a polysulfide linkage that bridges the two C(α)-centers. As shown in Figure 1.2, this core is found among the ETPs in combination with a variety of peripheral structures. These appendages can be as simple as the unmodified phenylalanine and serine residues of hyalodendrin (**4**)⁵ to the highly oxygenated polycyclic ring system of sirodesmin (**6**).⁶ As in the case of acetylaranotin (**11**),⁷ some structures are C_2 -symmetric about the ETP core, whereas others represent dimerization of two ETP-containing fragments adjoined at their periphery (as in **7–10**).^{8,9} Though sub-families can roughly be designated based on structure, they are not mutually exclusive; for example, apoaranotin (**12**)^{7f} possesses the cyclohexadienol monomer unit found in gliotoxin (**1**) as well as the dihydrooxepine unit found in acetylaranotin (**11**), whereas MPC1001B (**13**)¹⁰ contains the acetylaranotin monomer unit embedded within a macrocyclic framework. Finally, the characteristic polysulfide bridge can exist as the di-, tri-, or tetrasulfide (as with **7–9**). Though the disulfide structures are most common, in many cases all three polysulfides are isolated

together, and the tri- and tetrasulfides are hypothesized to exert their biological activities following reduction to the disulfide (or alternatively, the dithiol) to generate the active pharmacophore.¹¹

Figure 1.2. Epipolythiodiketopiperazine natural products

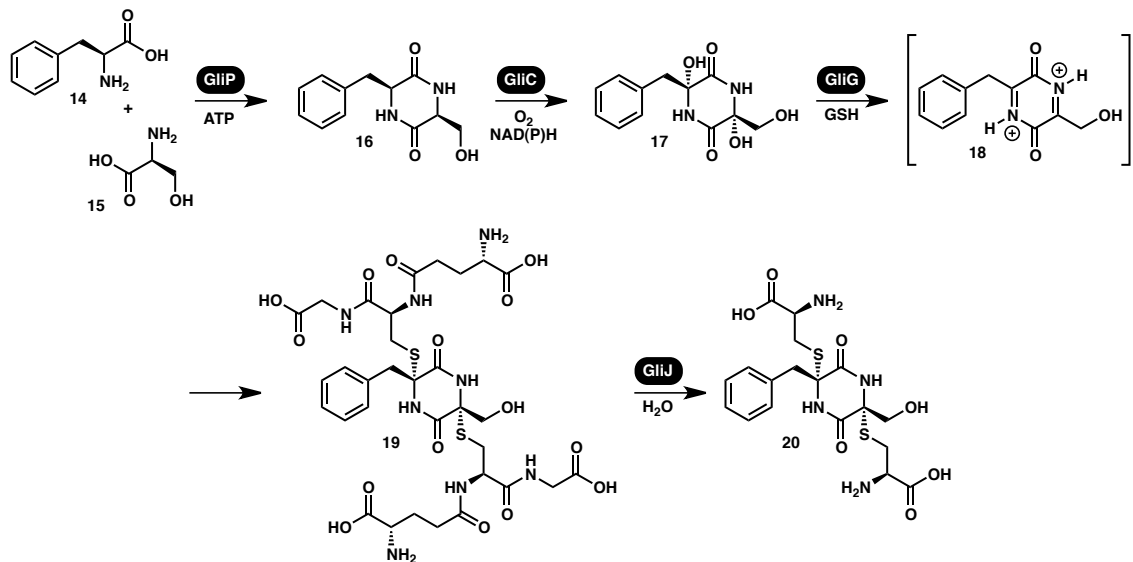


As suggested by the isolation sources listed in Figure 1.2, ETP natural products are found exclusively as secondary metabolites in fungal species. In many cases, they are hypothesized to serve as virulence and/or defense factors,¹² and generally exhibit various antimicrobial activities as well as cytotoxicity.

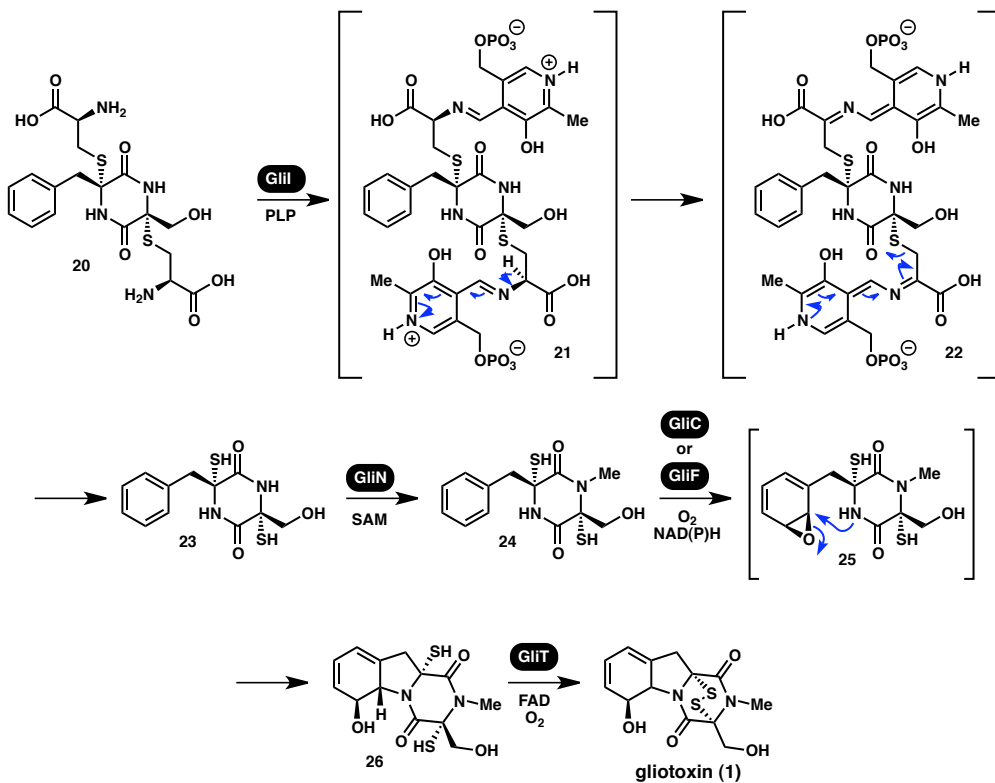
1.2.1 Biosynthesis

Though feeding studies have suggested that all ETP natural products derive from cyclic dipeptides,¹³ and that the sulfur atoms generally derive from cysteine residues,¹⁴ efforts to elucidate the details of biosynthetic pathway, including the associated gene clusters, have only been carried out for a few species: *Aspergillus fumigatus* (a producer of gliotoxin, **1**),¹⁵ *Leptosphaeria maculans* (a producer of sirodesmin PL, not shown),¹⁶ and *Aspergillus terreus* (a producer of acetylalarotin, **11**).¹⁷ Of these investigations, the best-understood pathway to date is that for gliotoxin (**1**).

Based on a combination of feeding experiments, directed mutagenesis, and BLAST primary sequence analyses, it is proposed that gliotoxin biosynthesis begins with the synthesis of diketopiperazine **16** from phenylalanine (**14**) and serine (**15**), catalyzed by GliP, a non-ribosomal peptide synthetase (NRPS) (See Scheme 1.1).^{15,18} Subsequent C–H oxidation by cytochrome P450 monooxygenase GliC then furnishes the dihydroxylated diketopiperazine **17**. The nascent hydroxyl groups are next displaced by two equivalents of glutathione (GSH), a reaction catalyzed by glutathione S-transferase GliG and presumed to involve the intermediacy of an iminium electrophile **18**, to afford the bis-GSH adduct **19**.¹⁹ Hydrolytic degradation by peptidase GliJ renders the corresponding bis-Cys adduct **20**.

Scheme 1.1. C–S bond formation during gliotoxin (**1**) biosynthesis

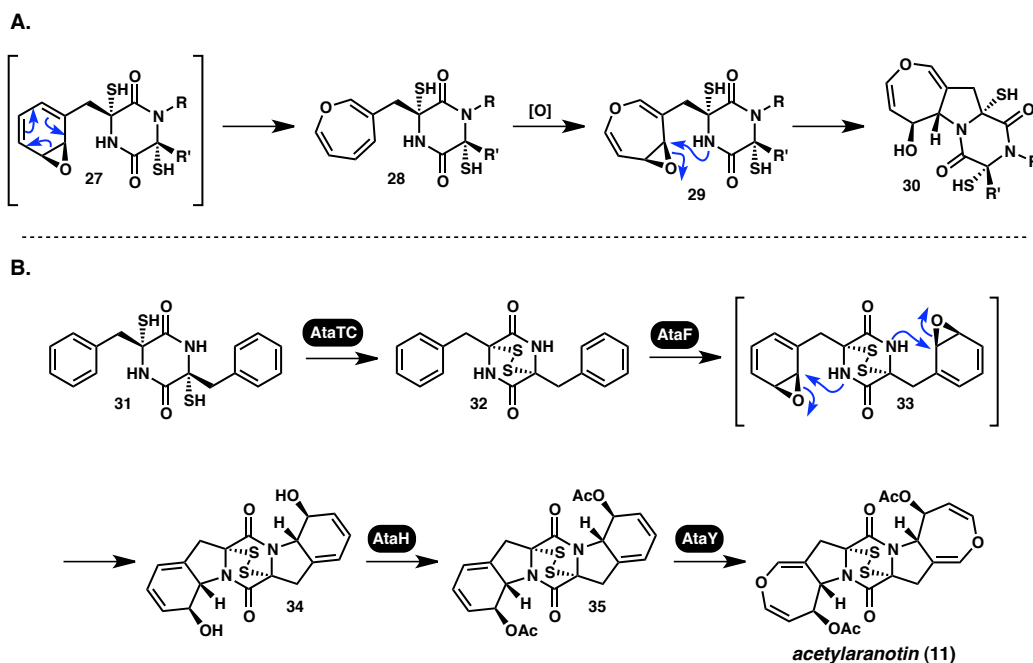
C–S bond cleavage to deliver the free dithiol **23** is mediated by GliI, a homodimeric pyridoxal phosphate (PLP)-dependent carbon–sulfur lyase that is homologous to 1-aminocyclopropane-1-carboxylic acid synthases (ACCS) (Scheme 1.2).²⁰ Significantly, this is the first confirmed example of C–S lyase activity in the biosynthesis of a secondary metabolite. Furthermore, the absence of detectable amounts of the mono-Cys adduct during the process suggests that GliI cleaves the two C–S bonds *simultaneously*. Next, *N*-methylation is accomplished by *N*-methyltransferase GliN to afford **24**, and subsequent cytochrome P450-mediated oxidative cyclization furnishes the polycyclic cyclohexadienol ring system of the natural product, via the intermediacy of epoxide **25**.²¹ Finally, the oxidase GliT promotes oxidation of the penultimate dithiol (**26**) to the disulfide, thus completing the biosynthesis of **1**.²²

Scheme 1.2. Completion of the biosynthesis of gliotoxin (**1**)

Classically, the biosynthesis of acetylaranotin has been hypothesized to occur via a benzene oxide intermediate (**27**) similar to that for the biosynthesis of gliotoxin (see Scheme 1.3, part A). Whereas the diketopiperazine attacks the epoxide **25** directly to give the gliotoxin ring system, it was envisioned that epoxide **27** might instead undergo electrocyclic ring opening to afford oxepine **28**. It was proposed that subsequent oxidation to *sym*-oxepine oxide **29** followed by cyclization would furnish dihydrooxepine **30**.^{7a} Recent genome-based deletion analyses reported by Wang and coworkers affirm the biogenetic relationship between gliotoxin (**1**) and acetylaranotin (**11**).¹⁷ They propose a biosynthetic pathway similar to that outlined for **1** above (see Scheme 1.3, part B), in which cyclic dipeptide **32** undergoes cytochrome P450 AtaF-promoted oxidative cyclization to afford bis(cyclohexadienol) **34**. This intermediate is then acetylated by

acetyltransferase AtaH to furnish diacetate **35**, which undergoes sequential AtaY-mediated oxidative ring expansion to afford acetylaranotin (**11**). Feeding experiments confirmed that cyclization to provide the cyclohexadienol moiety occurs *prior* to dihydrooxepine formation, in contrast to the traditional mechanistic hypothesis.

Scheme 1.3. Proposed biosynthetic transformations en route to acetylaranotin (**11**)

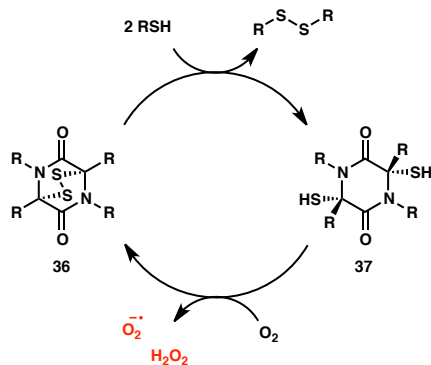


1.2.2 Biological Activity

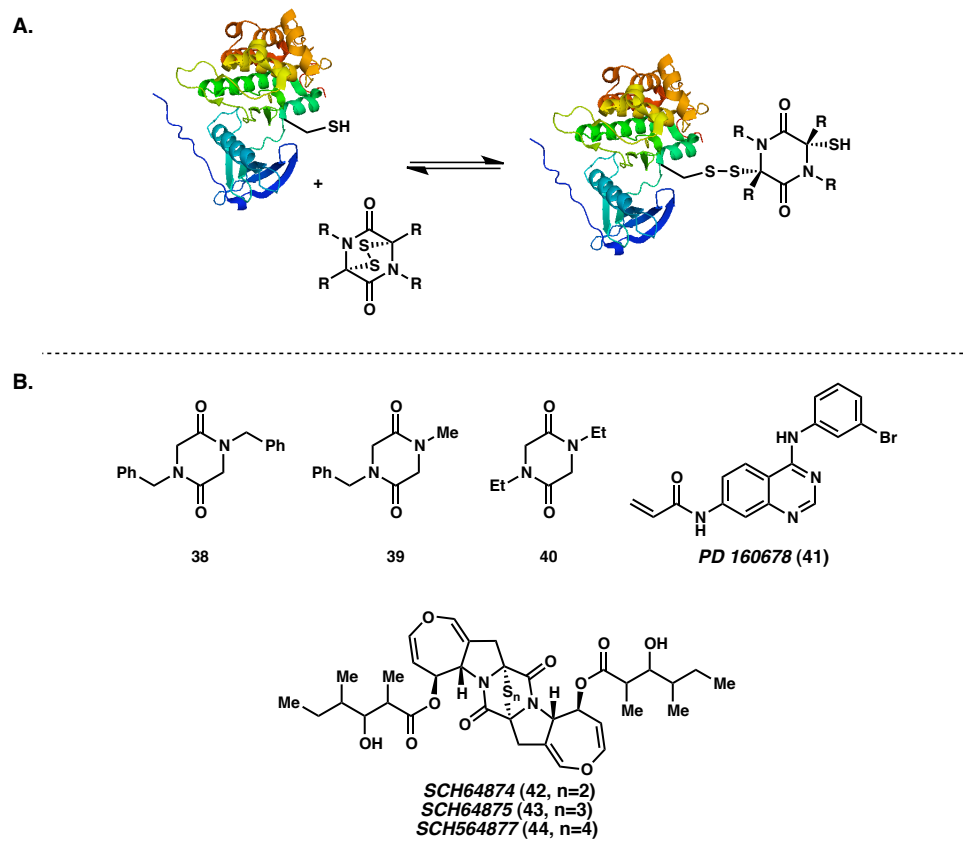
In addition to the general antimicrobial activity mentioned above, ETPs demonstrate cytotoxicity and/or antiproliferative effects against a variety of human cancer cell lines.^{10,11,23,24} Observed differences in efficacy from one agent to the next suggest a correlation between structure and specificity. Though it is generally agreed that the ETP core represents the primary pharmacophore of ETP natural products, the mechanism by which this moiety exerts its biological effects, as well as the role of peripheral structural elements, remains a topic of ongoing investigation. The two classical

hypotheses can be termed the redox cycling mechanism and the covalent modification mechanism, though recently strong evidence has been provided for a metal chelation mechanism as well.

The redox cycling hypothesis states that ETP cytotoxicity is mediated by the redox activity of the highly strained disulfide moiety. Once inside the cell, the toxin (**36**) is reduced by various cellular reductants (e.g., glutathione) to the corresponding dithiol (**37**, see Figure 1.3). The increased polarity of the dithiol relative to the disulfide causes sequestration and accumulation within the cell. The dithiol's low redox potential, on the other hand, allows for reoxidation to the disulfide by molecular oxygen, resulting in the formation of reactive oxygen species (ROS) such as superoxide and hydrogen peroxide. The resulting cycle of cellular reductant depletion and ROS generation ultimately causes cell death.^{1a} It is notable that this mechanism should be minimally affected by the peripheral structure of ETP agents, aside from effects on solubility and the ability to permeate the cell membrane. In support of this mechanism is the toxicity of sporidesmin (**5**) toward erythrocytes, and that of chaetocin (**7**) toward myeloma cells, both of which have been correlated with increased cellular levels of superoxide radical.^{25,26} On the other hand, the observed ability of gliotoxin (**1**) to modulate cellular calcium flux suggests that ETPs can induce oxidative stress via other, indirect pathways as well.²⁷

Figure 1.3. The redox cycling mechanism for ETP bioactivity

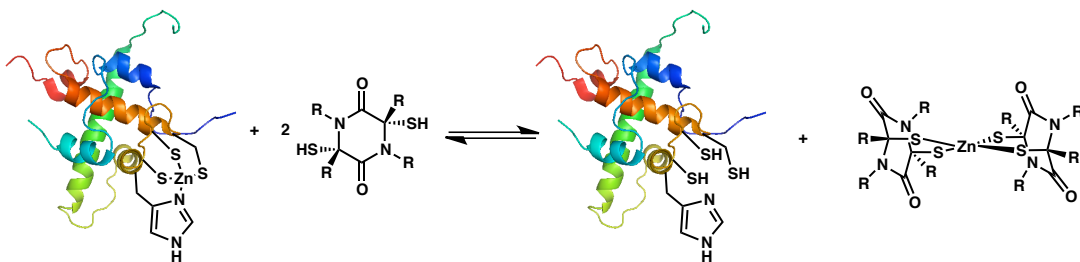
Perhaps more in line with the typical mode of action for bioactive small molecules is the covalent modification hypothesis, which states that ETPs deactivate specific molecular targets by reacting with susceptible cysteine residues to form mixed disulfides (see Figure 1.4, part A). This proposal is supported by a number of *in vitro* biochemical studies; for example, gliotoxin (**1**) has been identified to form covalent adducts with alcohol dehydrogenase.²⁸ As a part of their investigation of the inhibition of glutaredoxin (GRx) by sporidesmin A (**5**), Mieyal and coworkers found that the synthetic ETPs **38** and **39** exhibited similar inhibitory action, whereas **40** demonstrated negligible activity (see Figure 1.4, part B).²⁹ Epidermal Growth Factor Receptor (EGFR), a known molecular target of fungal metabolites **42–44**,³⁰ contains an active site cysteine residue in its kinase domain that has been targeted by covalent inhibitors (such as **41**)³¹ providing indirect evidence for mixed disulfide formation with the aforementioned ETPs. Though in the case of this mechanism, peripheral ETP structure would strongly influence bioactivity by contributing various secondary binding interactions between small molecule and protein target, there remains a lack of evidence for covalent adduct formation *in vivo*.

Figure 1.4. Deactivation of molecular targets by mixed disulfide formation

The dimeric ETPs chaetocin (**7**) and chaetomin (**10**) are known to inhibit the interaction between hypoxia inducible factor 1 (HIF-1) and the transcriptional coactivator p300, an activity with potential therapeutic potential in cancer biology.³² In an effort to elucidate the mechanism of this inhibition and identify structure-activity relationships, Figg and coworkers investigated a small panel of ETPs, including several natural products and synthetic compounds, and found that they were all effective at blocking the binding interaction between HIF-1 α and p300.³³ Using a non-denaturing ESI-MS technique, they found that in the presence of each ETP agent, structurally crucial Zn(II) ions appeared to have been removed from the HIF-1-binding domain of p300, presumably via chelation as shown in Figure 1.5. The authors have termed this the “zinc

ejection” mechanism, and although it is unclear what role peripheral ETP structure might have in determining target specificity,³⁴ it certainly represents a novel mode of action for small molecule inhibitors.

Figure 1.5. Deactivation of transcriptional regulators via Zn(II) ejection



Though evidence for each of the above mechanisms remains limited (particularly with respect to *in vivo* experiments), they represent reasonable hypotheses, and it is unlikely that they are mutually exclusive. Indeed, each ETP may exhibit some combination of these three modes of activity, and modulation of the scaffold surrounding the ETP core may ultimately allow for the tuning of this combination. As an increasing number of synthetic routes towards ETP natural products are developed, the ability to produce structural analogs and chemical probes for target pull-down will likely shed light on the mechanistic questions that remain.

1.3 PREVIOUS/CONCURRENT SYNTHETIC EFFORTS

As evidenced by the abundance of degradation product literature for gliotoxin (**1**) alone, the epidithiodiketopiperazine core is quite labile. In their full account of the total synthesis of **1** and other ETP natural products, Kishi and coworkers note the particular sensitivity of the compounds to oxidative, reductive, and basic conditions.³⁵ Additionally, many ETPs contain *acid*-sensitive functionality. These challenges have inspired the

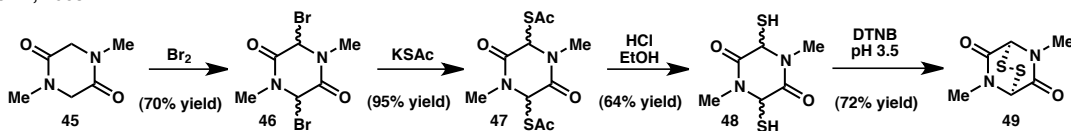
evolution of a variety of strategies for the protection of thiols, selective late-stage oxidation, and direct enolate sulfenylation.

1.3.1 Early Strategies for Installing the ETP Core

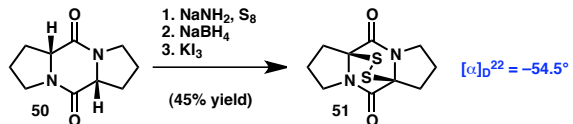
In 1968, Town reported the first synthetic procedure for constructing the ETP core (see Scheme 1.4).³⁶ The sequence involved bromination of sarcosine dimer **45** with molecular bromine, followed by bromide displacement with thioacetate anion and subsequent acidic hydrolysis to afford dithiol **48**. Final oxidation with Ellman's reagent (5,5'-dithiobis(2-nitrobenzoic acid), DTNB) revealed the simple ETP bicyclic **49**. Several years later, Schmidt and coworkers disclosed a strategy involving direct enolate sulfenylation; they found that they could readily sulfenylate proline dimer **50** with S₈ in the presence of NaNH₂, with sequential reductive and oxidative workups affording ETP **51**.³⁷ Notably, this process exhibits some degree of stereoretention, as **51** was shown to be optically active. The same authors later reported a procedure for converting **50** to *trans*-diacetate **52** by oxidation with Pb(OAc)₄.³⁸ This product was hydrolyzed to afford dihydroxydiketopiperazine **53**, which could be converted to ETP **51** by direct displacement by H₂S under Lewis acidic conditions, followed by oxidation with KI₃. These basic strategies continue to be used for the construction of ETPs, though their application to the synthesis of complex structures has been greatly facilitated by the development of more selective oxidants as well as robust protecting group strategies.

Scheme 1.4. “Classical” procedures for ETP synthesis

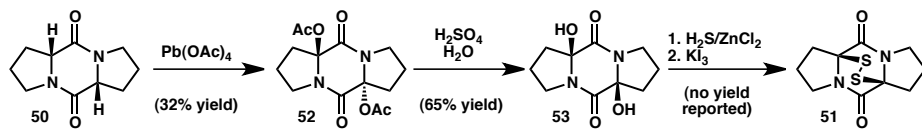
Trown, 1968:



Schmidt, 1972:



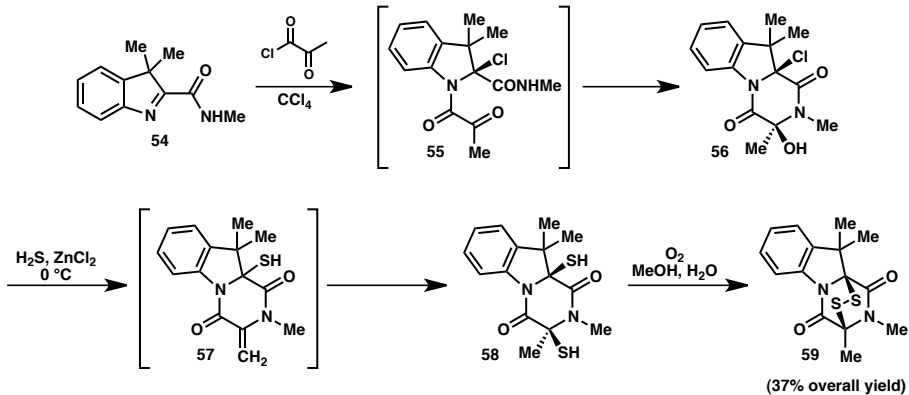
Schmidt, 1973:



In 1975, Ottenheijm and coworkers reported the development of a rapid, redox manipulation-free sequence for the synthesis of ETP **59** (see Scheme 1.5).³⁹ Imino amide **54** was first condensed with an equivalent of pyruvoyl chloride to yield α -chloro- α' -hydroxydiketopiperazine **56**. Displacement by H_2S in the presence of ZnCl_2 and subsequent aerobic oxidation furnished the final ETP product (**59**).

Scheme 1.5. A “redox neutral” synthesis of ETP **59**

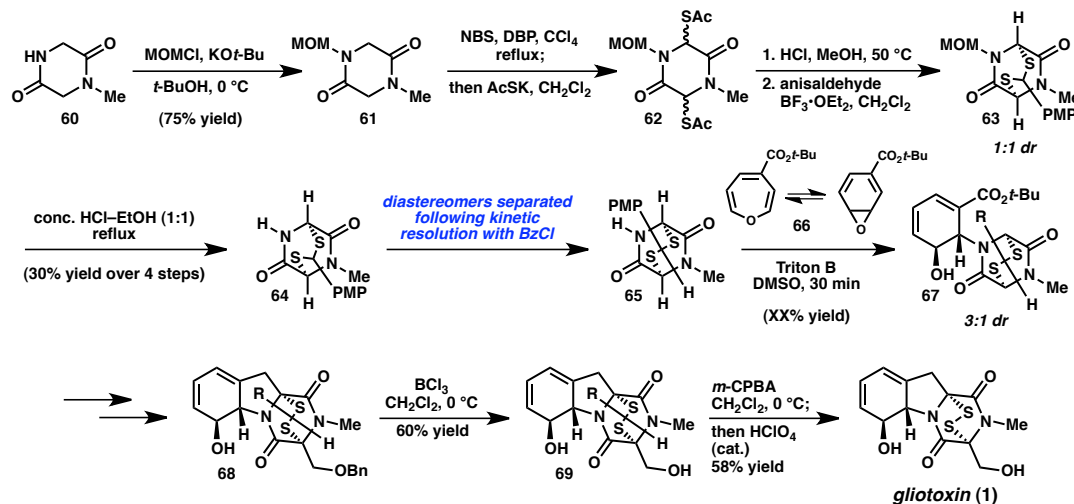
Ottenheijm, 1975:



1.3.2 The Thioacetal Protecting Group Strategy

In order to gain synthetic access to more complex ETP structures, Kishi and coworkers developed a thioacetal protecting group strategy that allowed them to install the required C–S bonds at an early stage of a synthetic route, but reserve completion of the ETP disulfide linkage for the end of the sequence.^{35,40} In their synthesis of gliotoxin (see Scheme 1.6), MOM-protected diketopiperazine **61** was advanced to *p*-anisaldehyde-derived thioacetal **64** in four steps and 30% overall yield. Following separation of diastereomers, nucleophilic addition of fragment **65** into oxepine electrophile **66** provided cyclohexadienol adduct **67** as a 3:1 mixture of diastereomers. This material was advanced to tetracycle **69**, at which point oxidation with *m*-CPBA and subsequent acidic workup revealed the ETP core of **1**.

Scheme 1.6. Total synthesis of gliotoxin (**1**)

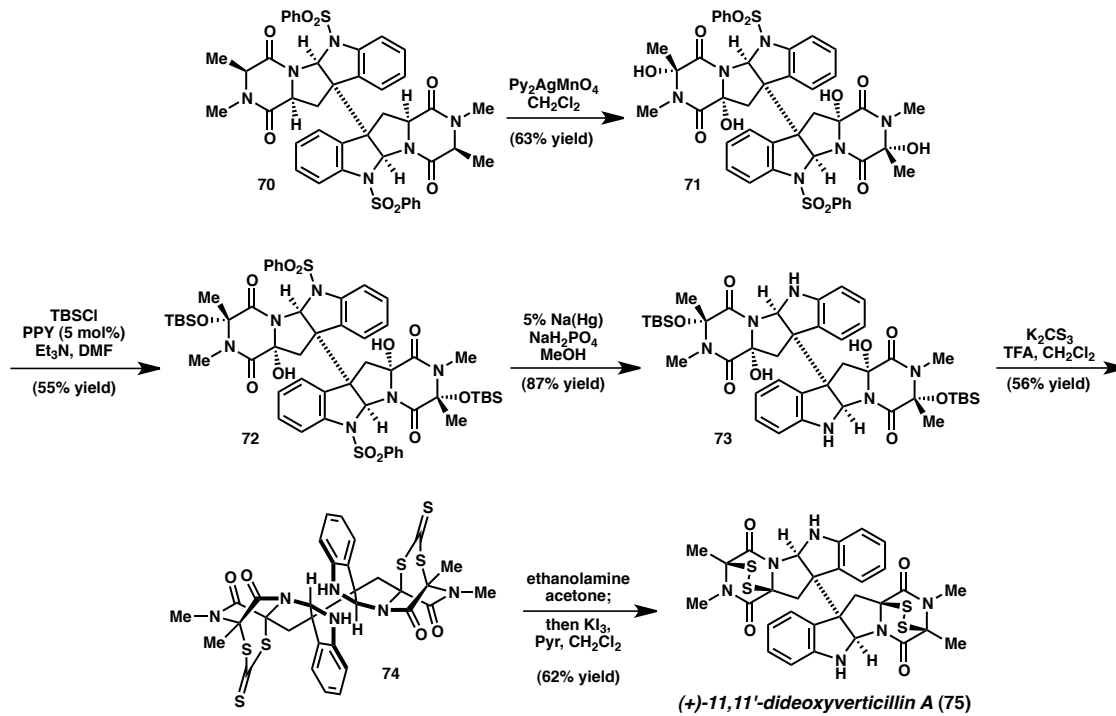


1.3.3 Recent Advances: Late Stage Oxidation/Displacement

For nearly three decades, Kishi's thioacetal protecting group strategy represented the state-of-the-art in complex ETP synthesis. Then, in 2009, Movassaghi and coworkers

reported the total synthesis of (+)-11,11'-dideoxyverticillin A (**75**).⁴¹ This seminal effort involved the mild, stereoretentive, and late-stage oxidation of bis-diketopiperazine **70** by $[\text{Ag}(\text{pyr})_2][\text{MnO}_4]$ to afford tetraol **71**. Following protecting group manipulation (it was noted that the free tetraol was unstable to a variety of acidic and basic conditions), nucleophilic displacement by trithiocarbonate under acidic conditions furnished bis-trithiocarbonate **74**. The natural product (**75**) was then obtained by ethanolaminolysis of the trithiocarbonate rings and KI_3 -mediated oxidation of the resulting dithiol.

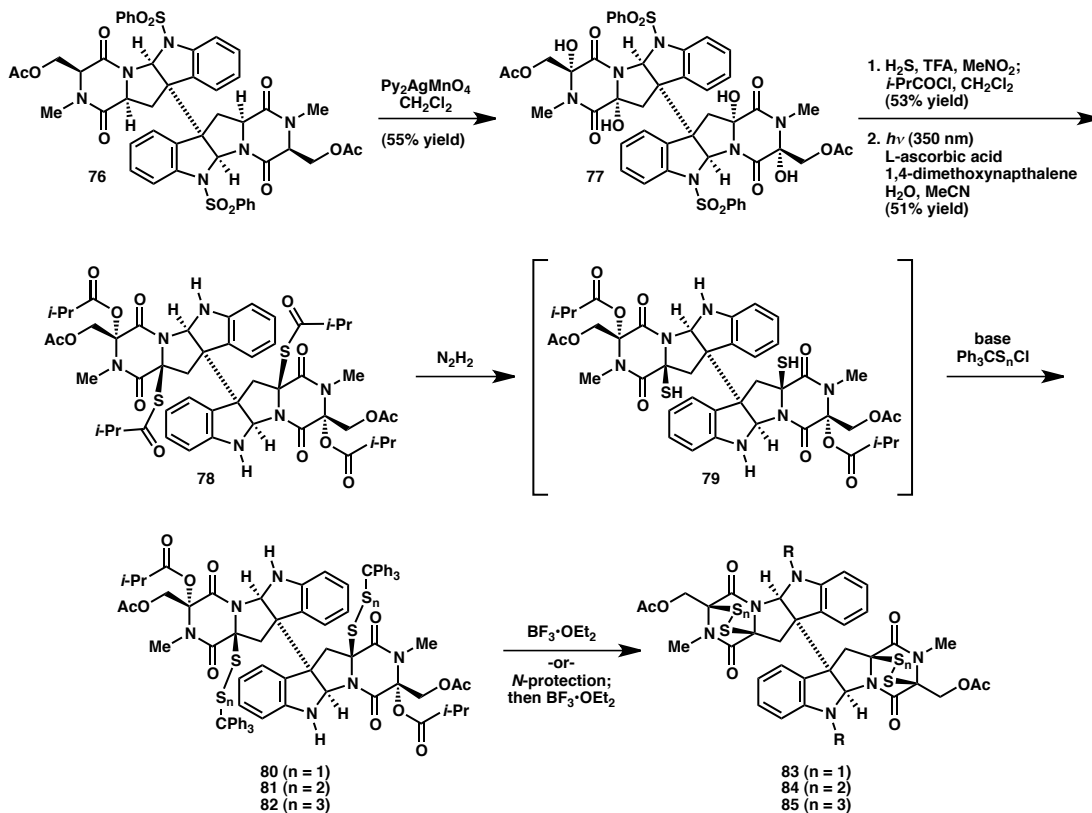
Scheme 1.7. Total synthesis of (+)-11,11'-dideoxyverticillin A (**75**)



In a follow-up communication, Movassaghi and Kim reported that a modification to the strategy used for the synthesis of **75** allowed for the selective preparation of related molecules as the di-, tri-, or tetrasulfide congener (see Scheme 1.8).⁴² Using the conditions developed during their previous efforts, bis(diketopiperazine) **76** was oxidized to tetraol **77**. However, treatment of **77** with H_2S and TFA in MeNO_2 promoted thiol

installation via S_N1-type displacement at only the C(11) and C(11') positions, and subsequent exhaustive acylation afforded tetra-*iso*-butyryl intermediate **78**. Treatment with hydrazine selectively liberated the thiol groups to give intermediate **79**, which could be trapped with Ph₃CSCl, Ph₃CSSCl, or Ph₃CSSSCl to afford protected disulfide **80**, trisulfide **81**, or tetrasulfide **82**, respectively. Subjection of these intermediates to BF₃•OEt₂ (following *N*-protection in the cases of **81** and **82**) resulted in cyclization of the polysulfide with concomitant loss of trityl cation to reveal the epidisulfide **83**, epitrisulfide **84**, or epitetrathiodiketopiperazines **85**, respectively.

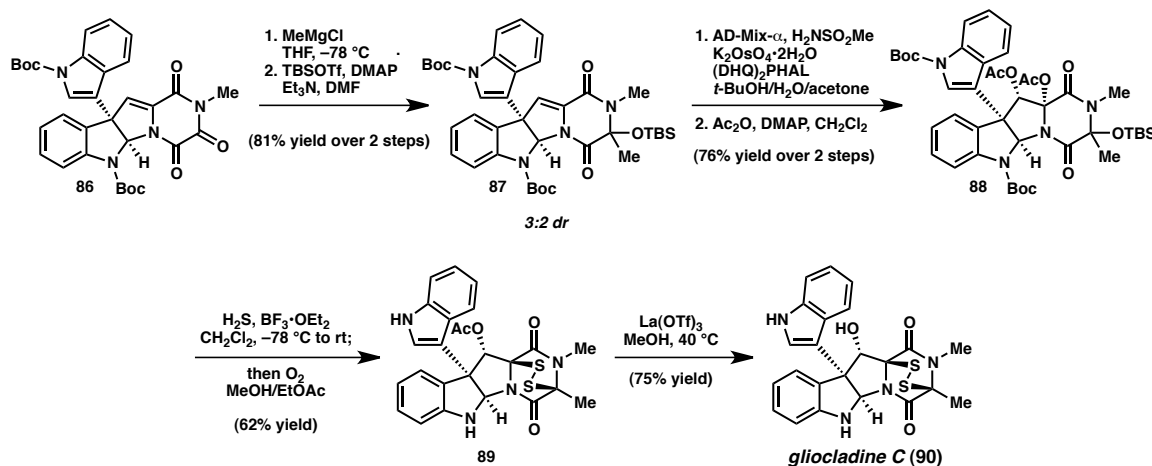
Scheme 1.8. Selective access to epidi-, epitri-, and epitetrathiodiketopiperazines



In 2011, Overman and coworkers reported a late-stage oxidation strategy for the synthesis of pyrroloindoline ETP natural products containing oxygenation at the C(12) position (see Scheme 1.9).⁴³ Reaction of triketopiperazine **86** with MeMgCl followed by

protection with TBSOTf afforded α,β -unsaturated diketopiperazine **87** as a 3:2 mixture of diastereomers. Dihydroxylation using AD-Mix- α resulted in the formation of the corresponding diol (>14:1 diastereoselectivity), which was subsequently converted to diacetate **88**. Displacement of the C(11)-hydroxyl and C(15)-siloxyl groups by H_2S was carried out in the presence of $BF_3 \cdot OEt_2$, and subsequent aerobic oxidation to the disulfide and deprotection of the C(12) acetate revealed gliocladiine C (**90**). In a follow-up report, the authors demonstrated that this strategy could be generally applied to the total synthesis of similar ETP natural products.²³

Scheme 1.9. Total synthesis of gliocladiine C (**90**)



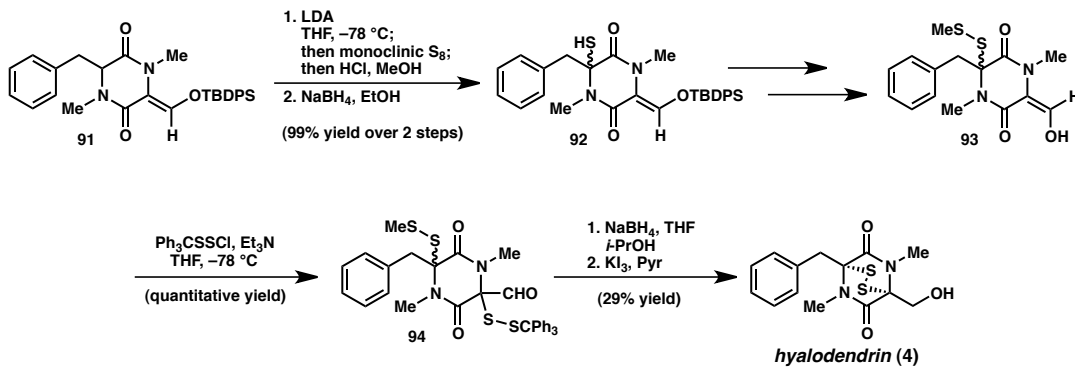
1.3.4 Recent Advances: Direct Diketopiperazine Sulfenylation

With the exception of the conditions reported by Schmidt and coworkers for the direct sulfenylation of proline dimer **50** under basic conditions, all of the examples of ETP syntheses reviewed above have involved the use of moderately to strongly acidic conditions for the displacement of various leaving groups by sulfur-containing nucleophiles. However, many natural products possess acid-labile functional groups in addition to a base- and redox-labile ETP core. Accordingly, the further development of

direct enolate sulfenylation methodologies has greatly facilitated total synthesis efforts targeting these structures.

Though the peripheral appendages of hyalodendrin (**4**) do not appear to be particularly acid-sensitive, the preparation of this natural product reported by Williams and Rastetter in 1980 constitutes one of the first examples of an enolate sulfenylation strategy in the context of natural product total synthesis (see Scheme 1.10).⁴⁴ In the first sulfenylation reaction, the lithium enolate of diketopiperazine **91** was trapped by *monoclinic* S₈ (the authors point out that the use of this form of sulfur—obtained by briefly heating the more stable orthorhombic form under vacuum—is critical to the success of the reaction), generating thiol **92**. The second sulfenylation event involved soft enolization of the more acidic α -formyl diketopiperazine **93** and subsequent trapping with Ph₃CSSCl to afford bis(disulfide) **94**. Reductive deprotection of the two disulfides followed by KI₃-mediated oxidation completed the synthesis of **4**.

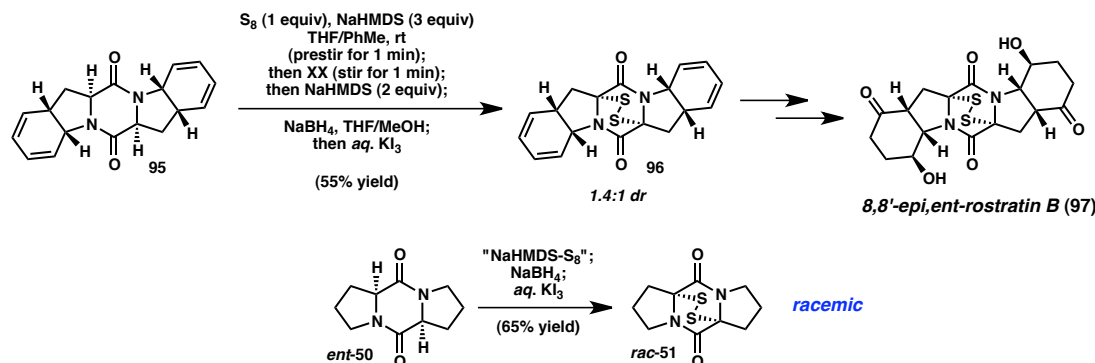
Scheme 1.10. Enolate sulfenylation in the total synthesis of hyalodendrin (**4**)



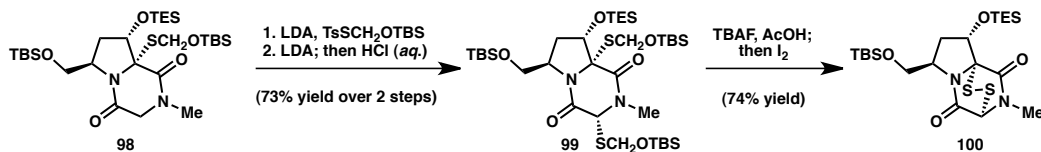
More recently, Nicolaou and coworkers have developed a modification to the conditions for direct enolate sulfenylation reported by Schmidt and coworkers that is better suited for complex substrates (see Scheme 1.11).⁴⁵ In their initial communication of the total synthesis of epicoccin G (not shown) and 8,8'-*epi,ent*-rostratin B (**97**),^{45a} the

authors describe having treated diketopiperazine **95** with a reagent mixture obtained by pre-stirring one equivalent of S₈ with three equivalents of NaHMDS in THF, followed by another two equivalents of NaHMDS. The resulting crude mixture of polysulfides was then reduced to the dithiol using NaBH₄, and workup with *aqueous* KI₃ furnished the disulfide **96** in 55% yield as a 1.4:1 mixture of epidisulfide diastereomers. This intermediate was then advanced to **97**. In contrast with the stereoretention observed by Schmidt and coworkers, a follow-up report by Nicolaou and coworkers revealed that sulfenylation of proline dimer *ent*-**50** under the “NaHMDS-S₈” conditions results in formation of *racemic* ETP **51**.^{45b}

Scheme 1.11. Direct sulfenylation of diketopiperazines with S₈/NaHMDS



Finally, Clive and coworkers recently reported that TsSCH₂OTBS can be used to sulfenylate diketopiperazine-derived enolates to afford the *protected* thiol product.⁴⁶ As shown in Scheme 1.12, the resulting siloxymethyl thioether (e.g., **99**) can be cleaved by buffered TBAF solution, with oxidative workup providing the ETP core (e.g., **100**). Though use of this reagent has yet to be reported in the context of a total synthesis, it may prove to be quite useful for sequences in which late stage sulfenylation is desirable, but subsequent conversion to the ETP must be delayed for the duration of multiple reactions.

Scheme 1.12. Introducing protected thiols via sulfenylation with $TsSCH_2OTBS$ 

1.4 CONCLUSIONS

ETP natural products have a rich history, yet continue to stimulate the chemist. The hypothesized modes of biological activity underscore Nature's abilities to evolve diverse mechanisms for the manipulation of biological systems, and will likely inspire the development of novel therapeutic strategies. Likewise, the complex structures and biosynthetic transformations described above demonstrate that the bar set by Nature for the synthetic chemist remains high. Though efforts at the total synthesis of these molecules have led to an evolution of innovative synthetic methodologies and strategies, challenges remain—particularly with respect to acid-sensitive and highly oxygenated ETP structures. Ultimately, comprehension of the molecular processes underlying ETP bioactivity requires that these challenges be addressed.

1.5 NOTES AND REFERENCES

-
- (1) For reviews of ETP natural products, see: (a) Gardiner, D. M.; Waring, P.; Howlett, B. J. *Microbiology* **2005**, *151*, 1021. (b) Waring, P.; Eichner, R. D.; Müllbacher, A. *Med. Res. Rev.*, **1988**, *8*, 499. (c) Iwasa, E.; Hamashima, Y.; Sodeoka, M. *Isr. J. Chem.* **2011**, *51*, 420. (d) Borthwick, A. D. *Chem. Rev.* **2012**, *112*, 3641. (e) Jiang, C.-S.; Guo, Y.-W. *Mini-Reviews in Medicinal Chemistry* **2011**, *11*, 728. (f) Jordan, T. W.; Cordiner, S. J. *Trends Pharmacol. Sci.* **1987**, *8*, 144. (g) Patron, N. J.; Waller, R. F.; Cozijnsen, A. J.; Straney, D. C.; Gardiner, D. M.; Nierman, W. C.; Howlett, B. J. *BMC Evol. Biol.* **2007**, *7*, 174. (h) Huang, R.; Zhou, X.; Xu, T.; Yang, X.; Liu, Y. *Chem. Biodiversity* **2010**, *7*, 2809.
- (2) Weindling, R.; Emerson, O. H. *Phytopathology* **1936**, *26*, 1068.
- (3) (a) Johnson, J. R.; McCrone, W. C., Jr.; Bruce, W. F. *J. Am. Chem. Soc.* **1944**, *66*, 501. (b) Bruce, W. F.; Dutcher, J. D.; Johnson, J. R.; Miller, L. L. *J. Am. Chem. Soc.* **1944**, *66*, 614. (c) Dutcher, J. D.; Johnson, J. R.; Bruce, W. F. *J. Am. Chem. Soc.* **1944**, *66*, 617. (d) Dutcher, J. D.; Johnson, J. R.; Bruce, W. F. *J. Am. Chem. Soc.* **1944**, *66*, 619. (e) Johnson, J. R.; Hasbrouck, R. B.; Dutcher, J. D.; Bruce, W. F. *J. Am. Chem. Soc.* **1945**, *67*, 423. (f) Dutcher, J. D.; Johnson, J. R.; Bruce, W. F. *J. Am. Chem. Soc.* **1945**, *67*, 1736. (g) Johnson, J. R.; Larsen, A. A.; Holley, A. D.; Gerzon, K. *J. Am. Chem. Soc.* **1947**, *69*, 2364. (h) Johnson, J. R.; Andreen, J. H. *J. Am. Chem. Soc.* **1950**, *72*, 2862. (i) Johnson, J. R.; Buchanan, J. B. *J. Am. Chem. Soc.* **1951**, *73*, 3749. (j) Dutcher, J. D.; Kjaer, A. *J. Am. Chem. Soc.* **1951**, *73*, 4139. (k) Johnson, J. R.; Buchanan, J. B. *J. Am. Chem. Soc.* **1953**, *75*, 2103.

-
- (l) Johnson, J. R.; Kidwai, A. R.; Warner, J. S. *J. Am. Chem. Soc.* **1953**, *75*, 2110.
- (m) Bell, M. R.; Johnson, J. R.; Wildi, B. S.; Woodward, R. B. *J. Am. Chem. Soc.* **1958**, *80*, 1001.
- (4) The connectivity proposed by Woodward and coworkers in 1958 was later confirmed by single-crystal X-ray diffraction analysis: Fridrichsons, J.; Mathieson, A. M. *Acta Cryst.* **1967**, *23*, 439.
- (5) Stillwell, M. A.; Magasi, L. P.; Strunz, G. M. *Can. J. Microbiol.* **1974**, *20*, 759.
- (6) (a) Curtis, P. J.; Greatbanks, D.; Hesp, B.; Cameron, A. F.; Freer, A. A. *J. Chem. Soc. Perkin Trans. I*, **1977**, 180. (b) Ferezou, J.-P.; Riche, C.; Quesneau-Thierry, A.; Pascard-Billy, C.; Barbier, M; Bousquet, J. F.; Boudart, G. *Nouv. J. Chim.* **1977**, *I*, 327.
- (7) (a) Neuss, N.; Boeck, L. D.; Brannon, D. R.; Cline, J. C.; DeLong, D. C.; Gorman, M.; Huckstep, L. L.; Lively, D. H.; Mabe, J.; Marsh, M. M.; Molloy, B. B.; Nagarajan, R.; Nelson, J. D.; Stark, W. M. *Antimicrob. Agents Chemother.* **1968**, 213. (b) Town, P. W.; Lindh, K. P.; Milstrey, K. P.; Gallo, V. M.; Mayberry, B. R.; Lindsay, H. L.; Miller, P. A. *Antimicrob. Agents Chemother.* **1968**, 225. (c) Nagarajan, R.; Huckstep, L. L.; Lively, D. H.; Delong, D. C.; Marsh, M. M.; Neuss, N. *J. Am. Chem. Soc.* **1968**, *90*, 2980. (d) Nagarajan, R.; Neuss, N.; Marsh, M. M. *J. Am. Chem. Soc.* **1968**, *90*, 6518. (e) Cosulich, D. B.; Nelson, N. R.; Van den Hende, J. H. *J. Am. Chem. Soc.* **1968**, *90*, 6519. (f) Neuss, N.; Nagarajan, R.; Molloy, B. B.; Huckstep, L. L. *Tetrahedron Lett.* **1968**, *42*, 4467.
- (8) Sekita, S.; Yoshira, K.; Natori, S.; Udagawa, S.; Muroi, T.; Sugiyama, Y.; Kurata, H.; Umeda, M. *Can. J. Microbiol.* **1981**, *27*, 766.

-
- (9) Saito, T.; Suzuki, Y.; Koyama, K.; Natori, S.; Iitaka, Y.; Knoshita, T. *Chem. Pharm. Bull.* **1988**, 36, 1942.
- (10) Onodera, H.; Hasegawa, A.; Tsumagari, N.; Nakai, R.; Ogawa, T.; Kanda, Y. *Org. Lett.* **2004**, 6, 4101.
- (11) Boyer, N.; Morrison, K. C.; Kim, J.; Hergenrother, P. J.; Movassaghi, M. *Chem. Sci.* **2013**, 4, 1646.
- (12) For a presentation of circumstantial evidence for the role of ETPs as virulence and/or defense factors, see ref. 1a and references therein.
- (13) (a) Ferezou, J.-P.; Quesneau-Thierry, A.; Servy, C.; Zissman, E.; Barbier, M. *J. Chem. Soc. Perkin Trans. I* **1980**, 1739. (b) Kirby, G. W.; Patrick, G. L.; Robins, D. J. *J. Chem. Soc. Perkin Trans. I* **1978**, 1336.
- (14) Kirby, G. W.; Robins, D. J. *The Biosynthesis of Mycotoxins 1980*, Edited by P. S. Steyn. New York: Academic Press.
- (15) Gardiner, D. M.; Howlett, B. J. *FEMS Microbiol. Lett.* **2005**, 248, 241.
- (16) Gardiner, D. M.; Cozijnsen, A. J.; Wilson, L. M.; Pedras, M. S.; Howlett, B. J. *Mol. Microbiol.* **2004**, 53, 1307.
- (17) Guo, C.-J.; Yeh, H.-H.; C., Y.-M.; Sanchez, J. F.; Chang, S.-L.; Bruno, K. S.; Wang, C. C. *C. J. Am. Chem. Soc.* **2013**, 135, 7205.
- (18) (a) Cramer, R. A., Jr.; Gamcsik, M. P.; Brooking, R. M.; Najvar, L.K.; Kirkpatrick, W. R.; Patterson, T. F.; Balibar, C. J.; Graybill, J. R.; Perfect, J. R.; Abraham, S. N.; Steinbach, W. J. *Eukaryotic Cell* **2006**, 5, 972. (b) Kupfahl, C.; Heinekamp, T.; Geginat, G.; Ruppert, T.; Hartl, A.; Hof, H.; Brakhage, A. A.

-
- Mol. Microbiol.* **2006**, *62*, 292. (c) Balibar, C. J.; Walsh, C. T. *Biochemistry* **2006**, *45*, 15029.
- (19) (a) Scharf, D. H.; Remme, N.; Habel, A.; Chankhamjon, P.; Scherlach, K.; Heinekamp, T.; Hortschansky, P.; Brakhage, A. A.; Hertweck, C. *J. Am. Chem. Soc.* **2011**, *133*, 12322. (b) Davis, C.; Carberry, S.; Schrettl, M.; Singh, I.; Stephens, J. C.; Barry, S. M.; Kavanagh, K.; Challis, G. L.; Brougham, D.; Doyle, S. *Chemistry & Biology* **2011**, *18*, 542.
- (20) Scharf, D. H.; Chankhamjon, P.; Scherlach, K.; Heinekamp, T.; Roth, M.; Brakhage, A. A.; Hertweck, C. *Angew. Chem. Int. Ed.* **2012**, *51*, 10064.
- (21) Forseth, R. R.; Fox, E. M.; Chung, D.; Howlett, B. J.; Keller, N. P.; Schroeder, F. *C. J. Am. Chem. Soc.* **2011**, *133*, 9678.
- (22) (a) Scharf, D. H.; Remme, N.; Heinekamp, T.; Hortschansky, P.; Brakhage, A. A.; Hertweck, C. *J. Am. Chem. Soc.* **2010**, *132*, 10136. (b) Schrettl, M.; Carberry, S.; Kavanagh, K.; Haas, H.; Jones, G. W.; O'Brien, J.; Stephens, J.; Fenelon, O.; Nolan, A.; Doyle, S. *PLoS Pathog.* **2010**, *6*, e1000952.
- (23) DeLorbe, J. E.; Horne, D.; Jove, R.; Mennen, S. M.; Nam, S.; Zhang, F.-L.; Overman, L. E. *J. Am. Chem. Soc.* **2013**, *135*, 4117.
- (24) Choi, E. J.; Park, J.-S.; Kim, Y.-J.; Jung, J.-H.; Lee, J. K.; Kwon, H. C.; Yang, H. O. *Journal of Applied Microbiology* **2010**, *110*, 304.
- (25) Munday, R. *Chem. Biol. Interact.* **1982**, *41*, 361.
- (26) Isham, C. R.; Tibodeau, J. D.; Jin, W.; Xu, R.; Timm, M. M.; Bible, K. C. *Blood* **2007**, *109*, 2579.

-
- (27) Hurne, A. M.; Chai, C. L.; Moerman, K.; Waring, P. *J. Biol. Chem.* **2002**, *277*, 31631.
- (28) Waring, P.; Sjaarda, A.; Lin, Q. H. *Biochem. Pharmacol.* **1995**, *49*, 1195.
- (29) Srinivasan, U.; Bala, A.; Jao, S.-C.; Starke, D. W.; Jordan, T. W.; Mieyal, J. J. *Biochemistry* **2006**, *45*, 8978.
- (30) Hegde, V. R.; Dai, P.; Patel, M.; Das, P. R.; Puar, M. S. *Tetrahedron Lett.* **1997**, *38*, 911.
- (31) Fry, D. W.; Bridges, A. J.; Denny, W. A.; Doherty, A.; Greis, K. D.; Hicks, J. L.; Hook, K. E.; Keller, P. R.; Leopold, W. R.; Loo, J. A.; McNamara, D. J.; Nelson, J. M.; Sherwood, V.; Smaill, J. B.; Trumpp-Kallmeyer, S.; Dobrusin, E. M. *Proc. Natl. Acad. Sci. USA* **1998**, *95*, 12022.
- (32) Kung, A. L.; Zabludoff, S. D.; France, D. S.; Freedman, S. J.; Tanner, E. A.; Vieira, A.; Cornel-Kennon, S.; Lee, J.; Wang, B.; Wang, J.; Memmert, K.; Naegeli, H.-U.; Petersen, F.; Eck, M. J.; Bair, K. W.; Wood, A. W.; Livingston, D. M. *Cancer Cell* **2004**, *6*, 33.
- (33) Cook, K. M.; Hilton, S. T.; Mecinovic, J.; Motherwell, W. B.; Figg, W. D.; Schofield, C. J. *Journal of Biological Chemistry* **2009**, *284*, 26831.
- (34) Whereas Figg and coworkers saw no statistically significant difference in efficacy between compounds containing a single ETP core versus those with two ETP cores, Olenyuk and coworkers have evidence to suggest that dimeric ETPs (both natural and synthetic) are more effective at inhibiting the HIF-1a-p300/CPB interaction. See: (a) Block, L. M.; Wang, H.; Szabó, L. Z.; Polaske, N. W.; Henchey, L. K.; Dubey, R.; Kushal, S.; László, C. F.; Makhoul, J.; Song, Z.;

-
- Meuillet, E. J.; Olenyuk, B. Z. *J. Am. Chem. Soc.* **2009**, *131*, 18078. (b) Dubey, R.; Levin, M. D.; Szabo, L. Z.; Laszlo, C. F.; Kushal, S.; Singh, J. B.; Oh, P.; Schnitzer, J. E.; Olenyuk, B. Z.
- (35) Fukuyama, T.; Nakatsuka, S.-I.; Kishi, Y. *Tetrahedron* **1981**, *37*, 2045.
- (36) Trown, P. W. *Biochemical and Biophysical Research Communications* **1968**, *33*, 402.
- (37) Öhler, E.; Poisel, H.; Tataruch, F.; Schmidt, U. *Chem. Ber.* **1972**, *105*, 635.
- (38) Öhler, E.; Tataruch, F.; Schmidt, U. *Chem. Ber.* **1973**, *106*, 396.
- (39) Ottenheim, H. C. J.; Kerkhoff, G. P. C.; Bijen, J. W. H. A.; Spande, T. F. *J. Chem. Soc., Chem. Comm.* **1975**, 768.
- (40) (a) Kishi, Y.; Fukuyama, T.; Nakatsuka, S. *J. Am. Chem. Soc.* **1973**, *95*, 6490. (b) Fukuyama, T.; Kishi, Y. *J. Am. Chem. Soc.* **1976**, *98*, 6723. (c) Kishi, Y.; Fukuyama, T.; Nakatsuka, S. *J. Am. Chem. Soc.* **1973**, *95*, 6492. (d) Kishi, Y.; Nakatsuka, S.; Fukuyama, T.; Havel, M. *J. Am. Chem. Soc.* **1973**, *95*, 6493. (e) Nakatsuka, S.; Fukuyama, T.; Kishi, Y. *Tetrahedron Lett.* **1974**, *16*, 1549. (f) Sasaki, K.; Fukuyama, T.; Nakatsuka, S.; Kishi, Y. *J. Chem. Soc., Chem. Comm.* **1975**, 542.
- (41) Kim, J.; Ashenhurst, J. A.; Movassaghi, M. *Science*, **2009**, *324*, 238.
- (42) Kim, J.; Movassaghi, M. *J. Am. Chem. Soc.* **2010**, *132*, 14376.
- (43) DeLorbe, J. E.; Jabri, S. Y.; Mennen, S. M.; Overman, L. E.; Zhang, F.-L. *J. Am. Chem. Soc.* **2011**, *133*, 6549.
- (44) Williams, R. M.; Rastetter, W. H. *J. Org. Chem.* **1980**, *45*, 2625.

- (45) (a) Nicolaou, K. C.; Totokotsopoulos, S.; Giguère, D.; Sun, Y.-P.; Sarlah, D. *J. Am. Chem. Soc.* **2011**, *133*, 8150. (b) Nicolaou, K. C.; Giguère, D.; Totokotsopoulos, S.; Sun, Y.-P. *Angew. Chem. Int. Ed.* **2012**, *51*, 728. (c) Nicolaou, K. C.; Lu, M.; Totokotsopoulos, S.; Heretsch, P.; Giguère, D.; Sun, Y.-P.; Sarlah, D.; Nguyen, T. H.; Wolf, I. C.; Smee, D. F.; Day, C. W.; Bopp, S.; Winzeler, E. A. *J. Am. Chem. Soc.* **2012**, *134*, 17320.
- (46) (a) Wang, L.; Clive, D. L. *J. Org. Lett.* **2011**, *13*, 1734. (b) Wang, L.; Clive, D. L. *J. Tetrahedron Lett.* **2012**, *53*, 1504.

Chapter 2

Development of a Synthetic Strategy Towards Dihydrooxepine-Containing Epipolythiodiketopiperazine Natural Products: Enantioselective Total Synthesis of (–)-Acetylalaranotin[†]

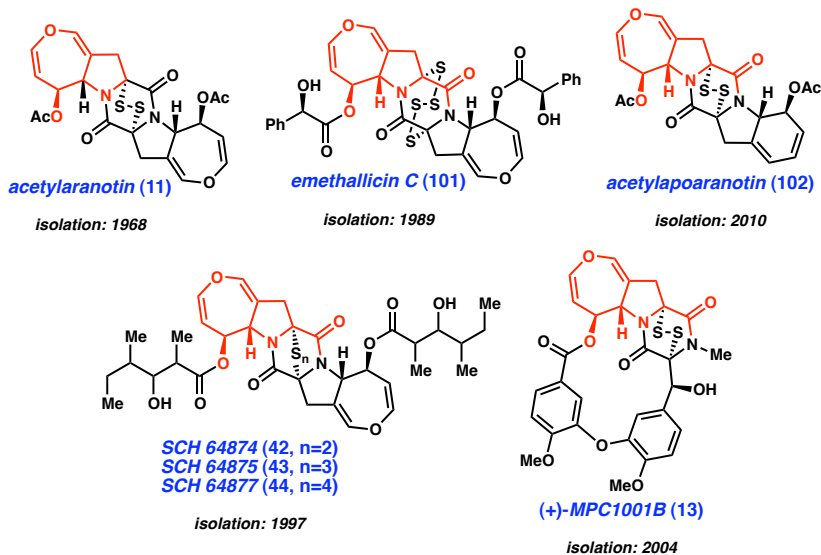
2.1 INTRODUCTION

The dihydrooxepine-containing epidithiodiketopiperazine natural product acetylalaranotin (**11**) was isolated in 1968 from the two fungal species *Arachniotus aureus* and *Aspergillus terreus* (see Figure 2.1).¹ As a C_2 -symmetric homodimer it is also the most simple of the dihydrooxepine-containing ETPs to be isolated in the past 45 years. Similar C_2 -symmetric structures include the epitetralsulfide emethallicin C (**101**),² which possesses the same carbocyclic core as **11** but is adorned by (*R*)-mandelate appendages, as well as the epidisulfide SCH64874 (**42**), epitriflalsulfide SCH64875 (**43**), and epitetralsulfide SCH64877 (**44**),³ which instead possess 2,4-dimethyl-3-hydroxyhexanoate appendages. Other natural products that contain the same dihydrooxepine monomer

[†] Part of this chapter was published as the following communication: Codelli, J. A.; Puchlopek, A. L. A.; Reisman, S. E. *J. Am. Chem. Soc.* **2012**, *134*, 1930. The research discussed in this chapter was completed in collaboration with Angela L. A. Puchlopek, a postdoctoral researcher in the Reisman Lab.

subunit include the heterodimer acetylapoaranotin (**102**)^{1f, 4} and the macrocycle MPC1001B (**13**).⁵

Figure 2.1. Dihydrooxepine-containing ETP natural products



In the 40 years from the initial isolation of **11** until the initiation of our research program, there were no reports of any successful efforts at the total synthesis of any of the structures shown in Figure 2.1—despite several reported approaches⁶—indicating the challenge that this ETP sub-family poses to modern synthetic techniques. For this reason, as part of a broad research program targeting ETP natural products, we initially selected to pursue a synthetic strategy towards dihydrooxepine-containing ETPs.

2.1.1 Biological Activity

Though dihydrooxepine-containing ETP natural products have been found to possess a variety of therapeutically relevant biological properties, from antiviral properties to selective cytotoxicity (see Table 2.1),^{2,3,4,5, 7} there have been no comprehensive studies comparing a panel of such agents against the same cellular or molecular targets. Considering that biochemical assays have suggested viral RNA

polymerases and epidermal growth factor receptor (EGFR) as molecular targets for acetylalaranotin (**11**) and the SCH series (**42–44**), respectively, such experiments would be invaluable in the ongoing efforts to elucidate ETP mechanisms of action. For example, by comparing the effects of peripheral structure in cell viability assays to those in biochemical assays, one might gain insight into the role of these structures in the modulation of physical properties (e.g., solubility, membrane permeability) versus modulation of target-binding affinities. With this in mind, a secondary goal of our research program has been to produce such a panel of dihydrooxepine-containing agents for comprehensive biological screening.

Table 2.1. Activities of dihydrooxepine ETPs against various cell lines and molecular targets

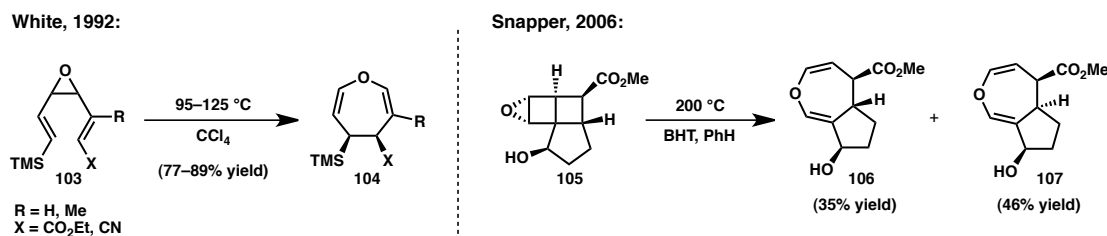
	IC₅₀ (μM)	Cellular/Molecular Target
acetylalaranotin (11)	0.20	RNA polymerase (Coxsackie A-21)
acetylalaranotin (11)	23	A549 (human alveolar adenocarcinoma)
acetylapoalaranotin (102)	2	“
acetylalaranotin (11)	21.2	HCT116 (human colon cancer)
acetylapoalaranotin (102)	13.8	“
SCH64874 (42)	1.4	EGFR Kinase
SCH64877 (44)	1.6	“
MPC1001B (13)	0.039	DU 145 (human prostate cancer)
emethallicin C (101)	1.0	Induced histamine release from mast cells

2.1.2 Previous Synthetic Approaches

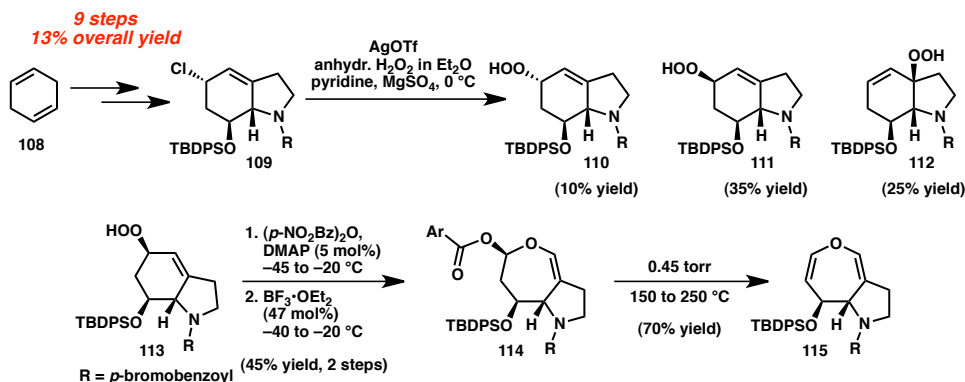
The dihydrooxepine-containing ETP natural products have remained particularly challenging as the targets of modern synthetic endeavors due to their chemical lability as well as the relative dearth of methods for rapid construction of the dihydrooxepine ring itself. Indeed, at the outset of our investigations, there existed only two reported *general* methods for the synthesis of dihydrooxepine rings.

In 1992, White and coworkers reported the thermal [3,3]-sigmatropic rearrangement of divinyl epoxides **103** to give dihydrooxepines **104**.⁸ More recently, Snapper and coworkers reported the thermal rearrangement of highly strained polycyclic epoxides such as **105** to give dihydrooxepines such as **106** and **107**.⁹ Unfortunately, it is not apparent how either of the required precursor structures could be incorporated into a readily accessible intermediate in the context of a total synthesis of a dihydrooxepine-containing ETP.

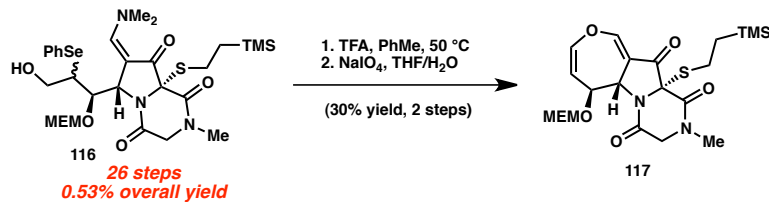
Scheme 2.1. General methods for constructing dihydrooxepine rings



Because the dihydrooxepine ring is found almost exclusively in ETP natural products, most of the remaining efforts towards their synthesis have been in the context of total synthesis endeavors. Kishi and coworkers reported the synthesis of **115**, a model for the aranotin ring system (Scheme 2.2).^{6e} Key to their approach was the use of the Criegee rearrangement to convert allylic hydroperoxide **113** to vinyl ether **114**,^{6d} with subsequent thermal carboxylate elimination to furnish the dihydrooxepine ring. Once more, however, the authors find that the required intermediate **113** can be accessed only in low yield as a racemate, and extension of this strategy to a total synthesis does not appear to have been pursued.

Scheme 2.2. Synthesis of model dihydrooxepine **115**

In reports of progress toward the macrocyclic structure of MPC1001, Clive and coworkers found that they could construct the dihydrooxepine ring of model ring system **117** by acid-promoted vinylogous lactonization of intermediate **116**, followed by selenoxide elimination to furnish the desired unsaturation.^{6b,c} However, preparation of intermediate **116** requires a 26-step synthetic sequence, and advancement to the natural product using this strategy has yet to be reported.

Scheme 2.3. Construction of dihydrooxepine model system **117**

With these reports in mind, we sought to pursue a novel synthetic method for constructing the dihydrooxepine ring that would simultaneously allow for rapid access to required precursors.

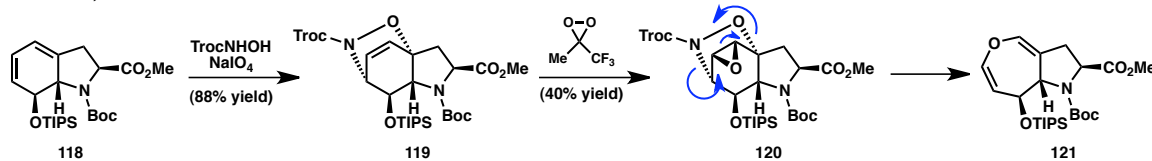
2.1.3 Concurrent Synthetic Approaches

Since our initial communication of the research described in this chapter, several investigations pertaining to the synthesis of dihydrooxepine-containing ETPs have been

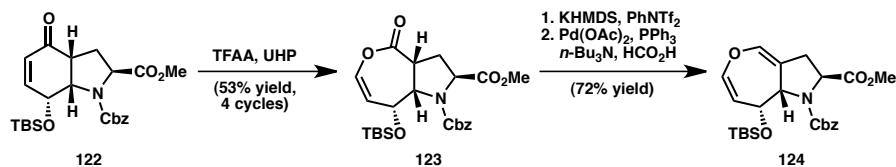
published. In their detailed account of the synthesis and biological evaluation of various perhydroindolone-containing ETP natural products, Nicolaou and coworkers reported the conversion of a gliotoxin-type monomer (**118**) to the acetylalaranotin-type monomer (**121**) via a [4+2]/oxidation/retro [4+2] sequence as shown in Scheme 2.4.¹⁰ Tokuyama and coworkers reported the second total synthesis of acetylalaranotin (**11**) in late 2012, using a Baeyer-Villiger oxidation/vinyl triflate reduction strategy to construct the dihydrooxepine ring (**124**).¹¹ Shortly thereafter, Nicolaou and coworkers published an optimized general method for the synthesis of dihydrooxepines starting from cyclohexenones (e.g. **125**) via a Baeyer-Villiger/vinyl phosphate reduction sequence.¹² Such developments greatly complement the work described in this chapter, and will likely provide access to an increased diversity of structural analogs to assist in biological studies.

Scheme 2.4. Recently disclosed reports pertaining to the synthesis of dihydrooxepine-containing ETPs

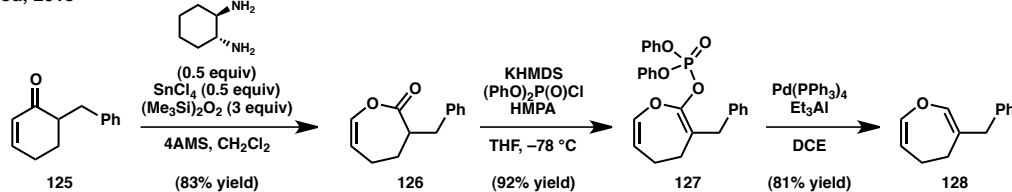
Nicolaou, 2012



Tokuyama, 2012



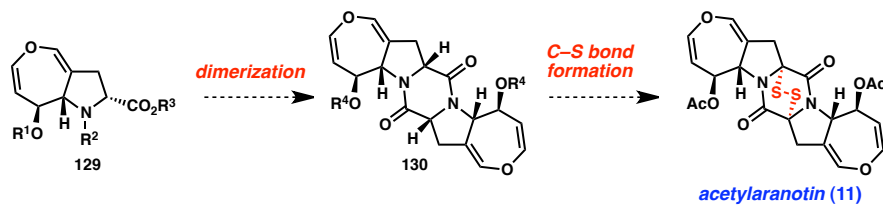
Nicolaou, 2013



2.1.4 Retrosynthetic Analysis

Our initial consideration during the planning of our synthetic approach towards dihydrooxepine-containing ETP natural products was one of target selection. We chose to initially pursue a total synthesis of the natural product acetylalaranotin (**11**), with the expectation that a successful strategy for synthesis of the corresponding monomer fragment (see Figure 2.1) would ultimately allow us to target other members of the subfamily. In the present case, dimerization of such a monomer unit (**129**) would provide diketopiperazine **130** (see Scheme 2.5). We anticipated that C–S bond formation prior to dimerization might lead to opening of the pyrrolidine ring or otherwise complicate the coupling of monomer units. Accordingly, installation of the C–S bonds of the ETP was to be reserved for the final stages of the synthesis.

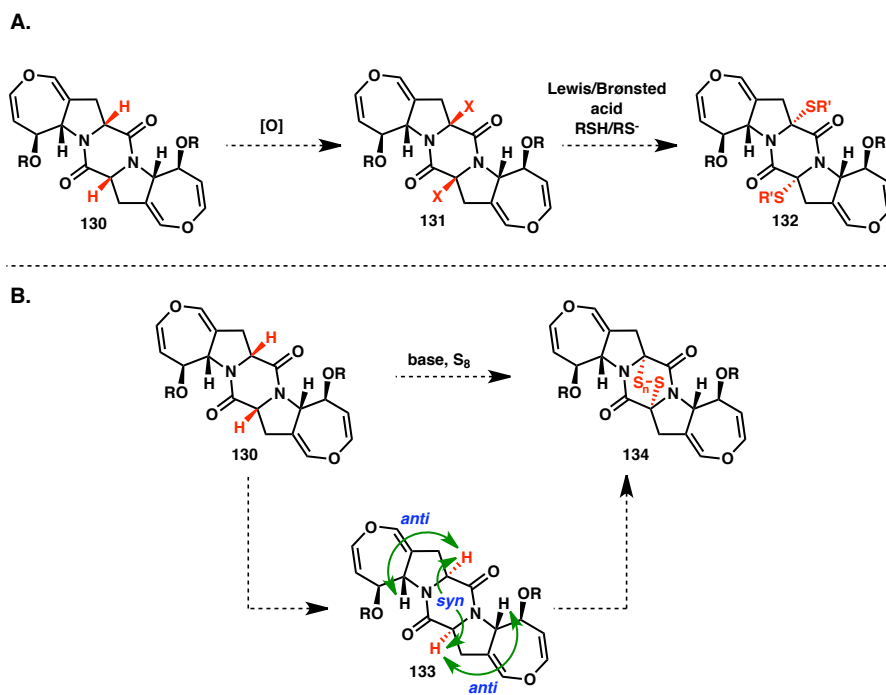
Scheme 2.5. Endgame strategy for the synthesis of acetylalaranotin (**11**)



In considering how best to accomplish late stage C–S bond formation, a major concern was the potential instability of the dihydrooxepine ring. Embedded within this structure is a divinyl ether moiety, as well as a vinylogous acetal, both of which were expected to be sensitive to acidic as well as oxidative reaction conditions. We therefore reasoned that it would be challenging to carry out a sequence involving late stage oxidation of diketopiperazine **130** followed by displacement with sulfur-containing nucleophiles under acidic conditions (Scheme 2.6, part A), and realized that direct sulfenylation of diketopiperazine **130** under basic conditions was likely a more practical

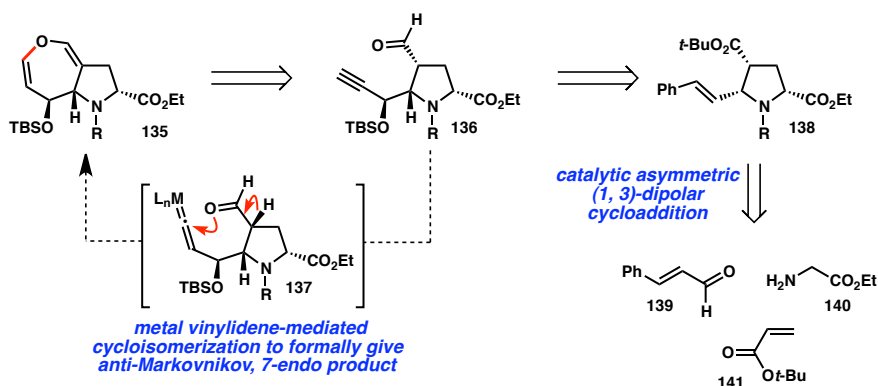
approach (Scheme 2.6, part B). It was unclear *a priori* what influence, if any, the stereochemistry of diketopiperazine **130** would have on the facial selectivity of this process. Romo and coworkers have demonstrated that for cyclo(Pro,Pro) electrophilic trapping of the kinetically generated monoenolate proceeds with retention of stereochemistry.¹³ Thus, we were cognizant that it might be necessary to epimerize diketopiperazine **130** from the *syn,syn,syn* configuration to the *anti,syn,anti* diketopiperazine (**133**) prior to sulfenylation.

Scheme 2.6. Possible strategies for C–S bond formation



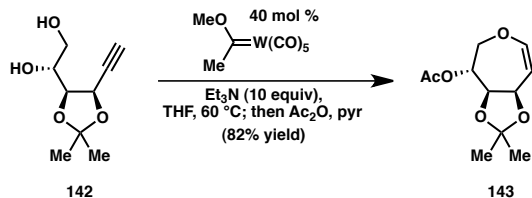
Turning our attention to construction of the acetylalaranotin monomer unit **129**, we envisioned forming the C(11)–O bond (Scheme 2.7) via transition-metal catalyzed cycloisomerization of alkynyl aldehyde **136**. In turn, we anticipated that the densely functionalized pyrrolidine scaffold of this intermediate could be rapidly accessed via a (1,3)-dipolar cycloaddition between an acrylate (**141**) and a glycinate-derived imine.

Scheme 2.7. Retrosynthetic analysis for dihydrooxepine-containing monomer unit 135

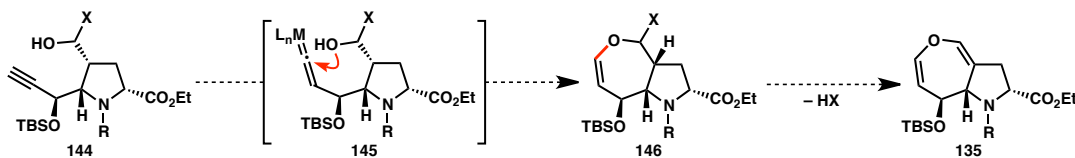


The anti-Markovnikov *7-endo* cyclization of an aldehyde onto a terminal alkyne, as described above, is relatively unprecedented. Transition metal complexes that favor reactions of alkynes via π -activation would likely result in the undesired Markovnikov 6-*exo* cyclization. On the other hand, transition metal catalysts that promote reactions of alkynes via metal vinylidene intermediates, in which the carbon terminus is electrophilic in character,¹⁴ were expected to provide the desired dihydrooxepine, the formal product of *7-endo* cyclization.

The anti-Markovnikov cyclization of primary alcohols onto terminal alkynes via metal vinylidene intermediates is well preceded. Complexes of transition metals belonging to groups 6 (Cr, Mo, W),¹⁵ 8 (Ru, Os),¹⁶ and 9 (Rh, Ir)¹⁷ are commonly used for the catalytic synthesis of cyclic vinyl ethers (an example of *7-endo* cyclization of an alkynyl alcohol is shown in Figure 2.8)^{15d} as well as other vinylidene-mediated transformations, and we were optimistic at the outset of our investigation that the properties of such catalysts could be tuned to accomplish similar reactions with alkynyl aldehydes.

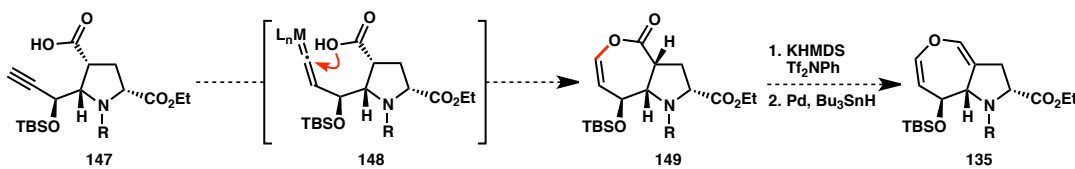
Scheme 2.8. Tungsten-catalyzed 7-*endo* cycloisomerization of an alkynyl alcohol

Additionally, aldehyde **136** would provide rapid access to several alternative cyclization substrates. For example, various aldehyde 1,2-adducts (**144**) could be formed via addition of HX, which could potentially demonstrate reactivity similar to alkynyl alcohols (see Scheme 2.9).¹⁸ Subsequent elimination of HX would then furnish the desired dihydrooxepine ring (**135**).

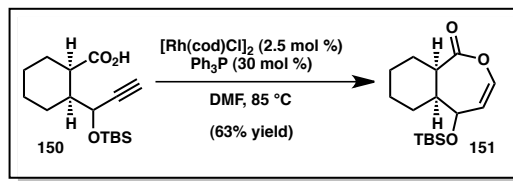
Scheme 2.9. Cyclization of alkynyl aldehyde 1,2-adducts followed by elimination to afford the dihydrooxepine ring

On the other hand, oxidation of the aldehyde would provide the corresponding carboxylic acid substrate (**147**, see Scheme 2.10). Such alkynyl acids have been shown to undergo cycloisomerization to give the 7-*endo* adducts, presumably via metal vinylidene intermediates.^{17b,19} Conceivably, subsequent conversion of the resulting enol lactone **149** to the vinyl triflate or analogous vinyl halide surrogate would allow for palladium-mediated reduction to furnish dihydrooxepine **135**. Indeed, preliminary studies using model alkynyl carboxylic acid **150** revealed the anti-Markovnikov 7-*endo* cyclization could readily be accomplished using Rh(I) catalysis.²⁰

Scheme 2.10. Cyclization of alkynyl carboxylic acids followed by vinyl triflate reduction to afford the dihydrooxepine ring



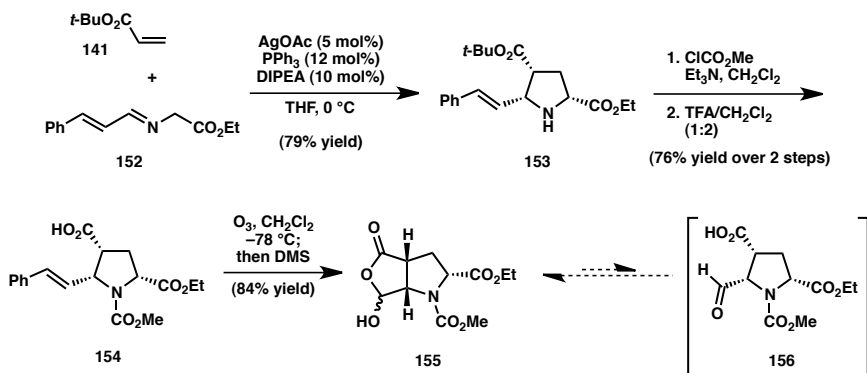
Scheme 2.11. Rh(I)-catalyzed cycloisomerization of a model alkynyl acid (**150**)



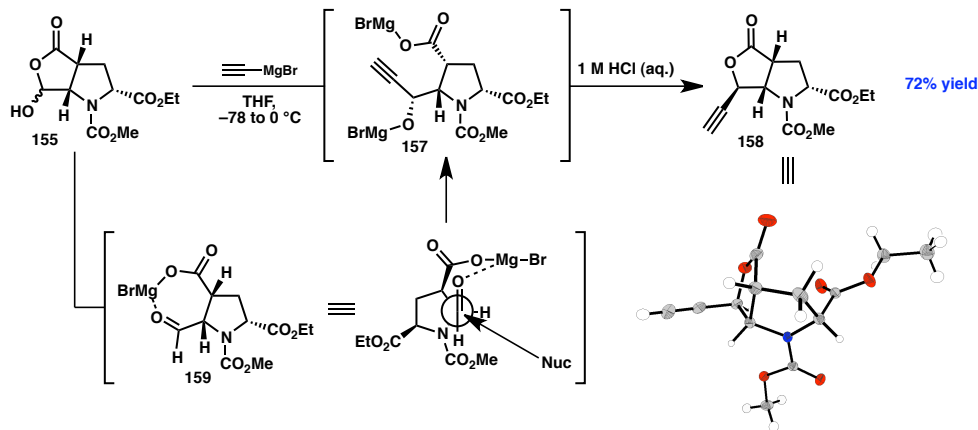
2.2 FORWARD SYNTHETIC EFFORTS

In the forward sense, our first objective was the construction of functionalized pyrrolidine scaffold **138**. To this end, racemic styrenyl pyrrolidine **153** was synthesized using a silver-catalyzed (1,3)-dipolar cycloaddition between α -imino glycinate ester **152** and *tert*-butyl acrylate (**141**, see Scheme 2.12).²¹ Protection of the amine as a methyl carbamate and subsequent cleavage of the *tert*-butyl ester under acidic conditions afforded carboxylic acid **154**. Finally, ozonolytic cleavage of the styrene moiety resulted in formation of hydroxylactone **155**, which was envisioned to serve as a masked aldehyde substrate for acetylide addition, providing access to a variety of potential cycloisomerization substrates.

Scheme 2.12. Construction of the functionalized pyrrolidine scaffold and synthesis of masked aldehyde substrate **155**

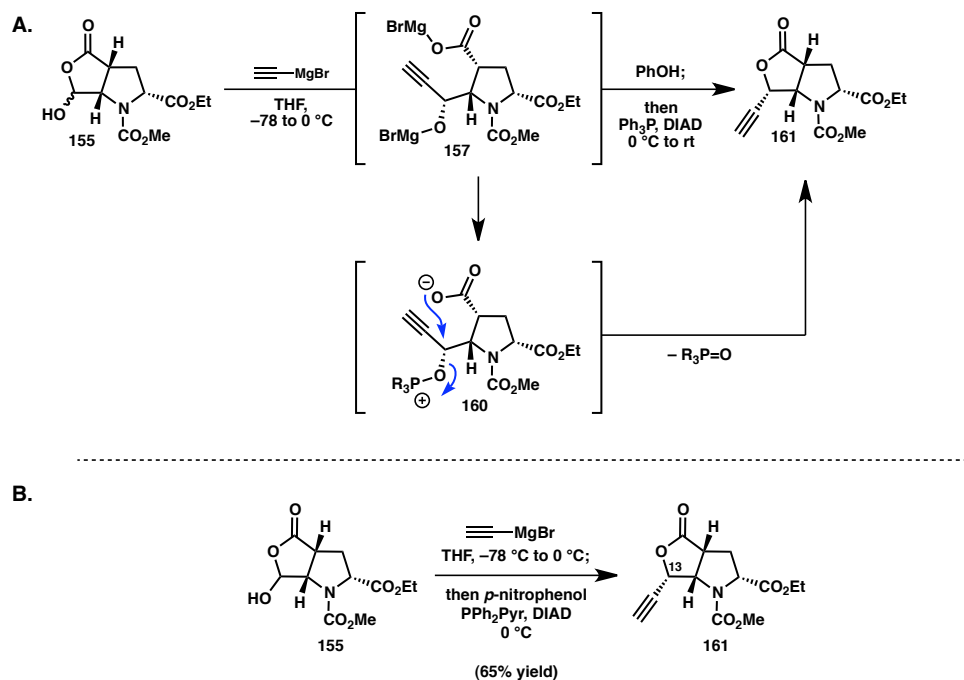


Preliminary investigation of acetylide addition to substrate **155** revealed that treatment with commercially available ethynylmagnesium bromide followed by acidic workup resulted in formation of alkynyl lactone **158** with good diastereoselectivity (Scheme 2.13). Unfortunately, single crystal X-ray diffraction revealed that **158** did not possess the desired stereochemistry at the propargylic position for advancement to the natural product. This observation can be rationalized mechanistically; initial deprotonation of hydroxylactone **155** by the first equivalent of the Grignard reagent presumably results in opening of the cyclic acetal to afford aldehyde carboxylate **159**, in which a cyclic chelation complex is formed. Approach of the nucleophile to the convex face of the resulting ring system affords propargylic alkoxide **157**, which lactonizes upon workup to provide the observed product. Unfortunately, attempts at reversing the observed selectivity by disrupting the proposed activated chelation complex (either by altering the nature of the counterion, or by using strongly coordinating additives) did not prove fruitful.

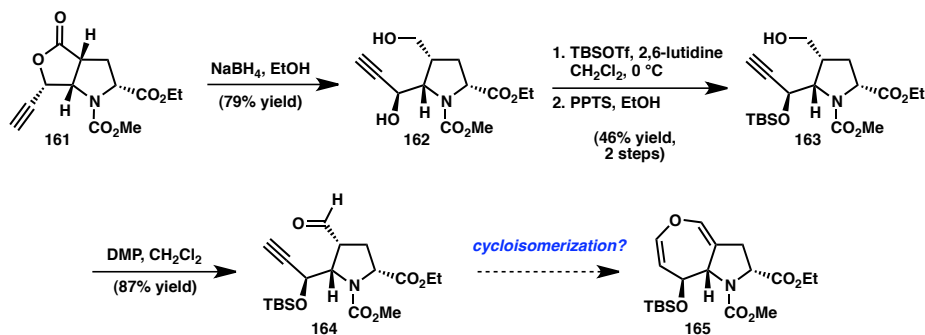
Scheme 2.13. Diastereoselective acetylide addition to afford alkynyl lactone **158**

Based on the above mechanistic hypothesis, we envisioned that intermediate species **157** might be intercepted with inversion at the propargylic center via a Mitsunobu lactonization protocol.²² Gratifyingly, it was found that quenching of the Grignard reaction with phenol, followed by addition of PPh_3 and DIAD afforded the desired epimer of the alkynyl lactone product (**161**) (see Scheme 2.14, part A). Though it was quite difficult to separate **161** from the triphenylphosphine oxide byproduct of the reaction, this purification challenge could be obviated by using *p*-nitrophenol as the quenching reagent and diphenyl 2-pyridylphosphine (PyrPPh_2) as the phosphine (Scheme 2.14, part B).²³

Scheme 2.14. Grignard addition and subsequent Mitsunobu lactonization to provide alkynyl lactone **161**



Conversion of alkynyl lactone **161** to the aldehyde **164** would formally require a reductive opening of the lactone ring. Unfortunately, attempts at partial reduction of lactone to give the aldehyde directly were largely unfruitful. On the other hand, it was found that lactone **161** could be reduced to diol **162** using an excess of NaBH_4 in ethanol. Protection of the two hydroxyl groups as TBS ethers, followed by selective deprotection with PPTS in ethanol furnished primary alcohol **163**, which was subsequently oxidized to aldehyde **164** on treatment with buffered Dess-Martin periodinane.²⁴ Thus, the stage was set for examination of transition metal catalysts for the direct cycloisomerization of aldehyde **164** to give dihydroooxepine **165**.

Scheme 2.15. Advancement of lactone **161** to aldehyde **164**

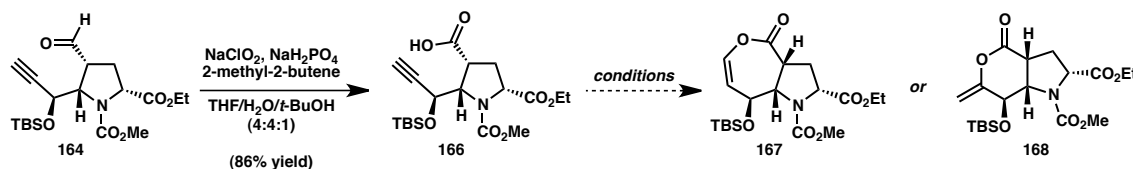
Initial attempts at cycloisomerization of substrate **164** were carried out using catalyst systems that are readily available and known to promote anti-Markovnikov cyclization of alcohols onto alkynes (as described above). In all cases, however, such conditions led either to complete decomposition or epimerization of aldehyde **164** (Table 2.2). Furthermore, experiments using gold(I) salts, which were anticipated to afford the 6-*exo* cyclization product, also demonstrated little reactivity other than slow decomposition of the starting material. Finally, cycloisomerization of several 1,2-adducts derived from aldehyde **164** (either isolated prior to cyclization or formed *in situ*) using a variety of transition metal catalysts could not be successfully accomplished.

Table 2.2. Attempted cycloisomerization of alkynyl aldehyde **164**

entry	catalyst	ligand	additive	solvent, temp.	result
1	[Rh(cod)Cl] ₂ (5 mol %)	(<i>p</i> -FC ₆ H ₄) ₃ P (60 mol %)	DIPEA	DMF, 85 °C	epimerization
2	[Rh(cod)Cl] ₂ (5 mol %)	Ph ₃ P (60 mol %)	TMG	DMF, 85 °C	decomposition
3	CpRuCl[P(<i>p</i> -FC ₆ H ₄) ₃] ₂ (5 mol %)	(<i>p</i> -FC ₆ H ₄) ₃ P (20 mol %)	NaHCO ₃ <i>n</i> -Bu ₄ NPF ₆	DMF, 85 °C	epimerization
4	(CO) ₅ W=C(OMe)Me (1 equiv)	—	Et ₃ N	PhMe, 85 °C	decomposition
5	AuCl (30 mol %)	—	—	PhMe, 23 °C	decomposition

Encouraged by our preliminary work with model system **150**, we next chose to investigate the possibility of cycloisomerization of an alkynyl carboxylic acid substrate. To this end, aldehyde **164** was converted to carboxylic acid **166** under Pinnick oxidation conditions.²⁵ Surprisingly, we found that the conditions identified for cycloisomerization of model substrate **150** to **151** could not be successfully extended to substrate **166**, and in fact demonstrated no reactivity whatsoever (Table 2.3). On the other hand, Fisher carbene precatalyst $(CO)_5W=C(OMe)Me$ promoted only decomposition, whereas ruthenium catalysts promoted varying combinations of decomposition and Markovnikov 6-*exo* cyclization. As expected, catalysis with gold(I) salts resulted in rapid, selective formation of 6-*exo* cyclization product **168** (as confirmed by 1D and 2D 1H and ^{13}C NMR spectroscopy).²⁶

Table 2.3. Synthesis and attempted cycloisomerization of alkynyl carboxylic acid **166**

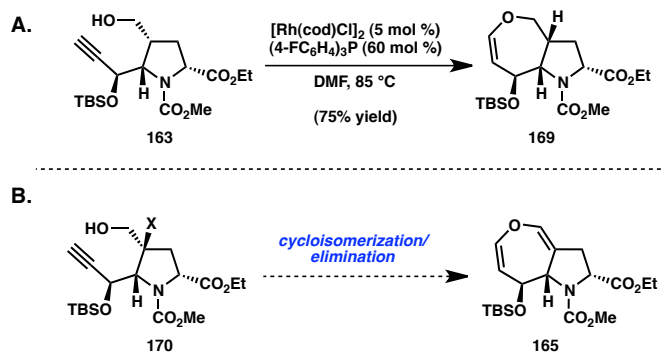


entry	catalyst	ligand	additive	solvent, temp.	result
1	$[Rh(cod)Cl]_2$ (5 mol %)	$(p-FC_6H_4)_3P$ (60 mol %)	—	DMF, 85 °C	no reaction
2	$(CO)_5W=C(OMe)Me$ (30 mol %)	—	Et ₃ N	THF 60 °C	decomposition
3	$[(p\text{-cumene})RuCl_2]_2$ (5 mol %)	$(p-FC_6H_4)_3P$ (15 mol %)	DMAP (20 mol %)	PhMe, 85 °C	6- <i>exo</i> cyclization
4	TpRuH(PPh ₃) ₂ (10 mol %)	—	—	PhMe, 85 °C	6- <i>exo</i> cyclization
5	AuCl (10 mol %)	—	—	CH ₂ Cl ₂ , 23 °C	6- <i>exo</i> cyclization

The difficulty encountered in trying to promote the desired anti-Markovnikov 6-*endo* cyclization of either the aldehyde **164** or the carboxylic acid **166** prompted us to investigate the cycloisomerization of the previous alcohol intermediate **163**. In the event,

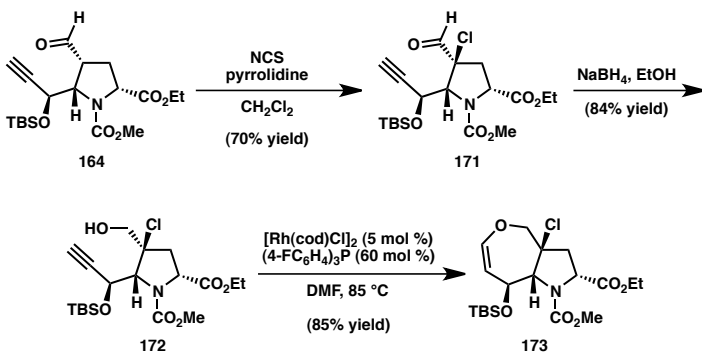
we were delighted to find that using the previously identified conditions ($[\text{Rh}(\text{cod})\text{Cl}]_2$ and $(p\text{-FC}_6\text{H}_4)_3\text{P}$ in DMF at 85 °C), alkynyl alcohol **163** smoothly underwent 7-*endo* cycloisomerization to provide tetrahydroooxepine **169** (Scheme 2.16). While it is unclear whether the facility of cycloisomerization for this particular substrate is due to steric or geometric parameters, it is apparent that the primary alcohol **163** represents an optimal structure for cycloisomerization among the substrates investigated. Accordingly, we hypothesized that halohydrins **170** might serve as viable aldehyde surrogates by providing the favorable reactivity of the primary alcohol while possessing a suitable functional handle for subsequent conversion to the dihydroooxepine.

Scheme 2.16. Successful cycloisomerization of alkynyl alcohol **163** and halohydrins **170** as potential aldehyde surrogates



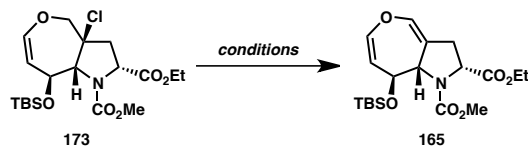
Aldehyde **164** was readily chlorinated by NCS in the presence of pyrrolidine to afford chloraldehyde **171** as a single diastereomer (relative stereochemistry as shown was confirmed by NOESY spectroscopy, see Scheme 2.17). Subsequent reduction with NaBH_4 provided the desired chlorohydrin **172** in 59% overall yield from **164**. Chlorohydrin **172** proved to be a suitable substrate for rhodium(I)-catalyzed cycloisomerization, providing chlorotetrahydroooxepine **173** in 57% yield.

Scheme 2.17. Synthesis and cycloisomerization of chlorohydrin 172



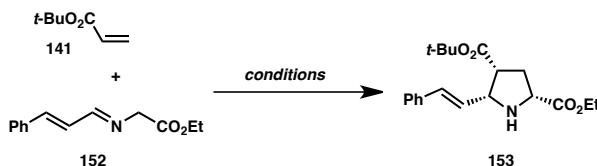
With chlorotetrahydrooxepine **173** in hand, we were very pleased to observe that treatment with DBU in DMF at elevated temperatures did in fact provide the desired dihydrooxepine ring to complete acetylaranotin monomer **165** (Table 2.4, Entry 1). However, under these conditions, **165** was isolated in only 10% yield despite proceeding to full conversion of **173**. Other strong non-ionic organic bases gave similar results, and reaction attempts employing less basic amine bases (e.g. DIPEA) or Ag(I) salts demonstrated no reactivity (Entries 2 and 3). Interestingly, we found that greatly improved yields for the reaction could be achieved using a mixture of LiCl and Li₂CO₃ in DMF at 100 °C, which provided the dihydrooxepine **165** in 50% isolated yield (Entry 4). Similar conditions have historically been used for the elimination of halides from relatively unfunctionalized molecules, and are not typically used in reactions involving structures as complex or highly oxidized as **173**.²⁷

Table 2.4. Identification of reaction conditions for elimination of HCl from chlorotetrahydrooxepine **173** to afford dihydrooxepine **165**

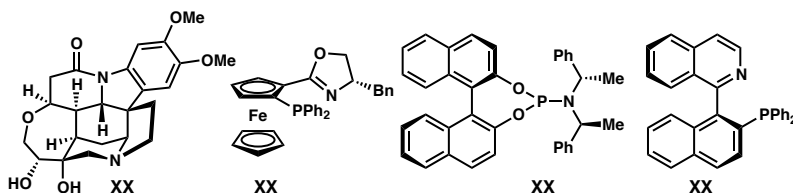


entry	base/additive	solvent, temp.	result
1	DBU	DMF, 85 °C	10% yield (no recovered SM)
2	DIPEA	DMF, 85 °C	no reaction
3	Ag(TFA), Ag ₂ CO ₃	PhMe, 85 °C	no reaction
4	LiCl, Li ₂ CO ₃	DMF, 100 °C	50% yield

Having accomplished a viable synthetic route towards racemic dihydrooxepine **165**, we turned our attention to the development of an enantioselective sequence. A brief survey of known catalyst systems for asymmetric (1,3)-dipolar cycloaddition reactions between alkyl acrylates and aryl glycinate imines revealed that both Ag(I)/(*S*)-QUINAP (**177**) and Cu(I)/Brucin-OL (**174**) catalyzed the reaction between **141** and **152** to give styrenyl pyrrolidine **153** in good *ee* (see Table 2.5, Entries 3 and 4).²⁸ Because they provided material of greater optical activity, and because Brucin-OL is substantially less expensive per mole than (*S*)-QUINAP, we opted to use the conditions in entry 4 for the preparation of **153** on scale.

Table 2.5. Survey of catalyst systems for the enantioselective synthesis of pyrrolidine **153**

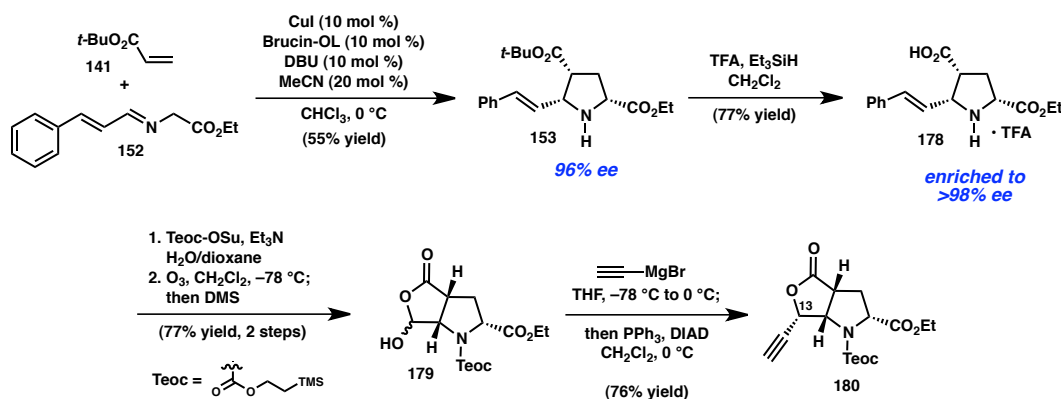
entry	catalyst/ligand/additive	solvent	temp. (°C)	yield (%)	ee (%)
1	AgOAc, 175	Et ₂ O	0	53	–63
2	AgClO ₄ , 176 , DABCO	PhMe	0	59	46
3	AgOAc, 177 , DIPEA	THF	–45	62	90
4	CuI, 174 , DBU	CHCl ₃	0	50	96



With access to ample quantities of pyrrolidine **153**,²⁹ we next reconsidered our protecting group strategy, knowing that the methyl carbamate protecting group used in our preliminary investigations was not optimal for deprotection and advancement of monomer **165** to the corresponding diketopiperazine. Ultimately, we opted to employ a trimethylsilylethyl carbamate (Teoc) protecting group, which can be removed using fluoride ion under neutral or basic conditions.³⁰ However, because of the acid sensitivity of this group, the order of protecting group manipulations was also modified relative to the preliminary sequence, so as to avoid subjection of the Teoc group to high concentrations of TFA. Accordingly, the *tert*-butyl ester of pyrrolidine **153** was first cleaved using TFA/Et₃SiH to afford trifluoroacetate salt **178** as a crystalline solid in 77% yield (see Scheme 2.18). Notably, the trituration procedure used to isolate this material resulted in enrichment of optical activity to >98% ee. Subsequent protection of the pyrrolidine nitrogen as the Teoc carbamate and ozonolytic cleavage of the styrene as

before provided hydroxylactone **179** in 77% yield over two steps. In contrast to the methyl carbamate-protected system (**155**), this substrate required an aqueous workup following reaction with ethynylmagnesium bromide in order for the subsequent Mitsunobu inversion to succeed. On the other hand, the decreased polarity of **180** versus **161** allowed for the use of Ph_3P , rather than the more expensive reagent Ph_2PPyr , without the previously encountered challenges to purification.

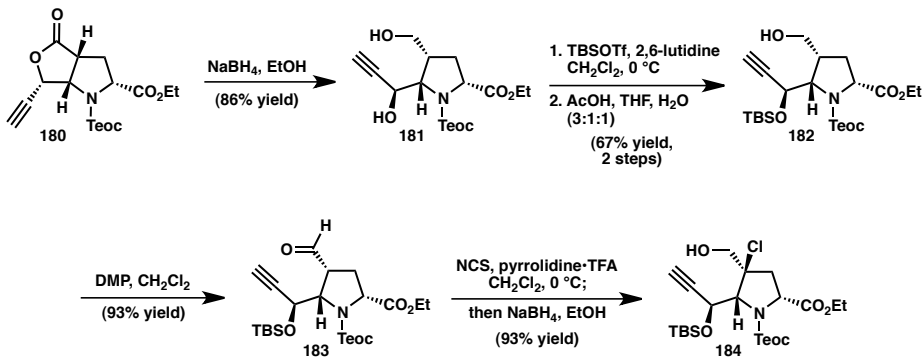
Scheme 2.18. Synthesis of enantioenriched, Teoc-protected alkynyl lactone **180**



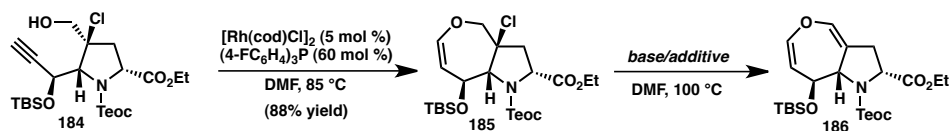
Alkynyl lactone **180** was advanced to chlorohydrin **184** using an analogous sequence to that developed for the methyl carbamate-protected variant, but with two notable exceptions (see Scheme 2.19). First, conditions employing $\text{AcOH}/\text{THF}/\text{H}_2\text{O}$ were used to selectively cleave the primary TBS ether following treatment of **181** with TBSOTf . These conditions demonstrated substantially reduced reaction times and greater selectivity for cleavage of the primary versus the secondary silyl ether (relative to PPTS/EtOH). Additionally, pyrrolidine-mediated chlorination of Teoc-protected aldehyde **183** was sluggish and resulted in consistently low conversion regardless of reaction time. By instead using pyrrolidine•TFA complex, the reaction progressed to completion over the course of 30 h. Furthermore, isolated yields for the

chlorination/aldehyde reduction sequence were greatly improved by performing the two processes in one flask, with no intermediate workup.

Scheme 2.19. Advancement of alkynyl lactone **180** to chlorohydrin **184**

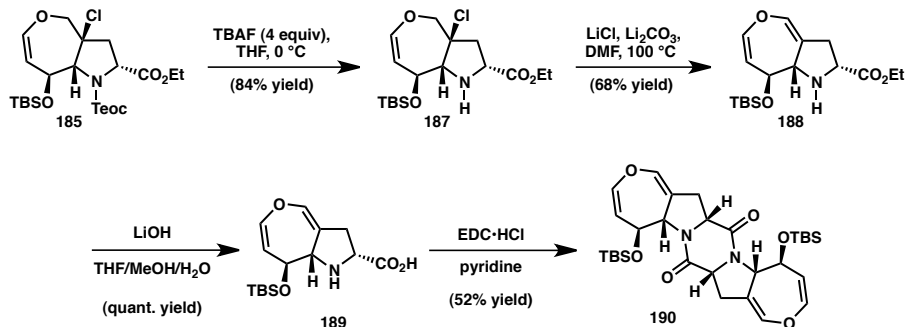


As expected, Teoc-protected chlorohydrin **184** proved to be an excellent substrate for Rh(I)-catalyzed cycloisomerization, affording chlorotetrahydrooxepine **185** in 87% yield. Though the combination of LiCl and Li₂CO₃ remained optimal for elimination of HCl from **185** to afford dihydrooxepine **186**, our curiosity about the role of each lithium salt in this reaction prompted us to perform a series of control experiments. In the absence of LiCl no reaction occurs (Table 2.6, Entry 2), whereas in the absence of Li₂CO₃ the reaction proceeds, but is accompanied by increased formation of decomposition products (Entry 3). Given that LiCl is quite soluble in DMF, whereas Li₂CO₃ is almost completely insoluble, we hypothesized that perhaps the high concentration of lithium cations in solution was critical to activation of the chloride leaving group. However, employing LiClO₄ rather than LiCl as the soluble source of lithium cation resulted in no reaction (Entry 4). These results suggest that the chloride ion itself is acting as a base during the elimination reaction, while the carbonate salt is simply acting as an insoluble buffer. Unfortunately, attempts to employ more basic lithium salts or more soluble carbonate salts led only to greatly increased levels of decomposition (Entries 5 and 6).

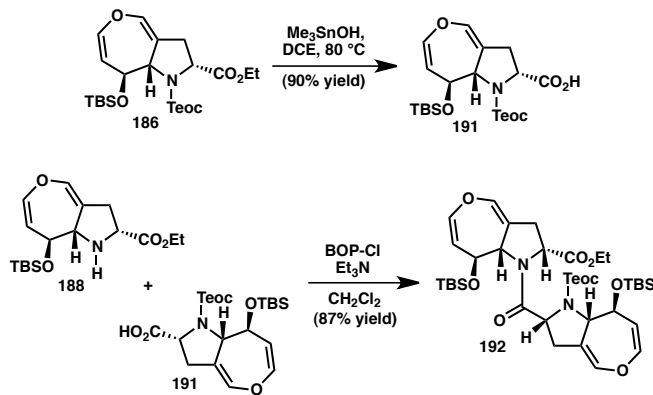
Table 2.6. Advancement of chlorohydrin **184** to Teoc-protected dihydrooxepine monomer **186**

entry	base/additive	result
1	$\text{LiCl}, \text{Li}_2\text{CO}_3$	53% yield
2	Li_2CO_3	no reaction
3	LiCl	complex product mixture
4	$\text{LiClO}_4, \text{Li}_2\text{CO}_3$	no reaction
5	$\text{LiOAc}, \text{Li}_2\text{CO}_3$	complex product mixture
6	Cs_2CO_3	complex product mixture

Perhaps unsurprisingly, we found it difficult to selectively cleave the Teoc protecting group from **186** in the presence of the TBS ether. In contrast, removal of the carbamate protecting group from chlorotetrahydrooxepine **185** proved to be quite facile, providing pyrrolidine **187** in 84% yield (Scheme 2.20). Furthermore, elimination of HCl from this substrate occurred in even greater yield than for the Teoc-protected substrate, affording dihydrooxepine pyrrolidine **188** in 65% yield. Subsequent saponification proceeded smoothly to provide amino acid **189**. Ultimately, it was determined that amino acid **189** could be dimerized using EDC in pyridine; however, our inability to achieve greater than 50% yield of diketopiperazine **190** under these conditions prompted us to investigate a stepwise approach, starting from two orthogonally protected monomer units.

Scheme 2.20. Synthesis and dimerization of dihydrooxepine amino acid **189**

Having previously established a sequence for the preparation of pyrrolidine **188**, saponification of **186** to give the corresponding carboxylic acid component for amide coupling was required. Though the fully protected monomer unit **186** was unstable to standard saponification conditions using LiOH, the ethyl ester could be cleaved using an excess of Me₃SnOH in dichloroethane at elevated temperatures to produce carboxylic acid **191** in 90% yield. Pyrrolidine **188** and carboxylic acid **191** could be readily coupled using BOP-Cl, affording protected dipeptide **192** in excellent yield.

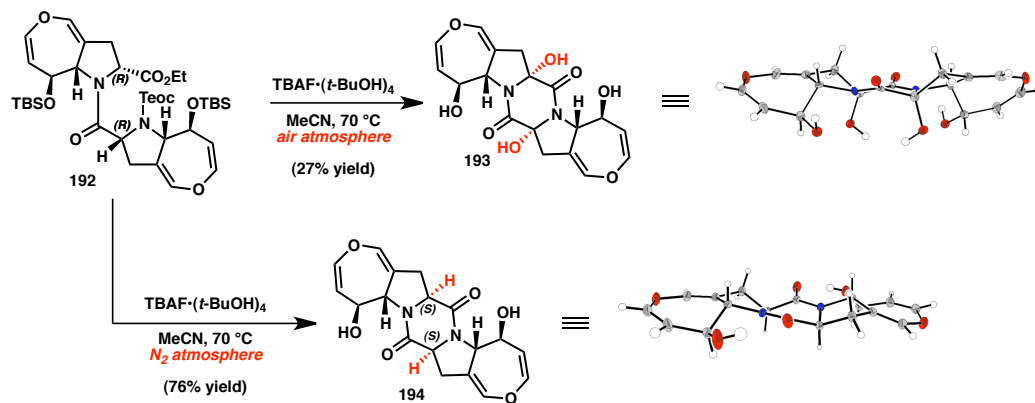
Scheme 2.21. Synthesis of dipeptide **192**

Initial attempts to deprotect dipeptide **192** using TBAF in THF resulted in various mixtures of partially or fully deprotected products. Though trace amounts of diketopiperazine were observed in the crude mixtures of some reactions, the material

recovery was consistently low. Together with the apparent instability of dihydrooxepine **186** to basic conditions, these results suggested that less basic conditions for deprotection of **192** were desirable. Unfortunately, no other fluoride sources appeared to promote the cleavage of the Teoc carbamate *at all*.

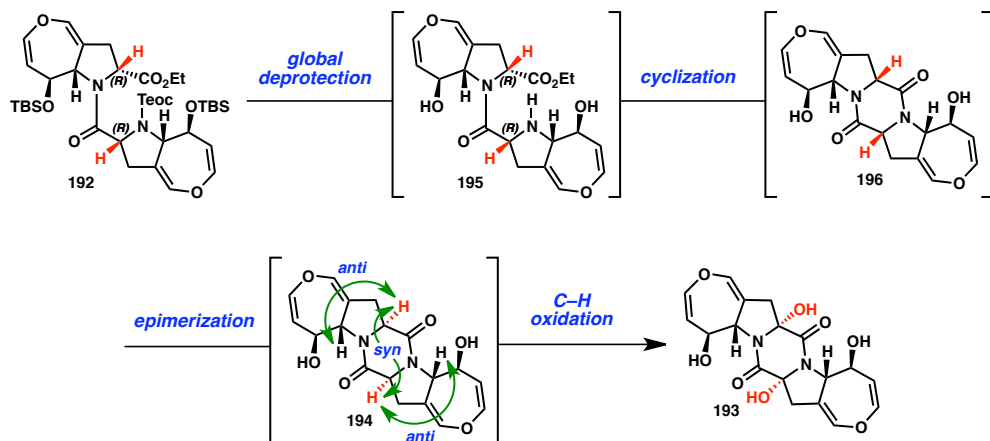
Turning our attention to attenuating the basicity of TBAF itself, we became interested in a report from Kim and coworkers, who determined that TBAF•(*t*-BuOH)₄ is not only substantially less hygroscopic than solid TBAF•(H₂O)₃, but also less *basic* than typical TBAF solutions.³¹ We were pleased to find that treatment of dipeptide **192** with TBAF•(*t*-BuOH)₄ in MeCN at 70 °C effected global deprotection and cyclization to deliver a *C*₂-symmetric compound as the major product. Interestingly, initial characterization of this compound using standard NMR techniques and high-resolution mass spectrometry suggested that it was a *syn*-diol (**193**), the result of a double C–H oxidation process (see Scheme 2.22). On the basis of the hypothesis that the oxidant was oxygen in the ambient atmosphere, the reaction was repeated under a nitrogen atmosphere using rigorously degassed solvent, which provided diketopiperazine **194** as a single diastereomer in 76% yield. The structures of **193** and **194** were confirmed by single-crystal X-ray diffraction. Notably, the (*S*, *S*)-stereochemistry of the central diketopiperazine of **194** is the result of epimerization at both of the diketopiperazine methine positions under the cyclization conditions.

Scheme 2.22. Unexpected aerobic oxidation and advancement of dipeptide **192** to diketopiperazine **194**



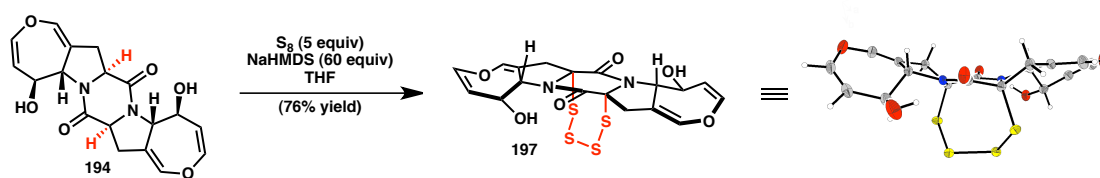
Based on a series of control experiments,³² we hypothesize that the processes described above are proceeding via the sequence shown in Scheme 2.23. First, fluoride-promoted global desilylation of **192** provides deprotected dipeptide **195**, which cyclizes to give the expected *syn,syn,syn* diketopiperazine **196**. Subsequent epimerization to the thermodynamically favored *anti,syn,anti* configuration affords the observed diketopiperazine **194**. Under aerobic conditions, **194** then undergoes a *stereoretentive* radical-mediated C–H oxidation to afford the tetraol **193**.

Scheme 2.23. Proposed $\text{TBAF}\bullet(\text{t-BuOH})_4$ -promoted diketopiperazine formation/oxidation sequence



Though we were unable to advance oxidized product **193** to the natural product, we were nevertheless encouraged by the above results, as they suggested that an analogous sulfenylation reaction might proceed with the correct facial selectivity for C–S bond formation. After several attempts at sulfenyling diketopiperazine **194** by kinetic deprotonation with LDA followed by trapping with sulfur electrophiles (e.g. monoclinic S₈, *p*-methoxybenzyl disulfide, etc.), we found that we could obtain tetrasulfide **197** (Scheme 2.24) as the sole isolable sulfenylated product using the conditions reported by Nicolaou and coworkers (see Chapter 1).^{10,33} By using the exact ratios of base to sulfur described in the literature, **197** was consistently obtained in 50% yield. However, by using a much larger excess of base relative to sulfur, the yield could be improved to 76%. Gratifyingly, single-crystal X-ray diffraction analysis revealed that oxidation had selectively occurred to give the C–S bonds in the desired orientation for advancement to the natural product.

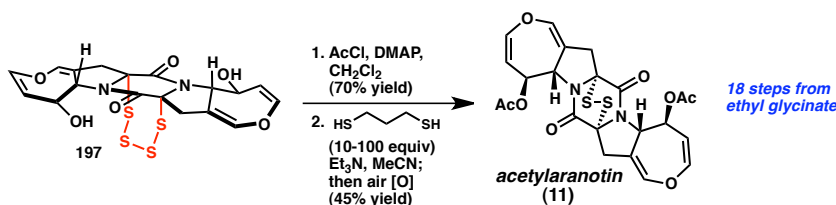
Scheme 2.X. Sulfenylation of diketopiperazine **194** to obtain tetrasulfide **197**



Tetrasulfide **197** was found to be unstable to NaBH_4 under conditions typically used to reduce similar cyclic epipolythiodiketopiperazines. Instead, acetylation of the two peripheral hydroxyl groups furnished the diacetate, and the tetrasulfide was reduced under mild conditions using propanedithiol and Et_3N in MeCN. Aerobic oxidation of the

resulting dithiol delivered the natural product, **11**. The spectroscopic data for synthetic (–)-acetylalaranotin were identical to the original isolation data.

Scheme 2.25. Conversion of tetrasulfide **197** to acetylalaranotin (**11**)



2.3 CONCLUDING REMARKS

In conclusion, we have achieved the enantioselective total synthesis of (–)-acetylalaranotin (**11**), the first total synthesis of any dihydrooxepine-containing ETP natural product, in 18 steps from inexpensive, commercially available materials. Essential to the development of this route was the successful execution of a rhodium-catalyzed cycloisomerization/chloride elimination sequence to furnish the dihydrooxepine ring and complete the monomer unit **186**. This strategy allowed us to exploit the power of an azomethine ylide (1,3)-dipolar cycloaddition reaction in order to enantio- and diastereoselectively construct the densely functionalized pyrrolidine scaffold of the requisite alkynyl alcohol substrate **184**. Notably, diketopiperazine **194** was obtained as a single diastereomer, which underwent direct sulfenylation with *complete retention of stereochemistry* to provide epitetrathiodiketopiperazine **197**. Access to monomer unit **186** has enabled the synthesis of related dihydrooxepine-containing ETP natural products and analogs, as described in Chapter 3.

2.4 EXPERIMENTAL SECTION

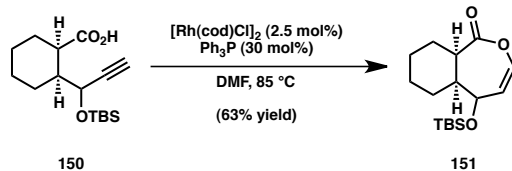
2.4.1 Materials and Methods

Unless otherwise stated, reactions were performed under a nitrogen atmosphere using freshly dried solvents. Tetrahydrofuran (THF), methylene chloride (CH_2Cl_2), acetonitrile (MeCN), dimethylformamide (DMF), and toluene (PhMe) were dried by passing through activated alumina columns. Unless otherwise stated, chemicals and reagents were used as received. Triethylamine (Et_3N) was distilled over calcium hydride prior to use. All reactions were monitored by thin-layer chromatography using EMD/Merck silica gel 60 F254 pre-coated plates (0.25 mm) and were visualized by UV, *p*-anisaldehyde, or KMnO_4 staining. Flash column chromatography was performed either as described by Still et al.³⁴ using silica gel (particle size 0.032-0.063) purchased from Silicycle or using pre-packaged RediSep[®]Rf columns on a CombiFlash Rf system (Teledyne ISCO Inc.). Optical rotations were measured on a Jasco P-2000 polarimeter using a 100 mm path-length cell at 589 nm. ^1H and ^{13}C NMR spectra were recorded on a Varian 400 MR (at 400 MHz and 101 MHz, respectively), a Varian Inova 500 (at 500 MHz and 126 MHz, respectively), or a Varian Inova 600 (at 600 MHz and 150 MHz, respectively), and are reported relative to internal CHCl_3 (^1H , δ = 7.26), MeCN (^1H , δ = 1.94), or DMSO (^1H , δ = 2.50), and CDCl_3 (^{13}C , δ = 77.0), MeCN (^{13}C , δ = 118.26), or DMSO (^{13}C , δ = 40.0). Data for ^1H NMR spectra are reported as follows: chemical shift (δ ppm) (multiplicity, coupling constant (Hz), integration). Multiplicity and qualifier abbreviations are as follows: s = singlet, d = doublet, t = triplet, q = quartet, m = multiplet, br = broad, app = apparent. IR spectra were recorded on a Perkin Elmer Paragon 1000 spectrometer and are reported in frequency of absorption (cm^{-1}). HRMS

were acquired using an Agilent 6200 Series TOF with an Agilent G1978A Multimode source in electrospray ionization (ESI), atmospheric pressure chemical ionization (APCI), or mixed (MM) ionization mode. Analytical chiral HPLC was performed with an Agilent 1100 Series HPLC utilizing Chiralpak AD or Chiralcel OD-H columns (4.6 mm x 25 cm) obtained from Daicel Chemical Industries, Ltd with visualization at 254 nm. Preparative HPLC was performed with an Agilent 1100 Series HPLC utilizing an Agilent Eclipse XDB-C18 5 μ m column (9.4 x 250 mm) or an Agilent Zorbax RX-SIL 5 μ m column (9.4 x 250 mm). Melting points were determined using a Büchi B-545 capillary melting point apparatus and the values reported are uncorrected.

2.4.2 *Preparative Procedures and Spectroscopic Data*

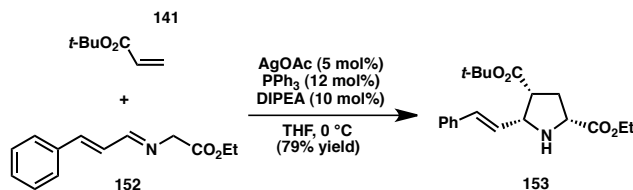
Preparation of enol lactone **151**



In the glove box, [Rh(cod)Cl]₂ (6.3 mg, 0.0127 mmol) was weighed into an oven-dried 1-dram vial. This was removed from the glove box, and charged with cycloisomerization substrate **150** (75 mg, 0.253 mmol), PPh₃ (39.9 mg, 0.152 mmol), and a magnetic stir bar. The vial was sealed with a rubber septum, and flushed with N₂. DMF (2.5 mL, dried over 4 \AA molecular sieves and degassed with Ar for 30 min) was then added, and the mixture was stirred until all solids had dissolved. The resulting solution was then heated to 85 °C. After 4 h, the reaction solution was cooled to rt, then transferred to a separatory funnel containing 50 mL sat. NaHCO₃. The mixture was extracted with Et₂O (3 x 15 mL), and the combined organic layers were washed with sat.

NaHCO_3 (15 mL), dried over Na_2SO_4 , and concentrated to give an orange oil. The crude material was purified by flash chromatography (1 \rightarrow 2% EtOAc/hexanes) to afford *endo*-enol lactone **151** (46.7 mg, 62% yield) as a pale yellow oil that solidifies upon standing at -20°C . ^1H NMR (500 MHz, CDCl_3) δ 6.31 (dd, $J = 5.9, 2.0$ Hz, 1H), 5.45 (t, $J = 5.1$ Hz, 1H), 4.22 – 4.15 (m, 1H), 3.12 (t, $J = 5.6$ Hz, 1H), 2.15 – 1.99 (m, 3H), 1.87 (dd, $J = 26.3, 13.1$ Hz, 1H), 1.78 (app d, $J = 12.2$ Hz, 1H), 1.56 (app d, $J = 13.7$ Hz, 1H), 1.35 (tt, $J = 13.4, 4.9$ Hz, 1H), 1.20 – 1.03 (m, 2H), 0.88 (s, 9H), 0.03 (s, 6H); ^{13}C NMR (126 MHz, CDCl_3) δ 173.1, 137.6, 121.8, 72.9, 50.5, 37.7, 28.8, 27.4, 25.7, 24.9, 21.5, 17.9, -4.6, -5.0; IR (NaCl/thin film): 2934, 2897, 2856, 1764, 1645 cm^{-1} ; HRMS (Multimode-ESI/APCI) calc'd for $\text{C}_{16}\text{H}_{29}\text{O}_3\text{Si}$ [M+H] $^+$ 297.1881, found 297.1881.

Preparation of styrenyl pyrrolidine **153**

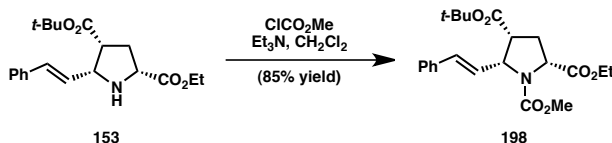


Ethyl glycinate hydrochloride (30 g) was ground together with K_2CO_3 (60 g) and several drops of brine using a mortar and pestle to give a white paste. This material was extracted with several portions of Et_2O , and the combined extracts were dried over Na_2SO_4 , filtered, and concentrated to afford ethyl glycinate (~81 wt %, contains a significant amount of Et_2O) as a nearly colorless oil (a white solid—presumably the cyclic glycine dimer—forms upon prolonged storage of this material at -20°C). An oven-dried flask equipped with a magnetic stir bar is charged with silica gel (15.0 g) then sealed with a rubber septum and flushed with N_2 . THF (250 mL) is then added, and the suspension is cooled to 0°C with stirring. The freshly prepared ethyl glycinate (81 wt %,

6.40 g, 50.0 mmol) was then added, followed by cinnamaldehyde (6.30 mL, 50.0 mmol), and the mixture was stirred at 0 °C. After 6 h, the resulting solution of imine **152** was filtered into an oven-dried flask to remove silica gel, and this flask was sealed with a rubber septum, flushed with N₂, and cooled to 0 °C.

Prior to filtration of the imine solution, an oven-dried flask equipped with a magnetic stir bar was charged with AgOAc (417 mg, 2.50 mmol) and PPh₃ (1.57 g, 6.00 mmol), then sealed with a rubber septum and flushed with N₂. The solids were dissolved in THF (250 mL) and the resulting solution was stirred for 15 min before being cooled to 0 °C. *t*-Butyl acrylate (11.0 mL, 75.0 mmol) was then added, followed by DIPEA (871 μL, 5.00 mmol). The cold imine solution was then transferred dropwise via cannula to the stirring solution of the catalyst system and dipolarophile over ~50 min. After 30 min of further stirring, the reaction solution was concentrated to an orange oil and purified by flash chromatography (14→50% EtOAc/hexanes) to afford pyrrolidine **153** (13.6 g, 79% yield) as a viscous green oil. ¹H NMR (500 MHz, CDCl₃) δ 7.36 – 7.33 (m, 2H), 7.32 – 7.27 (m, 2H), 7.24 – 7.19 (m, 1H), 6.59 (d, *J* = 15.8 Hz, 1H), 6.18 (dd, *J* = 15.8, 7.7 Hz, 1H), 4.29 – 4.19 (m, 2H), 4.02 (dd, *J* = 7.6, 7.6 Hz, 1H), 3.87 (dd, *J* = 8.4, 8.4 Hz, 1H), 3.11 (ddd, *J* = 7.6, 7.6, 7.6 Hz, 1H), 2.51 (s, 1H), 2.37 (ddd, *J* = 13.2, 8.4, 7.8 Hz, 1H), 2.26 (ddd, *J* = 13.3, 8.2, 7.8 Hz, 1H), 1.33 (s, 9H), 1.30 (t, *J* = 7.1 Hz, 3H); ¹³C NMR (126 MHz, CDCl₃) δ 173.8, 171.6, 136.5, 131.9, 128.5, 127.6, 127.0, 126.4, 80.9, 63.9, 61.1, 59.7, 49.6, 33.0, 28.0, 14.2; IR (NaCl/thin film): 2978, 1737, 1732, 1729, 1495, 1478, 1450, 1392, 1367, 1248, 1210, 1151, 1030, 966, 847, 750, 693 cm⁻¹; HRMS (Multimode-ESI/APCI) calc'd for C₂₀H₂₈NO₄ [M+H]⁺ 346.2013, found 346.2006.

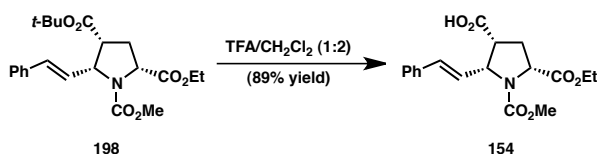
Preparation of methyl carbamate **198**



An oven-dried flask was charged with pyrrolidine **153** (667 mg, 1.93 mmol) and a magnetic stir bar, then was sealed with a rubber septum and flushed with N₂. The material was dissolved in CH₂Cl₂ (20 mL) and Et₃N (807 μ L, 5.79 mmol) was added. Methyl chloroformate (224 μ L, 2.90 mmol) was then added dropwise with stirring. After 1 h, the reaction was quenched with 20 mL of sat. NaHCO₃. The phases were separated, and the aqueous layer was extracted with CH₂Cl₂ (2 x 20 mL). The combined organic layers were washed with sat. NaHCO₃ (50 mL), dried over Na₂SO₄, filtered, and concentrated under reduced pressure. The crude material was purified by flash chromatography (20% EtOAc/hexanes) to afford methyl carbamate **198** (664 mg, 85% yield) as a viscous green oil. ¹H NMR (500 MHz, CDCl₃; compound exists as a 1.1:1 mixture of rotamers, the major rotamer is designated by *, minor rotamer denoted by \ddagger) δ 7.38 – 7.33 (m, 2H*), 2H \ddagger), 7.32 – 7.24 (m, 2H*, 2H \ddagger), 7.24 – 7.17 (m, 1H*, 1H \ddagger), 6.80 (d, J = 15.7 Hz, 1H \ddagger), 6.74 (d, J = 15.7 Hz, 1H*), 6.16 (dd, J = 16.1, 8.1 Hz, 1H*), 6.14 (dd, J = 16.3, 8.5 Hz, 1H \ddagger), 4.90 (t, J = 8.0 Hz, 1H \ddagger), 4.78 (t, J = 7.9 Hz, 1H*), 4.36 – 4.19 (m, 3H*, 3H \ddagger), 3.69 (s, 3H*), 3.67 (s, 3H \ddagger), 3.24 – 3.15 (m, 1H*, 1H \ddagger), 2.49 – 2.30 (m, 2H*, 2H \ddagger), 1.36 (s, 9H*, 9H \ddagger), 1.30 (dd, J = 6.5 Hz, 6.5 Hz, 3H*, 3H \ddagger); ¹³C NMR (126 MHz, CDCl₃; compound exists as a mixture of rotamers) δ 172.1, 172.0, 168.6, 168.6, 155.2, 154.3, 136.5, 136.4, 133.8, 133.4, 128.5, 128.3, 127.8, 127.6, 126.7, 126.6, 124.7, 124.2, 81.6, 61.9, 61.3, 61.3, 61.2, 59.0, 58.7, 52.8, 52.7, 48.6, 47.8, 30.6, 29.7, 29.5, 28.1, 14.2, 14.2; IR (NaCl/thin film): 2978, 2928, 1748, 1733, 1716, 1698, 1454, 1446, 1385, 1370, 1288,

1251, 1187, 1155, 1118, 1073, 1029, 962, 843, 752 cm⁻¹; HRMS (Multimode-ESI/APCI) calc'd for C₁₈H₂₂NO₆ [M-C₄H₈+H]⁺ 348.1442, found 348.1453 (detected fragment has undergone elimination of *iso*-butylene from the *t*-butyl ester).

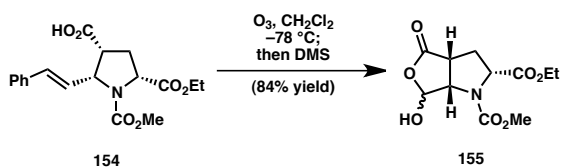
Preparation of carboxylic acid 154



An oven-dried flask equipped with a magnetic stir bar was charged with *t*-butyl ester **198** (1.31 g, 3.25 mmol), then was sealed with a rubber septum and flushed with N₂. CH₂Cl₂ (12 mL) was then added, followed by TFA (6 mL), and the resulting solution was stirred for 10 h at room temperature. During this time, the color of the solution changed from light green to bright red. The reaction solution was concentrated under reduced pressure to give an orange-red to brown oil, which partially solidified under high vacuum. The material was purified by flash chromatography (2:1 hexanes/EtOAc with 1% AcOH) to give carboxylic acid **154** (1.00 g, 89% yield) as an orange solid. It was later found that the crude material could also be purified and the color removed by trituration with Et₂O. ¹H NMR (500 MHz, CD₃CN; compound exists as a 1.2:1 mixture of rotamers, the major rotamer is designated by *, minor rotamer denoted by [§]) δ 7.38 (d, *J* = 7.7 Hz, 2H*, 2H[§]), 7.33 (t, *J* = 7.5 Hz, 2H*, 2H[§]), 7.26 (t, *J* = 6.9 Hz, 1H*, 1H[§]), 6.79 (d, *J* = 15.8 Hz, 1H*, 1H[§]), 6.18 (dd, *J* = 15.8, 7.5 Hz, 1H*, 1H[§]), 4.80 (dt, *J* = 14.8, 7.8 Hz, 1H*, 1H[§]), 4.28 (dt, *J* = 10.9, 6.8 Hz, 1H*, 1H[§]), 4.24 – 4.15 (m, 2H*, 2H[§]), 3.61 (s, 3H*), 3.59 (s, 3H[§]), 3.36 (dq, *J* = 15.3, 8.0, 7.5 Hz, 1H*, 1H[§]), 2.44 (apt tt, *J* = 13.8, 7.2 Hz, 1H*, 1H[§]), 2.29 (q, *J* = 11.8 Hz, 1H[§]), 2.23 (q, *J* = 11.9 Hz, 1H*), 1.26 (t, *J* = 7.1 Hz, 3H*, 3H[§]); ¹³C NMR (126 MHz, CD₃CN; compound exists as a 1.2:1 mixture of

rotamers) δ 173.2, 173.0, 171.2, 171.2, 156.0, 155.1, 137.5, 133.6, 133.5, 129.6, 128.7, 127.3, 126.4, 126.2, 62.2, 62.0, 61.9, 61.7, 60.0, 59.6, 53.2, 53.0, 48.0, 47.3, 31.4, 30.4, 14.5; IR (NaCl/thin film): 2987, 2596, 1743, 1711, 1452, 1384, 1287, 1242, 1190, 1122, 1076, 1029, 966, 862, 833, 771, 739 cm⁻¹; HRMS (Multimode-ESI/APCI) calc'd for C₁₈H₂₂NO₆ [M+H]⁺ 348.1442, found 348.1444.

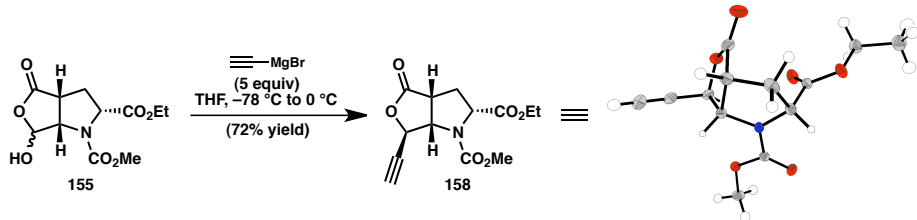
Preparation of hydroxylactone 155



An oven-dried 3-neck flask equipped with a magnetic stir bar was charged with styrene **154** (900 mg, 2.59 mmol) and CH₂Cl₂ (26 mL). The middle neck was fitted with an adaptor for the ozone line, one of the side necks was stoppered with a punctured plastic stopper as an outlet, and the third neck was stoppered with a glass stopper. The solution was cooled to -78 °C with stirring, and O₂ was bubbled through for several minutes. O₃ was then bubbled through the solution. When the solution had turned a blue color, the O₃ was bubbled through for an additional 15 min, and then the solution and reaction vessel were purged with O₂. When the blue color had disappeared, the solution was allowed to warm to room temperature, the punctured plastic stopper was replaced with a glass stopper, and the adapter in the center neck replaced with a rubber septum. N₂ was then bubbled through the solution for 15 min to remove O₂, and DMS (7.57 mL, 104 mmol) was added. The resulting solution was allowed to stir under N₂ overnight, and then was concentrated under reduced pressure and purified by flash chromatography (50→67% EtOAc/hexanes) to afford hydroxy lactone **155** (596 mg, 84% yield) as an

extremely viscous oil. ^1H NMR (500 MHz, $\text{DMSO}-d_6$; compound exists as a 1.1:1 mixture of rotamers, the major rotamer is designated by $*$, minor rotamer denoted by \ddagger) δ 7.92 (dd, $J = 10.5, 6.0$ Hz, 1 H^* , 1 H^\ddagger), 5.71 (d, $J = 4.6$ Hz, 1 H^*), 5.67 (d, $J = 4.8$ Hz, 1 H^\ddagger), 4.45 (t, $J = 11.0$ Hz, 1 H^* , 1 H^\ddagger), 4.20 (dd, $J = 7.3, 3.3$ Hz, 1 H^* , 1 H^\ddagger), 4.15 – 3.97 (m, 2 H^* , 2 H^\ddagger), 3.68 (s, 3 H^\ddagger), 3.60 (s, 3 H^*), 3.55 (dt, $J = 15.3, 8.1$ Hz, 1 H^* , 1 H^\ddagger), 2.68 – 2.53 (m, 1 H^* , 1 H^\ddagger), 2.17 (dd, $J = 21.3, 13.5$ Hz, 1 H^* , 1 H^\ddagger), 1.14 (t, $J = 7.0$ Hz, 3 H^* , 3 H^\ddagger); ^{13}C NMR (126 MHz, $\text{DMSO}-d_6$; compound exists as a 1.1:1 mixture of rotamers, the major rotamer is designated by $*$, minor rotamer denoted by \ddagger) δ 177.6*, 177.5 \ddagger , 171.8*, 171.7 \ddagger , 154.6*, 154.5 \ddagger , 101.9 \ddagger , 101.1*, 66.0*, 65.4 \ddagger , 61.6*, 61.5 \ddagger , 59.6 \ddagger , 59.0*, 53.5 \ddagger , 53.3*, 43.5 \ddagger , 42.5*, 31.7*, 30.7 \ddagger , 14.2* \ddagger ; IR (NaCl/thin film): 3382, 2963, 1782, 1743, 1712, 1454, 1387, 1352, 1293, 1254, 1200, 1157, 1122, 1057, 1038, 1022, 975, 954, 933, 856, 775 cm^{-1} ; HRMS (Multimode-ESI/APCI) calc'd for $\text{C}_{11}\text{H}_{14}\text{NO}_7$ [M–H] $^-$ 272.0776, found 272.0733.

Preparation of alkynyl lactone **158**

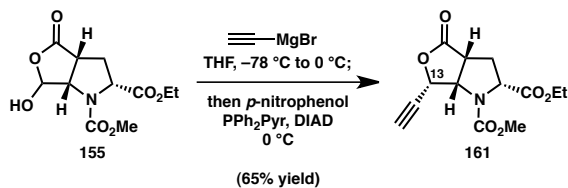


Hydroxylactone **155** (1.34 g, 4.90 mmol) was transferred to an oven-dried flask as a solution in benzene, then concentrated under reduced pressure. A magnetic stir bar was added, and the flask was sealed with a rubber septum and flushed with N_2 . THF (25 mL) was added, and the resulting solution was cooled to -78 $^\circ\text{C}$ with stirring. Ethynylmagnesium bromide (0.5 M solution in THF, 49.0 mL, 24.5 mmol) was added

dropwise over 25 min via syringe pump (this appears to be somewhat exothermic, and the addition was paused twice during addition of the first equivalent of reagent due to violent bubbling of the dry ice bath). The resulting yellow-brown suspension was stirred for another 5 min at $-78\text{ }^{\circ}\text{C}$, then allowed to warm to $0\text{ }^{\circ}\text{C}$ over 25 min. During this time, the reaction contents solubilized to give a pale yellow-brown solution. The reaction was quenched with 20 mL 2 M HCl, and the THF was removed under reduced pressure. The resulting mixture was extracted with EtOAc (75 mL, then 3 x 50 mL), then saturated with NaCl and extracted again with EtOAc (50 mL). The combined organics were washed with brine (100 mL), dried over Na_2SO_4 , filtered, and concentrated under reduced pressure. The crude material was stored at $-20\text{ }^{\circ}\text{C}$ overnight to allow complete lactonization, and then was purified by flash chromatography (40 \rightarrow 75% EtOAc/hexanes) to afford alkynyl lactone **158** (993 mg, 72% yield) as a viscous oil, which could be precipitated from EtOH to form a white solid. Crystals suitable for X-ray diffraction were obtained by vapor diffusion of pentane into a saturated solution of alkynyl lactone **158** in PhMe at room temperature. ^1H NMR (500 MHz, CDCl_3 ; compound exists as a 1.4:1 mixture of rotamers, the major rotamer is designated by $*$, minor rotamer denoted by \ddagger) δ 5.42 (d, $J = 2.0\text{ Hz}$, 1H $*$), 5.30 (d, $J = 1.3\text{ Hz}$, 1H \ddagger), 4.68 (d, $J = 7.8\text{ Hz}$, 1H $*$), 4.61 (d, $J = 7.3\text{ Hz}$, 1H \ddagger), 4.58 – 4.54 (m, 1H \ddagger), 4.47 – 4.42 (m, 1H $*$), 4.21 – 4.08 (m, 2H $*$, 2H \ddagger), 3.80 (s, 3H \ddagger), 3.71 (s, 3H $*$), 3.44 – 3.34 (m, 1H $*$, 1H \ddagger), 2.71 – 2.69 (m, 1H $*$, 1H \ddagger), 2.62 – 2.49 (m, 2H $*$, 2H \ddagger), 1.24 (t, $J = 7.1\text{ Hz}$, 3H $*$, 3H \ddagger); ^{13}C NMR (126 MHz, CDCl_3 ; compound exists as mixture of rotamers) δ 176.0, 175.7, 170.9, 154.4, 154.0, 78.5, 78.4, 76.9, 73.6, 72.9, 65.3, 64.6, 62.0, 59.2, 58.8, 53.4, 53.2, 43.4, 42.4, 31.7, 30.8, 13.8; IR (NaCl/thin film): 3263, 2961, 2125, 1784, 1742, 1709, 1451, 1386, 1348, 1292, 1248,

1200, 1147, 1126, 1021, 977, 950, 773 cm⁻¹; HRMS (Multimode-ESI/APCI) calc'd for C₁₃H₁₆NO₆ [M+H]⁺ 282.0972, found 282.0967.

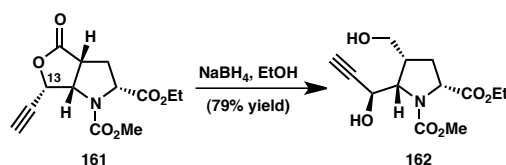
Preparation of alkynyl lactone **161**



To a flame dried 250 mL round bottom flask containing hydroxylactone **155** (3.36 g, 12.3 mmol) was added 62 mL of THF and the stirred solution was cooled to -78 °C. Ethynylmagnesium bromide (0.5 M solution in THF, 123 mL, 61.5 mmol) was added via syringe pump over one hour and the solution was then allowed to stir for five minutes at -78 °C before being warmed to 0 °C and stirred for another 25 min. The reaction was then quenched with *p*-nitrophenol (10.3 g, 73.8 mmol), and allowed to stir for 10 min, resulting in a bright yellow suspension. (2-Pyridyl)diphenylphosphine (6.48 g, 24.6 mmol) was then added, and the mixture was stirred for another 10 min before DIAD (4.8 mL, 25 mmol) was added dropwise via syringe. After stirring for 28 h, the mixture was concentrated *in vacuo*, taken up in 1 M *aq.* HCl, saturated with NaCl, and extracted with EtOAc (500 mL, then 2x250 mL). The combined organic layers were then washed with brine (200 mL), dried over Na₂SO₄, filtered, and concentrated *in vacuo* to give a dark brown-orange oil. Purification via silica gel flash chromatography (gradient elution, 1:1→1:2 hexanes-EtOAc) afforded 2.25 g of alkynyl lactone **161** (65% yield) as a pale yellow oil. ¹H NMR (500 MHz, CDCl₃; compound exists as a 1.2:1 mixture of rotamers, the major rotamer is designated by *, minor rotamer denoted by §) δ 5.34 (dd, *J* = 5.7, 2.3 Hz, 1H[§]), 5.30 (dd, *J* = 5.7, 2.3 Hz, 1H*), 4.96 (dd, *J* = 8.3, 5.7 Hz, 1H[§]), 4.85 (dd, *J* =

8.1, 5.6 Hz, 1H*), 4.61 (dd, J = 9.4, 1.7 Hz, 1H*), 4.56 (d, J = 9.0 Hz, 1H $^{\$}$), 4.15 (apt q, J = 7.2 Hz, 2H*, 2H $^{\$}$), 3.72 (s, 3H $^{\$}$), 3.70 (s, 3H*), 3.41 – 3.33 (m, 1H*, 1H $^{\$}$), 2.68 (d, J = 2.3 Hz, 1H*), 2.63 (d, J = 2.3 Hz, 1H $^{\$}$), 2.58 – 2.42 (m, 2H*, 2H $^{\$}$), 1.29 – 1.21 (m, 3H*, 3H $^{\$}$); ^{13}C NMR (126 MHz, CDCl_3 ; compound exists as a 1.2:1 mixture of rotamers, the major rotamer is designated by *, minor rotamer denoted by $^{\$}$) δ 175.5 $^{\$}$, 175.3*, 170.6*, 170.6 $^{\$}$, 155.0 $^{\$}$, 154.5*, 77.9 $^{\$}$, 77.6*, 75.8*, 75.6 $^{\$}$, 72.9*, 72.8 $^{\$}$, 61.8 $^{\$}$, 61.8*, 61.0 $^{\$}$, 60.3*, 59.9*, 59.7 $^{\$}$, 53.3 $^{\$}$, 52.6*, 44.4*, 43.5 $^{\$}$, 32.0 $^{\$}$, 31.2*, 13.8*, 13.8 $^{\$}$; IR (NaCl/thin film): 3262, 2958, 2131, 1779, 1709, 1447, 1385, 1286, 1245, 1195, 1163, 1126, 1042, 1016, 987, 920, 893, 856, 765, 733 cm^{-1} ; HRMS (Multimode-ESI/APCI) calc'd for $\text{C}_{13}\text{H}_{16}\text{NO}_6$ [M+H] $^+$ 282.0972, found 282.0968.

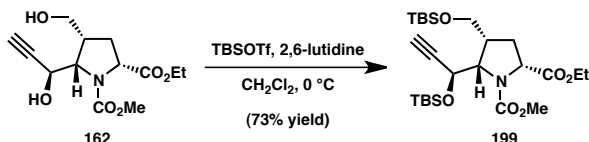
Preparation of diol 162



To a 500 mL round bottom flask containing alkynyl lactone **161** (2.04 g, 7.25 mmol) dissolved in 145 mL of EtOH, sodium borohydride (1.10 g, 29.0 mmol) was added and the reaction was stirred vigorously. Following completion of the reaction as judged by TLC (45 min), the reaction was cooled to 0 °C and quenched carefully with 60 mL of 1N *aq.* HCl. The solution was then saturated with NaCl, extracted with CHCl₃ (3x320 mL), then EtOAc (3x320 mL). The combined organic layers were dried over Na₂SO₄, filtered, and concentrated *in vacuo*. Purification through silica gel flash chromatography (isocratic elution, 1:2 hexanes–EtOAc) afforded **162** as a colorless oil in 79% yield (1.64 g). ¹H NMR (500 MHz, CDCl₃; compound exists as a 1.2:1 mixture of

rotamers, the major rotamer is designated by $*$, minor rotamer denoted by \ddagger) δ 4.68 (s, 1H \ddagger), 4.56 (s, 1H $*$), 4.44 – 4.27 (m, 2H $*$, 2H \ddagger), 4.27 – 4.15 (m, 2H $*$, 2H \ddagger), 4.03 (t, J = 10.7 Hz, 1H \ddagger), 3.92 (t, J = 10.2 Hz, 1H $*$), 3.81 – 3.72 (m, 1H $*$, 1H \ddagger), 3.69 (s, 3H $*$, 3H \ddagger), 2.61 (apt dp, J = 15.0, 7.5 Hz, 1H $*$, 1H \ddagger), 2.49 (s, 1H $*$), 2.49 (s, 1H \ddagger), 2.32 (apt dt, J = 12.8, 8.2 Hz, 1H $*$, 1H \ddagger), 2.10 (ddd, J = 12.1, 12.1, 12.1 Hz, 1H \ddagger), 1.99 (ddd, J = 11.5, 11.5, 11.5 Hz, 1H $*$), 1.27 (t, J = 7.1 Hz, 3H $*$, 3H \ddagger); ^{13}C NMR (126 MHz, CDCl_3 ; compound exists as a 1.2:1 mixture of rotamers, the major rotamer is designated by $*$, minor rotamer denoted by \ddagger) δ 174.7*, 173.7 \ddagger , 156.0*, 155.9 \ddagger , 83.1* \ddagger , 74.8 \ddagger , 74.2*, 63.3 \ddagger , 62.6*, 61.9*, 61.7*, 61.7 \ddagger , 61.5 \ddagger , 60.8* \ddagger , 59.3*, 59.1 \ddagger , 53.1 \ddagger , 52.7*, 44.4*, 43.8 \ddagger , 32.0 \ddagger , 30.9*, 14.0* \ddagger ; IR (NaCl/thin film): 3415, 3285, 2956, 2114, 1702, 1452, 1379, 1315, 1277, 1200, 1124, 1096, 1040, 918, 865, 819, 784, 769, 718 cm^{-1} ; HRMS (ESI) calc'd for $\text{C}_{13}\text{H}_{20}\text{NO}_6$ [$\text{M}+\text{H}]^+$ 286.1285, found 286.1293.

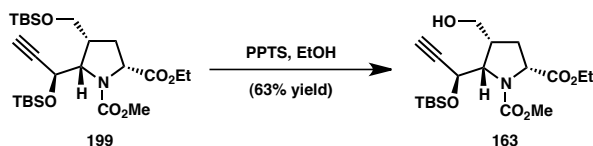
Preparation of bis(*tert*-butyldimethylsilyl) ether **199**



To a flame dried 250 mL round bottom flask equipped with diol **162** (1.62 g, 5.68 mmol) was added 57 mL of CH_2Cl_2 and the solution was cooled to 0 °C with stirring. Following addition of 2,6-lutidine (3.3 mL, 28 mmol), *tert*-butyldimethylsilyl trifluoromethanesulfonate (3.3 mL, 14 mmol) was added dropwise to the reaction. Upon completion of the reaction as judged by TLC (~1 h), the reaction was quenched with a small amount of MeOH, diluted with EtOAc (180 mL), and washed with brine (180 mL). The resulting organic layer was dried over Na_2SO_4 , filtered, and concentrated *in vacuo*. Purification through silica gel flash chromatography (isocratic elution, 6:1 hexanes-

EtOAc) afforded 2.13 g of **199** as a clear, colorless oil (73% yield). ¹H NMR (500 MHz, CD₃CN; compound exists as a 1:1 mixture of rotamers) δ 4.78 (s, 1H), 4.69 (s, 1H), 4.19 (t, *J* = 8.5 Hz, 2H), 4.15 – 4.00 (m, 6H), 3.91 (q, *J* = 4.9 Hz, 2H), 3.65 (s, 3H), 3.60 (s, 3H), 2.70 (s, 2H), 2.55 (dq, *J* = 14.1, 7.9 Hz, 2H), 2.45 – 2.24 (m, 4H), 1.21 (t, *J* = 7.1 Hz, 6H), 0.90 (s, 18H), 0.90 (s, 18H), 0.15 – 0.11 (m, 12H), 0.05 (s, 12H); ¹³C NMR (126 MHz, CD₃CN; compound exists as a 1:1 mixture of rotamers) δ 172.5, 172.1, 156.6, 118.3, 84.8, 77.2, 64.8, 64.2, 63.8, 63.0, 63.0, 63.0, 61.5, 61.4, 60.7, 60.3, 53.2, 45.5, 44.8, 34.5, 33.4, 26.4, 26.1, 19.0, 18.7, 14.7, -4.5, -5.0, -5.0; IR (NaCl/thin film): 3311, 3257, 2954, 2929, 2887, 2857, 2114, 1760, 1711, 1448, 1371, 1297, 1257, 1186, 1167, 1130, 1078, 1041, 1005, 993, 939, 838, 809, 778, 716 cm⁻¹; HRMS (Multimode-ESI/APCI) calc'd for C₂₅H₄₈NO₆Si₂ [M+H]⁺ 514.3015, found 514.3029.

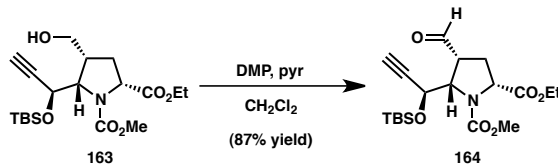
Preparation of primary alcohol 163



To a solution of bis(*tert*-butyldimethylsilyl) ether **199** (2.12 g, 4.13 mmol) in EtOH (41 mL) was added PPTS (1.04 g, 4.13 mmol), and the resulting solution was stirred for 14.5 h. The reaction mixture was then diluted with sat. *aq.* NaHCO₃ (20 mL) and brine (20 mL), then extracted with EtOAc (100 mL, then 3x50 mL). The combined organics were washed with brine (100 mL), dried over Na₂SO₄, filtered, and concentrated *in vacuo*. Purification via silica gel flash chromatography (gradient elution, 4:1→1:2 hexanes–EtOAc) afforded **163** as a clear, colorless oil in 63% yield (1.04 g), along with 29% yield of recovered starting material (616 mg). ¹H NMR (500 MHz, CD₃CN; compound exists as a 1:1 mixture of rotamers) δ 4.84 (s, 1H), 4.75 (s, 1H), 4.24 – 4.16

(m, 2H), 4.16 – 4.06 (m, 6H), 3.99 (apt dd, J = 8.2, 3.7 Hz, 2H), 3.71 (apt dt, J = 11.4, 8.0 Hz, 2H), 3.65 (s, 3H), 3.60 (s, 3H), 3.07 – 2.99 (m, 2H), 2.73 (s, 2H), 2.67 – 2.55 (m, 2H), 2.31 – 2.17 (m, 4H), 1.21 (t, J = 7.2 Hz, 6H), 0.92 (s, 18H), 0.18 (s, 12H); ^{13}C NMR (126 MHz, CD_3CN ; compound exists as a 1:1 mixture of rotamers) δ 172.3, 172.0, 156.5, 84.3, 77.5, 64.9, 64.2, 64.0, 63.2, 61.4, 61.4, 61.4, 60.5, 60.1, 53.1, 45.7, 45.0, 33.2, 32.2, 26.0, 18.7, 14.5, -4.8, -5.2, -5.2; IR (NaCl/thin film): 3506, 3255, 2955, 2932, 2888, 2858, 2114, 1759, 1709, 1450, 1372, 1301, 1255, 1190, 1125, 1068, 1041, 1009, 987, 939, 865, 834, 781, 715 cm^{-1} ; HRMS (Multimode-ESI/APCI) calc'd for $\text{C}_{19}\text{H}_{34}\text{NO}_6\text{Si}$ [$\text{M}+\text{H}]^+$ 400.2150, found 400.2148.

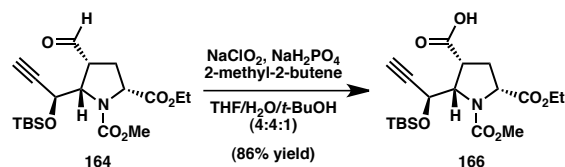
Preparation of aldehyde **164**



To a solution of primary alcohol **163** (1.04 g, 2.60 mmol) dissolved in 26 mL of CH_2Cl_2 (bulk solvent, not dried), was added pyridine (2.1 mL, 26 mmol), and Dess–Martin periodinane²⁴ (2.21 g, 5.20 mmol), and the cloudy white suspension was stirred vigorously. After 3 h, the reaction was quenched with sat. *aq.* $\text{Na}_2\text{S}_2\text{O}_3$ solution (30 mL) and sat. *aq.* NaHCO_3 solution (30 mL) and stirred vigorously for an additional 10 min. The layers were then separated and the aqueous layer was washed with EtOAc (2 x 100 mL). The combined organics were washed with sat. *aq.* NaHCO_3 solution (100 mL), then brine (100 mL), dried over Na_2SO_4 , and concentrated *in vacuo*. Purification through silica gel flash chromatography (isocratic elution, 3:1 hexanes– EtOAc) afforded **164** as a white amorphous solid in 87% yield (899 mg). ^1H NMR (500 MHz, CDCl_3 ; compound exists as

a 1.3:1 mixture of rotamers, the major rotamer is designated by *, minor rotamer denoted by §) δ 10.07 (s, 1H*), 10.05 (s, 1H§), 4.96 (s, 1H*), 4.82 (s, 1H§), 4.41 – 4.32 (m, 1H*, 1H§), 4.32 – 4.25 (m, 1H*, 1H§), 4.25 – 4.12 (m, 2H*, 2H§), 3.75 (s, 3H§), 3.69 (s, 3H*), 3.15 – 3.06 (m, 1H*, 1H§), 2.91 (apt dq, J = 23.2, 12.0 Hz, 1H*, 1H§), 2.46 (s, 1H§), 2.44 (s, 1H*), 2.39 (dt, J = 14.1, 7.9 Hz, 1H*, 1H§), 1.26 (apt t, J = 7.1 Hz, 3H*, 3H§), 0.88 (s, 9H*, 9H§), 0.17 – 0.09 (m, 6H*, 6H§); ^{13}C NMR (126 MHz, CDCl_3 ; compound exists as a 1.3:1 mixture of rotamers, the major rotamer is designated by *, minor rotamer denoted by §) δ 198.3*, 198.2§, 170.8*, 170.5§, 155.4*, 155.2§, 82.7*, 82.4§, 76.8§, 76.4*, 64.6*, 63.9§, 62.8§, 62.0*, 61.1§, 61.0*, 59.4§, 59.1*, 53.2§, 53.1§, 53.0*, 52.4*, 30.1*, 29.0§, 25.5*§, 18.0§, 18.0*, 14.2*, 14.2§, -5.0*§, -5.4*, -5.5§; IR (NaCl/thin film): 3262, 2956, 2931, 2886, 2858, 2116, 1756, 1714, 1448, 1373, 1289, 1255, 1192, 1126, 1080, 1037, 1006, 987, 939, 864, 839, 780, 721 cm^{-1} ; HRMS (Multimode-ESI/APCI) calc'd for $\text{C}_{19}\text{H}_{32}\text{NO}_6\text{Si} [\text{M}+\text{H}]^+$ 398.1993, found 398.1998.

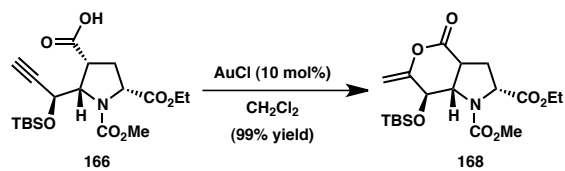
Preparation of carboxylic acid 166



Aldehyde **164** (60.0 mg, 0.151 mmol) was dissolved in a solution of 2-methyl-2-butene in THF (2.0 M, 1.2 mL, 2.4 mmol) and *tert*-butanol (0.3 mL) was added. To the resulting solution was added a solution of sodium chlorite (80 wt %, 25.7 mg, 0.227 mmol) and sodium dihydrogen phosphate monohydrate (62.5 mg, 0.453 mmol) in water (1.2 mL) via pipet with stirring. After 3 h, the reaction mixture was diluted with sat. *aq.* NH₄Cl, and extracted with EtOAc (3x4 mL). The combined organic layers were

subsequently washed with brine (20 mL), dried over Na_2SO_4 , filtered, and concentrated *in vacuo* to provide the crude product, which was purified by silica gel flash chromatography (isocratic elution, 1:1 hexanes–EtOAc containing 1% AcOH) to afford carboxylic acid **166** (54.0 mg, 86% yield) as a white foam. ^1H NMR (500 MHz, CDCl_3 ; compound exists as a 1.1:1 mixture of rotamers, the major rotamer is designated by *, minor rotamer denoted by \ddagger) δ 4.94 (s, 1H*), 4.82 (s, 1H \ddagger), 4.44 (dd, J = 7.8, 4.1 Hz, 1H*), 4.36 (t, J = 7.5 Hz, 2H \ddagger), 4.28 (t, J = 9.0 Hz, 1H*), 4.25 – 4.12 (m, 2H*, 2H \ddagger), 3.73 (s, 3H \ddagger), 3.70 (s, 3H*), 3.21 (dt, J = 13.8, 7.7 Hz, 1H*, 1H \ddagger), 2.91 (ddd, J = 12.2, 12.2, 12.2 Hz, 1H*), 2.84 (ddd, J = 12.1, 12.1, 11.8 Hz, 1H \ddagger), 2.57 – 2.47 (m, 1H*, 1H \ddagger), 2.45 (d, J = 2.2 Hz, 1H*, 1H \ddagger), 1.26 (t, J = 7.1 Hz, 3H*, 3H \ddagger), 0.88 (s, 9H*, 9H \ddagger), 0.18 – 0.10 (m, 6H*, 6H \ddagger); ^{13}C NMR (126 MHz, CDCl_3 ; compound exists as a mixture of rotamers) δ 174.2, 173.9, 170.7, 170.4, 155.6, 81.8, 81.7, 76.1, 63.4, 63.0, 63.0, 62.6, 61.1, 58.7, 58.5, 53.0, 52.9, 45.3, 44.7, 31.6, 30.3, 25.6, 18.1, 14.2, -4.9, -5.4; IR (NaCl/thin film): 3270, 2956, 2929, 2117, 1712, 1451, 1381, 1252, 1189, 1090, 1031, 1003, 939, 891, 839, 779 cm^{-1} ; HRMS (ESI) calc'd for $\text{C}_{19}\text{H}_{32}\text{NO}_7\text{Si}$ [M+H] $^+$ 414.1943, found 414.1946.

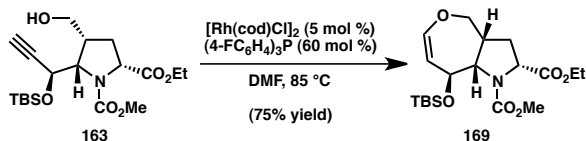
Preparation of enol lactone 168



Carboxylic acid **166** (18.7 mg, 45.2 μmol) was dissolved in CH_2Cl_2 (230 μL) and AuCl (1.1 mg, 4.52 μmol) was added. The resulting solution was stirred for 5 min, then filtered through SiO_2 (eluting with 1:1 hexanes–EtOAc) and concentrated *in vacuo* to afford 18.5 mg of enol lactone **168** (99% yield). ^1H NMR (500 MHz, CDCl_3 ; compound

exists as a 2:1 mixture of rotamers, the major rotamer is designated by $*$, minor rotamer denoted by \ddagger) δ 5.00 (s, 1H $*$), 4.91 – 4.80 (m, 1H $*$, 1H \ddagger), 4.71 – 4.58 (m, 1H $*$, 2H \ddagger), 4.42 (br s, 1H \ddagger), 4.37 (br s, 2H $*$), 4.20 – 4.10 (m, 2H $*$, 2H \ddagger), 4.07 (dd, J = 7.4, 3.4 Hz, 1H $*$, 1H \ddagger), 3.77 (s, 3H \ddagger), 3.70 (s, 3H $*$), 3.44 – 3.34 (m, 1H $*$, 1H \ddagger), 2.61 – 2.36 (m, 2H $*$, 2H \ddagger), 1.24 (t, J = 7.1 Hz, 3H $*$, 3H \ddagger), 0.87 (s, 9H $*$, 9H \ddagger), 0.18 – 0.07 (m, 6H $*$, 6H \ddagger); ^{13}C NMR (126 MHz, CDCl_3 ; compound exists as a mixture of rotamers) δ 170.8, 168.9, 155.4, 153.7, 110.0, 98.5, 98.3, 69.0, 66.8, 62.4, 62.3, 61.5, 60.1, 59.8, 53.2, 53.0, 42.2, 41.0, 32.7, 32.0, 29.7, 25.6, 18.0, 14.0, -5.0, -5.1; IR (NaCl/thin film): 2955, 2929, 2857, 1757, 1718, 1669, 1448, 1375, 1260, 1217, 1192, 1131, 1087, 1044, 1003, 967, 939, 866, 839, 779 cm^{-1} ; HRMS (ESI) calc'd for $\text{C}_{13}\text{H}_{18}\text{NO}_7$ [M– $\text{C}_6\text{H}_{15}\text{OSi} + \text{H}_2\text{O}]^+$ 300.1078, found 300.1086 (detected fragment has undergone loss of *tert*-butyldimethylsilanolate anion and gain of water).

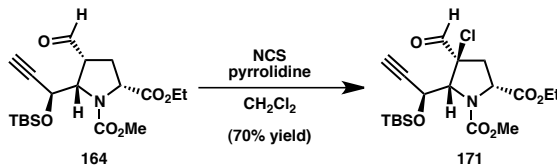
Preparation of tetrahydrooxepine 169



Alcohol **163** (28.7 mg, 71.8 μmol) was dissolved in dry, degassed DMF (360 μL) and transferred via syringe to a microwave vial equipped with a magnetic stir bar and sealed with a septum cap under an N_2 atmosphere. A stock solution of $[\text{Rh}(\text{cod})\text{Cl}]_2$ (0.01 M) and $(4-\text{FC}_6\text{H}_4)_3\text{P}$ (0.12 M) in dry, degassed DMF (360 μL) was added, and the resulting solution was heated with stirring to 85 $^\circ\text{C}$ in an oil bath. After 22 h, the reaction mixture was cooled to rt, diluted with sat. *aq.* NaHCO_3 , and extracted with EtOAc (5x5 mL). The combined organic layers were dried over Na_2SO_4 , filtered, and concentrated *in vacuo*, and the resulting material was purified via silica gel flash chromatography

(gradient elution, 5:1→4:1 hexanes–EtOAc, the SiO₂ was deactivated using 0.5 % Et₃N in 5:1 hexanes–EtOAc) to afford 21.5 mg of tetrahydrooxepine **169** (75% yield) as a clear, colorless oil. ¹H NMR (500 MHz, CDCl₃; compound exists as a mixture of rotamers) δ 6.06 (s, 2H), 4.93 – 4.42 (m, 3H), 4.34 (s, 1H), 4.25 – 4.11 (m, 3H), 3.84 (dd, *J* = 12.3, 7.0 Hz, 1H), 3.68 (s, 3H), 2.75 (s, 1H), 2.38 – 1.97 (m, 2H), 1.25 (t, *J* = 7.1 Hz, 3H), 0.88 (s, 9H), 0.09 (s, 6H); ¹³C NMR (126 MHz, CDCl₃; compound exists as a mixture of rotamers) δ 172.1, 156.4, 155.8, 147.0, 146.4, 105.7, 104.9, 68.8, 68.5, 68.1, 67.7, 67.3, 66.6, 60.9, 60.1, 60.0, 52.6, 41.4, 40.5, 30.8, 29.9, 25.8, 17.9, 14.1, -4.7, -5.0; IR (NaCl/thin film): 3054, 2954, 2929, 2894, 2856, 1754, 1707, 1648, 1448, 1375, 1336, 1301, 1291, 1257, 1190, 1126, 1099, 1038, 1004, 939, 918, 900, 871, 837, 777 cm⁻¹; HRMS (ESI) calc'd for C₁₃H₁₈NO₅ [M–C₆H₁₅OSi]⁺ 268.1180, found 268.1186 (detected fragment has undergone loss of *tert*-butyldimethylsilylanolate anion).

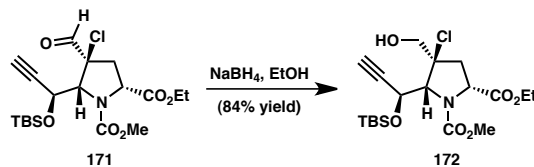
Preparation of chloroaldehyde **171**



To a solution of aldehyde **164** (283 mg, 0.712 mmol) in CH₂Cl₂ (7 mL, bulk solvent, not dried) was added pyrrolidine (60 μL, 0.712 mmol) followed by *N*-chlorosuccinimide (143 mg, 1.07 mmol). The resulting solution was stirred under an air atmosphere for 2.5 h, and was subsequently quenched with sat. *aq.* Na₂S₂O₃. The resulting mixture was extracted with CH₂Cl₂ (8 mL, then 2x15 mL), and the combined organic layers were dried over Na₂SO₄, filtered, and concentrated *in vacuo*. Purification via silica gel flash chromatography (gradient elution, 8:1→4:1 hexanes–EtOAc) afforded 215 mg of

chloroaldehyde **171** (70% yield) as a pale yellow oil. ¹H NMR (500 MHz, CDCl₃; compound exists as a 1.3:1 mixture of rotamers, the major rotamer is designated by *, minor rotamer denoted by \$) δ 9.64 (s, 1H*), 9.62 (s, 1H\$), 4.92 (dd, *J* = 5.0, 2.3 Hz, 1H*), 4.79 (dd, *J* = 5.0, 2.3 Hz, 1H\$), 4.66 (dd, *J* = 10.8, 7.3 Hz, 1H\$), 4.58 (dd, *J* = 10.8, 7.1 Hz, 1H*), 4.48 (d, *J* = 4.5 Hz, 1H*), 4.38 (d, *J* = 4.5 Hz, 1H\$), 4.27 – 4.14 (m, 2H*, 2H\$), 3.78 (s, 3H\$), 3.74 (s, 3H*), 3.46 (dd, *J* = 14.4, 10.8 Hz, 2H*), 3.42 (dd, *J* = 14.5, 10.9 Hz, 1H\$), 2.52 – 2.43 (m, 2H*, 2H\$), 1.27 (t, *J* = 7.1 Hz, 2H*, 2H\$), 0.89 (s, 9H*, 9H\$), 0.15 (s, 6H*, 6H\$); ¹³C NMR (126 MHz, CDCl₃; compound exists as a 1.3:1 mixture of rotamers, the major rotamer is designated by *, minor rotamer denoted by \$) δ 187.7*, 187.6\$, 170.1*, 169.8\$, 155.5*, 155.2\$, 128.9*, 128.6\$, 80.9*, 80.6\$, 77.7\$, 77.6*, 74.3*, 73.7\$, 63.0\$, 62.3*, 61.4\$, 61.3*, 58.3\$, 58.0*, 53.3\$, 53.3*, 39.0*, 37.9\$, 25.5*, 25.5\$, 18.0\$, 18.0*, 14.2*, 14.1\$, -5.0\$, -5.1*, -5.5*, -5.5\$; IR (NaCl/thin film): 3263, 2956, 2930, 2885, 2859, 2116, 1762, 1719, 1448, 1371, 1307, 1255, 1198, 1165, 1134, 1082, 1033, 1006, 988, 939, 860, 838, 782, 726 cm⁻¹; HRMS (ESI) calc'd for C₁₄H₁₉ClNO₆ [M–C₆H₁₅OSi+MeOH]⁺ 332.0895, found 332.0900 (detected fragment has undergone loss of *tert*-butyldimethylsilanolate anion and gain of methanol).

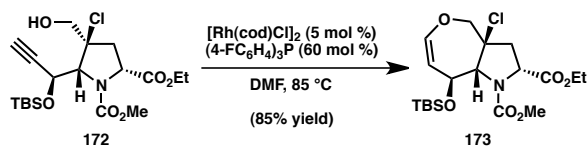
Preparation of chlorohydrin **172**



A solution of chloroaldehyde **171** (215 mg, 0.498 mmol) in EtOH (5 mL) was treated with NaBH₄ (75.3 mg, 1.99 mmol). After 15 min, the reaction mixture was cooled to 0 °C and slowly quenched with 1 M *aq.* HCl (15 mL). The mixture was then diluted

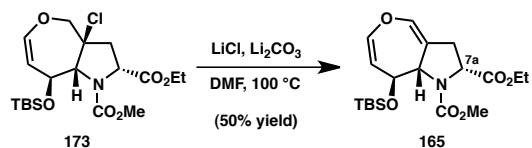
with brine (5 mL), and further saturated with solid NaCl, then extracted with CHCl_3 (3x15 mL) followed by EtOAc (3x15 mL). The combined organic layers were dried over Na_2SO_4 , filtered, and concentrated *in vacuo*. Purification via silica gel flash chromatography (gradient elution, 4:1 \rightarrow 2:1 hexanes–EtOAc) afforded 182 mg of chlorohydrin **172** (84% yield) as a clear, colorless oil. ^1H NMR (500 MHz, CDCl_3 ; compound exists as a 1.3:1 mixture of rotamers, the major rotamer is designated by *, minor rotamer denoted by \ddagger) δ 4.97 (dd, J = 4.3, 2.3 Hz, 1H*), 4.85 (dd, J = 4.1, 2.3 Hz, 1H \ddagger), 4.66 (dd, J = 10.6, 7.4 Hz, 1H \ddagger), 4.58 (dd, J = 10.5, 7.2 Hz, 1H*), 4.44 – 4.38 (m, 1H*, 1H \ddagger), 4.34 (dd, J = 4.3, 1.3 Hz, 1H*), 4.26 (dd, J = 4.2, 1.3 Hz, 1H \ddagger), 4.25 – 4.14 (m, 2H*, 2H \ddagger), 3.93 (dd, J = 12.8, 10.3 Hz, 1H*, 1H \ddagger), 3.76 (s, 3H \ddagger), 3.73 (s, 3H*), 3.54 (dd, J = 11.2, 3.9 Hz, 1H*), 3.45 (dd, J = 10.8, 4.1 Hz, 1H \ddagger), 2.88 (dd, J = 13.7, 10.6 Hz, 1H*), 2.85 (dd, J = 14.0, 10.7 Hz, 1H \ddagger), 2.57 – 2.49 (m, 2H*, 2H \ddagger), 1.26 (t, J = 7.2 Hz, 3H \ddagger), 1.26 (t, J = 7.2 Hz, 3H*), 0.94 (s, 9H*, 9H \ddagger), 0.22 (s, 3H*), 0.22 (s, 3H \ddagger), 0.20 (s, 6H \ddagger); ^{13}C NMR (126 MHz, CDCl_3 ; compound exists as a 1.3:1 mixture of rotamers, the major rotamer is designated by *, minor rotamer denoted by \ddagger) δ 170.6*, 170.3 \ddagger , 155.6*, 155.3 \ddagger , 81.7*, 81.3 \ddagger , 80.3 \ddagger , 79.4*, 77.2 \ddagger , 76.8*, 73.3*, 72.9 \ddagger , 65.8** \ddagger , 63.9 \ddagger , 63.1*, 61.2 \ddagger , 61.1*, 58.5 \ddagger , 58.1*, 53.2 \ddagger , 53.2*, 41.0*, 39.8 \ddagger , 25.6*, 25.6 \ddagger , 18.1 \ddagger , 18.1*, 14.2*, 14.2 \ddagger , -5.1 \ddagger , -5.2*, -5.4*, -5.5 \ddagger ; IR (NaCl/thin film): 3486, 3255, 2955, 2930, 2858, 2112, 1761, 1714, 1448, 1371, 1308, 1254, 1194, 1156, 1140, 1082, 862, 838, 782 cm^{-1} ; HRMS (ESI) calc'd for $\text{C}_{19}\text{H}_{33}\text{ClNO}_6\text{Si}$ [M+H] $^+$ 434.1760, found 434.1764.

Preparation of chlorotetrahydroxepine 173



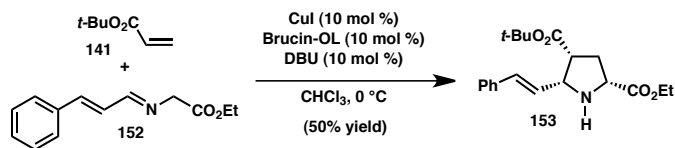
Chlorohydrin **172** (53.0 mg, 0.122 mmol) was dissolved in dry, degassed DMF (0.61 mL) and transferred via syringe to a Schlenk tube equipped with a magnetic stir bar and sealed with a septum cap under an N₂ atmosphere. A stock solution of [Rh(cod)Cl]₂ (0.01 M) and (4-FC₆H₄)₃P (0.12 M) in dry, degassed DMF (0.61 mL) was added. The resulting yellow solution was degassed using the freeze-pump-thaw technique. The vessel was sealed and the solution frozen by submersion in a bath of liquid N₂. The vessel was then placed under vacuum for approximately five minutes before once again being sealed and allowed to thaw under static vacuum by removal from the liquid N₂ bath. This procedure was repeated twice before the head-space was finally backfilled with N₂, the vessel sealed, and the solution heated to 85 °C with stirring. After 25 h, the reaction mixture was cooled to rt, diluted with sat. *aq.* NaHCO₃ (10 mL), and extracted with EtOAc (5x5 mL). The combined organic layers were dried over Na₂SO₄, filtered, and concentrated *in vacuo*, and the resulting material was purified via silica gel flash chromatography (gradient elution, 8:1→6:1 hexanes–EtOAc) to afford 45.0 mg of chlorotetrahydrooxepine **173** (85% yield) as a pale yellow oil. ¹H NMR (500 MHz, CDCl₃; compound exists as a mixture of rotamers) δ 6.21 – 6.04 (m, 1H), 5.20 – 4.30 (m, 5H), 4.29 – 4.13 (m, 2H), 4.09 (d, *J* = 12.8 Hz, 1H), 3.72 (s, 3H), 2.77 – 2.42 (m, 1H), 2.52 (dd, *J* = 13.4, 7.5 Hz, 1H), 1.27 (apt q, *J* = 7.9, 7.5 Hz, 3H), 0.90 (s, 9H), 0.19 – 0.04 (m, 6H); ¹³C NMR (126 MHz, CDCl₃; compound exists as a mixture of rotamers) δ 171.6, 145.7, 129.0, 128.6, 68.3, 61.3, 59.0, 58.7, 53.0, 40.4, 39.6, 25.7, 17.9, 14.2, -4.7, -5.1; IR (NaCl/thin film): 2954, 2929, 2856, 1752, 1710, 1647, 1447, 1373, 1340, 1263, 1194, 1130, 1035, 902, 871, 838, 777, 720 cm⁻¹; HRMS (Multimode-ESI/APCI) calc'd for C₁₃H₁₇ClNO₅ [M–C₆H₁₅OSi]⁺ 302.0790, found 302.0797.

Preparation of dihydroooxepine 165



A suspension of chlorotetrahydrooxepine **173** (8.7 mg, 20 μmol), LiCl (17.0 mg, 0.402 mmol), and Li_2CO_3 (59.4 mg, 0.804 mmol) in dry DMF (270 μL) was stirred vigorously at 100 °C for 48 h. After cooling to rt, the reaction mixture was diluted with Et_2O (to precipitate lithium salts), filtered (rinsing with EtOAc), further diluted with Et_2O , and filtered a second time. The resulting solution was concentrated *in vacuo*, then purified via silica gel flash chromatography (gradient elution, 12:1→10:1 hexanes– EtOAc) to afford 4.0 mg of dihydrooxepine **165** (50% yield) as a clear, colorless oil. ^1H NMR (400 MHz, CDCl_3) δ 6.37 (s, 1H), 6.12 (dd, J = 8.1, 2.3 Hz, 1H), 4.80 (br s, 1H), 4.71 (d, J = 8.2 Hz, 1H), 4.59 (br s, 1H), 4.42 (d, J = 7.0 Hz, 1H), 4.18 (q, J = 7.1 Hz, 2H), 3.71 (s, 3H), 2.95 (dd, J = 15.1, 9.8 Hz, 1H), 2.60 (d, J = 15.1 Hz, 1H), 1.27 (t, J = 7.2 Hz, 3H), 0.91 (s, 9H), 0.11 (s, 3H), 0.05 (s, 3H); ^{13}C NMR (101 MHz, CDCl_3) δ 172.0, 138.0, 135.8, 111.2 (br), 71.2 (br), 63.5, 61.2, 58.5, 52.8, 33.6 (br), 25.8, 18.0, 14.2, -4.8 (br), -5.4 (br); IR (NaCl/thin film): 2953, 2929, 2855, 1749, 1705, 1654, 1446, 1369, 1340, 1301, 1285, 1250, 1182, 1141, 1101, 1066, 1032, 970, 898, 874, 838, 771, 742 cm^{-1} ; HRMS (ESI) calc'd for $\text{C}_{13}\text{H}_{16}\text{NO}_5$ [$\text{M} - \text{C}_6\text{H}_{15}\text{OSi}$] $^+$ 266.1023, found 266.1024 (detected fragment has undergone loss of *tert*-butyldimethylsilanolate anion).

Enantioselective preparation of styrenyl pyrrolidine 153 (published procedure)



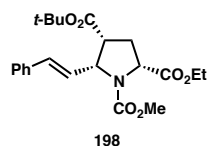
Generation of brucin-OL catalyst solution: To a flame dried 2 L three neck round bottom flask was added brucin-OL (1.50 g, 3.50 mmol) and CuI (667 mg, 3.50 mmol). The solids were then evacuated under vacuum, backfilled under N₂ atmosphere, cooled to 0 °C for 10 min, and then suspended in 74 mL of CHCl₃ and stirred for 24 h at 0 °C. Note: brucin-OL was prepared according to the method of Oh and co-workers.²⁸

Generation of imine 152: In a separate 250 mL flame dried round bottom flask, ethyl glycinate hydrochloride (7.33 g, 52.5 mmol) and 20 g of MgSO₄ were suspended in 70 mL of CHCl₃. To the stirred suspension was added Et₃N (7.3 mL, 52 mmol) and the mixture was allowed to stir for 20 min after which *trans*-cinnamaldehyde (4.4 mL, 35 mmol) was added. After the mixture was stirred for an additional 1.5 h, the MgSO₄ was removed by vacuum filtration, and the resulting solution was washed with H₂O (5 x 70 mL) and 70 mL of sat. *aq.* brine solution. The combined organic layers were dried over MgSO₄, filtered, and concentrated *in vacuo*. The resulting yellow-green oil was dissolved in 35 mL of CHCl₃ and cooled to 0 °C.

(1, 3)-Dipolar cycloaddition reaction: Following generation of the catalyst for 24 h, 1,8-diazabicycloundec-7-ene (520 µL, 3.5 mmol) was added to the brucin-OL catalyst suspension and it was allowed to stir for 15 min at 0 °C. To the resulting green solution was added *t*-butyl acrylate (7.7 mL, 53 mmol), followed by dropwise addition via cannula of the cooled solution of imine **152** in CHCl₃ over approximately 15 min. The brown solution was allowed to stir at 0 °C for 24 h after which the reaction was diluted with EtOAc (700 mL), washed with 5% NH₄OH solution (1 x 200 mL, followed by 2 x 100 mL), and sat. *aq.* Na₂SO₃ solution (2 x 100 mL), dried over Na₂SO₄, filtered, and concentrated *in vacuo* to yield a brown oil. Purification through silica gel flash

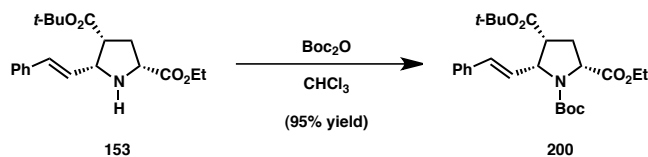
chromatography (gradient elution, 9:1→1:1 hexanes–EtOAc with 0.5% Et₃N) afforded 6.07 g (50% yield) of **153** as a yellow oil. Spectroscopic data for this product were identical to those described for the corresponding racemic material; [α]_D^{25.0} = +31.1° (c = 1.15, CHCl₃) (96% ee, as assessed by conversion to the corresponding methyl carbamate **198**, as described above). Note: On scale up, it was found that *tert*-butylcarbonyl (Boc) protection of pyrrolidine **153** to furnish **200** resulted in less cumbersome chromatographic separations. *t*-Butyl carbamate **200** could subsequently be subjected to TFA, Et₃SiH, DCM as described to yield trifluoroacetate salt **178** (see below). Additionally, an improved cycloaddition procedure was ultimately identified (see below), which resulted in more reproducible results on large scale, and obviated the need for conversion to **200** for the purposes of purification.

Methyl carbamate 198 (96% ee)



$[\alpha]_D^{25.0} = +21.9^\circ$ ($c = 0.41$, CHCl_3); HPLC (Chiracel AD); 5% isopropanol/hexanes; flow rate = 1.0 mL/min; t_r (major ent.) = 15.3 min, t_r (minor ent.) = 21.4 min.

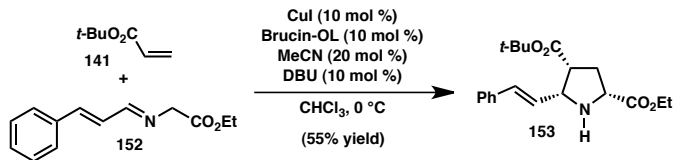
Preparation of *tert*-butyl carbamate 200



In order to achieve less cumbersome chromatographic separations and improved material purity on scale up, crude mixtures of pyrrolidine **153** were converted to *t*-butyl carbamate **200** (following initial silica gel chromatography as described above to remove

excess reagents/major impurities). Crude pyrrolidine **153** (25.0 g, 72.4 mmol) was dissolved in CHCl₃ (220 mL) and di-*tert*-butyl dicarbonate (17.4 g, 79.7 mmol) was added with stirring. After 1 h, the reaction mixture was concentrated *in vacuo*. The resulting residue was purified via silica gel flash chromatography (isocratic elution, 7:1 hexanes:EtOAc) to afford *tert*-butyl carbamate **200** (30.6 g, 95% yield). Note: although attempts were made to advance crude pyrrolidine **153** directly to trifluoroacetate salt **178** in order to avoid chromatography, it was observed that the purity of **153** greatly influenced the isolated yield of **178**. On large scale, the above procedure allowed sufficiently pure material to be obtained more readily than by direct chromatography of pyrrolidine **153**. $[\alpha]_D^{25.0} = +28.6^\circ$ (*c* = 1.13, CHCl₃); ¹H NMR (500 MHz, CDCl₃; compound exists as a mixture of rotamers) δ 7.34 (d, *J* = 7.5 Hz, 4H), 7.32 – 7.15 (m, 6H), 6.77 (d, *J* = 15.7 Hz, 1H), 6.65 (d, *J* = 15.6 Hz, 1H), 6.14 (dd, *J* = 15.7, 8.2 Hz, 2H), 4.83 (dd, *J* = 8.0, 8.0 Hz, 1H), 4.66 (dd, *J* = 8.2, 8.2 Hz, 1H), 4.30 – 4.13 (m, 6H), 3.24 – 3.13 (m, 2H), 2.44 – 2.29 (m, 4H), 1.40 (s, 18H), 1.34 (s, 9H), 1.34 (s, 9H), 1.32 – 1.25 (m, 6H); ¹³C NMR (126 MHz, CDCl₃; compound exists as a 1:1 mixture of rotamers) δ 172.5, 172.2, 168.8, 168.7, 153.7, 152.9, 146.7, 136.6, 133.4, 133.3, 128.5, 128.3, 127.5, 127.4, 126.6, 126.3, 125.1, 124.7, 85.1, 81.4, 81.4, 80.4, 80.3, 61.7, 61.2, 61.0, 59.0, 58.6, 48.3, 47.8, 30.4, 29.6, 28.3, 28.2, 28.0, 27.3, 14.2, 14.1; IR (NaCl/thin film): 2979, 2933, 1810, 1731, 1702, 1478, 1457, 1392, 1369, 1290, 1252, 1185, 1119, 1076, 960, 847, 757, 694 cm^{−1}; HRMS (Multimode-ESI/APCI) calc'd for C₂₀H₂₈NO₄ [M–C₄H₈–CO₂+H]⁺ 346.2013, found 346.2019 (detected fragment has undergone elimination of *iso*-butylene and CO₂ from the Boc protecting group).

Enantioselective preparation of styrenyl pyrrolidine 153 (improved procedure)



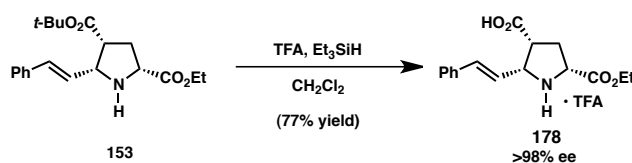
Preparation of ethyl glycinate: ethyl glycinate hydrochloride salt (29.3 g, 210 mmol) was suspended in 150 mL of DCM and 3.56 M KOH (77 mL, 273 mmol) was added with vigorous swirling. The layers were separated, and the aqueous layer was further extracted with DCM (2 x 80 mL), dried over MgSO₄, and concentrated to yield 12.1 g (56% yield) of the free amine. The amine was used immediately to avoid dimerization.

Generation of imine 152: The free amine (12.1 g, 117 mmol) was dissolved in 235 mL CHCl₃. Silica gel (35.1 g, 0.3 g SiO₂ per mmol substrate) was added and the resulting suspension was cooled to 0 °C while open to the atmosphere. *trans*-Cinnamaldehyde (14.7 mL, 117 mmol) was added dropwise and the reaction was left to stir at 0°C for an additional 3.5 hours, during which it turned from colorless to bright yellow. The silica gel was removed via filtration and rinsed with 50 mL CHCl₃, and the resulting imine solution was used immediately to avoid decomposition.

(1,3)-Dipolar cycloaddition reaction: A round-bottom flask was charged with CuI (2.23 g, 11.7 mmol), BrucinOL (5.01 g, 11.7 mmol), and 235 mL of CHCl₃. The resulting suspension was cooled to 0 °C under air, and MeCN (1.22 mL, 23.4 mmol) was added dropwise and with stirring. After a five minute prestir, DBU (1.75 mL, 11.7 mmol) was added and the solution was stirred vigorously for twenty minutes during which it went from a cloudy brown to a dark green. *tert*-Butyl acrylate (25.8 mL, 176 mmol) was

then added, followed by the solution of imine **152** (precooled to 0 °C and transferred via cannula over 5 min). After 5 h, the reaction mixture was loaded directly onto SiO₂ and subjected to flash chromatography (gradient elution, 5:1 → 1:1 hexanes–EtOAc with 0.5% Et₃N) to afford 22.4 g (55% yield) of **153** as an orange oil (97% *ee*, as assessed by conversion to the corresponding methyl carbamate **198**, as described above).

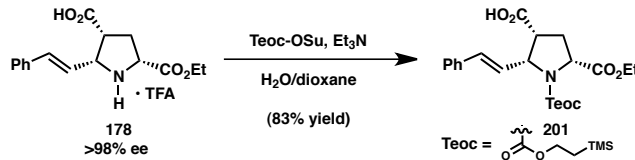
Preparation of pyrrolidinium trifluoroacetate salt **178**



Pyrrolidine **153** (5.43 g, 15.7 mmol) was dissolved in 56 mL of CH₂Cl₂ in a flame dried 250 mL round bottom flask. To the solution was added Et₃SiH (12.5 mL, 78.5 mmol) followed by trifluoroacetic acid (23 mL) and the solution was allowed to stir overnight. The solution was then concentrated *in vacuo*, redissolved in CHCl₃ and azeotroped (3x), and subsequently azeotroped from toluene (3x). Upon further addition of toluene and CHCl₃, white crystals crashed out of solution and were isolated by vacuum filtration to afford **178**. The mother liquor was concentrated *in vacuo* and crystallized further from toluene and CHCl₃, producing additional crops of **178** (over several iterations). Further recrystallization from hot CHCl₃ affords 4.87 g (77% yield) of **178** as a white solid (>98% *ee*, as assessed by conversion to the methyl ester **202** following protection as the trimethylsilylethyl carbamate, as described below). Note: *t*-butyl carbamate **200** could also be subjected to the conditions described above to afford trifluoroacetate salt **178**. $[\alpha]_D^{25.0} = -63.3^\circ$ (*c* = 0.70, CHCl₃); mp 108–111 °C; ¹H NMR (500 MHz, CD₃CN) δ 10.34 (s, 1H), 7.42 (dd, *J* = 7.9, 1.5 Hz, 2H), 7.38 – 7.30 (m, 3H),

6.85 (d, $J = 15.8$ Hz, 1H), 6.28 (dd, $J = 8.9, 15.8$ Hz, 1H), 4.66 – 4.60 (m, 2H), 4.20 – 4.30 (m, 2H), 3.36 (ddd, $J = 7.3, 7.3, 4.2$ Hz, 1H), 2.70 (ddd, $J = 14.0, 10.7, 7.5$ Hz, 1H), 2.54 (ddd, $J = 14.0, 5.7, 4.3$ Hz, 1H), 1.25 (t, $J = 7.1$ Hz, 3H); ^{13}C NMR (126 MHz, CD_3CN) δ 173.8, 169.8, 161.8 (q, $J_{\text{C}-\text{F}} = 35.1$ Hz), 138.9, 136.3, 129.9, 129.8, 127.8, 120.1, 117.6 (q, $J_{\text{C}-\text{F}} = 293.0$ Hz), 65.1, 64.0, 58.9, 47.4, 31.6, 14.2; IR (NaCl/thin film): 3189, 2981, 2913, 2730, 2532, 1726, 1661, 1652, 1565, 1474, 1436, 1251, 1189, 1137, 973, 798, 746, 691 cm^{-1} ; HRMS (Multimode-ESI/APCI) calc'd for $\text{C}_{16}\text{H}_{20}\text{NO}_4$ [M – $\text{C}_2\text{O}_2\text{F}_3$] $^+$ 290.1387, found 290.1381 (detected cation does not include the trifluoroacetate counterion).

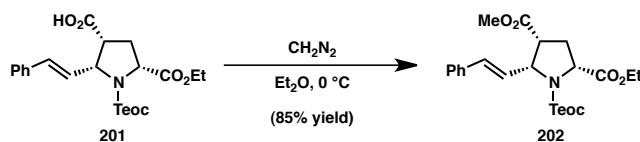
Preparation of trimethylsilylethyl carbamate 201



Trifluoroacetate salt **178** (7.93 g, 19.7 mmol) was suspended in 39 mL of H_2O and 39 mL of dioxane in a 250 mL round bottom flask. 1-[2-(Trimethylsilyl)ethoxycarbonyloxy]pyrrolidin-2,5-dione (7.64 g, 29.5 mmol) and Et_3N (8.2 mL, 59 mmol) were added to the stirred suspension and the reaction mixture was allowed to stir overnight. The reaction mixture was then acidified with sat. *aq.* NaHSO_4 solution, extracted with EtOAc (3x), dried over Na_2SO_4 , filtered, and concentrated *in vacuo* to yield a faint yellow oil. Purification through silica gel flash chromatography (isocratic elution, 30:1 CH_2Cl_2 –MeOH) afforded 7.10 g of **201** as a colorless oil (83% yield). $[\alpha]_D^{25.0} = -6.0^\circ$ ($c = 1.12$, CHCl_3); ^1H NMR (500 MHz, CD_3CN ; compound exists as a mixture of rotamers) δ 7.39 – 7.31 (m, 4H), 7.28 – 7.24 (m, 1H), 6.80 (d, $J = 15.8$

Hz, 1H), 6.17 (dd, $J = 15.8, 7.5$ Hz, 1H), 4.80 (dd, $J = 7.3, 7.3$ Hz, 1H), 4.32 – 4.23 (m, 1H), 4.23 – 4.15 (m, 2H), 4.15 – 4.06 (m, 2H), 3.40 – 3.30 (m, 1H), 2.48 – 2.37 (m, 1H), 2.34 – 2.17 (m, 1H), 1.29 – 1.23 (m, 3H), 0.98 – 0.89 (m, 2H), 0.02 and 0.00 (s, 9H); ^{13}C NMR (126 MHz, CD_3CN ; compound exists as a mixture of rotamers) δ 173.4, 173.1, 171.3, 171.3, 155.7, 154.9, 137.7, 133.7, 133.6, 129.7, 128.7, 127.3, 126.5, 126.4, 64.4, 64.3, 62.1, 62.0, 61.9, 61.7, 59.9, 59.7, 48.0, 47.4, 31.4, 30.4, 18.3, 14.5, –1.5, –1.5; IR (NaCl/thin film): 3059, 2982, 2954, 2900, 1745, 1705, 1668, 1404, 1349, 1284, 1250, 1186, 1114, 1075, 1061, 1038, 960, 860, 838, 740, 694 cm^{–1}; HRMS (Multimode-ESI/APCI) calc'd for $\text{C}_{20}\text{H}_{28}\text{NO}_6\text{Si}$ [M–C₂H₄+H]⁺ 406.1680, found 406.1689 (detected fragment has undergone elimination of ethylene from the Teoc protecting group).

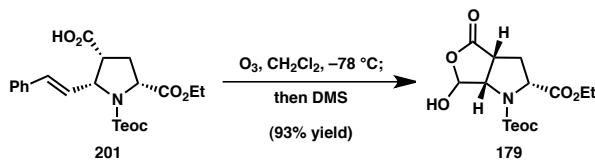
Preparation of methyl ester 202



In order to determine the extent of enantioenrichment resulting from crystallization of trifluoroacetate salt **178**, an aliquot of material was protected as the trimethylsilylethyl carbamate (**201**) as described above, then converted to methyl ester **202**. Carboxylic acid **201** (18.1 mg, 41.7 μmol) was dissolved in Et_2O (0.42 mL) and cooled to 0 °C with stirring. A solution of diazomethane in Et_2O was titrated into the reaction solution until a yellow color persisted. After 5 min, excess diazomethane was quenched by dropwise addition of AcOH (until the yellow color no longer persisted). The resulting solution was diluted with Et_2O (2 mL) and 10% aqueous K_2CO_3 (2 mL), the phases were separated, and the aqueous layer was further extracted with Et_2O (2 x 2 mL). The combined organic layers were dried over MgSO_4 , filtered, and concentrated *in vacuo*.

to afford methyl ester **202** (15.9 mg, 85% yield) as a clear, colorless oil. $[\alpha]_D^{25.0} = -5.9^\circ (c = 0.87, \text{CHCl}_3)$; ^1H NMR (500 MHz, CD_3CN ; compound mixture of rotamers) δ 7.38 – 7.31 (m, 4H), 7.28 – 7.24 (m, 1H), 6.76 (d, $J = 15.8$ Hz, 1H), 6.11 (dd, $J = 15.8, 7.4$ Hz, 1H), 4.79 (dd, $J = 7.8, 7.8$ Hz, 1H), 4.33 – 4.24 (m, 1H), 4.24 – 4.15 (m, 2H), 4.15 – 4.06 (m, 2H), 3.59 (s, 3H), 3.43 – 3.33 (m, 1H), 2.50 – 2.39 (m, 1H), 2.37 – 2.31 (m, 1H) 1.30 – 1.22 (m, 3H), 0.98 – 0.89 (m, 2H), 0.01 and 0.00 (s, 9H); ^{13}C NMR (126 MHz, CD_3CN ; compound exists as a mixture of rotamers) δ 173.4, 173.1, 171.2, 171.1, 155.7, 154.8, 137.6, 133.6, 133.5, 129.6, 128.8, 127.3, 126.7, 64.4, 64.3, 62.3, 62.0, 61.9, 61.8, 60.0, 59.7, 52.5, 48.3, 47.7, 31.4, 30.4, 18.3, 14.5, –1.5, –1.6; IR (NaCl/thin film): 2952, 1740, 1701, 1451, 1409, 1374, 1343, 1285, 1250, 1186, 1109, 1031, 860, 837, 750 cm^{-1} ; HRMS (Multimode-ESI/APCI) calc'd for $\text{C}_{21}\text{H}_{30}\text{NO}_6\text{Si} [\text{M} - \text{C}_2\text{H}_4 + \text{H}]^+$ 420.1837, found 420.1845 (detected fragment has undergone elimination of ethylene from the Teoc protecting group); HPLC (Chiracel OD); 5% isopropanol/hexanes; flow rate = 1.0 mL/min; t_r (major ent.) = 21.6 min, t_r (minor ent.) = 13.2 min.

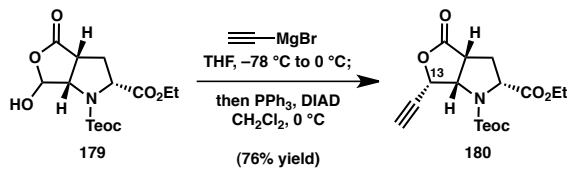
Preparation of hydroxylactone 179



A solution of styrenyl carboxylic acid **201** (1.93 g, 4.45 mmol) in 45 mL of CH_2Cl_2 was cooled to -78°C in a flame dried three-neck round bottom flask. Ozone was bubbled through the cooled solution until the solution turned bright blue. The solution was then sparged with Oxygen (until the blue color no longer persisted), warmed to room temperature, and sparged with nitrogen for 15 min, at which point dimethylsulfide (13.1

mL, 178 mmol) was added and the solution was stirred overnight. The pale yellow solution was then concentrated *in vacuo* to afford a pale yellow oil. Purification by silica gel flash chromatography (gradient elution, 2:1 → 3:2 hexanes–EtOAc) afforded 1.49 g of **179** as a colorless oil (93% yield). $[\alpha]_D^{25.0} = -42.4^\circ$ ($c = 1.04$, CHCl_3); ^1H NMR (400 MHz, DMSO, 60 °C) δ 7.69 (s, 1H), 5.72 (s, 1H), 4.43 (dd, $J = 10.3, 1.3$ Hz, 1H), 4.22 (d, $J = 7.3$ Hz, 1H), 4.19 – 4.10 (m, 2H), 4.12 – 3.99 (m, 2H), 3.51 (dd, $J = 8.1, 8.1$ Hz, 1H), 2.69 – 2.55 (m, 1H), 2.20 (d, $J = 13.3$ Hz, 1H), 1.16 (t, $J = 7.1$ Hz, 3H), 1.09 – 0.84 (m, 2H), 0.03 (s, 9H); ^{13}C NMR (101 MHz, DMSO, 60 °C) δ 176.6, 170.9, 153.4, 101.2 (br), 100.5 (br), 65.1 (br), 64.8 (br), 63.2, 60.6, 58.7 (br), 58.5 (br), 58.4 (br), 42.8 (br), 41.8 (br), 31.0, 30.9 (br), 30.0 (br), 28.0, 21.8, 17.1 (br), 13.5, 13.4, –1.8; IR (NaCl/thin film): 3380, 2957, 2901, 1783, 1747, 1706, 1682, 1417, 1347, 1251, 1198, 1119, 1038, 944, 860, 839, 773, 696, 620 cm^{–1}; HRMS (Multimode-ESI/APCI) calc'd for $\text{C}_{15}\text{H}_{24}\text{NO}_7\text{Si}$ [M–H][–] 358.1328, found 358.1309.

Preparation of alkynyl lactone **180**



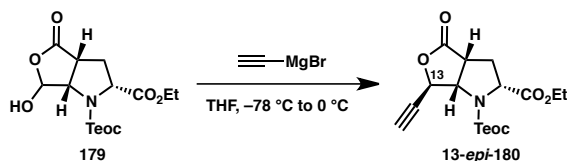
To a flame dried 250 mL round bottom flask containing hydroxylactone **179** (2.69 g, 7.48 mmol) was added 37 mL of THF and the stirred solution was cooled to –78 °C. Ethynylmagnesium bromide (0.5 M solution in THF, 75.0 mL, 37.4 mmol) was added via syringe pump over one hour and the solution was then allowed to stir for five minutes at –78 °C before being warmed to 0 °C and stirred for another 20 min. The reaction was then quenched with 20 mL of sat. *aq.* NaHCO₃ solution and the reaction mixture was

concentrated *in vacuo*. Following dilution with CH₂Cl₂ (500 mL) the mixture was acidified to pH = 2.5 with Na₂HPO₄/KHSO₄ buffer (pH = 2.5, prepared from a 10% w/v *aq.* Na₂HPO₄ solution by acidification with KHSO₄). The mixture was then further diluted with CH₂Cl₂ and NaCl was added to further saturate the aqueous phase. The phases were separated and the aqueous layer was washed twice with CH₂Cl₂. The combined organic layers were then dried over Na₂SO₄, filtered, and concentrated *in vacuo* to a volume of 300 mL (0.025 M solution, achieved by marking the flask for the desired volume prior to use). The solution was then cooled to 0 °C and triphenylphosphine (5.88 g, 22.4 mmol) was added and allowed to stir for 10 min. Diisopropylazodicarboxylate (3.0 mL, 15 mmol) was then added to the reaction and it was allowed to stir while warming to room temperature overnight. The orange solution was then concentrated *in vacuo* to yield an orange oil. Purification by silica gel flash chromatography (gradient elution, 3:1→1:1 hexanes–EtOAc) afforded **180** as a colorless oil in 76% yield (2.08 g).

$[\alpha]_D^{25.0} = -73.0^\circ$ (*c* = 1.01, CHCl₃); ¹H NMR (500 MHz, CDCl₃; compound exists as a 1:1 mixture of rotamers) δ 5.33 (dd, *J* = 5.7, 2.0 Hz, 1H), 5.29 (dd, *J* = 5.7, 2.0 Hz, 1H), 4.96 (dd, *J* = 8.0, 6.1 Hz, 1H), 4.85 (dd, *J* = 8.0, 6.1 Hz, 1H), 4.61 (d, *J* = 8.7 Hz, 1H), 4.56 (d, *J* = 9.0 Hz, 1H), 4.27 – 4.06 (m, 4H), 4.14 (q, *J* = 7.2 Hz, 4H), 3.40 – 3.32 (m, 2H), 2.65 (d, *J* = 2.0 Hz, 1H), 2.60 (d, *J* = 2.0 Hz, 1H), 2.56 – 2.41 (m, 4H), 1.29 – 1.19 (m, 6H), 1.04 – 0.91 (m, 4H), 0.01 (s, 9H), 0.00 (s, 9H); ¹³C NMR (126 MHz, CDCl₃; compound exists as a mixture of rotamers) δ 175.5, 175.3, 170.7, 154.7, 154.3, 77.8, 77.7, 76.0, 75.8, 73.0, 72.9, 64.5, 64.3, 61.6, 61.0, 60.2, 59.8, 59.6, 44.4, 43.5, 32.0, 31.2, 17.6, 17.6, 13.8, –1.6; IR (NaCl/thin film): 3262, 2955, 2900, 2132, 1782, 1741, 1706, 1455, 1407, 1349, 1283, 1250, 1190, 1163, 1118, 1042, 1014, 978, 938, 861, 839, 765 cm^{–1}; HRMS

(Multimode-ESI/APCI) calc'd for C₁₅H₂₂NO₆Si [M–C₂H₄+H]⁺ 340.1211, found 340.1192 (detected fragment has undergone elimination of ethylene from the Teoc protecting group).

Preparation of alkynyl lactone **13-*epi*-180**



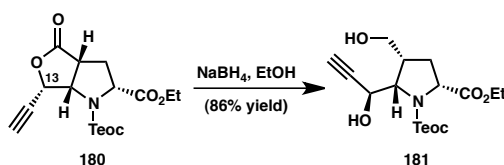
To a stirred solution of hydroxylactone **179** (12.0 mg, 33.4 μ mol) in 0.17 mL of THF at $-78\text{ }^{\circ}\text{C}$ was added ethynylmagnesium bromide (0.5 M solution in THF, 0.33 mL, 0.167 mmol) dropwise. The solution was then allowed to stir for five minutes at $-78\text{ }^{\circ}\text{C}$ before being warmed to $0\text{ }^{\circ}\text{C}$ and stirred for another 15 min. The reaction was then quenched with 0.5 mL of 1M *aq.* HCl solution and the reaction mixture was concentrated *in vacuo*. The resulting aqueous mixture was saturated with NaCl and extracted with EtOAc (5x), and the combined organic layers were dried over Na₂SO₄, filtered, and concentrated *in vacuo*. The crude material (~5:1 dr by ¹H NMR) was purified by silica gel flash chromatography (gradient elution, 2:1→1:1 hexanes–EtOAc) to afford alkynyl lactones **13-*epi*-180** (8.5 mg, 69% yield) and **180** (1.6 mg, 13% yield). NOTE: the relative configuration of the propargylic stereocenter of **13-*epi*-180** was initially assigned by analogy to the alkynyl lactone **158**.

Alkynyl lactone **13-*epi*-180**

$[\alpha]_D^{25.0} = -13.5^\circ$ ($c = 0.42$, CHCl₃); ¹H NMR (500 MHz, CDCl₃; compound exists as a 1.3:1 mixture of rotamers, the major rotamer is designated by *; minor rotamer denoted by \$) δ 5.46 – 5.44 (m, 1H*), 5.35 – 5.33 (m, 1H\$), 4.68 (d, $J = 7.4$ Hz, 1H*),

4.62 (d, $J = 7.6$ Hz, 1H $^{\delta}$), 4.59 – 4.53 (m, 1H $^{\delta}$), 4.49 – 4.42 (m, 1H *), 4.31 – 4.10 (m, 4H * , 4H $^{\delta}$), 3.44 – 3.36 (m, 1H * , 1H $^{\delta}$), 2.70 (d, $J = 2.4$ Hz, 1H $^{\delta}$), 2.70 (d, $J = 2.4$ Hz, 1H *), 2.62 – 2.49 (m, 2H * , 2H $^{\delta}$), 1.25 (t, $J = 7.1$ Hz, 3H * , 3H $^{\delta}$), 1.10 – 1.04 (m, 2H $^{\delta}$), 1.00 – 0.94 (m, 2H *), 0.06 (s, 9H $^{\delta}$), 0.02 (s, 9H *); ^{13}C NMR (126 MHz, CDCl_3 ; compound exists as a mixture of rotamers) δ 176.1, 175.8, 171.1, 171.0, 154.1, 153.7, 78.6, 78.5, 76.9, 76.8, 73.8, 73.0, 65.2, 64.9, 64.7, 64.5, 62.0, 62.0, 59.1, 58.8, 43.4, 42.4, 31.7, 30.9, 17.8, 13.8, –1.5, –1.6; IR (NaCl/thin film): 3260, 2956, 2900, 2125, 1788, 1744, 1703, 1457, 1410, 1354, 1290, 1250, 1200, 1146, 1117, 1057, 1035, 970, 941, 861, 839, 772 cm^{-1} ; HRMS (Multimode-ESI/APCI) calc'd for $\text{C}_{17}\text{H}_{24}\text{NO}_6\text{Si} [\text{M}–\text{H}]^-$ 366.1378, found 366.1400.

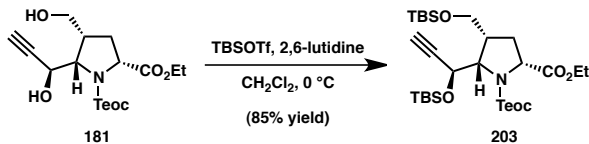
Preparation of diol **181**



To a flame dried 500 mL round bottom flask equipped with alkynyl lactone **180** (4.84 g, 13.2 mmol) dissolved in 264 mL of EtOH, sodium borohydride (2.00 g, 52.8 mmol) was added and the reaction was stirred vigorously. Following completion of the reaction as judged by TLC (\sim 1.75 h), the reaction was cooled to 0 °C and quenched carefully with 250 mL of 1N *aq.* HCl. The solution was then saturated with NaCl, diluted with CHCl_3 , and extracted (1 x 500 mL, then 2 x 250 mL). The aqueous layer was then extracted with EtOAc (3 x 250 mL), and the combined organic layers were dried over Na_2SO_4 , filtered, and concentrated *in vacuo*. Purification through silica gel flash chromatography (gradient elution, 2:1 → 1:1 hexanes–EtOAc) afforded **181** as a colorless

oil in 86% yield (4.20 g). $[\alpha]_D^{25.0} = +8.0^\circ$ ($c = 1.22, \text{CHCl}_3$); ^1H NMR (500 MHz, CD_3CN ; compound exists as a mixture of rotamers) δ 4.56 – 4.41 (m, 2H), 4.30 (dd, $J = 9.8, 8.3$ Hz, 1H), 4.23 – 4.05 (m, 5H), 3.93 – 3.75 (m, 1H), 3.64 (ddd, $J = 11.2, 6.0, 6.0$ Hz, 1H), 3.23 – 3.10 (m, 1H), 2.72 – 2.62 (m, 1H), 2.62 – 2.51 (m, 1H), 2.34 – 2.25 (m, 1H), 2.04 – 1.84 (m, 1H), 1.24 (t, $J = 7.1$ Hz, 3H), 1.06 – 0.89 (m, 2H), 0.03 (s, 9H); ^{13}C NMR (126 MHz, CD_3CN ; compound exists as a mixture of rotamers) δ 175.8, 175.1, 156.7, 156.4, 84.9, 75.5 (br), 75.4 (br), 65.0, 64.3 (br), 63.6 (br), 62.6 (br), 62.3 (br), 61.4, 60.6 (br), 60.2 (br), 45.3, 44.6, 33.3, 32.3, 18.3, 14.5, –1.5; IR (NaCl/thin film): 3422, 3307, 2953, 2898, 2114, 1718, 1701, 1406, 1348, 1314, 1250, 1198, 1171, 1041, 1006, 860, 838 cm^{-1} ; HRMS (Multimode-ESI/APCI) calc'd for $\text{C}_{15}\text{H}_{26}\text{NO}_6\text{Si}$ [$\text{M}-\text{C}_2\text{H}_4+\text{H}]^+$ 344.1524, found 344.1535 (detected fragment has undergone elimination of ethylene from the Teoc protecting group).

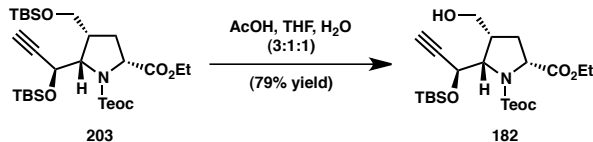
Preparation of bis(*tert*-butyldimethylsilyl) ether **203**



To a flame dried 250 mL round bottom flask equipped with diol **181** (4.20 g, 11.3 mmol) was added 113 mL of CH_2Cl_2 and the solution was cooled to 0 °C with stirring. Following addition of 2,6-lutidine (6.5 mL, 56 mmol), *tert*-butyldimethylsilyl trifluoromethanesulfonate (6.5 mL, 28 mmol) was added dropwise to the reaction. Upon completion of the reaction as judged by TLC (~1.5 h), the reaction was quenched with 3.0 mL of MeOH and 300 mL of sat. *aq.* NaHCO_3 solution was added. The mixture was then washed with CH_2Cl_2 (3 x 300 mL), and the organics were dried over Na_2SO_4 , filtered, and concentrated *in vacuo* to yield a faint yellow oil. Purification through silica

gel flash chromatography (gradient elution, 16:1 → 12:1 hexanes–EtOAc) afforded 5.75 g of **203** as a colorless oil (85% yield). $[\alpha]_D^{25.0} = -11.5^\circ$ ($c = 1.19$, CHCl_3); ^1H NMR (500 MHz, CD_3CN ; compound exists as a 1:1 mixture of rotamers) δ 4.78 (dd, $J = 4.2, 2.3$ Hz, 1H), 4.72 (dd, $J = 4.1, 2.2$ Hz, 1H), 4.21 – 4.01 (m, 14H), 3.91 (dd, $J = 8.0, 4.2$ Hz, 1H), 3.90 (dd, $J = 8.0, 4.0$ Hz, 1H), 2.68 (br d, $J = 2.4$ Hz, 2H), 2.61 – 2.50 (m, 2H), 2.44 – 2.25 (m, 2H), 1.22 (t, $J = 6.7$ Hz, 3H), 1.21 (t, $J = 6.7$ Hz, 3H), 1.07 – 0.97 (m, 2H), 0.91 (s, 18H), 0.90 (s, 18H), 0.95 – 0.86 (m, 2H), 0.14 (br s, 6H), 0.13 (s, 6H), 0.05 (s, 12H), 0.03 (s, 9H), 0.03 (s, 9H); ^{13}C NMR (126 MHz, CD_3CN ; compound exists as a mixture of rotamers) δ 172.6, 172.2, 156.3, 84.9, 84.9, 77.3, 77.2, 64.7, 64.5, 64.5, 64.1, 63.9, 63.1, 61.5, 61.3, 60.7, 60.4, 45.7, 44.9, 34.6, 33.5, 26.5, 26.2, 19.1, 18.8, 18.7, 18.4, 14.7, –1.3, –4.4, –4.5, –4.8, –4.9, –4.9, –5.0; IR (NaCl/thin film): 3312, 3257, 2955, 2931, 2895, 2858, 2114, 1762, 1736, 1706, 1472, 1406, 1351, 1252, 1185, 1126, 1079, 839, 778 cm^{-1} ; HRMS (Multimode-ESI/APCI) calc'd for $\text{C}_{27}\text{H}_{54}\text{NO}_6\text{Si}_3$ [$\text{M}-\text{C}_2\text{H}_4+\text{H}]^+$ 572.3253, found 572.3254 (detected fragment has undergone elimination of ethylene from the Teoc protecting group).

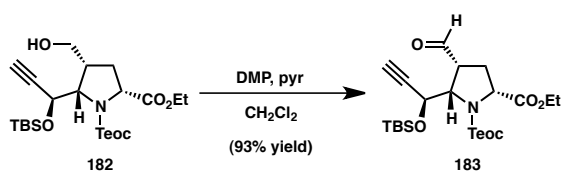
Preparation of primary alcohol **182**



To a 250 mL round bottom flask equipped with bis(*tert*-butyldimethylsilyl) ether **203** (1.00 g, 1.67 mmol) was added 22 mL of a 1:1 mixture of THF:H₂O and 33 mL of acetic acid. The reaction was monitored by TLC for disappearance of starting material and conversion to mono(*tert*-butyldimethylsilyl) ether **182** (with minimal formation of

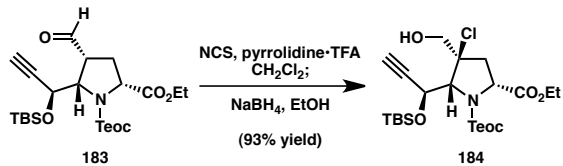
diol **181**). After 6 h, the reaction was cooled to 0 °C and quenched dropwise with 520 mL of 1N *aq.* NaOH (vigorous bubbling occurs initially) and excess sat. *aq.* NaHCO₃ solution until the reaction stopped bubbling. The reaction was then extracted with CHCl₃ (3x) followed by EtOAc (3x), and the combined organic layers were dried over Na₂SO₄, filtered, and concentrated *in vacuo*. Purification through silica gel flash chromatography (gradient elution, 16:1 → 1:1 hexanes–EtOAc) afforded **182** as a colorless oil in 79% yield (637 mg). [α]_D^{25.0} = -12.4° (*c* = 1.22, CHCl₃); ¹H NMR (500 MHz, CD₃CN; compound exists as a 1:1 mixture of rotamers) δ 4.85 (dd, *J* = 3.1, 3.1 Hz, 1H), 4.77 (dd, *J* = 2.9, 2.9 Hz, 1H), 4.23 – 4.04 (m, 12H), 4.01 – 3.91 (m, 2H), 3.72 (dd, *J* = 11.5, 7.1 Hz, 2H), 3.13 (br s, 2H), 2.73 (d, *J* = 2.3 Hz, 1H), 2.72 (d, *J* = 2.3 Hz, 1H), 2.65 – 2.55 (m, 2H), 2.30 – 2.22 (m, 4H), 1.22 (t, *J* = 6.9 Hz, 3H), 1.20 (t, *J* = 6.9 Hz, 3H), 1.09 – 0.96 (m, 2H), 0.92 (s, 18H), 0.18 (s, 12H), 0.18 (s, 12H), 0.03 (s, 18H), 0.03 (s, 18H); ¹³C NMR (126 MHz, CD₃CN; compound exists as a mixture of rotamers) δ 172.5, 172.1, 156.3, 84.5, 77.8, 77.7, 64.9, 64.6, 64.6, 64.3, 64.2, 63.4, 61.6, 61.5, 61.4, 60.6, 60.3, 46.0, 45.2, 33.4, 32.4, 26.3, 18.9, 18.8, 18.4, 14.8, -1.3, -4.4, -4.5, -4.8, -4.9; IR (NaCl/thin film): 3503, 3254, 2954, 2896, 2857, 2113, 1759, 1734, 1704, 1472, 1405, 1348, 1251, 1185, 1042, 838, 780 cm⁻¹; HRMS (Multimode-ESI/APCI) calc'd for C₂₁H₄₀NO₆Si₂ [M–C₂H₄+H]⁺ 458.2389, found 458.2412 (detected fragment has undergone elimination of ethylene from the Teoc protecting group).

Preparation of aldehyde 183



To a 250 mL round bottom flask equipped with primary alcohol **182** (2.29 g, 4.71 mmol) dissolved in 47 mL of CH₂Cl₂ (bulk solvent, not dried), was added pyridine (3.8 mL, 47.1 mmol), and Dess–Martin periodinane²⁴ (4.00 g, 9.42 mmol), and the cloudy white suspension was stirred vigorously. After 3.5 h, the reaction was quenched with sat. *aq.* Na₂S₂O₃ solution (50 mL) and sat. *aq.* NaHCO₃ solution (50 mL), diluted with EtOAc (50 mL), and stirred vigorously for an additional 20 min. The layers were then separated and the aqueous layer was washed with EtOAc (3 x 100 mL). The combined organics were washed with sat. *aq.* NaHCO₃ solution (400 mL), dried over Na₂SO₄, and concentrated *in vacuo*. Purification through silica gel flash chromatography (gradient elution, 8:1→4:1 hexanes–EtOAc) afforded **183** as a white oil in 93% yield (2.11 g). [α]_D^{25.0} = −35.2° (c = 1.18, CHCl₃); ¹H NMR (500 MHz, CD₃CN; compound exists as a 1:1 mixture of rotamers) δ 9.98 (s, 1H), 9.95 (s, 1H), 4.87 (br s, 1H), 4.82 (br s, 1H), 4.33 (dd, *J* = 8.7, 4.5 Hz, 2H), 4.29 – 4.22 (m, 2H), 4.21 – 4.08 (m, 8H), 3.25 – 3.17 (m, 2H), 2.77 (ddd, *J* = 11.4, 11.4, 11.4 Hz, 2H), 2.69 (s, 2H), 2.34 – 2.26 (m, 4H), 1.23 (t, *J* = 5.7 Hz, 3H), 1.22 (t, *J* = 5.7 Hz, 3H), 1.07 – 0.99 (m, 2H), 0.98 – 0.85 (m, 2H), 0.89 (s, 18H), 0.14 (s, 12H), 0.04 (s, 9H), 0.03 (s, 9H); ¹³C NMR (126 MHz, CD₃CN; compound exists as a mixture of rotamers) δ 199.4, 199.3, 172.1, 171.7, 156.2, 156.1, 83.7, 78.0, 77.9, 65.3, 64.8, 64.7, 64.6, 63.9, 63.3, 61.7, 61.6, 60.4, 60.1, 53.9, 53.2, 30.7, 29.7, 26.0, 18.8, 18.7, 18.3, 14.6, −1.5, −4.6, −4.7, −5.0, −5.0; IR (NaCl/thin film): 3262, 2954, 2930, 2897, 2857, 2116, 1758, 1706, 1472, 1405, 1348, 1251, 1188, 1079, 838, 779 cm^{−1}; HRMS (Multimode-ESI/APCI) calc'd for C₂₁H₃₈NO₆Si₂ [M–C₂H₄+H]⁺ 456.2232, found 456.2242 (detected fragment has undergone elimination of ethylene from the Teoc protecting group).

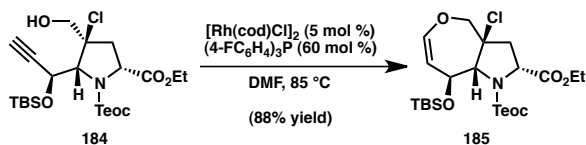
Preparation of chlorohydrin **184**



To a solution of aldehyde **183** (2.11 g, 4.36 mmol) in CH_2Cl_2 (87 mL, bulk solvent, not dried) was added pyrrolidinium trifluoroacetate (1.61 g, 8.72 mmol) followed by *N*-chlorosuccinimide (1.46 g, 10.9 mmol). The resulting solution was stirred under an air atmosphere for 30 h, and was subsequently diluted with EtOH (120 mL) and treated with NaBH_4 (1.65 g, 43.6 mmol). After 1.5 h, the reaction mixture was cooled to 0 °C and carefully quenched with 1M *aq.* HCl (200 mL). The resulting mixture was saturated with NaCl, then extracted with CHCl_3 (3 x 200 mL) followed by EtOAc (200 mL). The combined organic layers were washed with brine (400 mL), dried over Na_2SO_4 , filtered and concentrated *in vacuo* to provide the crude product, which was purified by silica gel flash chromatography (gradient elution, 12:1→6:1 hexanes–EtOAc) to afford chlorohydrin **184** (2.11 g, 93% yield) as a clear, colorless oil. $[\alpha]_D^{25.0} = -8.2^\circ$ ($c = 0.98$, CHCl_3); ^1H NMR (500 MHz, CDCl_3 ; compound exists as a 1.25:1 mixture of rotamers, the major rotamer is designated by *, minor rotamer denoted by \ddagger) δ 4.96 (dd, $J = 4.3, 2.3$ Hz, 1H*), 4.85 (dd, $J = 4.2, 2.3$ Hz, 1H \ddagger), 4.64 (dd, $J = 10.6, 7.4$ Hz, 1H \ddagger), 4.56 (dd, $J = 10.6, 7.1$ Hz, 1H*), 4.38 (ddd, $J = 13.3, 13.3, 4.1$ Hz, 1H*, 1H \ddagger), 4.32 (dd, $J = 4.4, 1.3$ Hz, 1H*), 4.27 (m, 1H \ddagger), 4.26 – 4.11 (m, 3H*, 3H \ddagger), 3.96 – 3.88 (m, 1H*, 1H \ddagger), 3.53 (dd, $J = 10.8, 4.3$ Hz, 1H*), 3.42 (dd, $J = 10.7, 4.4$ Hz, 1H \ddagger), 2.90 – 2.81 (m, 1H*, 1H \ddagger), 2.55 – 2.47 (m, 2H*, 2H \ddagger), 1.25 (t, $J = 7.0, 3\text{H}^*$), 1.25 (t, $J = 7.0, 3\text{H}^\ddagger$), 1.04 – 0.91 (m, 2H*, 2H \ddagger), 0.93 (s, 9H*, 9H \ddagger), 0.21 (3H*), 0.21 (3H*), 0.19 (3H \ddagger), 0.19 (3H \ddagger), 0.03 (s, 9H \ddagger),

0.01 (s, 9H*); ^{13}C NMR (126 MHz, CDCl_3 ; compound exists as a mixture of rotamers) δ 170.7, 170.3, 155.3, 155.1, 81.7, 81.4, 80.4, 79.5, 77.2, 76.8 (obscured by CDCl_3 signal, observable by acquiring spectrum in CD_2Cl_2), 73.1, 72.6, 65.8, 64.6, 64.5, 63.9, 63.1, 61.1, 61.0, 58.4, 58.1, 40.9, 39.8, 25.6, 18.0, 18.0, 17.5, 14.2, 14.1, –1.6, –1.6, –5.0, –5.2, –5.4, –5.4; IR (NaCl/thin film): 3494, 3309, 3255, 2955, 2931, 2898, 2859, 2113, 1761, 1708, 1404, 1350, 1307, 1252, 1191, 1082, 839, 781 cm^{-1} ; HRMS (Multimode-ESI/APCI) calc'd for $\text{C}_{21}\text{H}_{39}\text{ClNO}_6\text{Si}_2$ [$\text{M}-\text{C}_2\text{H}_4+\text{H}$] $^+$ 492.1999, found 492.2002 (detected fragment has undergone elimination of ethylene from the Teoc protecting group).

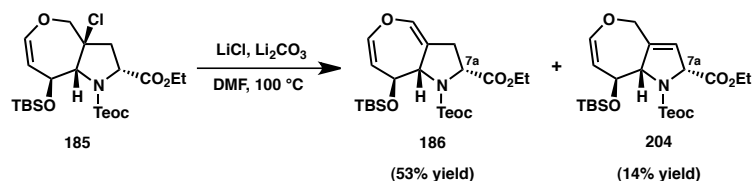
Preparation of chlorotetrahydroooxepine 185



A flame-dried Schlenk tube equipped with a magnetic stir bar was charged with $[\text{Rh}(1,5\text{-cyclooctadiene})\text{Cl}]_2$ (26.1 mg, 0.053 mmol, 5 mol %) and tris(4-fluorophenyl)phosphine (201 mg, 0.636 mmol, 60 mol %). An atmosphere of N_2 was established by evacuation/backfilling (three cycles) and a solution of chlorohydrin **184** (553 mg, 1.06 mmol) in dry DMF (10.6 mL, including two rinses to ensure quantitative transfer) was added via syringe. The resulting yellow solution was degassed using the freeze-pump-thaw technique. The vessel was sealed and the solution frozen by submersion in a bath of liquid N_2 . The vessel was then placed under vacuum for approximately five minutes before once again being sealed and allowed to thaw under static vacuum by removal from the liquid N_2 bath. This procedure was repeated twice before the head-space was finally backfilled with N_2 , the vessel sealed, and the solution heated to 85 °C with stirring. After 26 h, the reaction mixture was cooled to rt, diluted

with 50 mL sat. *aq.* NaHCO₃ solution, and extracted with EtOAc (3 x 50 mL). The combined organic layers were washed with water (2 x 50 mL) followed by brine (50 mL), dried over Na₂SO₄, filtered, and concentrated *in vacuo* to provide the crude product, which was purified by silica gel flash chromatography (gradient elution, 24:1 → 12:1 hexanes–EtOAc) to afford chlorotetrahydrooxepine **185** (483 mg, 88% yield) as a pale yellow oil. [α]_D^{25.0} = +91.9° (*c* = 1.14, CHCl₃); ¹H NMR (400 MHz, CD₃CN, 60 °C) δ 6.23 (dd, *J* = 7.5, 1.1 Hz, 1H), 4.66 (dd, *J* = 7.5, 3.7 Hz, 1H), 4.60 (d, *J* = 13.2 Hz, 1H), 4.57 – 4.49 (m, 2H), 4.41 (dd, *J* = 7.8, 1.0 Hz, 1H), 4.26 – 4.07 (m, 5H), 2.57 (ddd, *J* = 14.3, 7.6, 1.0 Hz, 1H), 2.49 (dd, *J* = 14.5, 10.0 Hz, 1H), 1.26 (t, *J* = 7.1 Hz, 3H), 1.04 – 0.97 (m, 2H), 0.92 (s, 9H), 0.14 (s, 3H), 0.12 (s, 3H), 0.05 (s, 9H); ¹³C NMR (101 MHz, CD₃CN, 60 °C; compound exists as a mixture of rotamers) δ 172.7, 157.3, 146.9, 109.4 (br), 77.9, 76.8 (br), 74.8, 70.0, 65.1, 62.2, 60.5, 41.5 (br), 26.6, 18.9, 18.8, 14.8, –1.1, –4.1, –4.3; IR (NaCl/thin film): 2954, 2929, 2896, 2856, 1757, 1707, 1647, 1406, 1352, 1336, 1313, 1251, 1192, 1131, 1037, 863, 837, 777 cm^{–1}; HRMS (Multimode-ESI/APCI) calc'd for C₁₅H₂₃ClNO₅Si [M–C₂H₄–C₆H₁₅OSi]⁺ 360.1029, found 360.1030 (detected fragment has undergone elimination of ethylene from the Teoc protecting group, as well as loss of *tert*-butyldimethylsilanolate anion).

Preparation of dihydrooxepine **186**



An oven-dried Schlenk tube was charged with a magnetic stir bar and dry LiCl (149 mg, 3.52 mmol), and its contents were flame-dried under vacuum. The headspace

was then backfilled with N₂, and Li₂CO₃ (519 mg, 7.03 mmol) was quickly added to the vessel. The tube was then evacuated and backfilled with N₂, and this procedure was repeated twice to establish an inert atmosphere. Finally, chlorotetrahydrooxepine **185** (30.5 mg, 58.6 μmol) was added as a solution in DMF (rinsing twice for a total volume of 2.3 mL), and the mixture was heated to 100 °C with vigorous stirring. After 75 h, the reaction mixture was cooled to room temperature and filtered through celite, rinsing the vessel and filter pad with EtOAc, followed by excess Et₂O. The resulting off-white suspension was again filtered through celite and concentrated *in vacuo*. This material was purified by preparative HPLC (normal phase, isocratic elution, 6% EtOAc in hexanes) to afford dihydrooxepine **186** (14.9 mg, 53% yield) and olefin isomer **204** (4.0 mg, 14% yield) as colorless oils.

Dihydrooxepine **186**.

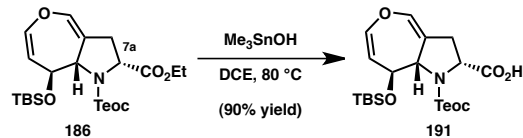
$[\alpha]_D^{25.0} = -70.5^\circ$ (*c* = 0.94, CHCl₃); ¹H NMR (400 MHz, CDCl₃, 50 °C) δ 6.37 (ddd, *J* = 2.5, 2.5, 1.1 Hz, 1H), 6.11 (dd, *J* = 8.2, 2.2 Hz, 1H), 4.81 – 4.68 (m, 2H), 4.62 (br d, *J* = 7.6 Hz, 1H), 4.42 (ddd, *J* = 7.5, 2.1, 2.1 Hz, 1H), 4.34 – 4.02 (m, 4H), 2.92 (dddd, *J* = 15.1, 9.8, 2.1, 2.1 Hz, 1H), 2.59 (dddd, *J* = 15.1, 1.6, 1.6, 1.6 Hz, 1H), 1.27 (t, *J* = 7.1 Hz, 3H), 1.06 – 0.98 (m, 2H), 0.91 (s, 9H), 0.11 (s, 3H), 0.06 (s, 3H), 0.03 (s, 9H); ¹³C NMR (101 MHz, CDCl₃, 50 °C) δ 172.1, 156.3 (br), 138.0, 135.8, 114.4 (br), 111.6, 71.6, 63.9, 63.7, 61.0, 58.5, 33.9 (br), 25.9, 18.0, 17.9, 14.2, –1.5, –4.7, –5.2; IR (NaCl/thin film): 2954, 2928, 2897, 2855, 1750, 1723, 1699, 1687, 1652, 1407, 1330, 1250, 1180, 1142, 1098, 1031, 860, 837, 778 cm^{–1}; HRMS (Multimode-ESI/APCI) calc'd for C₁₅H₂₂NO₅Si [M–C₂H₄–C₆H₁₅OSi]⁺ 324.1262, found 324.1267 (detected fragment has

undergone elimination of ethylene from the Teoc protecting group, as well as loss of *tert*-butyldimethylsilanolate anion).

Olefin isomer 204.

$[\alpha]_D^{25.0} = +121.9^\circ$ ($c = 1.02$, CHCl_3); ^1H NMR (400 MHz, CD_3CN ; 60 °C) δ 6.16 (d, $J = 7.2, 1.2$ Hz, 1H), 5.86 (br s, 1H), 5.08 (q, $J = 1.6$ Hz, 1H), 4.80 (dd, $J = 7.6, 4.4$ Hz, 1H), 4.66 (dt, $J = 5.6, 1.6$ Hz, 1H), 4.52 (d, $J = 12.4$ Hz, 1H), 4.44 – 4.38 (m, 2H), 4.28 – 4.18 (m, 4H), 1.25 (t, $J = 7.2$ Hz, 3H), 1.01 (t, $J = 8.4$ Hz, 2H), 0.93 (s, 9H), 0.12 (s, 3H), 0.11 (s, 3H), 0.05 (s, 9H); ^{13}C NMR (101 MHz, CD_3CN , 60 °C) δ 171.1, 146.2, 141.8, 125.9, 113.2, 73.8, 72.9, 69.0, 66.8, 64.7, 62.4, 26.7, 19.0, 18.9, 14.9, –1.1, –4.0, –4.2; IR (NaCl/thin film): 2953, 2928, 2893, 2854, 1755, 1703, 1639, 1404, 1348, 1328, 1251, 1189, 1128, 1103, 1058, 1027, 861, 836, 777 cm^{-1} ; HRMS (Multimode-ESI/APCI) calc'd for $\text{C}_{15}\text{H}_{22}\text{NO}_5\text{Si}$ [M– C_2H_4 – $\text{C}_6\text{H}_{15}\text{OSi}$] $^+$ 324.1262, found 324.1264 (detected fragment has undergone elimination of ethylene from the Teoc protecting group, as well as loss of *tert*-butyldimethylsilanolate anion).

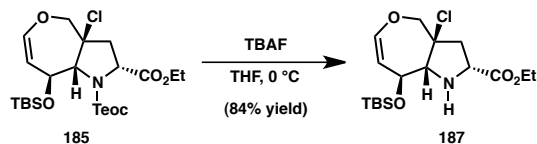
Preparation of carboxylic acid 191



To a solution of ethyl ester **186** (47.3 mg, 97.8 μmol) in DCE (1.0 mL) was added trimethyltin hydroxide (177 mg, 0.978 mmol), and the resulting solution was heated 80 °C with stirring. After 30 h, the reaction mixture was cooled to room temperature and diluted with $\text{Na}_2\text{HPO}_4/\text{KHSO}_4$ buffer (pH = 2.5, prepared from a 10% w/v *aq.* Na_2HPO_4 solution by acidification with KHSO_4), then extracted with EtOAc (5x). The combined

organic layers were washed with H₂O followed by brine, then dried over Na₂SO₄, filtered, and concentrated *in vacuo* to provide the crude product, which was purified by silica gel flash chromatography (gradient elution, 40:1 → 20:1 CH₂Cl₂–MeOH) to afford carboxylic acid **191** (40.3 mg, 90% yield) as a white foam. [α]_D^{25.0} = −68.6° (*c* = 0.890, CHCl₃); ¹H NMR (400 MHz, CDCl₃, 50 °C) δ 6.43 (ddd, *J* = 2.1, 2.1, 2.1 Hz, 1H), 6.14 (dd, *J* = 8.2, 2.2 Hz, 1H), 4.72 – 4.67 (m, 2H), 4.64 (dddd, *J* = 7.8, 1.8, 1.8, 1.8 Hz, 1H), 4.42 – 4.31 (m, 1H), 4.20 – 4.10 (m, 2H), 3.03 (d, *J* = 16.0 Hz, 1H), 2.91 (dddd, *J* = 15.5, 9.6, 1.7, 1.7 Hz, 1H), 1.13 – 1.01 (m, 2H), 0.91 (s, 9H), 0.09 (s, 3H), 0.05 (s, 9H), 0.04 (s, 3H); ¹³C NMR (101 MHz, CDCl₃, 50 °C) δ 174.7 (br), 157.5 (br), 138.5, 136.4, 114.6 (br), 111.1, 71.4, 64.8, 63.9, 58.6, 31.9 (br), 25.9, 18.0, 17.9, −1.5, −4.8, −5.1; IR (NaCl/thin film): 3088, 2954, 2928, 2897, 2855, 1750, 1722, 1684, 1652, 1418, 1336, 1250, 1180, 1142, 1101, 859, 837, 777 cm^{−1}; HRMS (Multimode-ESI/APCI) calc'd for C₁₃H₁₈NO₅Si [M–C₂H₄–C₆H₁₅OSi]⁺ 296.0949, found 296.0958 (detected fragment has undergone elimination of ethylene from the Teoc protecting group, as well as loss of *tert*-butyldimethylsilanolate anion).

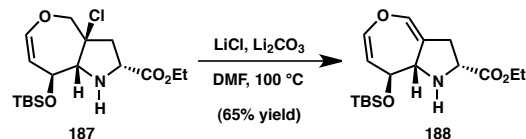
Preparation of amine **187**



To a stirred solution of trimethylsilylethyl carbamate **185** (677 mg, 1.30 mmol) in THF (26 mL) at 0 °C was added a solution of TBAF (1.0 M in THF, 5.2 mL, 5.20 mmol). After 2.5 h, the solution was diluted with sat. *aq.* Na₂SO₄ solution (125 mL) and H₂O (250 mL) and extracted with EtOAc (4 x 125 mL). The combined organic layers were

washed with sat. *aq.* Na₂SO₄ solution (250 mL), H₂O (2 x 250 mL), and brine (250 mL), then dried over Na₂SO₄, filtered, and concentrated *in vacuo* to provide the crude product, which was purified by silica gel flash chromatography (isocratic elution, 6:1 hexanes–EtOAc) to afford pyrrolidine **187** (412 mg, 84% yield) as a pale brown oil. [α]_D^{25.0} = +117.4° (*c* = 1.07, CHCl₃); ¹H NMR (500 MHz, CDCl₃) δ 6.19 (dd, *J* = 7.5, 0.7 Hz, 1H), 4.66 (d, *J* = 11.6 Hz, 1H), 4.54 (dd, *J* = 7.4, 5.1 Hz, 1H), 4.31 (ddd, *J* = 6.9, 5.2, 0.8 Hz, 1H), 4.24 – 4.14 (m, 2H), 4.08 (d, *J* = 12.2 Hz, 2H), 3.74 (s, 1H), 2.42 (dd, *J* = 13.7, 5.9 Hz, 2H), 2.30 (dd, *J* = 13.7, 10.8 Hz, 1H), 1.27 (t, *J* = 7.1 Hz, 3H), 0.90 (s, 9H), 0.09 (s, 3H), 0.08 (s, 3H); ¹³C NMR (126 MHz, CDCl₃) δ 172.4, 146.8, 105.5, 76.3, 74.5, 74.4, 68.5, 61.1, 58.1, 43.6, 25.7, 18.0, 14.2, –4.6, –4.9; IR (NaCl/thin film): 2954, 2929, 2886, 2856, 1741, 1646, 1472, 1286, 1252, 1192, 1138, 1088, 1057, 1035, 872, 838, 778 cm^{–1}; HRMS (Multimode-ESI/APCI) calc'd for C₁₇H₃₁ClNO₄Si [M+H]⁺ 376.1705, found 376.1728.

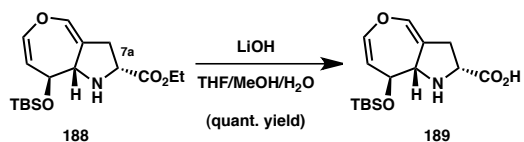
Preparation of dihydrooxepine amine **188**



An oven-dried Schlenk tube was charged with a magnetic stir bar and dry LiCl (454 mg, 10.7 mmol), and its contents were flame-dried under vacuum. The headspace was then backfilled with N₂, and Li₂CO₃ (1.58 g, 21.4 mmol) was quickly added to the vessel. The tube was then evacuated and backfilled with N₂, and this procedure was repeated twice to establish an inert atmosphere. Finally, chlorotetrahydrooxepine **187** (67.0 mg, 0.178 mmol) was added as a solution in DMF (rinsing twice for a total volume of 7.1 mL), and the mixture was heated to 100 °C with vigorous stirring. After 48 h, the

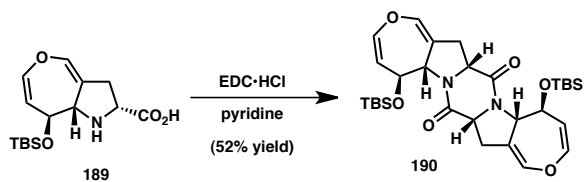
reaction mixture was cooled to room temperature and filtered through celite, rinsing the vessel and filter pad with EtOAc, followed by excess Et₂O. The resulting off-white suspension was again filtered through celite and concentrated *in vacuo*. Residual DMF was removed by distillation under high vacuum with gentle heating (water bath, 40 °C) to give the crude product as a brown oil. This material was purified by silica gel flash chromatography (isocratic elution, 8:1 hexanes–EtOAc) to afford dihydrooxepine **188** (41.1 mg) as a pale brown oil. NOTE: This material was contaminated with ~5 wt% starting material, giving a corrected yield of 65%. Material of this purity was typically used without further purification; however, analytically pure samples could be obtained with further purification by silica gel flash chromatography (gradient elution, 0→5% EtOAc–CH₂Cl₂ with 0.5% Et₃N). [α]_D^{25.0} = −28.2° (c = 1.30, CHCl₃); ¹H NMR (500 MHz, CDCl₃) δ 6.33 (ddd, *J* = 2.1, 2.1, 2.1 Hz, 1H), 6.09 (dd, *J* = 8.2, 2.3 Hz, 1H), 4.62 (dd, *J* = 8.2, 1.8 Hz, 1H), 4.20 – 4.13 (m, 3H), 3.86 (dd, *J* = 7.7, 5.8 Hz, 1H), 3.81 (dddd, *J* = 7.2, 2.0, 2.0, 2.0 Hz, 1H), 2.85 (dddd, *J* = 14.9, 7.7, 1.7, 1.7 Hz, 1H), 2.64 (dddd, *J* = 14.9, 5.8, 1.9, 1.9 Hz, 1H), 2.74 – 2.49 (br s, 1H), 1.26 (t, *J* = 7.1 Hz, 3H), 0.93 (s, 9H), 0.18 (s, 3H), 0.15 (s, 3H); ¹³C NMR (126 MHz, CDCl₃) δ 173.9, 138.5, 135.0, 115.7, 110.2, 71.7, 64.8, 60.8, 58.3, 33.8, 25.8, 18.1, 14.2, −4.5, −4.5; IR (NaCl/thin film): 3376, 2955, 2929, 2886, 2856, 1737, 1688, 1651, 1472, 1463, 1368, 1295, 1279, 1252, 1203, 1175, 1119, 1090, 1035, 1005, 882, 838, 778 cm^{−1}; HRMS (Multimode-ESI/APCI) calc'd for C₁₇H₃₀NO₄Si [M+H]⁺ 340.1939, found 340.1941.

Preparation of amino acid 189



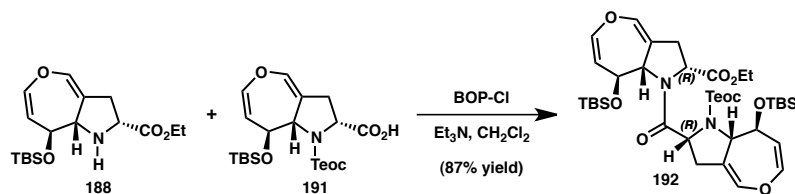
LiOH (242 mg, 10.1 mmol) was dissolved in 7 mL H₂O, and the resulting solution was added via pipet to a stirring solution of ethyl ester **188** (343 mg, 1.01 mmol) in 14 mL of THF/MeOH (1:1) under an air atmosphere. The resulting biphasic mixture was stirred vigorously for 1 h, then diluted with 100 mL sat. *aq.* Na₂HPO₄ and extracted with CHCl₃ (3 x 100 mL). The combined organic layers were then dried over Na₂SO₄, filtered, and concentrated to afford 321 mg (quantitative yield) of amino acid **189** as a yellow solid. Though this material was generally used without further purification, it was found that the yellow color as well as minor impurities could be removed via trituration with THF. [α]_D^{25,0} = -60.5 ° (c = 1.59, CHCl₃); ¹H NMR (500 MHz, CDCl₃) δ 6.35 (ddd, *J* = 1.9, 1.9, 1.9 Hz, 1H), 6.13 (dd, *J* = 7.8, 2.3 Hz, 1H), 4.76 (dd, *J* = 8.0, 2.1 Hz, 1H), 4.43 (ddd, *J* = 8.0, 2.3, 2.3 Hz, 1H), 4.22 (dd, *J* = 8.2, 2.2 Hz, 1H), 4.10 (dd, *J* = 8.2, 2.1 Hz, 1H), 3.09 – 2.93 (m, 2H), 0.90 (s, 9H), 0.20 (s, 3H), 0.13 (s, 3H); ¹³C NMR (126 MHz, CDCl₃) δ 173.1, 138.8, 136.2, 110.5, 110.0, 69.2, 62.2, 57.5, 34.1, 25.8, 17.8, -4.3, -4.9; IR (NaCl/thin film): 3067, 2954, 2929, 2886, 2858, 2368, 1688, 1652, 1472, 1464, 1444, 1368, 1332, 1300, 1260, 1220, 1190, 1142, 1108, 1080, 1006, 960, 938, 872, 839, 780, 754, 724 cm⁻¹; LRMS (ESI/APCI) calc'd for C₁₅H₂₆NO₄Si [M+H]⁺ 312.2, found 312.1.

Preparation of diketopiperazine 190



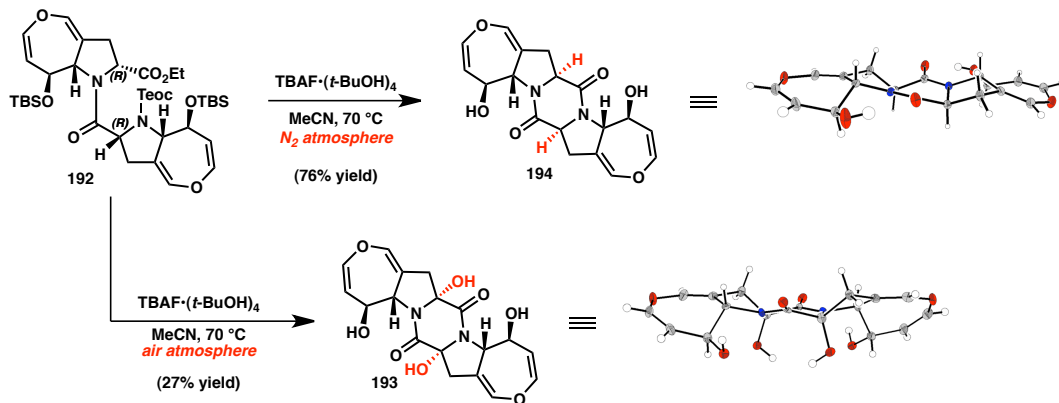
In a 1-dram vial equipped with a magnetic stir bar, amino acid **189** (40.6 mg, 0.130 mmol) was dissolved in 1.3 mL pyridine. Solid EDC•HCl (125 mg, 0.650 mmol) was then added in one portion, and the resulting suspension was stirred vigorously for 18 hours. The mixture was then diluted with H₂O, giving a yellow precipitate that was filtered off through a cotton plug and rinsed with an excess of further H₂O. The crude product was then recovered by elution through the cotton plug with CH₂Cl₂. Purification via flash chromatography (gradient elution, 2:1→1:1 hexanes–EtOAc) afforded diketopiperazine **190** (19.9 mg, 52% yield) as an off-white solid. [α]_D^{25.0} = −92.3 ° (c = 1.29, CHCl₃); ¹H NMR (500 MHz, CDCl₃) δ 6.53 (dd, *J* = 2.0, 2.0 Hz, 2H), 6.22 (dd, *J* = 8.3, 1.9 Hz, 2H), 4.68 (ddd, *J* = 8.2, 2.1, 2.1 Hz, 2H), 4.61 (dd, *J* = 8.3, 1.4 Hz, 2H), 4.25 (dd, *J* = 11.6, 7.2 Hz, 2H), 4.06 (ddd, *J* = 8.2, 1.7, 1.7 Hz, 2H), 2.94 (ddd, *J* = 15.7, 7.2, 1.0 Hz, 2H), 2.68 (dddd, *J* = 15.8, 11.8, 2.7, 2.7 Hz, 2H), 0.92 (s, 18H), 0.10 (s, 6H), 0.06 (s, 6H); ¹³C NMR (126 MHz, CDCl₃) δ 169.9, 140.6, 138.2, 117.7, 109.3, 71.1, 64.0, 63.5, 29.0, 25.8, 18.1, -3.8, -4.5; IR (NaCl/thin film): 3391, 3059, 2947, 2926, 2854, 1702, 1645, 1470, 1462, 1360, 1330, 1289, 1256, 1245, 1231, 1197, 1163, 1138, 1127, 1097, 1062, 993, 980, 956, 937, 897, 860, 836, 775, 713 cm⁻¹; LRMS (ESI/APCI) calc'd for C₂₄H₃₁N₂O₅Si [M–C₆H₁₅OSi]⁺ 455.2, found 455.2 (detected fragment has undergone loss of *tert*-butyldimethylsilanolate anion).

Preparation of dipeptide **192**



To a stirred solution of amine **188** (59.2 mg, 0.174 mmol) and carboxylic acid **191** (73.9 mg, 0.162 mmol) in CH₂Cl₂ (1.6 mL) was added triethylamine (226 μ L, 1.62 mmol) followed by BOP-Cl (206 mg, 0.810 mmol). After 24 h, the reaction mixture was diluted with sat. *aq.* NaHCO₃ solution and extracted with EtOAc (5x). Each organic fraction was filtered individually through a plug of SiO₂, which was then rinsed with excess EtOAc. The combined organic filtrates were concentrated *in vacuo* to provide the crude product, which was purified by silica gel flash chromatography (gradient elution, 16:1 \rightarrow 4:1 hexanes–EtOAc) to afford dipeptide **192** (109.5 mg, 87% yield) as a white foam. $[\alpha]_D^{25.0} = -46.8^\circ$ ($c = 1.86$, CHCl₃); ¹H NMR (400 MHz, CDCl₃, 50 °C) δ 6.43 – 6.36 (m, 2H), 6.15 (dd, $J = 8.2, 2.2$ Hz, 1H), 6.12 (dd, $J = 8.2, 2.2$ Hz, 1H), 5.63 (s, 1H), 5.34 (d, $J = 8.2$ Hz, 1H), 5.01 (d, $J = 9.9$ Hz, 1H), 4.80 (dd, $J = 8.2, 2.1$ Hz, 1H), 4.66 (dd, $J = 8.2, 1.7$ Hz, 1H), 4.60 (d, $J = 7.3$ Hz, 1H), 4.50 (apt dddd, $J = 12.3, 7.9, 2.0, 2.0$ Hz, 2H), 4.28 – 4.01 (m, 4H), 2.97 – 2.87 (m, 1H), 2.87 – 2.77 (m, 1H), 2.76 – 2.68 (m, 1H), 2.67 – 2.58 (m, 1H), 1.26 (t, $J = 7.1$ Hz, 3H), 1.01 (apt dd, $J = 9.9, 8.1$ Hz, 2H), 0.94 (s, 9H), 0.88 (s, 9H), 0.17 (s, 3H), 0.09 (s, 3H), 0.04 (s, 3H), 0.02 (s, 9H), –0.08 (s, 3H); ¹³C NMR (101 MHz, CDCl₃, 50 °C) δ 172.8, 171.7, 156.5, 138.3, 138.0, 136.0, 134.6, 116.1, 115.4, 111.1, 110.7, 71.4, 70.7, 64.6, 64.1, 63.3, 61.2, 57.1, 55.7, 34.5, 32.6, 26.3, 25.8, 18.3, 18.0, 18.0, 14.2, –1.6, –3.3, –4.7, –5.2, –5.8; IR (NaCl/thin film): 2954, 2929, 2896, 2856, 1746, 1718, 1685, 1653, 1430, 1331, 1302, 1251, 1190, 1179, 1141, 1091, 865, 837, 780 cm^{–1}; HRMS (Multimode-ESI/APCI) calc'd for C₂₆H₃₃N₂O₇Si [M–C₆H₁₆OSi–C₆H₁₅OSi]⁺ 513.2052, found 513.2051 (detected fragment has undergone elimination of *tert*-butyldimethylsilanol, as well as loss of *tert*-butyldimethylsilanolate anion).

Preparation of diketopiperazine 194 (or tetraol 193)



An oven-dried Schlenk tube was charged with a magnetic stir bar, TBAF(*t*-BuOH)₄³¹ (248 mg, 0.445 mmol), and a solution of dipeptide **192** (57.6 mg, 74.1 μ mol) in dry MeCN (1.5 mL). The resulting solution was degassed using the freeze-pump-thaw technique. The vessel was sealed and the solution frozen by submersion in a bath of liquid N₂. The vessel was then placed under vacuum for ca. five minutes before once again being sealed and allowed to thaw under static vacuum by removal from the liquid N₂ bath. This procedure was repeated three times before the head-space was finally backfilled with N₂, the vessel sealed, and the solution heated to 70 °C with stirring. After 2 h and 20 min, the reaction mixture was cooled to rt, was diluted with sat. *aq.* Na₂SO₄ solution, and extracted with EtOAc (5x). Each organic fraction was passed individually through a plug of SiO₂, which was then rinsed with excess EtOAc. The combined organic filtrates were then concentrated *in vacuo* to provide the crude product, which was purified by silica gel flash chromatography (isocratic elution, 1% MeOH in 1:1 CH₂Cl₂–EtOAc) to afford diketopiperazine **194** (20.3 mg, 76% yield) as a white solid. Crystals suitable for X-ray diffraction were obtained by slow evaporation of a solution of diketopiperazine **194** in THF at ambient temperature. NOTE: It was observed that if this reaction was

performed under an air atmosphere, tetraol **193** was formed. This oxidation process displays a great degree of apparent diastereoselectivity, as no other diastereomers of the dihydroxylated product are observed in significant quantities. Tetraol **193** could be isolated as a white solid (27% yield) by preparative HPLC (reverse phase, gradient elution, 20→40% MeCN in H₂O). Crystals suitable for X-ray diffraction were obtained as follows: the material was dissolved in a minimal amount of THF and diluted with CH₂Cl₂, then benzene and *iso*-octane were sequentially layered over the resulting solution and the phases were allowed to slowly diffuse at ambient temperature.

Diketopiperazine **194**

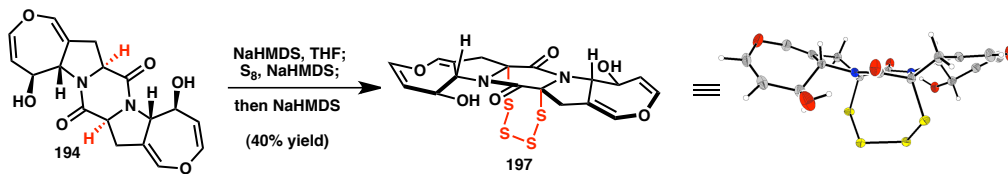
$[\alpha]_D^{25.0} = -624.5^\circ$ ($c = 1.01$, CHCl₃); mp 200–222 °C (dec); ¹H NMR (500 MHz, CDCl₃) δ 6.53 (ddd, $J = 2.6, 2.6, 1.0$ Hz, 2H), 6.18 (dd, $J = 8.2, 2.3$ Hz, 2H), 5.07 (s, 2H), 4.91 (dddd, $J = 7.9, 1.7, 1.7, 1.7$ Hz, 2H), 4.87 (dd, $J = 8.2, 1.9$ Hz, 2H), 4.50 – 4.44 (m, 2H), 4.35 (ddd, $J = 7.9, 2.1$ Hz, 2H), 3.01 (dddd, $J = 14.9, 6.9, 1.2, 1.2$ Hz, 2H), 2.84 (dddd, $J = 15.1, 11.2, 2.2, 2.2$ Hz, 2H); ¹³C NMR (126 MHz, CDCl₃) δ 167.1, 138.3, 137.8, 110.3, 109.6, 71.0, 64.1, 57.8, 33.9; IR (NaCl/thin film): 3244, 3164, 2923, 2895, 2848, 1675, 1638, 1623, 1438, 1284, 1187, 1131, 1046, 749 cm^{−1}; HRMS (Multimode-ESI/APCI) calc'd for C₁₈H₁₇N₂O₆ [M–H][−] 357.1092, found 357.1089.

Tetraol **193**

¹H NMR (500 MHz, CD₃CN) δ 6.54 (ddd, $J = 2.6, 2.6, 0.9$ Hz, 2H), 6.25 (dd, $J = 8.3, 2.3$ Hz, 2H), 4.82 – 4.76 (m, 4H), 4.39 (ddd, $J = 7.7, 2.2, 2.2$ Hz, 2H), 2.95 (ddd, $J = 15.4, 2.4, 2.4$ Hz, 2H), 2.78 (ddd, $J = 15.4, 1.5, 1.0$ Hz, 2H); ¹³C NMR (126 MHz, CD₃CN) δ 167.9, 139.1, 138.2, 111.2, 111.1, 87.8, 73.1, 65.0, 42.0; IR (NaCl/thin film):

3583, 3300, 2916, 2848, 1653, 1647, 1420, 1320, 1197, 1148, 1063, 1014 cm⁻¹; HRMS (Multimode-ESI/APCI) calc'd for C₁₈H₁₇N₂O₈ [M–H][–] 389.0990, found 389.0960.

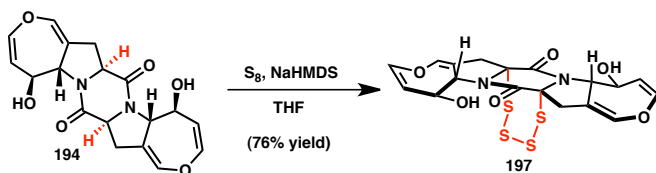
Preparation of epitetrathiodiketopiperazine 197 (published procedure)



To a stirred suspension of S₈ (22.4 mg, 87.3 μmol) in THF (5.8 mL) under a N₂ atmosphere was added a solution of NaHMDS in PhMe (0.6 M, 437 μL, 0.262 mmol) over two minutes. The S₈ solids dissolved over the course of the addition, giving initially a dark green solution that evolved to an orange-brown color towards the end of the addition. While this solution was allowed to stir for an additional one minute, a solution of NaHMDS in PhMe (0.6 M, 145 μL, 87.3 μmol) was added to a stirred solution of diketopiperazine 194 (3.13 mg, 8.73 μmol) in THF (1.0 mL) under a N₂ atmosphere. The resulting pale brown solution was then added dropwise via syringe to the previously described solution of reagents over one minute, rinsing once with THF (0.25 mL) (rinsings transferred over an additional one minute) to give a slightly opaque yellow-orange solution. After an additional one minute, a solution of NaHMDS in PhMe (0.6 M, 292 μL, 0.175 mmol) was added dropwise to the reaction mixture. After 50 min, the reaction was quenched with sat. *aq.* NaHCO₃ solution and extracted with EtOAc. The combined organic layers were dried over Na₂SO₄, filtered, and concentrated *in vacuo* to provide the crude product, which was purified by silica gel flash chromatography (gradient elution, 3:1→3:2 hexanes–EtOAc) to afford epitetrathiodiketopiperazine 197 (1.67 mg, 40% yield) as a yellow solid. Crystals suitable for X-ray diffraction were

obtained as follows: *iso*-octane was carefully layered over a solution of epitetrathiodiketopiperazine **197** in CHCl₃ and the resulting phases were allowed to slowly diffuse at ambient temperature. [α]_D^{25.0} = −548.9° (*c* = 0.135, CHCl₃); mp 148–165 °C (dec); ¹H NMR (500 MHz, CDCl₃) δ 6.54 (dd, *J* = 2.5 Hz, 2H), 6.21 (dd, *J* = 8.2, 2.3 Hz, 2H), 5.02 (d, *J* = 7.6 Hz, 2H), 4.92 (dd, *J* = 8.1, 1.9 Hz, 2H), 4.73 (s, 2H), 4.49 – 4.43 (m, 2H), 3.29 (ddd, *J* = 16.0, 2.2 Hz, 2H), 3.03 (d, *J* = 16.1 Hz, 2H); ¹³C NMR (126 MHz, CDCl₃) δ 169.5, 138.9, 138.0, 110.4, 106.4, 74.5, 71.4, 65.4, 41.1; IR (NaCl/thin film): 3369, 2919, 2849, 1689, 1662, 1391, 1337, 1193, 1133, 1082, 1046, 748 cm^{−1}; HRMS (Multimode-ESI/APCI) calc'd for C₁₈H₁₆ClN₂O₆S₄ [M+Cl][−] 518.9585, found 518.9614.

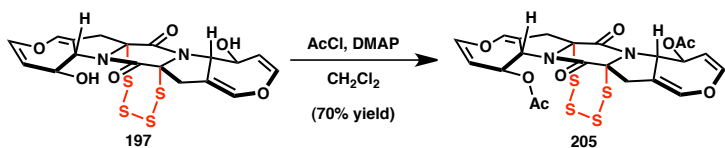
Preparation of epitetrathiodiketopiperazine **197** (improved procedure)



To a stirred suspension of S₈ (212 mg, 0.825 mmol) in THF (27 mL) under a N₂ atmosphere was added a solution of NaHMDS in PhMe (0.6 M, 16.5 mL, 9.90 mmol) over two minutes. After an additional 1 minute, a solution of diketopiperazine **194** (59.2 mg, 0.165 mmol) in 18 mL THF was added dropwise via syringe to the previously described solution of reagents over 1.5 minutes (the flask that had contained the solution of **194** was rinsed with an additional 9 mL portion of THF, which was transferred to the reaction vessel). After 50 min, the reaction was quenched with sat. *aq.* NaHCO₃ solution and extracted with EtOAc (3x). The combined organic layers were dried over Na₂SO₄, filtered, and concentrated *in vacuo* to provide the crude product, which was purified by silica gel flash chromatography (gradient elution, 3:1→3:2 hexanes–EtOAc followed by

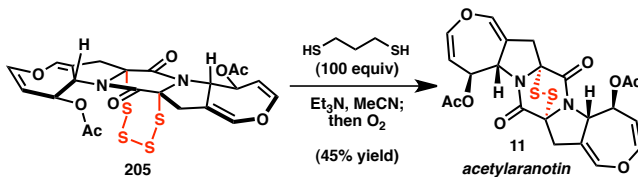
100% EtOAc) to afford epitetrathiodiketopiperazine **197** (61.0 mg, 76% yield) as a yellow solid.

Preparation of diacetate 205



To a stirred solution of diol **197** (3.11 mg, 6.43 μmol) and DMAP (20 mg, 0.16 mmol) in CH_2Cl_2 (0.64 mL) at 0 °C was added acetyl chloride (6.9 μL , 97 μmol). After 10 min, the ice bath was removed and the reaction mixture was allowed to warm to room temperature. After an additional 30 min, the reaction mixture was quenched with H_2O and extracted five times with a mixture of hexanes and EtOAc (1:1). Each organic fraction was passed individually through a plug of SiO_2 , which was subsequently rinsed with excess hexanes/EtOAc. The combined filtrates were concentrated *in vacuo* to provide the crude product, which was purified by silica gel flash chromatography (gradient elution, 3:1 → 3:2 hexanes–EtOAc) to afford diacetate **205** (2.57 mg, 70% yield) as a yellow solid. $[\alpha]_D^{25.0} = -476.6^\circ$ ($c = 0.1285$, CHCl_3); ^1H NMR (500 MHz, CDCl_3) δ 6.57 (ddd, $J = 2.5, 2.5, 0.9$ Hz, 2H), 6.27 (dd, $J = 8.2, 2.4$ Hz, 2H), 5.30 (ddd, $J = 8.5, 2.6, 1.4$ Hz, 2H), 5.20 (ddd, $J = 8.4, 2.2, 2.2$ Hz, 2H), 4.70 (dd, $J = 8.2, 1.9$ Hz, 2H), 3.36 (ddd, $J = 16.4, 2.2, 2.2$ Hz, 2H), 3.07 (ddd, $J = 16.3, 1.2, 1.2$ Hz, 2H), 2.18 (s, 6H); ^{13}C NMR (126 MHz, CDCl_3) δ 170.4, 165.7, 139.7, 138.7, 108.0, 106.0, 75.7, 71.1, 60.8, 41.7, 21.5; IR (NaCl/thin film): 2917, 2849, 1739, 1695, 1370, 1237, 1136 cm^{-1} ; HRMS (Multimode-ESI/APCI) calc'd for $\text{C}_{20}\text{H}_{17}\text{N}_2\text{O}_6\text{S}_4$ [$\text{M}-\text{C}_2\text{H}_3\text{O}_2$] $^+$ 508.9964, found 508.9961 (detected fragment has undergone loss of acetate anion).

Preparation of acetylaranotin (**11**)



A solution of tetrasulfide **205** (2.40 mg, 4.22 μmol) in CH_2Cl_2 (0.5 mL) was diluted with MeCN (12 mL), then treated with a solution of Et_3N in MeCN (0.2 μL , 1.4 μmol in 50 μL of MeCN), followed by propanedithiol (42 μL , 0.42 mmol). The resulting mixture was allowed to stand for 20 min, and was then washed with hexanes (5 x 8 mL, the final hexanes wash was back-extracted once with MeCN to ensure material recovery), and concentrated *in vacuo*. The resulting residue was dissolved in $\text{CH}_2\text{Cl}_2/\text{PhMe}$ and loaded onto a short plug of SiO_2 . Residual propanedithiol and other nonpolar impurities were eluted with 4:1 hexanes– EtOAc before the presumed dithiol intermediate was eluted with 100% EtOAc . The EtOAc fractions (~25 mL total) were combined and diluted with EtOAc (10 mL) and MeOH (70 mL), and the resulting solution was sparged with O_2 for 15 min, then allowed to stand under an O_2 atmosphere for ~6 h. The solution was then concentrated *in vacuo*, and purified by preparative HPLC (normal phase, isocratic elution, 33% EtOAc in hexanes) to afford acetylaranotin (**11**) (0.96 mg, 45% yield) as a white solid. $[\alpha]_D^{25.0} = -401.5^\circ$ ($c = 0.048$, CHCl_3); ^1H NMR (400 MHz, CDCl_3) δ 6.61 (ddd, $J = 2.1, 2.1, 2.1$ Hz, 2H), 6.30 (dd, $J = 8.2, 2.2$ Hz, 2H), 5.67 (ddd, $J = 8.5, 2.0, 2.0$ Hz, 2H), 5.10 (dddd, $J = 8.4, 1.7, 1.7, 1.7$ Hz, 2H), 4.60 (dd, $J = 8.2, 1.8$ Hz, 2H), 4.10 (ddd, $J = 18.2, 2.3, 1.3$ Hz, 2H), 2.98 (ddd, $J = 18.2, 1.7, 1.7$ Hz, 2H), 2.02 (s, 6H); ^1H NMR (500 MHz, $\text{DMSO}-d_6$) δ 6.82 (ddd, $J = 2.1, 2.1, 2.1$ Hz, 2H), 6.45 (dd, $J = 8.2, 2.2$ Hz, 2H), 5.42 (ddd, $J = 8.5, 2.0, 2.0$ Hz, 2H), 5.02 (dddd, $J = 8.5, 1.9, 1.4, 1.4$ Hz, 2H),

4.60 (dd, $J = 8.0, 1.8$ Hz, 2H), 3.85 (ddd, $J = 18.3, 2.5, 1.3$ Hz, 2H), 3.23 (ddd, $J = 18.3, 1.6, 1.6$ Hz, 2H), 1.90 (s, 6H); ^{13}C NMR (126 MHz, DMSO- d_6) δ 169.7, 162.3, 141.6, 139.2, 114.0, 105.4, 76.4, 70.0, 62.9, 34.1, 21.2; IR (NaCl/thin film): 2917, 2849, 1739, 1709, 1652, 1356, 1231, 1141, 1040 cm^{-1} ; HRMS (Multimode-ESI/APCI) calc'd for $\text{C}_{20}\text{H}_{17}\text{N}_2\text{O}_6\text{S}_2$ [$\text{M}-\text{C}_2\text{H}_3\text{O}_2$] $^+$ 445.0523, found 445.0522 (detected fragment has undergone loss of acetate anion).

Table 2.7. Comparison of spectroscopic data for natural and synthetic acetylaranotin (**11**).

^1H NMR Data (CDCl₃, data for synthetic material referenced to CHCl₃ at 7.26 ppm)^a

Reported (τ) ^{1c}	Reported (δ)	Synthetic
3.37	6.63 (ddd, $J = 2.3, 2.2, 1.4$ Hz, 2H)	6.61 (ddd, $J = 2.1, 2.1, 2.1$ Hz, 2H)
3.68	6.32 (dd, $J = 7.5, 2.1$ Hz, 2H)	6.30 (dd, $J = 8.2, 2.2$ Hz, 2H)
4.32	5.68 (ddd, $J = 8.7, 2.1, 1.5$ Hz, 2H)	5.67 (ddd, $J = 8.5, 2.0, 2.0$ Hz, 2H)
4.91	5.09 (dddd, $J = 8.7, 2.3, 1.4, 1.3$ Hz, 2H)	5.10 (dddd, $J = 8.4, 1.7, 1.7, 1.7$ Hz, 2H)
5.37	4.63 (dd, $J = 7.5, 1.5$ Hz, 2H)	4.60 (dd, $J = 8.2, 2.2$ Hz, 2H)
5.88	4.12 (ddd, $J = 18.0, 2.2, 1.3$ Hz, 2H)	4.10 (ddd, $J = 18.2, 2.3, 1.3$ Hz, 2H)
7.03 ^b	2.97 (ddd, $J = 18.0, 1.4, 1.4$ Hz, 2H)	2.98 (ddd, $J = 18.2, 1.7, 1.7$ Hz, 2H)
— ^c	— ^c	2.02 (s, 6H)

^aReported data was referenced to TMS as an internal standard.

^bReported value is 7.30 ppm, but this is assumed to be a typographical error based on the plot of the spectrum.

^cValue not tabulated.

^1H NMR Data (DMSO- d_6 , data for synthetic material referenced to DMSO at 2.50 ppm)^a

Reported ⁴	Synthetic
6.82 (ddd, $J = 2.5, 2.0, 1.5$ Hz, 2H)	6.82 (ddd, $J = 2.1, 2.1, 2.1$ Hz, 2H)
6.45 (dd, $J = 8.0, 2.5$ Hz, 2H)	6.45 (dd, $J = 8.2, 2.2$ Hz, 2H)
5.42 (ddd, $J = 8.5, 2.5, 2.0$ Hz, 2H)	5.42 (ddd, $J = 8.5, 2.0, 2.0$ Hz, 2H)
5.01 (br ddt, $J = 8.5, 2.0, 1.5$ Hz, 2H)	5.02 (dddd, $J = 8.5, 1.9, 1.4, 1.4$ Hz, 2H)
4.59 (dd, $J = 8.0, 2.0$ Hz, 2H)	4.60 (dd, $J = 8.0, 1.8$ Hz, 2H)
3.84 (br ddd, $J = 18.0, 2.5, 1.5$ Hz, 2H)	3.85 (ddd, $J = 18.3, 2.5, 1.3$ Hz, 2H)
3.22 (br ddd, $J = 18.0, 1.5, 1.5$ Hz, 2H)	3.23 (ddd, $J = 18.3, 1.6, 1.6$ Hz, 2H)
1.90 (s, 6H)	1.90 (s, 6H)

^aReference value not provided for previously reported data.

¹³C NMR Data (DMSO-*d*₆, data for synthetic material referenced to DMSO-*d*₆ at 40.0 ppm)^a

Reported ⁴	Synthetic
169.7	169.7
162.3	162.3
141.6	141.6
139.2	139.2
114.0	114.0
105.4	105.4
76.4	76.4
69.9	70.0
62.9	62.9
34.1	34.1
21.2	21.2

^aReference value not provided for previously reported data.

2.5 NOTES AND REFERENCES

-
- (1) (a) Neuss, N.; Boeck, L. D.; Brannon, D. R.; Cline, J. C.; DeLong, D. C.; Gorman, M.; Huckstep, L. L.; Lively, D. H.; Mabe, J.; Marsh, M. M.; Molloy, B. B.; Nagarajan, R.; Nelson, J. D.; Stark, W. M. *Antimicrob. Agents Chemother.* **1968**, 213. (b) Town, P. W.; Lindh, K. P.; Milstrey, K. P.; Gallo, V. M.; Mayberry, B. R.; Lindsay, H. L.; Miller, P. A. *Antimicrob. Agents Chemother.* **1968**, 225. (c) Nagarajan, R.; Huckstep, L. L.; Lively, D. H.; Delong, D. C.; Marsh, M. M.; Neuss, N. *J. Am. Chem. Soc.* **1968**, 90, 2980. (d) Nagarajan, R.; Neuss, N.; Marsh, M. M. *J. Am. Chem. Soc.* **1968**, 90, 6518. (e) Cosulich, D. B.; Nelson, N. R.; Van den Hende, J. H. *J. Am. Chem. Soc.* **1968**, 90, 6519. (f) Neuss, N.; Nagarajan, R.; Molloy, B. B.; Huckstep, L. L. *Tetrahedron Lett.* **1968**, 42, 4467.
- (2) Kawahara, N.; Nozawa, K.; Nakajima, S.; Kawai, K.; Yamazaki, M. *J. Chem. Soc., Chem. Commun.* **1989**, 951.
- (3) Hegde, V. R.; Dai, P.; Patel, M.; Das, P. R.; Puar, M. S. *Tetrahedron Lett.* **1997**, 38, 911.
- (4) Choi, E. J.; Park, J.-S.; Kim, Y.-J.; Jung, J.-H.; Lee, J. K.; Kwon, H. C.; Yang, H. O. *Journal of Applied Microbiology* **2010**, 110, 304.
- (5) Onodera, H.; Hasegawa, A.; Tsumagari, N.; Nakai, R.; Ogawa, T.; Kanda, Y. *Org. Lett.* **2004**, 6, 4101.
- (6) Previous synthetic studies toward dihydrooxepine ETPs: (a) Gross, U.; Nieger, M.; Bräse, S. *Chem.—Eur. J.* **2010**, 16, 11624. (b) Peng, J. B.; Clive, D. L. J. *J. Org. Chem.* **2009**, 74, 513. (c) Peng, J. B.; Clive, D. L. J. *Org. Lett.* **2007**, 9, 2938.

-
- (d) Goodman, R. M.; Kishi, Y. *J. Am. Chem. Soc.* **1998**, *120*, 9392. (e) Goodman, R. M. Ph.D. Thesis, Harvard University, May **1998**. (f) Cebon, B. I. M. Ph.D. Thesis, University of Melbourne, November **2009**.
- (7) Murdock, K. *C. J. Med. Chem.* **1974**, *17*, 827.
- (8) Chou, W. N.; White, J. B.; Smith, W. B. *J. Am. Chem. Soc.* **1992**, *114*, 4658.
- (9) Leyhane, A. J.; Snapper, M. L. *Org. Lett.* **2006**, *8*, 5183.
- (10) Nicolaou, K. C.; Lu, M.; Totokotsopoulos, S.; Heretsch, P.; Giguère, D.; Sun, Y.-P.; Sarlah, D.; Nguyen, T. H.; Wolf, I. C.; Smee, D. F.; Day, C. W.; Bopp, S.; Winzeler, E. A. *J. Am. Chem. Soc.* **2012**, *134*, 17320.
- (11) Fujiwara, H.; Kurogi, T.; Okaya, S.; Okano, K.; Tokuyama, H. *Angew. Chem. Int. Ed.* **2012**, *51*, 13062.
- (12) Nicolaou, K. C.; Yu, R.; Shi, L.; Cai, Q.; Lu, M.; Heretsch, P. *Org. Lett.* **2013**, *15*, 1994.
- (13) This is presumably the result of directing effects exerted by the remaining diketopiperazine a-methine. See: Poullennec, K. G.; Kelly, A. T.; Romo, D. *Org. Lett.* **2002**, *4*, 2645.
- (14) For reviews of metal vinylidene-mediated transformations, see: (a) Bruneau, C.; Dixneuf, P. H. *Metal Vinylidenes and Allenylenes in Catalysis: From Reactivity to Applications in Synthesis*; Wiley-VCH: Weinheim, **2008**. (b) Trost, B. M.; McClory, A. *Chem.—Asian J.* **2008**, *3*, 164.
- (15) (a) McDonald, F. E.; Connolly, C. B.; Gleason, M. M.; Towne, T. B.; Treiber, K. D. *J. Org. Chem.* **1993**, *58*, 6952. (b) McDonald, F. E.; Schultz, C. C. *J. Am. Chem. Soc.* **1994**, *116*, 9363. (c) Alcázar, E.; Pletcher, J. M.; McDonald, F. E.

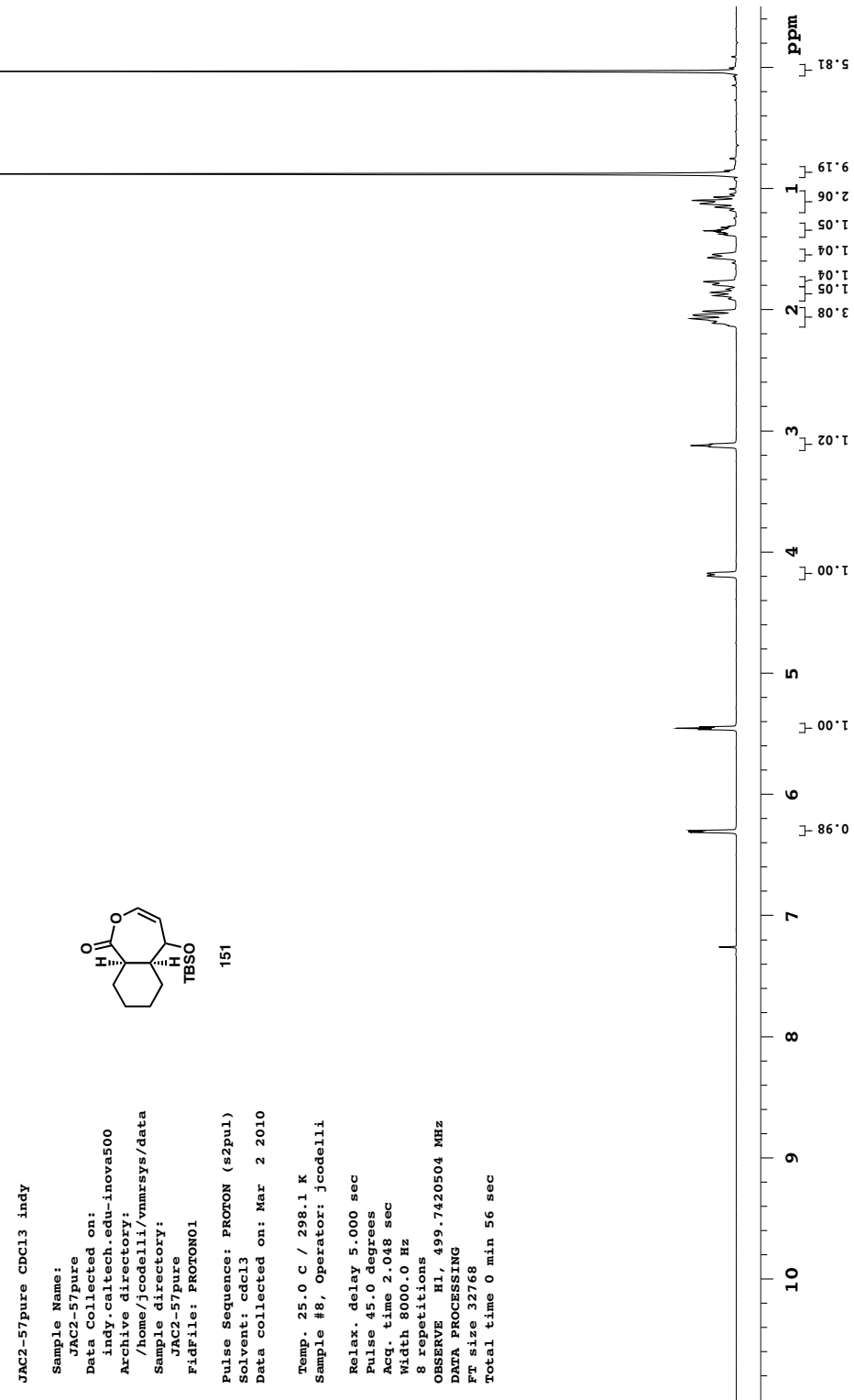
-
- Org. Lett.* **2004**, *6*, 3877. (d) Koo, B.; McDonald, F. E. *Org. Lett.* **2007**, *9*, 1737.
- (16) (a) Trost, B. M.; Rhee, Y. H. *J. Am. Chem. Soc.* **2002**, *124*, 2528. (b) Trost, B. M.; Rhee, Y. H. *J. Am. Chem. Soc.* **1999**, *121*, 11680. (c) Liu, P. N.; Su, F. H.; Wen, T. B.; Sung, H. H.-Y.; Williams, I. D.; Jia, G. *Chem.—Eur. J.* **2010**, *16*, 7889. (d) Varela-Fernández, A.; García-Yebra, C.; Varela, J. A.; Esteruelas, M. A.; Saá, C. *Angew. Chem., Int. Ed.* **2010**, *49*, 4278.
- (17) (a) Trost, B. M.; Rhee, Y. H. *J. Am. Chem. Soc.* **2003**, *125*, 7482. (b) Trost, B. M.; McClory, A. *Angew. Chem., Int. Ed.* **2007**, *46*, 2074.
- (18) Metal-catalyzed 6-endo cyclization of aldehydes onto terminal alkynes in the presence of secondary nucleophiles: (a) Yao, X.; Li, C.-J. *Org. Lett.* **2006**, *8*, 1953. (b) Patil, N. T.; Yamamoto, Y. *J. Org. Chem.* **2004**, *69*, 5139. (c) Asao, N.; Nogami, T.; Takahashi, K.; Yamamoto, Y. *J. Am. Chem. Soc.* **2002**, *124*, 764.
- (19) Jiménez-Tenorio, M.; Puerta, M. C.; Valerga, P.; Moreno-Dorado, F. J.; Guerra, F. M.; Massanet, G. M. *Chem. Commun.* **2001**, 2324.
- (20) Conditions were adapted from ref. 17
- (21) Conditions were adapted from those described by Schreiber and coworkers for the synthesis of racemic pyrrolidines. See the supporting information of: Chen, C.; Li, X. D.; Schreiber, S. L. *J. Am. Chem. Soc.* **2003**, *125*, 10174.
- (22) Mitsunobu, O. *Synthesis* **1981**, 1.
- (23) Kiankarimi, M.; Lowe, R.; McCarthy, J. R.; Whitten, J. P. *Tetrahedron Lett.* **1999**, *40*, 4497.
- (24) Dess, D. B.; Martin, J. C. *J. Org. Chem.* **1983**, *48*, 4155.
- (25) Bal, B. S.; Childers, W. E., Jr.; Pinnick, H. W. *Tetrahedron* **1981**, *37*, 2091.

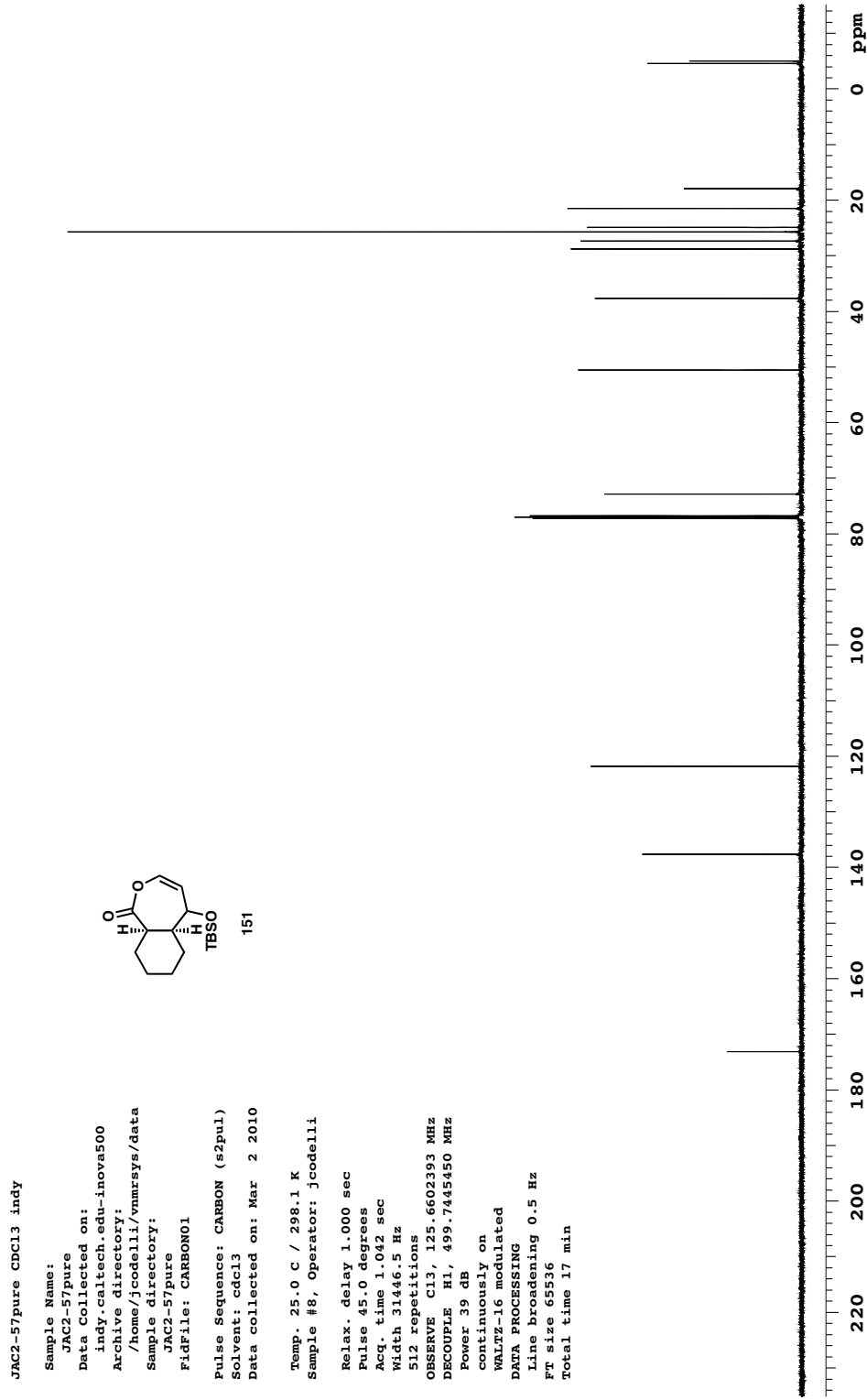
-
- (26) Examples of gold(I)-catalyzed 6-*exo* cyclization of alkynoic acids: (a) Harkat, H.; Dembelé, A. Y.; Weibel, J.-M.; Blanc, A.; Pale, P. *Tetrahedron* **2009**, *65*, 1871. (b) Marchal, E.; Uriac, P.; Legouin, B.; Toupet, L.; van de Weghe, P. *Tetrahedron* **2007**, *63*, 9979. (c) Harkat, H.; Weibel, J.-M.; Pale, P. *Tetrahedron Lett.* **2006**, *47*, 6273.
- (27) (a) Joly, R.; Warnant, J.; Nomine, G.; Bertin, D. *Bull. Soc. Chem. Fr.* **1958**, 366. (b) Ho, T.-L. *Synth. Commun.* **1981**, *11*, 7. (c) Weisz, A.; Mandelbaum, A. *J. Org. Chem.* **1984**, *49*, 2648. (d) Demuth, M. R.; Garrett, P. E.; White, J. D. *J. Am. Chem. Soc.* **1976**, *98*, 634.
- (28) Ag(I)/(S)-QUINAP: Chen, C.; Li, X. D.; Schreiber, S. L. *J. Am. Chem. Soc.* **2003**, *125*, 10174. Cu(I)/Brucin-OL: Kim, H. Y.; Shih, H.-J.; Knabe, W. E.; Oh, K. *Angew. Chem., Int. Ed.* **2009**, *48*, 7420. Ag(I)/**175**: Zeng, W.; Zhou, Y.-G. *Org. Lett.* **2005**, *7*, 5055. Ag(I)/**176**: Najera, C.; Retamosa, M. D.; Sansano, J. M. *Angew. Chem., Int. Ed.* **2008**, *47*, 6055. For a review of asymmetric (1,3)-dipolar cycloaddition reactions for the preparation of pyrrolidines, see: Pandey, G.; Banerjee, P.; Gadre, S. R. *Chem. Rev.* **2006**, *106*, 4484.
- (29) As part of our optimization to render the Cu(I)/Brucin-OL-catalyzed cycloaddition more scaleable, an alternative procedure was developed relative to that reported in our original communication, which includes a different method for imine preparation as well as acetonitrile as an additive. See the Experimental Section for details.

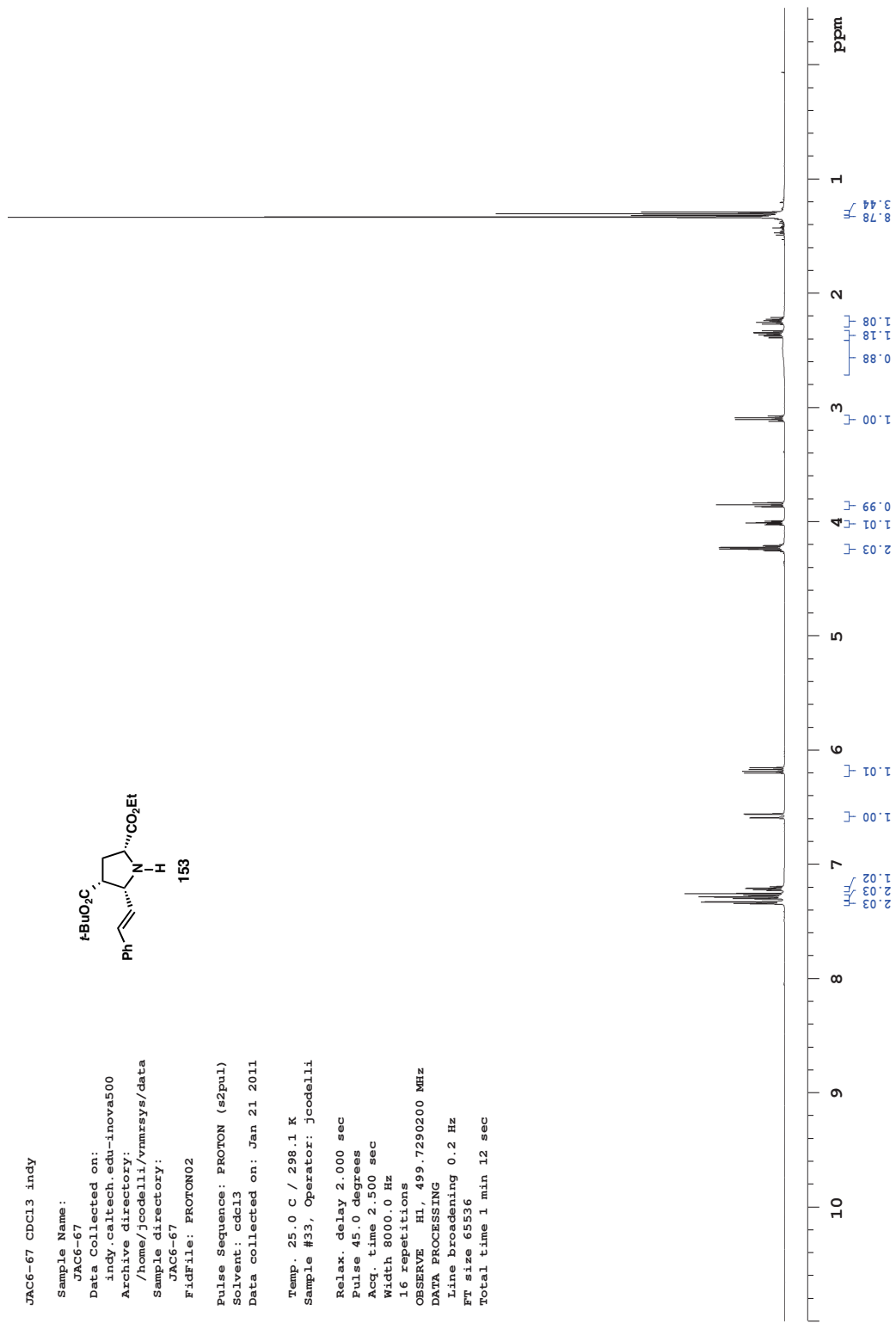
-
- (30) (a) Carpino, L. A.; Tsao, J.-H.; Ringsdorf, H.; Fell, E.; Hettrich, G. *J. Chem. Soc., Chem. Commun.* **1978**, 358. (b) Shute, R. E.; Rich, D. H. *Synthesis* **1987**, 346. (c) Paquet, A. *Can. J. Chem.* **1982**, 60, 976.
- (31) Kim, D.-W.; Jeong, H.-J.; Lim, S.-T.; Sohn, M.-H. *Angew. Chem., Int. Ed.* **2008**, 47, 8404.
- (32) See Chapter 4 for details.
- (33) (a) Nicolaou, K. C.; Totokotsopoulos, S.; Giguère, D.; Sun, Y.-P.; Sarlah, D. *J. Am. Chem. Soc.* **2011**, 133, 8150. (b) Nicolaou, K. C.; Giguère, D.; Totokotsopoulos, S.; Sun, Y.-P. *Angew. Chem., Int. Ed.* **2012**, 51, 728.
- (34) Still, W. C., Kahn, M.; Mitra, A. *J. Org. Chem.* **1978**, 43, 2923.

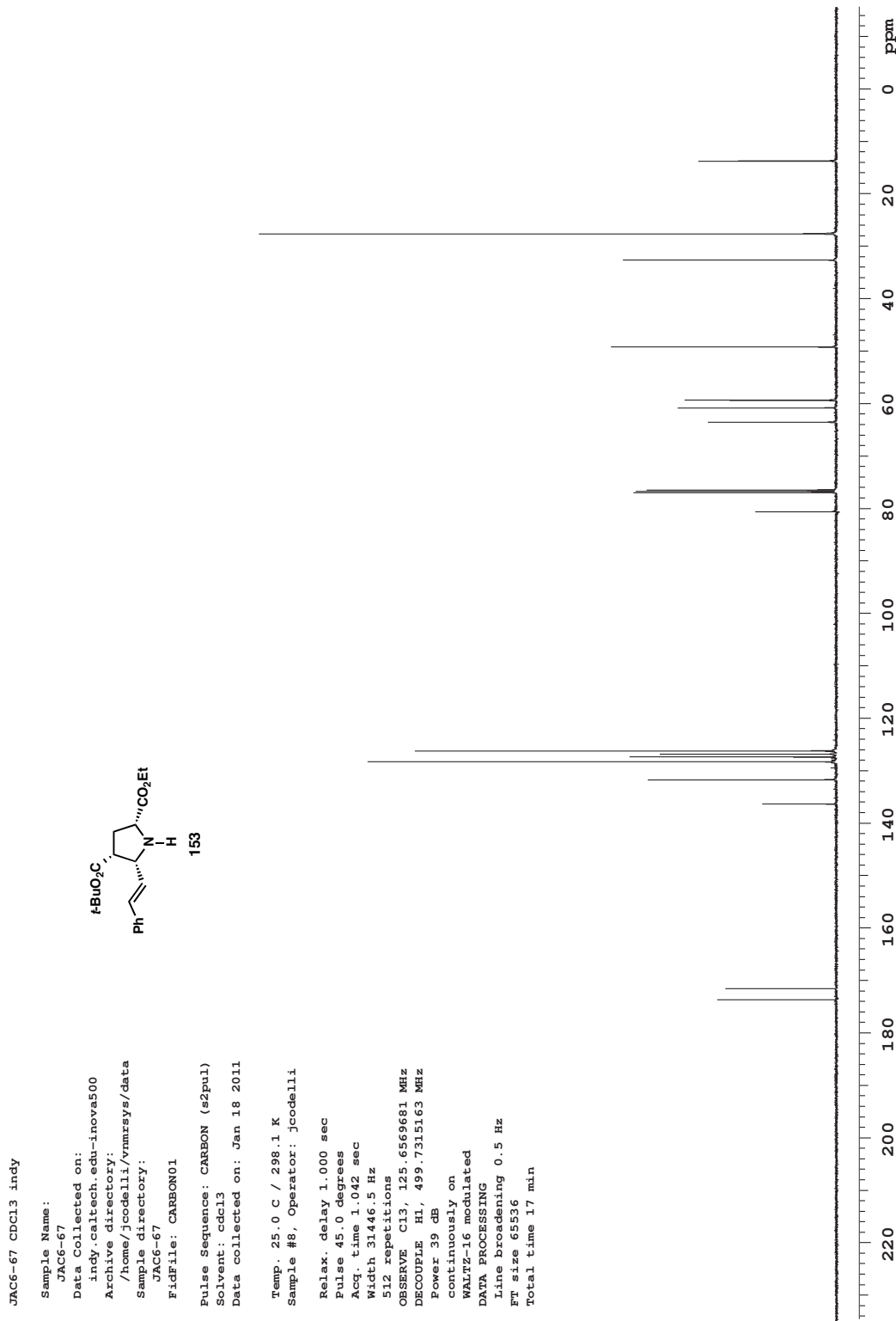
Appendix 1

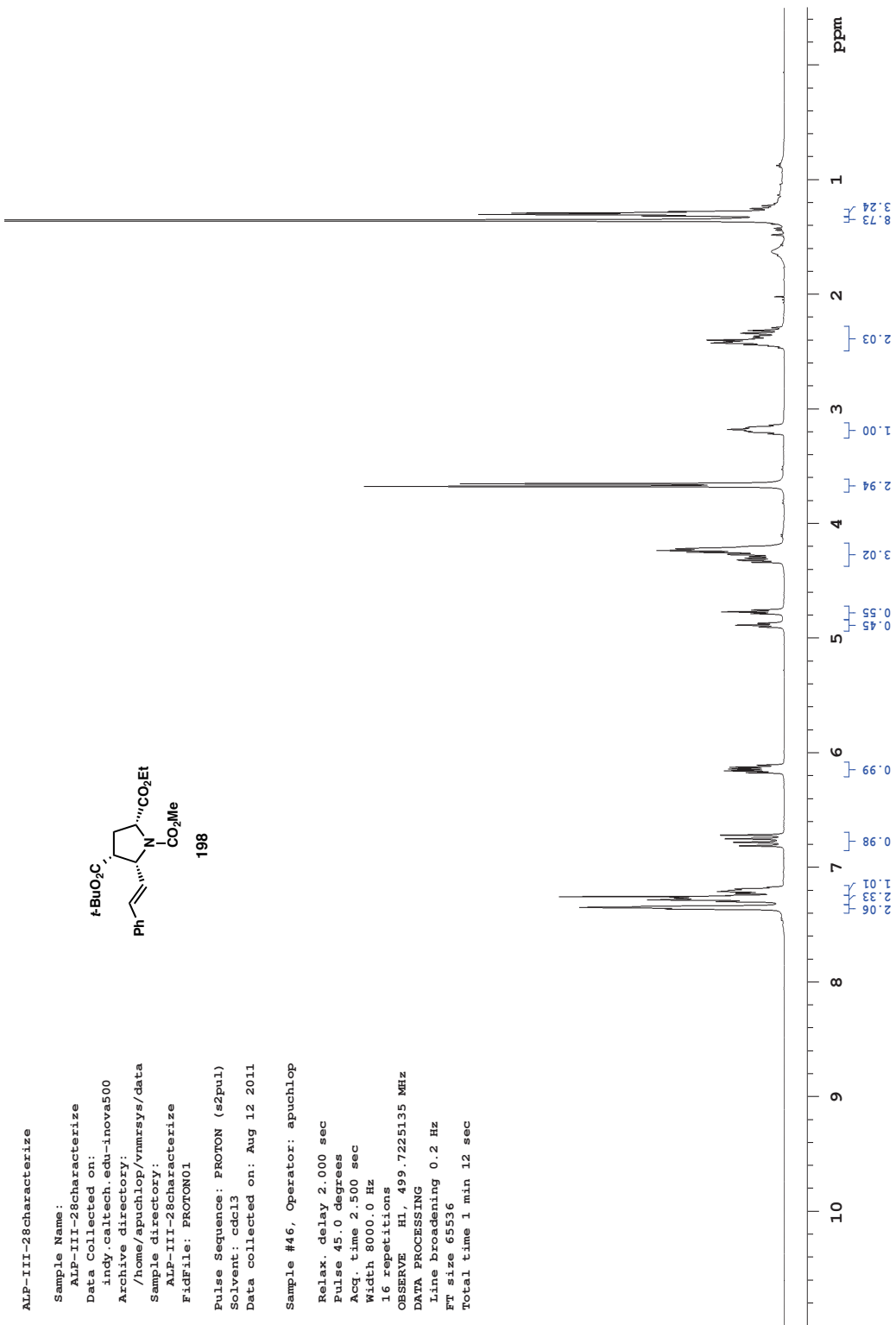
*Spectra Relevant to Chapter 2:
Enantioselective Total Synthesis of (–)-Acetylaranotin*

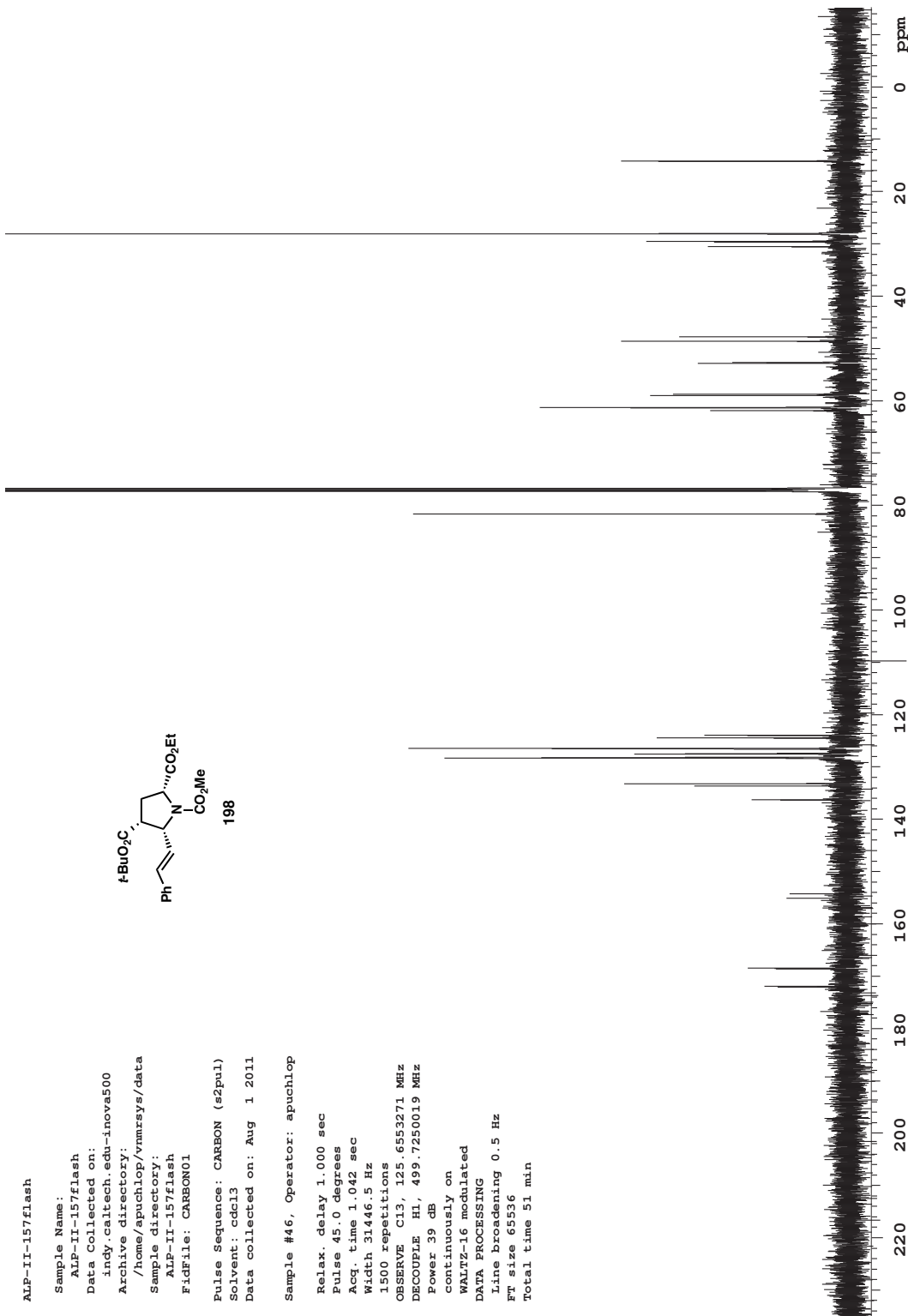


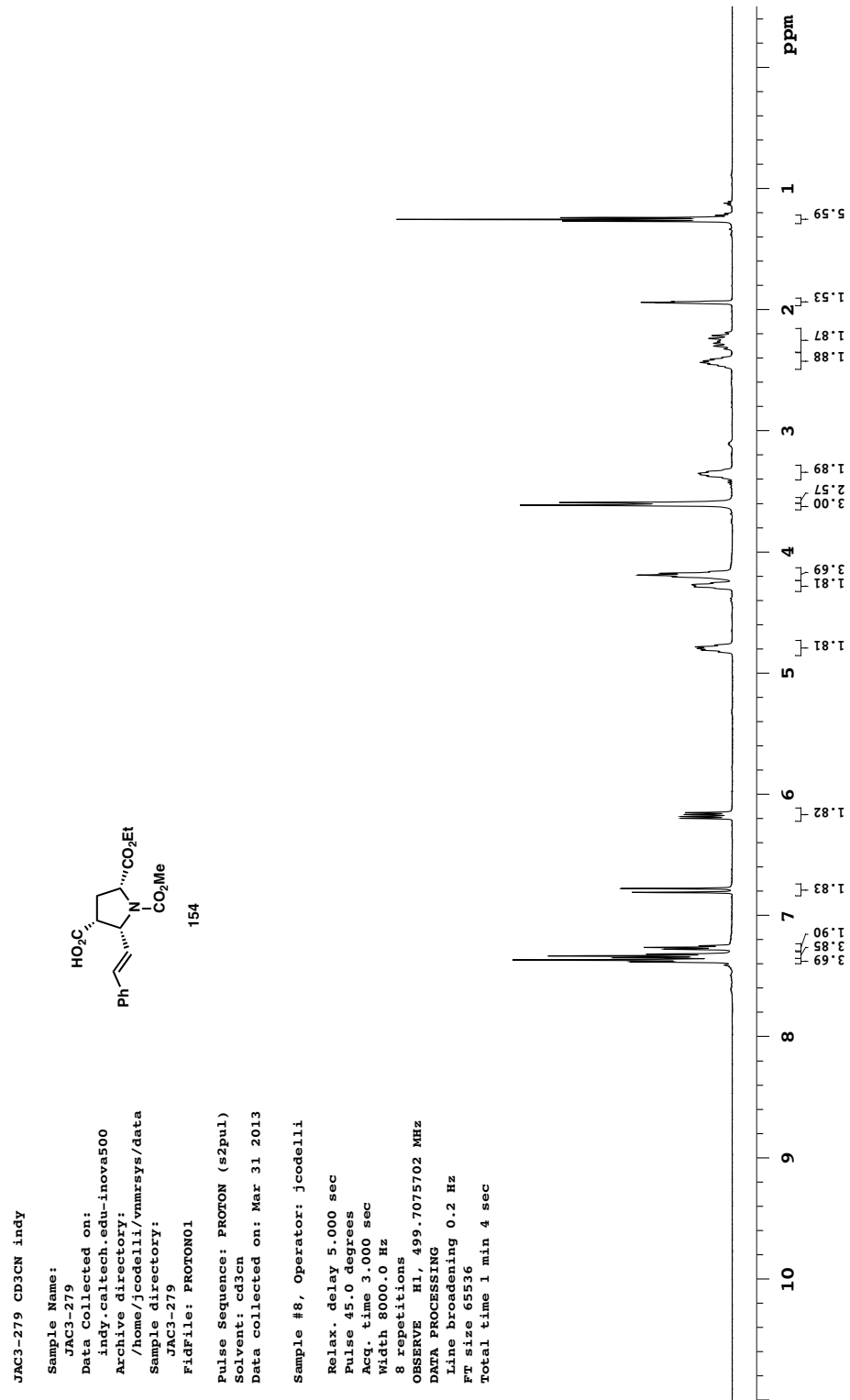


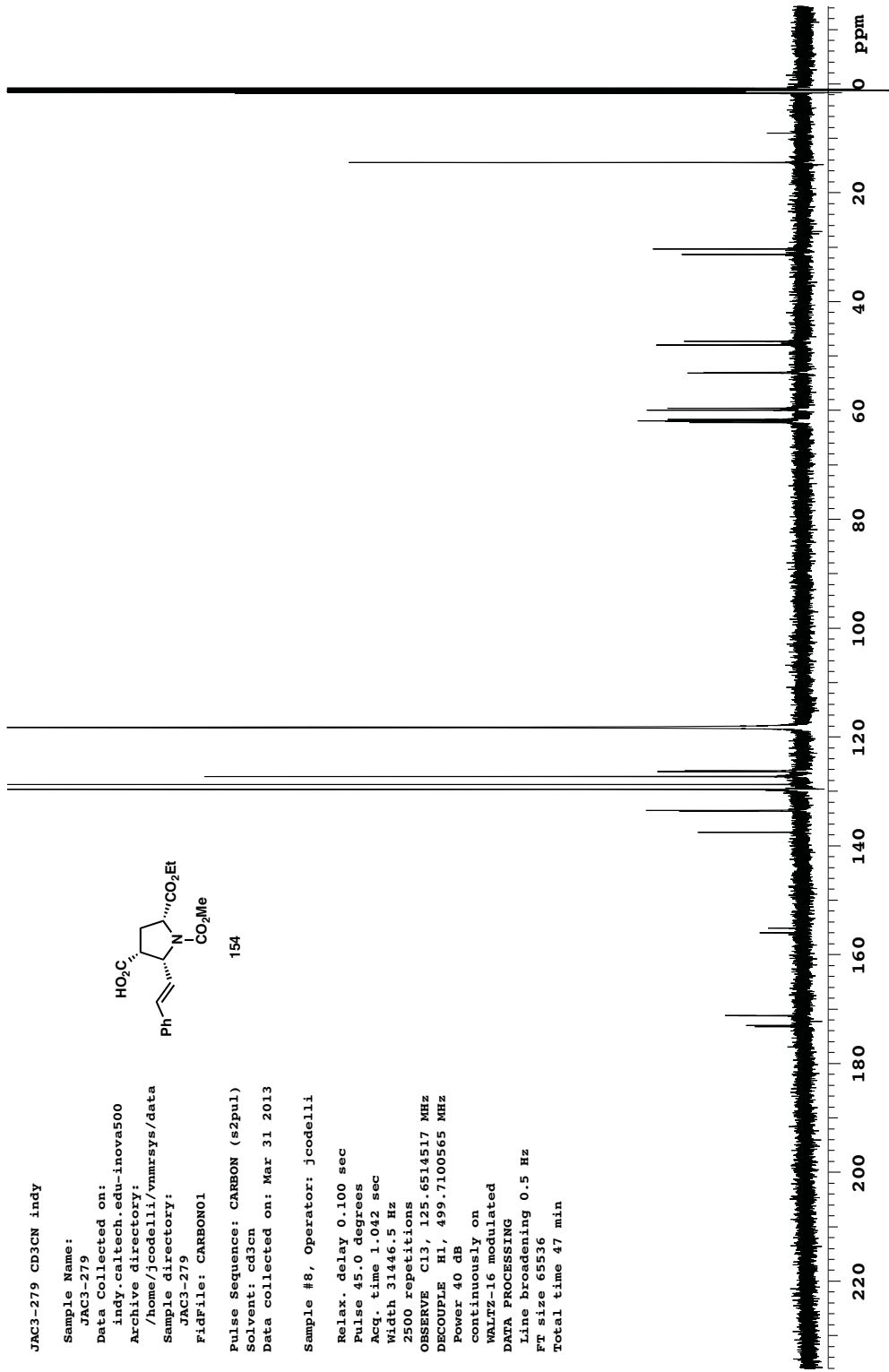


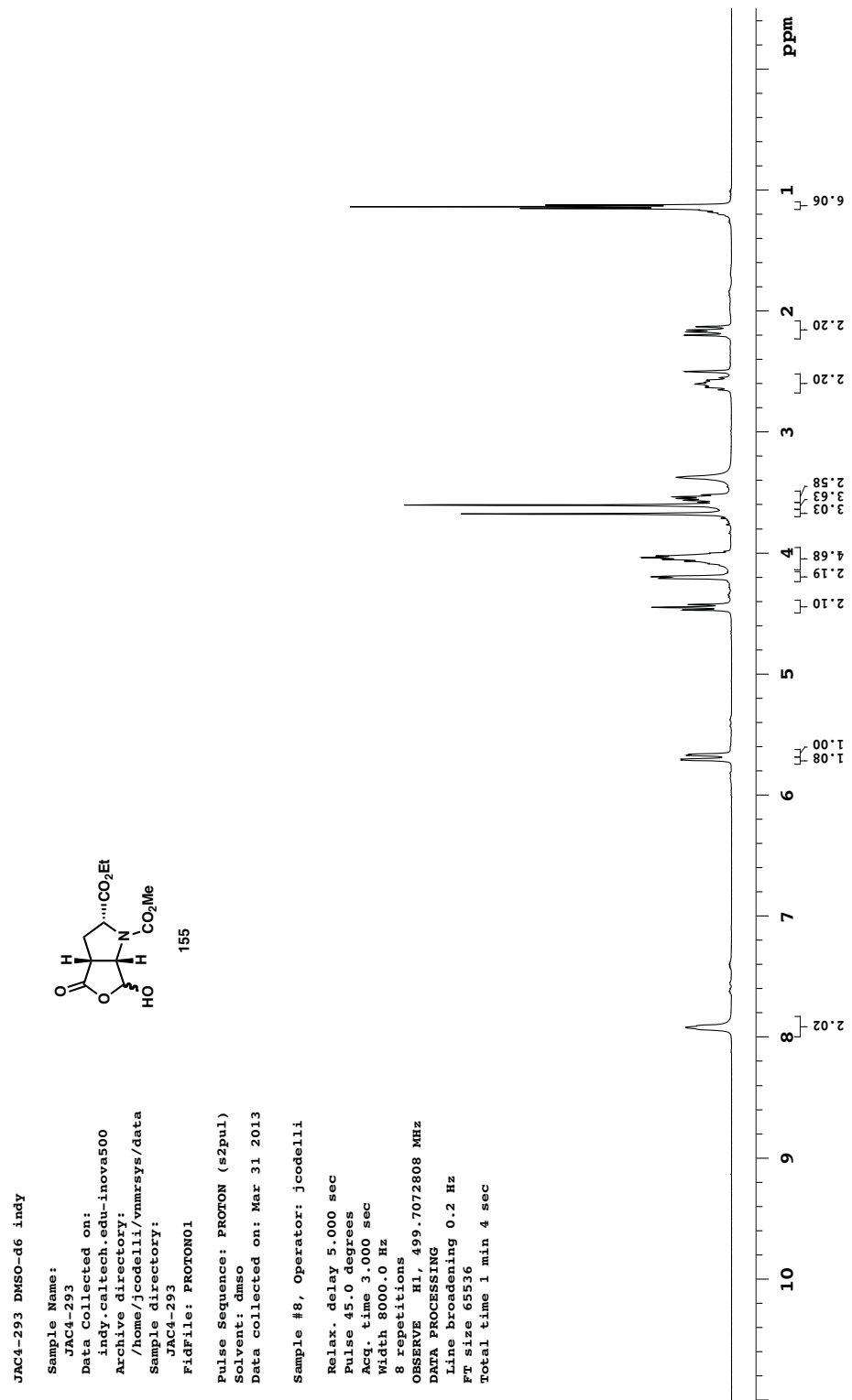


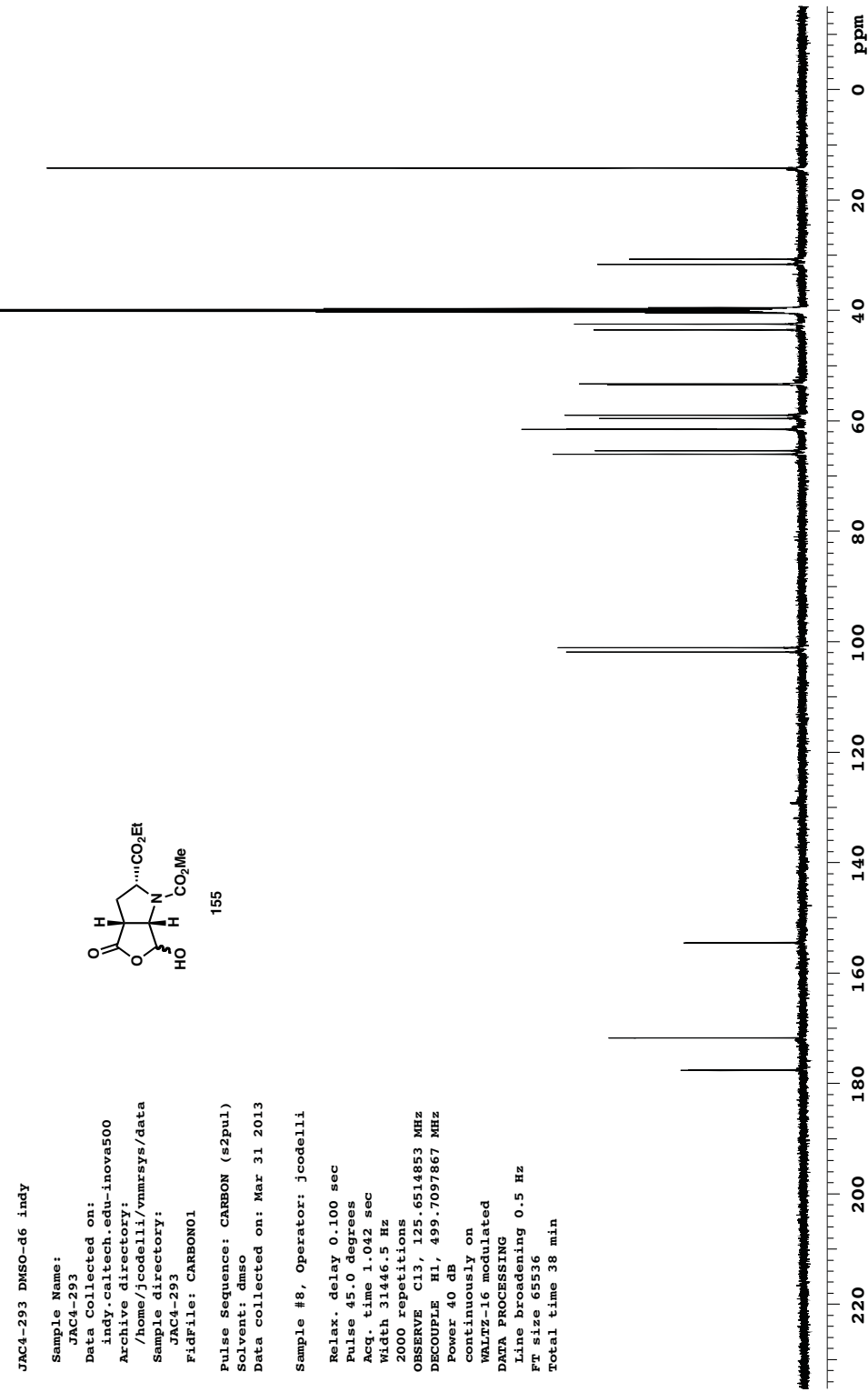


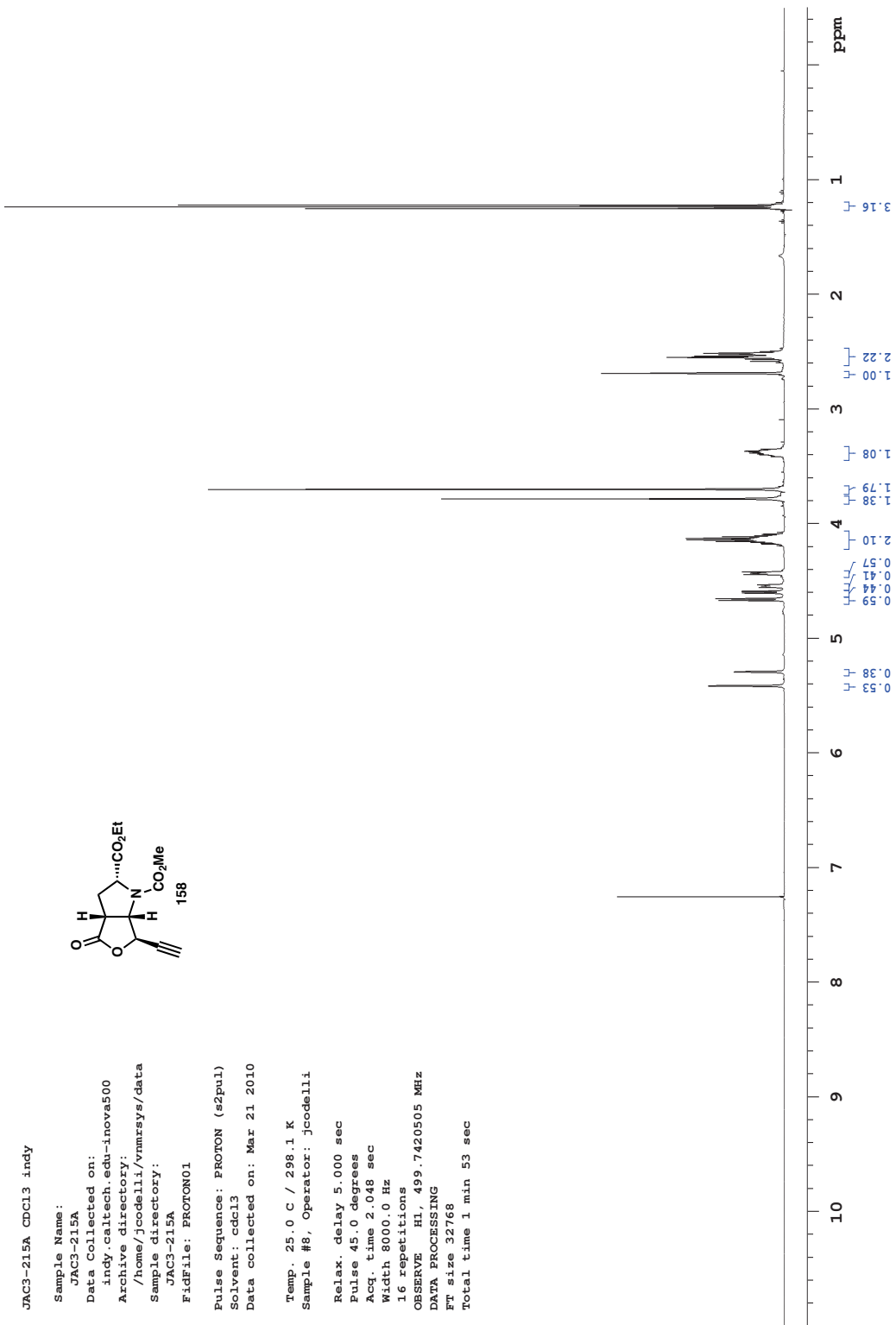


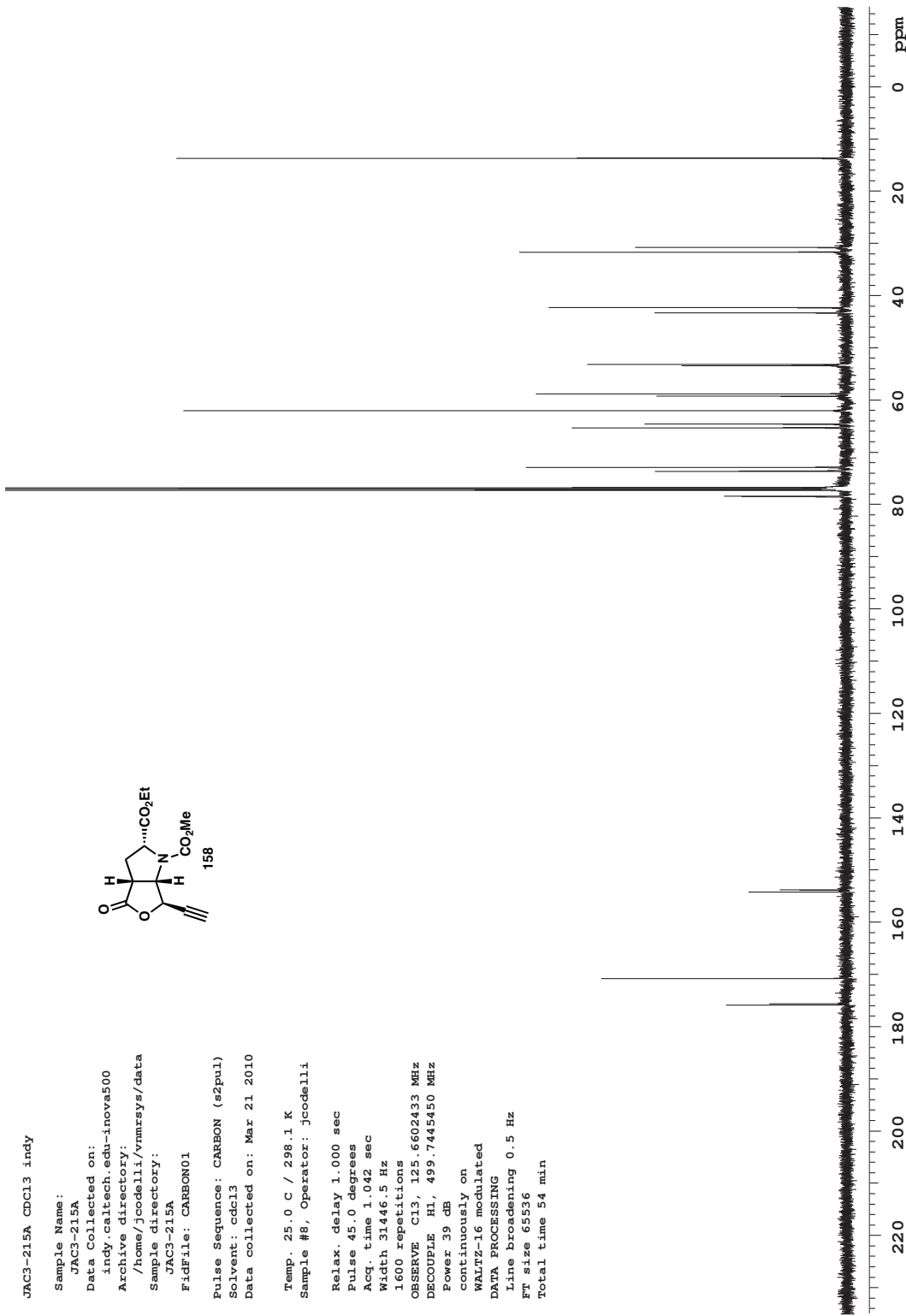


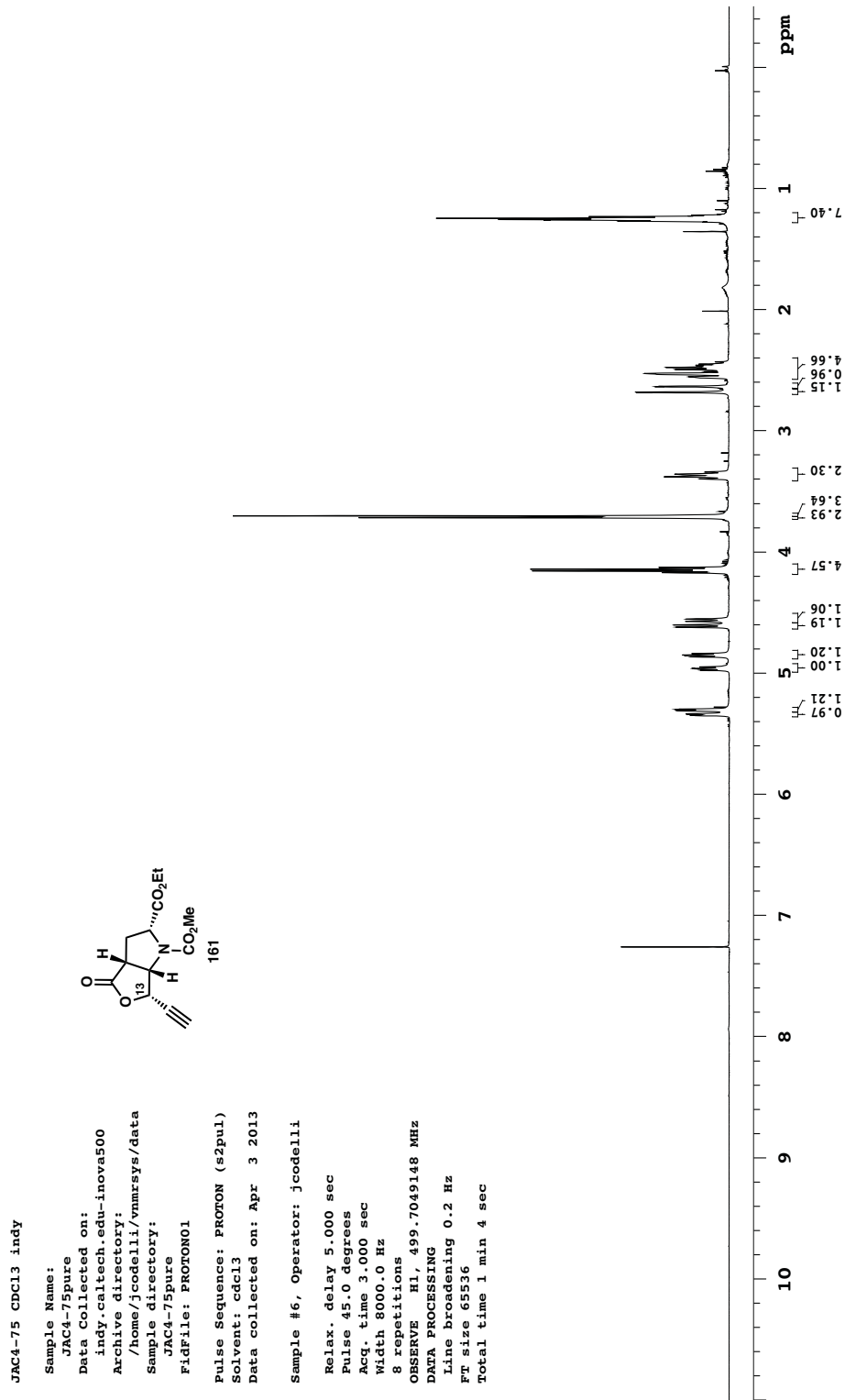


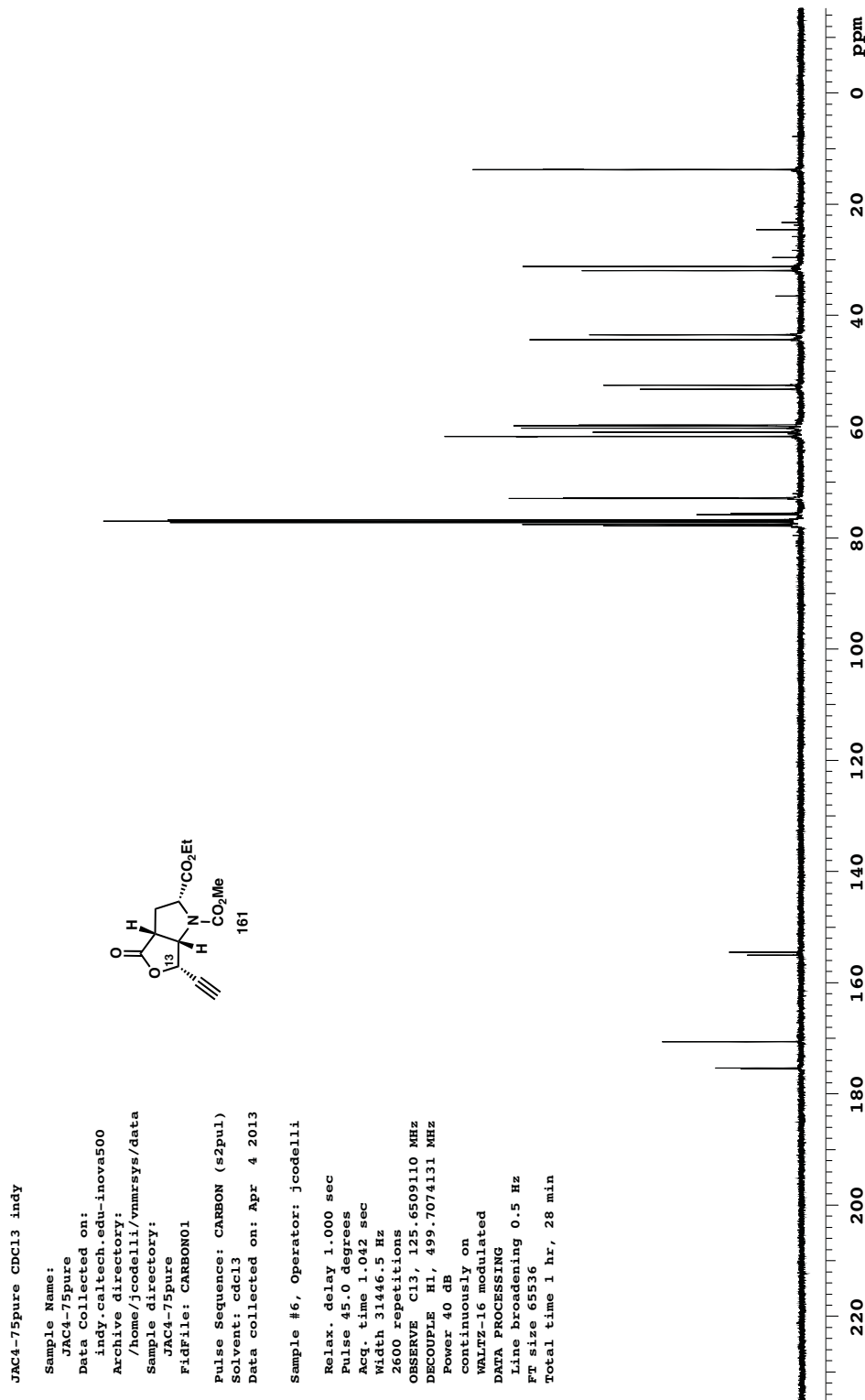


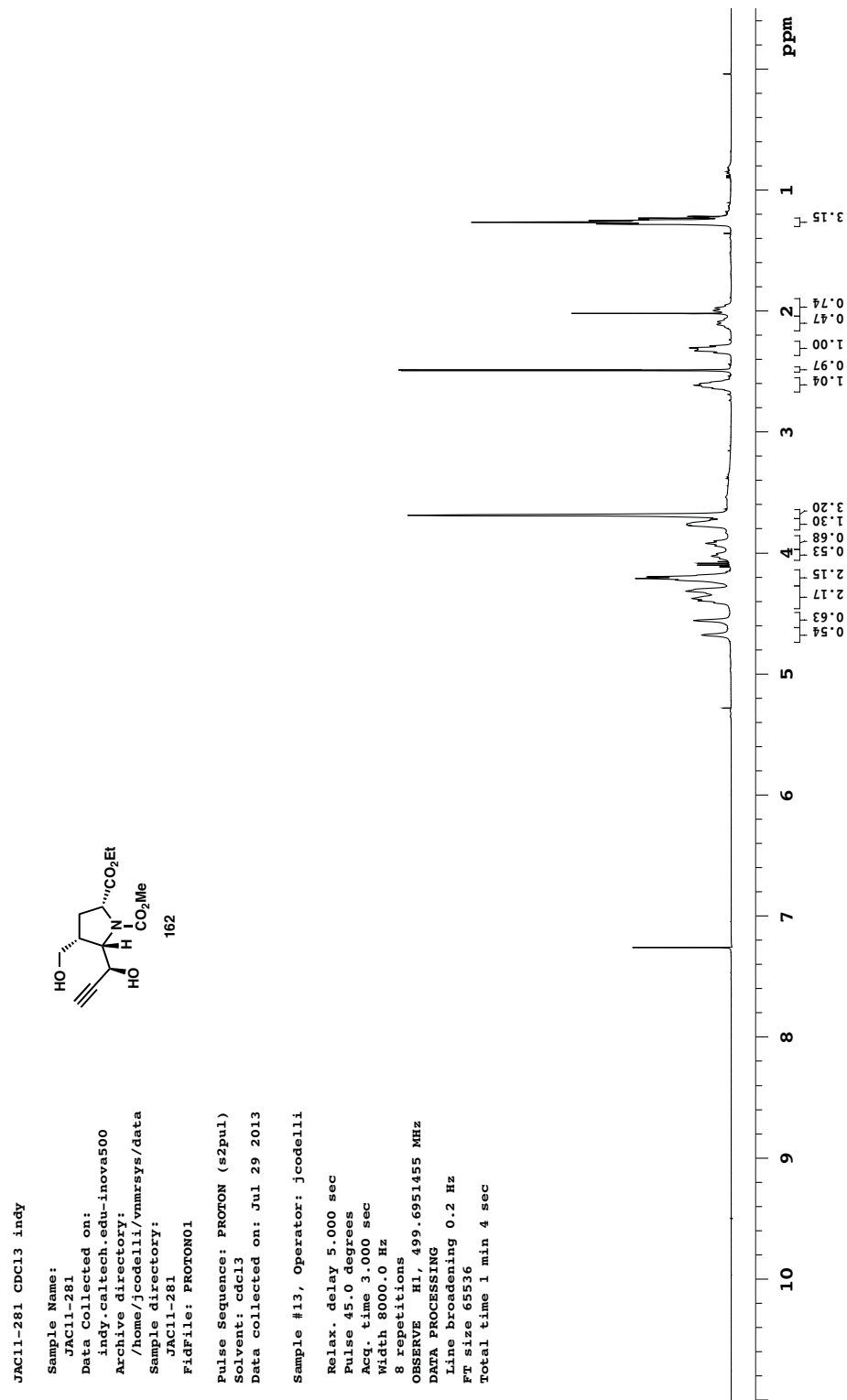


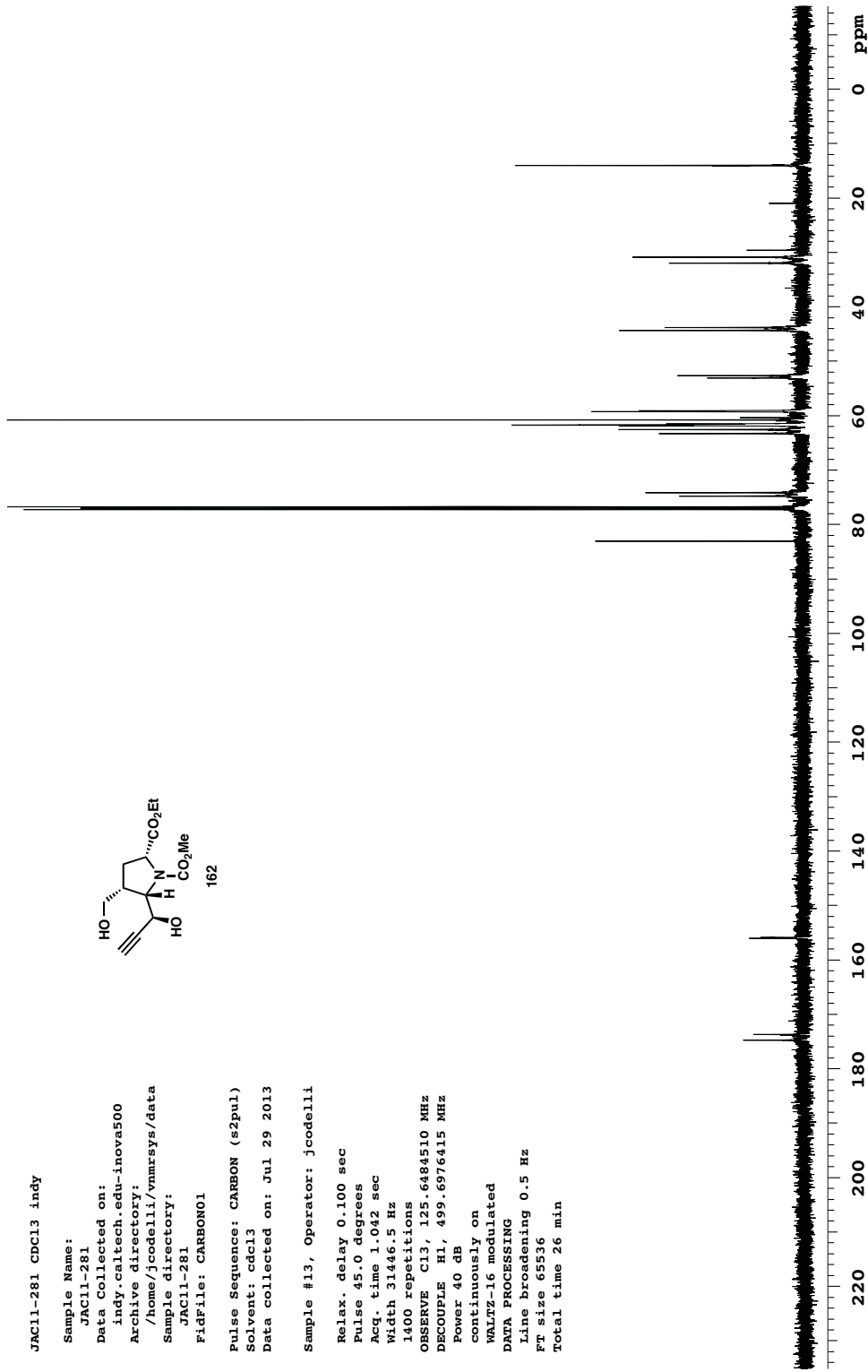


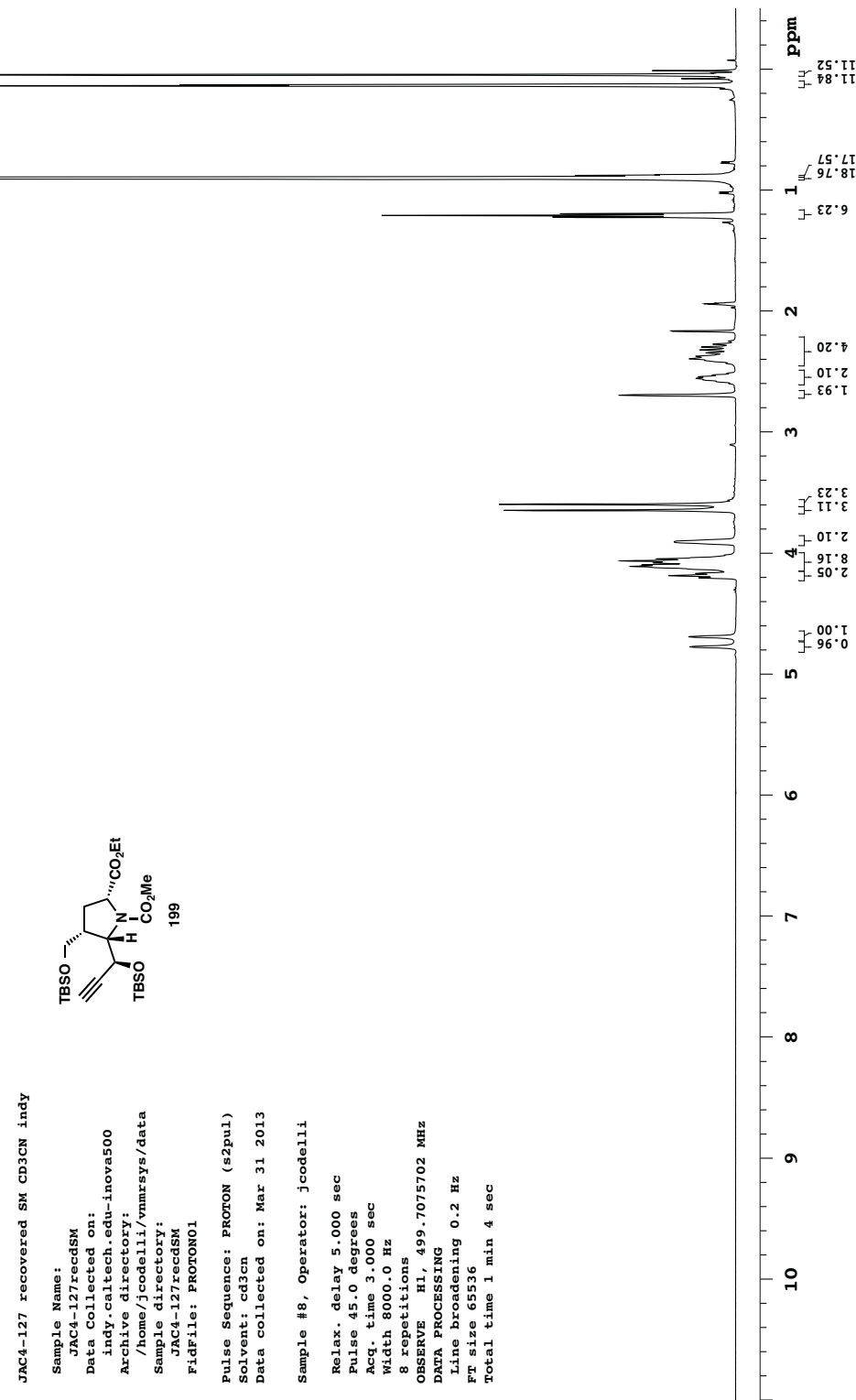


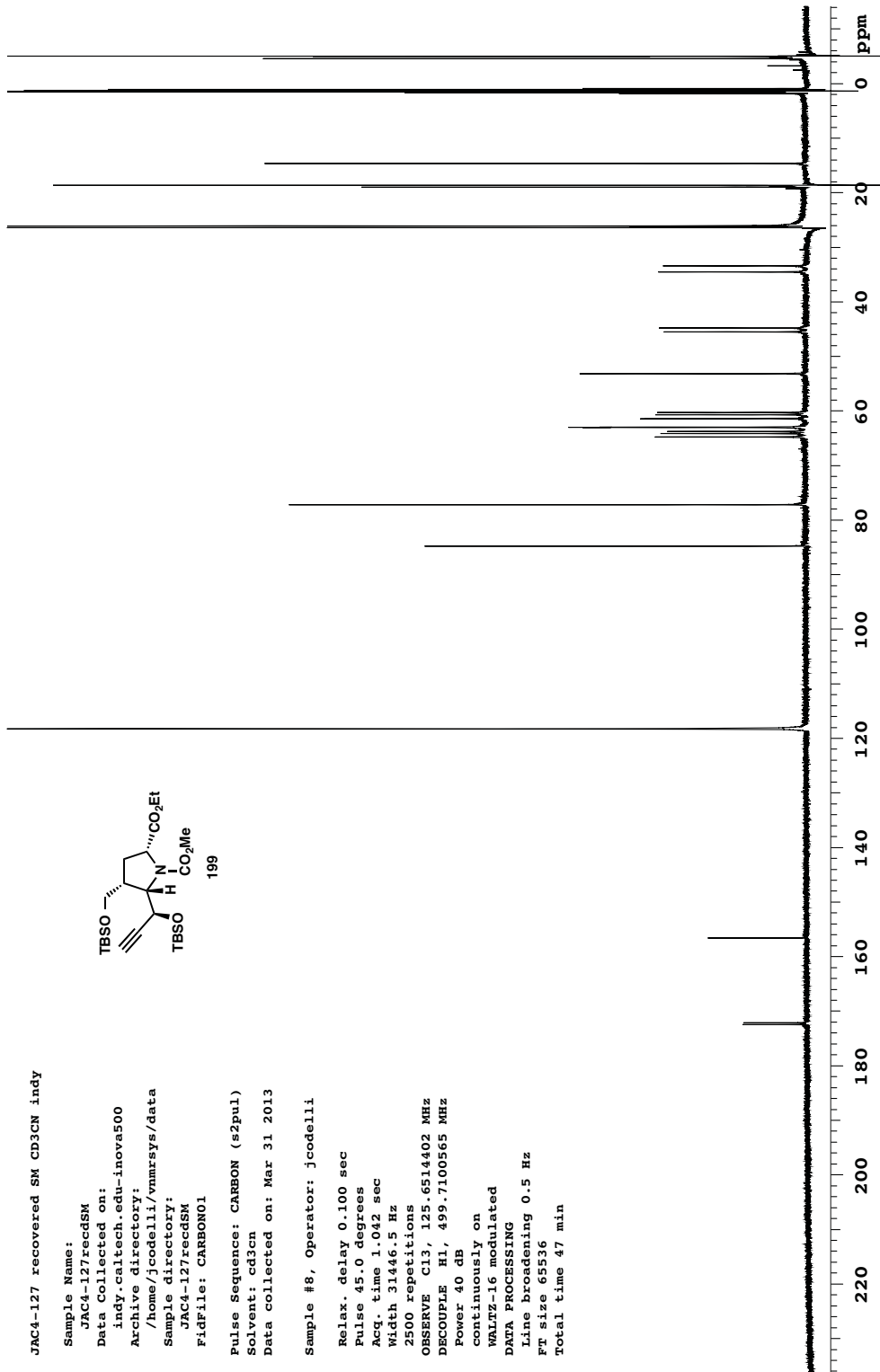


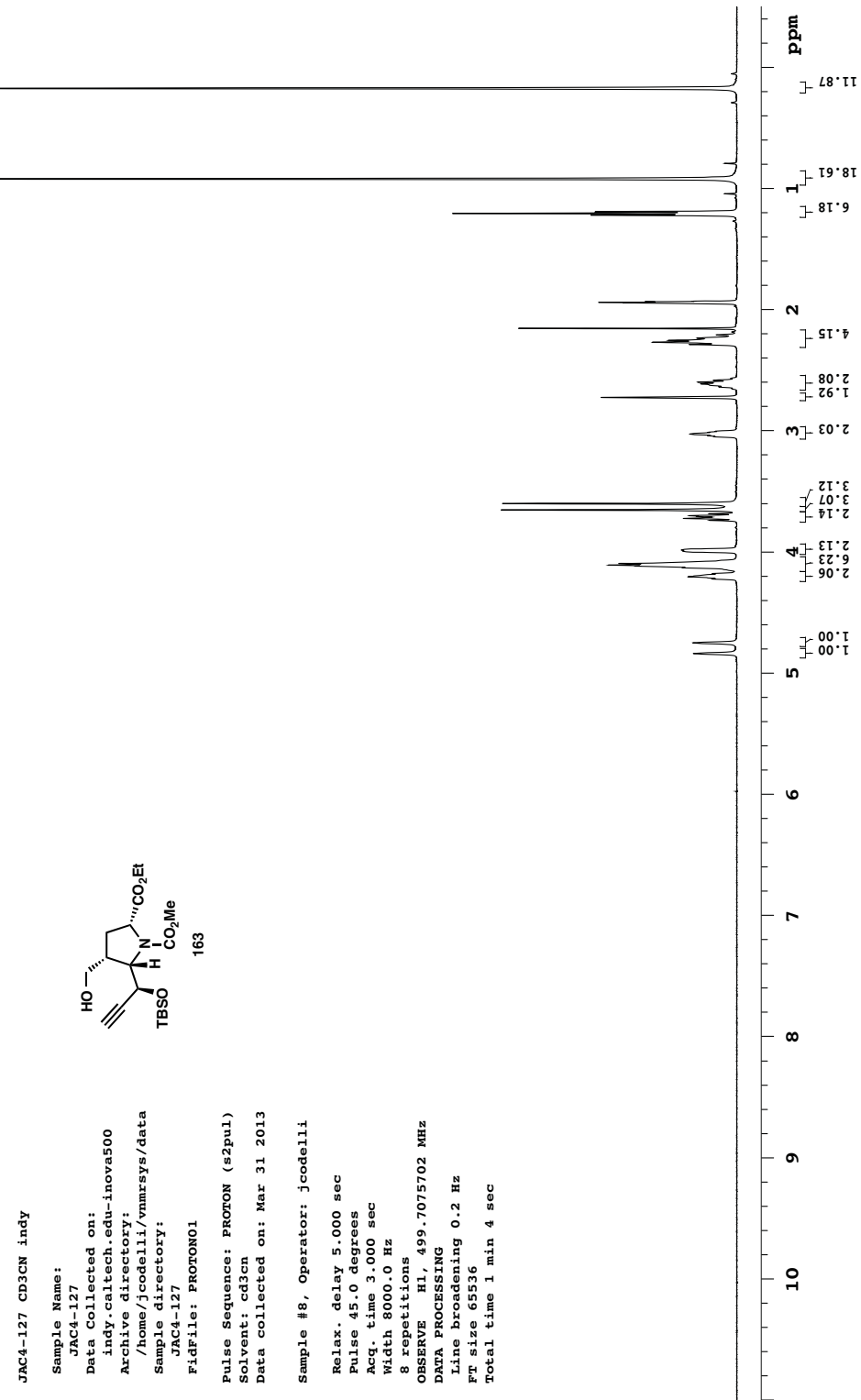


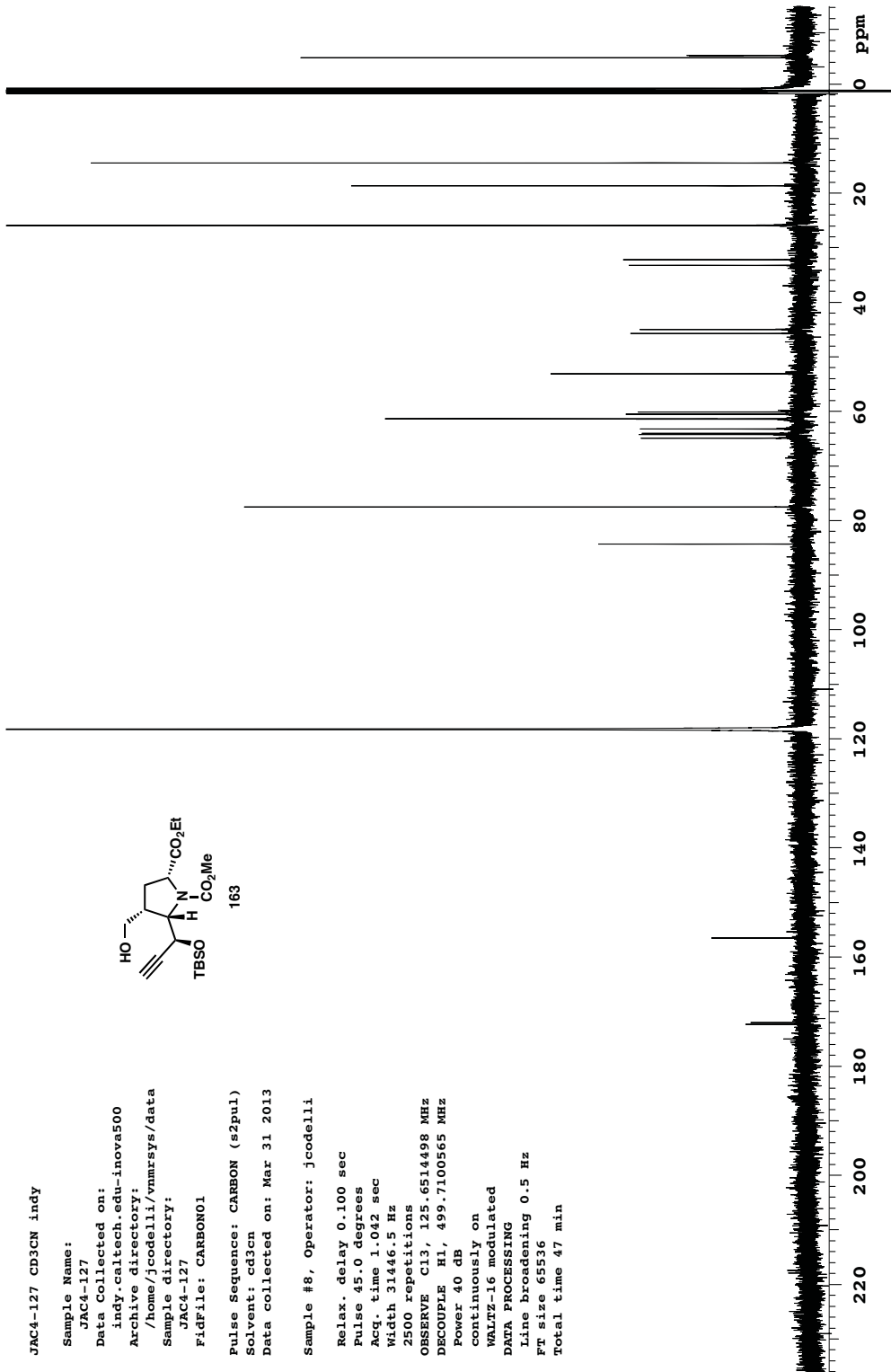


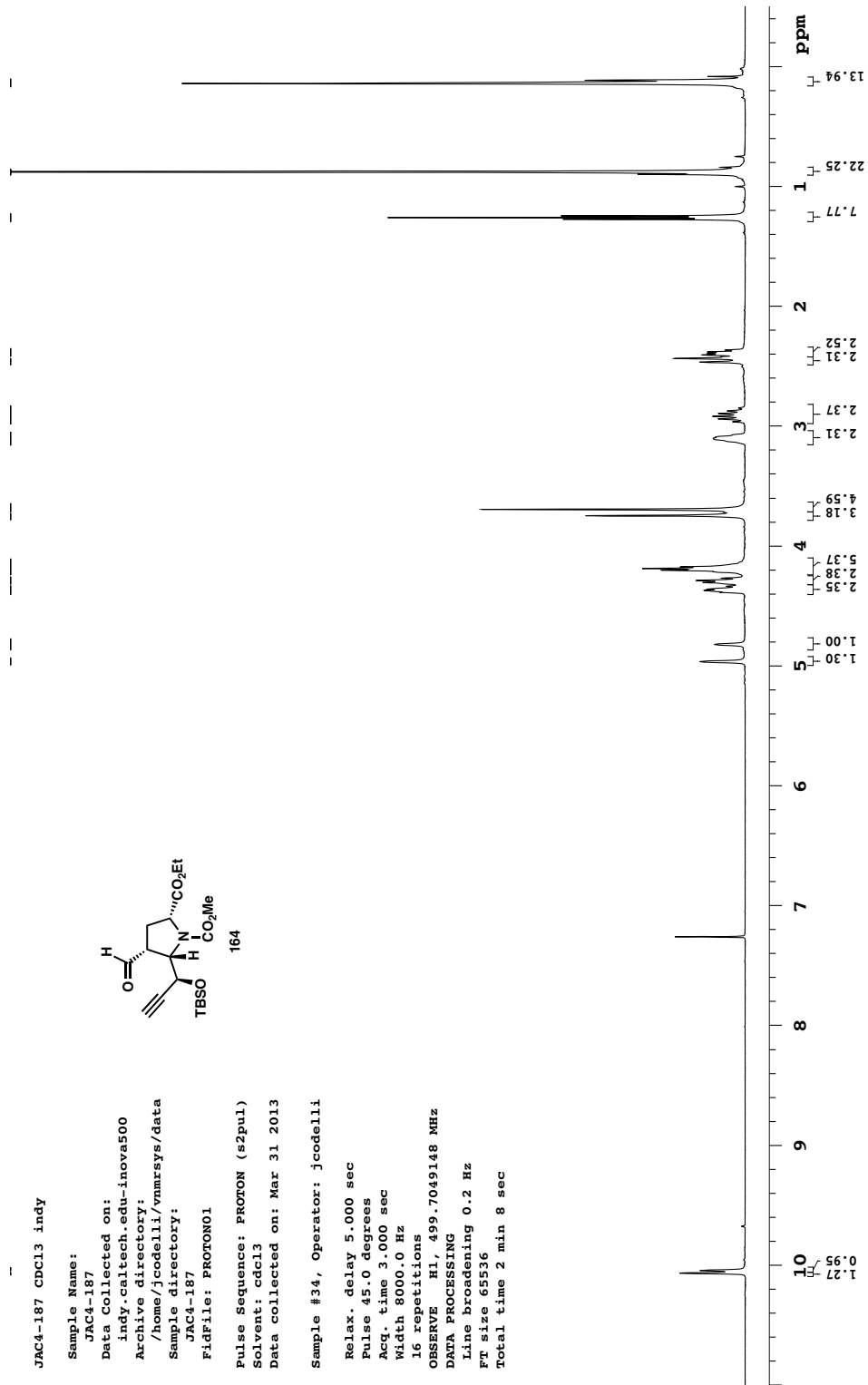


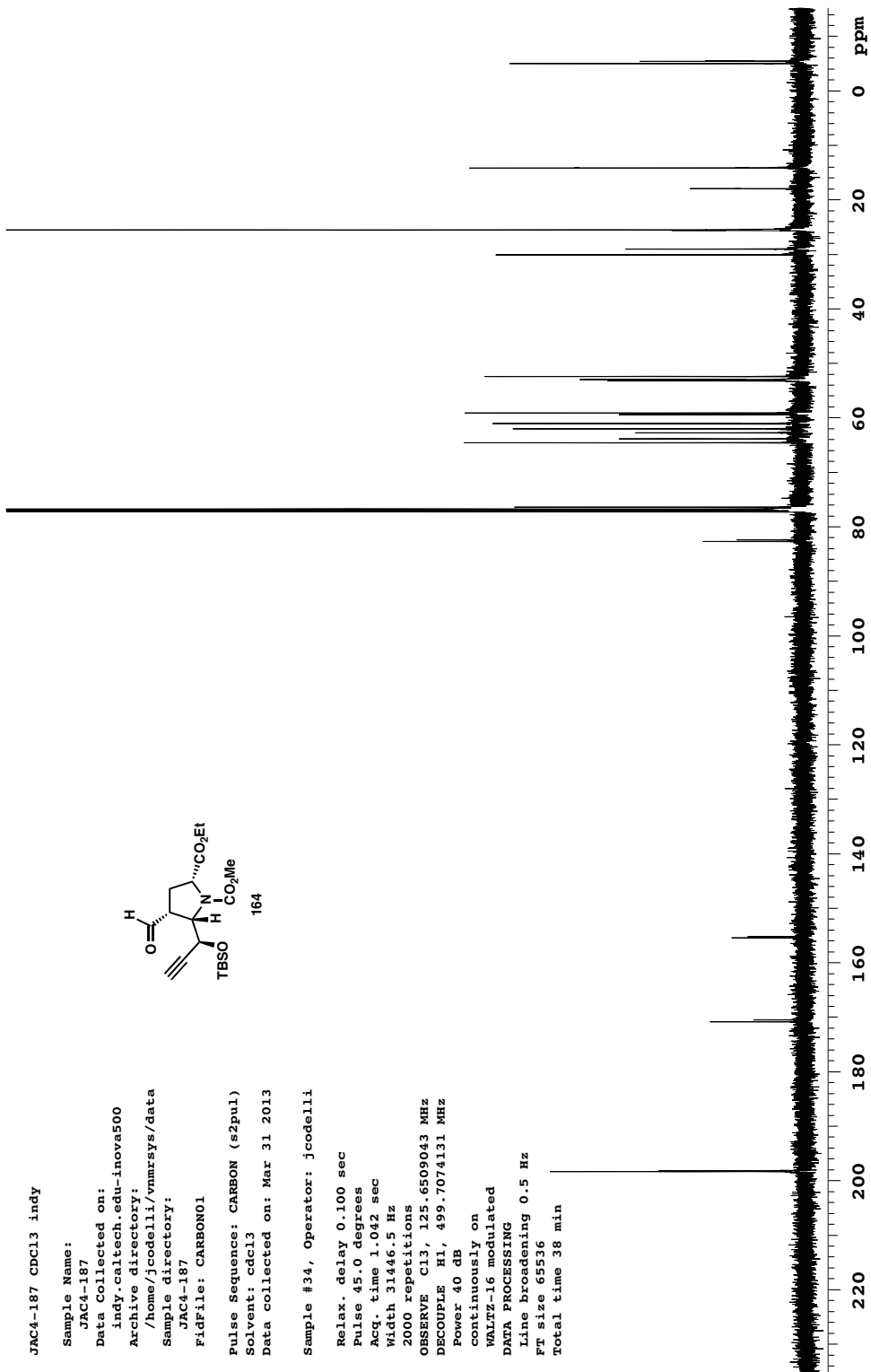


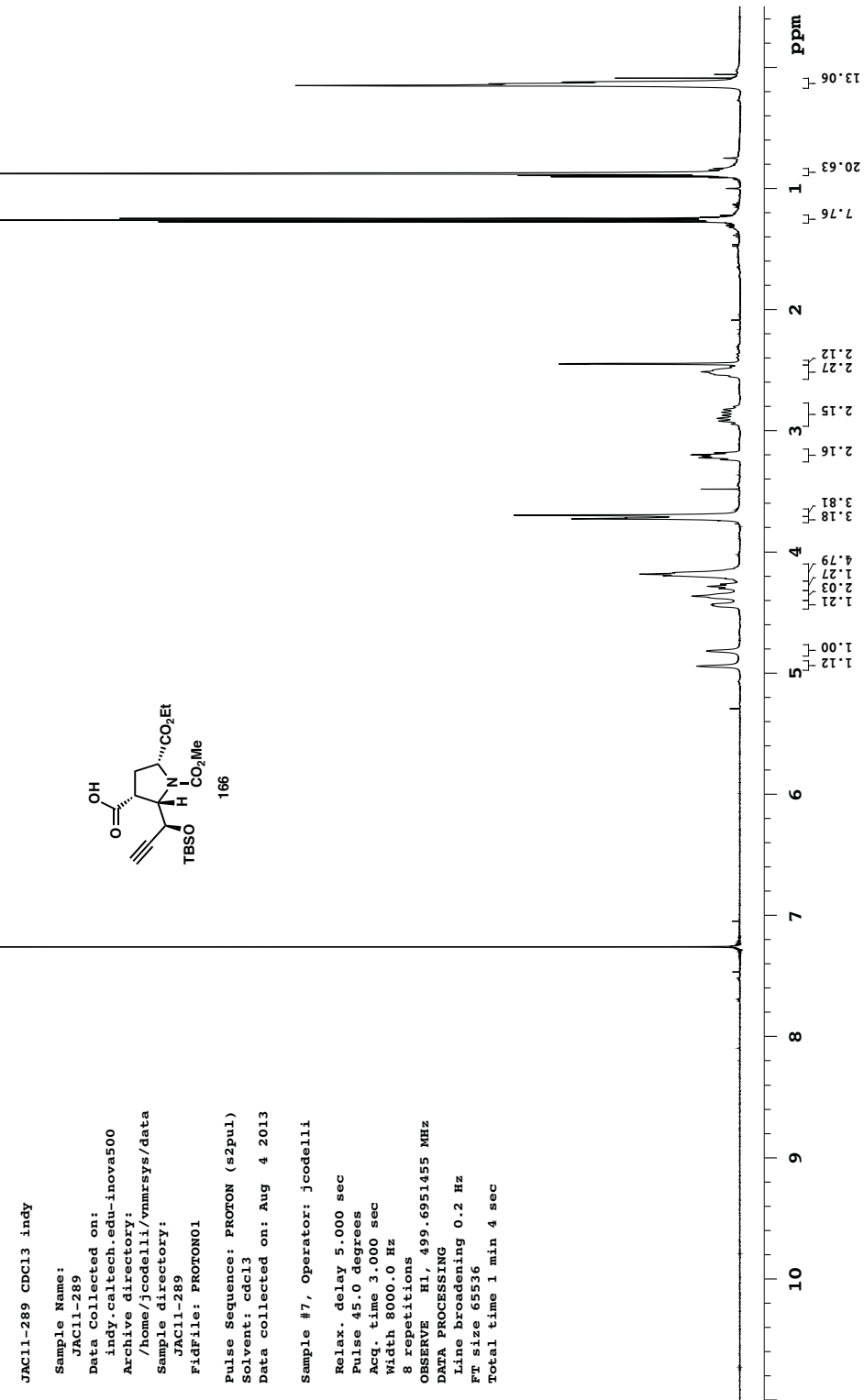


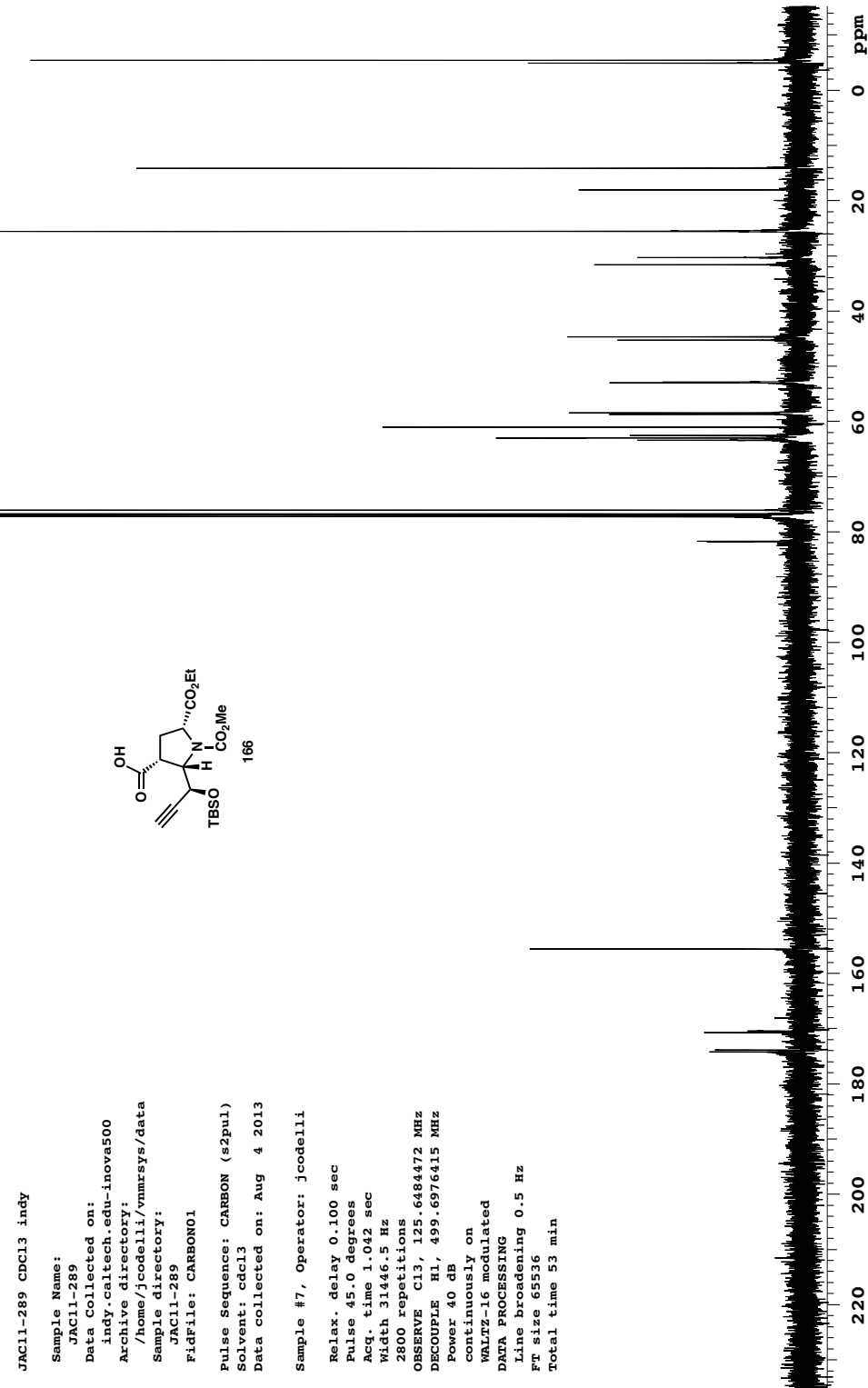


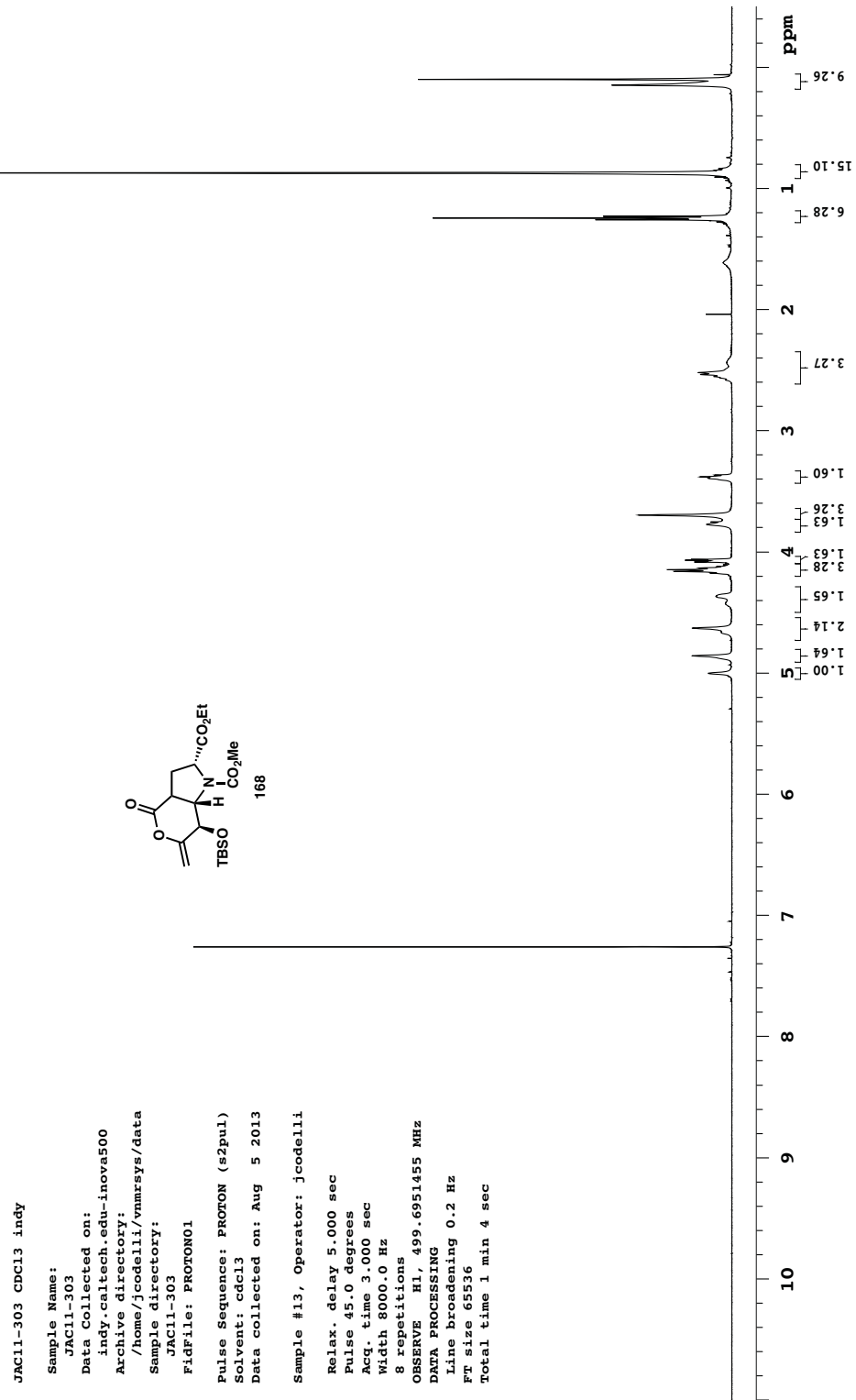


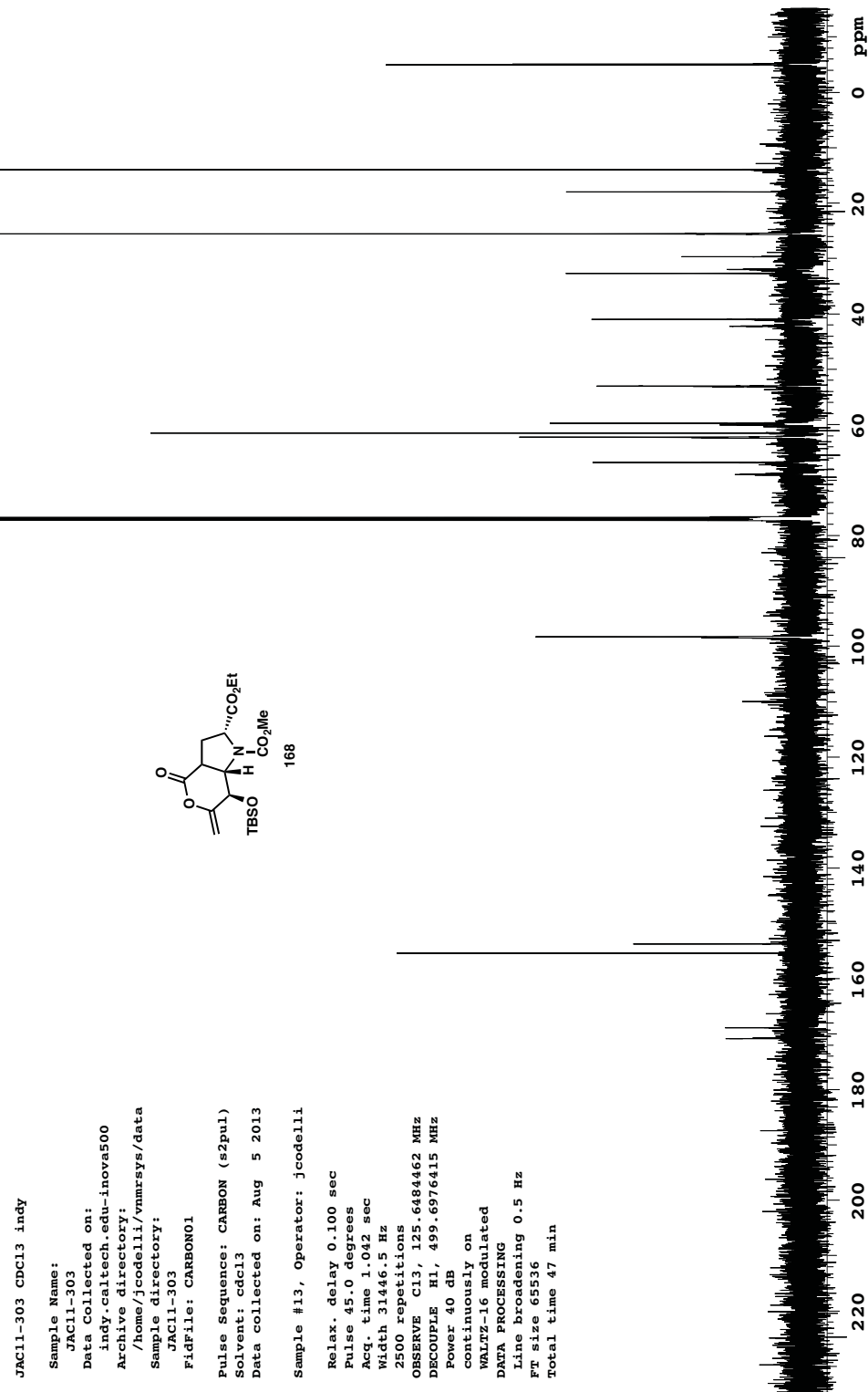


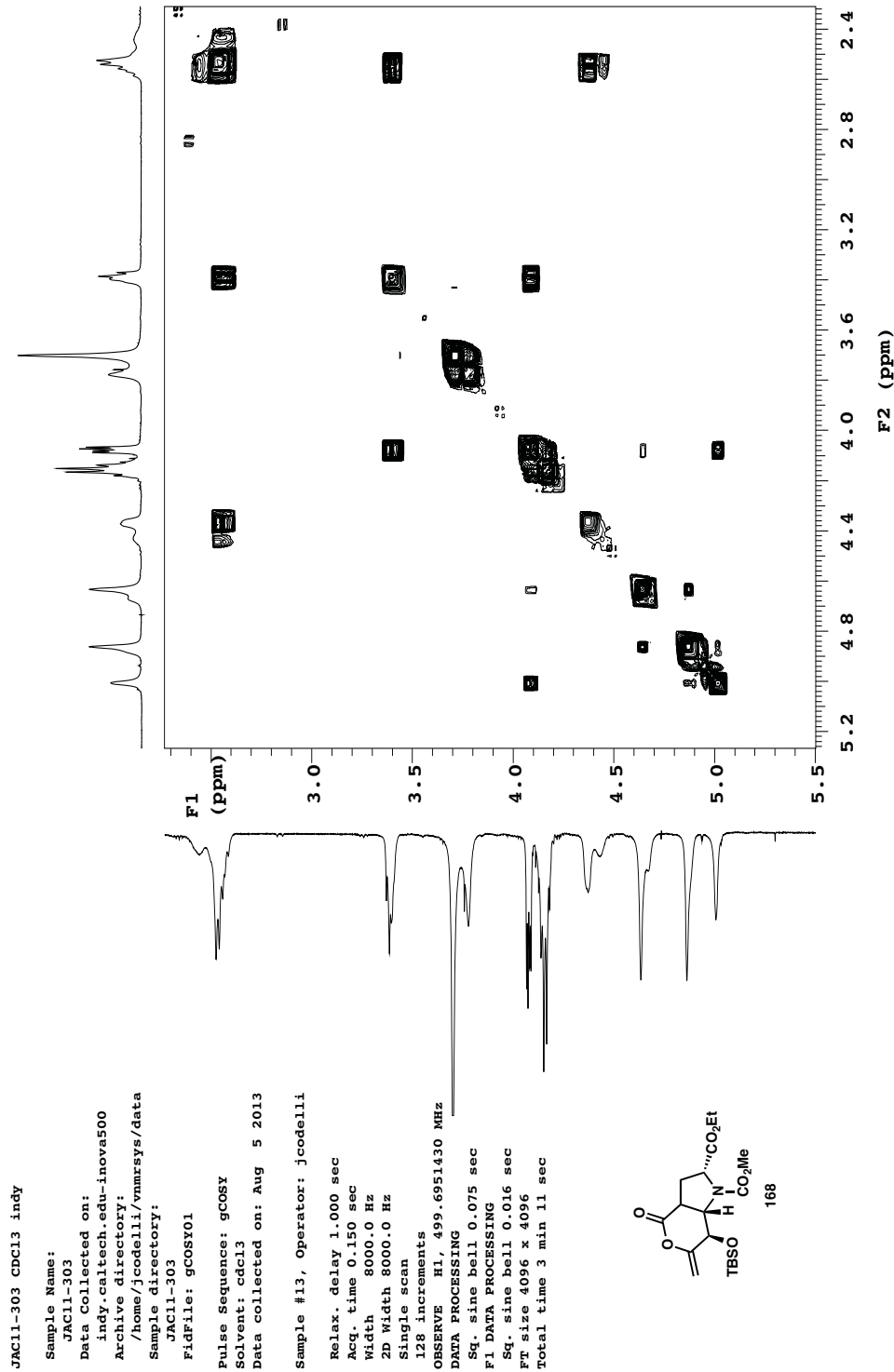


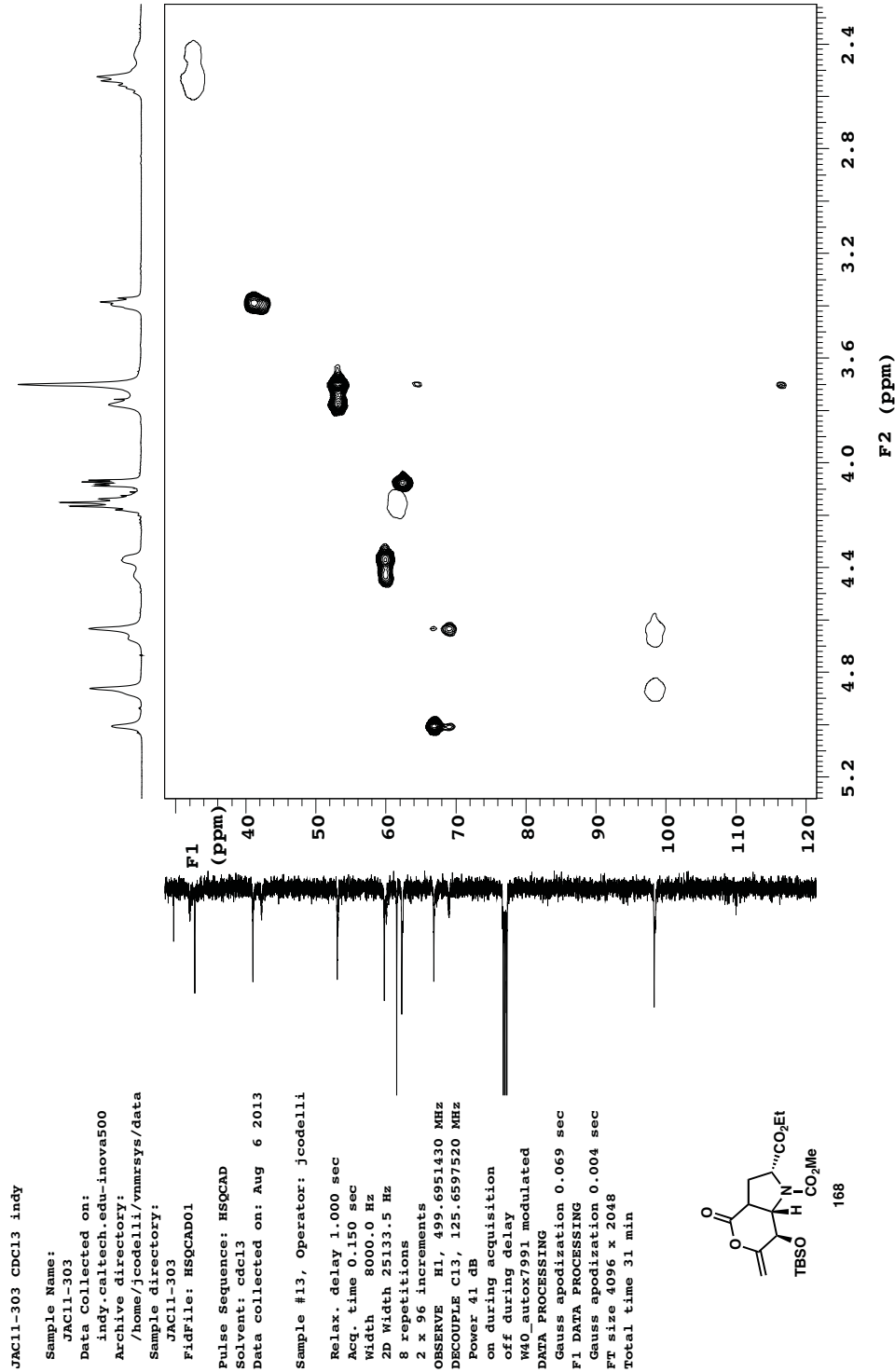


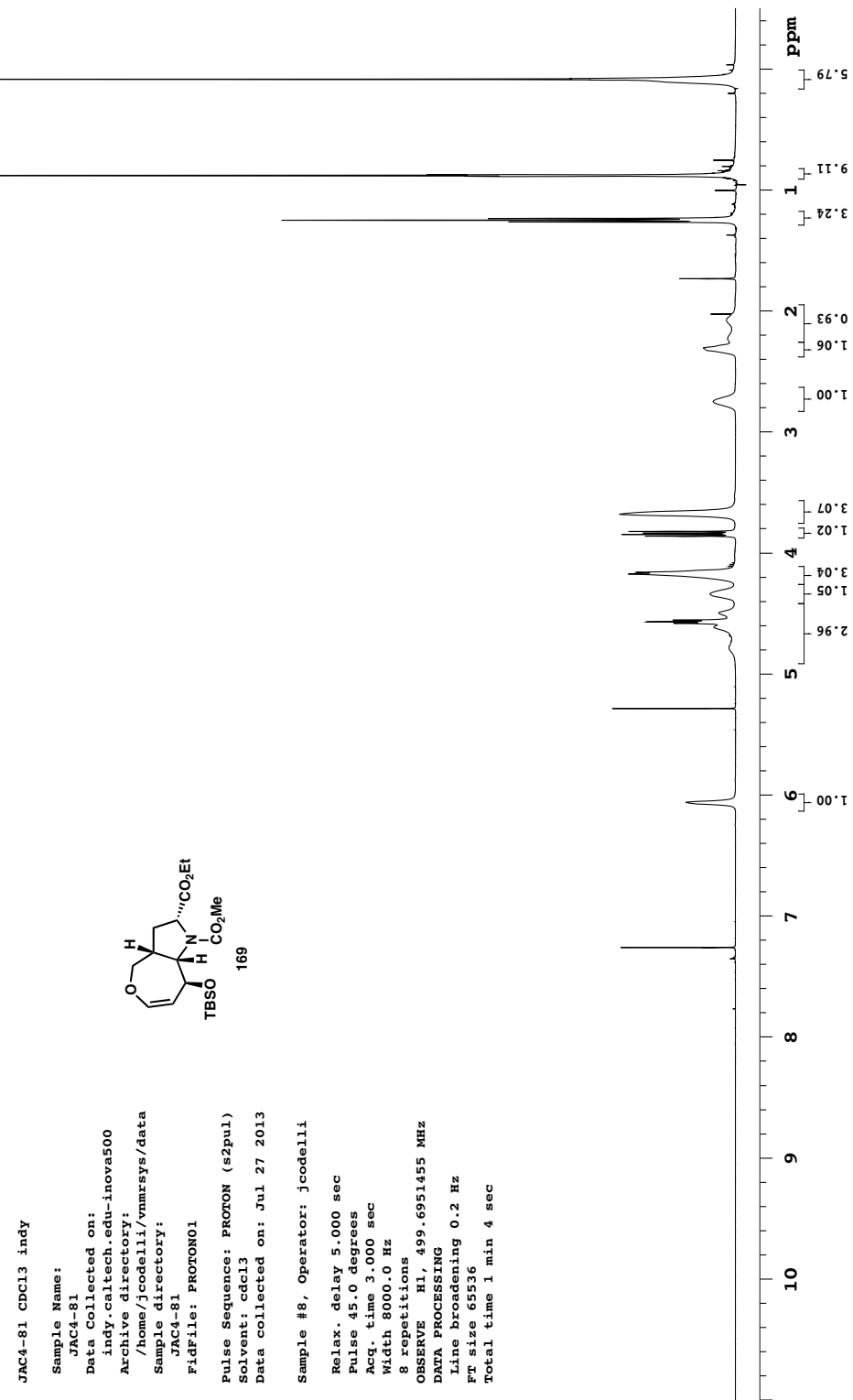


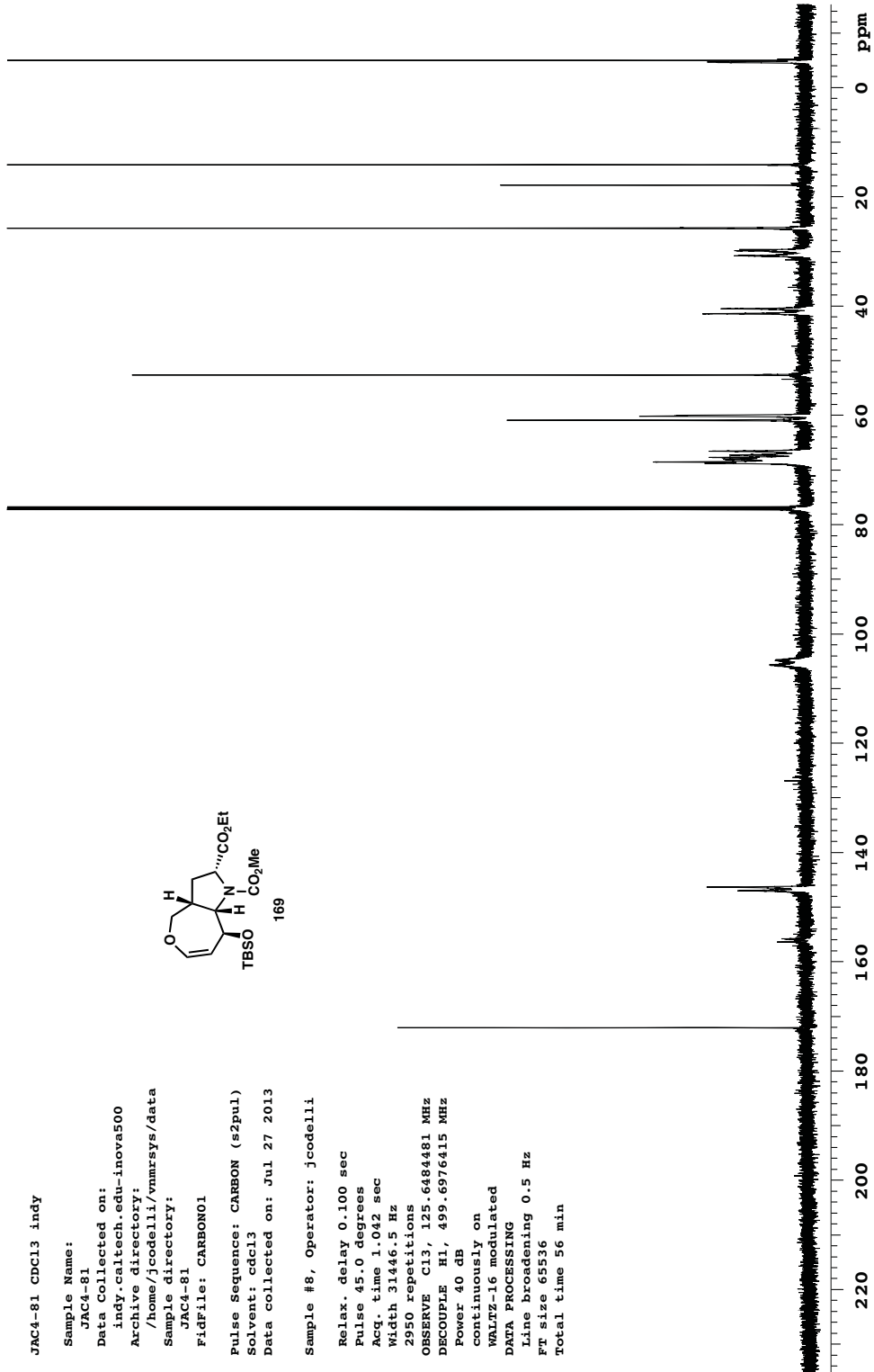


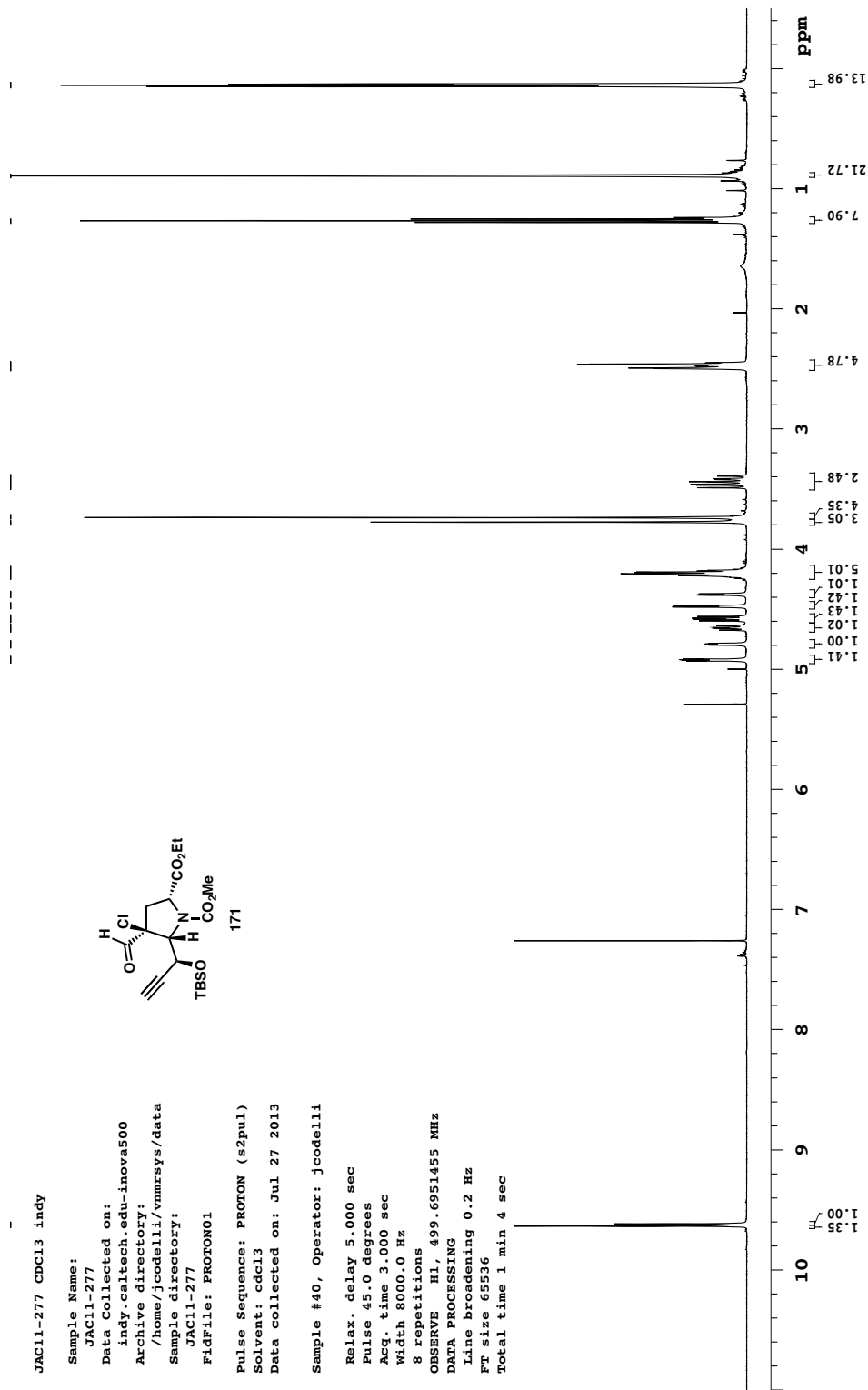


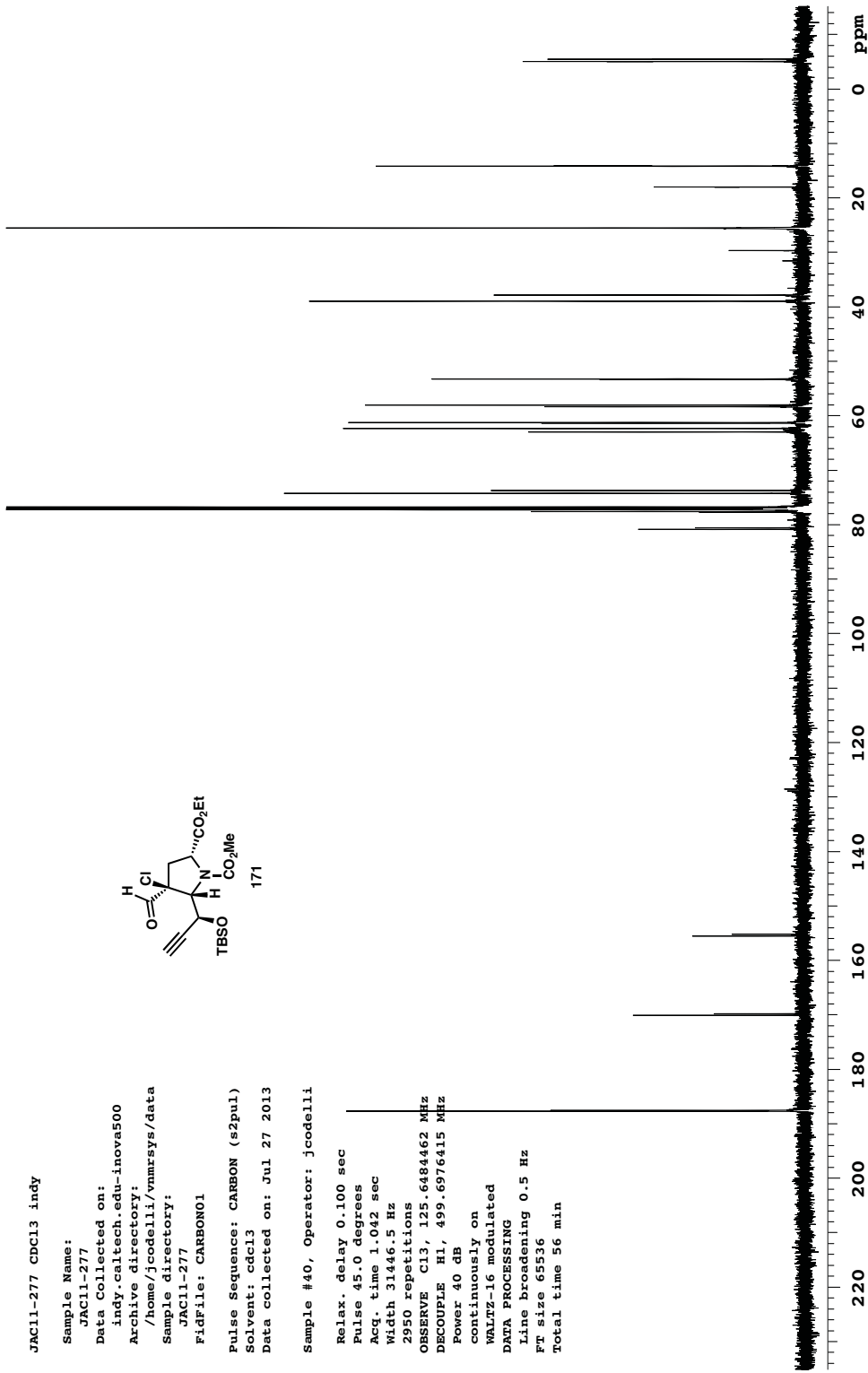


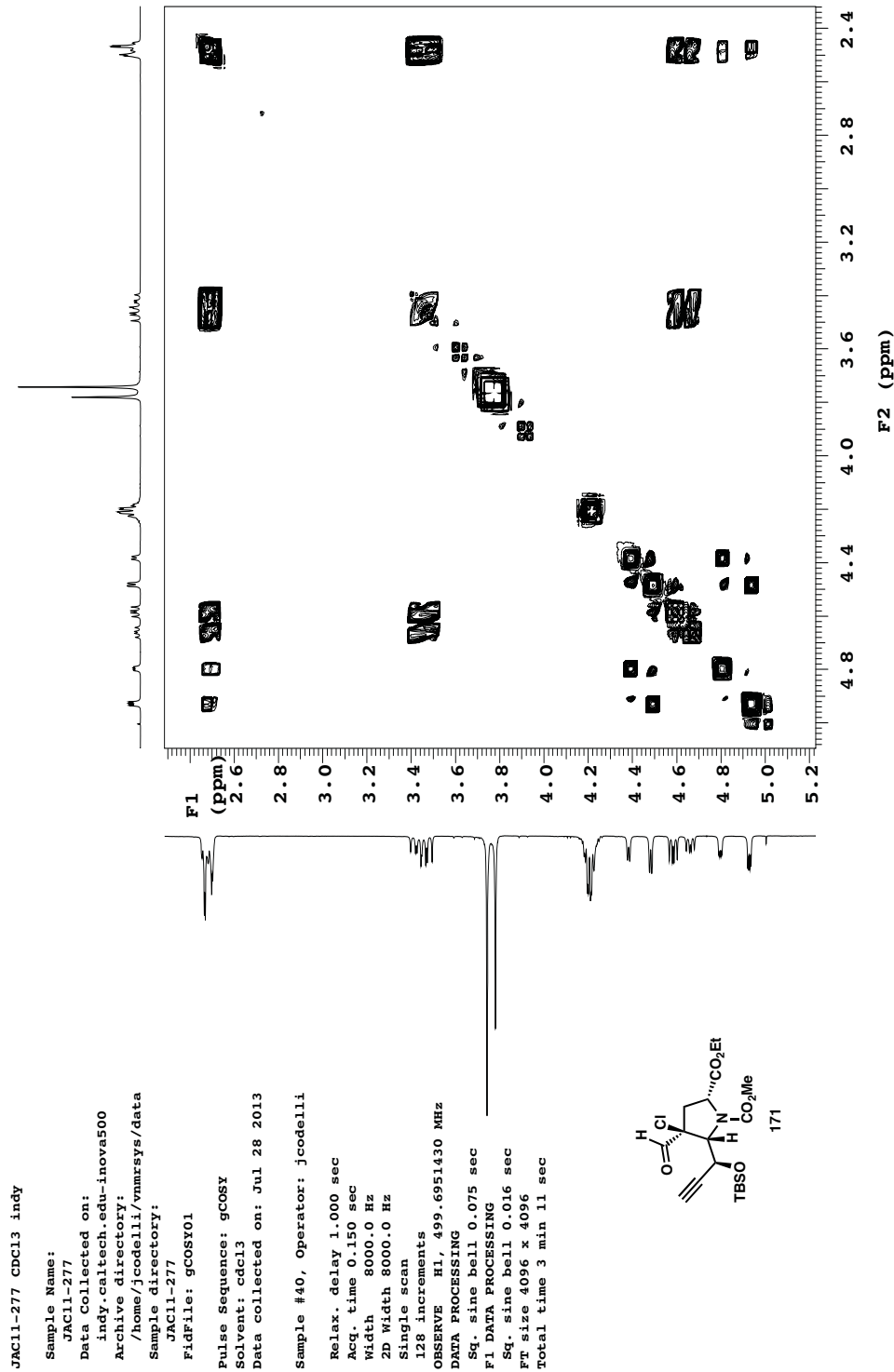


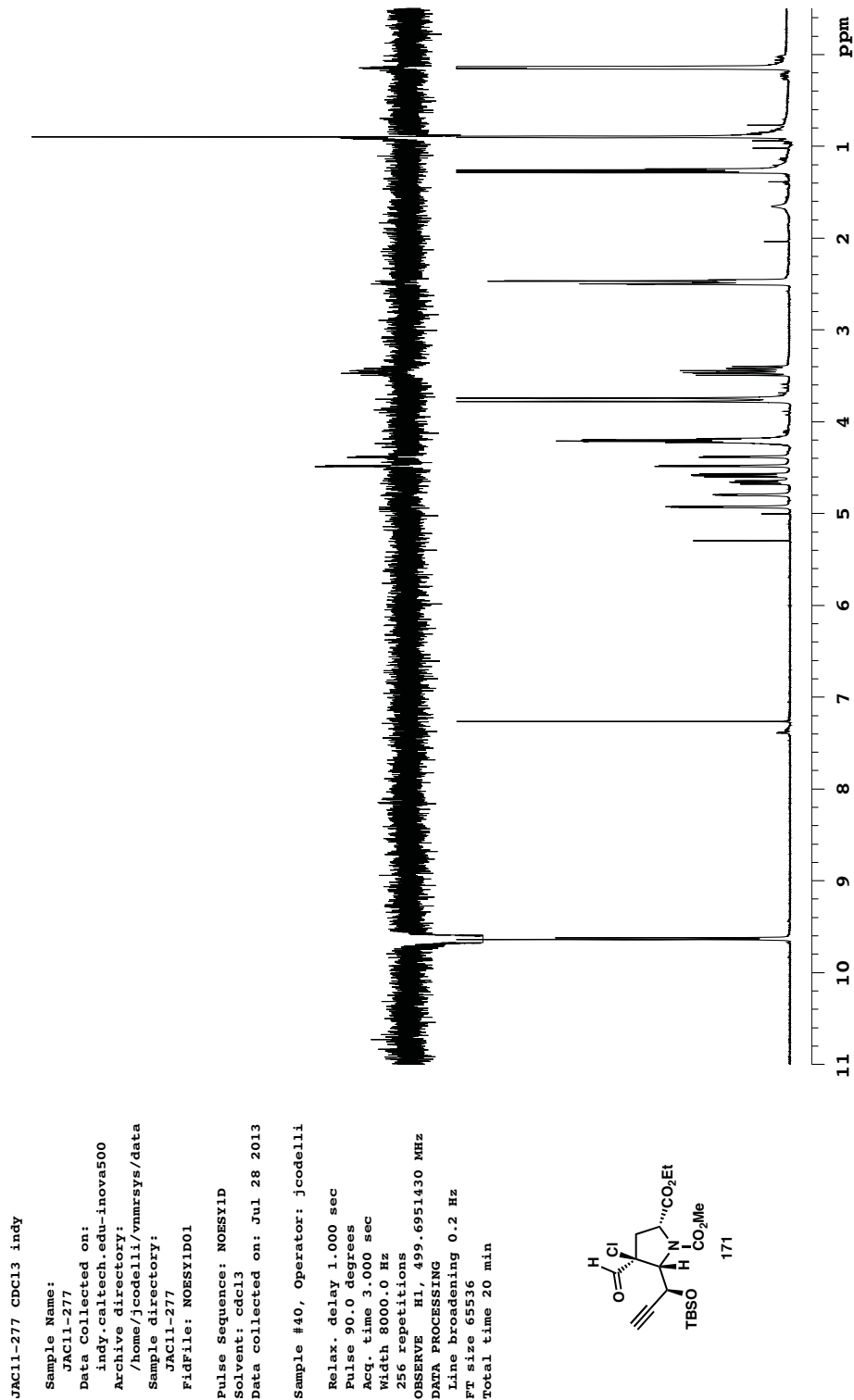


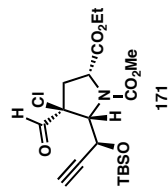
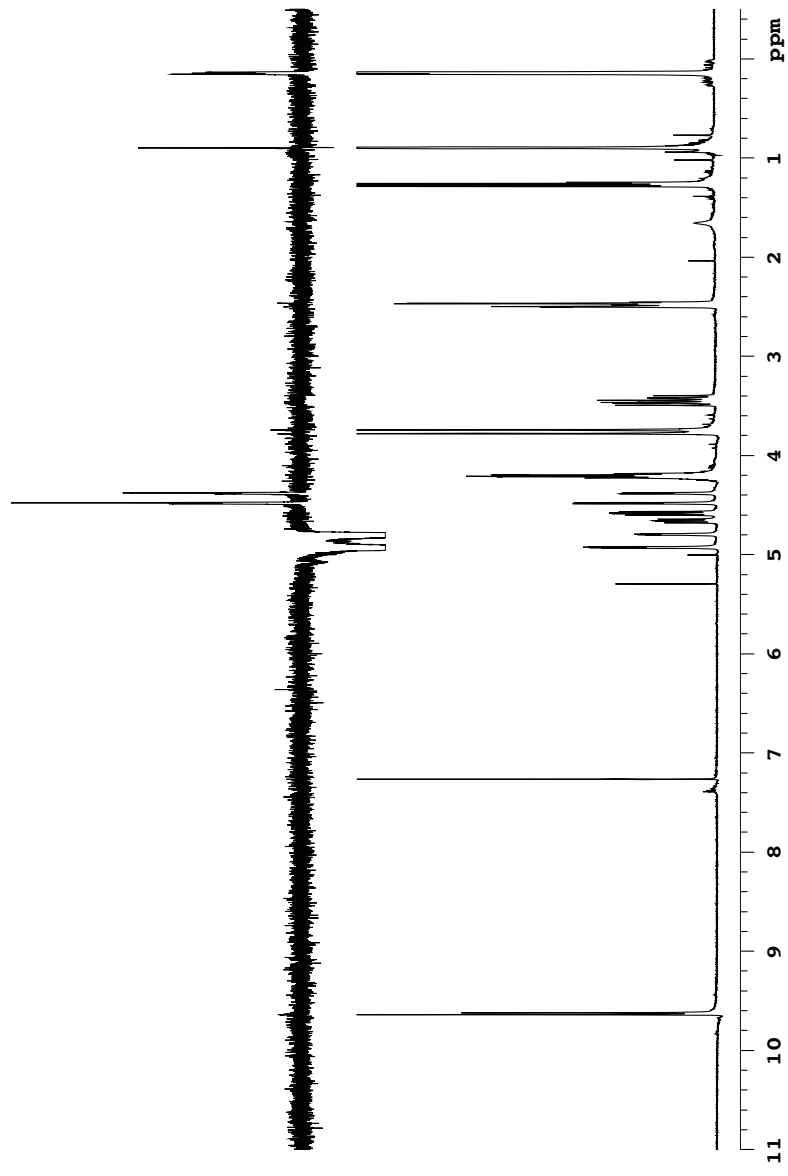


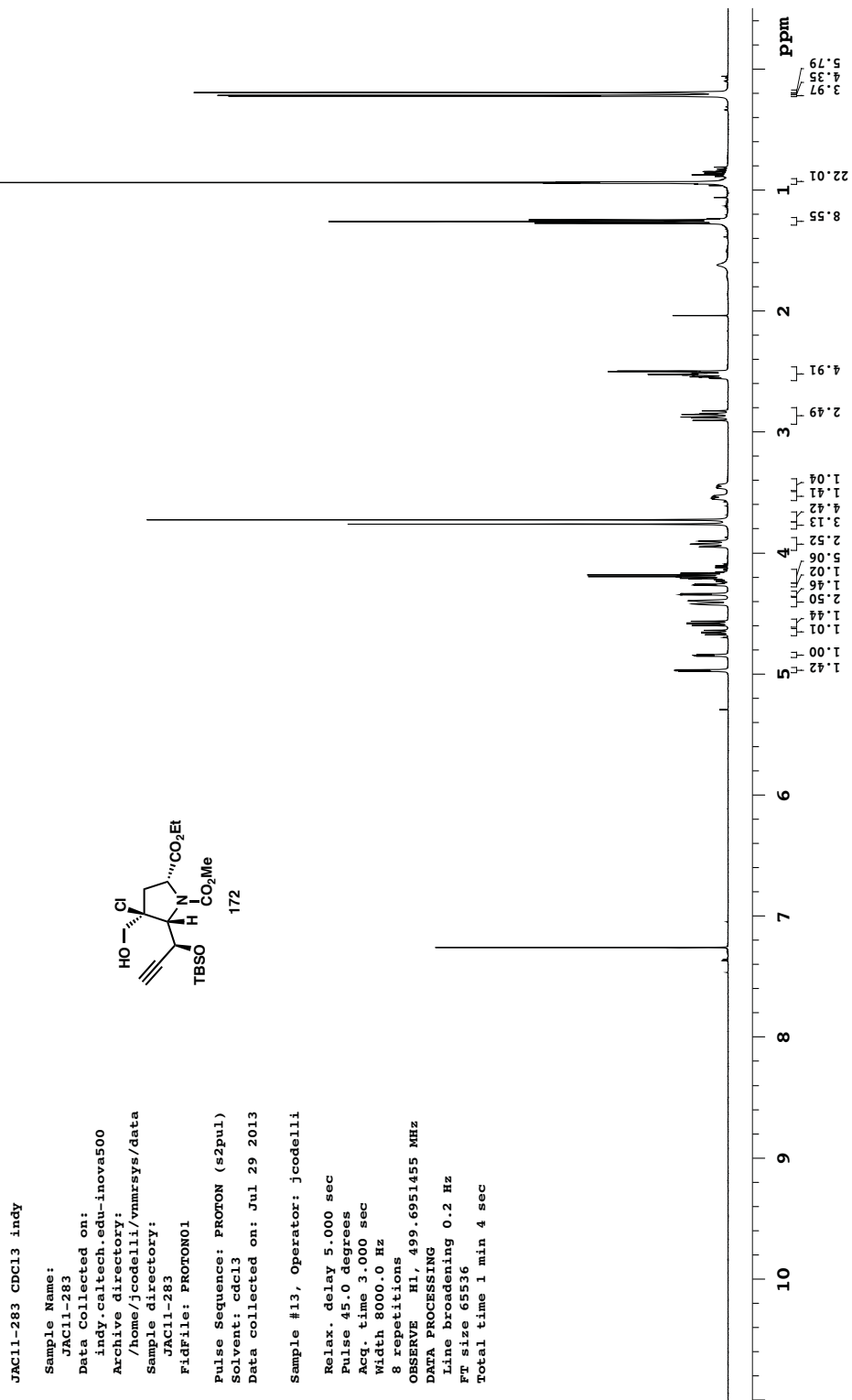


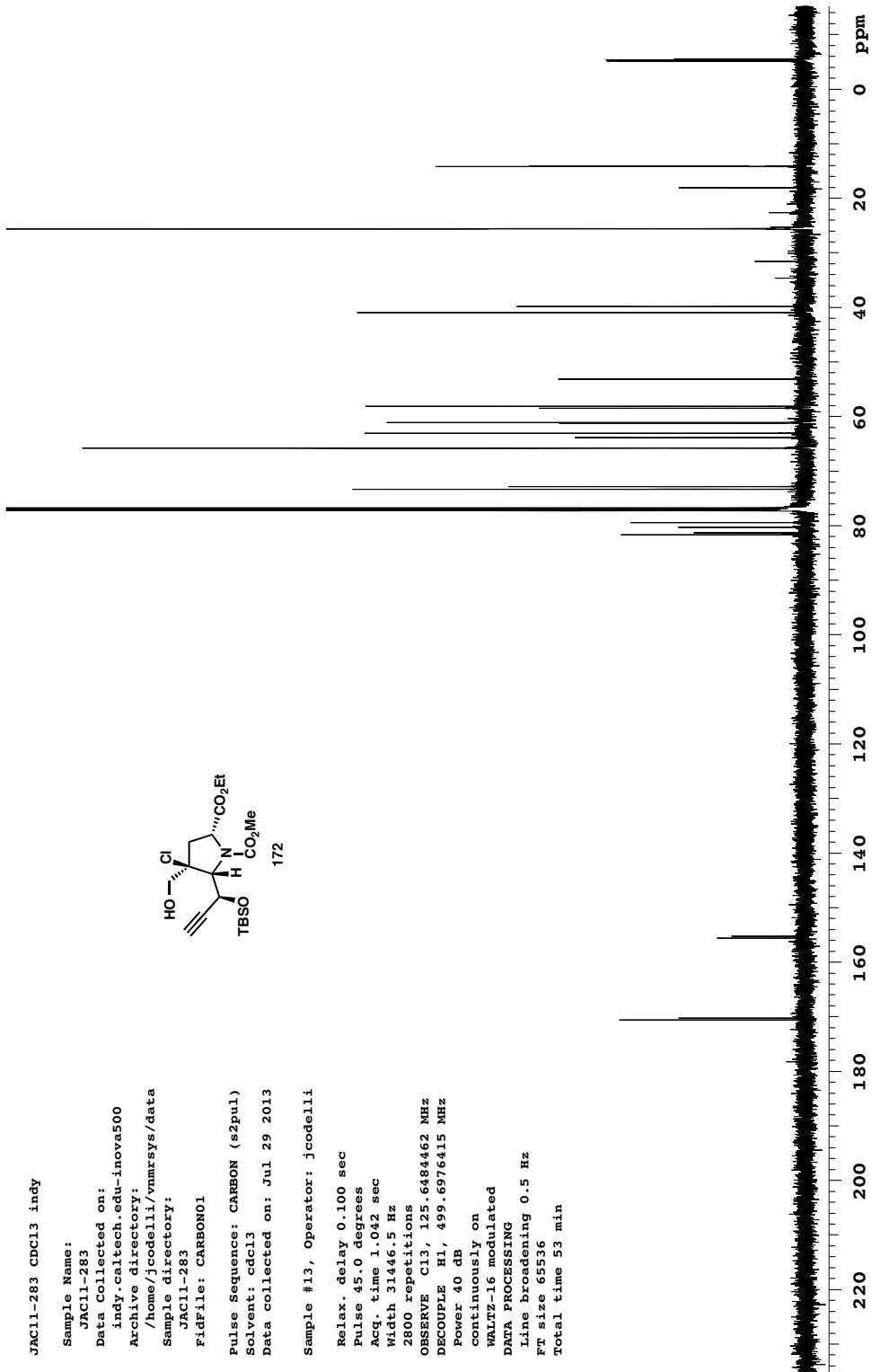


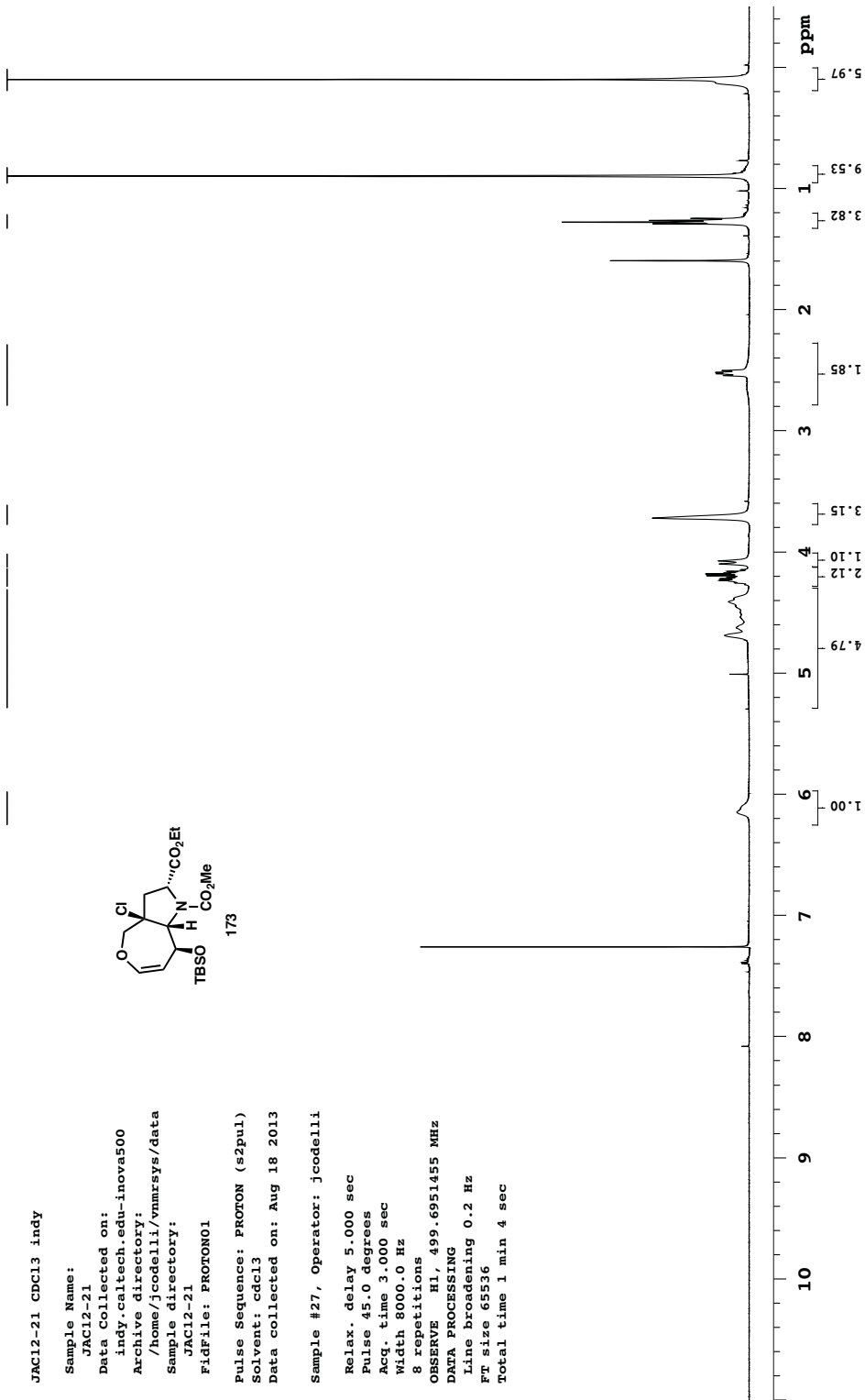


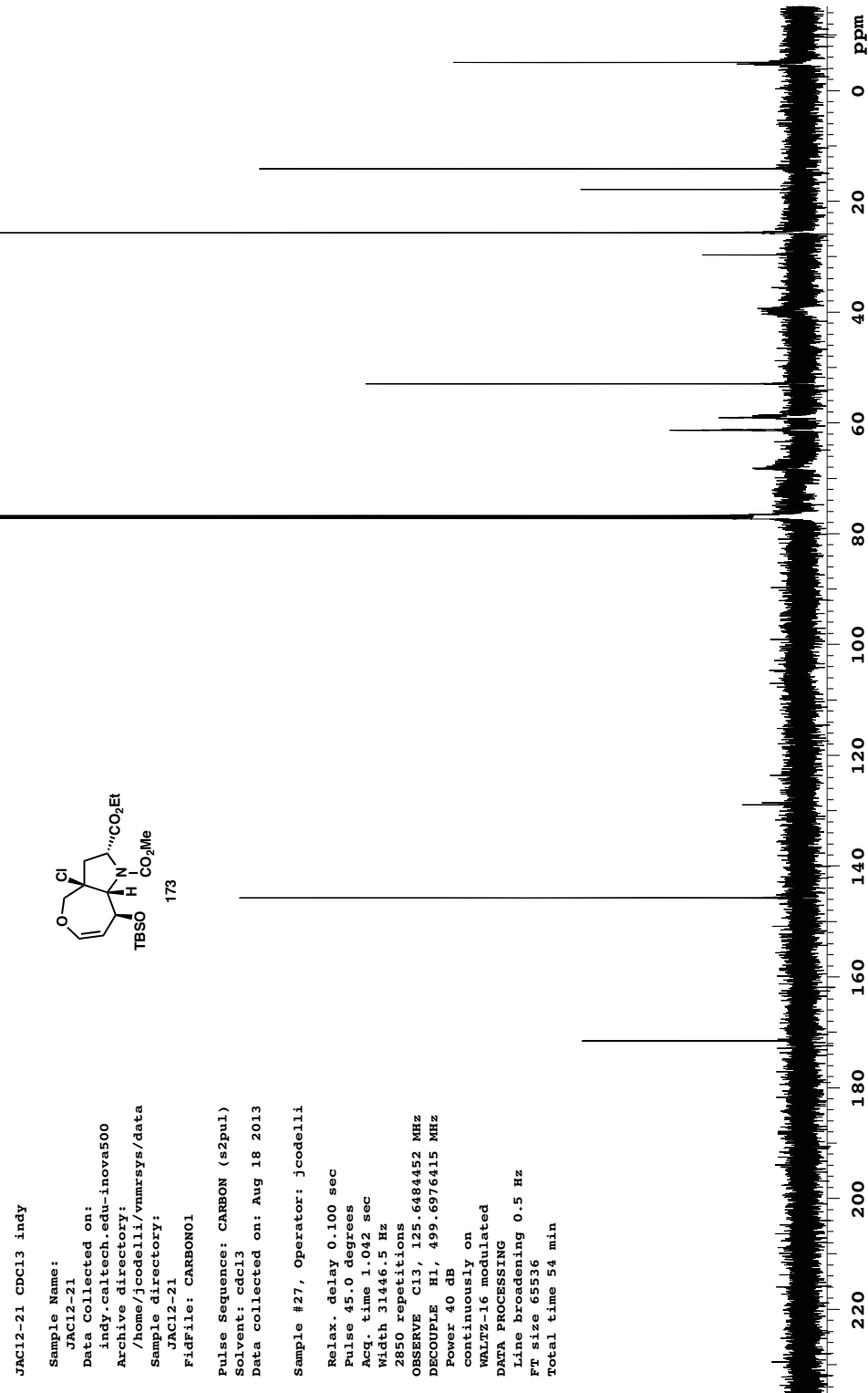


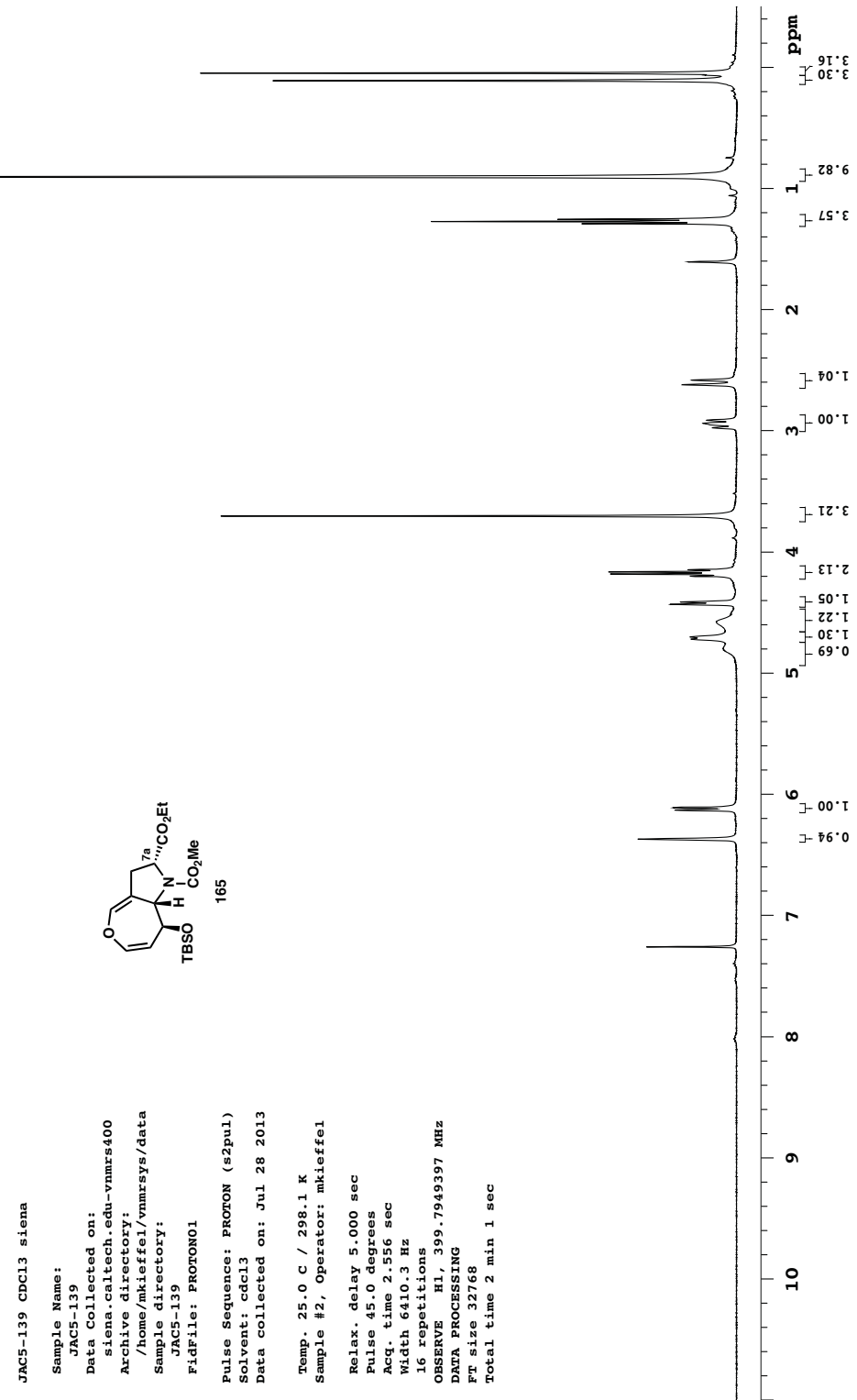


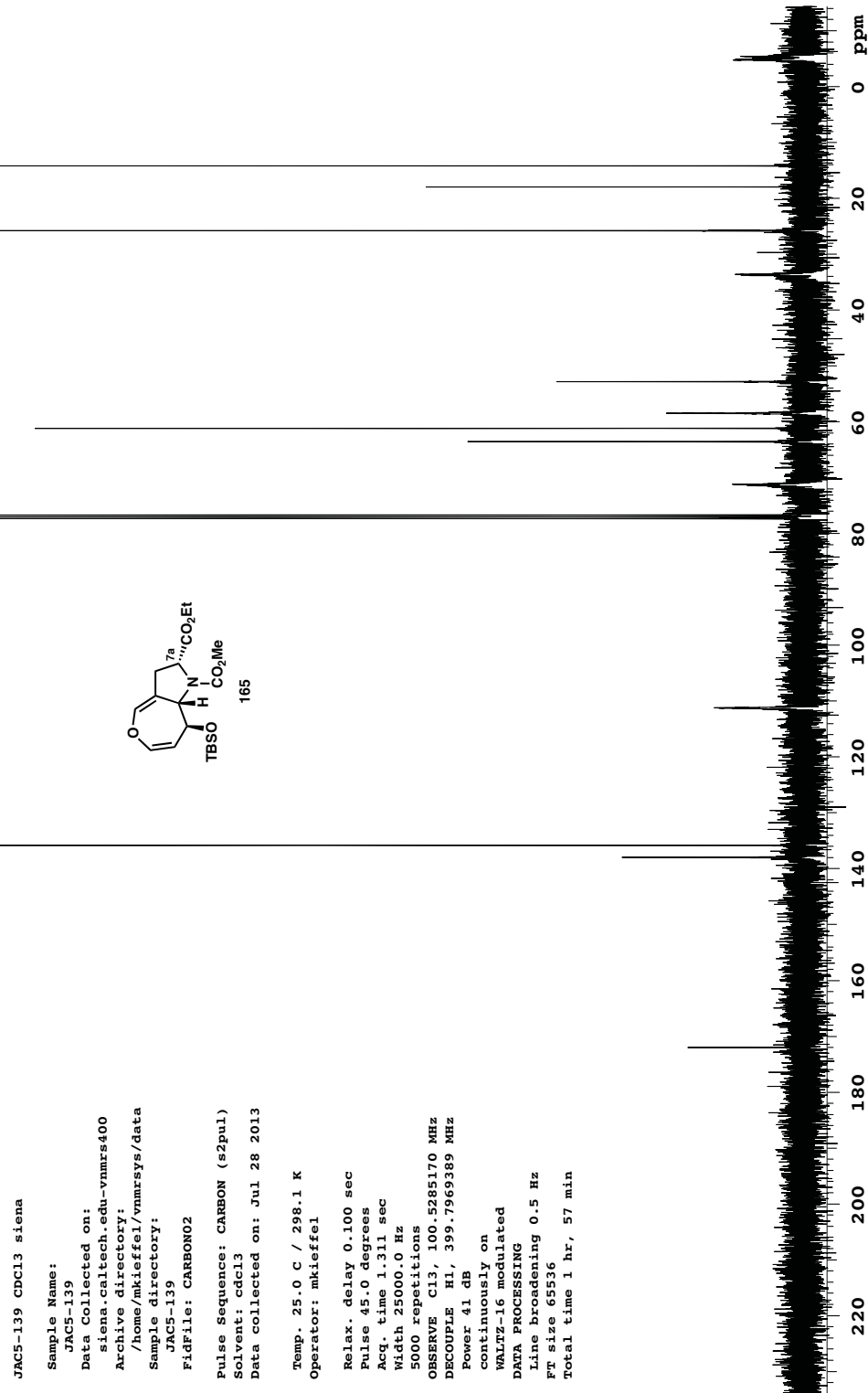


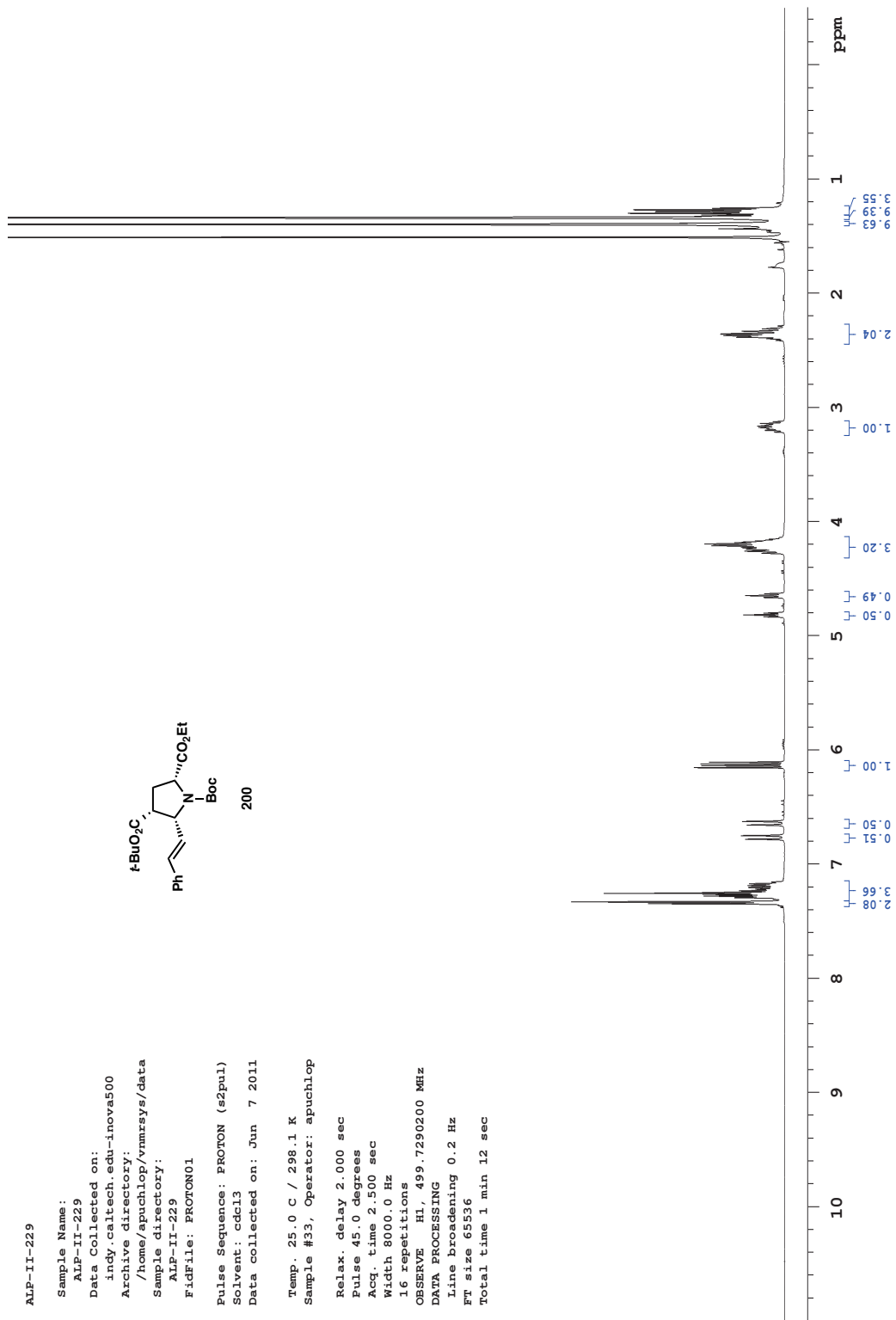


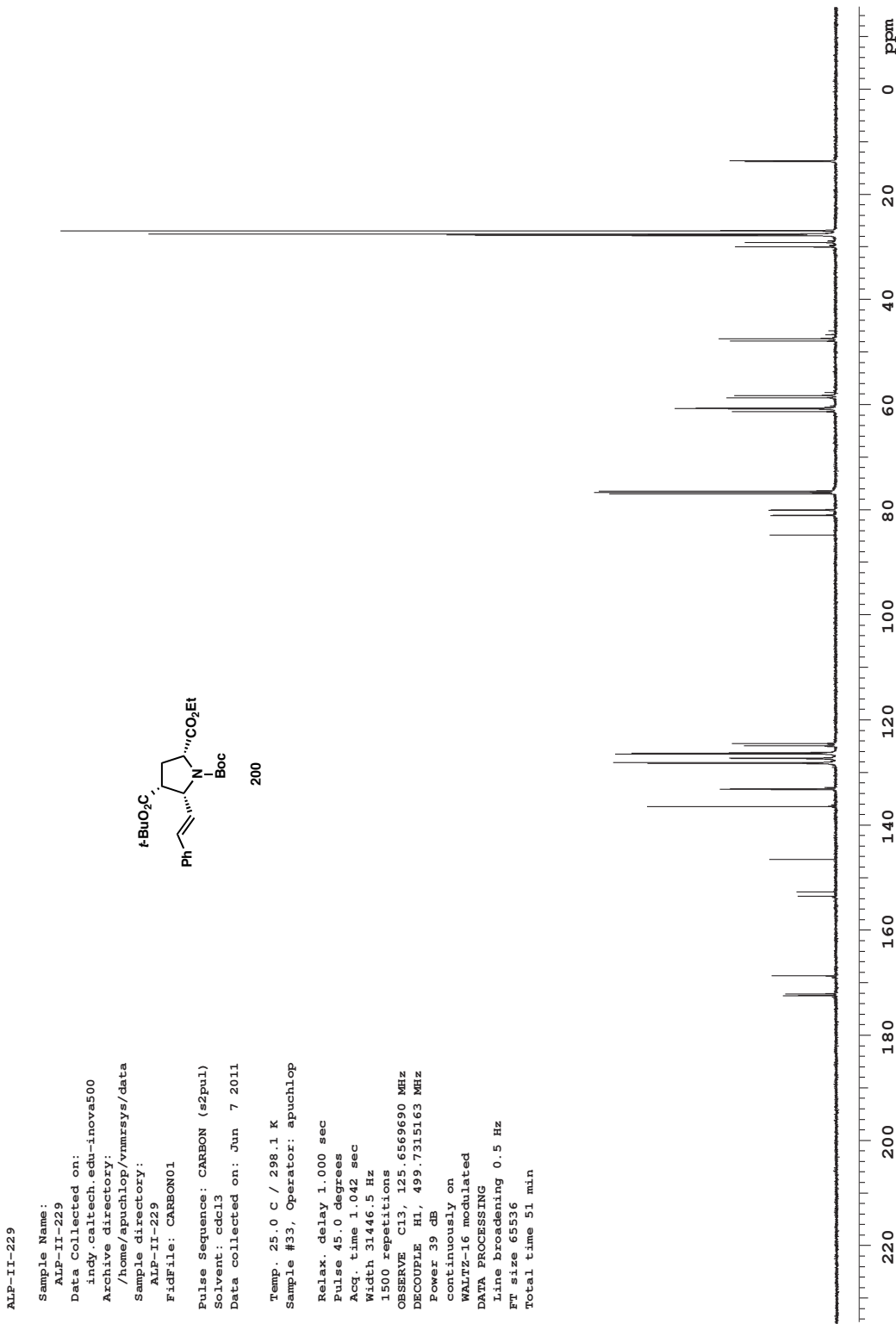


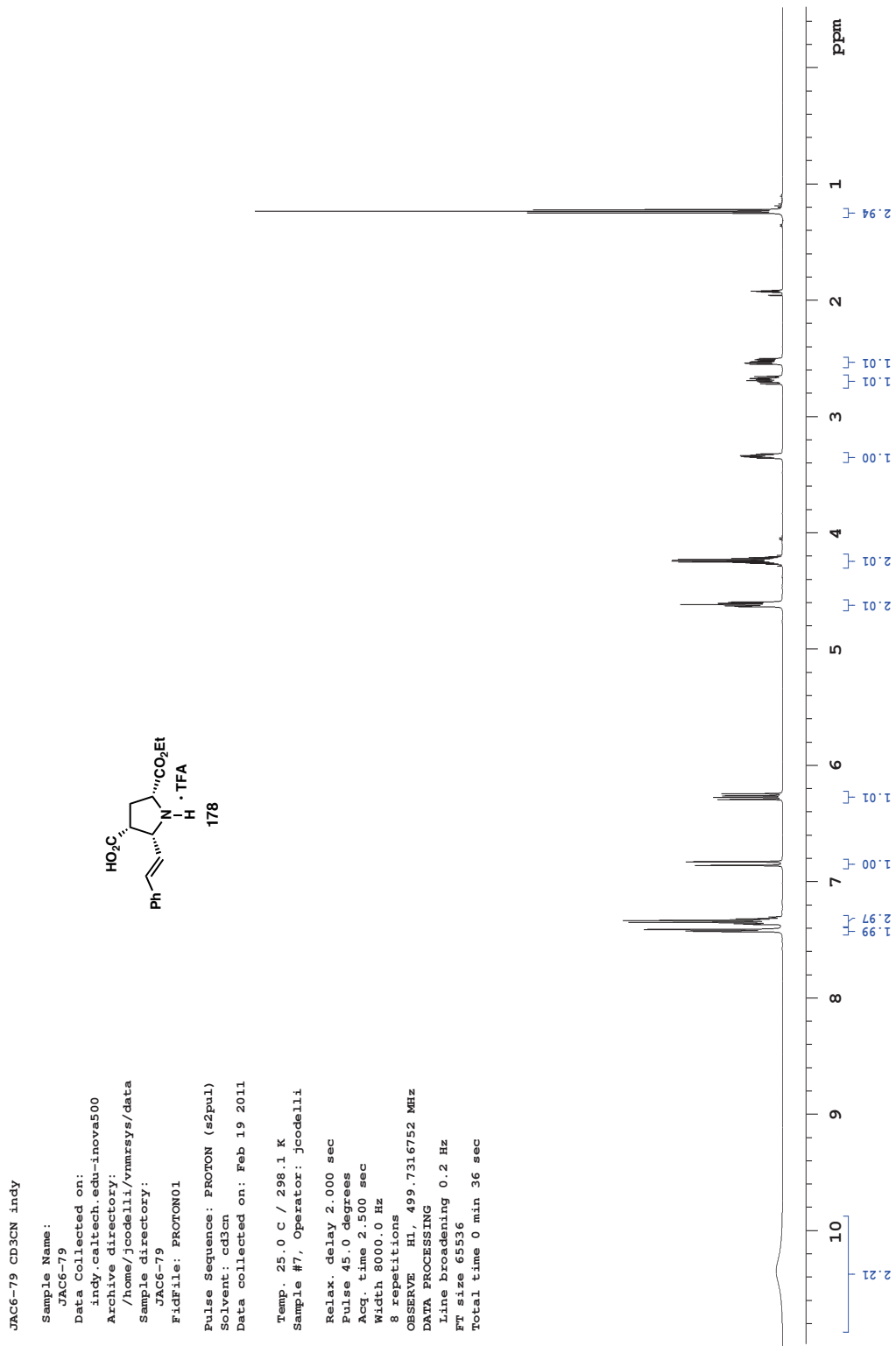


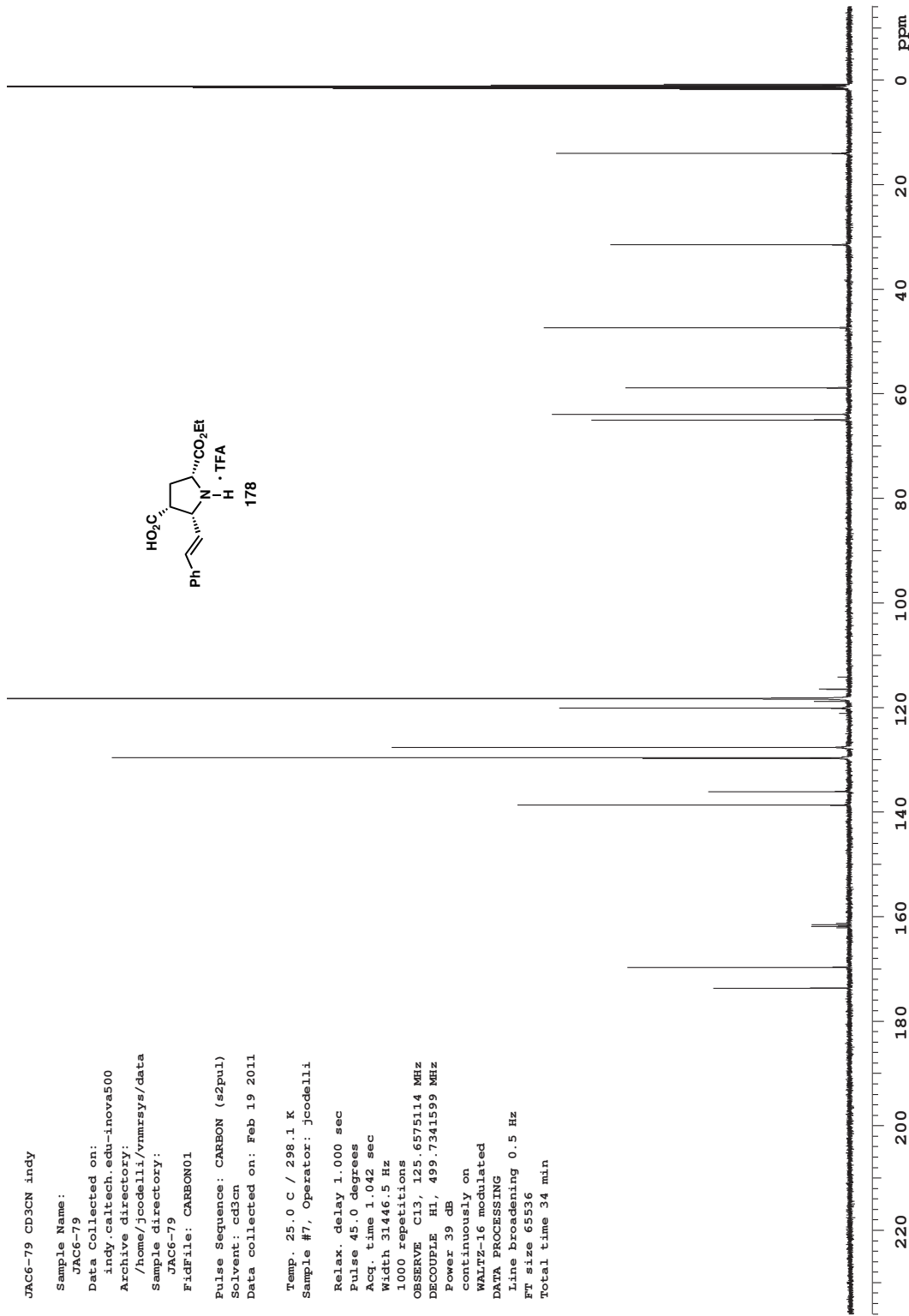


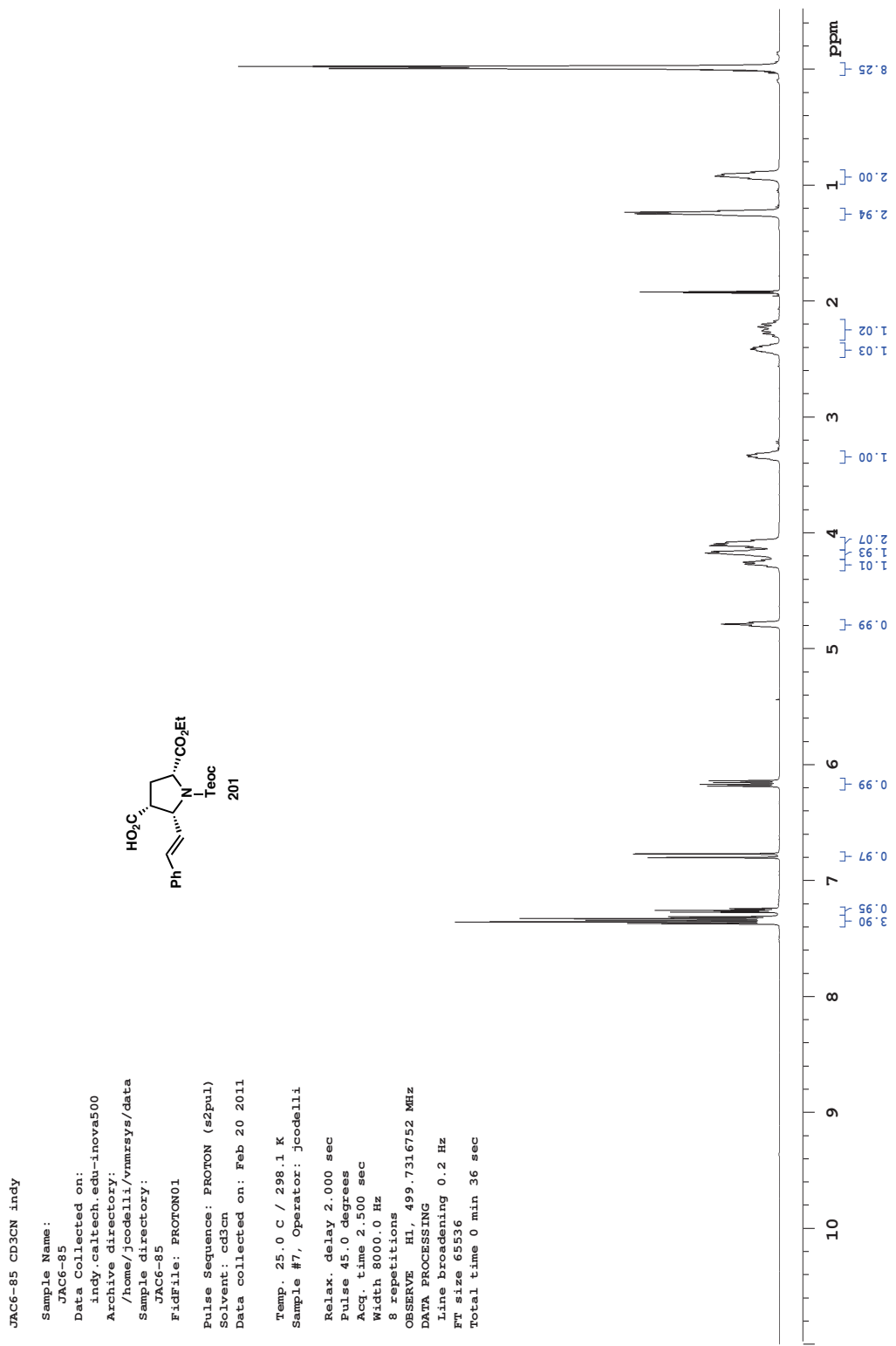


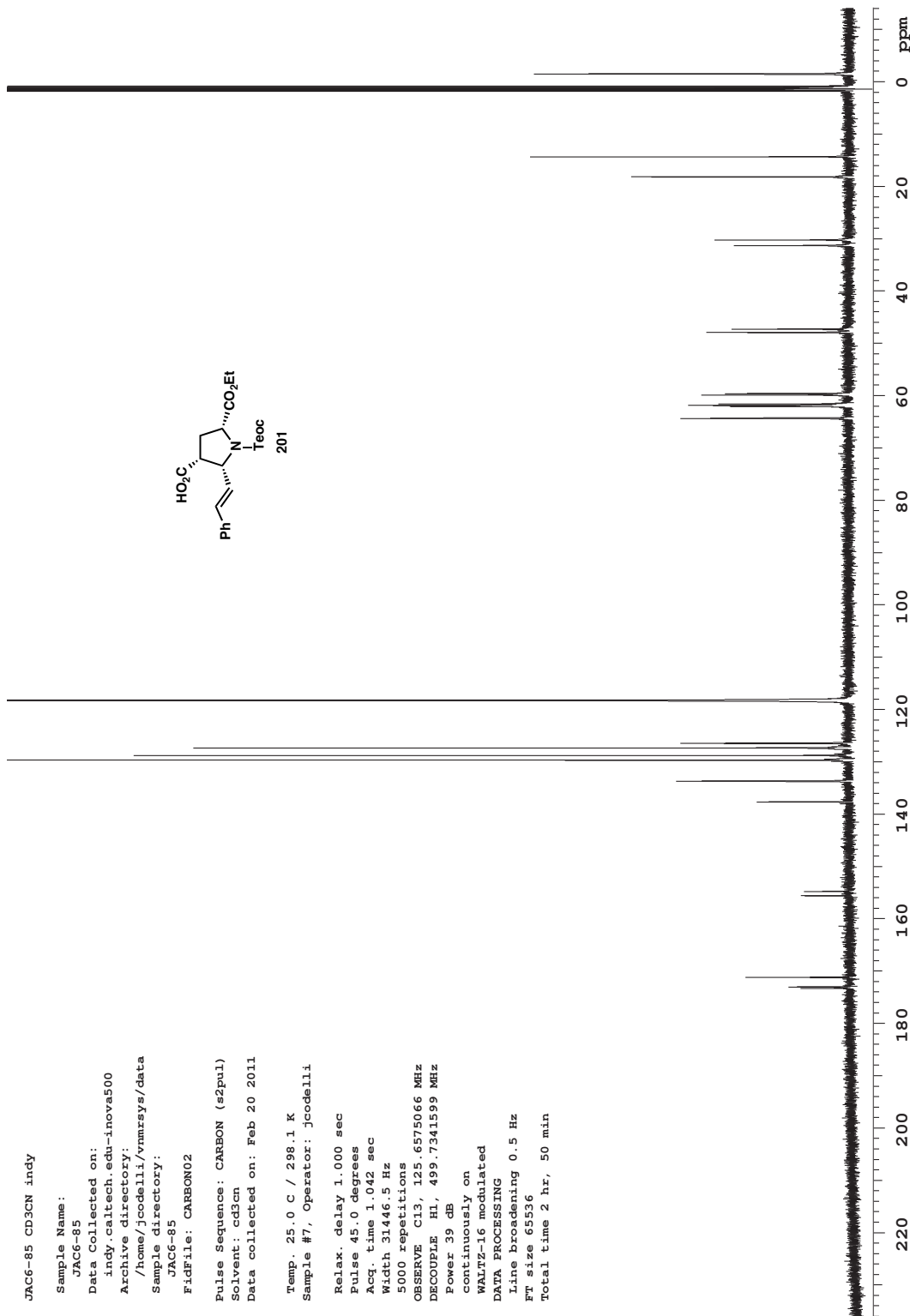


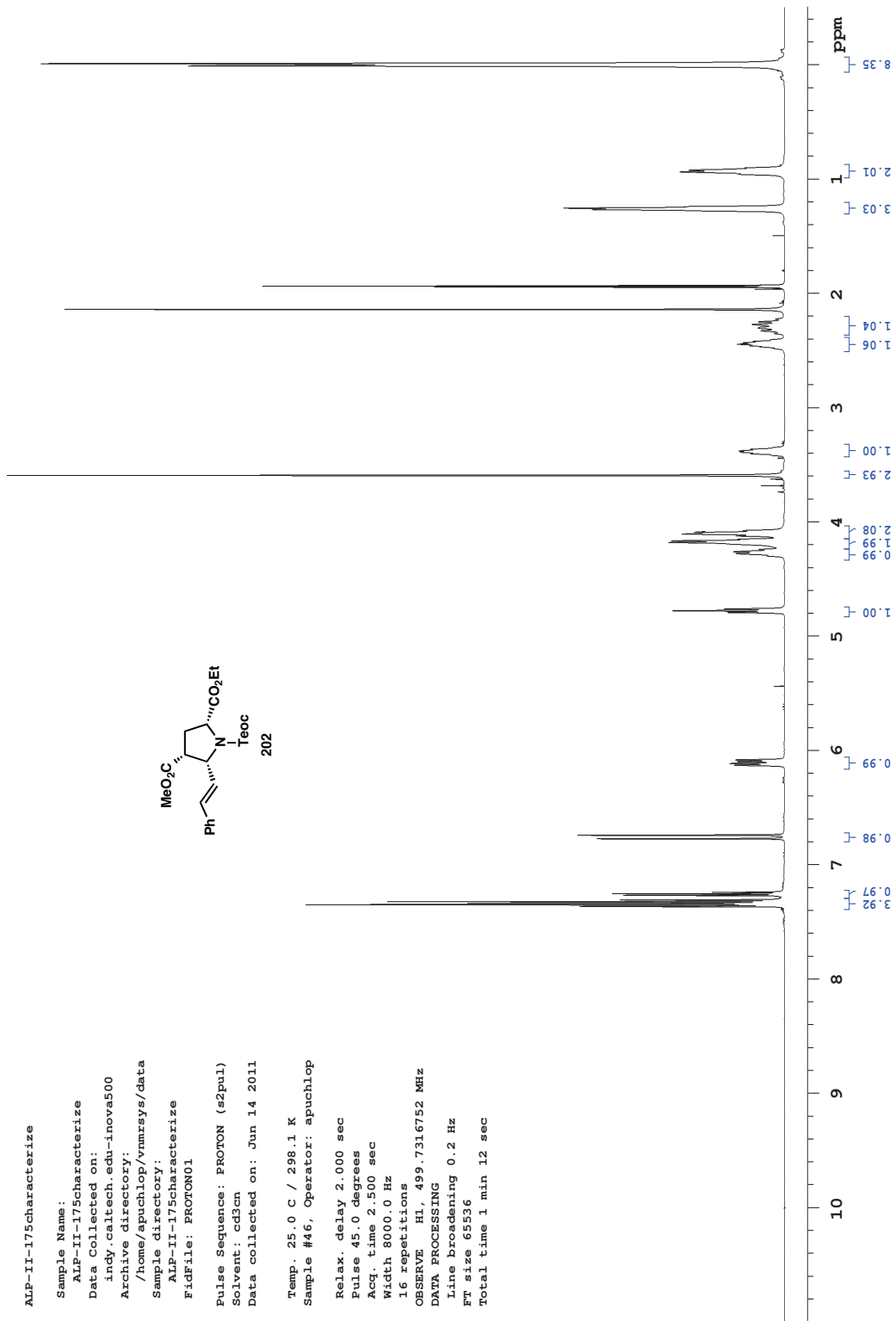


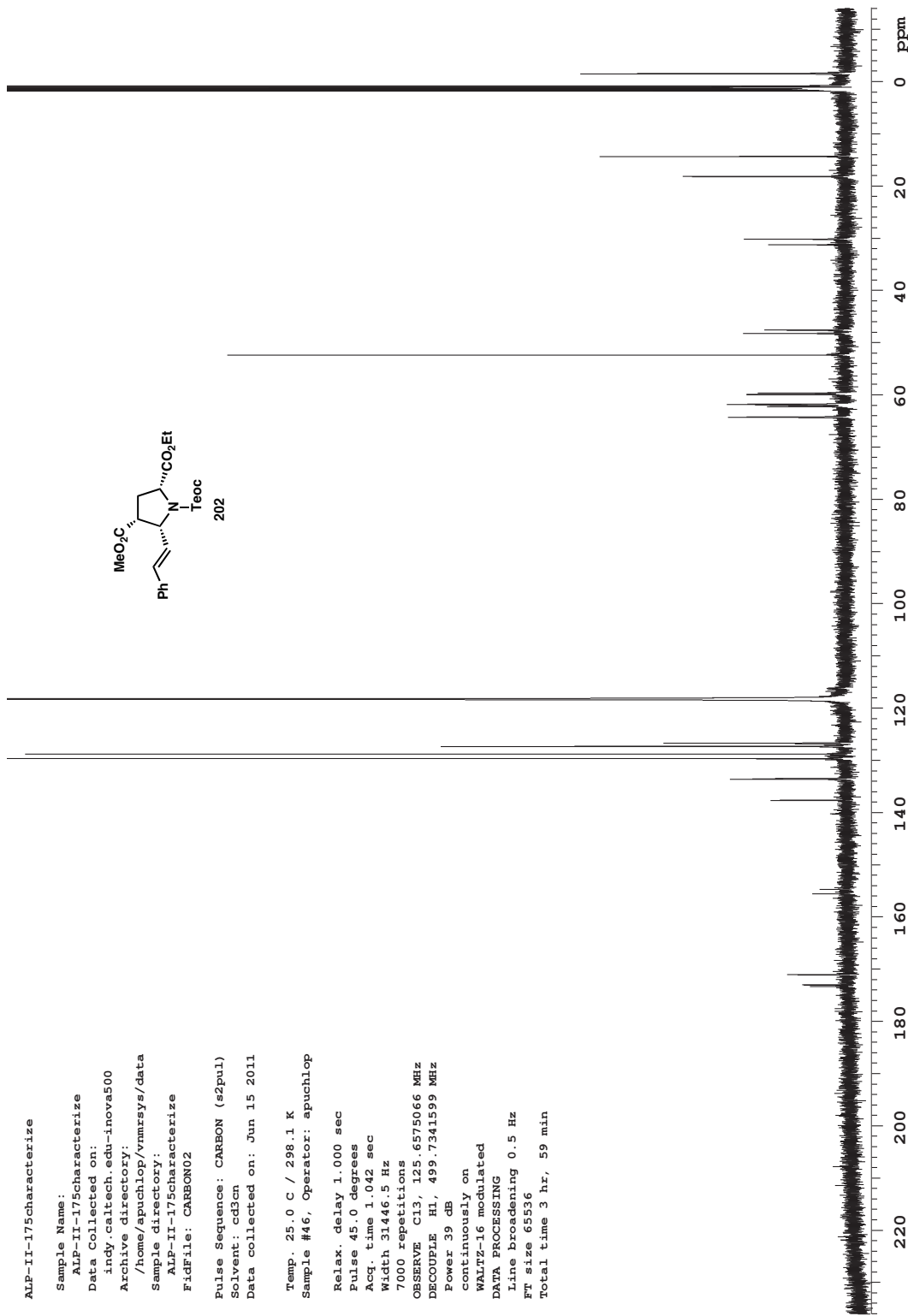


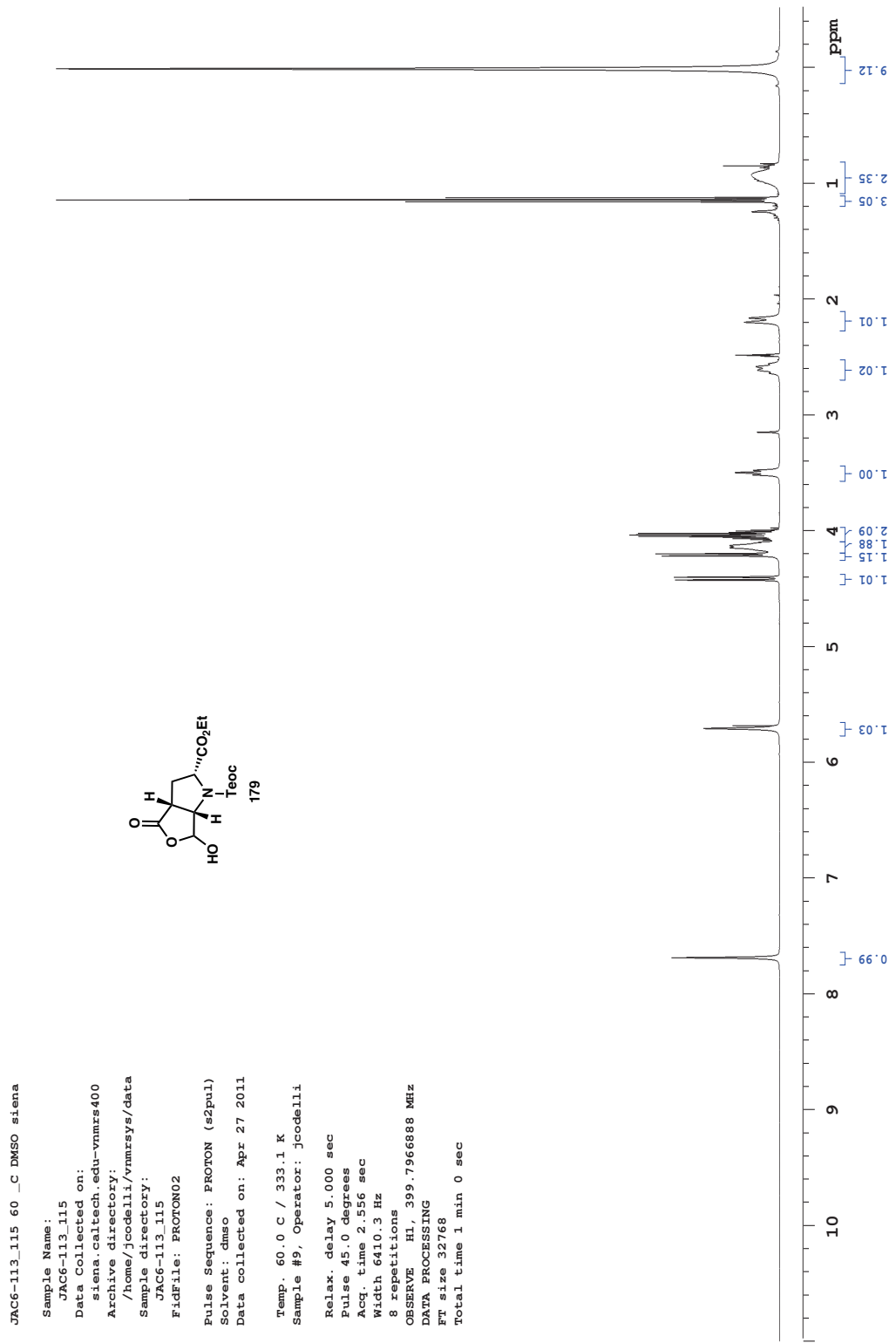


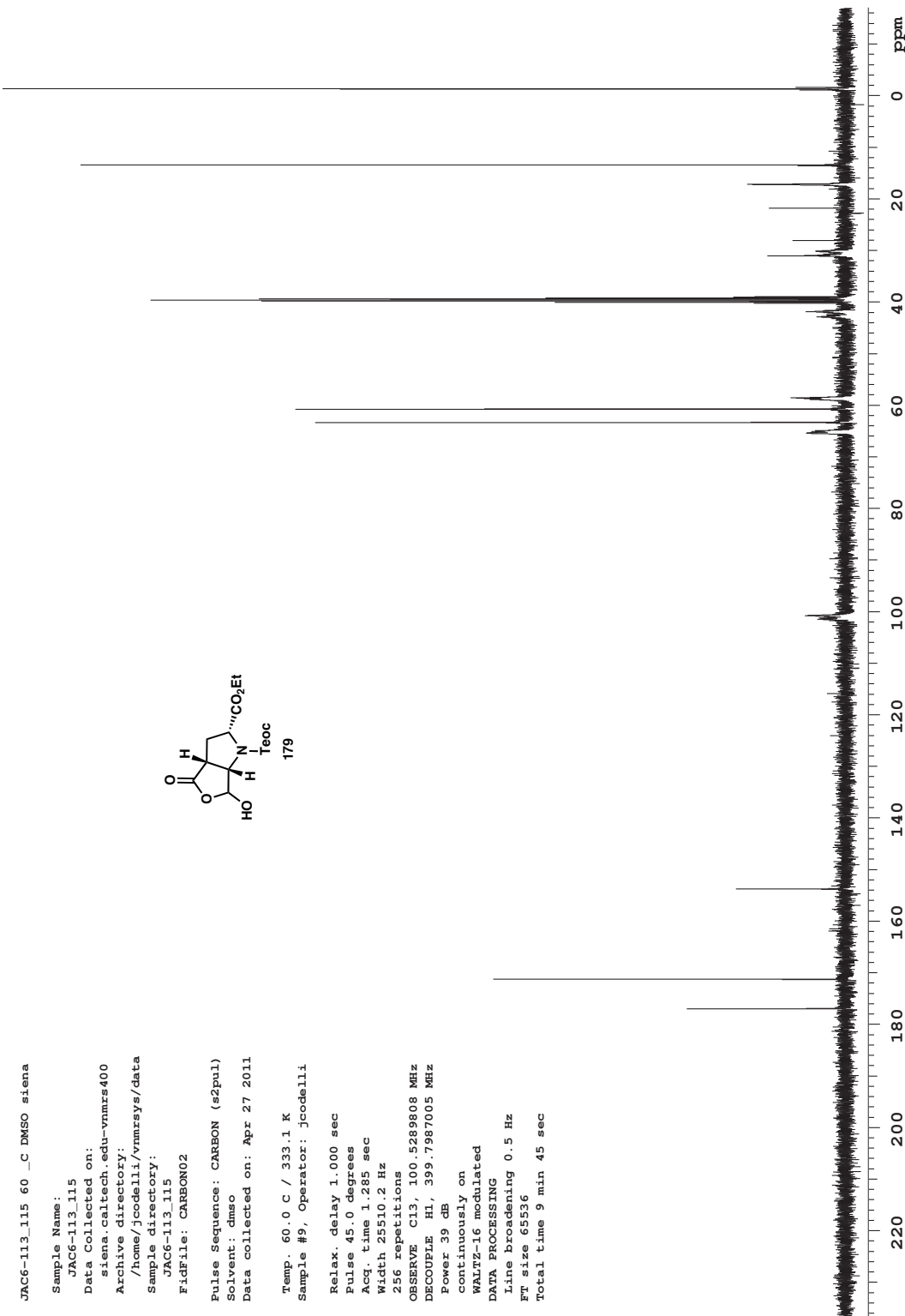


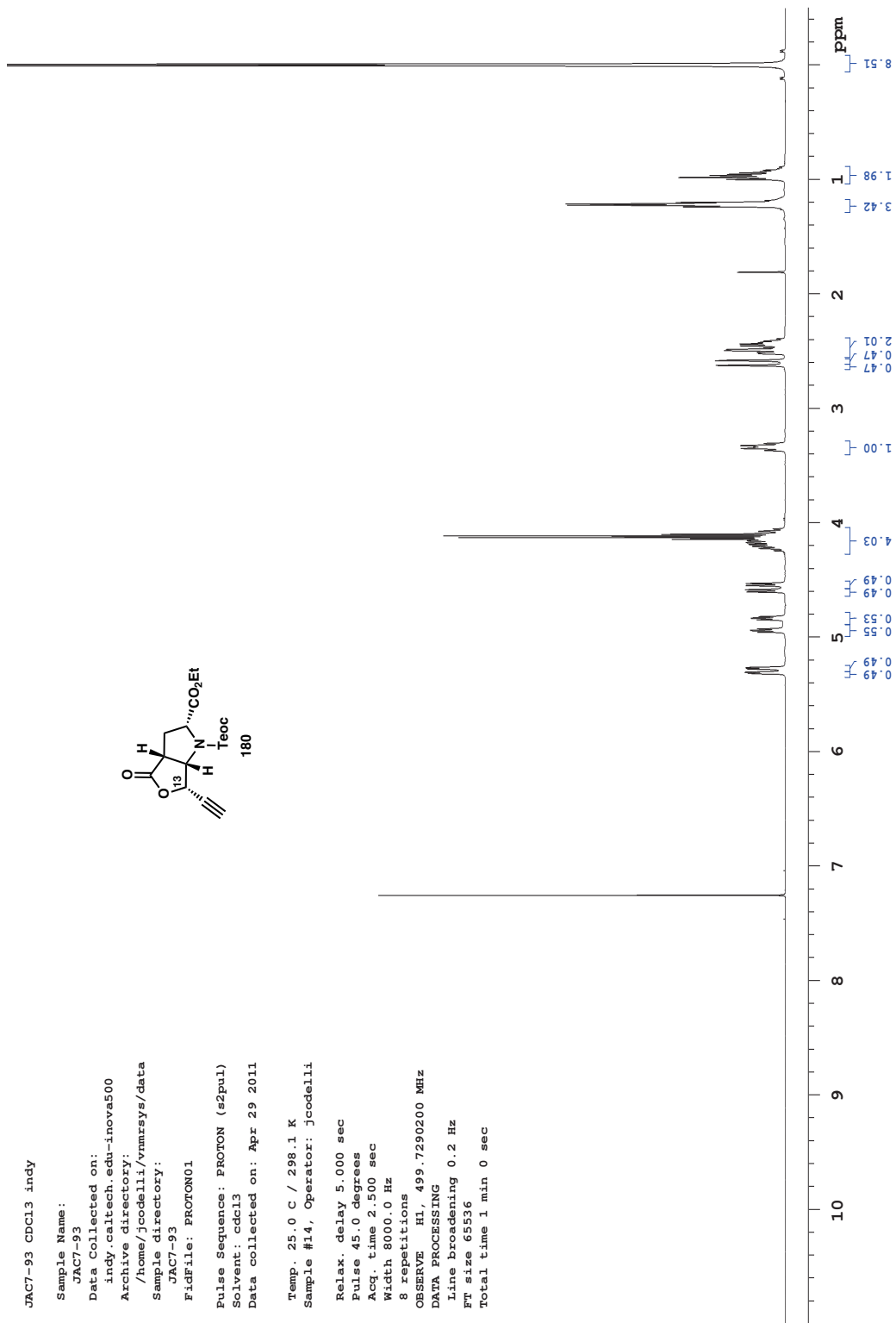


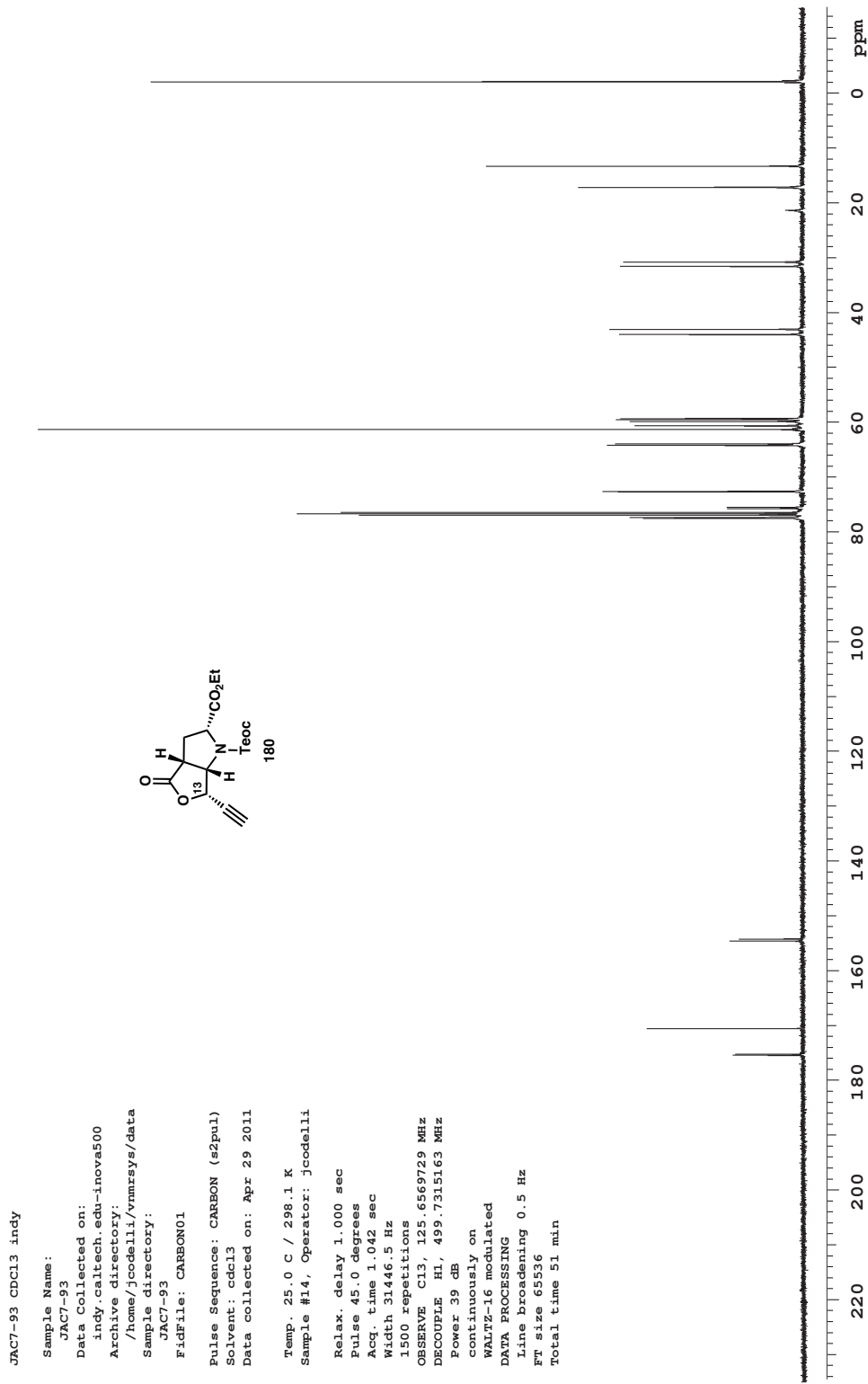


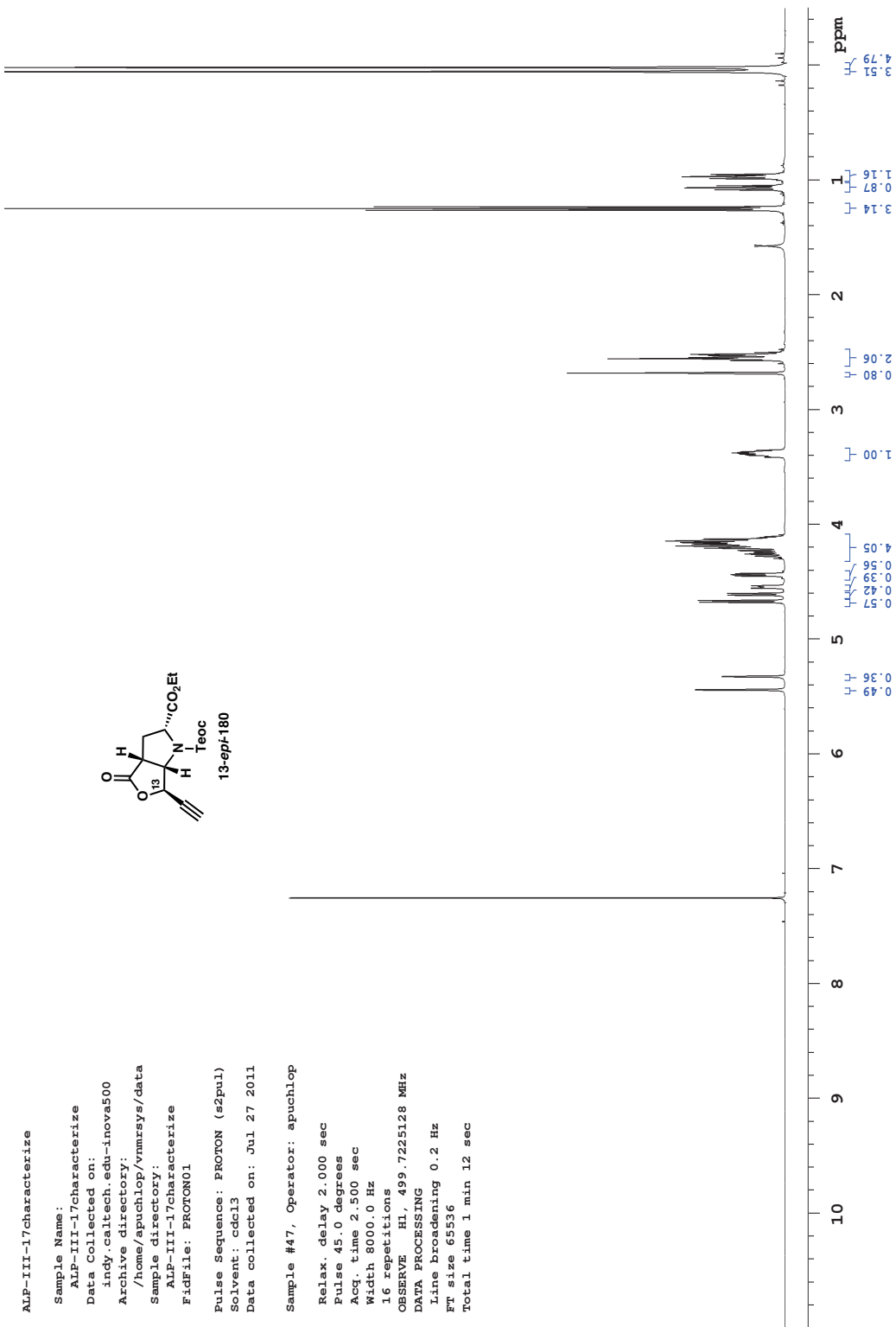


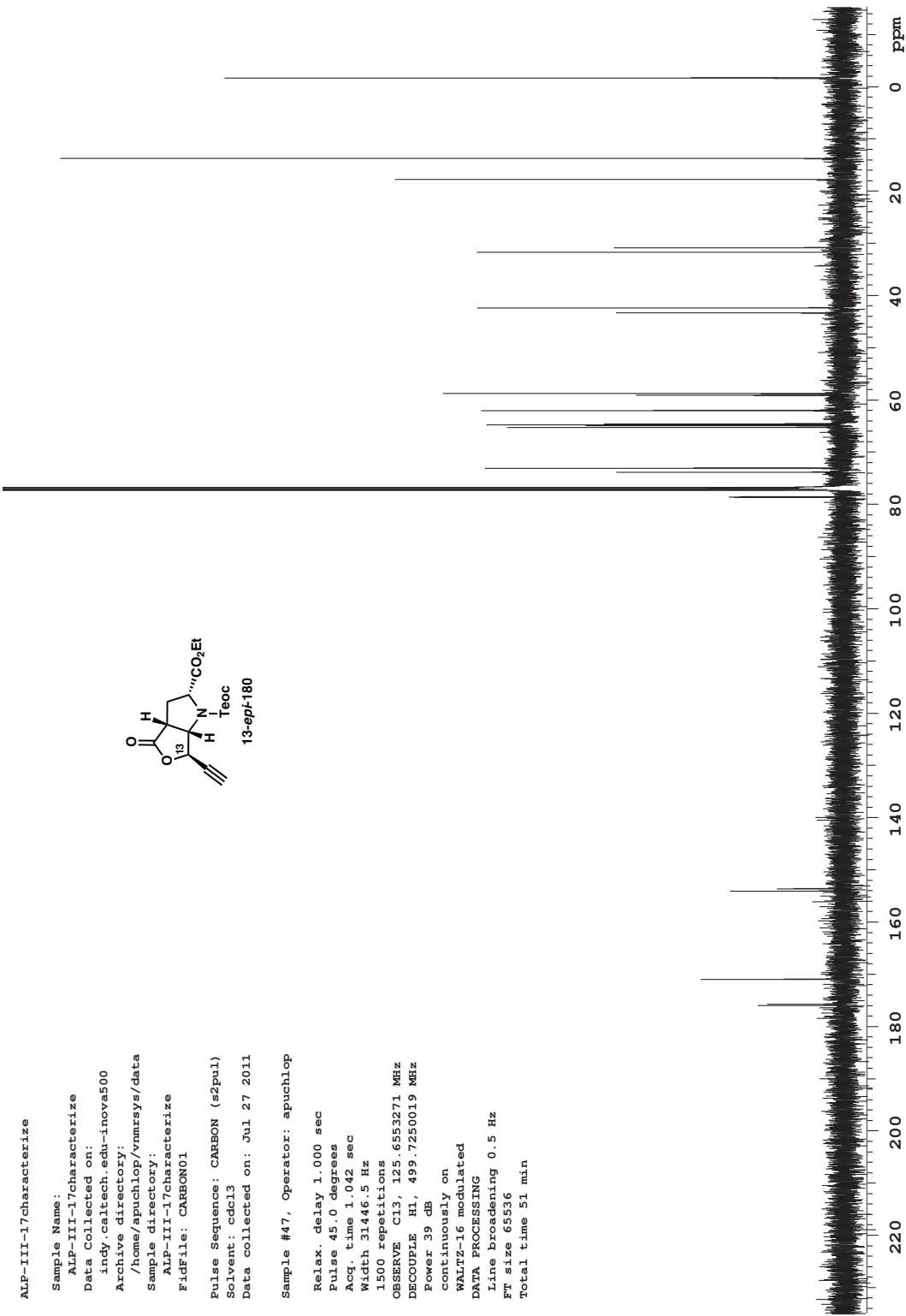


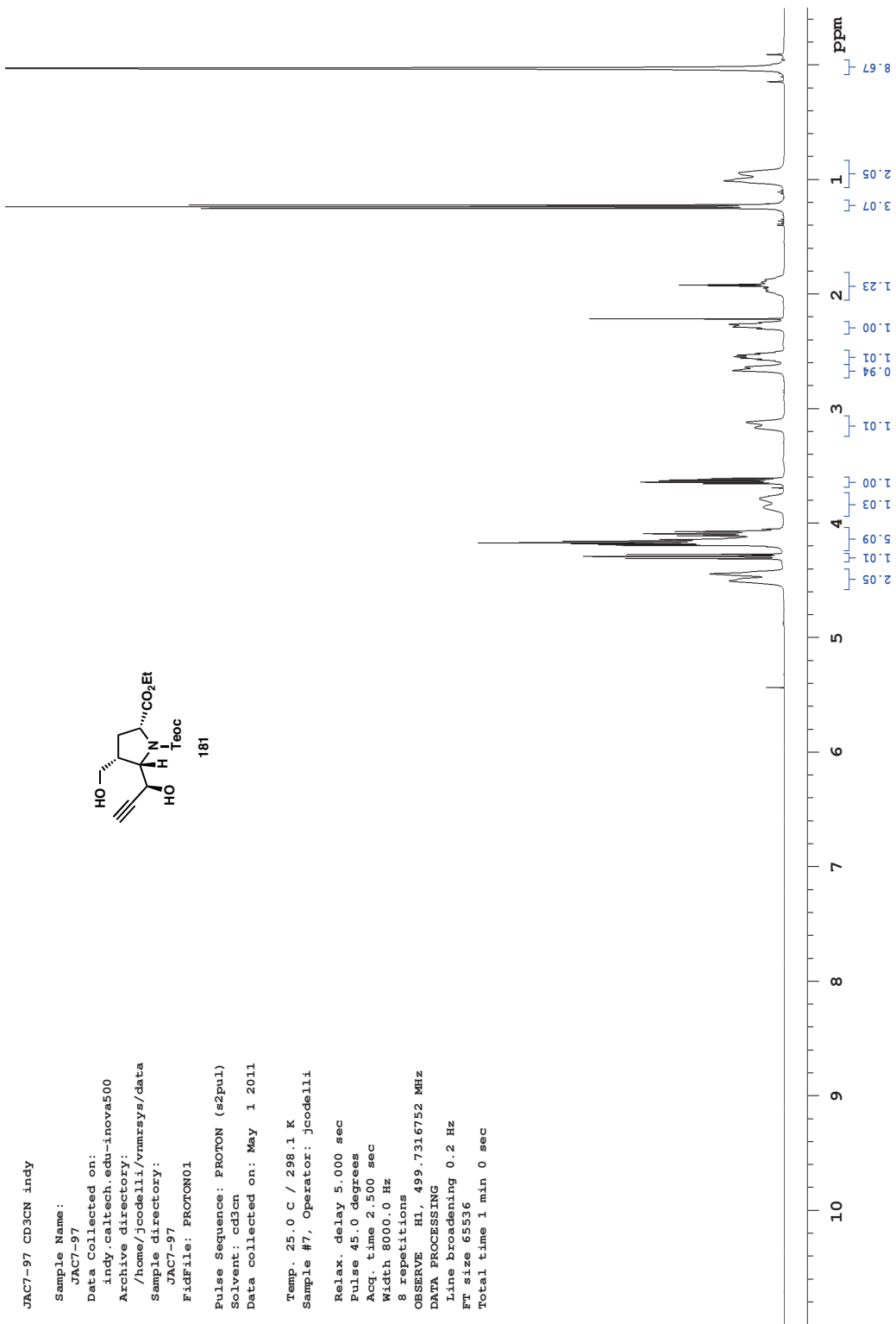


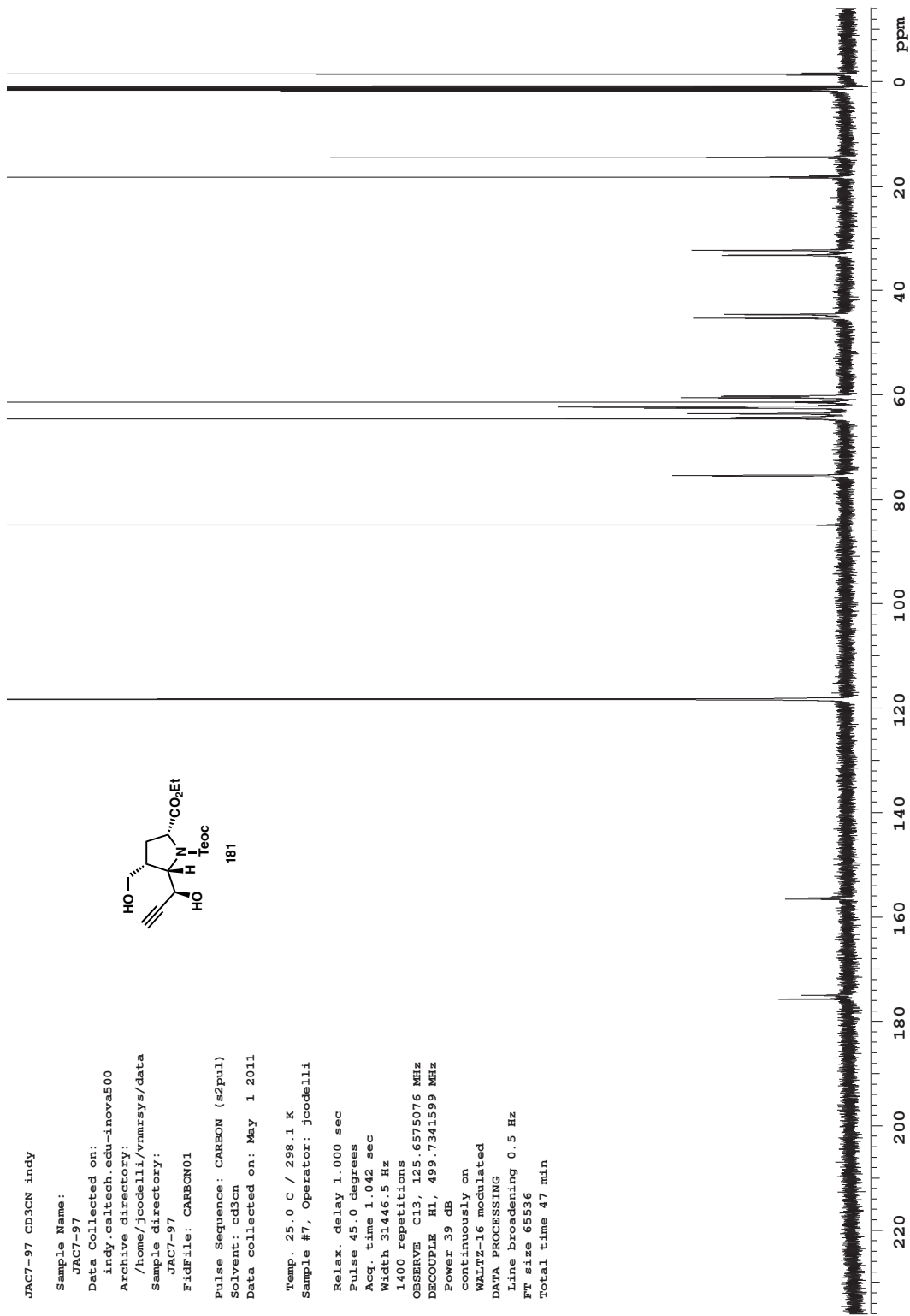


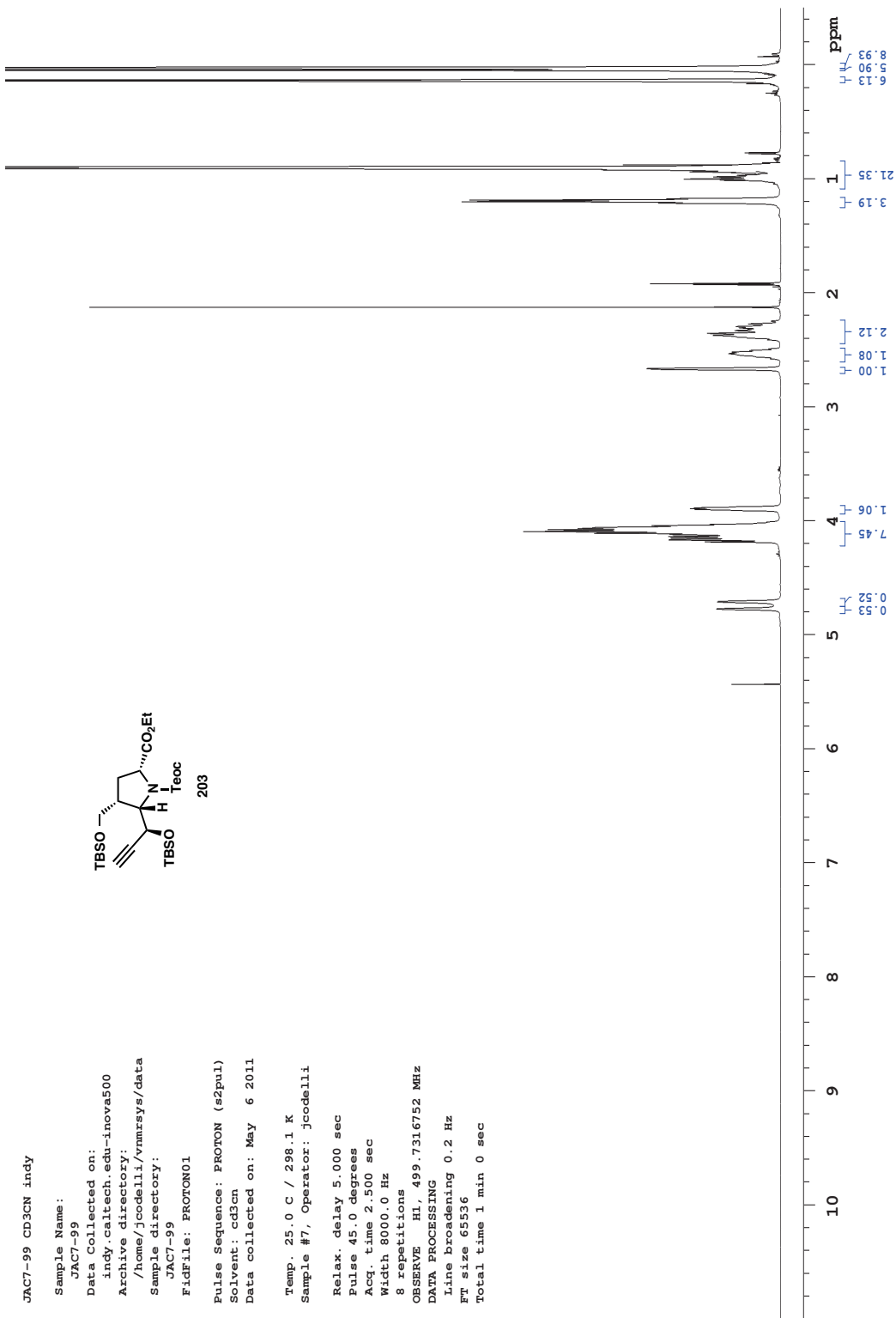


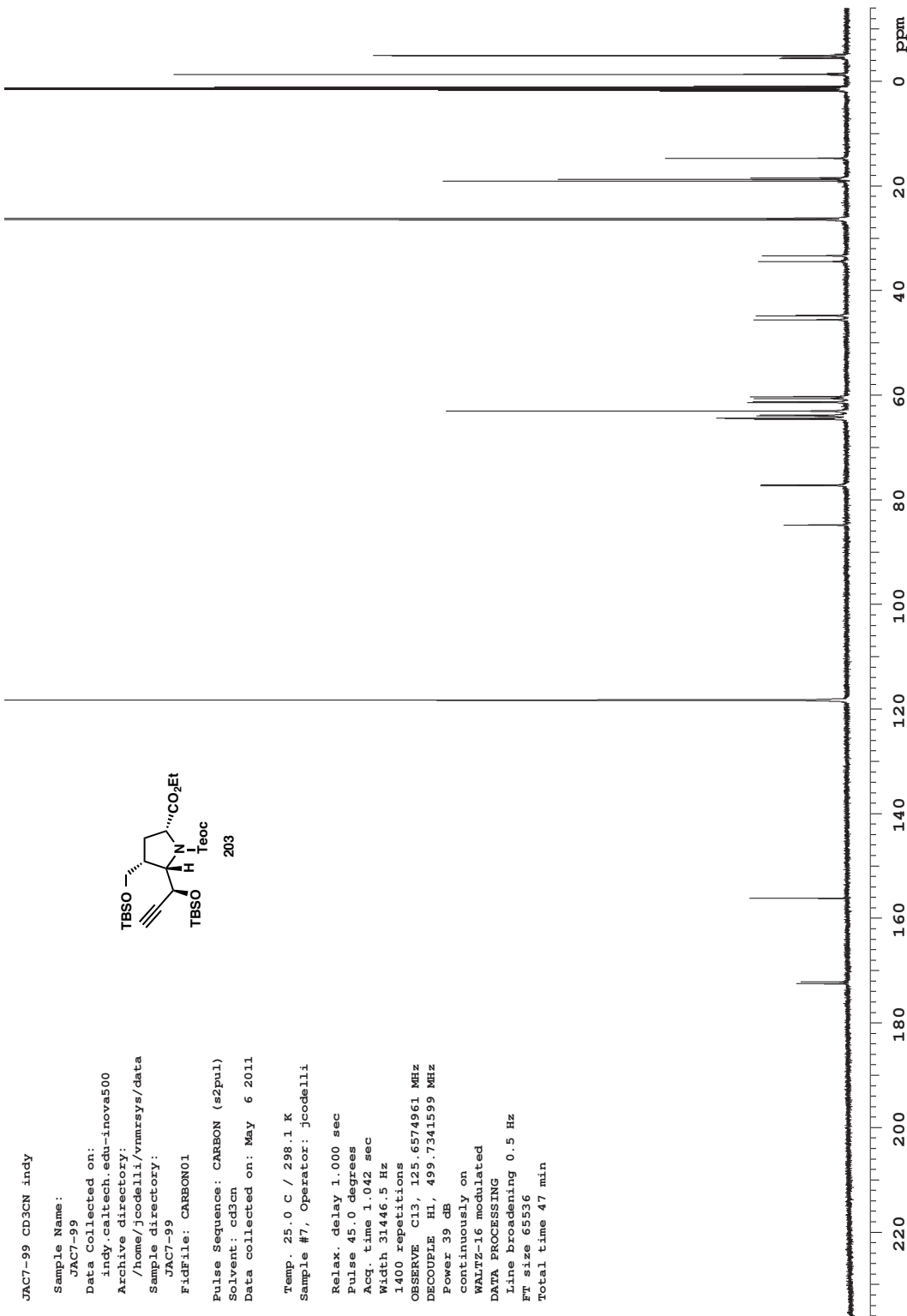


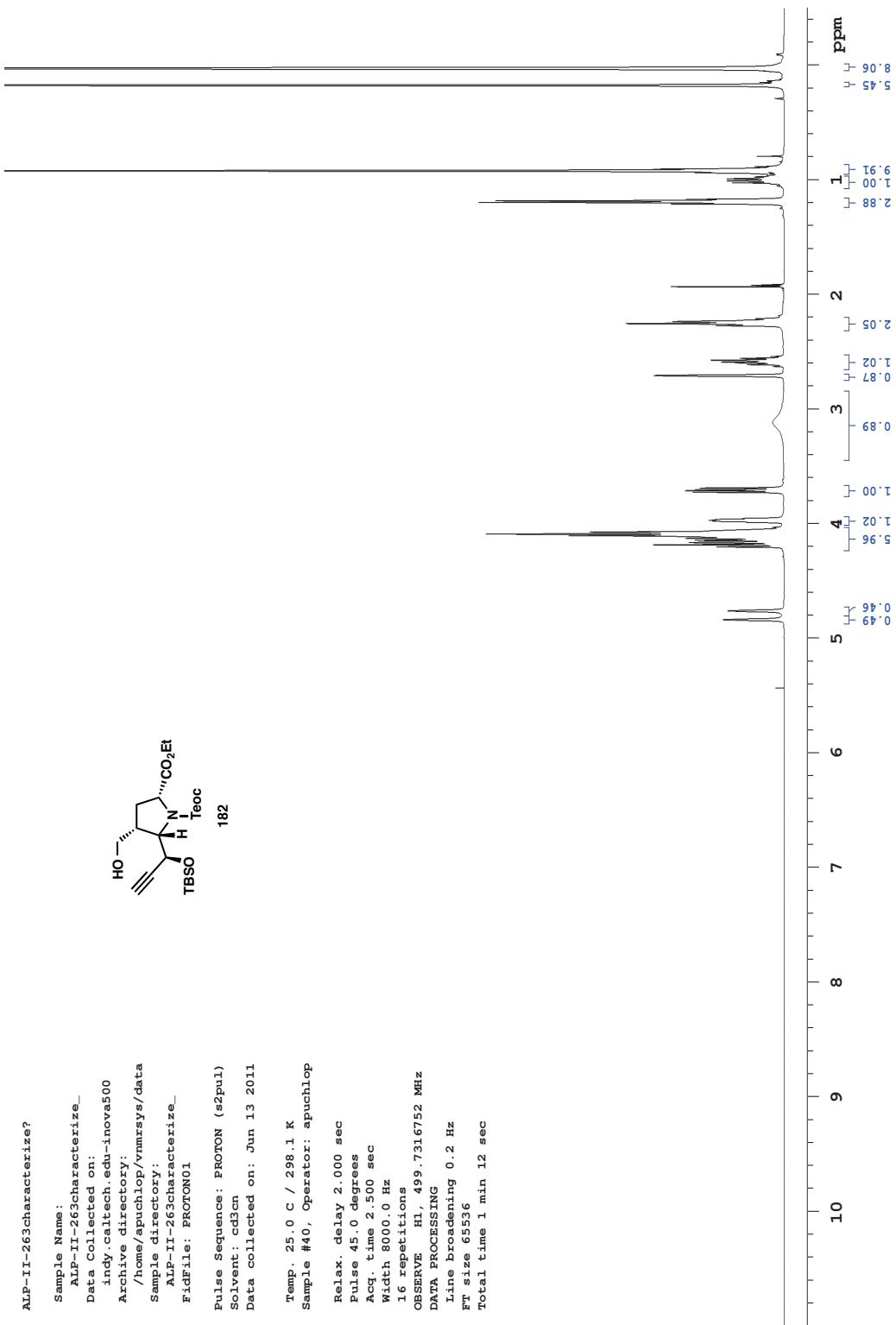


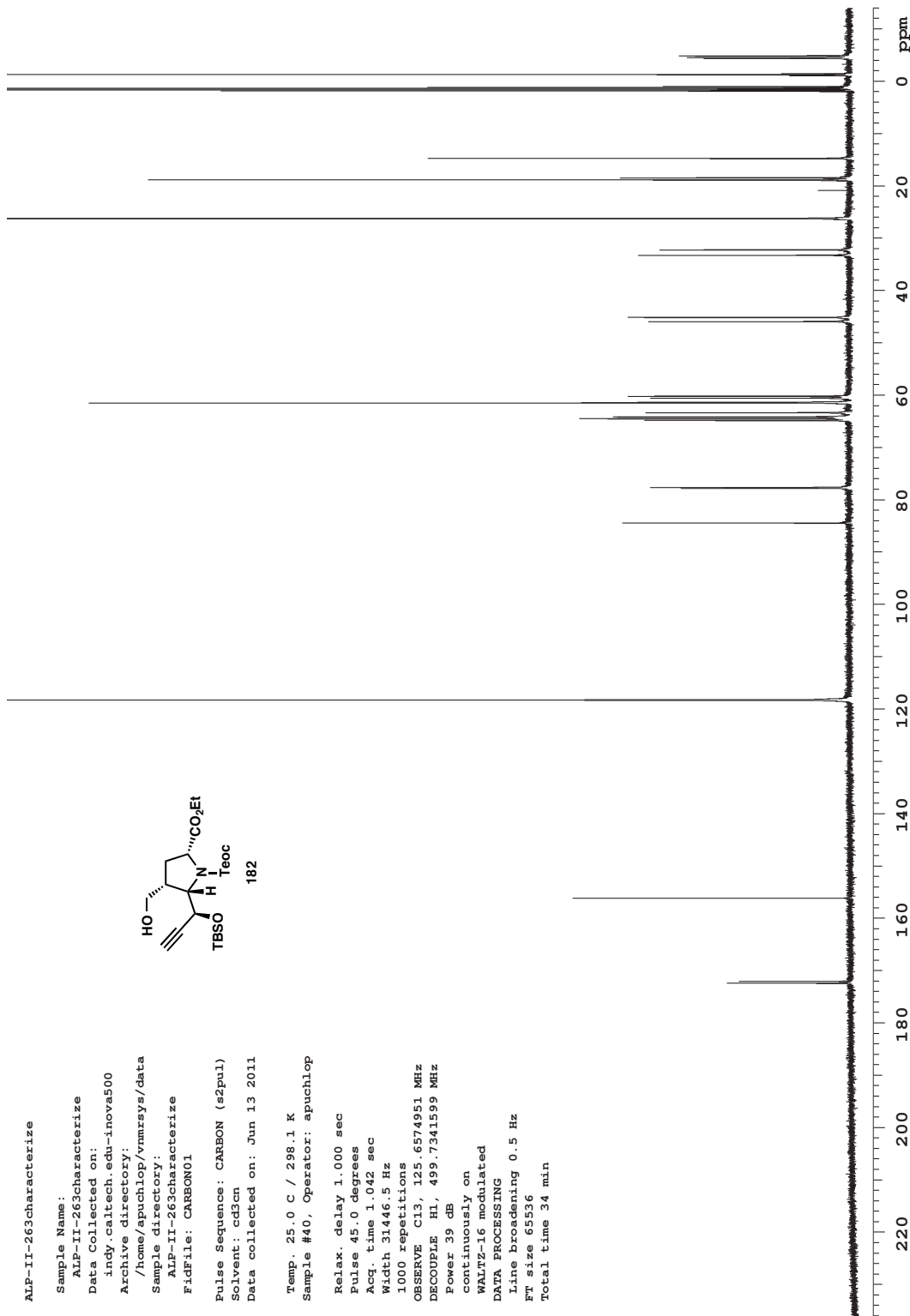


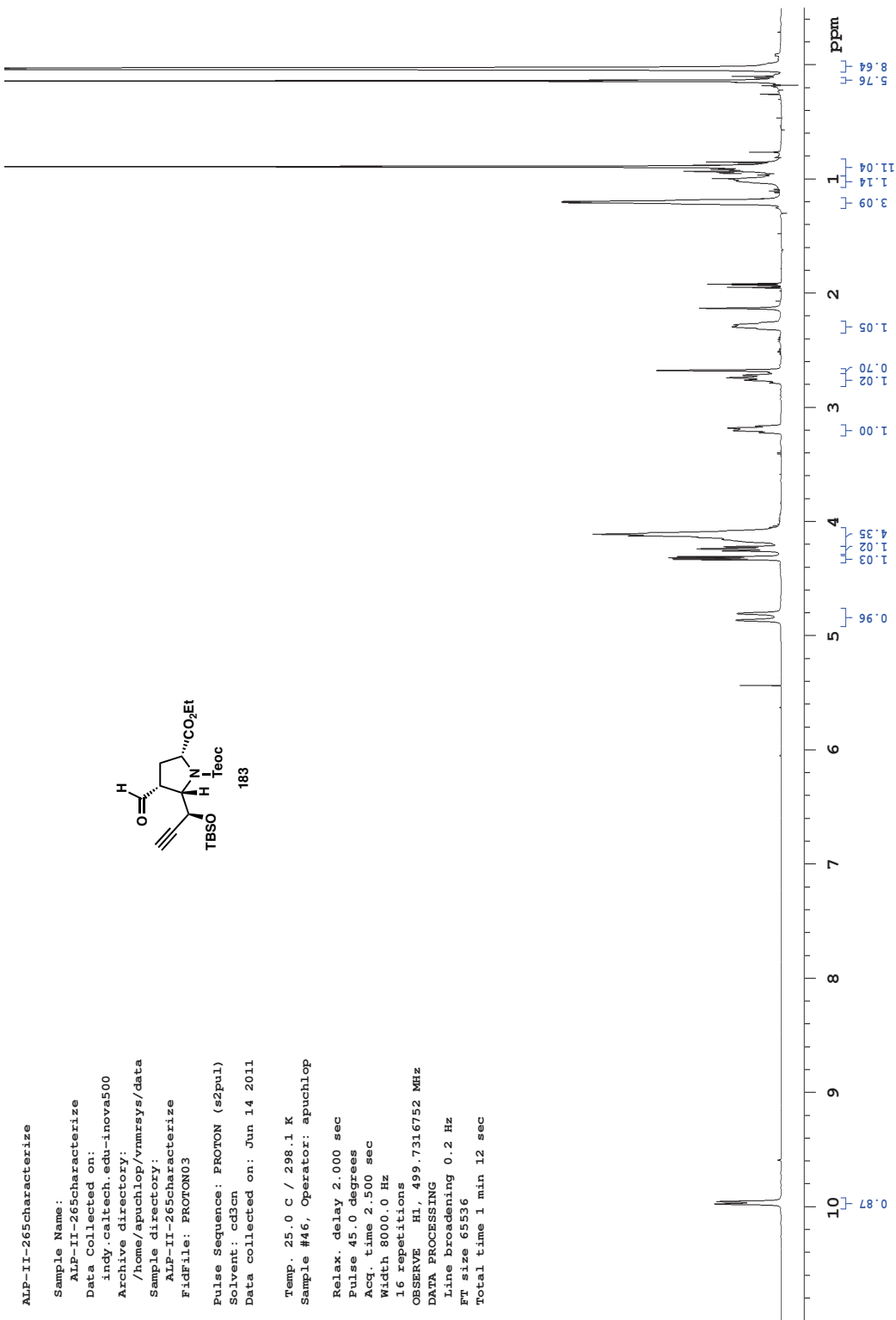


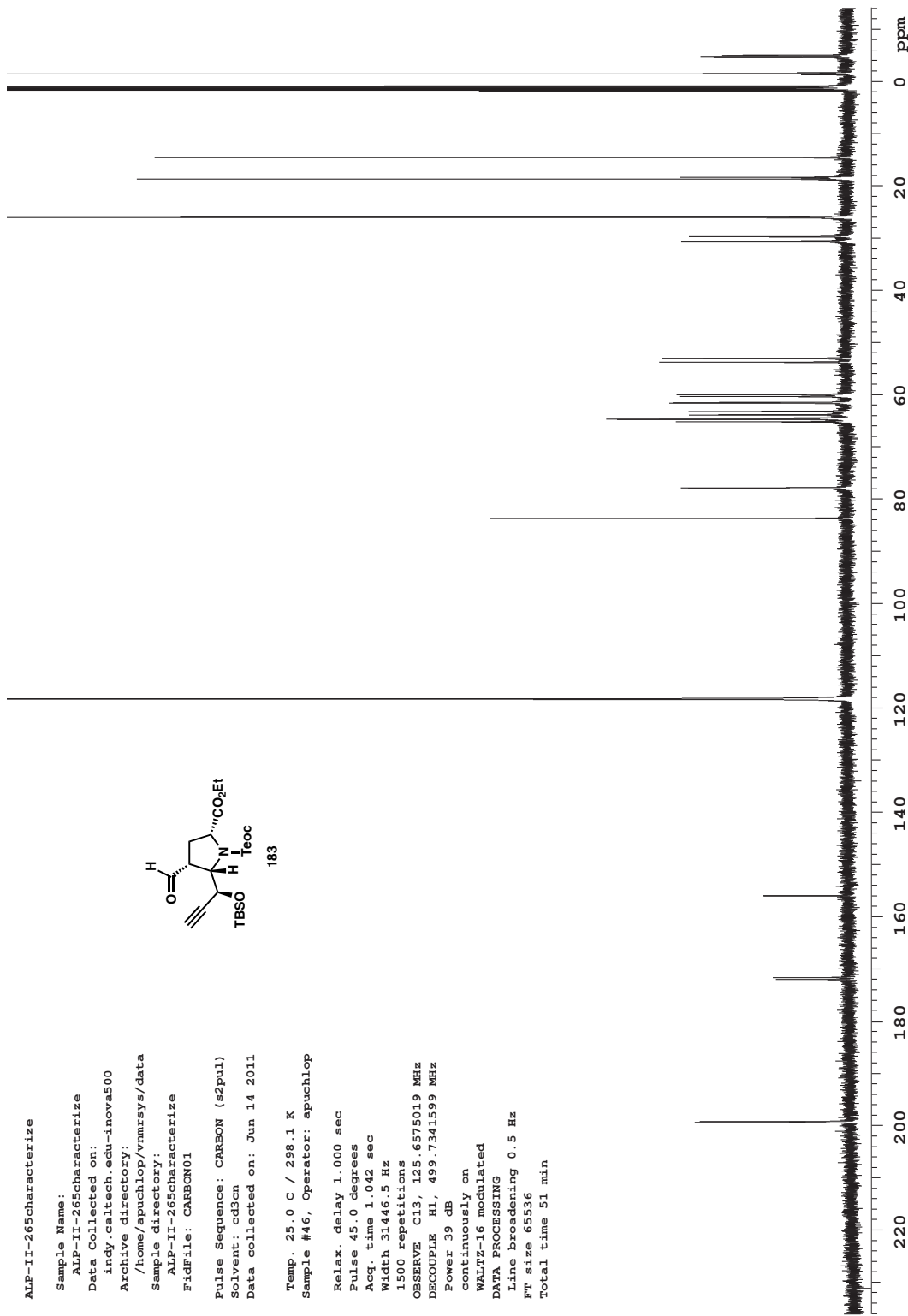


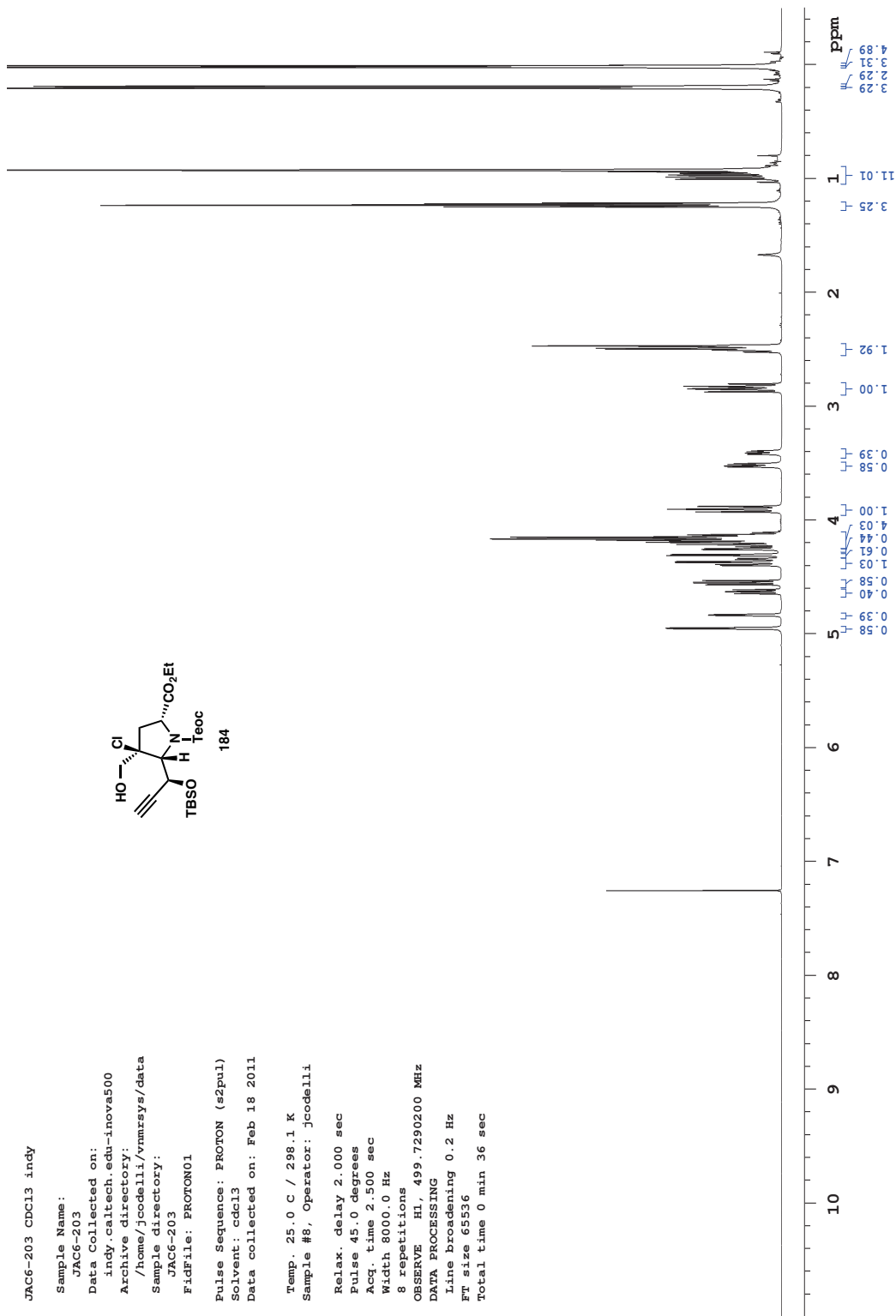


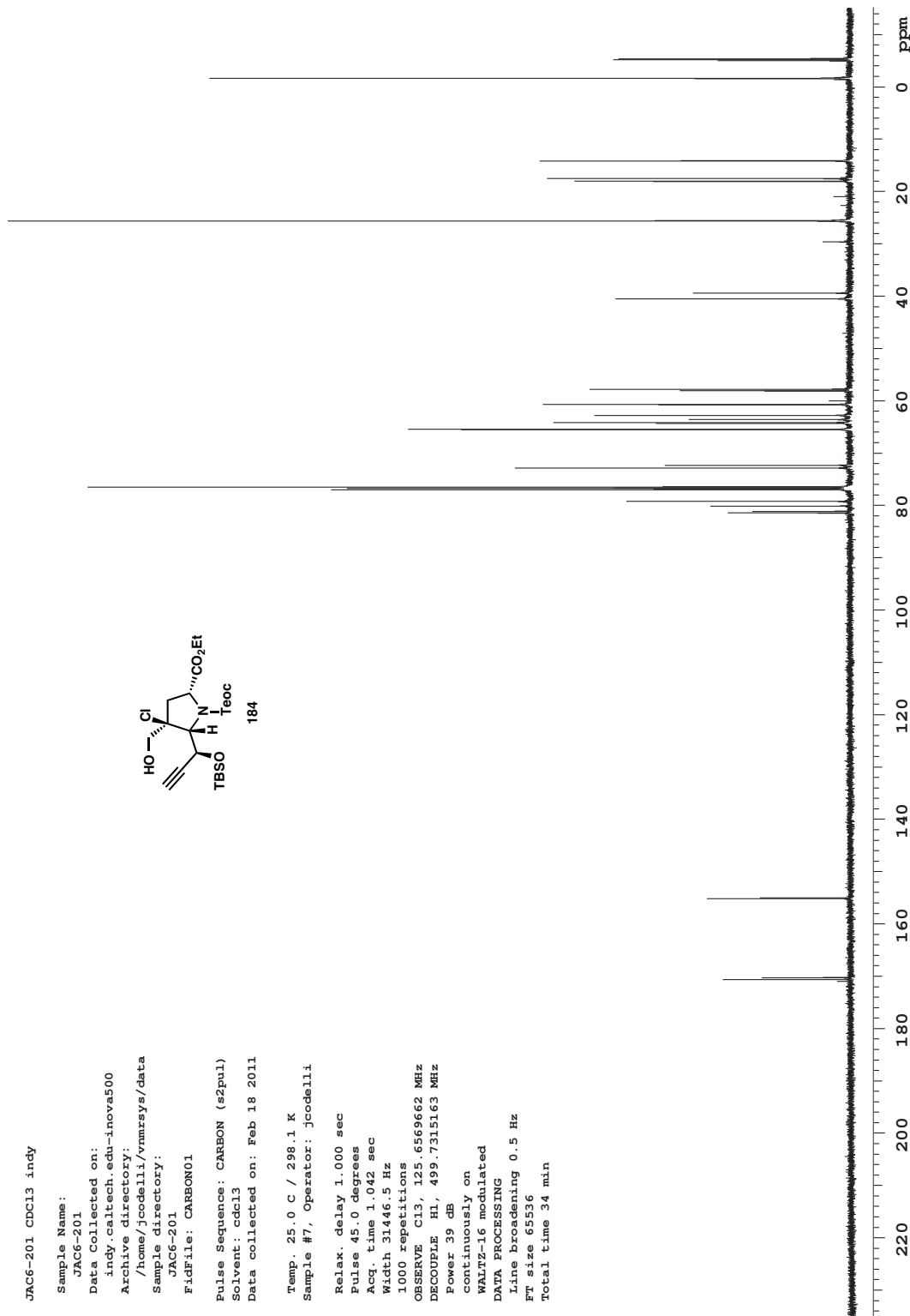


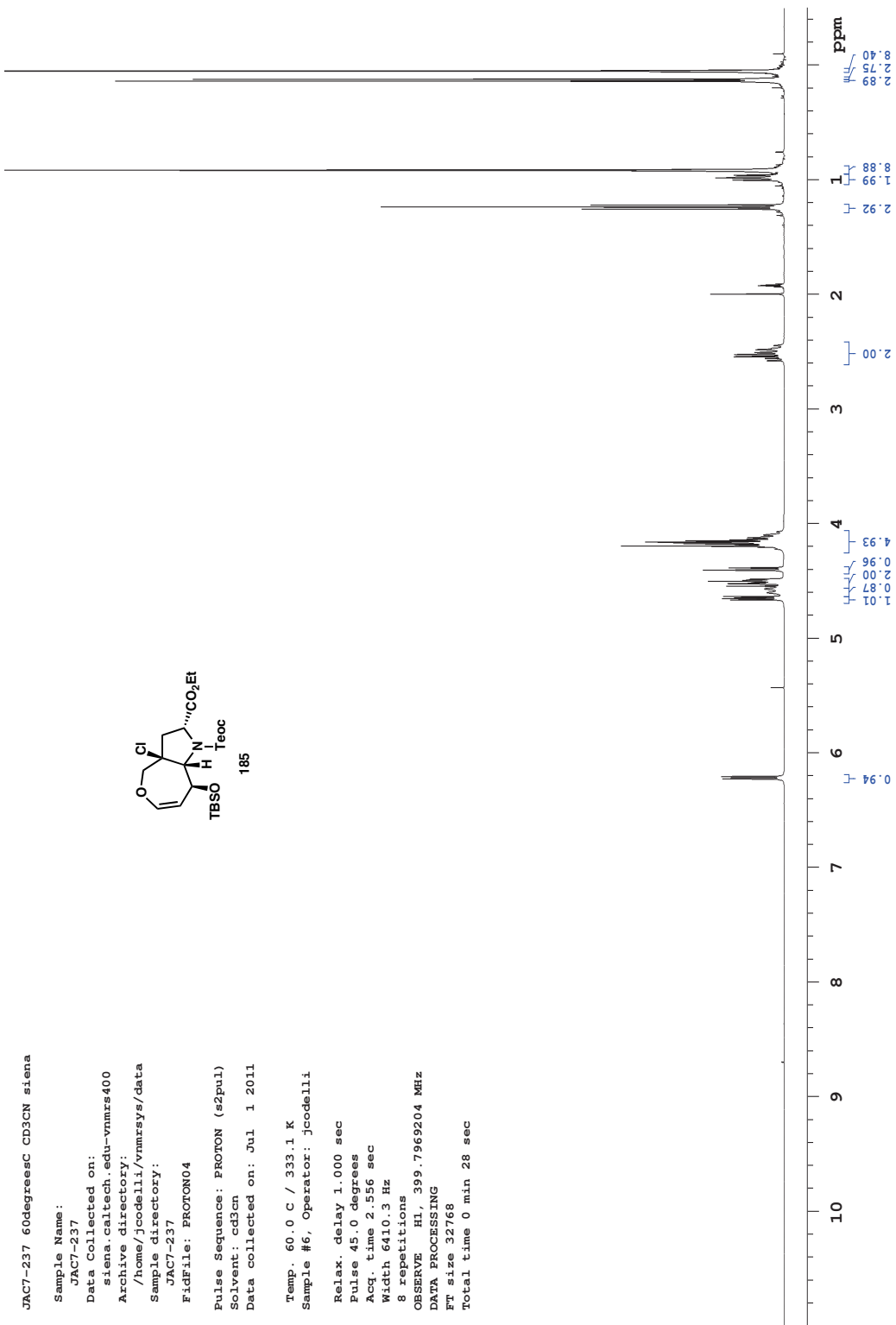


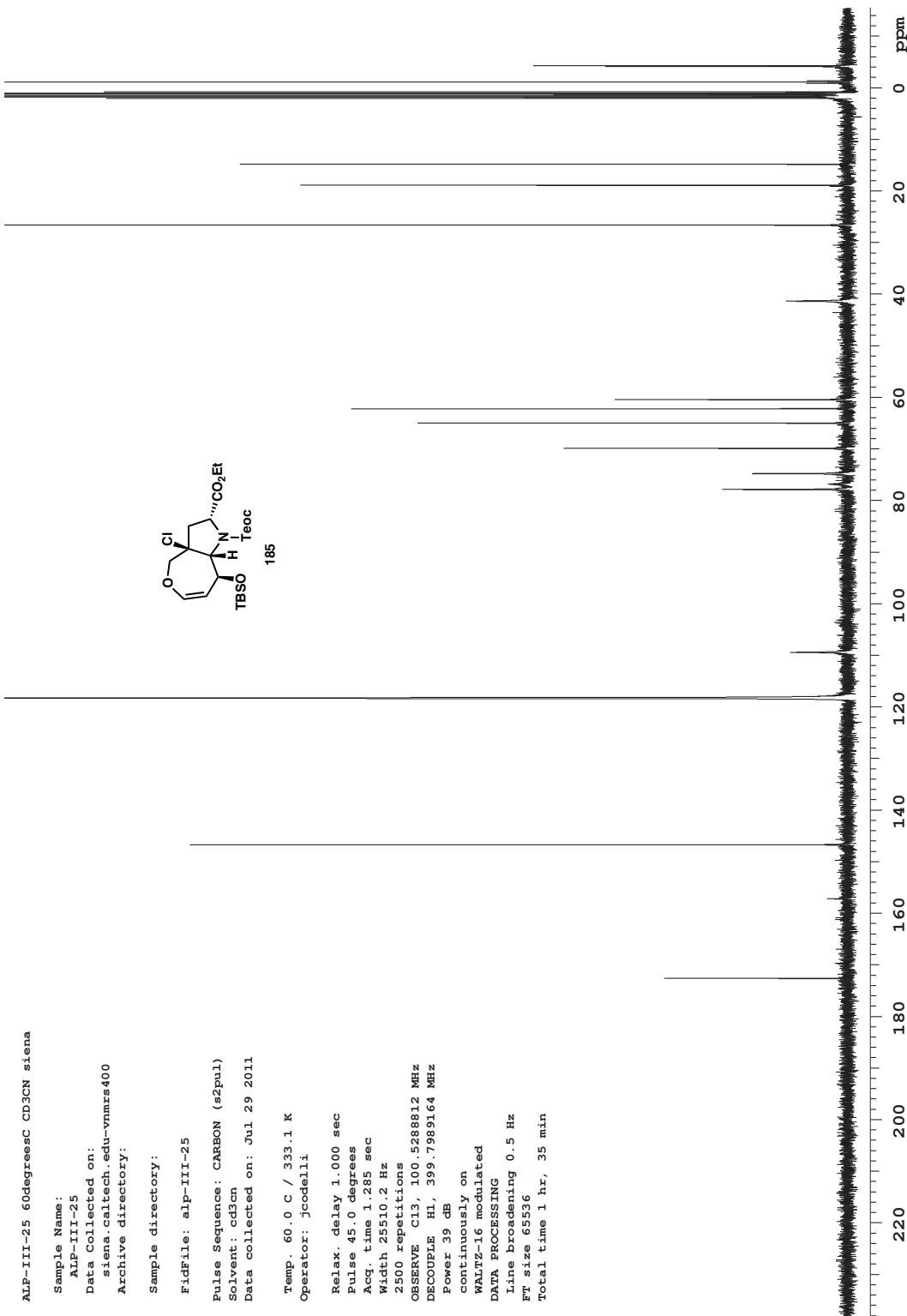


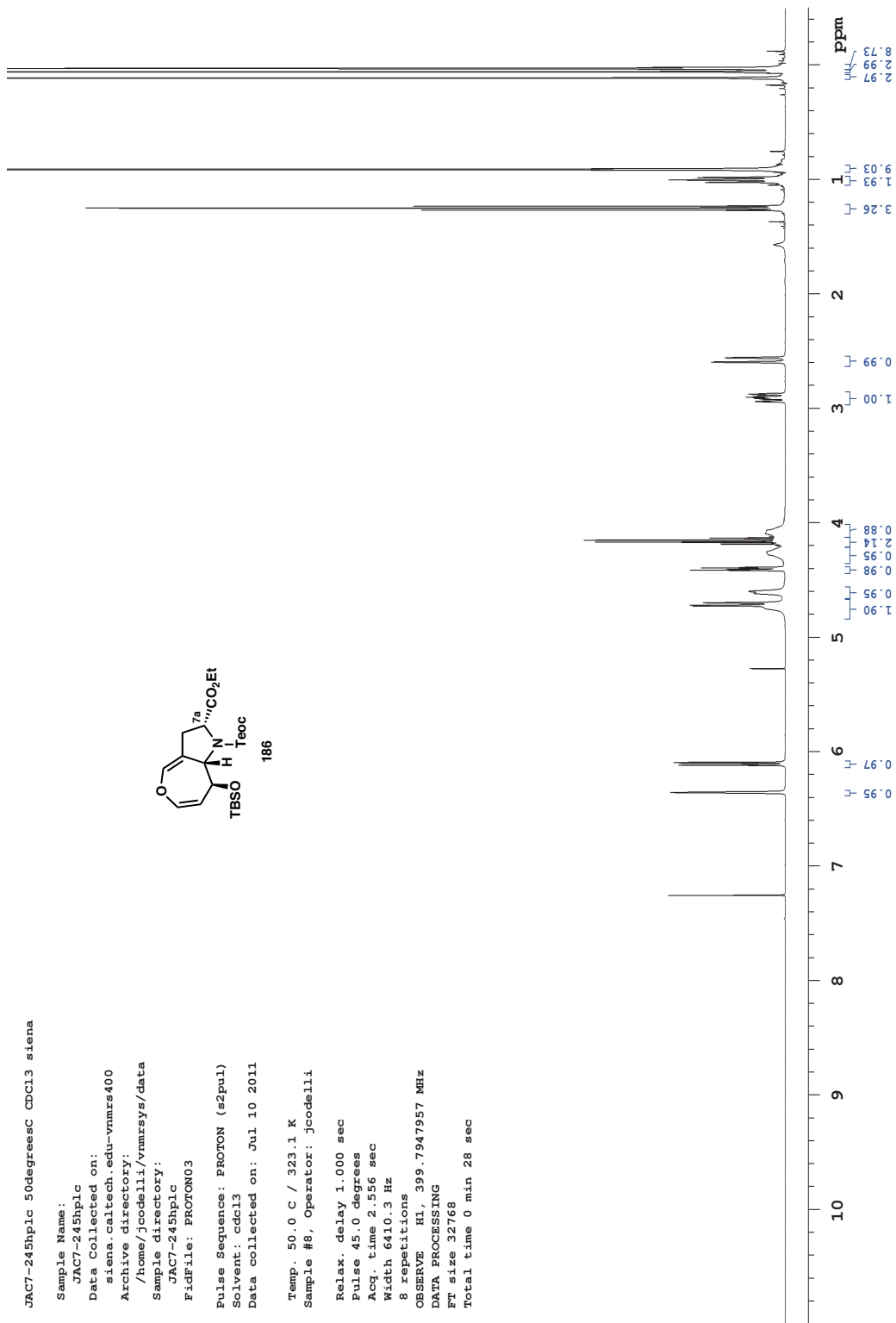












```

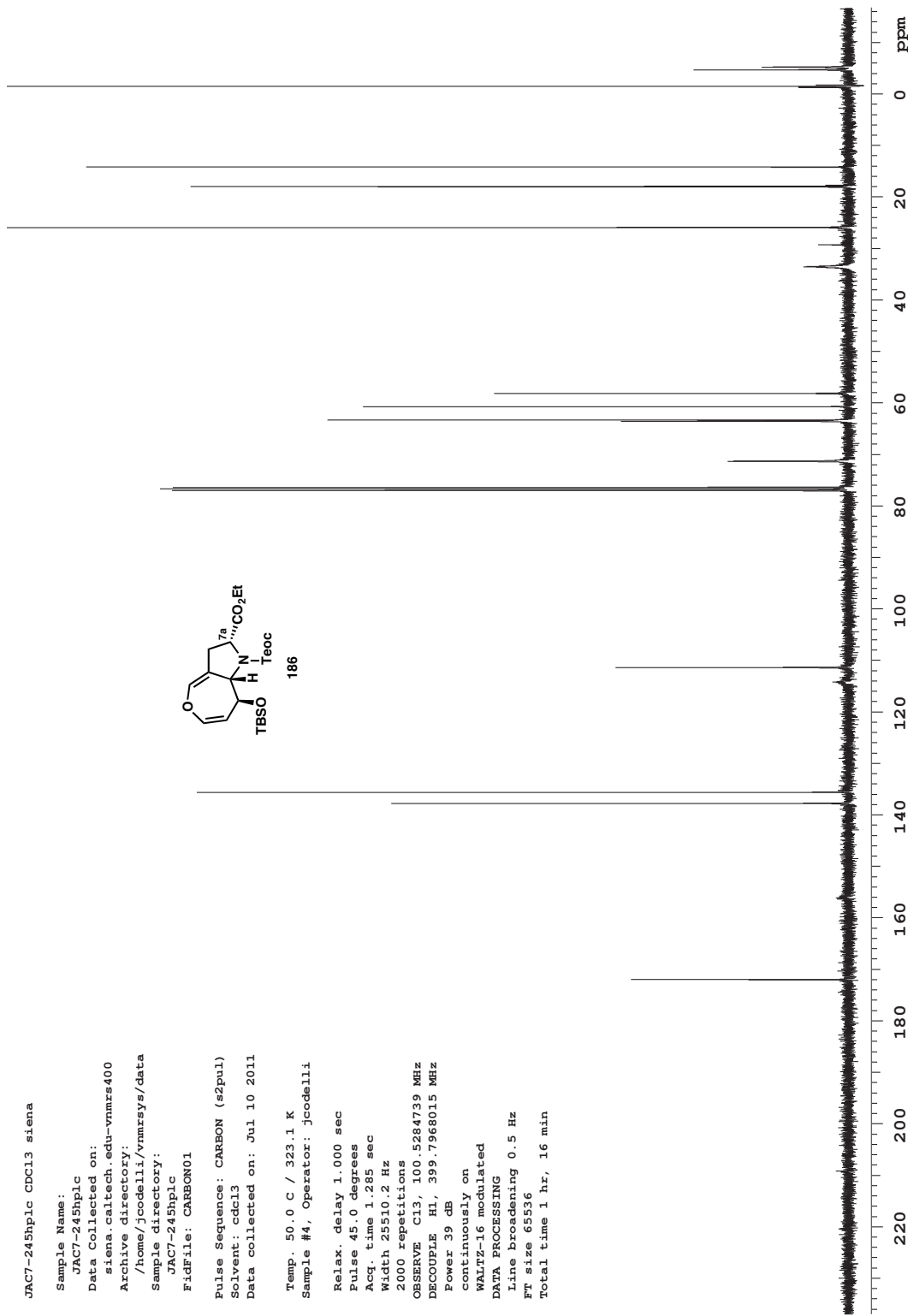
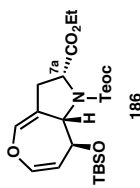
JAC7-245hplic CDCL3 siena

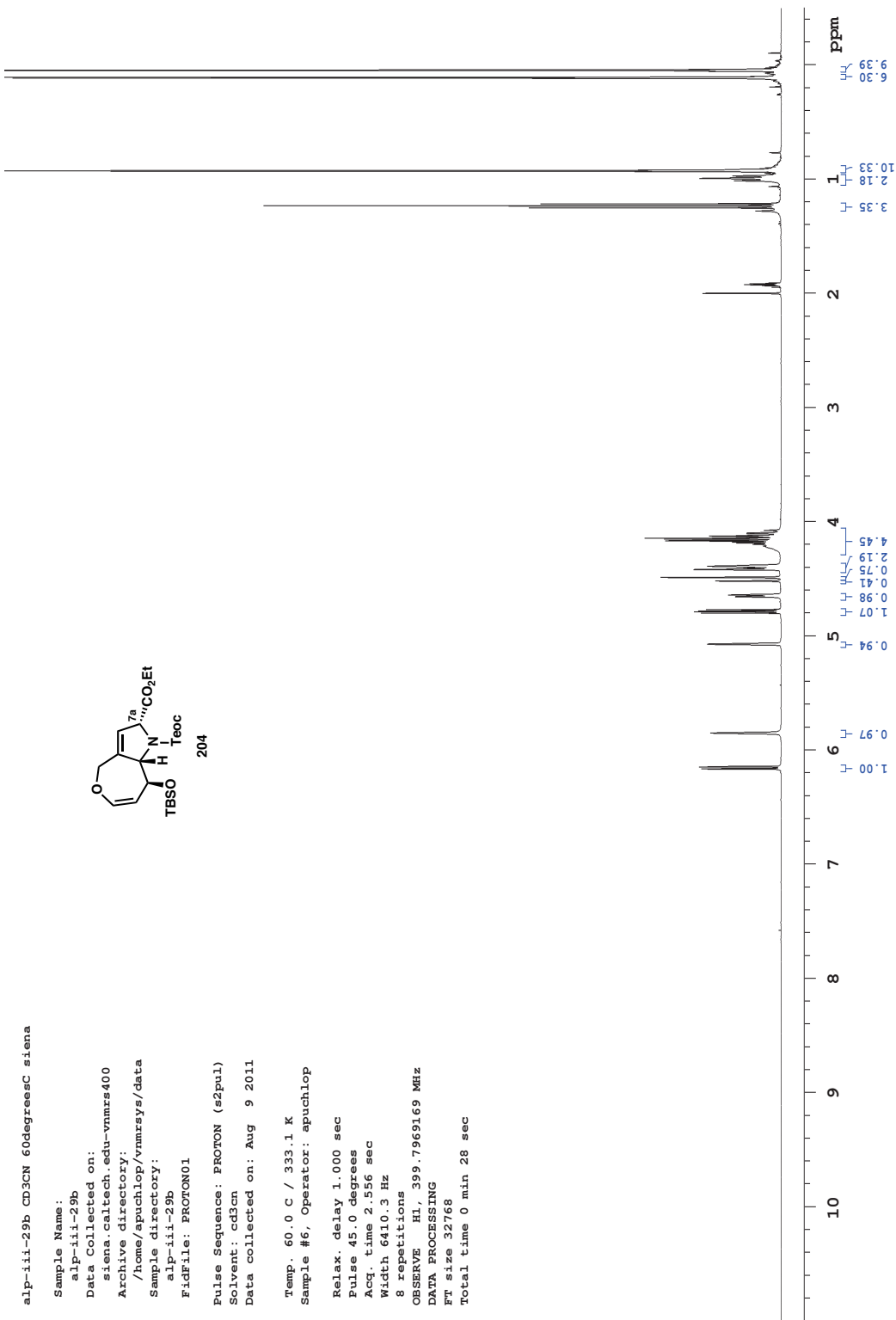
Sample Name : 
  JAC7-245hplic
Data Collected on: 
  siana.caltech.edu-vnmrsys/c
Archive directory: 
  /home/jcode/1i/vnmrsys/c
Sample directory: 
  JAC7-245hplic
FDfile: CARBON01

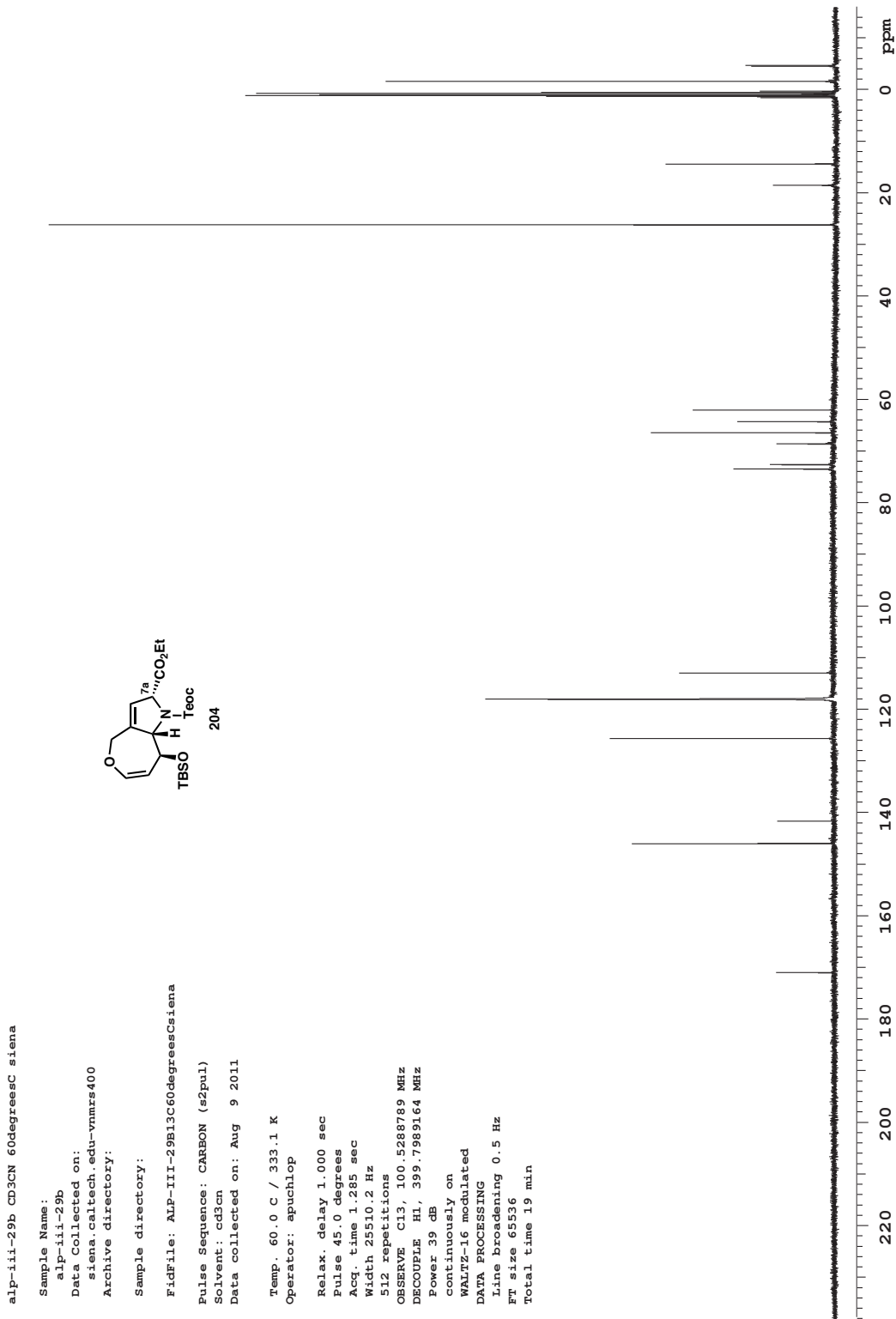
Pulse Sequence: CARBON (s2p)
CDfile: cdd13
Data collected on: Jul 10 2001
Temp. 50.0 C / 323.1 K
Sample #4, Operator: jcode

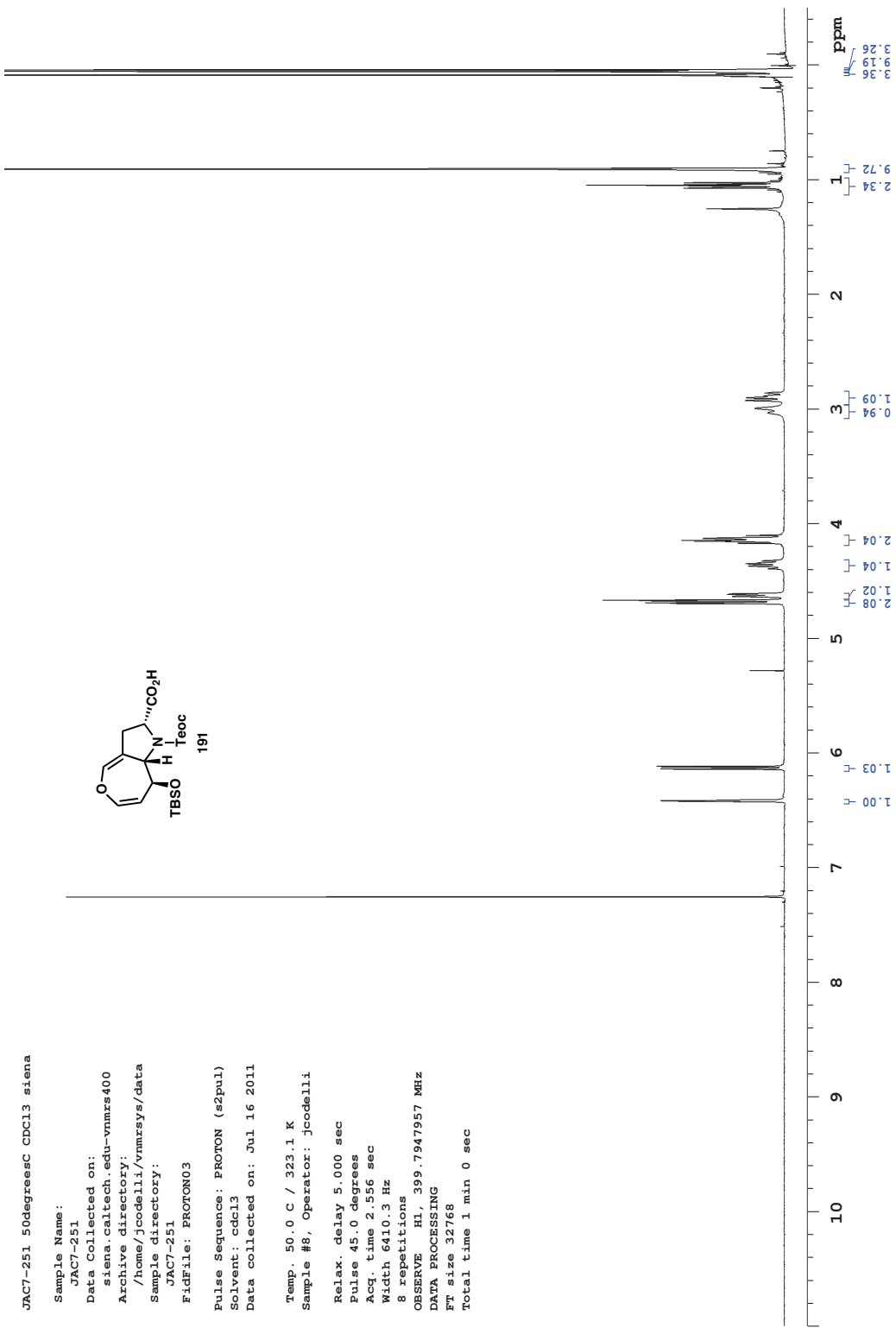
Relax. delay 1.000 sec
Pulse 45.0 degrees
Aqg. time 1.25 sec
Width 25210.2 Hz
2000 repetitions
OBSERVE C13, 100.522479 MHz
DECUPLE HI, 399.7968015 MHz
Power 39 dB
contINUOUSLY on
WALTZ-16 modulated
DATA PROCESSING
Line broadening 0.5 Hz
FT size 65536
Total time 1 hr, 16 min

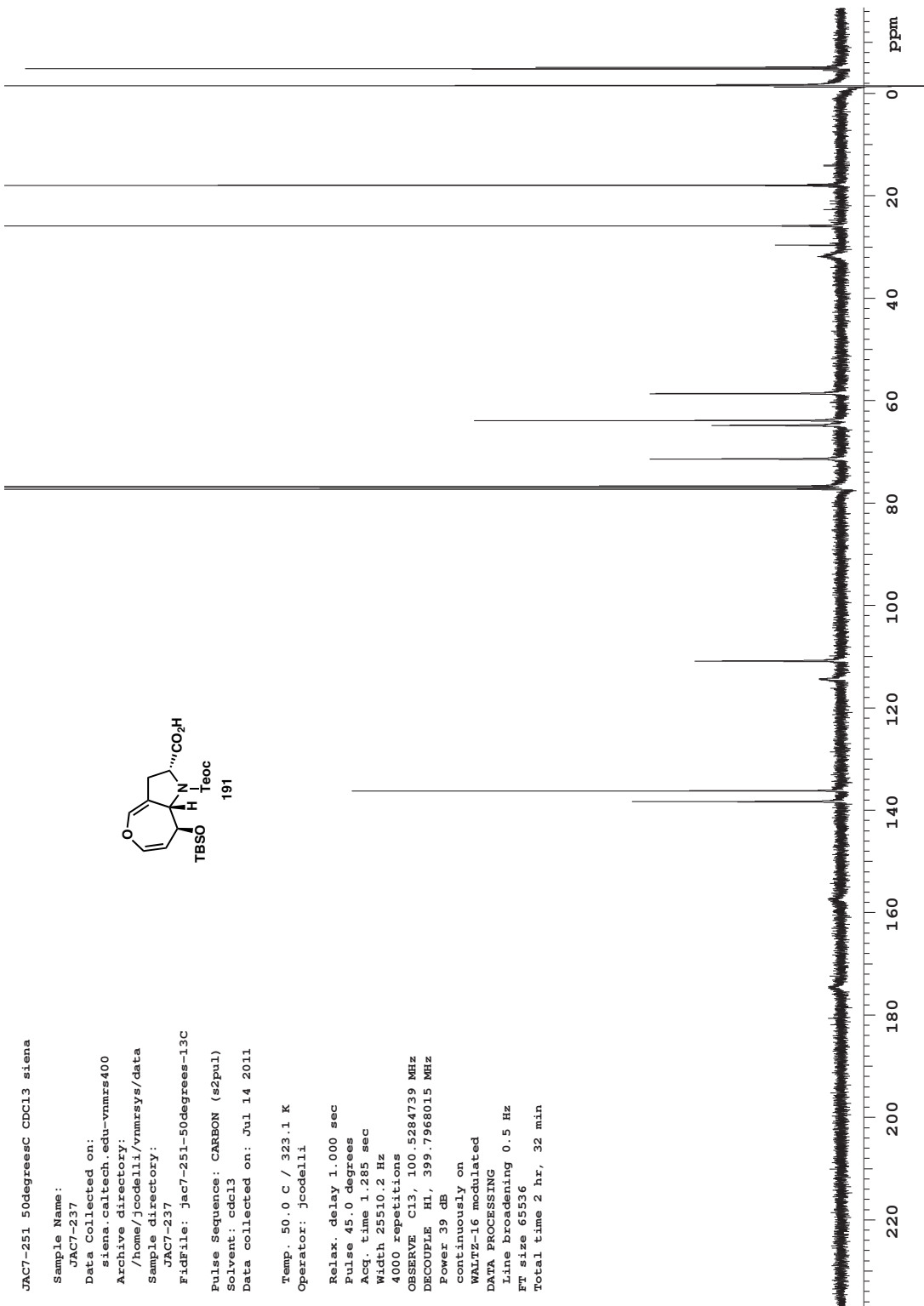
```

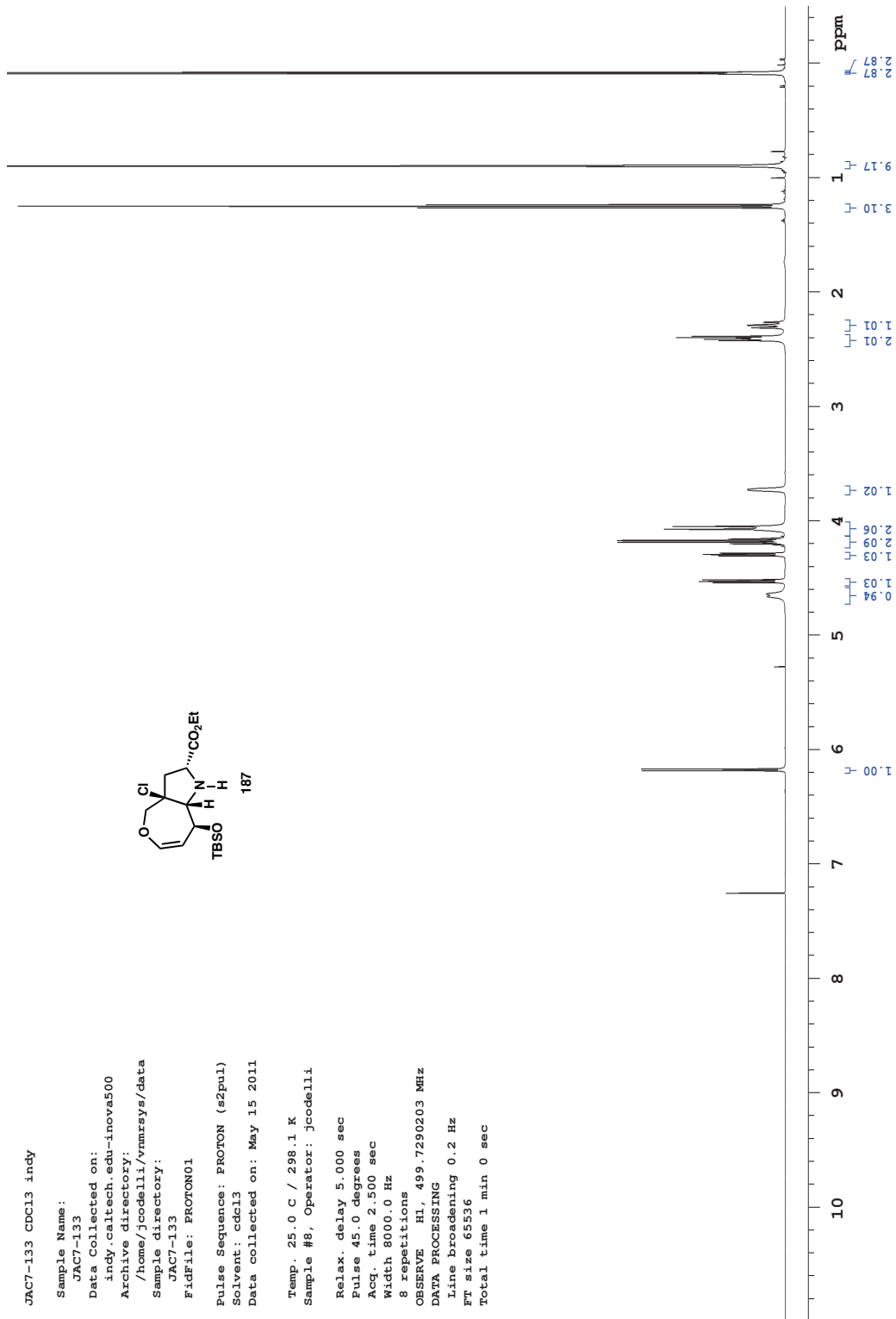


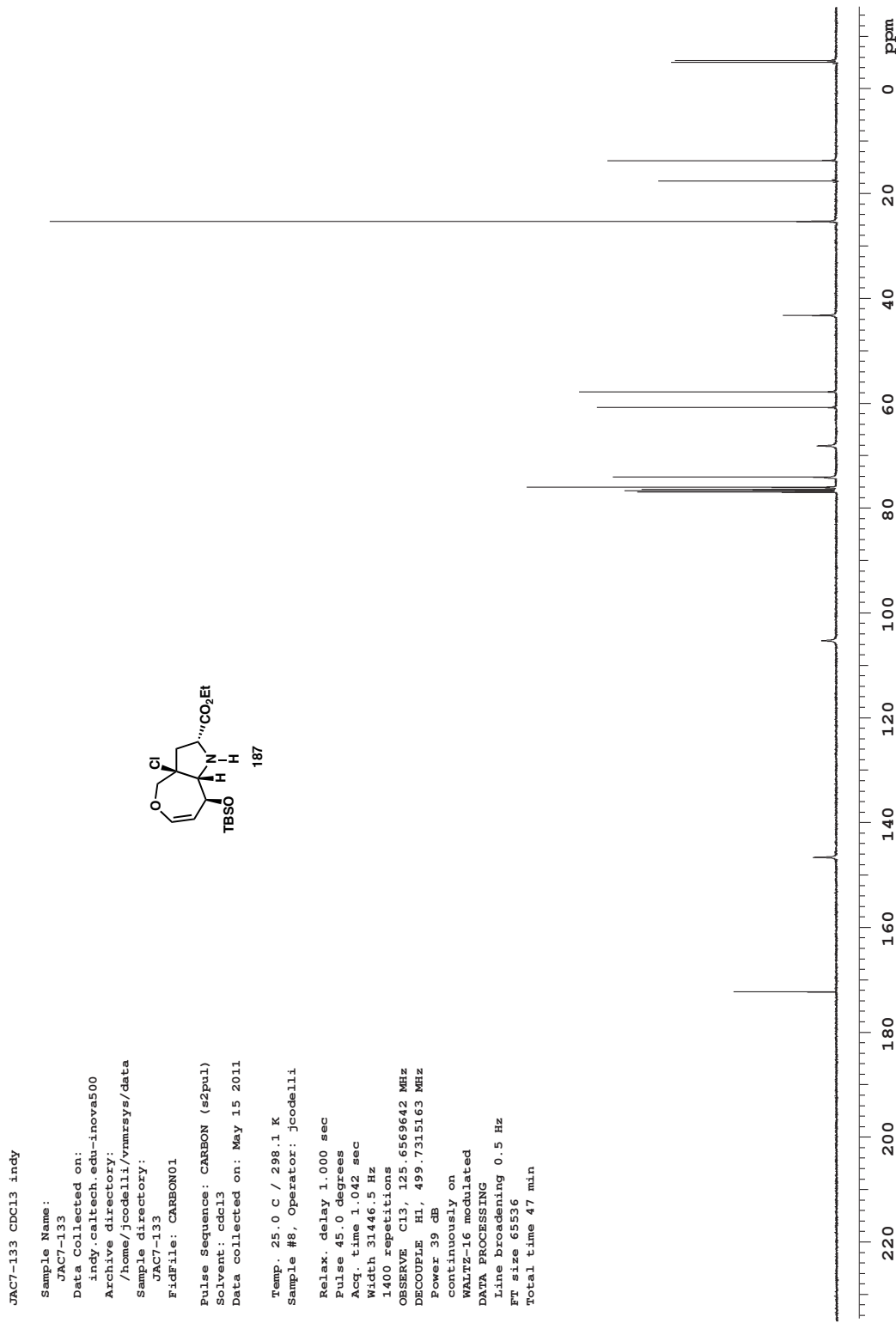


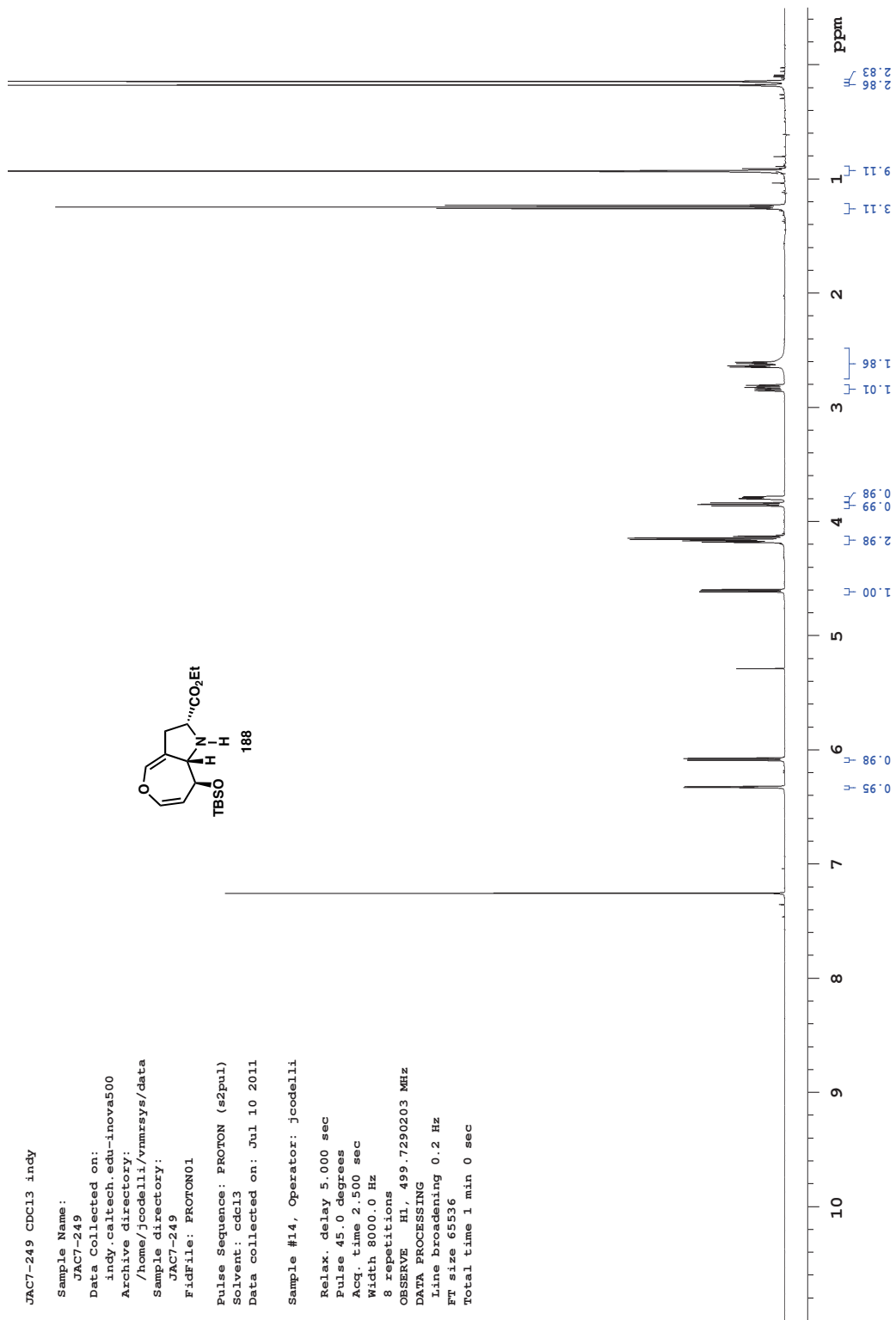


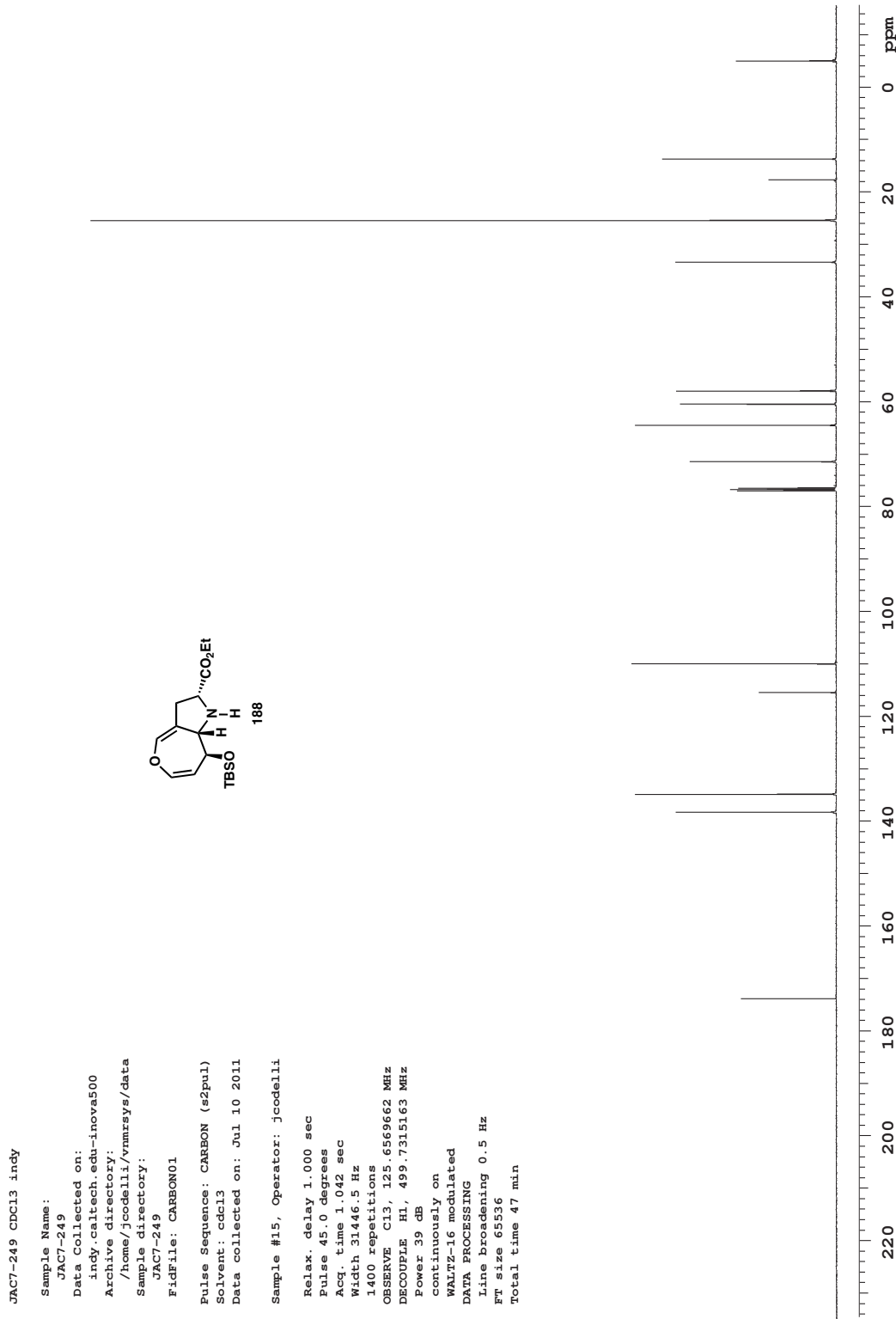


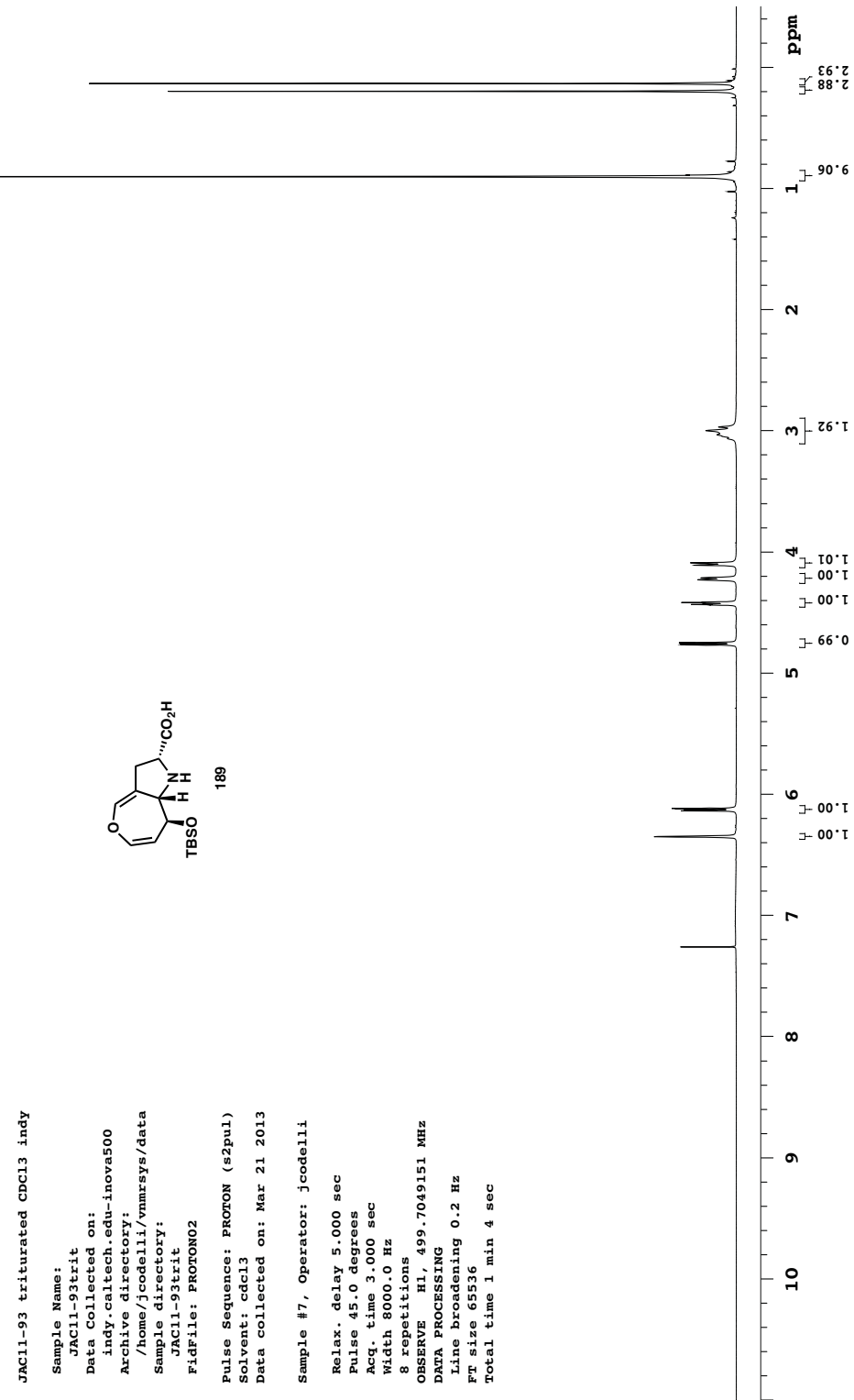


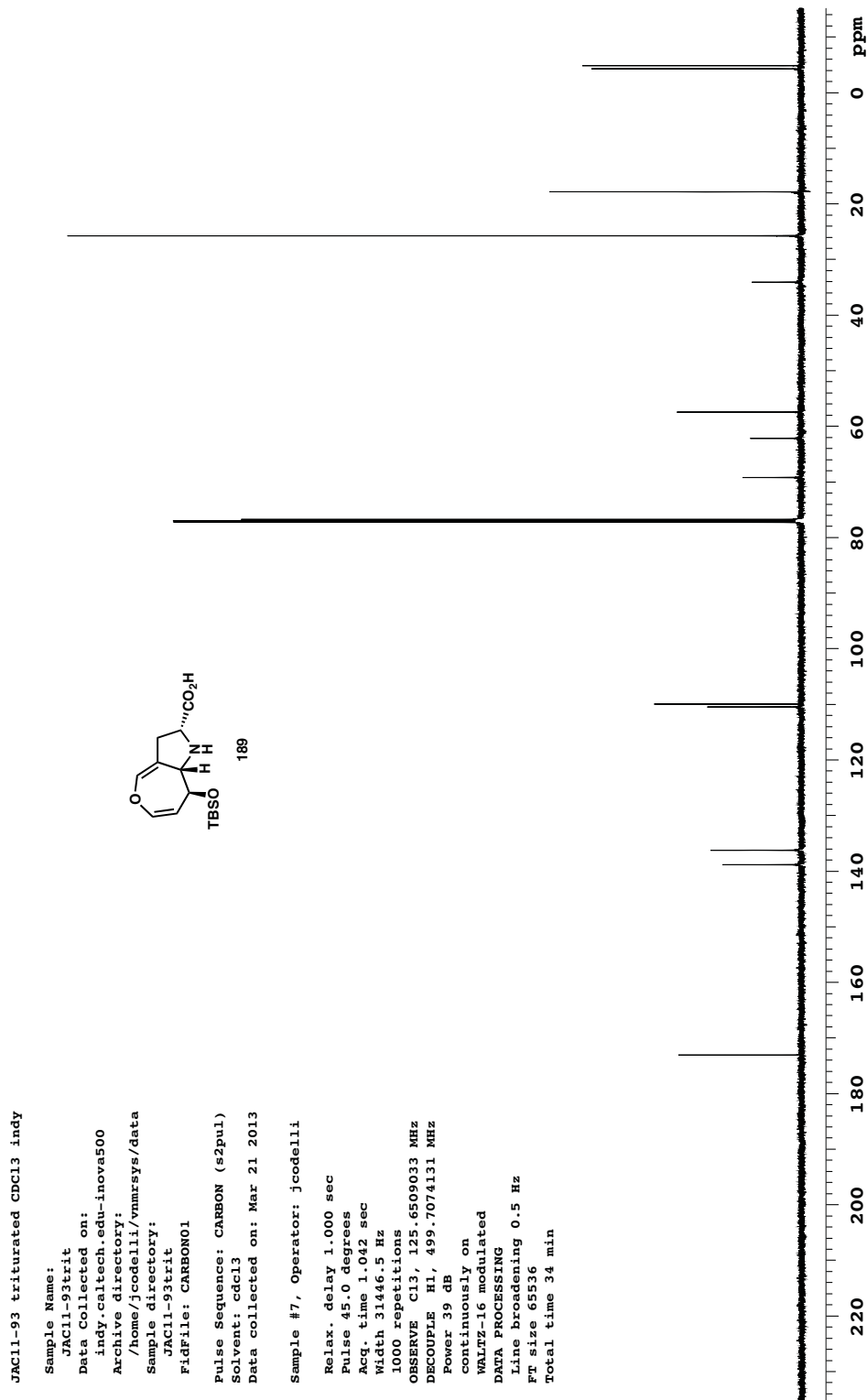


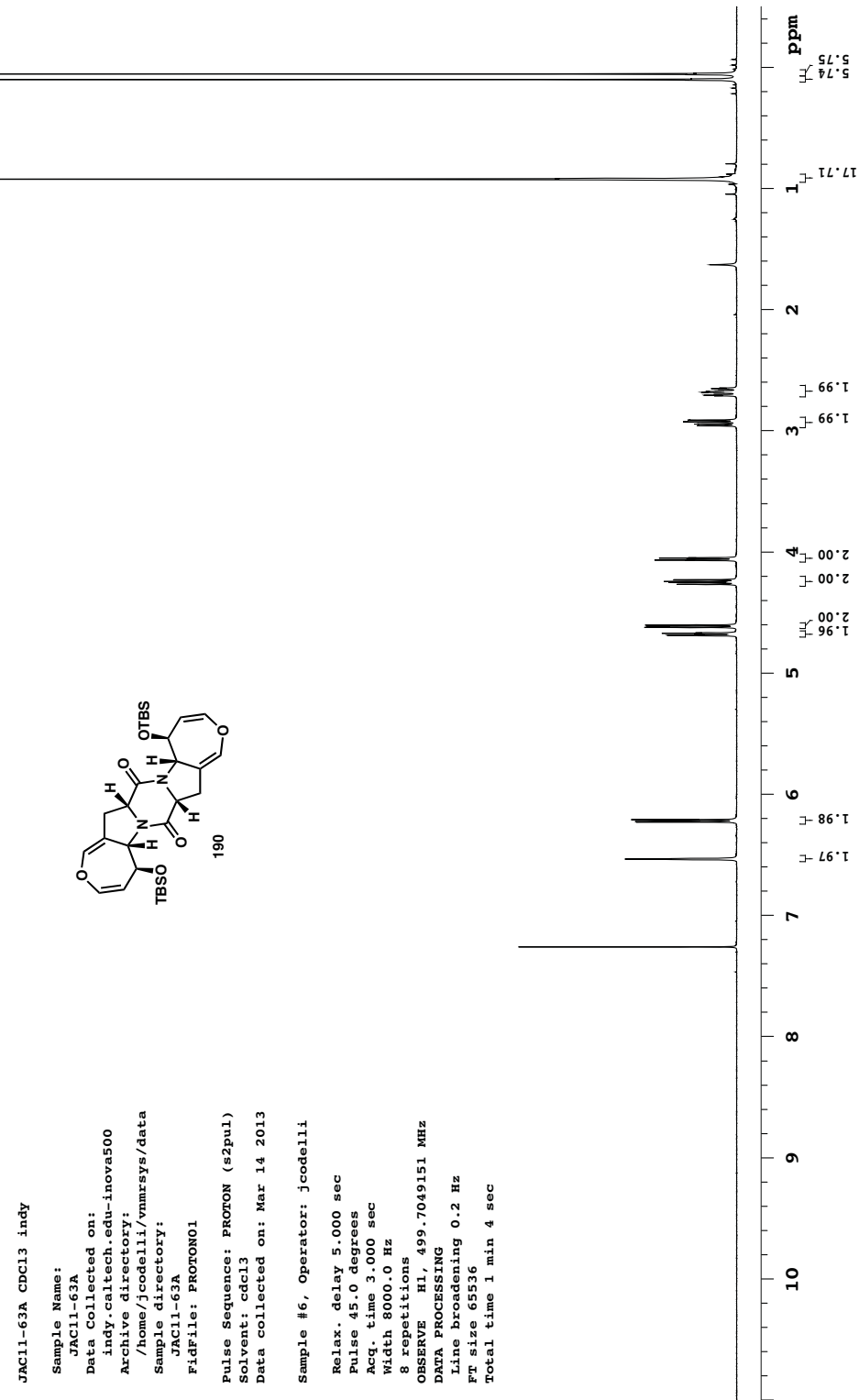


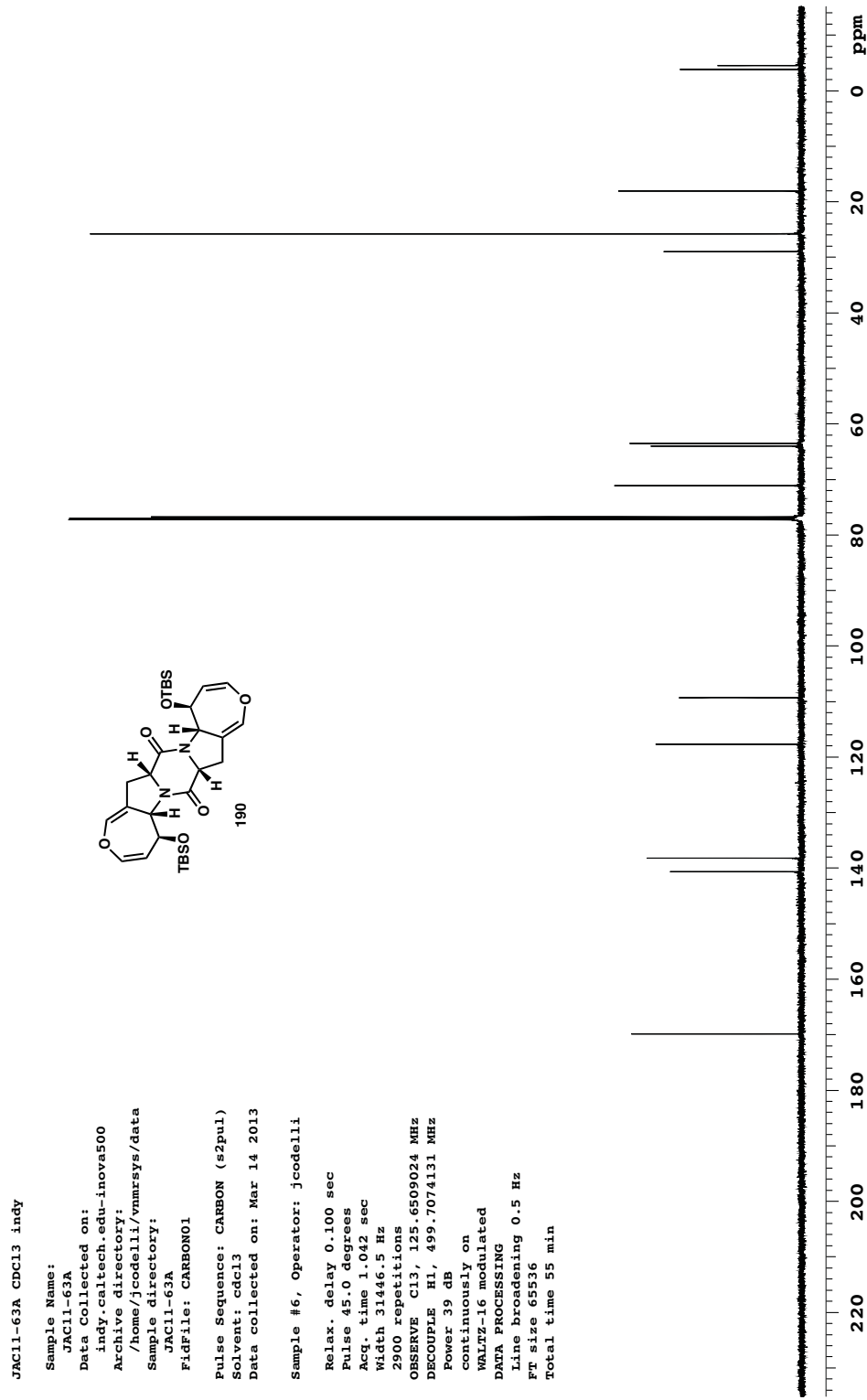


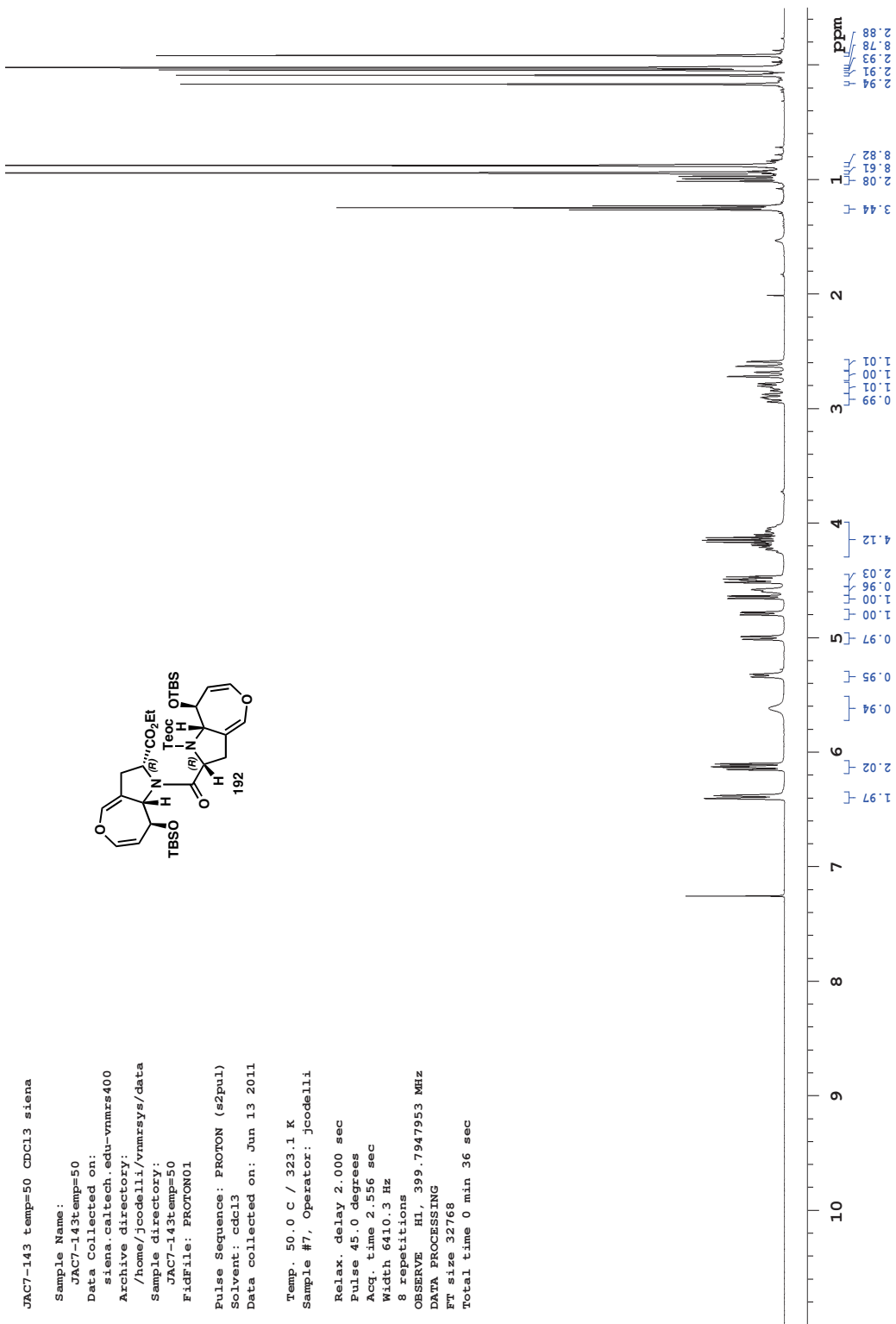


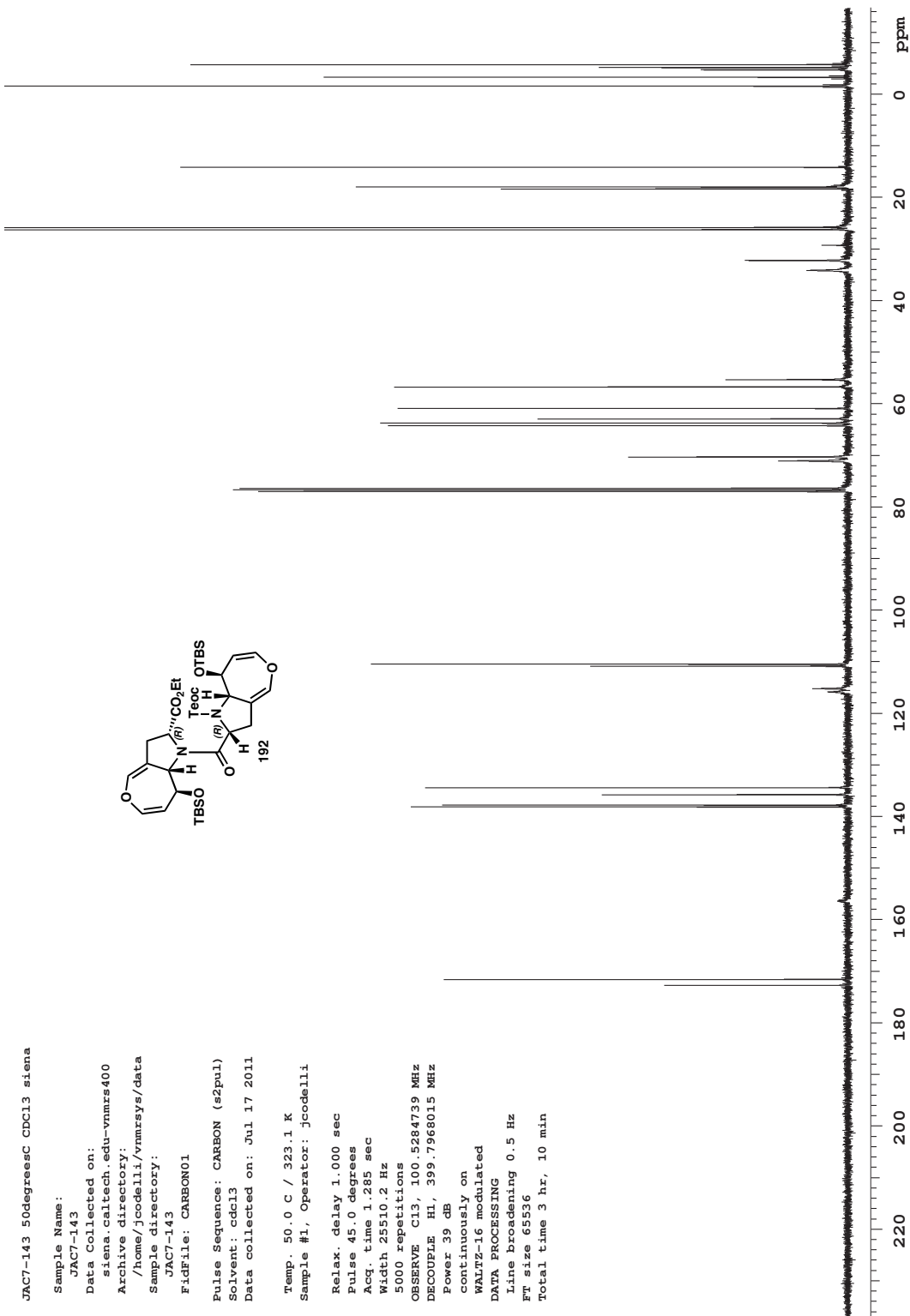


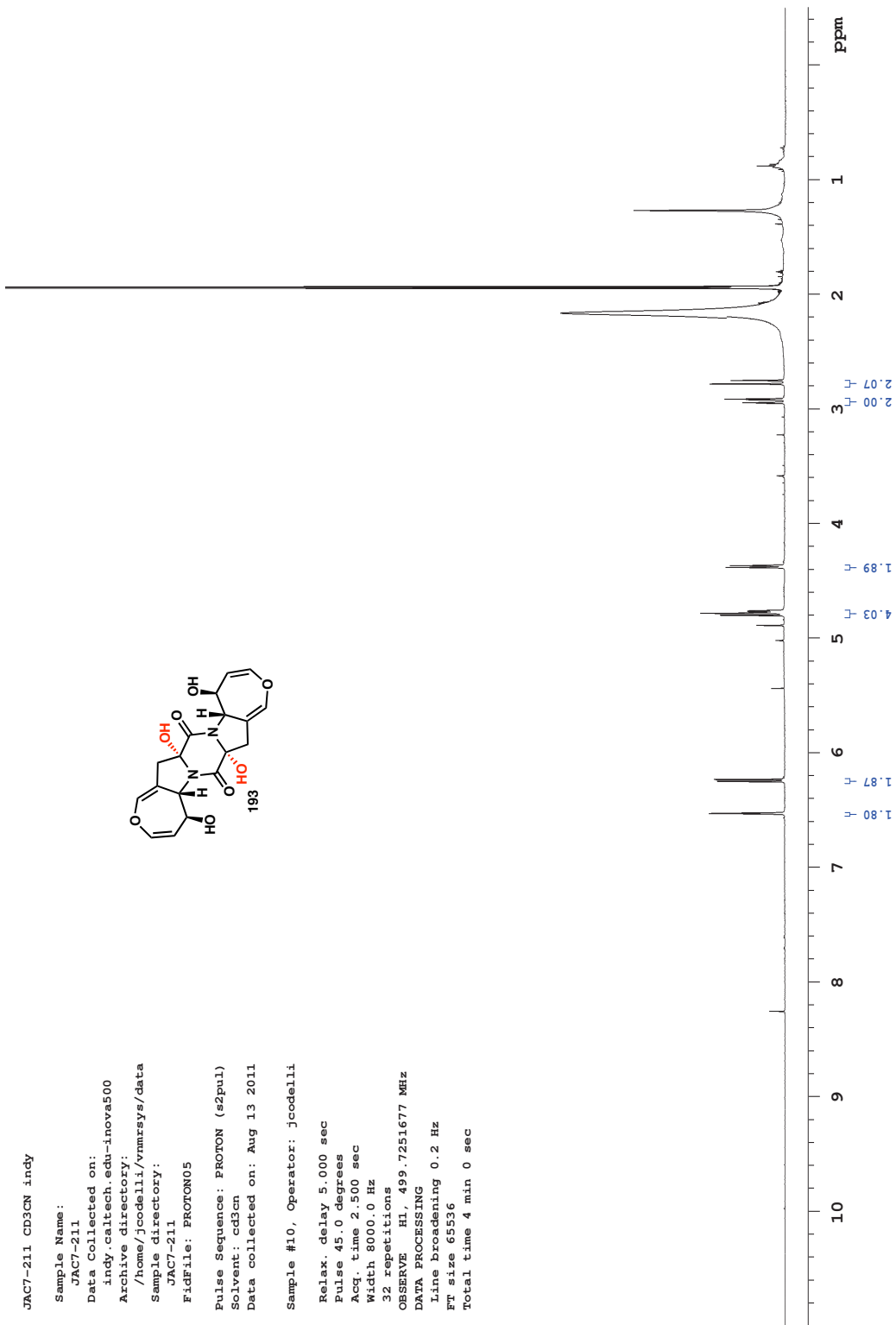


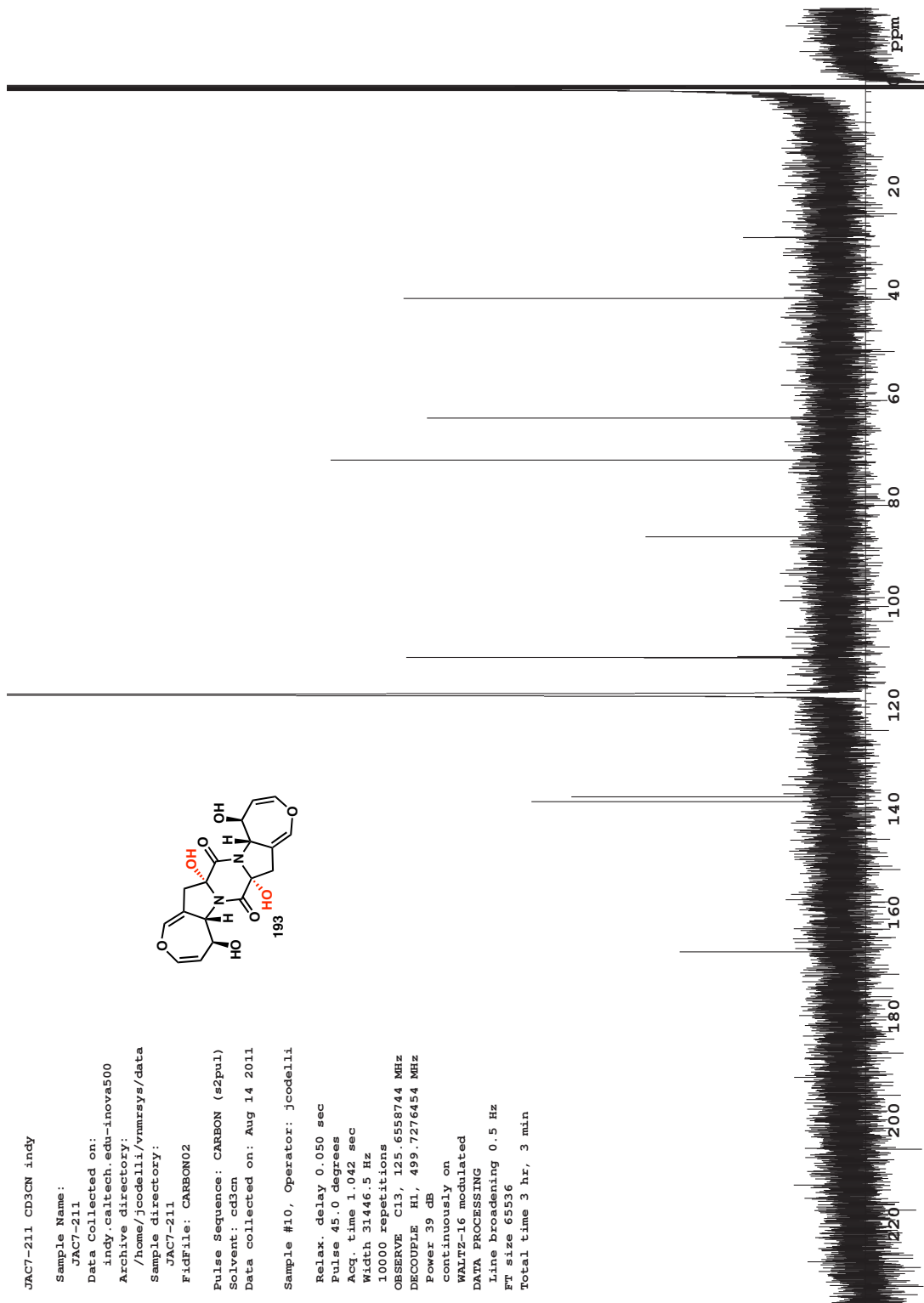


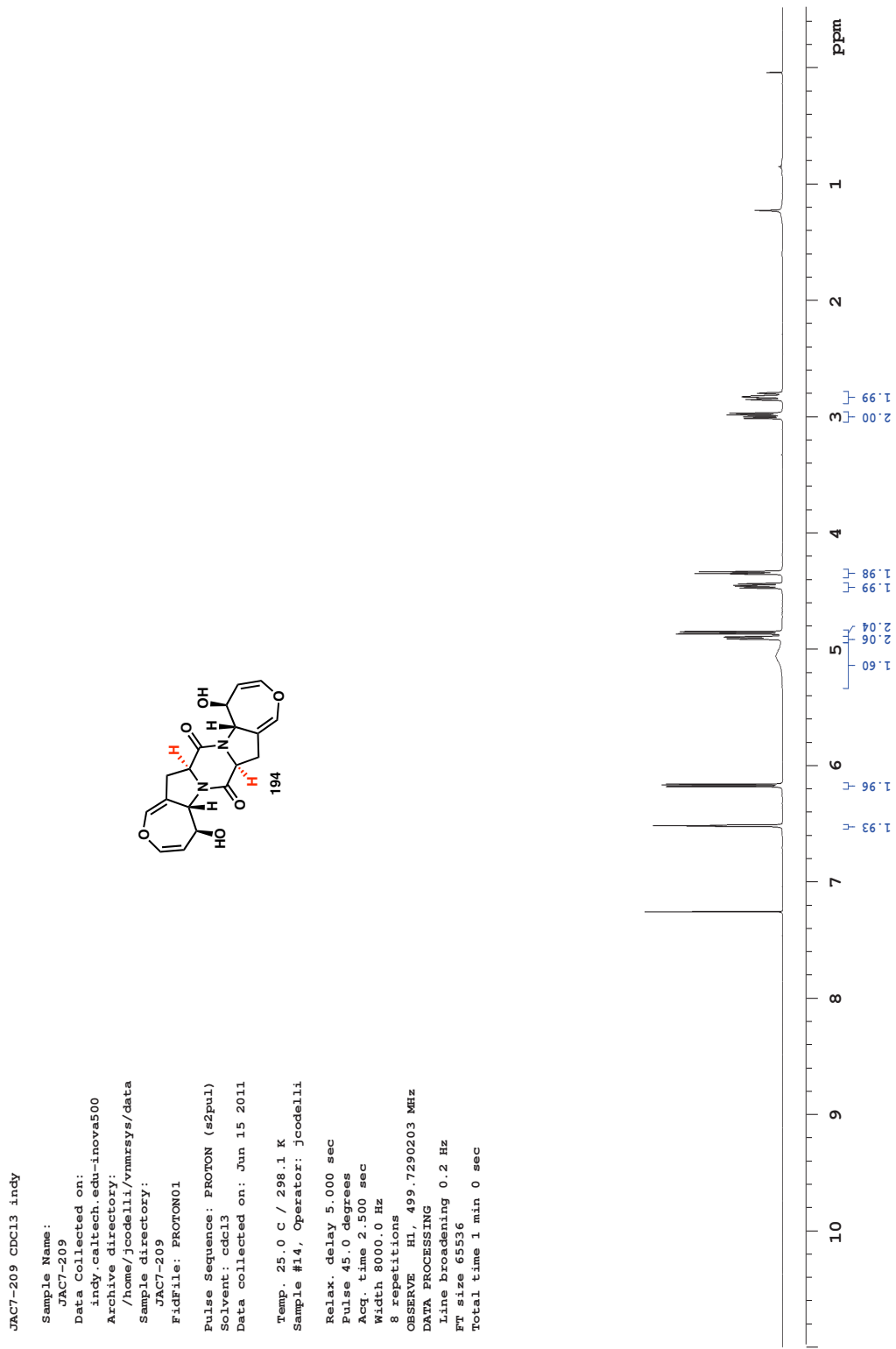


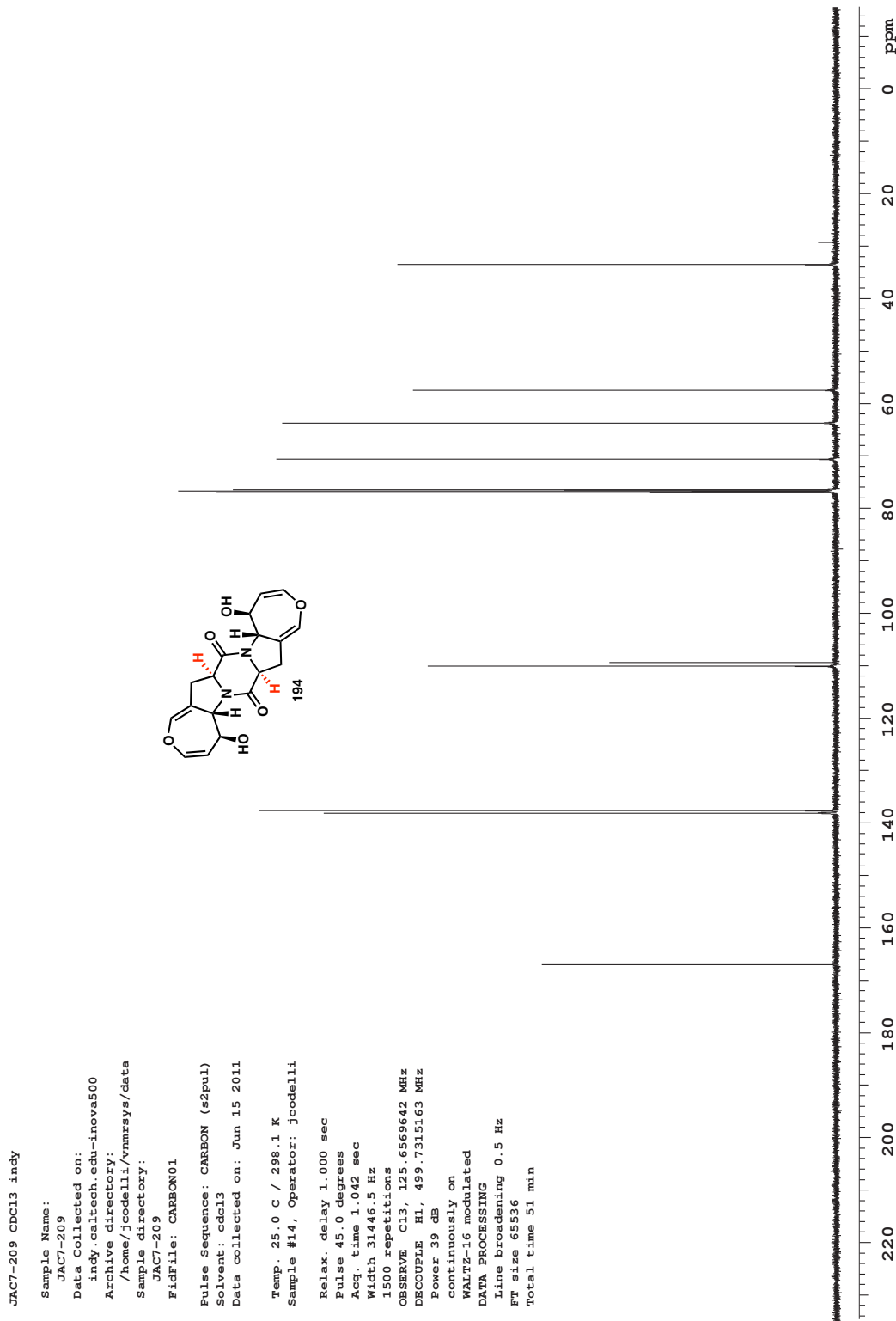












JAC7-221 CDC13 indy

Sample Name: _____

JAC 7-221

Data Collected on: 11/19/2018

indy : carltech.edu_innovatio Archive directory:

`/home/jcode11i/vnmrsys/data`

Sample directory:

JAC7-221

FidFile: PROTON01

Pulse Sequence: PROTON (s2pul)

Solvent: cdc13

Data collected on: Jun 21 2011

Temp. 25.0 C / 298.1 K

Sample #7, Operator: jcodelli

Relax. delay 2.000 sec

Pulse 45.0 degrees

Acq. time 2.500 sec

Width 8000.0 Hz

16 repetitions

OBSERVE H1, 499.7290210 MHz

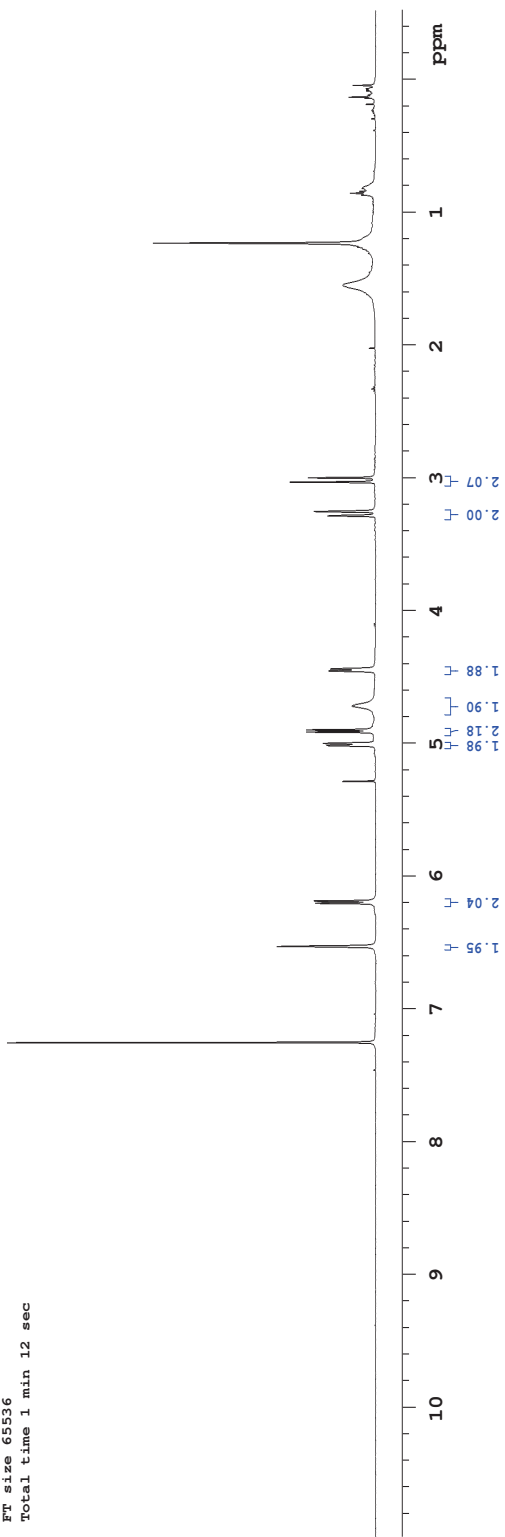
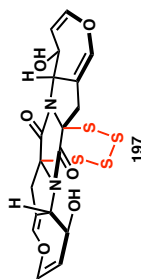
DATA PROCESSING 03 11

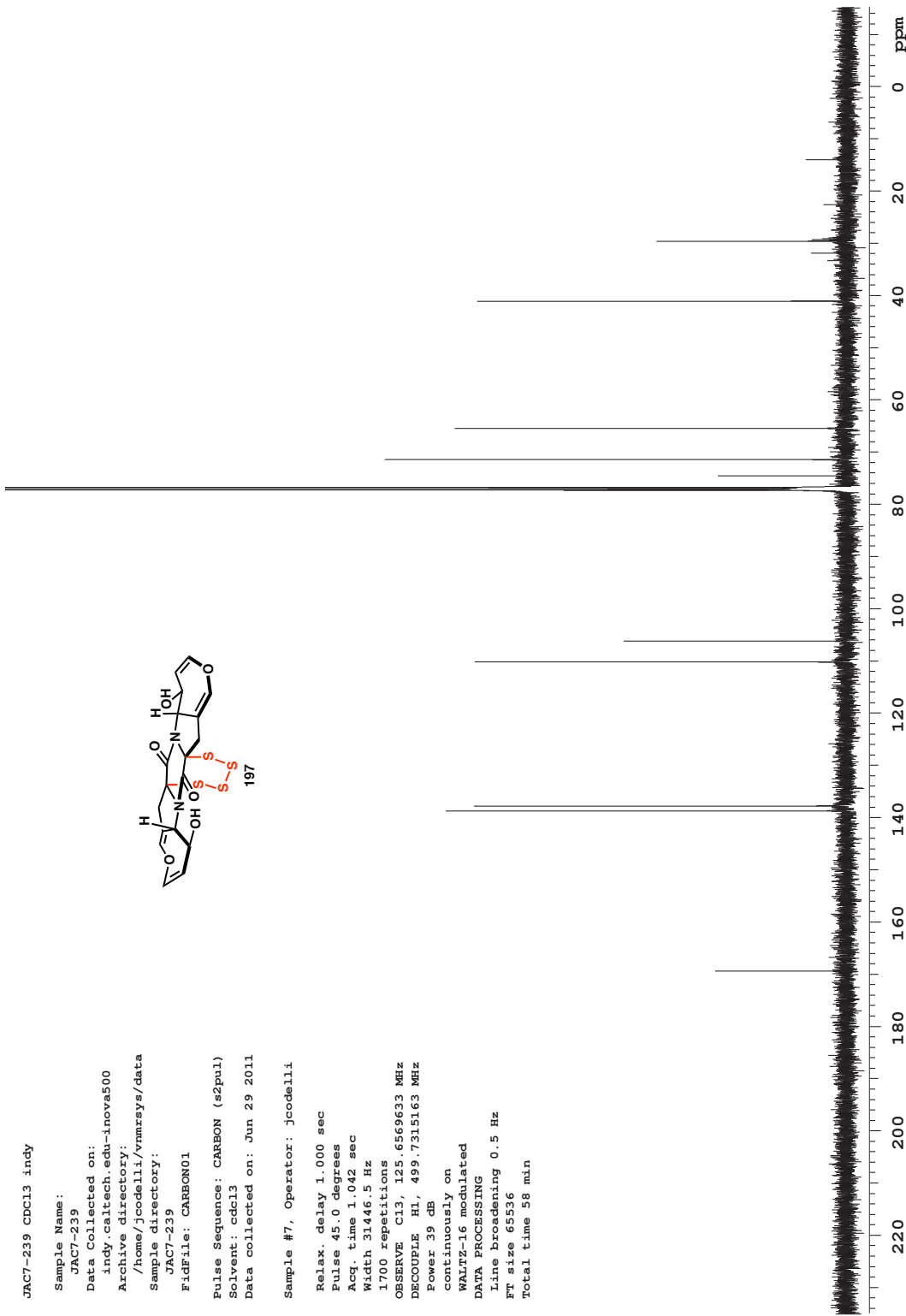
Line Broadening U.2 Hz

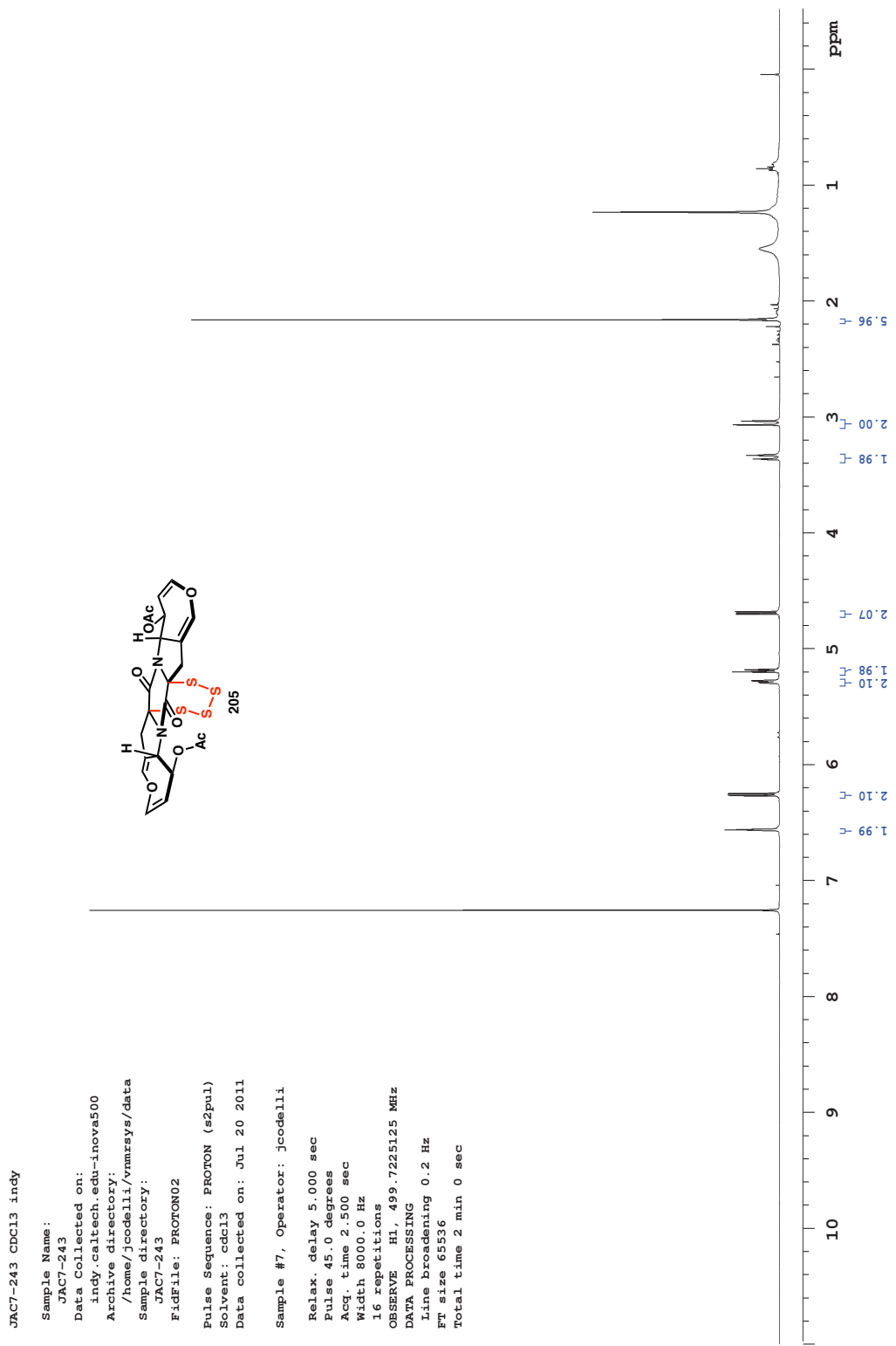
```

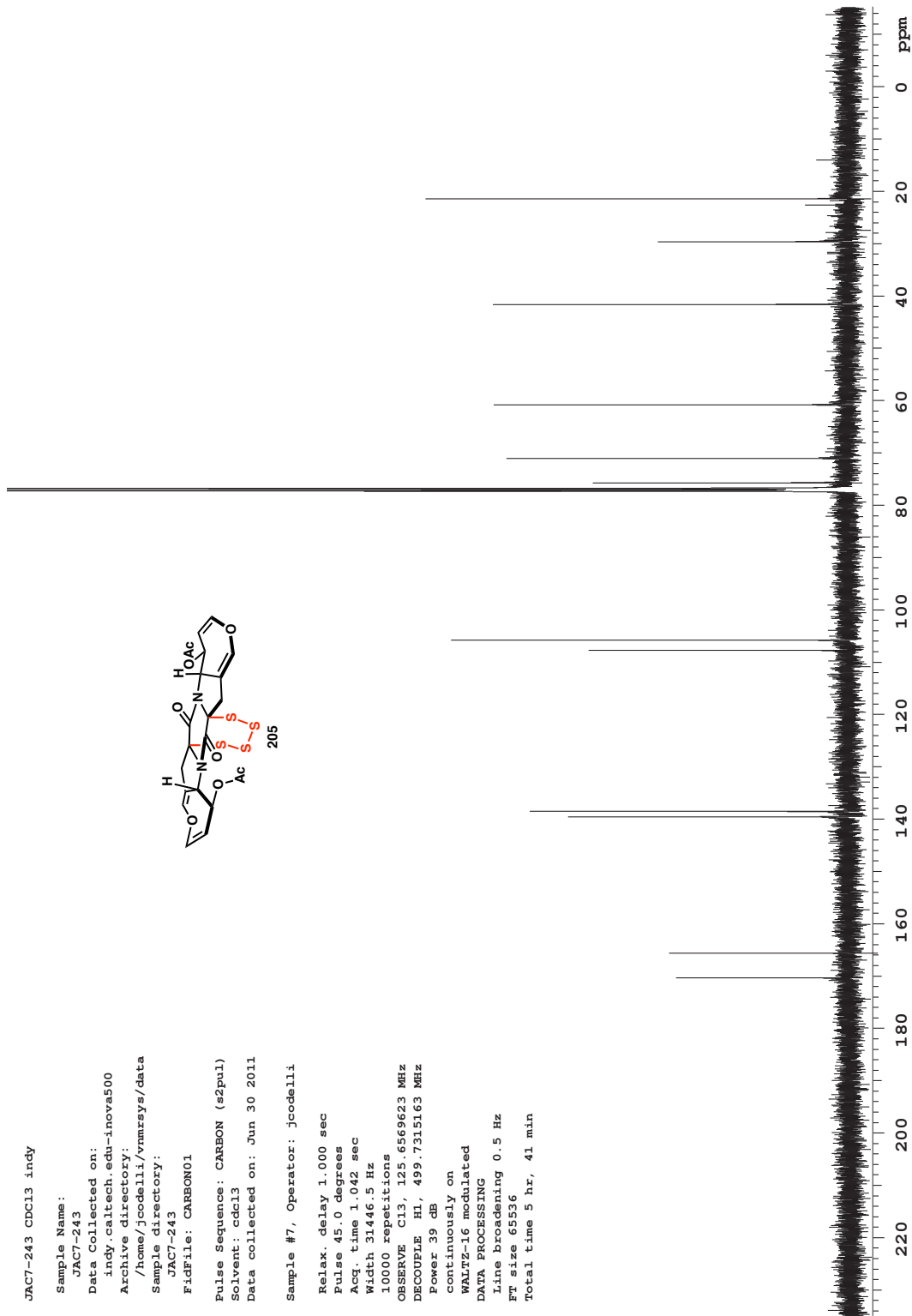
Relax. delay 2.000 sec
Pulse 45.0 deg
Acd. time 2.500 sec
Width 8000.0 Hz
16 repetitions
OBSERVE H1 499.71290210 MHz
DATA PROCESSING
Line broadening 0.2 Hz
FFT size 65536
Time constant 1 min 12 sec

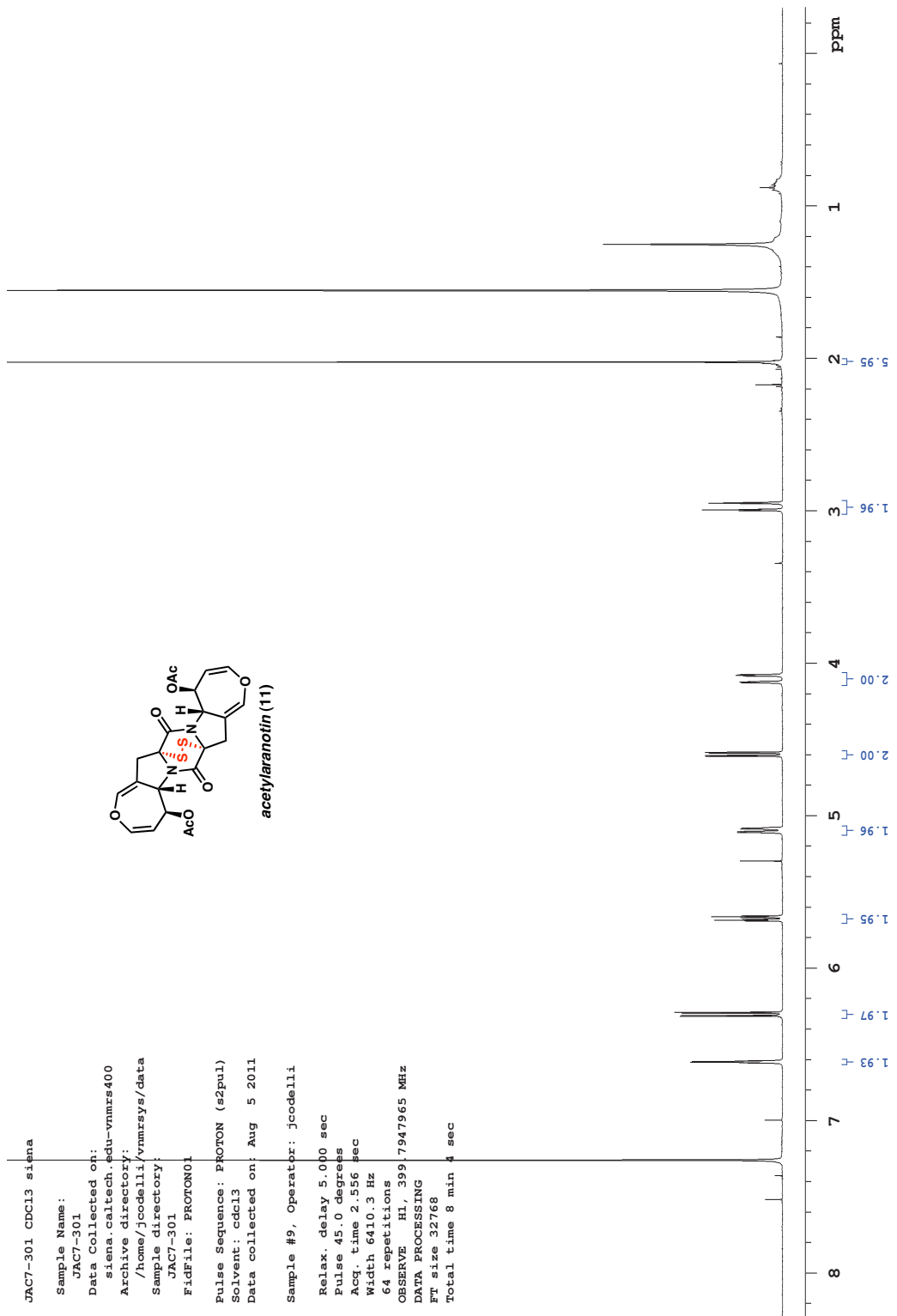
```

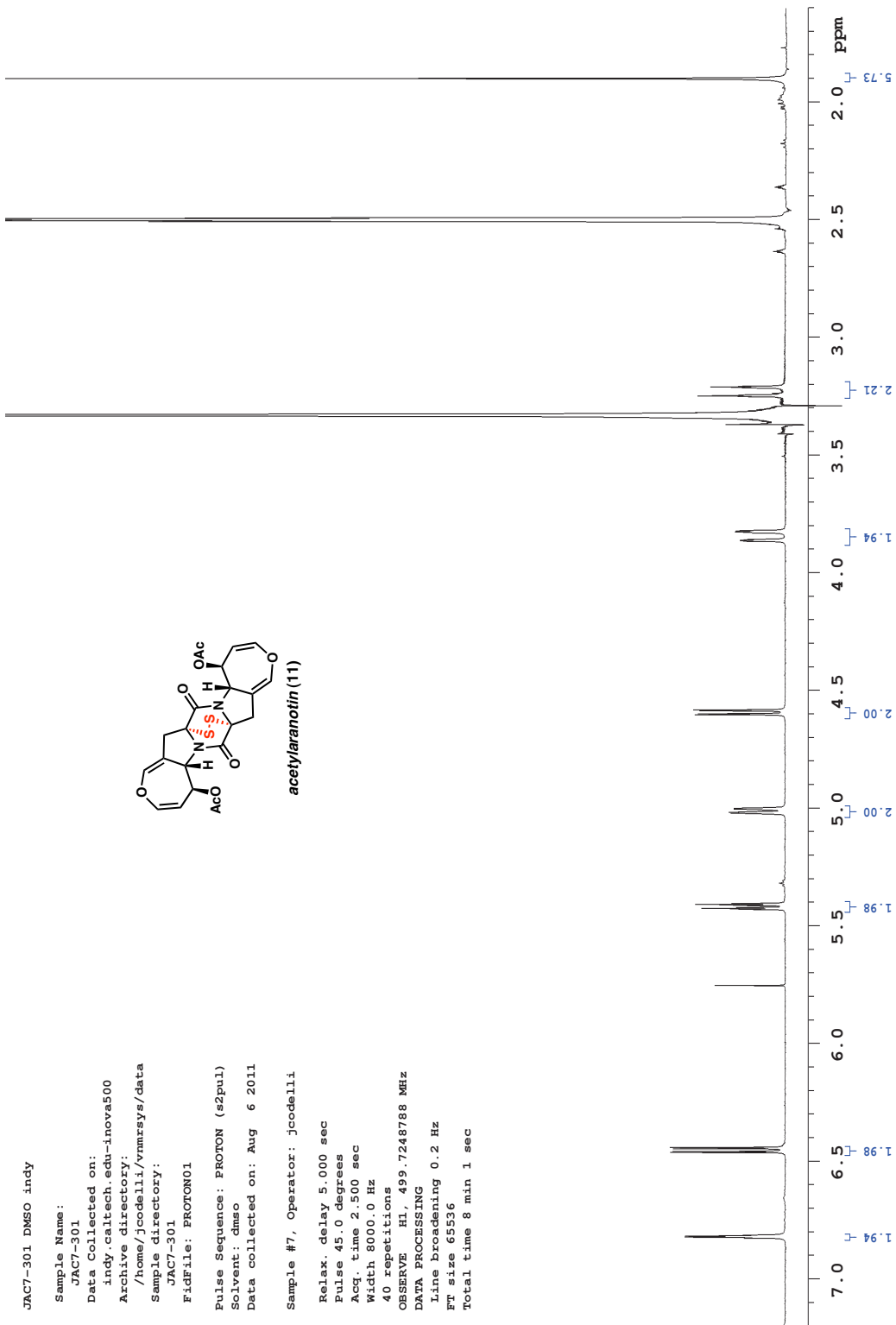


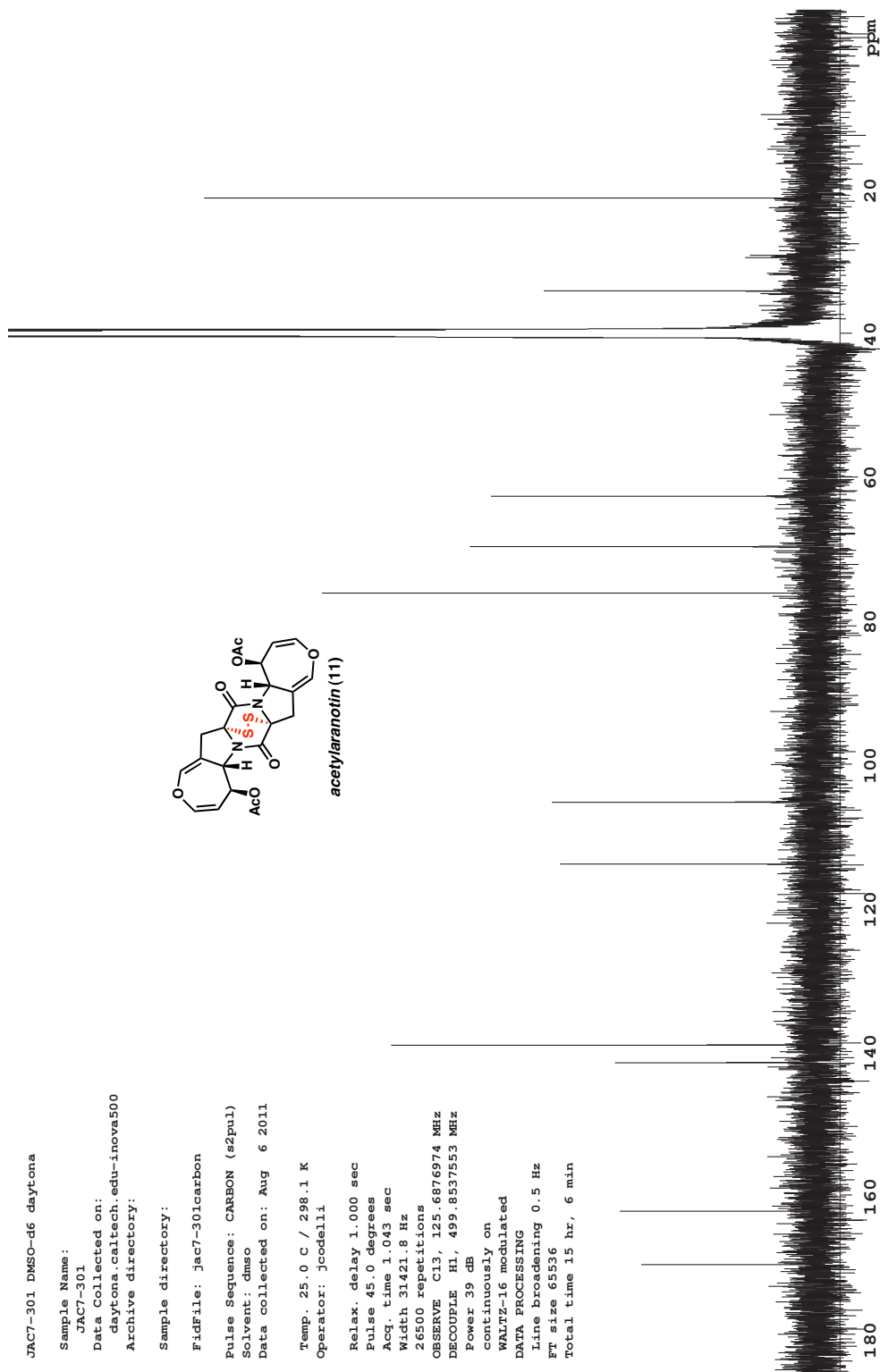












Appendix 2

*X-Ray Crystallography Reports Relevant to Chapter 2:
Enantioselective Total Synthesis of (–)-Acetylaranotin[†]*

[†] The work disclosed in this appendix for the X-ray crystallographic analysis of **158**, **193**, **194**, and **197** was completed entirely by Larry Henling and Dr. Michael Day in the Caltech X-ray crystallography lab.

A2.1 CRYSTAL STRUCTURE ANALYSIS OF ALKYNYL LACTONE 158

Figure A2.1. Alkynyl lactone **158**. Crystallographic data have been deposited at the CCDC, 12 Union Road, Cambridge CB2 1EZ, UK and copies can be obtained on request, free of charge, by quoting the publication citation and the deposition number 771581.

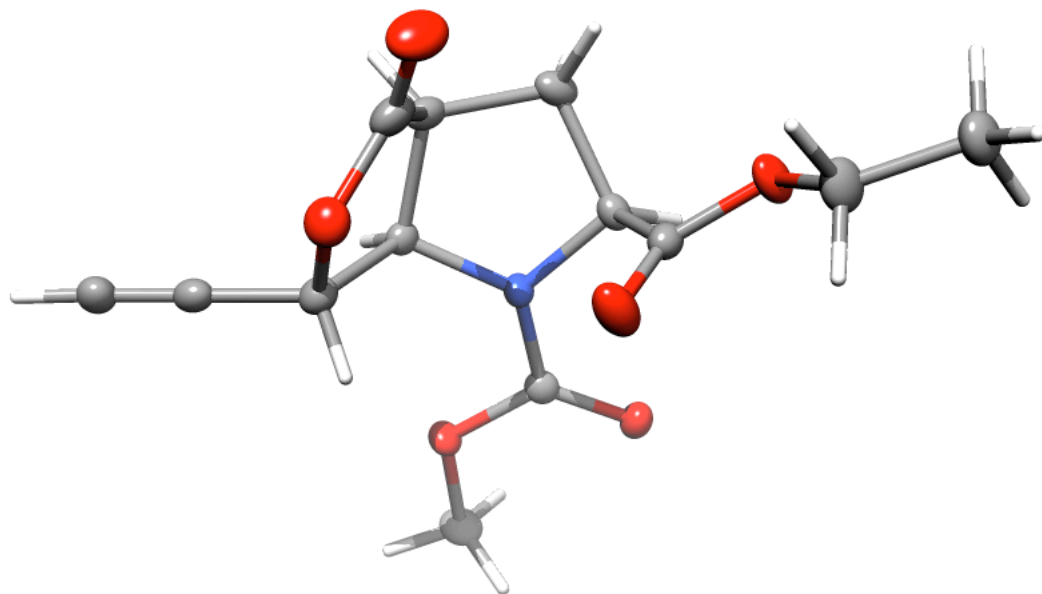


Table A2.1. Crystal data and structure refinement for alkynyl lactone **158** (CCDC 771581).

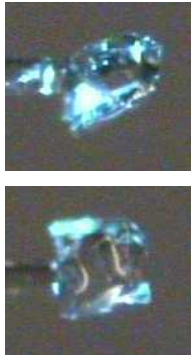
Empirical formula	C ₁₃ H ₁₅ NO ₆	
Formula weight	281.26	
Crystallization Solvent	Toluene/pentane	
Crystal Habit	Colorless	
Crystal size	0.21 x 0.17 x 0.10 mm ³	
Crystal color	Fragment	
Data Collection		
Type of diffractometer	Bruker KAPPA APEX II	
Wavelength	0.71073 Å MoKα	
Data Collection Temperature	100(2) K	
θ range for 9198 reflections used in lattice determination	2.39 to 31.03°	
Unit cell dimensions	a = 6.9163(3) Å b = 20.5882(8) Å c = 9.3847(3) Å	α= 90° β= 95.402(2)° γ = 90°
Volume	1330.39(9) Å ³	
Z	4	
Crystal system	Monoclinic	
Space group	P 2 ₁ /n	
Density (calculated)	1.404 Mg/m ³	
F(000)	592	
Data collection program	Bruker APEX2 v2009.7-0	
θ range for data collection	1.98 to 31.11°	
Completeness to θ = 31.11°	99.8 %	
Index ranges	-9 ≤ h ≤ 10, -29 ≤ k ≤ 29, -13 ≤ l ≤ 13	
Data collection scan type	ω scans; 10 settings	
Data reduction program	Bruker SAINT-Plus v7.66A	
Reflections collected	30667	
Independent reflections	4258 [R _{int} = 0.0413]	
Absorption coefficient	0.112 mm ⁻¹	
Absorption correction	None	
Max. and min. transmission	0.9889 and 0.9768	

Table A2.1 (cont.)**Structure Solution and Refinement**

Structure solution program	SHELXS-97 (Sheldrick, 2008)
Primary solution method	Direct methods
Secondary solution method	Difference Fourier map
Hydrogen placement	Difference Fourier map
Structure refinement program	SHELXL-97 (Sheldrick, 2008)
Refinement method	Full matrix least-squares on F^2
Data / restraints / parameters	4258 / 0 / 241
Treatment of hydrogen atoms	Unrestrained
Goodness-of-fit on F^2	2.394
Final R indices [$I > 2\sigma(I)$, 3426 reflections]	$R = 0.0424$, $wR2 = 0.0612$
R indices (all data)	$R = 0.0536$, $wR2 = 0.0618$
Type of weighting scheme used	Sigma
Weighting scheme used	$w = 1/\sigma^2(Fo^2)$
Max shift/error	0.001
Average shift/error	0.000
Largest diff. peak and hole	0.382 and -0.339 e. \AA^{-3}

Special Refinement Details

Crystals were mounted on a glass fiber using Paratone oil then placed on the diffractometer under a nitrogen stream at 100K.

Refinement of F^2 against ALL reflections. The weighted R-factor (wR) and goodness of fit (S) are based on F^2 , conventional R-factors (R) are based on F, with F set to zero for negative F^2 . The threshold expression of $F^2 > 2\sigma(F^2)$ is used only for calculating R-factors(gt) etc. and is not relevant to the choice of reflections for refinement. R-factors based on F^2 are statistically about twice as large as those based on F, and R-factors based on ALL data will be even larger.

All esds (except the esd in the dihedral angle between two l.s. planes) are estimated using the full covariance matrix. The cell esds are taken into account individually in the estimation of esds in distances, angles and torsion angles; correlations between esds in cell parameters are only used when they are defined

by crystal symmetry. An approximate (isotropic) treatment of cell esds is used for estimating esds involving l.s. planes.

Table A2.2. Atomic coordinates ($\times 10^4$) and equivalent isotropic displacement parameters ($\text{\AA}^2 \times 10^3$) for alkynyl lactone **158** (CCDC 771581). $U(\text{eq})$ is defined as the trace of the orthogonalized U^{ij} tensor.

	x	y	z	U_{eq}
O(1)	3264(1)	3891(1)	8422(1)	25(1)
O(2)	1757(1)	4780(1)	7535(1)	34(1)
O(3)	2341(1)	4207(1)	3372(1)	23(1)
O(4)	4388(1)	3848(1)	5210(1)	30(1)
O(5)	2648(1)	1926(1)	6592(1)	18(1)
O(6)	2464(1)	2173(1)	4217(1)	20(1)
N(1)	1720(1)	2918(1)	5876(1)	16(1)
C(1)	1757(2)	4201(1)	7692(1)	24(1)
C(2)	199(2)	3722(1)	7140(1)	20(1)
C(3)	1193(1)	3064(1)	7317(1)	16(1)
C(4)	2952(2)	3193(1)	8406(1)	20(1)
C(5)	2628(1)	2973(1)	9855(1)	21(1)
C(6)	2323(2)	2785(1)	11000(1)	27(1)
C(7)	-420(2)	3806(1)	5542(1)	22(1)
C(8)	1125(1)	3416(1)	4825(1)	18(1)
C(9)	2840(1)	3838(1)	4511(1)	18(1)
C(10)	3752(2)	4688(1)	2984(1)	26(1)
C(11)	3121(2)	4898(1)	1483(1)	28(1)
C(12)	2296(1)	2326(1)	5454(1)	16(1)
C(13)	3016(2)	1257(1)	6242(1)	24(1)

Table A2.3. Bond lengths [\AA] and angles [°] for alkynyl lactone **158** (CCDC 771581).

O(1)-C(1)	1.3532(13)	C(1)-C(2)-H(2)	107.9(6)
O(1)-C(4)	1.4520(13)	C(3)-C(2)-H(2)	112.5(7)
O(2)-C(1)	1.2015(13)	C(7)-C(2)-H(2)	112.6(7)
O(3)-C(9)	1.3300(12)	N(1)-C(3)-C(2)	103.40(8)
O(3)-C(10)	1.4601(13)	N(1)-C(3)-C(4)	113.57(8)
O(4)-C(9)	1.2022(11)	C(2)-C(3)-C(4)	103.88(8)
O(5)-C(12)	1.3522(12)	N(1)-C(3)-H(3)	111.1(6)
O(5)-C(13)	1.4453(13)	C(2)-C(3)-H(3)	115.1(5)
O(6)-C(12)	1.2184(11)	C(4)-C(3)-H(3)	109.6(5)
N(1)-C(12)	1.3522(13)	O(1)-C(4)-C(5)	109.35(9)
N(1)-C(8)	1.4560(13)	O(1)-C(4)-C(3)	106.58(8)
N(1)-C(3)	1.4645(12)	C(5)-C(4)-C(3)	112.45(9)
C(1)-C(2)	1.5150(15)	O(1)-C(4)-H(4)	105.8(6)
C(2)-C(3)	1.5211(14)	C(5)-C(4)-H(4)	111.4(6)
C(2)-C(7)	1.5305(15)	C(3)-C(4)-H(4)	110.9(6)
C(2)-H(2)	0.969(11)	C(6)-C(5)-C(4)	178.01(12)
C(3)-C(4)	1.5368(14)	C(5)-C(6)-H(6)	177.4(7)
C(3)-H(3)	0.965(9)	C(2)-C(7)-C(8)	103.17(8)
C(4)-C(5)	1.4700(15)	C(2)-C(7)-H(7A)	113.6(6)
C(4)-H(4)	0.974(10)	C(8)-C(7)-H(7A)	111.5(6)
C(5)-C(6)	1.1802(15)	C(2)-C(7)-H(7B)	111.7(6)
C(6)-H(6)	0.976(12)	C(8)-C(7)-H(7B)	108.8(6)
C(7)-C(8)	1.5406(15)	H(7A)-C(7)-H(7B)	108.0(8)
C(7)-H(7A)	0.988(11)	N(1)-C(8)-C(9)	110.94(8)
C(7)-H(7B)	1.024(10)	N(1)-C(8)-C(7)	103.56(8)
C(8)-C(9)	1.5210(14)	C(9)-C(8)-C(7)	111.92(9)
C(8)-H(8)	0.965(10)	N(1)-C(8)-H(8)	109.3(6)
C(10)-C(11)	1.4991(16)	C(9)-C(8)-H(8)	108.3(6)
C(10)-H(10A)	0.983(11)	C(7)-C(8)-H(8)	112.8(6)
C(10)-H(10B)	1.021(12)	O(4)-C(9)-O(3)	125.37(9)
C(11)-H(11A)	1.007(13)	O(4)-C(9)-C(8)	125.13(9)
C(11)-H(11B)	1.031(13)	O(3)-C(9)-C(8)	109.47(8)
C(11)-H(11C)	0.998(11)	O(3)-C(10)-C(11)	106.74(9)
C(13)-H(13A)	1.000(11)	O(3)-C(10)-H(10A)	107.3(7)
C(13)-H(13B)	0.959(12)	C(11)-C(10)-H(10A)	112.9(7)
C(13)-H(13C)	0.975(12)	O(3)-C(10)-H(10B)	107.9(7)
		C(11)-C(10)-H(10B)	112.8(7)
C(1)-O(1)-C(4)	110.81(8)	H(10A)-C(10)-H(10B)	109.0(9)
C(9)-O(3)-C(10)	117.29(8)	C(10)-C(11)-H(11A)	110.7(7)
C(12)-O(5)-C(13)	115.07(8)	C(10)-C(11)-H(11B)	107.9(8)
C(12)-N(1)-C(8)	120.57(9)	H(11A)-C(11)-H(11B)	109.4(10)
C(12)-N(1)-C(3)	124.17(8)	C(10)-C(11)-H(11C)	110.6(7)
C(8)-N(1)-C(3)	113.68(8)	H(11A)-C(11)-H(11C)	107.0(9)
O(2)-C(1)-O(1)	121.43(10)	H(11B)-C(11)-H(11C)	111.3(10)
O(2)-C(1)-C(2)	127.79(10)	O(6)-C(12)-N(1)	124.68(10)
O(1)-C(1)-C(2)	110.78(10)	O(6)-C(12)-O(5)	124.65(10)
C(1)-C(2)-C(3)	104.06(8)	N(1)-C(12)-O(5)	110.67(9)
C(1)-C(2)-C(7)	112.68(9)	O(5)-C(13)-H(13A)	108.5(7)
C(3)-C(2)-C(7)	106.81(9)	O(5)-C(13)-H(13B)	105.3(7)

H(13A)-C(13)-H(13B)	112.0(9)
O(5)-C(13)-H(13C)	110.1(7)
H(13A)-C(13)-H(13C)	110.8(9)
H(13B)-C(13)-H(13C)	110.0(9)

Table A2.4. Anisotropic displacement parameters ($\text{\AA}^2 \times 10^4$) for alkynyl lactone **158** (CCDC 771581). The anisotropic displacement factor exponent takes the form: $-2p^2[h^2a^{*2}U^{11} + \dots + 2hk a^* b^* U^{12}]$

	U ¹¹	U ²²	U ³³	U ²³	U ¹³	U ¹²
O(1)	280(4)	222(5)	254(4)	-47(3)	-6(3)	-56(3)
O(2)	413(5)	169(5)	459(6)	-39(4)	98(4)	-32(4)
O(3)	222(4)	237(5)	239(4)	101(3)	1(3)	-57(3)
O(4)	212(4)	369(5)	298(5)	107(4)	-25(3)	-50(4)
O(5)	246(4)	132(4)	170(4)	14(3)	7(3)	15(3)
O(6)	201(4)	238(4)	153(4)	-28(3)	18(3)	7(3)
N(1)	201(4)	143(5)	136(4)	14(3)	20(3)	8(4)
C(1)	252(6)	223(7)	249(6)	-59(5)	92(5)	-10(5)
C(2)	181(5)	172(6)	241(6)	-5(5)	69(4)	14(4)
C(3)	161(5)	163(6)	158(5)	2(4)	31(4)	-5(4)
C(4)	199(5)	194(6)	196(5)	-43(5)	20(4)	-2(5)
C(5)	184(5)	235(6)	218(6)	-47(5)	-12(4)	49(5)
C(6)	226(6)	355(8)	223(6)	-7(5)	0(5)	89(5)
C(7)	187(5)	188(6)	273(6)	56(5)	24(4)	17(5)
C(8)	185(5)	169(6)	167(5)	25(4)	-6(4)	-11(4)
C(9)	216(5)	162(6)	174(5)	8(4)	43(4)	12(4)
C(10)	266(6)	260(7)	255(6)	60(5)	43(5)	-86(5)
C(11)	312(7)	288(8)	252(6)	77(6)	53(5)	-41(6)
C(12)	136(5)	162(6)	178(5)	-1(4)	4(4)	-21(4)
C(13)	297(6)	131(6)	293(7)	-11(5)	1(5)	9(5)

Table A2.5. Hydrogen coordinates ($\times 10^4$) and isotropic displacement parameters ($\text{\AA}^2 \times 10^3$) for alkynyl lactone **158** (CCDC 771581).

	x	y	z	U_{iso}
H(2)	-877(16)	3765(5)	7724(12)	28(3)
H(3)	409(12)	2722(5)	7667(10)	11(3)
H(4)	4127(14)	3003(5)	8087(10)	17(3)
H(6)	2132(16)	2633(6)	11963(13)	48(4)
H(7A)	-460(15)	4264(6)	5225(11)	25(3)
H(7B)	-1755(15)	3605(5)	5260(11)	25(3)
H(8)	612(13)	3212(5)	3944(11)	14(3)
H(10A)	5033(17)	4477(5)	3075(12)	34(3)
H(10B)	3760(16)	5060(6)	3703(13)	37(4)
H(11A)	3197(17)	4525(7)	796(14)	48(4)
H(11B)	4040(19)	5264(7)	1218(14)	57(4)
H(11C)	1742(16)	5048(5)	1402(12)	32(3)
H(13A)	1871(16)	1088(6)	5623(12)	35(3)
H(13B)	3193(15)	1035(6)	7144(13)	34(3)
H(13C)	4195(17)	1226(6)	5752(13)	40(4)

A2.2 CRYSTAL STRUCTURE ANALYSIS OF TETRAOL 193

Figure A2.2. Tetraol 193. Crystallographic data have been deposited at the CCDC, 12 Union Road, Cambridge CB2 1EZ, UK and copies can be obtained on request, free of charge, by quoting the publication citation and the deposition number 844563.

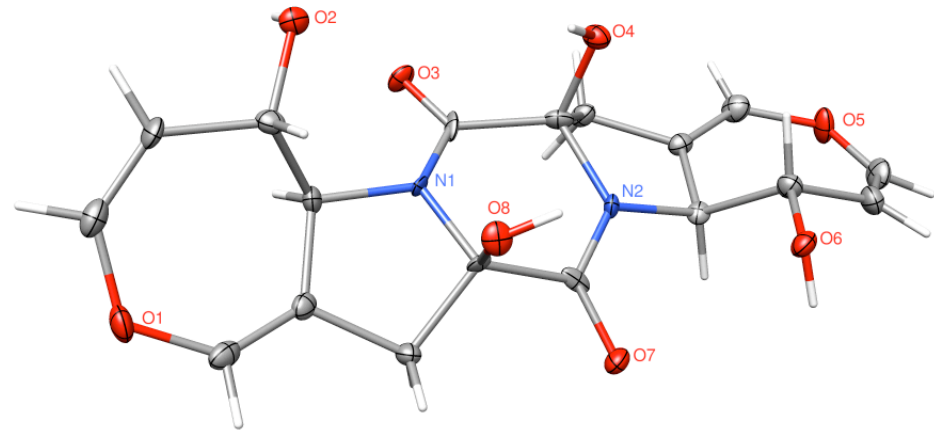


Table A2.6. Crystal data and structure refinement for tetraol **193** (CCDC 844563).

Empirical formula	$C_{18}H_{18}N_2O_8 \cdot 0.5(C_6H_6) \cdot H_2O$	
Formula weight	447.41	
Crystallization Solvent	Benzene	
Crystal Habit	Blade	
Crystal size	0.39 x 0.16 x 0.07 mm ³	
Crystal color	Colorless	

Data Collection

Type of diffractometer	Bruker KAPPA APEX II		
Wavelength	0.71073 Å MoKα		
Data Collection Temperature	100(2) K		
θ range for ? reflections used in lattice determination	? to ?°		
Unit cell dimensions	$a = 20.744(4)$ Å	$\alpha = 90^\circ$	$b = 7.7389(15)$ Å
		$\beta = 97.41(3)^\circ$	$c = 12.557(3)$ Å
		$\gamma = 90^\circ$	
Volume	1999.0(7) Å ³		
Z	4		
Crystal system	Monoclinic		
Space group	C 2		
Density (calculated)	1.487 Mg/m ³		
F(000)	940		
Data collection program	Bruker APEX2 v2009.7-0		
θ range for data collection	1.98 to 30.52°		
Completeness to θ = 30.52°	98.6 %		
Index ranges	$-29 \leq h \leq 29, 0 \leq k \leq 11, 0 \leq l \leq 17$		
Data collection scan type	ω scans; 8 settings		
Data reduction program	Bruker SAINT-Plus v7.68A		
Reflections collected	4904		
Independent reflections	4905 [$R_{int} = 0.0000$]		
Absorption coefficient	0.118 mm ⁻¹		
Absorption correction	Semi-empirical from equivalents		
Max. and min. transmission	0.7461 and 0.6457		

Table A2.6 (cont.)**Structure Solution and Refinement**

Structure solution program	SHELXS-97 (Sheldrick, 2008)
Primary solution method	Direct methods
Secondary solution method	Difference Fourier map
Hydrogen placement	Geometric positions
Structure refinement program	SHELXL-97 (Sheldrick, 2008)
Refinement method	Full matrix least-squares on F^2
Data / restraints / parameters	4905 / 1 / 295
Treatment of hydrogen atoms	Riding
Goodness-of-fit on F^2	2.523
Final R indices [I>2σ(I), 3856 reflections]	$R_1 = 0.0475, wR_2 = 0.0570$
R indices (all data)	$R_1 = 0.0724, wR_2 = 0.0586$
Type of weighting scheme used	Sigma
Weighting scheme used	$w=1/\sigma^2(Fo^2)$
Max shift/error	0.003
Average shift/error	0.000
Absolute structure determination	Unknown
Absolute structure parameter	0.0(15)
Largest diff. peak and hole	0.360 and -0.387 e. \AA^{-3}

Special Refinement Details

Crystals were mounted on a glass fiber using Paratone oil then placed on the diffractometer under a nitrogen stream at 100K.

The crystal is a twin. Below is a summary of cell_now[‡] and TWINABS results[§];

Cell for domain 1: 20.744 7.739 12.557 89.89 97.41 90.05

341 reflections within tolerance assigned to domain 1,

341 of them exclusively; 109 reflections not yet assigned to a domain

Cell for domain 2: 20.744 7.739 12.557 89.89 97.41 90.05

Rotated from first domain by 180.0 degrees about

reciprocal axis 1.000 0.000 -0.077 and real axis 1.000 0.002 0.003

[‡] cell_now v2008/2, Bruker-AXS, Madison, WI

[§] TWINABS v2008/4, Bruker-AXS, Madison, WI

319 reflections within tolerance assigned to domain 2,
107 of them exclusively; 2 reflections not yet assigned to a domain

PART 1 - Refinement of parameters to model systematic errors

4095 data (1047 unique) involve domain 1 only, mean I/sigma 7.3

4126 data (1039 unique) involve domain 2 only, mean I/sigma 7.7

12800 data (2820 unique) involve 2 domains, mean I/sigma 7.0

Table A2.7. Atomic coordinates ($\times 10^4$) and equivalent isotropic displacement parameters ($\text{\AA}^2 \times 10^3$) for tetraol **193** (CCDC 844563). $U(\text{eq})$ is defined as the trace of the orthogonalized U^{ij} tensor.

	x	y	z	U_{eq}
O(1)	8553(1)	4178(3)	4236(2)	21(1)
O(2)	9325(1)	5646(3)	1137(2)	15(1)
O(3)	8215(1)	4557(4)	-488(2)	15(1)
O(4)	9086(1)	2056(3)	-1515(2)	15(1)
O(5)	7924(2)	-1604(3)	-4248(2)	21(1)
O(6)	9132(1)	-3189(3)	-1136(2)	14(1)
O(7)	8311(1)	-2039(4)	519(2)	16(1)
O(8)	9346(1)	470(3)	1510(2)	16(1)
N(1)	8556(1)	2544(4)	781(3)	10(1)
N(2)	8441(1)	-47(4)	-763(3)	11(1)
C(1)	8832(2)	5634(6)	3838(3)	21(1)
C(2)	9097(2)	5893(5)	2959(3)	18(1)
C(3)	9160(2)	4676(5)	2034(3)	15(1)
C(4)	8514(2)	3673(6)	1726(3)	15(1)
C(5)	8410(2)	2421(5)	2610(3)	14(1)
C(6)	8462(2)	2676(6)	3657(3)	17(1)
C(7)	8399(2)	3089(7)	-234(4)	14(1)
C(8)	8487(2)	1779(5)	-1118(3)	14(1)
C(9)	7949(2)	1845(5)	-2059(3)	15(1)
C(10)	7994(2)	94(5)	-2581(3)	14(1)
C(11)	7903(2)	-121(6)	-3625(3)	19(1)
C(12)	8189(2)	-3099(6)	-3834(3)	20(1)
C(13)	8577(2)	-3429(5)	-2933(3)	19(1)
C(14)	8812(2)	-2223(5)	-2026(3)	14(1)
C(15)	8243(2)	-1186(6)	-1697(3)	11(1)
C(16)	8442(2)	-553(7)	253(4)	13(1)
C(17)	8679(2)	731(5)	1142(3)	12(1)
C(18)	8300(2)	625(5)	2108(3)	14(1)
O(21)	0	3462(6)	0	17(1)
O(22)	10000	8951(5)	10000	15(1)
C(21)	9865(2)	2553(5)	5484(3)	34(1)
C(22)	9715(2)	1029(6)	5951(3)	39(1)
C(23)	9852(2)	-546(5)	5471(3)	45(1)

Table A2.8. Bond lengths [\AA] and angles [°] for tetraol **193** (CCDC 844563).

O(1)-C(1)	1.389(5)	C(1)-C(2)-C(3)	129.7(4)
O(1)-C(6)	1.371(5)	O(2)-C(3)-C(2)	109.3(3)
O(2)-C(3)	1.432(4)	O(2)-C(3)-C(4)	110.6(3)
O(3)-C(7)	1.227(5)	C(2)-C(3)-C(4)	110.2(3)
O(4)-C(8)	1.413(4)	N(1)-C(4)-C(5)	103.8(3)
O(5)-C(11)	1.393(5)	N(1)-C(4)-C(3)	110.9(3)
O(5)-C(12)	1.355(5)	C(5)-C(4)-C(3)	109.8(3)
O(6)-C(14)	1.434(4)	C(6)-C(5)-C(18)	122.3(4)
O(7)-C(16)	1.238(5)	C(6)-C(5)-C(4)	129.5(4)
O(8)-C(17)	1.414(4)	C(18)-C(5)-C(4)	107.9(3)
N(1)-C(7)	1.342(6)	C(5)-C(6)-O(1)	130.0(4)
N(1)-C(4)	1.485(5)	O(3)-C(7)-N(1)	124.5(5)
N(1)-C(17)	1.486(5)	O(3)-C(7)-C(8)	119.1(5)
N(2)-C(16)	1.334(6)	N(1)-C(7)-C(8)	116.3(5)
N(2)-C(8)	1.489(5)	O(4)-C(8)-N(2)	110.0(3)
N(2)-C(15)	1.483(5)	O(4)-C(8)-C(9)	108.2(3)
C(1)-C(2)	1.310(5)	N(2)-C(8)-C(9)	101.3(3)
C(2)-C(3)	1.514(5)	O(4)-C(8)-C(7)	110.3(4)
C(3)-C(4)	1.553(5)	N(2)-C(8)-C(7)	113.2(4)
C(4)-C(5)	1.510(5)	C(9)-C(8)-C(7)	113.5(4)
C(5)-C(6)	1.320(5)	C(8)-C(9)-C(10)	103.1(4)
C(5)-C(18)	1.531(5)	C(11)-C(10)-C(9)	122.5(4)
C(7)-C(8)	1.531(6)	C(11)-C(10)-C(15)	129.5(4)
C(8)-C(9)	1.518(5)	C(9)-C(10)-C(15)	107.5(3)
C(9)-C(10)	1.514(5)	C(10)-C(11)-O(5)	130.9(4)
C(10)-C(11)	1.311(5)	C(13)-C(12)-O(5)	131.5(4)
C(10)-C(15)	1.527(6)	C(12)-C(13)-C(14)	129.0(4)
C(12)-C(13)	1.327(5)	O(6)-C(14)-C(13)	109.8(3)
C(13)-C(14)	1.505(5)	O(6)-C(14)-C(15)	111.1(3)
C(14)-C(15)	1.528(5)	C(13)-C(14)-C(15)	110.1(3)
C(16)-C(17)	1.528(6)	N(2)-C(15)-C(14)	112.4(3)
C(17)-C(18)	1.531(5)	N(2)-C(15)-C(10)	102.9(3)
C(21)-C(21)#1	1.403(8)	C(14)-C(15)-C(10)	110.2(3)
C(21)-C(22)	1.371(6)	O(7)-C(16)-N(2)	123.9(5)
C(22)-C(23)	1.405(6)	O(7)-C(16)-C(17)	117.9(4)
C(23)-C(23)#1	1.401(9)	N(2)-C(16)-C(17)	117.9(4)
		O(8)-C(17)-N(1)	110.9(3)
C(1)-O(1)-C(6)	122.1(3)	O(8)-C(17)-C(18)	108.3(3)
C(11)-O(5)-C(12)	121.9(3)	N(1)-C(17)-C(18)	101.9(3)
C(7)-N(1)-C(4)	122.8(4)	O(8)-C(17)-C(16)	110.8(3)
C(7)-N(1)-C(17)	126.7(4)	N(1)-C(17)-C(16)	111.4(3)
C(4)-N(1)-C(17)	109.7(3)	C(18)-C(17)-C(16)	113.2(3)
C(16)-N(2)-C(8)	125.0(4)	C(5)-C(18)-C(17)	102.3(3)
C(16)-N(2)-C(15)	123.2(4)	C(21)#1-C(21)-C(22)	120.6(3)
C(8)-N(2)-C(15)	110.4(3)	C(23)-C(22)-C(21)	119.5(4)
C(2)-C(1)-O(1)		C(23)#1-C(23)-C(22)	

Symmetry transformations used to generate equivalent atoms:

#1 -x+2,y,-z+1

Table A2.9. Anisotropic displacement parameters ($\text{\AA}^2 \times 10^4$) for tetraol **193** (CCDC 844563). The anisotropic displacement factor exponent takes the form: $-2p^2[h^2a^{*2}U^{11} + \dots + 2 h k a^* b^* U^{12}]$

	U ¹¹	U ²²	U ³³	U ²³	U ¹³	U ¹²
O(1)	251(17)	240(19)	131(15)	-80(14)	42(14)	-6(14)
O(2)	143(15)	152(17)	156(17)	9(13)	12(13)	-1(15)
O(3)	190(18)	78(18)	164(19)	26(14)	-25(14)	13(14)
O(4)	136(15)	179(17)	135(16)	-8(13)	22(13)	-34(14)
O(5)	286(16)	190(20)	141(14)	-62(13)	-5(16)	69(16)
O(6)	151(15)	94(16)	191(18)	-10(12)	23(13)	-17(15)
O(7)	178(18)	104(18)	180(20)	-22(14)	35(15)	-28(14)
O(8)	134(15)	179(17)	156(17)	5(13)	-20(13)	40(13)
N(1)	160(20)	29(18)	140(20)	-10(16)	54(16)	2(15)
N(2)	140(20)	75(19)	110(20)	-35(16)	30(16)	10(15)
C(1)	230(20)	150(30)	230(30)	-60(20)	-10(20)	-20(20)
C(2)	230(20)	130(20)	190(20)	-77(19)	24(19)	-70(20)
C(3)	140(20)	180(20)	140(20)	1(19)	40(18)	-40(20)
C(4)	200(30)	120(20)	130(20)	-40(20)	60(20)	0(20)
C(5)	130(20)	110(20)	170(20)	-15(19)	34(18)	8(17)
C(6)	170(20)	110(20)	240(30)	10(20)	50(20)	0(20)
C(7)	100(20)	130(30)	170(30)	-120(20)	20(20)	-40(20)
C(8)	140(20)	150(30)	130(20)	50(20)	18(18)	-20(20)
C(9)	190(20)	120(20)	130(20)	0(20)	2(18)	-29(19)
C(10)	120(20)	120(20)	160(20)	11(18)	16(18)	-10(17)
C(11)	210(20)	190(30)	170(30)	-20(20)	-10(20)	-40(20)
C(12)	220(20)	180(30)	190(30)	-90(20)	20(20)	-50(20)
C(13)	220(20)	190(30)	170(20)	-42(18)	80(20)	0(20)
C(14)	170(20)	140(20)	120(20)	5(18)	24(18)	0(20)
C(15)	70(20)	130(20)	135(19)	-10(20)	0(20)	-13(19)
C(16)	90(20)	190(30)	110(30)	70(20)	40(20)	90(20)
C(17)	190(20)	50(20)	130(20)	30(20)	36(18)	-10(20)
C(18)	180(20)	130(20)	120(20)	-4(19)	52(18)	-40(19)
O(21)	100(30)	100(30)	280(30)	0	-20(20)	0
O(22)	190(30)	120(30)	130(30)	0	10(20)	0
C(21)	280(20)	410(30)	320(30)	-60(20)	-80(20)	50(20)
C(22)	320(20)	570(30)	280(20)	80(30)	10(30)	-40(30)
C(23)	550(30)	350(30)	410(30)	90(20)	-100(30)	-20(30)

Table A2.10. Hydrogen bonds for tetraol **193** (CCDC 844563) [\AA and $^\circ$].

D-H...A	d(D-H)	d(H...A)	d(D...A)	\angle (DHA)
O(2)-H(2)...O(7) ^{#2}	0.84	1.97	2.795(4)	168.8
O(4)-H(4)...O(21) ^{#3}	0.84	1.92	2.733(3)	162.9
O(6)-H(6)...O(3) ^{#4}	0.84	1.95	2.779(4)	171.0
O(6)-H(6)...O(2) ^{#4}	0.84	2.69	2.970(3)	101.0
O(8)-H(8)...O(22) ^{#5}	0.84	1.90	2.736(3)	174.8
O(21)-H(21A)...O(2) ^{#6}	0.96	1.82	2.715(4)	153.3
O(22)-H(22A)...O(6) ^{#7}	0.84	1.92	2.712(4)	156.7

Symmetry transformations used to generate equivalent atoms:

#1 -x+2,y,-z+1
#2 x,y+1,z
#3 x+1,y,z
#4 x,y-1,z
#5 x,y-1,z-1
#6 -x+1,y,-z
#7 x,y+1,z+1

A2.3 CRYSTAL STRUCTURE ANALYSIS OF DIKETOPIPERAZINE 194

Figure A2.3. Diketopiperazine **194**. Crystallographic data have been deposited at the CCDC, 12 Union Road, Cambridge CB2 1EZ, UK and copies can be obtained on request, free of charge, by quoting the publication citation and the deposition number 832361.

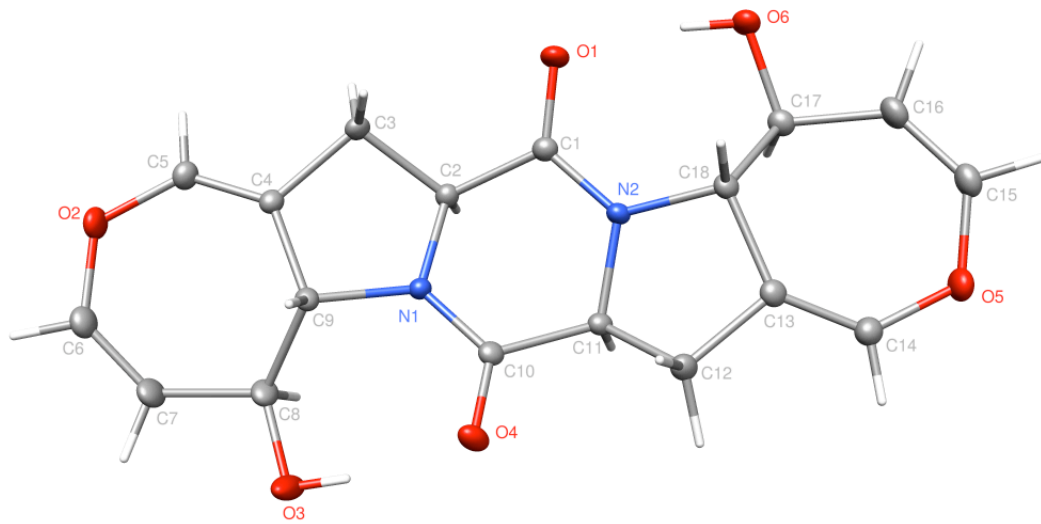


Table A2.11. Crystal data and structure refinement for diketopiperazine **194** (CCDC 832361).

Empirical formula	C ₁₈ H ₁₈ N ₂ O ₆
Formula weight	358.34
Crystallization Solvent	THF
Crystal Habit	Block
Crystal size	0.37 x 0.37 x 0.30 mm ³
Crystal color	Colorless

Data Collection

Type of diffractometer	Bruker SMART 1000
Wavelength	0.71073 Å MoKα
Data Collection Temperature	100(2) K
θ range for 6587 reflections used in lattice determination	2.18 to 27.57°
Unit cell dimensions	a = 9.8372(4) Å b = 7.2818(3) Å c = 11.6037(5) Å
	α= 90° β= 108.626(2)° γ = 90°
Volume	787.67(6) Å ³
Z	2
Crystal system	Monoclinic
Space group	P 2 ₁
Density (calculated)	1.511 Mg/m ³
F(000)	376
Data collection program	Bruker SMART v5.630
θ range for data collection	1.85 to 42.08°
Completeness to θ = 42.08°	97.7 %
Index ranges	-18 ≤ h ≤ 18, -13 ≤ k ≤ 13, -21 ≤ l ≤ 21
Data collection scan type	ω scans at 7 settings
Data reduction program	Bruker SAINT-Plus v7.66A
Reflections collected	24528
Independent reflections	10286 [R _{int} = 0.0425]
Absorption coefficient	0.115 mm ⁻¹
Absorption correction	None
Max. and min. transmission	0.9664 and 0.9587

Table A2.11 (cont.)**Structure Solution and Refinement**

Structure solution program	SHELXS-97 (Sheldrick, 2008)
Primary solution method	Direct methods
Secondary solution method	Difference Fourier map
Hydrogen placement	Difference Fourier map
Structure refinement program	SHELXL-97 (Sheldrick, 2008)
Refinement method	Full matrix least-squares on F^2
Data / restraints / parameters	10286 / 1 / 307
Treatment of hydrogen atoms	Unrestrained
Goodness-of-fit on F^2	1.822
Final R indices [$I > 2\sigma(I)$, 8534 reflections]	$R = 0.0456, wR2 = 0.0767$
R indices (all data)	$R = 0.0564, wR2 = 0.0781$
Type of weighting scheme used	Sigma
Weighting scheme used	$w = 1/\sigma^2(Fo^2)$
Max shift/error	0.001
Average shift/error	0.000
Absolute structure determination	Not determined
Absolute structure parameter	0.1(5)
Largest diff. peak and hole	0.524 and -0.394 e. \AA^{-3}

Special Refinement Details

Crystals were mounted on a glass fiber using Paratone oil then placed on the diffractometer under a nitrogen stream at 100K.

Refinement of F^2 against ALL reflections. The weighted R-factor (wR) and goodness of fit (S) are based on F^2 , conventional R-factors (R) are based on F, with F set to zero for negative F^2 . The threshold expression of $F^2 > 2\sigma(F^2)$ is used only for calculating R-factors(gt) etc. and is not relevant to the choice of reflections for refinement. R-factors based on F^2 are statistically about twice as large as those based on F, and R-factors based on ALL data will be even larger.

All esds (except the esd in the dihedral angle between two l.s. planes) are estimated using the full covariance matrix. The cell esds are taken into account individually in the estimation of esds in distances, angles and torsion angles; correlations between esds in cell parameters are only used when they are defined by crystal symmetry. An approximate (isotropic) treatment of cell esds is used for estimating esds involving l.s. planes.

Table A2.12. Atomic coordinates ($\times 10^4$) and equivalent isotropic displacement parameters ($\text{\AA}^2 \times 10^3$) for diketopiperazine **194** (CCDC 832361). $U(\text{eq})$ is defined as the trace of the orthogonalized U^{ij} tensor.

	x	y	z	U_{eq}
O(1)	8348(1)	-1783(1)	4697(1)	20(1)
O(2)	6071(1)	-327(1)	9389(1)	22(1)
O(3)	5737(1)	4976(1)	7307(1)	36(1)
O(4)	6036(1)	4590(1)	5142(1)	19(1)
O(5)	9107(1)	3564(1)	885(1)	22(1)
O(6)	9445(1)	-1772(1)	2927(1)	20(1)
N(1)	7024(1)	1926(1)	6068(1)	12(1)
N(2)	8058(1)	1240(1)	4124(1)	12(1)
C(1)	8126(1)	-153(1)	4894(1)	13(1)
C(2)	8002(1)	363(1)	6130(1)	13(1)
C(3)	7351(1)	-1162(1)	6684(1)	15(1)
C(4)	6691(1)	-122(1)	7499(1)	13(1)
C(5)	6665(1)	-897(2)	8531(1)	17(1)
C(6)	5583(1)	1426(2)	9415(1)	21(1)
C(7)	5717(1)	2919(2)	8810(1)	22(1)
C(8)	6405(1)	3310(1)	7852(1)	19(1)
C(9)	6176(1)	1723(1)	6930(1)	13(1)
C(10)	6855(1)	3264(1)	5249(1)	13(1)
C(11)	7799(1)	3142(1)	4437(1)	12(1)
C(12)	7135(1)	4037(1)	3200(1)	16(1)
C(13)	7916(1)	3080(1)	2440(1)	14(1)
C(14)	8397(1)	4055(2)	1682(1)	17(1)
C(15)	9449(1)	1776(2)	741(1)	19(1)
C(16)	9583(1)	353(2)	1481(1)	19(1)
C(17)	9450(1)	160(1)	2730(1)	15(1)
C(18)	8087(1)	1087(1)	2835(1)	13(1)

Table A2.13. Bond lengths [\AA] and angles [°] for diketopiperazine **194** (CCDC 832361).

O(1)-C(1)	1.2410(12)	C(6)-O(2)-C(5)	122.19(8)
O(2)-C(6)	1.3671(14)	C(8)-O(3)-H(3)	104.9(13)
O(2)-C(5)	1.3706(12)	C(15)-O(5)-C(14)	121.90(8)
O(3)-C(8)	1.4282(14)	C(17)-O(6)-H(6)	104.5(11)
O(3)-H(3)	0.834(15)	C(10)-N(1)-C(2)	121.93(7)
O(4)-C(10)	1.2378(12)	C(10)-N(1)-C(9)	125.25(7)
O(5)-C(15)	1.3685(13)	C(2)-N(1)-C(9)	112.58(7)
O(5)-C(14)	1.3719(12)	C(1)-N(2)-C(11)	121.51(7)
O(6)-C(17)	1.4250(13)	C(1)-N(2)-C(18)	126.34(8)
O(6)-H(6)	0.842(13)	C(11)-N(2)-C(18)	111.92(7)
N(1)-C(10)	1.3342(12)	O(1)-C(1)-N(2)	125.17(8)
N(1)-C(2)	1.4772(11)	O(1)-C(1)-C(2)	118.70(8)
N(1)-C(9)	1.5006(11)	N(2)-C(1)-C(2)	116.03(8)
N(2)-C(1)	1.3399(12)	N(1)-C(2)-C(3)	103.12(7)
N(2)-C(11)	1.4748(12)	N(1)-C(2)-C(1)	112.99(7)
N(2)-C(18)	1.5094(11)	C(3)-C(2)-C(1)	112.80(8)
C(1)-C(2)	1.5250(12)	N(1)-C(2)-H(2)	110.7(6)
C(2)-C(3)	1.5231(12)	C(3)-C(2)-H(2)	111.5(6)
C(2)-H(2)	0.998(10)	C(1)-C(2)-H(2)	105.9(6)
C(3)-C(4)	1.5107(13)	C(4)-C(3)-C(2)	102.78(7)
C(3)-H(3A)	0.960(11)	C(4)-C(3)-H(3A)	108.2(7)
C(3)-H(3B)	0.919(13)	C(2)-C(3)-H(3A)	107.4(7)
C(4)-C(5)	1.3312(13)	C(4)-C(3)-H(3B)	112.7(8)
C(4)-C(9)	1.5110(13)	C(2)-C(3)-H(3B)	111.0(8)
C(5)-H(5)	0.917(14)	H(3A)-C(3)-H(3B)	114.0(11)
C(6)-C(7)	1.3232(15)	C(5)-C(4)-C(3)	119.07(9)
C(6)-H(6A)	0.929(13)	C(5)-C(4)-C(9)	132.05(9)
C(7)-C(8)	1.5024(13)	C(3)-C(4)-C(9)	108.87(7)
C(7)-H(7)	0.935(14)	C(4)-C(5)-O(2)	131.33(10)
C(8)-C(9)	1.5415(13)	C(4)-C(5)-H(5)	117.6(8)
C(8)-H(8)	0.985(12)	O(2)-C(5)-H(5)	111.0(8)
C(9)-H(9)	0.972(11)	C(7)-C(6)-O(2)	131.33(9)
C(10)-C(11)	1.5222(12)	C(7)-C(6)-H(6A)	122.0(8)
C(11)-C(12)	1.5212(13)	O(2)-C(6)-H(6A)	106.7(8)
C(11)-H(11)	0.941(11)	C(6)-C(7)-C(8)	133.86(10)
C(12)-C(13)	1.5118(13)	C(6)-C(7)-H(7)	115.5(8)
C(12)-H(12A)	1.004(11)	C(8)-C(7)-H(7)	110.6(8)
C(12)-H(12B)	1.011(13)	O(3)-C(8)-C(7)	103.66(8)
C(13)-C(14)	1.3301(13)	O(3)-C(8)-C(9)	112.64(8)
C(13)-C(18)	1.5151(14)	C(7)-C(8)-C(9)	111.77(8)
C(14)-H(14)	0.910(13)	O(3)-C(8)-H(8)	105.1(8)
C(15)-C(16)	1.3255(15)	C(7)-C(8)-H(8)	113.9(7)
C(15)-H(15)	0.982(13)	C(9)-C(8)-H(8)	109.5(7)
C(16)-C(17)	1.5025(13)	N(1)-C(9)-C(4)	101.45(7)
C(16)-H(16)	0.958(12)	N(1)-C(9)-C(8)	113.55(7)
C(17)-C(18)	1.5405(13)	C(4)-C(9)-C(8)	114.14(8)
C(17)-H(17)	0.969(12)	N(1)-C(9)-H(9)	108.3(7)
C(18)-H(18)	0.969(12)	C(4)-C(9)-H(9)	111.6(7)

C(8)-C(9)-H(9)	107.6(7)
O(4)-C(10)-N(1)	124.78(8)
O(4)-C(10)-C(11)	119.31(8)
N(1)-C(10)-C(11)	115.86(8)
N(2)-C(11)-C(12)	103.03(7)
N(2)-C(11)-C(10)	113.26(8)
C(12)-C(11)-C(10)	113.34(7)
N(2)-C(11)-H(11)	108.7(7)
C(12)-C(11)-H(11)	110.3(7)
C(10)-C(11)-H(11)	108.1(6)
C(13)-C(12)-C(11)	101.98(8)
C(13)-C(12)-H(12A)	110.0(7)
C(11)-C(12)-H(12A)	108.1(6)
C(13)-C(12)-H(12B)	114.5(7)
C(11)-C(12)-H(12B)	112.3(7)
H(12A)-C(12)-H(12B)	109.5(10)
C(14)-C(13)-C(12)	119.65(9)
C(14)-C(13)-C(18)	133.03(9)
C(12)-C(13)-C(18)	107.08(8)
C(13)-C(14)-O(5)	132.25(10)
C(13)-C(14)-H(14)	121.0(8)
O(5)-C(14)-H(14)	106.7(8)
C(16)-C(15)-O(5)	129.93(9)
C(16)-C(15)-H(15)	119.4(8)
O(5)-C(15)-H(15)	110.7(8)
C(15)-C(16)-C(17)	132.62(10)
C(15)-C(16)-H(16)	114.5(7)
C(17)-C(16)-H(16)	112.9(7)
O(6)-C(17)-C(16)	104.65(8)
O(6)-C(17)-C(18)	111.84(8)
C(16)-C(17)-C(18)	112.40(8)
O(6)-C(17)-H(17)	108.1(7)
C(16)-C(17)-H(17)	111.9(7)
C(18)-C(17)-H(17)	107.9(7)
N(2)-C(18)-C(13)	101.13(7)
N(2)-C(18)-C(17)	113.78(7)
C(13)-C(18)-C(17)	114.32(7)
N(2)-C(18)-H(18)	105.9(7)
C(13)-C(18)-H(18)	113.6(7)
C(17)-C(18)-H(18)	107.8(7)

Table A2.14. Anisotropic displacement parameters ($\text{\AA}^2 \times 10^4$) for diketopiperazine **194** (CCDC 832361). The anisotropic displacement factor exponent takes the form: $-2p^2[h^2a^{*2}U^{11} + \dots + 2hk a^* b^* U^{12}]$

	U ¹¹	U ²²	U ³³	U ²³	U ¹³	U ¹²
O(1)	321(4)	98(3)	241(4)	6(3)	168(3)	39(3)
O(2)	327(4)	205(4)	204(3)	28(3)	179(3)	9(3)
O(3)	794(7)	123(4)	315(5)	22(4)	374(5)	66(4)
O(4)	269(4)	158(3)	171(3)	26(3)	99(3)	99(3)
O(5)	302(4)	203(4)	213(3)	19(3)	172(3)	7(3)
O(6)	285(4)	124(3)	235(4)	12(3)	156(3)	43(3)
N(1)	153(3)	88(3)	136(3)	10(3)	75(3)	11(3)
N(2)	169(3)	93(3)	126(3)	0(3)	70(3)	20(3)
C(1)	147(4)	114(4)	154(4)	4(3)	66(3)	9(3)
C(2)	142(4)	114(4)	140(4)	11(3)	66(3)	9(3)
C(3)	203(4)	102(4)	160(4)	25(3)	89(3)	19(3)
C(4)	157(4)	111(4)	148(4)	-7(3)	68(3)	-17(3)
C(5)	199(4)	159(4)	180(4)	21(4)	94(3)	2(4)
C(6)	266(5)	206(5)	184(4)	-18(4)	127(4)	-10(4)
C(7)	358(6)	174(5)	189(5)	-33(4)	165(4)	3(4)
C(8)	290(5)	139(4)	183(4)	-48(4)	128(4)	-44(4)
C(9)	149(4)	106(4)	141(4)	-17(3)	71(3)	-16(3)
C(10)	155(4)	111(4)	115(3)	-13(3)	46(3)	1(3)
C(11)	157(4)	100(3)	119(3)	-2(3)	52(3)	11(3)
C(12)	206(4)	134(4)	138(4)	25(3)	71(3)	45(3)
C(13)	164(4)	139(4)	113(4)	0(3)	39(3)	13(3)
C(14)	231(5)	149(4)	152(4)	7(4)	76(3)	12(4)
C(15)	216(4)	220(5)	158(4)	-17(4)	95(4)	11(4)
C(16)	223(5)	205(5)	181(4)	-23(4)	112(4)	26(4)
C(17)	157(4)	143(4)	154(4)	-6(3)	60(3)	15(3)
C(18)	152(4)	123(4)	113(3)	-9(3)	47(3)	1(3)

Table A2.15. Hydrogen coordinates ($\times 10^4$) and isotropic displacement parameters ($\text{\AA}^2 \times 10^3$) for diketopiperazine **194** (CCDC 832361).

	x	y	z	U_{iso}
H(3)	5794(18)	4960(30)	6606(14)	51(5)
H(6)	9043(14)	-1890(20)	3463(11)	32(4)
H(2)	8996(11)	669(14)	6656(9)	3(2)
H(3A)	6590(12)	-1706(18)	6037(10)	13(3)
H(3B)	8040(13)	-1983(19)	7104(11)	21(3)
H(5)	7075(13)	-2035(19)	8718(11)	22(3)
H(6A)	5086(14)	1432(17)	9974(13)	18(3)
H(7)	5272(15)	3970(20)	8980(12)	34(4)
H(8)	7436(13)	3600(18)	8181(10)	23(3)
H(9)	5163(12)	1697(17)	6458(10)	14(3)
H(11)	8687(12)	3694(16)	4850(9)	10(3)
H(12A)	6089(12)	3711(16)	2898(10)	13(3)
H(12B)	7244(13)	5419(18)	3235(11)	17(3)
H(14)	8278(13)	5295(18)	1621(11)	19(3)
H(15)	9612(13)	1605(18)	-45(12)	22(3)
H(16)	9814(11)	-782(17)	1168(9)	13(3)
H(17)	10269(13)	679(17)	3350(11)	15(3)
H(18)	7275(12)	325(16)	2409(10)	12(3)

Table A2.16. Hydrogen bonds for diketopiperazine **194** (CCDC 832361) [\AA and $^\circ$].

D-H...A	d(D-H)	d(H...A)	d(D...A)	\angle (DHA)
O(3)-H(3)...O(4)	0.834(15)	1.809(15)	2.6365(11)	171.2(19)
O(6)-H(6)...O(1)	0.842(13)	1.775(13)	2.6082(10)	169.9(15)

A2.4. CRYSTAL STRUCTURE ANALYSIS OF TETRA SULFIDE 197

Figure A2.4. Tetrasulfide **197**. Crystallographic data have been deposited at the CCDC, 12 Union Road, Cambridge CB2 1EZ, UK and copies can be obtained on request, free of charge, by quoting the publication citation and the deposition number 838235.

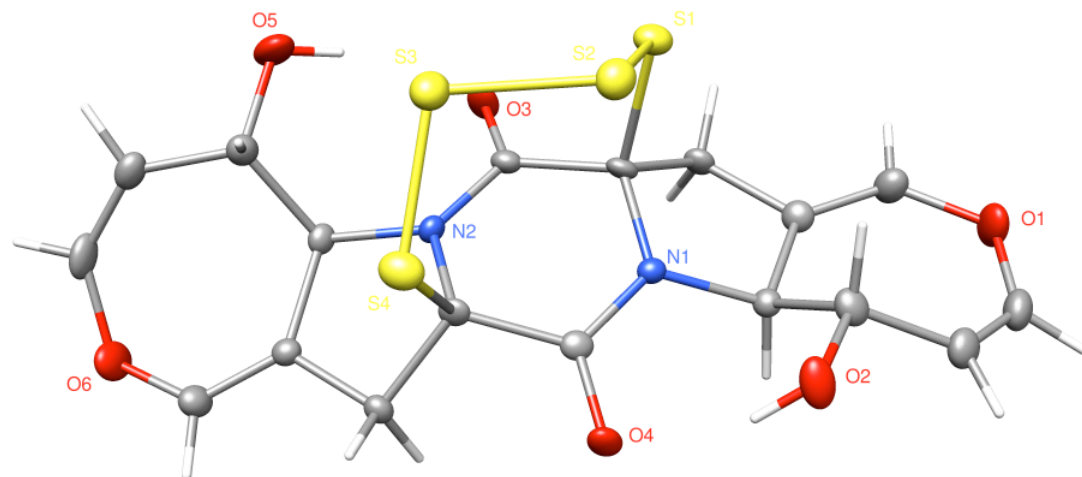


Table A2.17. Crystal data and structure refinement for tetrasulfide **197** (CCDC 838235).

Empirical formula	C ₁₈ H ₁₆ N ₂ O ₆ S ₄	
Formula weight	484.57	
Crystallization Solvent	Chloroform/isooctane	
Crystal Habit	Plate	
Crystal size	0.48 x 0.20 x 0.05 mm ³	
Crystal color	Light yellow	

Data Collection

Type of diffractometer	Bruker KAPPA APEX II
Wavelength	0.71073 Å MoKα
Data Collection Temperature	100(2) K
θ range for 9912 reflections used in lattice determination	2.61 to 29.28°
Unit cell dimensions	a = 7.6944(3) Å b = 9.6777(3) Å c = 26.3981(9) Å
	α= 90° β= 90° γ = 90°
Volume	1965.71(12) Å ³
Z	4
Crystal system	Orthorhombic
Space group	P 2 ₁ 2 ₁ 2 ₁
Density (calculated)	1.637 Mg/m ³
F(000)	1000
Data collection program	Bruker APEX2 v2009.7-0
θ range for data collection	2.24 to 29.30°
Completeness to θ = 29.30°	99.9 %
Index ranges	-10 ≤ h ≤ 10, -13 ≤ k ≤ 13, -36 ≤ l ≤ 36
Data collection scan type	ω scans; 9 settings
Data reduction program	Bruker SAINT-Plus v7.68A
Reflections collected	42286
Independent reflections	5365 [R _{int} = 0.0472]
Absorption coefficient	0.525 mm ⁻¹
Absorption correction	None
Max. and min. transmission	0.9742 and 0.7868

Table A2.17 (cont.)**Structure Solution and Refinement**

Structure solution program	SHELXS-97 (Sheldrick, 2008)
Primary solution method	Direct methods
Secondary solution method	Difference Fourier map
Hydrogen placement	Geometric positions
Structure refinement program	SHELXL-97 (Sheldrick, 2008)
Refinement method	Full matrix least-squares on F^2
Data / restraints / parameters	5365 / 0 / 273
Treatment of hydrogen atoms	Riding
Goodness-of-fit on F^2	2.797
Final R indices [$I > 2\sigma(I)$, 4892 reflections]	$R = 0.0433, wR2 = 0.0639$
R indices (all data)	$R = 0.0483, wR2 = 0.0642$
Type of weighting scheme used	Sigma
Weighting scheme used	$w = 1/\sigma^2(Fo^2)$
Max shift/error	0.000
Average shift/error	0.000
Absolute structure determination	Anomalous dispersion
Absolute structure parameter	-0.02(6)
Largest diff. peak and hole	1.078 and -0.643 e. \AA^{-3}

Special Refinement Details

Crystals were mounted on a glass fiber using Paratone oil then placed on the diffractometer under a nitrogen stream at 100K.

Refinement of F^2 against ALL reflections. The weighted R-factor (wR) and goodness of fit (S) are based on F^2 , conventional R-factors (R) are based on F, with F set to zero for negative F^2 . The threshold expression of $F^2 > 2\sigma(F^2)$ is used only for calculating R-factors(gt) etc. and is not relevant to the choice of reflections for refinement. R-factors based on F^2 are statistically about twice as large as those based on F, and R-factors based on ALL data will be even larger.

All esds (except the esd in the dihedral angle between two l.s. planes) are estimated using the full covariance matrix. The cell esds are taken into account individually in the estimation of esds in distances, angles and torsion angles; correlations between esds in cell parameters are only used when they are defined by crystal symmetry. An approximate (isotropic) treatment of cell esds is used for estimating esds involving l.s. planes.

Table A2.18. Atomic coordinates ($\times 10^4$) and equivalent isotropic displacement parameters ($\text{\AA}^2 \times 10^3$) for tetrasulfide **197** (CCDC 838235). $U(\text{eq})$ is defined as the trace of the orthogonalized U^{ij} tensor.

	x	y	z	U_{eq}
S(1)	3450(1)	7409(1)	3420(1)	21(1)
S(2)	1537(1)	5992(1)	3477(1)	23(1)
S(3)	429(1)	6398(1)	4176(1)	23(1)
S(4)	-1817(1)	7354(1)	3987(1)	23(1)
O(1)	4095(2)	9173(2)	1605(1)	31(1)
O(2)	-845(2)	7303(2)	2186(1)	24(1)
O(3)	3157(2)	10233(2)	4085(1)	23(1)
O(4)	-2156(2)	9030(2)	2905(1)	20(1)
O(5)	2022(2)	9505(2)	5062(1)	38(1)
O(6)	-2979(2)	11716(2)	5196(1)	28(1)
N(1)	760(3)	8971(2)	3011(1)	12(1)
N(2)	315(2)	9677(2)	4025(1)	13(1)
C(1)	2554(3)	8757(3)	1390(1)	25(1)
C(2)	1178(3)	8178(3)	1600(1)	22(1)
C(3)	847(3)	7836(3)	2144(1)	19(1)
C(4)	1153(3)	9144(3)	2464(1)	14(1)
C(5)	3062(3)	9543(3)	2471(1)	17(1)
C(6)	4231(4)	9471(3)	2113(1)	24(1)
C(7)	3548(3)	9946(3)	3003(1)	17(1)
C(8)	2289(3)	9089(3)	3326(1)	14(1)
C(9)	1969(3)	9709(3)	3845(1)	15(1)
C(10)	-888(3)	9024(2)	3189(1)	14(1)
C(11)	-1150(3)	9105(3)	3753(1)	14(1)
C(12)	-2663(3)	10049(3)	3900(1)	15(1)
C(13)	-3277(3)	11166(3)	4725(1)	21(1)
C(14)	-2160(3)	10581(3)	4418(1)	15(1)
C(15)	-220(3)	10389(3)	4500(1)	14(1)
C(16)	198(3)	9562(3)	4976(1)	20(1)
C(17)	-555(3)	10219(3)	5442(1)	22(1)
C(18)	-1787(4)	11133(3)	5517(1)	24(1)

Table A2.19. Bond lengths [\AA] and angles [$^\circ$] for tetrasulfide **197** (CCDC 838235).

S(1)-C(8)	1.872(3)	C(9)-N(2)-C(15)	122.8(2)
S(1)-S(2)	2.0170(9)	C(11)-N(2)-C(15)	112.32(18)
S(2)-S(3)	2.0698(10)	C(2)-C(1)-O(1)	130.0(3)
S(3)-S(4)	2.0224(10)	C(1)-C(2)-C(3)	129.4(3)
S(4)-C(11)	1.875(3)	O(2)-C(3)-C(2)	108.4(2)
O(1)-C(6)	1.376(3)	O(2)-C(3)-C(4)	113.6(2)
O(1)-C(1)	1.374(3)	C(2)-C(3)-C(4)	108.6(2)
O(2)-C(3)	1.405(3)	N(1)-C(4)-C(5)	102.42(19)
O(3)-C(9)	1.223(3)	N(1)-C(4)-C(3)	114.2(2)
O(4)-C(10)	1.230(3)	C(5)-C(4)-C(3)	111.3(2)
O(5)-C(16)	1.423(3)	C(6)-C(5)-C(7)	121.2(2)
O(6)-C(13)	1.372(3)	C(6)-C(5)-C(4)	130.1(2)
O(6)-C(18)	1.370(3)	C(7)-C(5)-C(4)	108.4(2)
N(1)-C(10)	1.352(3)	C(5)-C(6)-O(1)	131.6(3)
N(1)-C(8)	1.444(3)	C(5)-C(7)-C(8)	102.77(19)
N(1)-C(4)	1.485(3)	N(1)-C(8)-C(9)	114.8(2)
N(2)-C(9)	1.358(3)	N(1)-C(8)-C(7)	103.82(19)
N(2)-C(11)	1.447(3)	C(9)-C(8)-C(7)	113.0(2)
N(2)-C(15)	1.488(3)	N(1)-C(8)-S(1)	113.32(17)
C(1)-C(2)	1.320(4)	C(9)-C(8)-S(1)	107.53(17)
C(2)-C(3)	1.495(3)	C(7)-C(8)-S(1)	103.97(16)
C(3)-C(4)	1.540(3)	O(3)-C(9)-N(2)	122.0(2)
C(4)-C(5)	1.519(3)	O(3)-C(9)-C(8)	120.7(2)
C(5)-C(6)	1.306(3)	N(2)-C(9)-C(8)	117.3(2)
C(5)-C(7)	1.507(3)	O(4)-C(10)-N(1)	122.2(2)
C(7)-C(8)	1.533(3)	O(4)-C(10)-C(11)	119.7(2)
C(8)-C(9)	1.517(3)	N(1)-C(10)-C(11)	118.0(2)
C(10)-C(11)	1.505(3)	N(2)-C(11)-C(10)	114.00(19)
C(11)-C(12)	1.531(3)	N(2)-C(11)-C(12)	103.76(18)
C(12)-C(14)	1.510(3)	C(10)-C(11)-C(12)	112.7(2)
C(13)-C(14)	1.310(3)	N(2)-C(11)-S(4)	113.25(16)
C(14)-C(15)	1.520(3)	C(10)-C(11)-S(4)	108.43(17)
C(15)-C(16)	1.524(3)	C(12)-C(11)-S(4)	104.34(16)
C(16)-C(17)	1.502(3)	C(14)-C(12)-C(11)	103.83(19)
C(17)-C(18)	1.312(4)	C(14)-C(13)-O(6)	128.3(2)
		C(13)-C(14)-C(12)	122.6(2)
C(8)-S(1)-S(2)	104.59(8)	C(13)-C(14)-C(15)	127.5(2)
S(1)-S(2)-S(3)	103.82(4)	C(12)-C(14)-C(15)	109.8(2)
S(4)-S(3)-S(2)	102.66(4)	N(2)-C(15)-C(14)	102.0(2)
C(11)-S(4)-S(3)	105.14(8)	N(2)-C(15)-C(16)	113.2(2)
C(6)-O(1)-C(1)	121.9(2)	C(14)-C(15)-C(16)	112.9(2)
C(13)-O(6)-C(18)	120.8(2)	O(5)-C(16)-C(17)	105.5(2)
C(10)-N(1)-C(8)	124.18(19)	O(5)-C(16)-C(15)	111.1(2)
C(10)-N(1)-C(4)	121.56(19)	C(17)-C(16)-C(15)	111.9(2)
C(8)-N(1)-C(4)	112.57(18)	C(18)-C(17)-C(16)	133.5(3)
C(9)-N(2)-C(11)	124.4(2)	C(17)-C(18)-O(6)	131.9(2)

Table A2.20. Anisotropic displacement parameters ($\text{\AA}^2 \times 10^4$) for tetrasulfide **197** (CCDC 838235). The anisotropic displacement factor exponent takes the form: $-2p^2[h^2a^{*2}U^{11} + \dots + 2hka^*b^*U^{12}]$

	U ¹¹	U ²²	U ³³	U ²³	U ¹³	U ¹²
S(1)	186(3)	209(4)	241(4)	12(3)	-16(3)	49(3)
S(2)	258(4)	206(4)	214(4)	7(3)	-2(3)	3(3)
S(3)	254(4)	226(4)	216(4)	20(3)	3(3)	41(3)
S(4)	192(3)	189(4)	300(4)	44(3)	3(3)	-19(3)
O(1)	225(10)	517(14)	174(11)	-12(10)	67(9)	-18(10)
O(2)	245(10)	230(11)	243(11)	-85(9)	72(8)	-102(9)
O(3)	89(9)	382(12)	205(11)	-71(9)	-4(8)	-28(9)
O(4)	94(9)	311(11)	188(10)	-50(9)	-31(8)	-3(9)
O(5)	197(11)	697(17)	243(12)	143(12)	-46(9)	85(12)
O(6)	303(11)	320(12)	208(11)	-99(9)	-6(9)	68(10)
N(1)	120(11)	120(11)	126(11)	9(9)	-11(9)	5(9)
N(2)	129(11)	156(11)	102(11)	6(9)	-9(9)	-6(9)
C(1)	319(17)	277(17)	150(15)	-33(12)	20(12)	36(14)
C(2)	267(16)	211(15)	174(15)	-59(11)	-5(12)	5(12)
C(3)	187(14)	161(14)	210(15)	-41(11)	19(11)	-9(12)
C(4)	137(13)	136(13)	133(13)	13(10)	4(10)	0(11)
C(5)	164(14)	157(13)	181(14)	20(11)	9(12)	-22(12)
C(6)	185(15)	331(17)	189(16)	12(12)	-9(12)	-21(13)
C(7)	91(13)	232(14)	183(14)	3(11)	1(11)	10(12)
C(8)	85(12)	170(13)	177(14)	-1(11)	-11(10)	41(11)
C(9)	113(13)	179(14)	165(14)	30(11)	-5(11)	34(11)
C(10)	138(13)	101(12)	170(14)	2(11)	-11(11)	-13(11)
C(11)	80(12)	172(13)	162(14)	26(11)	1(10)	-31(11)
C(12)	105(12)	179(13)	154(14)	2(11)	10(10)	-2(11)
C(13)	185(14)	244(15)	193(14)	-12(12)	-6(12)	36(13)
C(14)	130(13)	172(14)	140(14)	37(11)	-5(11)	-4(11)
C(15)	166(14)	146(13)	120(13)	-7(10)	3(11)	-9(11)
C(16)	160(14)	269(16)	168(14)	14(12)	-3(12)	20(12)
C(17)	199(14)	298(16)	149(14)	25(12)	-13(12)	-64(13)
C(18)	321(16)	273(16)	123(13)	-38(12)	29(13)	-81(15)

Chapter 3

Enantioselective Total Synthesis of C₂-Symmetric Dihydrooxepine-Containing Epipolythiodiketopiperazine Natural Products and Progress Toward MPC1001B

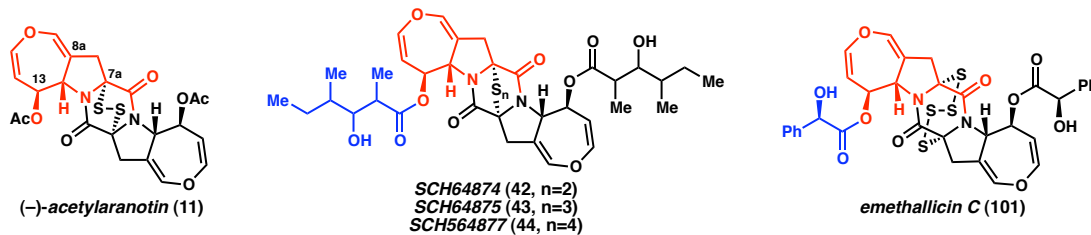
3.1 INTRODUCTION

Having completed an enantioselective total synthesis of acetylaranotin (**11**),¹ and in doing so developed a strategy towards the synthesis of dihydrooxepine-containing ETP natural products, our attention turned to the extention of this strategy to the preparation of related targets. These efforts have culminated in the synthesis of a small panel of epitetrathiodiketopiperazines, including natural products as well as analogs, which are currently being evaluated for biological activity. Furthermore, we have conducted preliminary investigations into the synthesis of dihydrooxepine-containing macrocycles, with a particular focus on the preparation of bis(*ortho*-methoxyaryl) ethers. Herein, a detailed account of these endeavors is presented.

3.2 C₂-SYMMETRIC DIHYDROOXEPINE-CONTAINING EPIPOLYTHIODIKETOPIPERAZINE NATURAL PRODUCTS

With access to tetrasulfide diol **197**, our successful completion of the total synthesis of acetylaranotin (**11**) left us well-positioned for preparation of related C₂-symmetric dihydrooxepine-containing ETP natural products, such as SCH64874 (**42**), SCH64877 (**44**),² and emethallicin C (**101**)³ (see Figure 3.1). We anticipated that the successful preparation of these natural products and related unnatural analogs might allow for a more comprehensive understanding of the role of their peripheral structure in biological target specificity and/or biophysical properties. Furthermore, a better understanding of structure/activity relationships might ultimately inform the synthesis of chemical probes for molecular target validation.

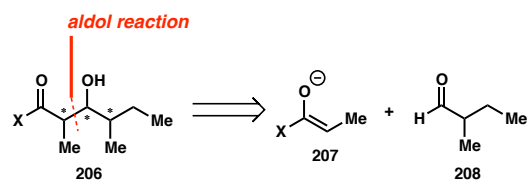
Figure 3.1. C₂-Symmetric ETP natural products containing the dimeric aranotin core



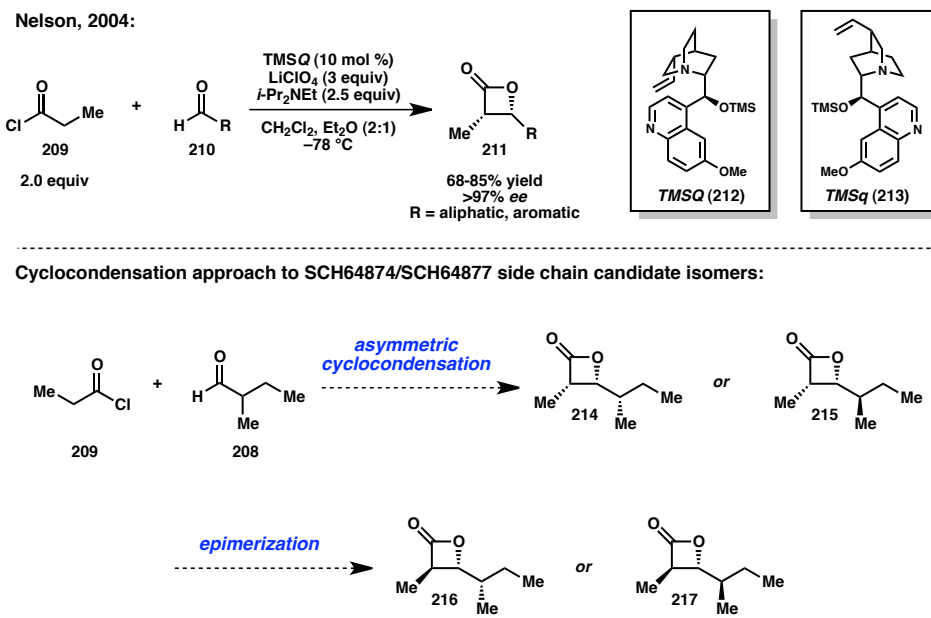
As the stereochemistry of the SCH sidechains was not disclosed in the original isolation report, we first sought to develop a divergent approach to access all eight isomers of 3-hydroxy-2,4-dimethylhexanoic acid derivatives (**206**). Classically, one might expect to form the desired stereotriad in a stereocontrolled manner using aldol chemistry (see Scheme 3.1). Nelson and coworkers have developed an enantioselective, organocatalytic cyclocondensation reaction for the preparation of β-lactones **211** from propionyl chloride (**209**) and aldehydes **210** (see Scheme 3.2),⁴ which represents an

attractive variant of the aldol reaction. This transformation is appealing because in addition to possessing all of the required stereocenters, the β -lactones themselves could potentially serve as acylating agents for the formation of the various candidate isomers of SCH64874 (**42**) and SCH64877 (**44**).

Scheme 3.1. Retrosynthetic analysis of the SCH64874 carboxylate side chain



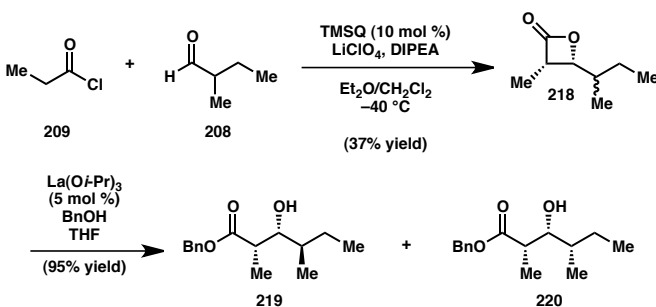
Scheme 3.2. Enantioselective cyclocondensation reaction to provide β -lactones



Our investigation began with the preparation of model 2,4-dimethyl-3-hydroxyhexanoate esters for spectroscopic analysis. To this end, synthetic studies commenced with the reaction between racemic 2-methylbutyraldehyde (**208**) and propionyl chloride (**209**) in the presence of quinidine-derived catalyst **212** (Scheme 3.3). The resulting mixture of enantioenriched β -lactone diastereomers (**218**) was then treated

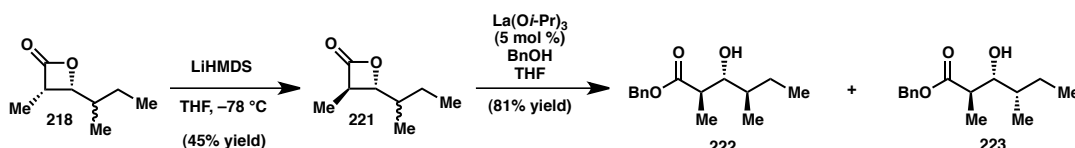
with excess benzyl alcohol in the presence of La(O*i*-Pr)₃ to afford the corresponding benzyl esters (**219** and **220**),⁵ which could be readily separated by simple flash chromatography.

Scheme 3.3. Synthesis of model *syn,anti*- and *syn,syn*- esters **219** and **220**



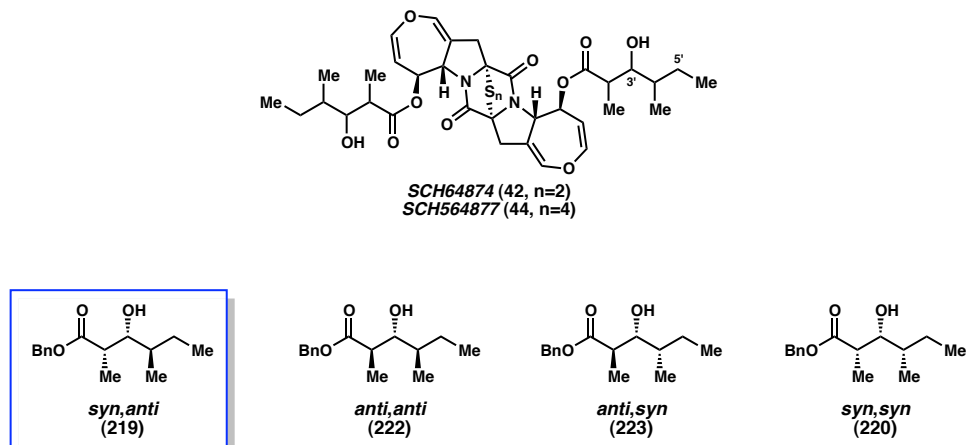
Likewise, epimerization of mixture **218** could be carried out with LiHMDS to formally give the *anti* aldol products (**221**), which could be converted to the benzyl esters **222** and **223** as before (Scheme 3.4). In this case, however, it was necessary to use preparative HPLC to separate the two diastereomers. Despite the low overall yields for these two routes, they allowed for rapid access to all four possible diastereomers of the 2,4-dimethyl-3-hydroxyhexanoate esters (**219**, **220**, **222**, and **223**) starting from inexpensive materials. Furthermore, the ability to use *either* the quinidine- or quinine-derived catalyst (**212** or **213**, respectively) provided access to either of the enantiomers of a particular ester.

Scheme 3.4. Synthesis of model *anti,anti*- and *anti,syn*- esters **222** and **223**



With isomers **219**, **220**, **222**, and **223** in hand, a comparison was made of their ¹H and ¹³C NMR spectra to those for SCH64874 (**42**) and SCH64877 (**44**). The carboxylate

appendages shared by the natural products each contain three methine hydrogens, two methylene hydrogens, and nine methyl hydrogens. Inspection of the corresponding chemical shifts of the four benzyl esters reveals that there are three diagnostic shifts for each stereotriad: those of the β -methine (C(3')–H) and the δ -methylene (C(5')–H_a and C(5')–H_b) (see Table 3.1). As assigned by Hegde and coworkers, the chemical shift for C(3')–H is 3.72 ppm for SCH64874 (**42**) and 3.81 ppm for SCH64877 (**44**). On the other hand, the chemical shift for the down-field C(5')–H_a is 1.84 ppm (**42**) and 1.85 ppm (**44**), and that for the up-field C(5')–H_b is 1.24–1.25 ppm (**42**) and 1.13–1.10 ppm (**44**). The *anti,anti* diastereomer (**222**) can be ruled out, as its chemical shift for C(3')–H is too far up-field (3.39 ppm). Likewise, the chemical shift for C(5')–H_a in *anti,syn* diastereomer **223** is too far up-field (1.51–1.39 ppm), whereas the chemical shift for C(5')–H_b is too far down-field (1.33–1.23 ppm). Similarly, the chemical shift for C(5')–H_a in *syn,syn* diastereomer **220** is too far up-field (1.46–1.33 ppm). By contrast, the ¹H NMR data for *syn,anti* diastereomer **219** appear to be consistent with those of **42** and **44**. Furthermore, the ¹³C shifts for the three methyl groups of **42** and **44** most closely match those of benzyl ester **219**. Taken together, these comparisons suggest that the SCH carboxylate side chain possesses the *syn,anti* configuration. Preliminary experiments revealed that the patterns described above are also observed when the individual carboxylates are coupled to the acetylarnanotin core.

Table 3.1. Comparison of relevant ¹H and ¹³C NMR data for SCH64874 (**42**), SCH64877 (**44**), and model carboxylates **219**, **220**, **222**, and **223****Important ¹H NMR Chemical Shifts (ppm) for **42**, **44**, **219**, **222**, **223**, and **220****

C#	SCH64874	SCH64877	219	222	223	220
1'	–	–	–	–	–	–
2'	2.67	2.8	2.72	2.77	2.69	2.72
3'	3.72	3.81	3.68	3.39	3.64	3.69
4'	1.49	1.5	1.50-1.41	1.44	1.51-1.39	1.46-1.33
5'	1.24-1.15 1.84	1.13-1.10 1.85	1.21-1.11 1.77	1.22-1.11 1.62	1.33-1.23 1.51-1.39	1.19-1.09 1.46-1.33
6'	0.94	0.95	0.89	0.88	0.90	0.87
7'	1.17	1.28	1.20	1.26	1.18	1.23
8'	0.83	0.84	0.82	0.90	0.87	0.94

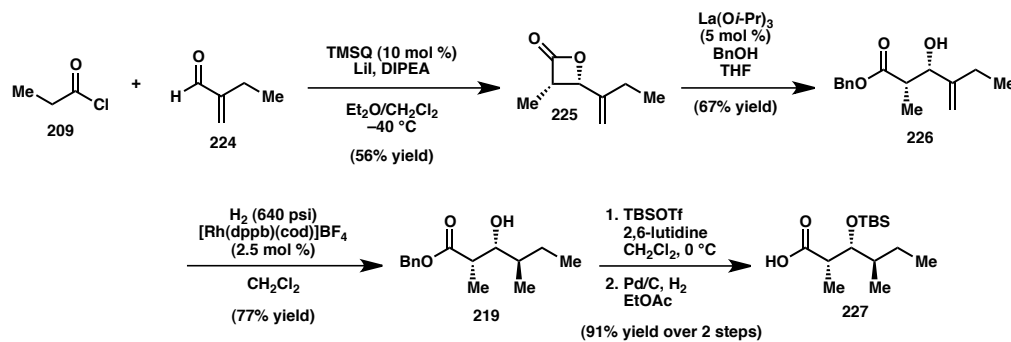
Important ¹³C NMR Chemical Shifts (ppm) for **42, **44**, **219**, **222**, **223**, and **220****

SCH64874	SCH64877	219	222	223	220
175.0	175.8	176.5	176.3	176.3	175.9
73.3	73.9	75.0	77.9	75.7	75.2
41.0	41.9	41.5	42.0	43.1	42.4
36.0	36.8	36.8	38.2	36.8	37.0
25.0	25.3	24.7	23.6	26.6	25.9
14.4	14.9	14.9	15.8	14.5	13.9
10.4	10.9	10.9	15.1	12.4	11.6
8.3	9.1	9.8	11.4	11.7	11.2

Though at this stage we were confident that we had identified the correct *relative* stereochemistry for the SCH carboxylate appendage, the question remained as to the *absolute* configuration. Furthermore, it was determined that benzyl ester **219** had only

been prepared in 60% *ee* using the sequence described above. We therefore sought to modify our sequence in such a way that it would provide not only diastereoselective access to either enantiomer of **219**, but also improved enantioselectivity. Inspired by Evans and coworkers' seminal studies on the hydroxyl-directed transformations of aldol adducts formed using chiral auxiliary technology,⁶ we hypothesized that a directed hydrogenation approach might address the former challenge. Thus, in analogy to the synthesis of **219** and **220**, cyclocondensation between propionyl chloride (**209**) and 2-ethylacrolein (**224**) was carried out in the presence of quinidine-derived catalyst **212**, and the resulting β-lactone opened to give benzyl ester **226** (Scheme 3.5). Gratifyingly, at 82% *ee*, the optical activity of this material was substantially improved. Furthermore, directed hydrogenation using 2.5 mol % of Brown's catalyst under 640 psi of hydrogen afforded the desired hydroxy ester **219** as a 9:1 mixture of readily separable diastereomers. Alcohol **219** was converted to TBS-protected hydroxy acid **227** by a two-step sequence involving treatment with TBSOTf and 2,6-lutidine followed by hydrogenolysis of the benzyl ester. An identical sequence was employed using quinine-derived catalyst **213** to obtain *ent*-**227**.

Scheme 3.5. Stereoselective synthesis of carboxylic acid **227**



With carboxylic acids **227** and *ent*-**227** in hand, what remained in the syntheses of the two putative SCH64877 candidates was the coupling of these fragments to the tetrasulfide diol core **197** and cleavage of the TBS ethers. Though the acid chloride derived from **227** and *ent*-**227** reacted sluggishly with **197**, it was ultimately determined that the desired ester formation could be accomplished using Yamaguchi's reagent⁷ in the presence of DMAP and DIPEA in CH₂Cl₂ to afford dicarboxylate **228** (when **227** was used as the coupling partner, see Scheme 3.6). The final deprotection step was carried out using aqueous H₂SiF₆ in MeCN to afford a product that was found to be spectroscopically identical to SCH64877 (**44**). Synthesis of **229** (Figure 3.2) using an identical sequence but with *ent*-**227** as the coupling partner confirmed that this structure was inconsistent with the natural product.

Scheme 3.6. Synthesis of SCH64877 (**44**)

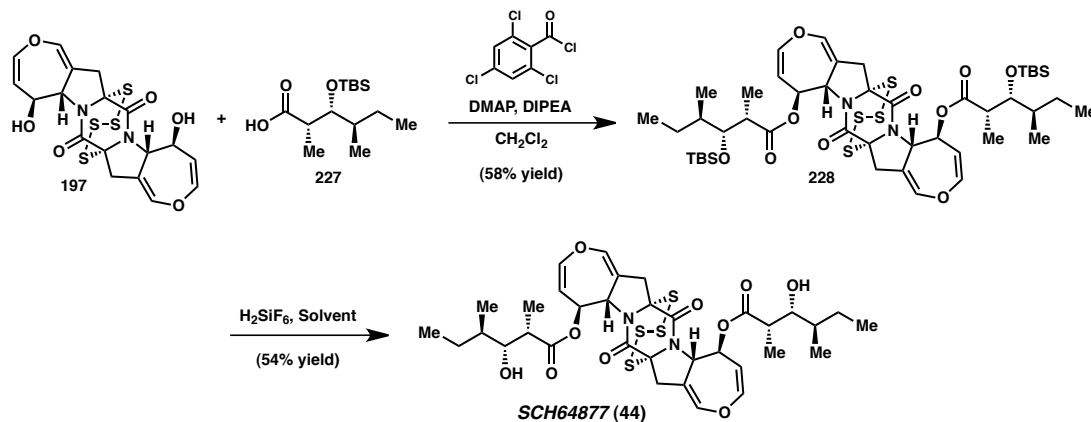
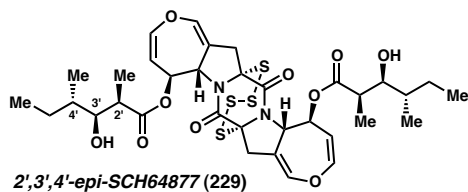
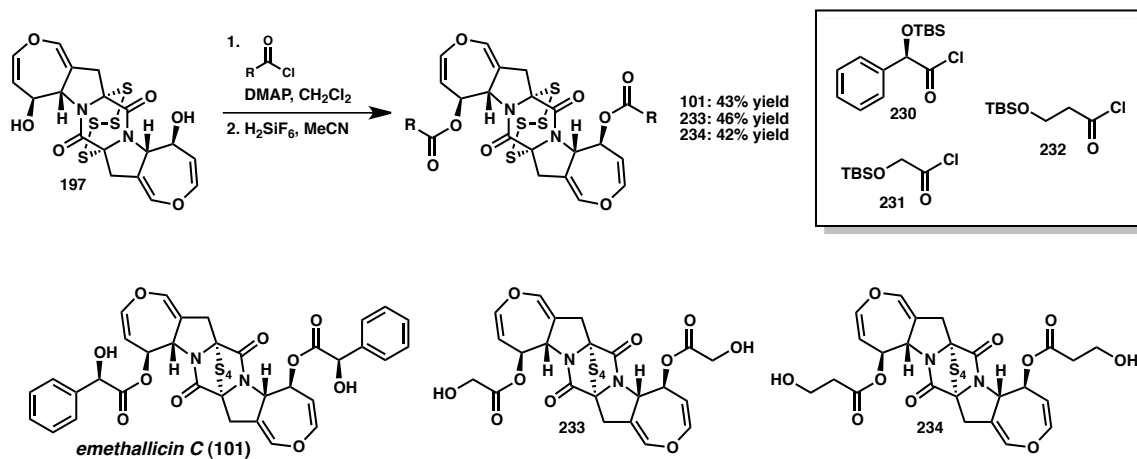


Figure 3.2. Structure of 2',3',4'-*epi*-SCH64877 (**229**)



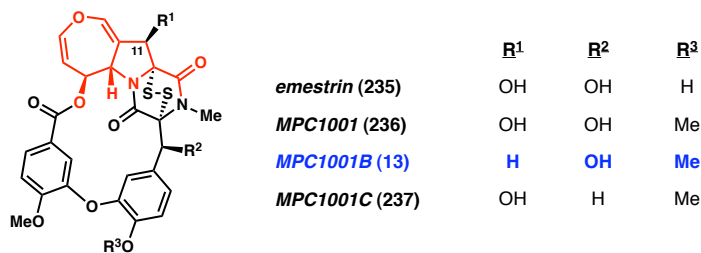
Having completed a total synthesis and structural assignment of SCH64877 (**44**) (and with epimeric analog **229** in hand), we next set out to prepare emethallicin C (**101**) as well as several structural analogs, in order to complete our desired panel of epitetrathiodiketopiperazines for biological evaluation. The synthesis of emethallicin C (**101**), as well as bis(hydroxyacetate) **233** and bis(β-hydroxypropionate) **234**, could be accomplished by DMAP-promoted reaction of diol **197** with acid chlorides **230**,⁸ **231**,⁹ or **232**,¹⁰ respectively, followed by subsequent removal of the TBS groups with H₂SiF₂ as described above (Scheme 3.7).

Scheme 3.7. Synthesis of emethallicin C (**101**) and unnatural analogs **233** and **234**

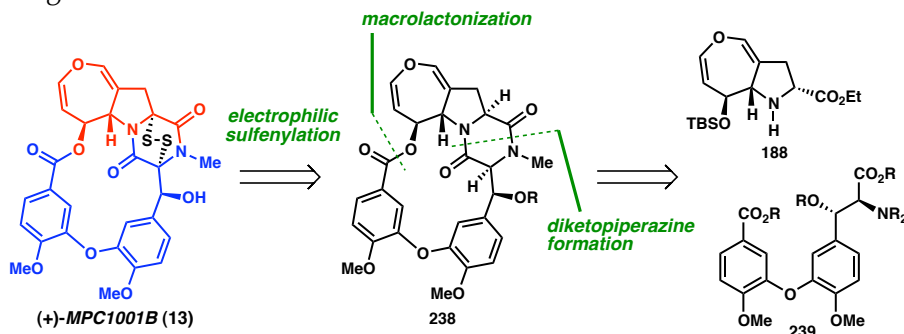


3.3 MACROCYCLIC DIHYDROOXEPINE-CONTAINING EPIDITHIODIKETOPIPERAZINE NATURAL PRODUCTS

Whereas the intrinsic symmetry of molecules like acetylaranotin (**11**) and SCH84877 (**44**) simplifies their chemical synthesis, the extension of our synthetic strategy towards the macrocyclic structures of emestrin (**235**)¹¹ or the MPC1001 congeners (**13**, **236**, **237**, see Figure 3.3)¹² requires examination of a larger array of possible retrosynthetic disconnections.

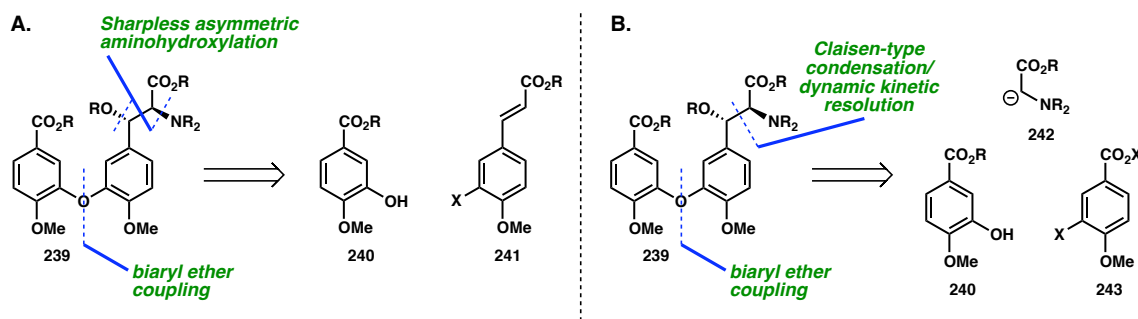
Figure 3.3. Macro cyclic ETP natural products containing the aranotin monomer

As it possesses the same oxidation pattern at C(11) as the monomer unit developed during our synthesis of C₂-symmetric dihydrooxepine-containing ETPs, our initial efforts towards accessing the macrocycles shown in Figure 3.3 have focused on MPC1001B (13).¹³ Retrosynthetically, the most straightforward initial disconnection involves late-stage diketopiperazine sulfenylation, as in the synthesis of acetylaranotin (11) described in Chapter 2 (see Scheme 3.8). This would involve the intermediacy of macrocycle 238, which can be further simplified to monomer unit 188 and biaryl ether-containing amino acid fragment 239. The joining of these two fragments could conceivably be carried out via a stepwise diketopiperazine formation (as in Chapter 2), followed by macrolactonization.

Scheme 3.8. Amino acid dimerization strategy for adjoining the northern and southern fragments

Construction of biaryl ether amino acid fragment **239**¹⁴ has been envisioned to proceed in one of two ways (see Scheme 3.9). In the first, Ullman-type coupling (or a variant thereof)¹⁵ between a phenol **240** and halostyrene **241** would furnish the desired ether, while Sharpless asymmetric aminohydroxylation¹⁶ would provide enantioselective access to the β-hydroxy amino acid moiety of **239**. Of course, depending on the coupling conditions employed, it might also be feasible to perform the aminohydroxylation prior to biaryl ether formation. Alternatively, the β-hydroxy amino acid moiety might be formed via condensation of a glycine-derived nucleophile **242** and carboxylic acid derivative **243** (or a biaryl ether-containing derivative), followed by dynamic kinetic resolution to obtain the desired stereochemistry at the benzylic position.^{17,18}

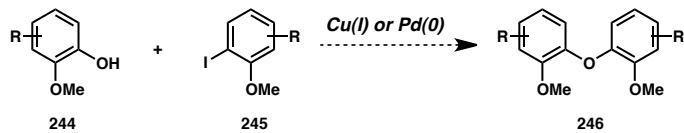
Scheme 3.9. Strategies for constructing biaryl ether amino acid **239**



Pivotal to these or any other strategies for the synthesis of MPC1001B (**13**) is the ability to successfully carry out the biaryl ether coupling to form a bis(*ortho*-methoxyaryl) ether. There is generally a lack of literature regarding the formation of such structural motifs, and indeed our preliminary efforts in this regard were largely met with failure. Attempts at coupling *ortho*-methoxy aryl iodides with *ortho*-methoxy phenols using a variety of transition metal catalysts suffered either from negligible conversion or substrate protodehalogenation (see Scheme 3.10).¹⁹ Likewise, attempts at Evans-Chan-

Lam-type coupling between *ortho*-methoxy aryl boronic acids and *ortho*-methoxy phenols were plagued by substrate protodeborylation.²⁰

Scheme 3.10. Unsuccessful approaches to the construction of bis(*ortho*-methoxyaryl) ethers (**246**)



Conditions Attempted:

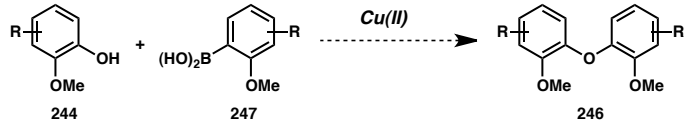
CuI, Cs₂CO₃, TMHD, DMF, 120 °C

Cu₂O, pyridine, reflux

CuBr·SMe₂, K₂CO₃, pyridine, MeCN, 75 °C

CuI, picolinic acid, K₃PO₄, DMSO, 100 °C

Pd(OAc)₂, di(*t*-Bu)XPhos (or *t*-BuBrettPhos), K₃PO₄, PhMe, 100 °C



Conditions Attempted:

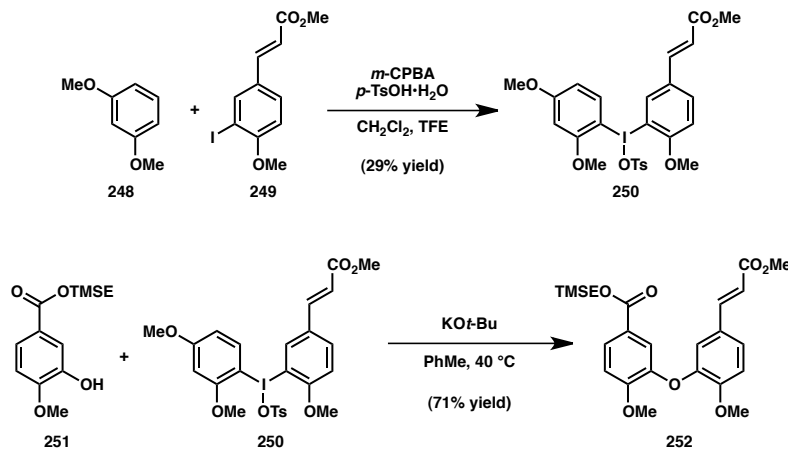
Cu(OAc)₂, base (Et₃N, pyridine, pyrazine, DMAP, etc.), CH₂Cl₂, 4ÅMS

Recently, diaryl iodonium salts have received much attention as highly reactive electrophiles for a variety of transition metal-mediated processes.²¹ In fact, Olofsson and coworkers have demonstrated that such iodonium reagents can undergo coupling with phenols under very mild, transition metal-free conditions.²² These reports have suggested that *para*-methoxyphenyl ligands on the I(III) center are electronically disfavored for transfer to nucleophiles. Furthermore, Pike and coworkers have demonstrated that although *ortho*-substituted aryl ligands are generally *more* favorable for transfer to nucleophiles relative to unsubstituted ligands,²³ *ortho*-methoxy ligands are the exception to this rule (being highly disfavored for transfer).²⁴ We therefore reasoned that an *ortho,para*-dimethoxyphenyl ligand might be an excellent non-transferable ligand, allowing for selective transfer of a less electron-rich *ortho*-methoxy ligand that is more

appropriately functionalized for advancement to the southern amino acid fragment of MPC1001B.

To test the above hypothesis, iodonium tosylate **250** was synthesized from aryl iodide **249** and 1,3-dimethoxybenzene (**248**) via oxidation in the presence of *m*-CPBA and *p*-TsOH•H₂O in CH₂Cl₂/TFE (see Scheme 3.11).²⁵ In the event, we observed that **250** readily underwent coupling with *ortho*-methoxy phenol **251** in the presence of KO*t*-Bu in PhMe at 40 °C, providing biaryl ether **252** in 69% yield. Ongoing efforts are focused on the application of this chemistry to the synthesis of MPC1001B (**13**).

Scheme 3.11. Synthesis and biaryl ether coupling of iodonium tosylate **250**



3.4 CONCLUDING REMARKS

We have successfully prepared a panel of epitetrathiodiketopiperazines, which includes the natural products SCH64877 (**44**) and emethallicin C (**101**), as well as several structural analogs (**229**, **233**, **234**) and previously described intermediates (diol **197**, diacetate **205**). These efforts involved elucidation of the stereochemical configuration of the carboxylate appendages of **44**, which was accomplished via rapid synthesis of four model esters using an acid chloride/aldehyde cyclocondensation strategy. Ongoing

efforts include the biological screening of these tetrasulfides in both cell viability and biochemical assays, with the goal of comprehensively examining structure-activity relationships. Though our studies toward the synthesis of MPC1001B (**13**) and related molecules are still preliminary, further development of the biaryl ether coupling reaction described above may ultimately allow for biological investigations of macrocyclic structures as well.

3.5 EXPERIMENTAL SECTION

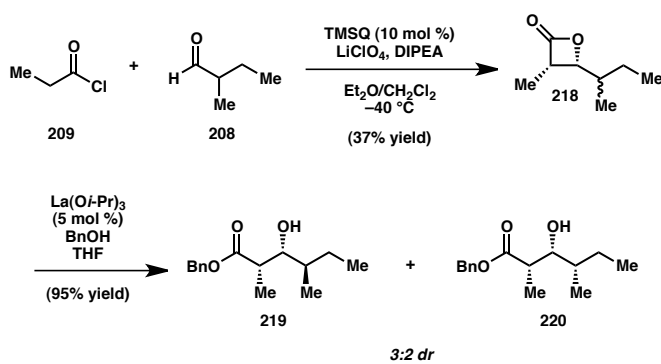
3.5.1 Materials and Methods

Unless otherwise stated, reactions were performed under a nitrogen atmosphere using freshly dried solvents. Tetrahydrofuran (THF), methylene chloride (CH₂Cl₂), acetonitrile (MeCN), dimethylformamide (DMF), and toluene (PhMe) were dried by passing through activated alumina columns. Unless otherwise stated, chemicals and reagents were used as received. *N,N*-Diisopropylethamine (DIPEA) was distilled over calcium hydride prior to use. All reactions were monitored by thin-layer chromatography using EMD/Merck silica gel 60 F254 pre-coated plates (0.25 mm) and were visualized by UV, *p*-anisaldehyde, or KMnO₄ staining. Flash column chromatography was performed either as described by Still et al.²⁶ using silica gel (particle size 0.032-0.063) purchased from Silicycle or using pre-packaged RediSep®Rf columns on a CombiFlash Rf system (Teledyne ISCO Inc.). Optical rotations were measured on a Jasco P-2000 polarimeter using a 100 mm path-length cell at 589 nm. ¹H and ¹³C NMR spectra were recorded on a Varian 400 MR (at 400 MHz and 101 MHz, respectively), a Varian Inova 500 (at 500 MHz and 126 MHz, respectively), or a Varian Inova 600 (at 600 MHz and 150 MHz, respectively), and are reported relative to internal CHCl₃ (¹H, δ = 7.26), MeCN (¹H, δ = 1.94), acetone (¹H, δ = 2.05), or DMSO (¹H, δ = 2.50), and CDCl₃ (¹³C, δ = 77.0), MeCN (¹³C, δ = 118.26), acetone-*d*₆ (¹³C, δ = 206.26) or DMSO (¹³C, δ = 40.0). Data for ¹H NMR spectra are reported as follows: chemical shift (δ ppm) (multiplicity, coupling constant (Hz), integration). Multiplicity and qualifier abbreviations are as follows: s = singlet, d = doublet, t = triplet, q = quartet, m = multiplet, br = broad, app = apparent. IR spectra were recorded on a Perkin Elmer Paragon 1000 spectrometer and are reported in

frequency of absorption (cm⁻¹). HRMS were acquired using an Agilent 6200 Series TOF with an Agilent G1978A Multimode source in electrospray ionization (ESI), atmospheric pressure chemical ionization (APCI), or mixed (MM) ionization mode. Analytical chiral HPLC was performed with an Agilent 1100 Series HPLC utilizing Chiraldpak AD or Chiralcel OD-H columns (4.6 mm x 25 cm) obtained from Daicel Chemical Industries, Ltd with visualization at 254 nm. Preparative HPLC was performed with an Agilent 1100 Series HPLC utilizing an Agilent Eclipse XDB-C18 5μm column (9.4 x 250 mm) or an Agilent Zorbax RX-SIL 5μm column (9.4 x 250 mm). Melting points were determined using a Büchi B-545 capillary melting point apparatus and the values reported are uncorrected.

3.5.2 Preparative Procedures and Spectroscopic Data

Preparation of benzyl esters 219 and 220



Preparation of β-lactone 218: In a glovebox under an N₂ atmosphere, a flame-dried round-bottom flask equipped with a magnetic stir bar was charged with anhydrous LiClO₄ (4.64 g, 43.6 mmol). The vessel was then sealed with a septum cap, removed from the glovebox, and placed under a positive pressure of N₂. Et₂O (13 mL) was then added, and the mixture was stirred vigorously until the LiClO₄ had completely dissolved.

To this solution was added a solution of TMSQ (**212**, 525 mg, 1.32 mmol) in CH₂Cl₂ (26 mL) via syringe, and the mixture was cooled to –40 °C. DIPEA (5.53 mL, 33.0 mmol) was then added dropwise, followed by 2-methylbutyraldehyde (**208**, 1.41 mL, 13.2 mmol). Finally, a solution of propionyl chloride (**209**, 2.31 mL, 26.4 mmol) in CH₂Cl₂ (6.6 mL) was added dropwise over 6 h (using a syringe pump). The resulting solution was allowed to stir overnight at –40 °C before being diluted with Et₂O and filtered through a plug of SiO₂, eluting with excess Et₂O and concentrating to afford a crude oil. Purification via column chromatography (gradient elution, 16:1→8:1 pentanes–Et₂O) afforded β-lactone **218** (686 mg, 37% yield, mixture of diastereomers) as a clear, colorless oil.

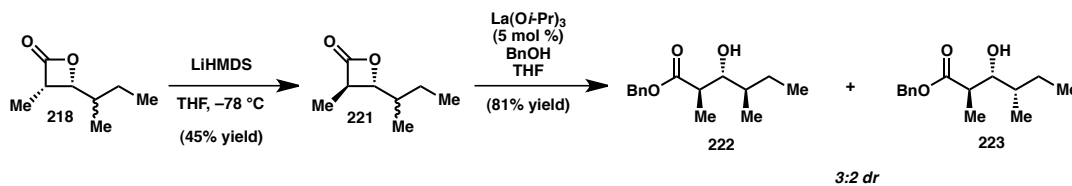
Preparation of benzyl esters **219 and **220**:** In a glovebox, a 20-mL scintillation vial equipped with a magnetic stir bar was charged with La(O*i*-Pr)₃ (29 mg, 0.092 mmol), then sealed with a septum cap, removed from the glovebox, and placed under a positive pressure of N₂. A solution of β-lactone **218** (300 mg, 2.11 mmol) and benzyl alcohol (952 μL, 9.2 mmol) in 9.2 mL of THF was then added via syringe, and the resulting mixture was stirred vigorously for 48 h. The reaction mixture was then diluted with sat. *aq.* NH₄Cl and extracted with Et₂O (3x). The combined organic layers were dried over MgSO₄, filtered, and concentrated, and the resulting crude oil was purified via flash chromatography (gradient elution, 0→15% hexanes–EtOAc) to afford diastereomerically pure benzyl esters **219** (207 mg, 39% yield) and **220** (131 mg, 25% yield) as well as 164 mg (31% yield) of a 1:1 mixture of **219** and **220**.

219 (syn,anti)²⁷: ¹H NMR (500 MHz, CDCl₃) δ 7.40 – 7.31 (m, 5H), 5.15 (s, 2H), 3.68 (ddd, *J* = 8.4, 3.1, 3.1 Hz, 1H), 2.72 (qd, *J* = 7.2, 3.1 Hz, 1H), 2.52 (d, *J* = 3.7 Hz,

1H), 1.77 (dq, *J* = 13.3, 7.6, 3.1 Hz, 1H), 1.50 – 1.41 (m, 1H), 1.20 (d, *J* = 7.2 Hz, 3H), 1.21 – 1.11 (m, 1H), 0.89 (t, *J* = 7.5 Hz, 3H), 0.82 (d, *J* = 6.8 Hz, 3H); ¹³C NMR (126 MHz, CDCl₃) δ 176.5, 135.7, 128.6, 128.3, 128.1, 75.0, 66.4, 41.5, 36.8, 24.7, 14.9, 10.9, 9.8; IR (NaCl/thin film): 3503, 3066, 3033, 2964, 2935, 2877, 1730, 1498, 1456, 1382, 1330, 1259, 1176, 1110, 1079, 1054, 1029, 971, 916, 751 cm⁻¹; HRMS (ESI) calc'd for C₁₅H₂₃O₃ [M+H]⁺ 251.1642, found 251.1642. (60% *ee*, as determined by conversion to the Mosher ester using (S)-(+)-α-methoxy-α-trifluoromethylphenylacetyl chloride followed by NMR analysis).

220 (syn,syn): ¹H NMR (500 MHz, CDCl₃) δ 7.39 – 7.31 (m, 5H), 5.14 (s, 2H), 3.69 (ddd, *J* = 5.9, 4.7, 4.7 Hz, 1H), 2.72 (qd, *J* = 7.1, 5.3 Hz, 1H), 2.20 (d, *J* = 4.8 Hz, 1H), 1.46 – 1.33 (m, 2H), 1.23 (d, *J* = 7.1 Hz, 3H), 1.19 – 1.09 (m, 1H), 0.94 (d, *J* = 6.6 Hz, 3H), 0.87 (t, *J* = 7.3 Hz, 3H); ¹³C NMR (126 MHz, CDCl₃) δ 175.9, 135.8, 128.6, 128.3, 128.1, 75.2, 66.3, 42.4, 37.0, 25.9, 13.9, 11.6, 11.2; IR (NaCl/thin film): 3497, 3066, 3034, 2963, 2935, 2877, 1730, 1498, 1456, 1380, 1336, 1261, 1167, 1109, 1052, 1028, 991, 957, 916, 752 cm⁻¹; HRMS (ESI) calc'd for C₁₅H₂₃O₃ [M+H]⁺ 251.1642, found 251.1647.

Preparation of benzyl esters **222** and **223**



Preparation of β-lactone **221:** In a flame-dried round-bottom flask, β-lactone **218** (193 mg, 1.36 mmol) was dissolved in 27 mL THF. The resulting solution was cooled to –78 °C with stirring and treated with LiHMDS (1.0 M solution in THF, 2.7 mL,

2.7 mmol). After 15 min, the reaction was quenched with 30 mL sat. *aq.* NH₄Cl, and allowed to warm to ambient temperature. The mixture was then extracted with Et₂O (60 mL, then 2x30 mL), and the combined organic layers were dried over MgSO₄, filtered, and concentrated to afford the crude product as a clear oil. Purification via flash chromatography (gradient elution, 16:1→4:1 pentanes–Et₂O) afforded β-lactone **221** (87.8 mg, 45% yield, mixture of diastereomers) as a clear, colorless oil.

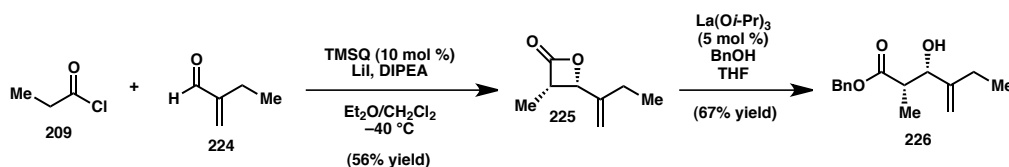
Preparation of benzyl esters **222 and **223**:** In a glovebox, a 20-mL scintillation vial equipped with a magnetic stir bar was charged with La(O*i*-Pr)₃ (9.2 mg, 0.029 mmol), then sealed with a septum cap, removed from the glovebox, and placed under a positive pressure of N₂. A solution of β-lactone **221** (82.3 mg, 0.579 mmol) and benzyl alcohol (300 μL, 2.90 mmol) in 2.9 mL of THF was then added via syringe, and the resulting mixture was stirred vigorously for 48 h. The reaction mixture was then diluted with sat. *aq.* NH₄Cl and extracted with Et₂O (3x). The combined organic layers were dried over MgSO₄, filtered, and concentrated, and the resulting crude oil was purified via flash chromatography (gradient elution, 8:1→4:1 pentanes–Et₂O) to afford benzyl esters **222** and **223** (118 mg, 81% yield) as a 3:2 mixture of diastereomers. Diastereomerically pure materials could be obtained via preparative HPLC (normal phase, gradient elution, 5→7.5% EtOAc in hexanes).

222 (anti,anti)²⁸: ¹H NMR (500 MHz, CDCl₃) δ 7.39 – 7.31 (m, 5H), 5.15 (s, 2H), 3.39 (ddd, *J* = 8.0, 5.9, 5.9 Hz, 1H), 2.77 (qd, *J* = 7.2, 5.4 Hz, 1H), 2.58 (d, *J* = 8.1 Hz, 1H), 1.62 (dq, *J* = 13.4, 7.5, 3.2 Hz, 1H), 1.44 (ddq, *J* = 9.9, 6.7, 6.7, 3.3 Hz, 1H), 1.26 (d, *J* = 7.2 Hz, 3H), 1.22 – 1.11 (m, 1H), 0.90 (d, *J* = 6.8 Hz, 3H), 0.88 (t, *J* = 7.5 Hz, 3H); ¹³C NMR (126 MHz, CDCl₃) δ 176.3, 135.7, 128.6, 128.3, 128.1, 77.9, 66.3, 42.0,

38.2, 23.6, 15.8, 15.1, 11.4; IR (NaCl/thin film): 3523, 3034, 2963, 2935, 2876, 1719, 1498, 1456, 1383, 1351, 1261, 1166, 1043, 996, 958, 750 cm⁻¹; HRMS (ESI) calc'd for C₁₅H₂₃O₃ [M+H]⁺ 251.1642, found 251.1643.

223 (anti,syn): ¹H NMR (500 MHz, CDCl₃) δ 7.39 – 7.31 (m, 5H), 5.16 (s, 2H), 3.64 (ddd, J = 7.7, 6.3, 3.5 Hz, 1H), 2.69 (dq, J = 7.3, 7.3 Hz, 1H), 2.41 (d, J = 6.4 Hz, 1H), 1.51 – 1.39 (m, 2H), 1.33 – 1.23 (m, 1H), 1.18 (d, J = 7.2 Hz, 3H), 0.90 (t, J = 7.3 Hz, 3H), 0.87 (d, J = 6.6 Hz, 3H); ¹³C NMR (126 MHz, CDCl₃) δ 176.3, 135.8, 128.6, 128.3, 128.1, 75.7, 66.4, 43.1, 36.8, 26.6, 14.5, 12.4, 11.7; IR (NaCl/thin film): 3514, 3034, 2963, 2935, 2877, 1728, 1498, 1456, 1383, 1351, 1311, 1262, 1166, 1037, 991, 958, 750 cm⁻¹; HRMS (ESI) calc'd for C₁₅H₂₃O₃ [M+H]⁺ 251.1642, found 251.1642.

Preparation of benzyl ester **226**



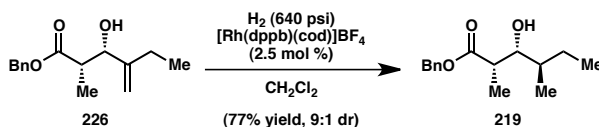
Preparation of β-lactone **225:** In a glovebox under an N₂ atmosphere, a flame-dried round-bottom flask equipped with a magnetic stir bar was charged with anhydrous LiI (402 mg, 3.00 mmol). The vessel was then sealed with a septum cap, removed from the glovebox, and placed under a positive pressure of N₂. To the flask was added a solution of TMSQ (**212**, 59 mg, 0.150 mmol) in 4.7 mL CH₂Cl₂, followed by 0.53 mL Et₂O. The resulting mixture was stirred vigorously until all of the LiI had dissolved, and then cooled to -40 °C. DIPEA (628 μL, 3.75 mmol) was then added dropwise, followed by 2-ethylacrolein (**224**, 85 wt%, 173 μL, 1.5 mmol). Finally, a solution of propionyl chloride (**209**, 328 μL, 3.75 mmol) in CH₂Cl₂ (1.0 mL) was added dropwise over 2 h

(using a syringe pump). The resulting solution was allowed to stir for an additional 3 h before being diluted with Et₂O and filtered through a plug of SiO₂, eluting with excess Et₂O and concentrating to afford a crude oil. Purification via column chromatography (gradient elution, 24:1→8:1 pentanes–Et₂O) afforded β-lactone **225** (149 mg, corrected for Et₂O contamination to 117 mg, 56% yield) as a clear, colorless, and volatile oil.

Preparation of benzyl ester 226: In a glovebox, a 20-mL scintillation vial equipped with a magnetic stir bar was charged with La(O*i*-Pr)₃ (13 mg, 0.042 mmol), then sealed with a septum cap, removed from the glovebox, and placed under a positive pressure of N₂. A solution of β-lactone **225** (117 mg, 0.835 mmol) and benzyl alcohol (433 μL, 4.18 mmol) in 4.2 mL of THF was then added via syringe, and the resulting mixture was stirred vigorously for 1.5 h. The reaction mixture was then diluted with sat. *aq.* NH₄Cl and extracted with Et₂O (3x). The combined organic layers were dried over MgSO₄, filtered, and concentrated, and the resulting crude oil was purified via flash chromatography (gradient elution, 12:1→6:1 hexanes–EtOAc) to afford benzyl ester **226** (139 mg, 67% yield) as a clear, colorless oil. [α]_D^{25.0} = -14.1° (*c* = 1.33, CHCl₃); ¹H NMR (500 MHz, CDCl₃) δ 7.40 – 7.31 (m, 5H), 5.17 (d, *J* = 12.3 Hz, 1H), 5.13 (d, *J* = 12.3 Hz, 1H), 5.12 (dd, *J* = 1.3, 1.3, 1.3, 1.3 Hz, 1H), 4.95 (dd, *J* = 1.5, 1.5, 1.5, 1.5 Hz, 1H), 4.48 (d, *J* = 3.6 Hz, 1H), 2.73 (qd, *J* = 7.2, 4.0 Hz, 1H), 2.43 (s, 1H), 2.07 – 1.90 (m, 2H), 1.15 (d, *J* = 7.1 Hz, 3H), 1.05 (t, *J* = 7.4 Hz, 3H); ¹³C NMR (126 MHz, CDCl₃) δ 175.6, 149.6, 135.7, 128.6, 128.3, 128.2, 109.7, 74.1, 66.5, 42.5, 25.0, 12.1, 10.3; IR (NaCl/thin film): 3488, 3090, 3066, 3034, 2967, 2939, 2880, 1734, 1648, 1498, 1456, 1382, 1340, 1257, 1213, 1174, 1123, 1081, 1063, 1028, 991, 955, 904, 752 cm⁻¹; HRMS (ESI) calc'd for C₁₅H₂₁O₃ [M+H]⁺ 249.1485, found 249.1489. (82% *ee*, as determined by conversion

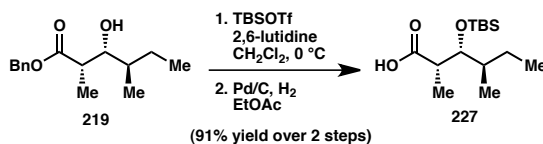
to the Mosher ester using (*S*)-(+)- α -methoxy- α -trifluoromethylphenylacetyl chloride followed by NMR analysis). The opposite enantiomer (**ent-226**) was prepared via an analogous sequence using TMSq (**213**) as the cyclocondensation catalyst. $[\alpha]_D^{25.0} = +14.6^\circ$ ($c = 1.38$, CHCl₃).

Diastereoselective preparation of benzyl ester **219**



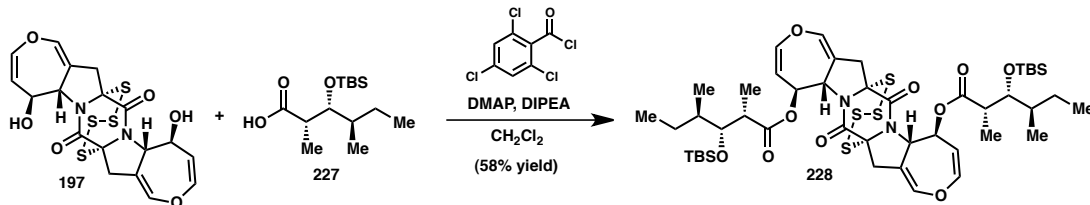
In a glovebox under a N₂ atmosphere, a stainless steel autoclave lined with a glass insert and equipped with a magnetic stir bar was charged with a solution of allylic alcohol **226** (66.7 mg, 0.269 mmol) and [Rh(dppb)(cod)]BF₄ (4.9 mg, 6.76 μ mol) in 9.7 mL CH₂Cl₂. The apparatus was then sealed, removed from the glovebox, and connected to a high-pressure hydrogen inlet. The vessel was pressurized to 200 psi with H₂, then carefully vented, and this process was repeated once more before pressurizing to a final H₂ pressure of 640 psi. The reaction was allowed to proceed with stirring behind a blast shield for 22 h, at which time it was carefully vented, and the reaction mixture was filtered through a plug of SiO₂, eluting with 1:1 hexanes–EtOAc. Purification of the resulting crude mixture (9:1 dr) via flash chromatography (gradient elution, 0 → 15% EtOAc in hexanes) afforded benzyl ester **219** (52.1 mg, 77% yield) as a clear, colorless oil. $[\alpha]_D^{25.0} = -4.38^\circ$ ($c = 1.30$, CHCl₃). **Ent-219** : $[\alpha]_D^{25.0} = +4.20^\circ$ ($c = 0.997$, CHCl₃).

Preparation of carboxylic acid **227**



A solution of benzyl ester **219** (51.6 mg, 0.206 mmol) in 4.1 mL of CH₂Cl₂ was cooled to 0 °C with stirring under a N₂ atmosphere. 2,6-lutidine (72 μL, 0.62 mmol) was then added followed by TBSOTf (71 μL, 0.31 mmol). After 2 h, the reaction mixture was quenched with a small amount of MeOH, diluted with sat. *aq.* NaHCO₃, and extracted with CH₂Cl₂ (3x). The combined organic extracts were dried over Na₂SO₄, filtered, and concentrated *in vacuo*. The resulting crude intermediate was then dissolved in 4.1 mL EtOAc and Pd/C (10 wt % Pd, 28.4 mg) was added. The resulting suspension was sealed with a septum cap, and the headspace purged with N₂. After 5 min, the headspace was purged with H₂ (for 5 min), and then left under a balloon of H₂ for 1 h. The headspace was once more purged with N₂, and the reaction mixture was filtered through celite, rinsing with excess EtOAc, and concentrated to afford carboxylic acid **227** (51.6 mg, 91% yield) as a clear, colorless oil. [α]_D^{25.0} = +4.31 ° (c = 1.18, CHCl₃); ¹H NMR (500 MHz, CDCl₃) δ 11.48 (s, 1H), 3.92 (dd, *J* = 4.9, 4.9 Hz, 1H), 2.63 (qd, *J* = 7.0, 4.7 Hz, 1H), 1.58 – 1.46 (m, 2H), 1.15 (d, *J* = 7.0 Hz, 3H), 1.14 – 1.02 (m, 1H), 0.92 – 0.86 (m, 15H), 0.07 (s, 3H), 0.03 (s, 3H); ¹³C NMR (126 MHz, CDCl₃) δ 181.8, 76.7, 42.6, 40.1, 26.0, 24.9, 18.3, 15.3, 12.0, 11.9, -4.3, -4.3; IR (NaCl/thin film): 2959, 2930, 2883, 2858, 1708, 1472, 1463, 1412, 1383, 1361, 1283, 1252, 1117, 1091, 1059, 1020, 1005, 938, 894, 836, 810, 774 cm⁻¹; HRMS (Multimode-ESI/APCI) calc'd for C₁₄H₂₉O₃Si [M–H]⁻ 273.1891, found 273.1893. **Ent-227:** [α]_D^{25.0} = -5.78 ° (c = 0.960, CHCl₃).

Preparation of bis(*tert*-butyldimethylsilyl) SCH64877 (**228**)



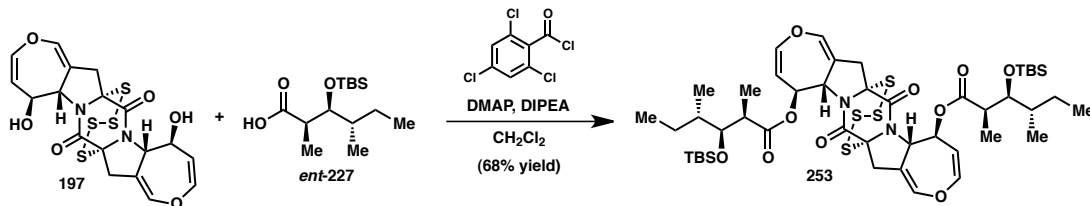
In a 1-dram vial, carboxylic acid **227** (52.4 mg, 0.191 mmol) was dissolved in a stock solution of DIPEA (43.2 μ L, 0.248 mmol) in CH₂Cl₂ (0.48 mL), solid DMAP (117 mg, 0.955 mmol) was added, and the mixture was swirled until homogeneous. A stock solution of Yamaguchi's reagent (35.8 μ L, 0.229 mmol) in CH₂Cl₂ (0.48 mL) was then added, and the resulting mixture was swirled until homogeneous and allowed to sit. After 10 min, the resulting acylating solution was added to a 1-dram vial containing a magnetic stir bar and solid diol **197** (18.5 mg, 0.0382 mmol). The resulting solution was capped and stirred for 20 h. The reaction mixture was then diluted with sat. *aq.* NaHCO₃ and extracted with CH₂Cl₂ (3x). The combined organic layers were dried over Na₂SO₄, then filtered through SiO₂, eluting with 3:1 hexanes–EtOAc. The resulting crude material was purified via flash chromatography (gradient elution, 8:1 → 4:1 hexanes–EtOAc) to afford dicarboxylate **228** (22.0 mg, 58% yield) as a white, amorphous solid. $[\alpha]_D^{25.0} = -306^\circ$ (*c* = 1.10, CHCl₃); ¹H NMR (500 MHz, CDCl₃) δ 6.56 (dd, *J* = 2.1, 2.1 Hz, 2H), 6.26 (dd, *J* = 8.2, 2.3 Hz, 2H), 5.29 (dddd, *J* = 8.5, 1.8, 1.8, 1.8 Hz, 2H), 5.19 (ddd, *J* = 8.5, 2.2, 2.2 Hz, 2H), 4.60 (dd, *J* = 8.2, 2.0 Hz, 2H), 4.12 (dd, *J* = 4.5, 4.5 Hz, 2H), 3.36 (ddd, *J* = 16.5, 2.2, 2.2 Hz, 2H), 3.06 (d, *J* = 16.3 Hz, 2H), 2.70 (qd, *J* = 7.2, 4.5 Hz, 2H), 1.56 – 1.45 (m, 4H), 1.30 (d, *J* = 7.2 Hz, 6H), 1.17 – 1.07 (m, 2H), 0.97 – 0.80 (m, 30H), 0.10 (s, 6H), 0.06 (s, 6H); ¹³C NMR (126 MHz, CDCl₃) δ 175.0, 165.3, 139.6, 138.6, 108.2, 106.1, 75.6, 74.7, 70.9, 60.8, 42.8, 41.7, 40.6, 26.1, 25.0, 18.4, 15.7, 12.7, 12.1, -3.9, -4.3; IR (NaCl/thin film): 3369, 2957, 2928, 2855, 1731, 1698, 1462, 1366, 1343, 1302, 1276, 1250, 1235, 1213, 1185, 1136, 1117, 1093, 1055, 971, 938, 895, 863, 836, 815, 774, 737, 721 cm⁻¹; HRMS (ESI) calc'd for C₃₂H₄₃N₂O₇S₄Si [M–C₁₄H₂₉O₃Si]⁺ 723.1717, found 723.1717 (detected fragment has undergone loss of one of the carboxylate side chains).

Preparation of SCH64877 (44)



A 1-dram vial equipped with a magnetic stir bar was charged with bis(*tert*-butyldimethylsilylether) **228** (22.0 mg, 0.0221 mmol), followed by MeCN (2 mL) and H₂SiF₆ (20–25 wt % *aq.* solution, 100 μL). The resulting suspension was stirred vigorously (with occasional shaking to ensure exposure of material to the reaction medium) for 24 h, then quenched with sat. *aq.* NaHCO₃, and extracted with EtOAc (5x). The combined organic layers were dried over Na₂SO₄, filtered, and concentrated *in vacuo*. The material was then purified via preparative HPLC (reverse phase, gradient elution, 60→95% MeCN in H₂O) to afford SCH64877 (**44**, 9.2 mg, 54% yield) as a white, amorphous solid. [α]_D^{25.0} = −411 ° (c = 0.46, CHCl₃); ¹H NMR (500 MHz, CDCl₃) δ 6.58 (dd, *J* = 1.8, 1.8 Hz, 2H), 6.28 (dd, *J* = 8.4, 1.9 Hz, 2H), 5.30 (s, 4H), 4.59 (dd, *J* = 8.3, 1.2 Hz, 2H), 3.81 (ddd, *J* = 9.5, 2.1, 2.1 Hz, 2H), 3.37 (ddd, *J* = 16.4, 2.5, 1.2 Hz, 2H), 3.11 (d, *J* = 16.7 Hz, 2H), 3.06 (d, *J* = 3.4 Hz, 2H), 2.79 (qd, *J* = 7.2, 1.8 Hz, 2H), 1.84 (dq, *J* = 13.5, 7.6, 3.1 Hz, 2H), 1.56 – 1.47 (m, 2H), 1.27 (d, *J* = 7.3 Hz, 6H), 1.25 – 1.16 (m, 2H), 0.92 (t, *J* = 7.5 Hz, 6H), 0.85 (d, *J* = 6.8 Hz, 6H); ¹³C NMR (126 MHz, CDCl₃) δ 175.8, 165.9, 139.9, 138.9, 108.0, 105.8, 75.4, 73.9, 70.9, 60.9, 41.9, 41.5, 36.7, 25.3, 14.9, 10.8, 9.1; IR (NaCl/thin film): 3529, 2962, 2929, 2874, 1719, 1693, 1457, 1370, 1343, 1301, 1279, 1243, 1183, 1136, 1052, 972, 739, 722 cm^{−1}; HRMS (Multimode-ESI/APCI) calc'd for C₃₄H₄₄ClN₂O₁₀S₄ [M+Cl][−] 803.1573, found 803.1574.

Preparation of bis(*tert*-butyldimethylsilyl) 2',3',4'-*epi*-SCH64877 (253)



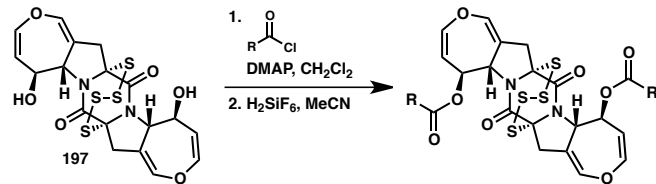
Following an analogous procedure to that for the conversion of **197** to **228**, coupling of diol **197** (9.27 mg, 0.0192 mmol) and carboxylic acid *ent*-**227** (26.3 mg, 0.0960 mmol) afforded dicarboxylate **253** (13.1 mg, 68% yield) as a white, amorphous solid. $[\alpha]_D^{25.0} = -336^\circ$ ($c = 0.655$, CHCl_3); ^1H NMR (500 MHz, CDCl_3) δ 6.57 (ddd, $J = 2.5, 2.5, 1.3$ Hz, 2H), 6.26 (dd, $J = 8.3, 2.2$ Hz, 2H), 5.31 – 5.26 (m, 2H), 5.22 (ddd, $J = 8.4, 2.1, 2.1$ Hz, 2H), 4.60 (dd, $J = 8.2, 1.9$ Hz, 2H), 3.96 (dd, $J = 6.0, 3.9$ Hz, 2H), 3.35 (ddd, $J = 16.5, 2.2, 2.2$ Hz, 2H), 3.05 (ddd, $J = 16.4, 1.2, 1.2$ Hz, 2H), 2.75 (dd, $J = 7.2, 6.0$ Hz, 2H), 1.63 – 1.53 (m, 2H), 1.53 – 1.44 (m, 2H), 1.26 (d, $J = 7.0$ Hz, 6H), 1.18 – 1.07 (m, 2H), 0.95 (d, $J = 6.8$ Hz, 6H), 0.91 (t, $J = 7.3$ Hz, 6H), 0.90 (s, 18H), 0.08 (s, 12H); ^{13}C NMR (126 MHz, CDCl_3) δ 175.2, 165.4, 139.7, 138.7, 108.3, 105.9, 76.5, 75.5, 70.7, 61.0, 42.7, 41.7, 40.8, 26.1, 24.5, 18.4, 15.9, 13.8, 12.3, -3.8, -3.9; IR (NaCl/thin film): 3364, 2957, 2929, 2881, 2856, 1721, 1697, 1463, 1372, 1348, 1305, 1278, 1235, 1212, 1186, 1138, 1109, 1061, 1005, 973, 866, 835, 815, 775, 738, 718 cm^{-1} ; HRMS (Multimode-ESI/APCI) calc'd for $\text{C}_{32}\text{H}_{43}\text{N}_2\text{O}_7\text{S}_4\text{Si}$ [$\text{M}-\text{C}_{14}\text{H}_{29}\text{O}_3\text{Si}$]⁺ 723.1717, found 723.1714 (detected fragment has undergone loss of one of the carboxylate side chains).

Preparation of 2',3',4'-*epi*-SCH64877 (229)



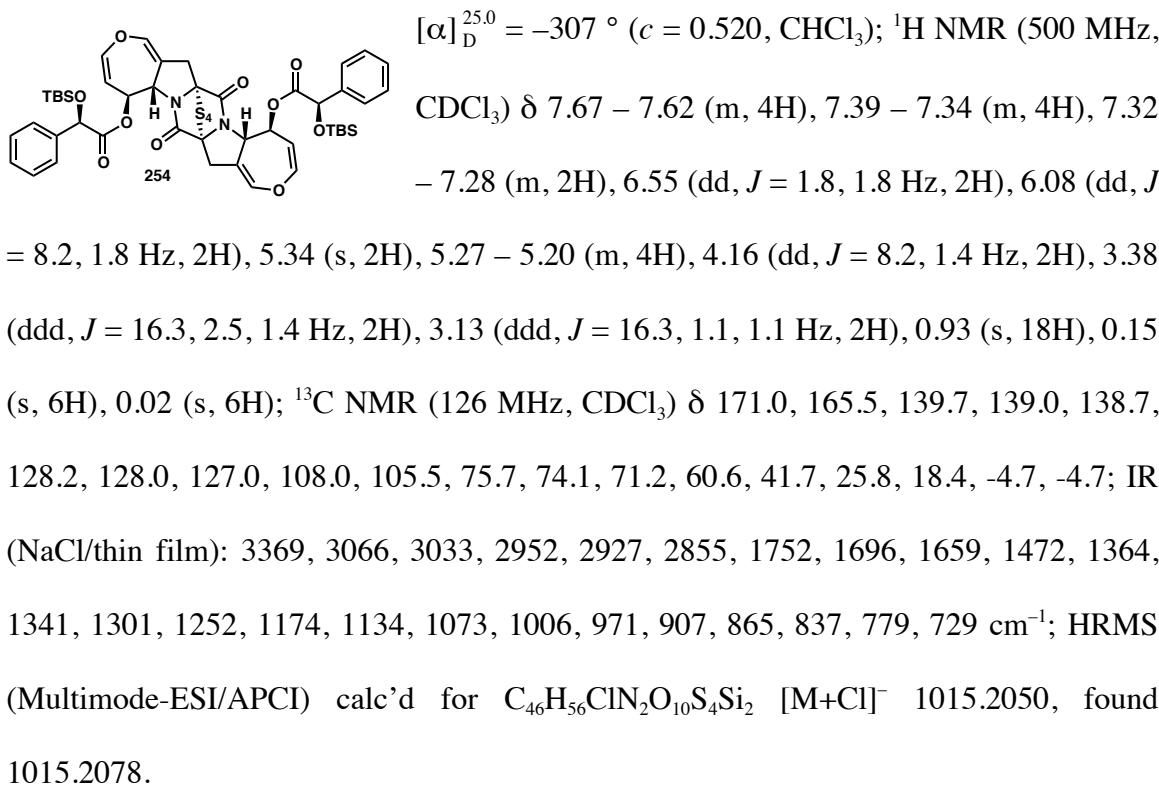
Following an analogous procedure to that for the conversion of **228** to **44**, deprotection of bis(*tert*-butyldimethylsilyl) ether **253** (13.1 mg, 0.0131 mmol) afforded 2',3',4'-*epi*-SCH64877 (**229**, 7.4 mg, 73% yield) as a pale yellow, amorphous solid. $[\alpha]_D^{25.0} = -357^\circ$ ($c = 0.37$, CHCl₃); ¹H NMR (500 MHz, CDCl₃) δ 6.59 (ddd, $J = 2.5, 2.5, 0.9$ Hz, 2H), 6.27 (dd, $J = 8.3, 2.3$ Hz, 2H), 5.32 (dddd, $J = 8.5, 2.8, 1.7, 1.7$ Hz, 2H), 5.24 (ddd, $J = 8.5, 2.1, 2.1$ Hz, 2H), 4.61 (dd, $J = 8.2, 1.9$ Hz, 2H), 3.84 (d, $J = 8.8$ Hz, 2H), 3.37 (ddd, $J = 16.5, 2.2, 2.2$ Hz, 2H), 3.08 (ddd, $J = 16.6, 1.2, 1.2$ Hz, 2H), 2.77 (qd, $J = 7.2, 2.3$ Hz, 2H), 2.73 (br s, 2H), 1.82 (dqd, $J = 13.4, 7.5, 3.2$ Hz, 2H), 1.55 – 1.46 (m, 2H), 1.27 (d, $J = 7.2$ Hz, 6H), 1.29 – 1.16 (m, 2H), 0.93 (t, $J = 7.4$ Hz, 6H), 0.86 (d, $J = 6.8$ Hz, 6H); ¹³C NMR (126 MHz, CDCl₃) δ 175.7, 165.8, 139.8, 138.9, 108.0, 105.9, 75.5, 74.0, 71.0, 60.9, 42.1, 41.5, 37.1, 25.2, 15.1, 11.0, 9.5; IR (NaCl/thin film): 3503, 2962, 2929, 2874, 1726, 1695, 1457, 1369, 1344, 1301, 1279, 1184, 1135, 971, 738, 723 cm⁻¹; HRMS (Multimode-ESI/APCI) calc'd for C₃₄H₄₄ClN₂O₁₀S₄ [M+Cl]⁺ 803.1573, found 803.1563.

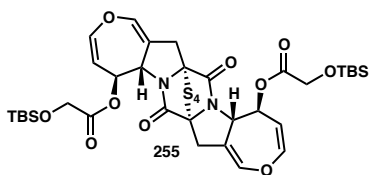
Typical procedure for the acylation of diol **197** using carboxylic acid chloride reagents



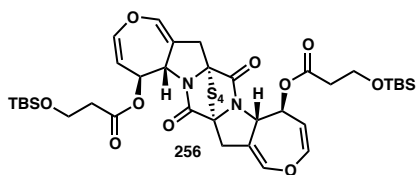
To a solution of diol **197** (8.74 mg, 0.0181 mmol) and DMAP (33.2 mg, 0.272 mmol) in 0.9 mL CH₂Cl₂ was added 0.9 mL (~0.181 mmol) of a stock solution of acid chloride **230** (0.320 mmol in 1.5 mL CH₂Cl₂). The resulting solution was stirred for 40 min, then diluted with sat. *aq.* NaHCO₃ and extracted with CH₂Cl₂ (3x). Each organic layer was individually passed through a plug of SiO₂, which was then flushed with excess 1:1 hexanes–EtOAc, and the resulting filtrate concentrated *in vacuo*. Purification via flash chromatography (gradient elution, 4:1→2:1 hexanes–EtOAc) afforded dicarboxylate **254** (10.4 mg, 59% yield) as a white, amorphous solid.

Bis(*tert*-butyldimethylsilyl) emethallicin C (**254**)



Bis[α -(*tert*-butyldimethylsiloxy)acetate] 255

Following the procedure described above for the conversion of **197** to **254**, coupling of diol **197** (8.74 mg, 0.0181 mmol) and acid chloride **231** (0.181 mmol) afforded dicarboxylate **255** (10.0 mg, 67% yield). $[\alpha]_D^{25.0} = -262^\circ$ ($c = 0.500$, CHCl₃); ¹H NMR (500 MHz, CDCl₃) δ 6.58 (ddd, $J = 2.5, 2.5, 0.9$ Hz, 2H), 6.27 (dd, $J = 8.2, 2.2$ Hz, 2H), 5.29 – 5.26 (m, 2H), 5.24 (ddd, $J = 8.4, 2.0, 2.0$ Hz, 2H), 4.69 (dd, $J = 8.2, 1.8$ Hz, 2H), 4.40 (d, $J = 17.4$ Hz, 2H), 4.35 (d, $J = 17.4$ Hz, 2H), 3.34 (ddd, $J = 16.4, 2.2, 2.2$ Hz, 2H), 3.06 (ddd, $J = 16.3, 1.1, 1.1$ Hz, 2H), 0.93 (s, 18H), 0.14 (s, 6H), 0.12 (s, 6H); ¹³C NMR (126 MHz, CDCl₃) δ 171.0, 165.7, 139.8, 138.8, 107.8, 105.7, 75.7, 71.2, 62.0, 60.8, 41.6, 25.8, 18.5, -5.2, -5.3; IR (NaCl/thin film): 3583, 2952, 2928, 2855, 1762, 1693, 1472, 1437, 1363, 1342, 1302, 1253, 1185, 1134, 1006, 838, 781 cm⁻¹; HRMS (ESI) calc'd for C₃₄H₄₈ClN₂O₁₀S₄Si₂ [M+Cl]⁻ 863.1424, found 863.1452.

Bis[β -(*tert*-butyldimethylsiloxy)propionate] 256

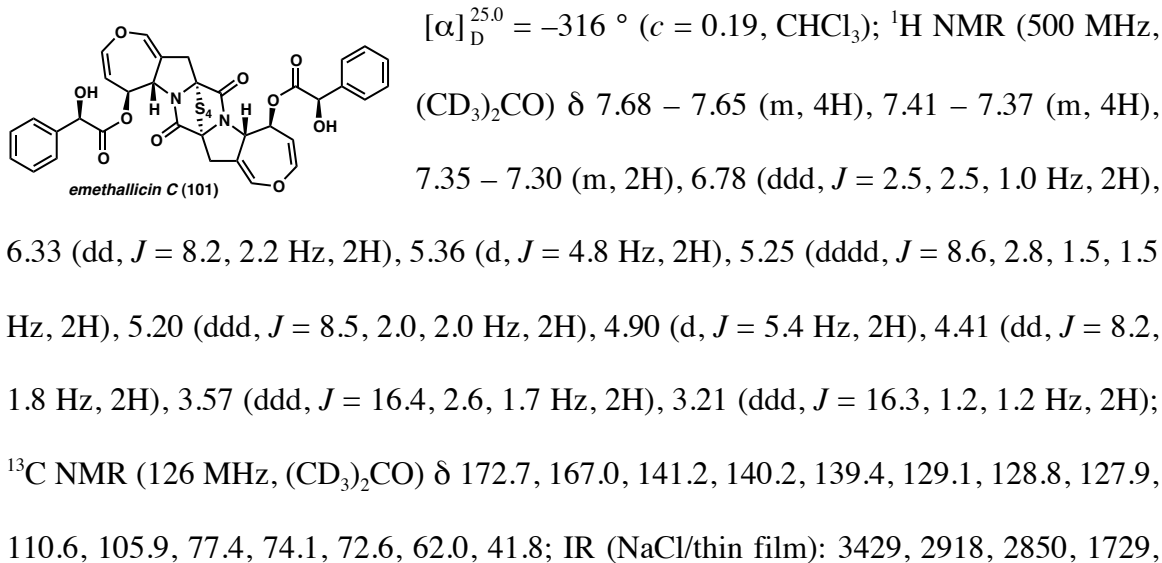
Following the procedure described above for the conversion of **197** to **254**, coupling of diol **197** (8.74 mg, 0.0181 mmol) and acid chloride **232** (0.181 mmol) afforded dicarboxylate **256** (9.0 mg, 58% yield). $[\alpha]_D^{25.0} = -343^\circ$ ($c = 0.450$, CHCl₃); ¹H NMR (500 MHz, CDCl₃) δ 6.57 (ddd, $J = 2.5, 2.5, 0.9$ Hz, 2H), 6.25 (dd, $J = 8.2, 2.3$ Hz, 2H), 5.29 (dddd, $J = 8.5, 2.9, 1.7, 1.7$ Hz, 2H), 5.22 (ddd, $J = 8.4, 2.1, 2.1$ Hz, 2H), 4.68 (dd, $J = 8.0, 1.8$ Hz, 2H), 3.97 (apt qt, $J = 10.2, 6.6$ Hz, 4H), 3.35 (ddd, $J = 16.4, 2.2, 2.2$ Hz, 2H), 3.05 (ddd, $J = 16.4, 1.2, 1.2$ Hz, 2H), 2.72 – 2.59 (m, 4H), 0.89 (s, 18H), 0.08 (s, 6H), 0.08 (s, 6H); ¹³C NMR (126 MHz, CDCl₃) δ 170.9, 165.6, 139.6, 138.7, 108.1,

106.1, 75.6, 70.9, 60.8, 58.7, 41.6, 38.4, 25.9, 18.3, -5.3, -5.3; IR (NaCl/thin film): 3583, 3369, 2952, 2927, 2854, 1734, 1696, 1473, 1364, 1343, 1302, 1255, 1181, 1137, 1099, 1064, 1006, 971, 939, 836, 812, 778, 723 cm⁻¹; HRMS (ESI) calc'd for C₃₆H₅₂ClN₂O₁₀S₄Si₂ [M+Cl]⁻ 891.1737, found 891.1745.

Typical procedure for the preparation of bis(hydroxycarboxylates) 101, 233, and 234

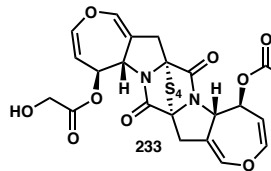
A 1-dram vial equipped with a magnetic stir bar was charged with bis(*tert*-butyldimethylsilylether) **254** (10.4 mg, 0.0106 mmol), followed by MeCN (1 mL) and H₂SiF₆ (20-25 wt % *aq.* Solution, 50 μL). The resulting suspension was stirred vigorously (with occasional shaking to ensure exposure of material to the reaction medium) for 17 h, then quenched with sat. *aq.* NaHCO₃, and extracted with EtOAc (3x). The combined organic layers were dried over Na₂SO₄, filtered, and concentrated *in vacuo*. The material was then purified via preparative TLC (2:1 PhMe–acetone) to afford emethallicin C (**101**, 5.8 mg, 73% yield) as a pale yellow, amorphous solid.

Emethallicin C (101)



1683, 1373, 1344, 1235, 1185, 1137, 1090, 1069, 1015, 968, 861, 815, 722 cm⁻¹; HRMS (Multimode-ESI/APCI) calc'd for C₃₄H₂₈ClN₂O₁₀S₄ [M+Cl]⁻ 787.0321, found 787.0298.

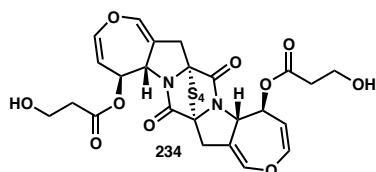
Bis(α-hydroxyacetate) 233



Following the procedure described above for the conversion of **254** to **101**, deprotection of bis(*tert*-butyldimethylsilylether) **255** (10.0 mg, 0.0121 mmol)

afforded bis(hydroxyacetate) analog **233** (5.0 mg, 69% yield). $[\alpha]_D^{25.0} = -462^\circ$ (*c* = 0.25, acetone); ¹H NMR (500 MHz, (CD₃)₂CO) δ 6.78 (ddd, *J* = 2.5, 2.5, 0.9 Hz, 2H), 6.42 (dd, *J* = 8.2, 2.2 Hz, 2H), 5.23 (dddd, *J* = 8.5, 2.6, 1.5, 1.5 Hz, 2H), 5.20 (ddd, *J* = 8.5, 2.0, 2.0 Hz, 2H), 4.76 (dd, *J* = 8.2, 1.7 Hz, 2H), 4.21 (d, *J* = 6.0 Hz, 4H), 4.09 (t, *J* = 6.5 Hz, 2H), 3.51 (ddd, *J* = 16.4, 2.6, 1.7 Hz, 2H), 3.13 (ddd, *J* = 16.3, 1.2, 1.2 Hz, 2H); ¹³C NMR (126 MHz, (CD₃)₂CO) δ 172.6, 167.0, 140.9, 139.4, 110.5, 106.5, 77.4, 72.0, 62.1, 61.9, 41.8; IR (NaCl/thin film): 3306, 2916, 2849, 1743, 1689, 1374, 1344, 1303, 1235, 1186, 1137, 1095, 816, 723 cm⁻¹; HRMS (Multimode-ESI/APCI) calc'd for C₂₂H₂₀ClN₂O₁₀S₄ [M+Cl]⁻ 634.9695, found 634.9686.

Bis(β-hydroxypropionate) 234

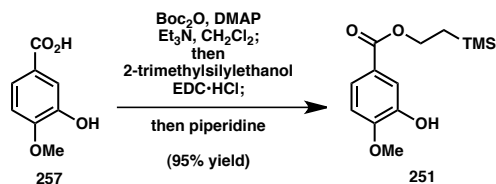


Following the procedure described above for the conversion of **254** to **101**, deprotection of bis(*tert*-butyldimethylsilylether) **256** (9.0 mg, 0.0105 mmol)

afforded bis(hydroxypropionate) analog **234** (4.8 mg, 73% yield). $[\alpha]_D^{25.0} = -404^\circ$ (*c* = 0.24, acetone); ¹H NMR (500 MHz, (CD₃)₂CO) δ 6.77 (ddd, *J* = 2.5, 2.5, 0.9 Hz, 2H), 6.39 (dd, *J* = 8.2, 2.3 Hz, 2H), 5.28 – 5.23 (m, 2H), 5.19 (ddd, *J* = 8.5, 2.1, 2.1 Hz, 2H), 4.72 (dd, *J* = 8.1, 1.9 Hz, 2H), 3.95 – 3.83 (m, 4H), 3.75 (t, *J* = 5.8 Hz, 2H), 3.52 (ddd, *J*

= 16.3, 2.1, 2.1 Hz, 2H), 3.12 (ddd, J = 16.4, 1.2, 1.2 Hz, 2H), 2.61 (t, J = 6.1 Hz, 4H); ¹³C NMR (126 MHz, (CD₃)₂CO) δ 171.9, 166.9, 140.7, 139.3, 110.8, 107.1, 77.3, 71.7, 62.0, 58.3, 41.8, 39.4; IR (NaCl/thin film): 3368, 2916, 2848, 1726, 1686, 1560, 1369, 1302, 1235, 1186, 1136, 1043, 815, 723 cm⁻¹; HRMS (Multimode-ESI/APCI) calc'd for C₂₄H₂₄ClN₂O₁₀S₄ [M+Cl]⁻ 663.0008, found 662.9992.

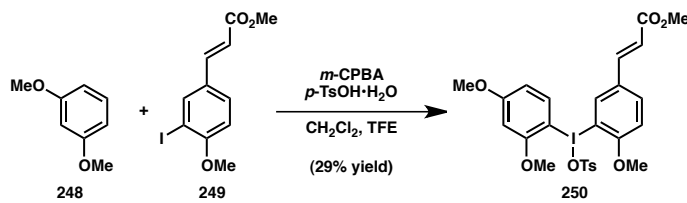
Preparation of (trimethylsilyl)ethyl ester **251**



To a solution of *iso*-vanillic acid (**257**, 500 mg, 2.97 mmol) and DMAP (72.6 mg, 0.594 mmol) in 3.0 mL CH₂Cl₂ were added Et₃N (414 μL, 2.97 mmol) and Boc₂O (1.57 mL, 6.83 mmol). NOTE: the resulting mixture effervesced for ~10 min. After 2 h, 2-(trimethylsilyl)ethanol (1.28 mL, 8.91 mmol) was added (resulting in slight effervescence). After 45 min, EDC•HCl (569 mg, 2.97 mmol) was added. After 6 h, piperidine (22 mL, 223 mmol) was added. After 1.5 h, the reaction mixture was diluted with EtOAc (100 mL), then washed with 1 M HCl (2x100 mL), H₂O (100 mL), and brine (100 mL). The organic layer was then dried over Na₂SO₄, filtered, and concentrated *in vacuo* (under high vacuum until most of the piperidine had evaporated). Purification via flash chromatography (gradient elution, 8:1→4:1 hexanes–EtOAc) afforded (trimethylsilyl)ethyl ester **251** (756 mg, 95% yield) as a white, amorphous solid with a melting point close to ambient temperature. ¹H NMR (500 MHz, CDCl₃) δ 7.62 – 7.58 (m, 2H), 6.86 (d, J = 8.3 Hz, 1H), 5.76 (s, 1H), 4.40 – 4.35 (m, 2H), 3.92 (s, 3H), 1.13 – 1.08 (m, 2H), 0.07 (s, 9H); ¹³C NMR (126 MHz, CDCl₃) δ 166.46, 150.24, 145.14,

123.81, 122.60, 115.50, 109.75, 62.98, 55.95, 17.34, -1.47; IR (NaCl/thin film): 3414, 2953, 2898, 2844, 1710, 1616, 1591, 1512, 1457, 1442, 1379, 1352, 1283, 1251, 1220, 1182, 1126, 1093, 1026, 965, 952, 860, 838, 763 cm⁻¹; HRMS (ESI) calc'd for C₁₁H₁₇O₄Si [M–C₂H₄+H]⁺ 241.0891, found 241.0896.

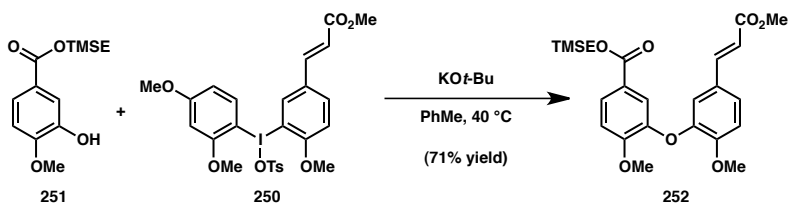
Preparation of λ³-iodane 250



A 1-dram vial equipped with a magnetic stir bar was charged with aryl iodide **249** (50 mg, 0.16 mmol), *m*-CPBA (85 wt %, 32 mg, 0.16 mmol), *p*-TsOH•H₂O (30 mg, 0.16 mmol), and 0.62 mL of CH₂Cl₂/TFE (1:1). To the resulting solution was added 1,3-dimethoxybenzene (**248**, 21 μL, 0.16 mmol) with stirring. After 3 h, the reaction mixture was concentrated *in vacuo* to give a dark brown residue. The residue was dissolved in acetone (~1 mL), then added dropwise via pipet to a vigorously stirring volume of Et₂O (~30 mL). The resulting precipitate was filtered off to afford λ³-iodane **250** (28 mg, 29% yield) as a pale purple solid. ¹H NMR (500 MHz, CDCl₃) δ 7.87 – 7.83 (m, 1H), 7.63 – 7.57 (m, 3H), 7.55 (d, *J* = 2.0 Hz, 1H), 7.45 (d, *J* = 16.0 Hz, 1H), 7.05 (d, *J* = 7.6 Hz, 2H), 6.99 (d, *J* = 8.6 Hz, 1H), 6.54 – 6.50 (m, 2H), 6.22 (d, *J* = 16.0 Hz, 1H), 3.95 (s, 3H), 3.85 (s, 3H), 3.83 (s, 3H), 3.78 (s, 3H), 2.31 (s, 3H); ¹³C NMR (126 MHz, CDCl₃) δ 166.9, 165.4, 158.6, 157.6, 142.7, 141.9, 139.3, 139.0, 133.7, 132.7, 130.2, 128.4, 126.0, 117.9, 112.3, 108.7, 104.6, 99.9, 91.4, 57.2, 56.9, 55.9, 51.8, 21.3; IR (NaCl/thin film): 3459, 2946, 2847, 1714, 1632, 1595, 1580, 1493, 1459, 1437, 1399, 1319, 1284, 1264, 1212, 1173, 1136, 1120, 1032, 1009, 816, 730 cm⁻¹; HRMS (ESI) calc'd for C₁₉H₂₀IO₅

$[M-C_7H_7O_3S]^+$ 455.0350, found 455.0371 (detected fragment does not include the *para*-toluenesulfonate ligand).

Preparation of diaryl ether 252



To a solution of phenol **251** (5.3 mg, 0.020 mmol) in 0.25 mL PhMe was added KO*t*-Bu (1.0 M in THF, 22 μ L, 0.022 mmol), and the resulting mixture was stirred for 15 min. Solid iodane **250** (15 mg, 0.024 mmol) was then added, and the mixture was heated to 40 °C. After 3 h, the reaction mixture was diluted with H₂O and extracted with CH₂Cl₂ (3x). The combined organic layers were dried over Na₂SO₄, filtered, and concentrated, and the resulting crude material was purified by flash chromatography (gradient elution, 8:1 → 4:1 hexanes–EtOAc) to afford biaryl ether **252** (6.5 mg, 71% yield) as a white, amorphous solid. ¹H NMR (500 MHz, CDCl₃) δ 7.84 (dd, *J* = 8.5, 2.1 Hz, 1H), 7.54 (d, *J* = 15.9 Hz, 1H), 7.49 (d, *J* = 2.0 Hz, 1H), 7.26 (dd, *J* = 8.5, 2.0 Hz, 1H), 7.01 (d, *J* = 8.6 Hz, 1H), 6.98 (s, 1H), 6.98 (d, *J* = 10.0 Hz, 1H), 6.17 (d, *J* = 15.9 Hz, 1H), 4.37 – 4.32 (m, 2H), 3.91 (s, 3H), 3.88 (s, 3H), 3.76 (s, 3H), 1.09 – 1.03 (m, 2H), 0.03 (s, 9H); ¹³C NMR (126 MHz, CDCl₃) δ 167.5, 166.0, 154.2, 152.3, 145.7, 145.0, 144.1, 127.5, 126.5, 125.2, 123.5, 119.8, 117.5, 115.9, 112.4, 111.5, 63.1, 56.1, 56.0, 51.6, 17.3, -1.5; IR (NaCl/thin film): 3400, 2952, 2840, 1712, 1636, 1607, 1573, 1511, 1430, 1378, 1266, 1219, 1175, 1124, 1094, 1025, 980, 946, 859, 838, 765 cm⁻¹; HRMS (ESI) calc'd for C₁₈H₁₅O₆ [M–C₃H₉Si–CH₃O–C₂H₄+H]⁺ 327.0863, found 327.0870 (detected fragment)

has undergone loss of trimethylsilyl cation, ethylene, and methoxide anion and gain of H⁺).

Table 3.2. Comparison of spectroscopic data for natural and synthetic SCH64877 (44)

¹H NMR Data (CDCl₃, data for synthetic material referenced to CHCl₃ at 7.26 ppm)

Reported chemical shift (δ) ²	Synthetic	Δ
3.28 ^a (dd, J = 15, 1 Hz, 2H)	3.37 (ddd, J = 16.4, 2.5, 1.2 Hz, 2H)	+0.09
3.11 (d, J = 15 Hz, 2H)	3.11 (d, J = 16.7 Hz, 2H)	0
5.30 (s, 2H)	5.30 (s, 2H)	0
5.30 (s, 2H)	5.30 (s, 2H)	0
4.6 (d, J = 10 Hz, 2H)	4.59 (dd, J = 8.3, 1.2 Hz, 2H)	-0.01
6.28 (d, J = 8 Hz, 2H)	6.28 (dd, J = 8.4, 1.9 Hz, 2H)	0
6.60 (s, 2H))	6.58 (dd, J = 1.8, 1.8 Hz, 2H)	-0.02
2.8 (dq ^b , J = 8, 2 Hz, 2H)	2.79 (qd, J = 7.2, 1.8 Hz, 2H)	-0.01
3.81 (dd, J = 10, 1 Hz, 2H)	3.81 (ddd, J = 9.5, 2.1, 2.1 Hz, 2H)	0
1.5 (m, 2H)	1.56 – 1.47 (m, 2H)	+0.02
1.13-1.10 ^c (m, 2H)	1.25 – 1.16 (m, 2H)	+0.09
1.85 (dq, J = 8, 2 Hz, 2H)	1.84 (dq, J = 13.5, 7.6, 3.1 Hz, 2H)	-0.01
0.95 (t, J = 8 Hz, 6H)	0.92 (t, J = 7.5 Hz, 6H)	-0.03
1.28 (d, J = 8 Hz, 6H)	1.27 (d, J = 7.3 Hz, 6H)	-0.01
0.84 (d, J = 8 Hz, 6H)	0.85 (d, J = 6.8 Hz, 6H)	+0.01

^aThis is suspected to be a typographical error. ^bThis is suspected to be a typographical error, based on the reported J value for the C(7') methyl group. ^cThis is suspected to be a typographical error, based on the reported chemical shift for SCH64874 (42).

¹³C NMR Data (CDCl₃, data for synthetic material referenced to CDCl₃ at 77.0 ppm)

Reported chemical shift (δ) ²	Synthetic	Δ
165.9	165.9	0
75.5	75.4	-0.1
41.5	41.5	0
108.0	108.0	0
61.0	60.9	-0.1
70.9	70.9	0
105.8	105.8	0
139.9	139.9	0
138.9	138.9	0
175.8	175.8	0
41.9	41.9	0
73.9	73.9	0
36.8	36.7	-0.1
25.3	25.3	0
10.9	10.8	-0.1
9.1	9.1	0
14.9	14.9	0

Table 3.3. Comparison of spectroscopic data for natural and synthetic emethallicin C (**101**)

¹H NMR Data (acetone-*d*₆, data for synthetic material referenced to acetone-*d*₅ at 2.05 ppm)

Reported chemical shift (δ) ³	Synthetic
3.212 (d, $J = 16.4$ Hz, 2H)	3.21 (ddd, $J = 16.3, 1.2, 1.2$ Hz, 2H)
3.566 (ddd, $J = 16.4, 2.5, 2.0$ Hz, 2H)	3.57 (ddd, $J = 16.4, 2.6, 1.7$ Hz, 2H)
4.409 (dd, $J = 8.2, 1.7$ Hz, 2H)	4.41 (dd, $J = 8.2, 1.8$ Hz, 2H)
4.873 (d, $J = 5.6$ Hz, 2H)	4.90 (d, $J = 5.4$ Hz, 2H)
5.202 (ddd, $J = 8.5, 2.0, 2.0$ Hz, 2H)	5.20 (ddd, $J = 8.5, 2.0, 2.0$ Hz, 2H)
5.256 (ddd, $J = 8.5, 2.2, 1.7$ Hz, 2H)	5.25 (dddd, $J = 8.6, 2.8, 1.5, 1.5$ Hz, 2H)
5.362 (d, $J = 5.6$ Hz, 2H)	5.36 (d, $J = 4.8$ Hz, 2H)
6.332 (dd, $J = 8.2, 2.2$ Hz, 2H)	6.33 (dd, $J = 8.2, 2.2$ Hz, 2H)
6.780 (dd, $J = 2.5, 2.0$ Hz, 2H)	6.78 (ddd, $J = 2.5, 2.5, 1.0$ Hz, 2H)
7.325 (br t, $J = 7.3$ Hz, 2H)	7.35 – 7.30 (m, 2H)
7.391 (br t, $J = 7.3$ Hz, 4H)	7.41 – 7.37 (m, 4H)
7.667 (br d, $J = 7.3$ Hz, 4H)	7.68 – 7.65 (m, 4H)

3.6 NOTES AND REFERENCES

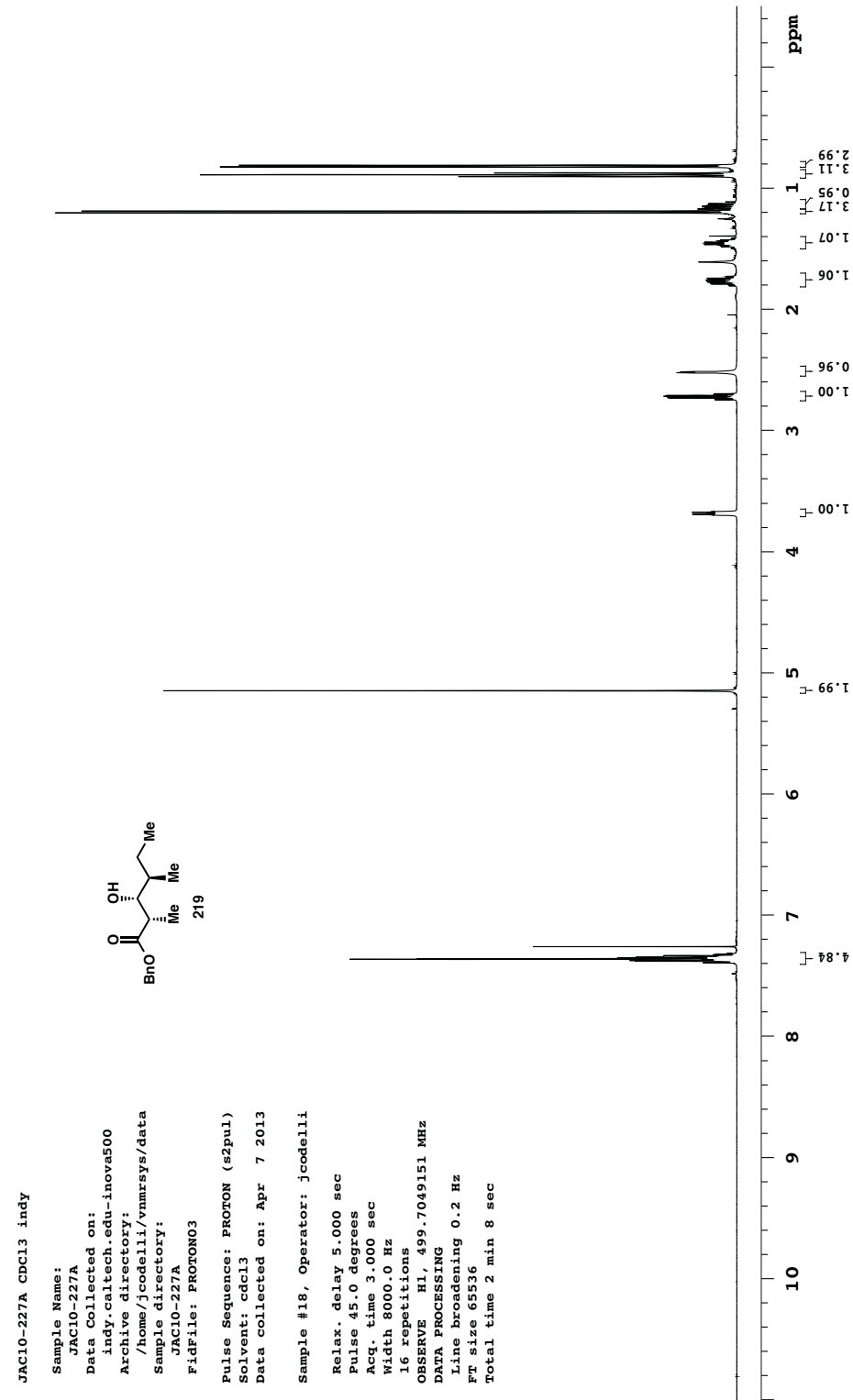
-
- (1) Codelli, J. A.; Puchlopek, A. L. A.; Reisman, S. E. *J. Am. Chem. Soc.* **2012**, *134*, 1930.
 - (2) Hegde, V. R.; Dai, P.; Patel, M.; Das, P. R.; Puar, M. S. *Tetrahedron Lett.* **1997**, *38*, 911.
 - (3) Kawahara, N.; Nozawa, K.; Nakajima, S.; Kawai, K.; Yamazaki, M. *J. Chem. Soc., Chem. Commun.* **1989**, 951.
 - (4) (a) Zhu, C.; Shen, X.; Nelson, S. G. *J. Am. Chem. Soc.* **2004**, *126*, 5352. (b) Shen, X.; Wasmuth, A. S.; Zhao, J.; Zhu, C.; Nelson, S. G. *J. Am. Chem. Soc.* **2006**, *128*, 7438. (c) Shen, X. Ph.D. Thesis, University of Pittsburgh, August **2007**.
 - (5) Nelson, S. G.; Wan, Z.; Peelen, T. J.; Spencer, K. L. *Tetrahedron Lett.* **1999**, *40*, 6535.
 - (6) Evans, D. A.; Morrissey, M. M. *J. Am. Chem. Soc.* **1984**, *106*, 3866.
 - (7) Inanaga, J.; Hirata, K.; Saeki, H.; Katsuki, T.; Yamaguchi, M. *Bull. Chem. Soc. Jpn.* **1979**, *52*, 1989.
 - (8) (a) Eidamshaus, C.; Reissig, H.-U. *Eur. J. Org. Chem.* **2011**, 6056. (b) Nieman, J. A.; Keay, B. A. *Tetrahedron, Asymmetry* **1995**, *6*, 1575.
 - (9) Zhang, K.; Peng, Q.; Hou, X.-L.; Wu, Y.-D. *Angew. Chem., Int. Ed.* **2008**, *47*, 1741.
 - (10) Qi, J.; Blanden, A. R.; Bane, S.; Kingston, D. G. I. *Bioorganic & Medicinal Chemistry* **2011**, *19*, 5247.

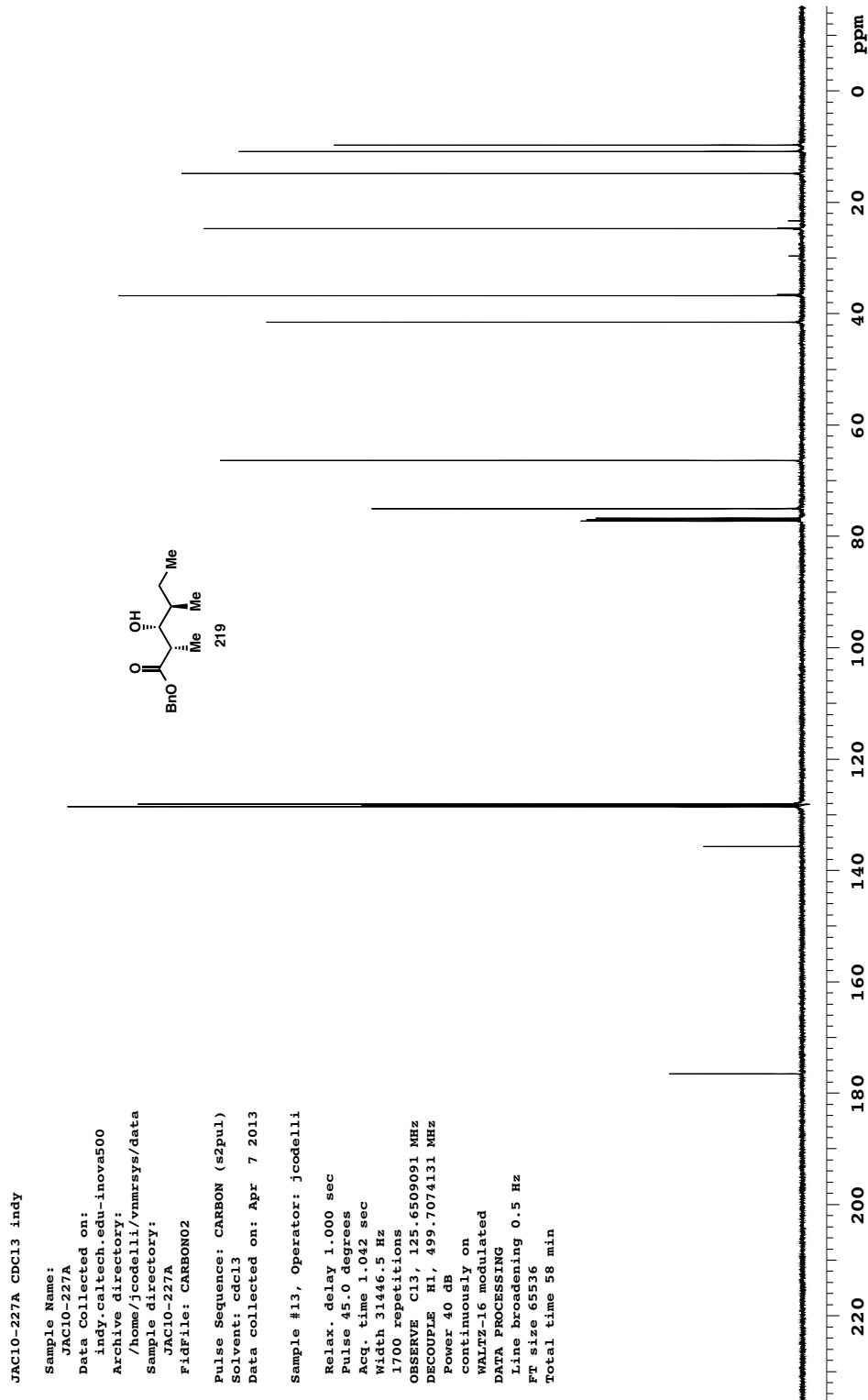
-
- (11) Seya, H.; Nakajima, S.; Kawai, K.; Udagawa, S. *J. Chem. Soc., Chem. Commun.* **1985**, 657.
- (12) Onodera, H.; Hasegawa, A.; Tsumagari, N.; Nakai, R.; Ogawa, T.; Kanda, Y. *Org. Lett.* **2004**, 6, 4101.
- (13) For a (1,3)-dipolar cycloaddition strategy that incorporates a C(11)-silyl functional handle for the purpose of accessing the natural products possessing C(11)-OH functionality, see: Schuber, P. T.; Williams, R. M. *Heterocycles* **2012**, 84, 1193.
- (14) Previous synthetic efforts toward this fragment: Schuber, P. T., Jr.; Williams, R. M. *Tetrahedron Lett.* **2012**, 53, 380.
- (15) (a) Ullman, F. *Ber.* **1904**, 37, 853. (b) Ullman, F.; Sponagel, P. *Ber.* **1905**, 38, 2211.
- (16) (a) Tao, B.; Schlingloff, G.; Sharpless, K. B. *Tetrahedron Lett.* **1998**, 39, 2507. (b) Sharpless, K. B.; Tao, B.; Schlingloff, G. U.S. Patent 6,057,473 May **2000**.
- (17) Noyori, R.; Ikeda, T.; Ohkuma, T.; Widhalm, M.; Kitamura, M.; Takaya, H.; Akutagawa, S.; Sayo, N.; Saito, T. *J. Am. Chem. Soc.* **1989**, 111, 9134.
- (18) (a) Vedejs, E.; Jure, M. *Angew. Chem., Int. Ed.* **2005**, 44, 3974. (b) Pellissier, H. *Tetrahedron* **2003**, 59, 8291. (c) Noyori, R.; Tokunaga, M.; Kitamura, M. *Bull. Chem. Soc. Jpn.* **1995**, 68, 36.
- (19) (a) Maiti, D.; Buchwald, S. L. *J. Org. Chem.* **2010**, 75, 1791. (b) Burgos, C. H.; Barder, T. E.; Huang, X.; Buchwald, S. L. *Angew. Chem., Int. Ed.* **2006**, 45, 4321. (c) Buck, E.; Song, Z. J.; Tschaen, D.; Dormer, P. G.; Volante, R. P.; Reider, P. J.

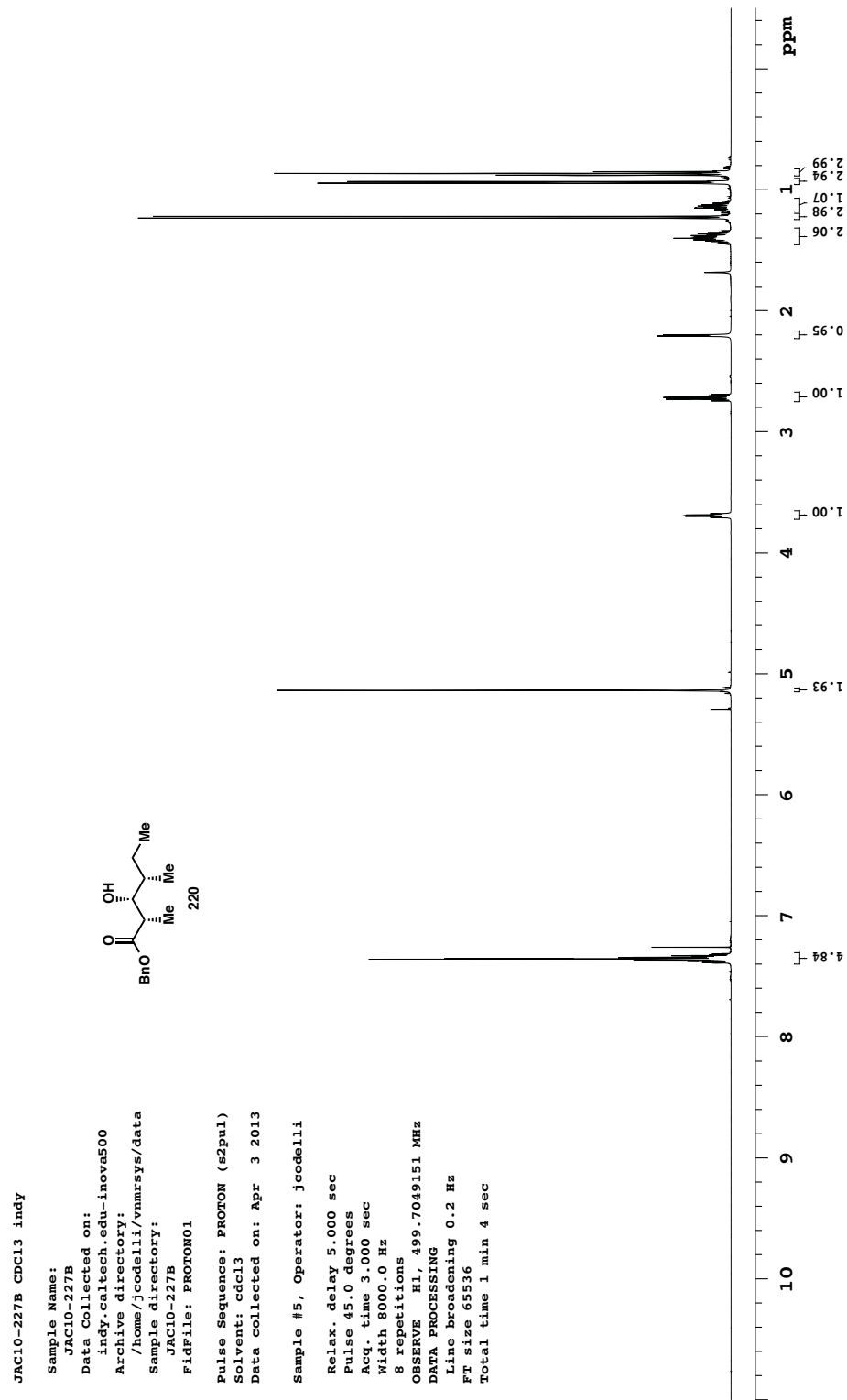
-
- Org. Lett.* **2002**, *4*, 1623. (d) Jung, N.; Bräse, S. *J. Comb. Chem.* **2009**, *11*, 47. (e) Wipf, P.; Jung, J.-K. *J. Org. Chem.* **2000**, *65*, 6319.
- (20) (a) Evans, D. A.; Katz, J. L.; West, T. R. *Tetrahedron Lett.* **1998**, *39*, 2937. (b) Chan, D. M. T.; Monaco, K. L.; Wang, R. P.; Winters, M. P. *Tetrahedron Lett.* **1998**, *39*, 2933. (c) Lam, P. Y. S.; Clark, C. G.; Saubern, S.; Adams, J.; Winters, M. P.; Chan, D. M. T.; Combs, A. *Tetrahedron Lett.* **1998**, *39*, 2941.
- (21) Review: Merritt, E. A.; Olofsson, B. *Angew. Chem., Int. Ed.* **2009**, *48*, 9052.
- (22) (a) Jalalian, N.; Ishikawa, E. E.; Silva, L. F., Jr.; Olofsson, B. *Org. Lett.* **2011**, *13*, 1552. (b) Jalalian, N.; Petersen, T. B.; Olofsson, B. *Chem. Eur. J.* **2012**, *18*, 14140.
- (23) Lancer, K. M.; Wiegand, G. H. *J. Org. Chem.* **1976**, *41*, 3360.
- (24) Chun, J.-H.; Lu, S.; Lee, Y.-S.; Pike, V. W. *J. Org. Chem.* **2010**, *75*, 3332.
- (25) Zhu, M.; Jalalian, N.; Olofsson, B. *Synlett* **2008**, 592.
- (26) Still, W. C., Kahn, M.; Mitra, A. *J. Org. Chem.* **1978**, *43*, 2923.
- (27) Relative stereochemistry was determined by conversion of **ent-291** to a known diol, (2*R*,3*R*,4*R*)-2,4-dimethylhexane-1,3-diol. See: Cooksey, J. P.; Ford, R.; Kocienski, P. J.; Pelotier, B.; Pons, J.-M. *Tetrahedron* **2010**, *66*, 6462.
- (28) Relative stereochemistry was determined by DBU-promoted epimerization of **ent-219**, which afforded a mixture of **ent-219** and **ent-222**.

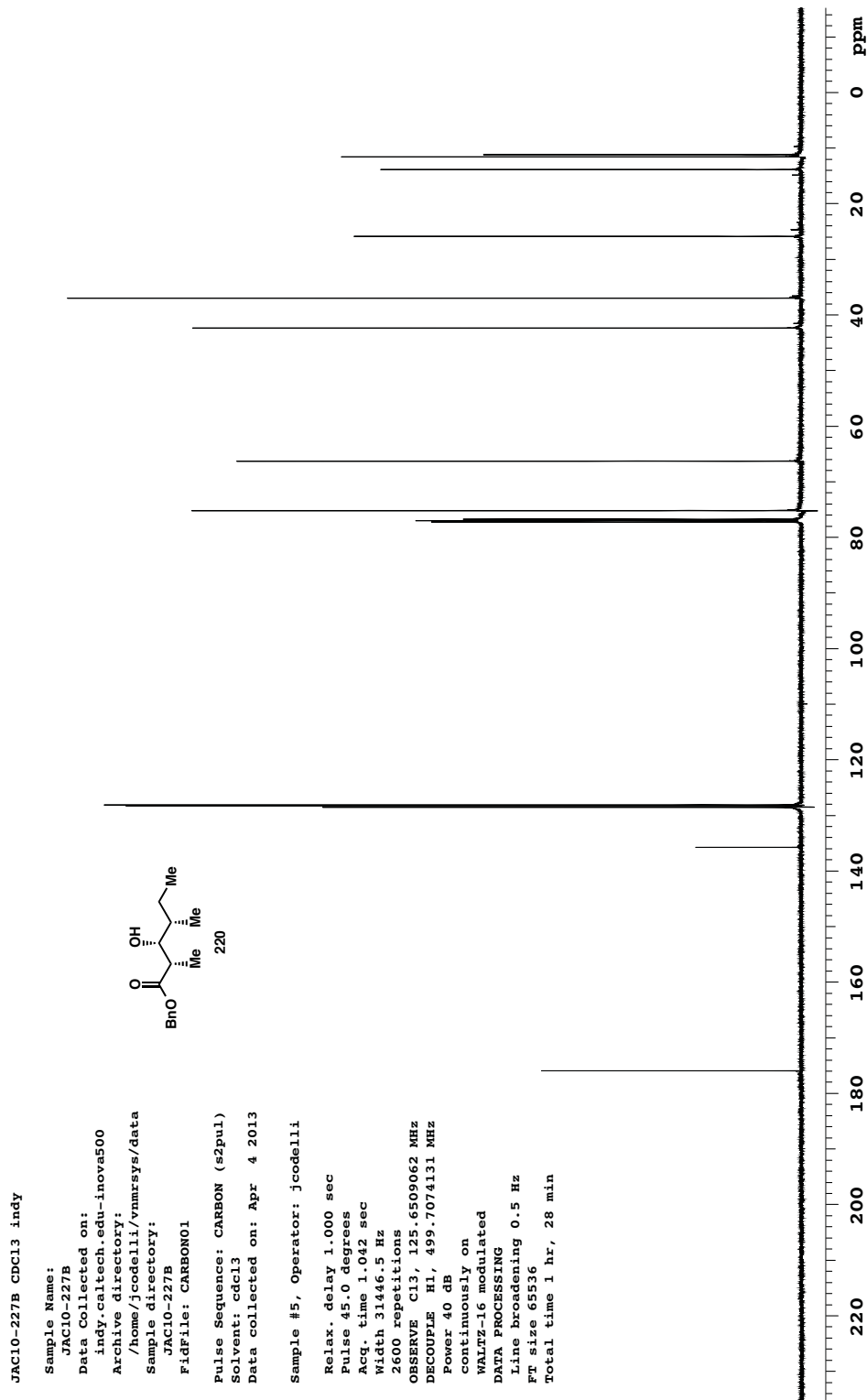
Appendix 3

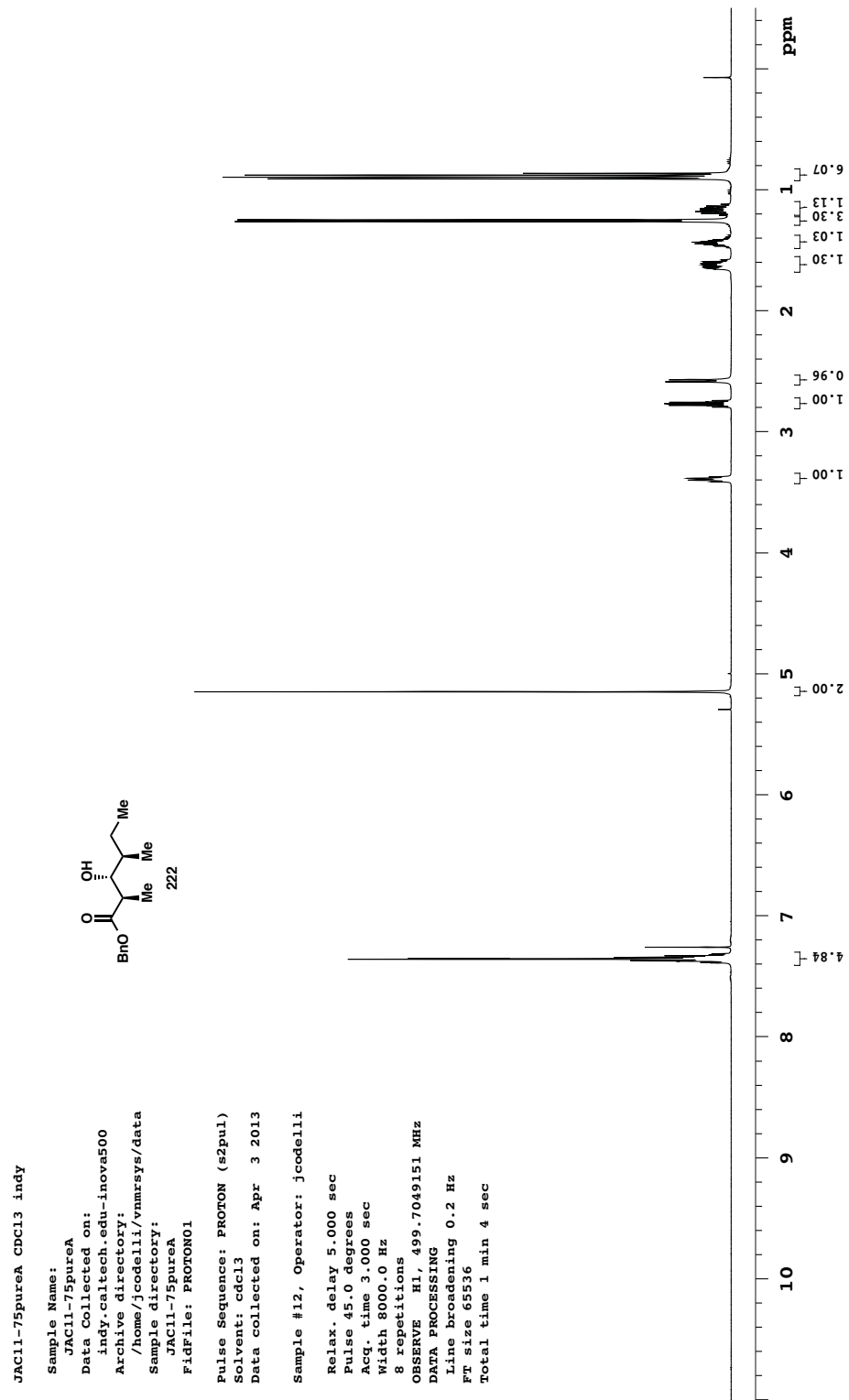
*Spectra Relevant to Chapter 3:
C₂-Symmetric Dihydrooxepine-Containing ETPs and MPC1001B*

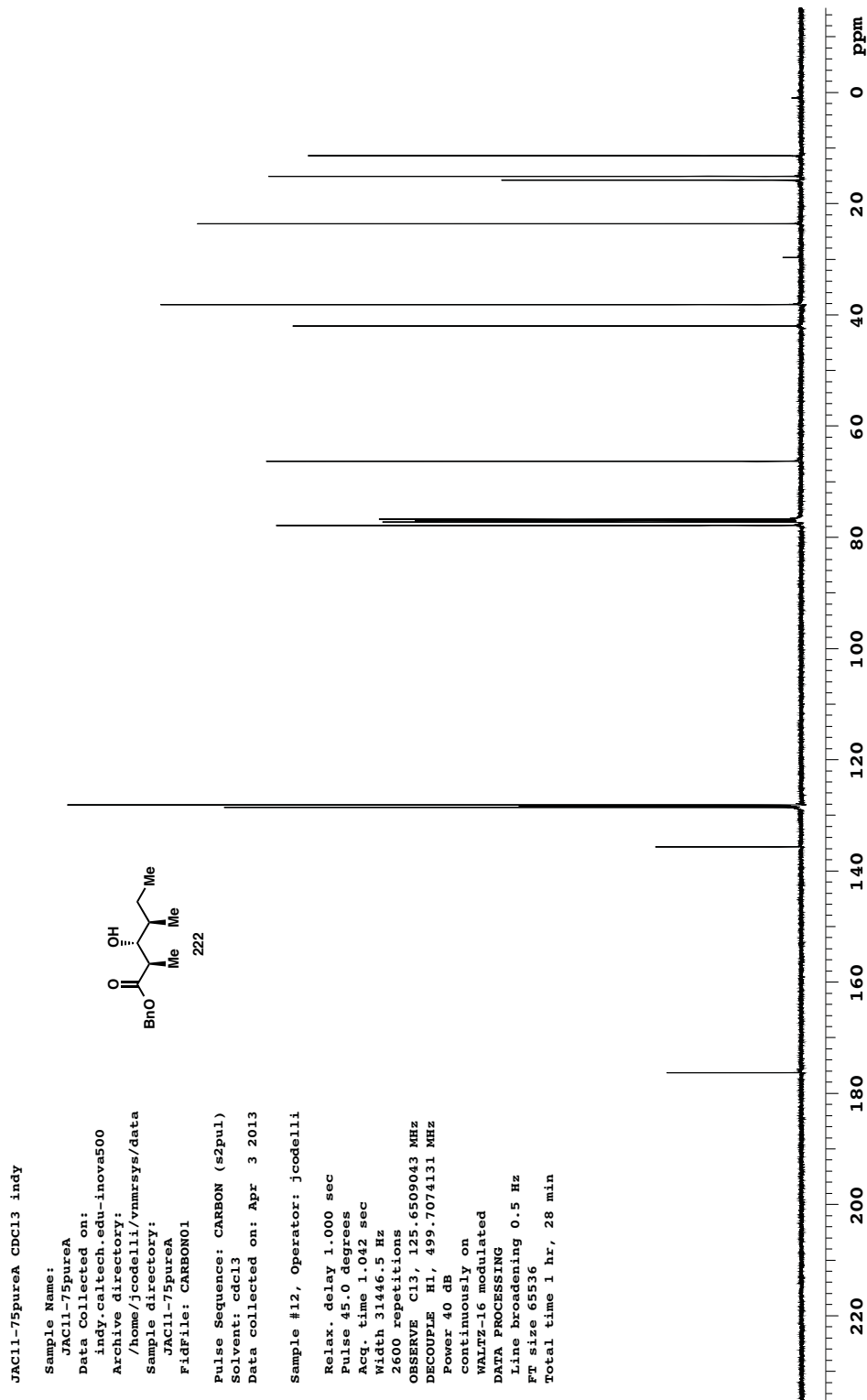


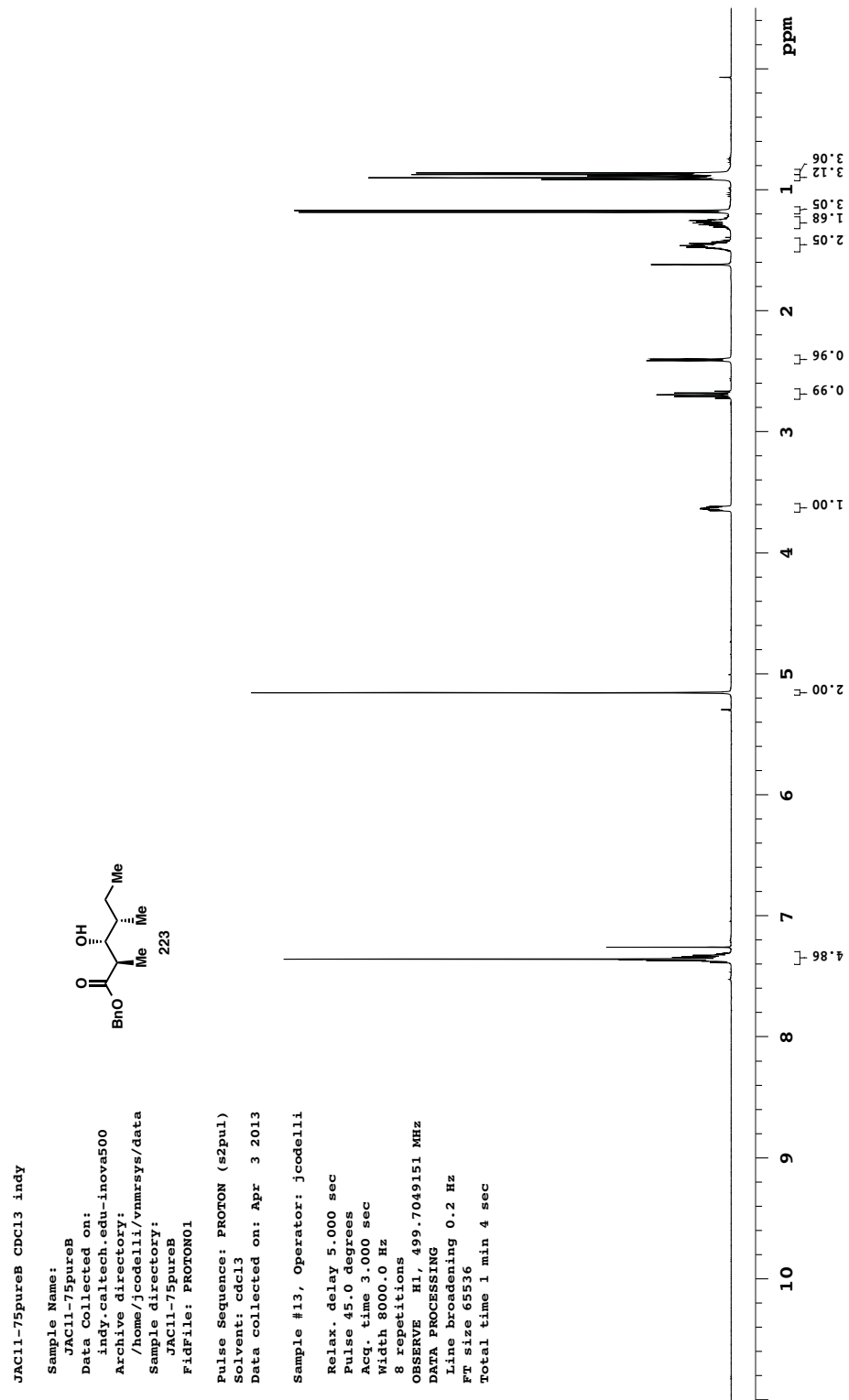


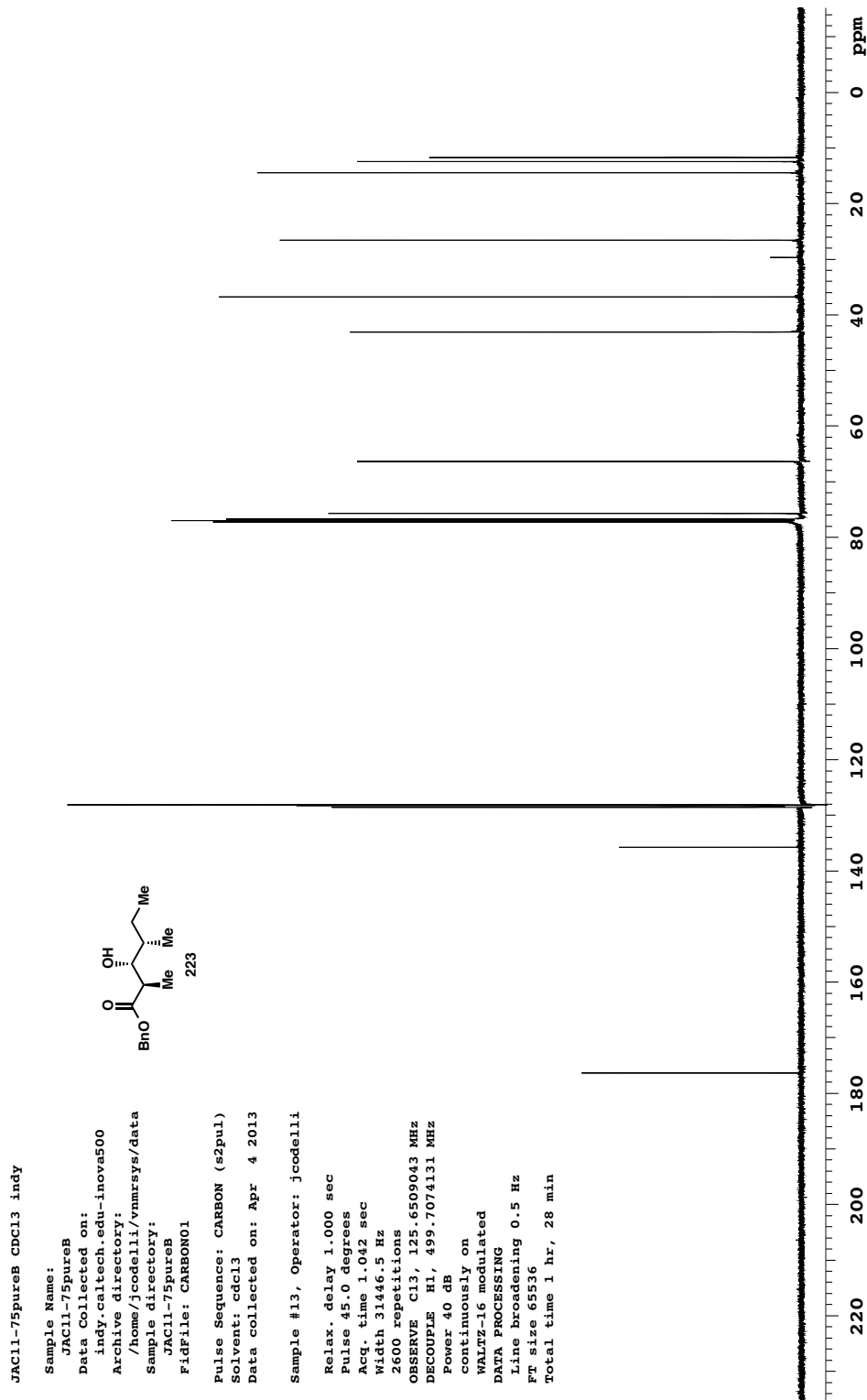


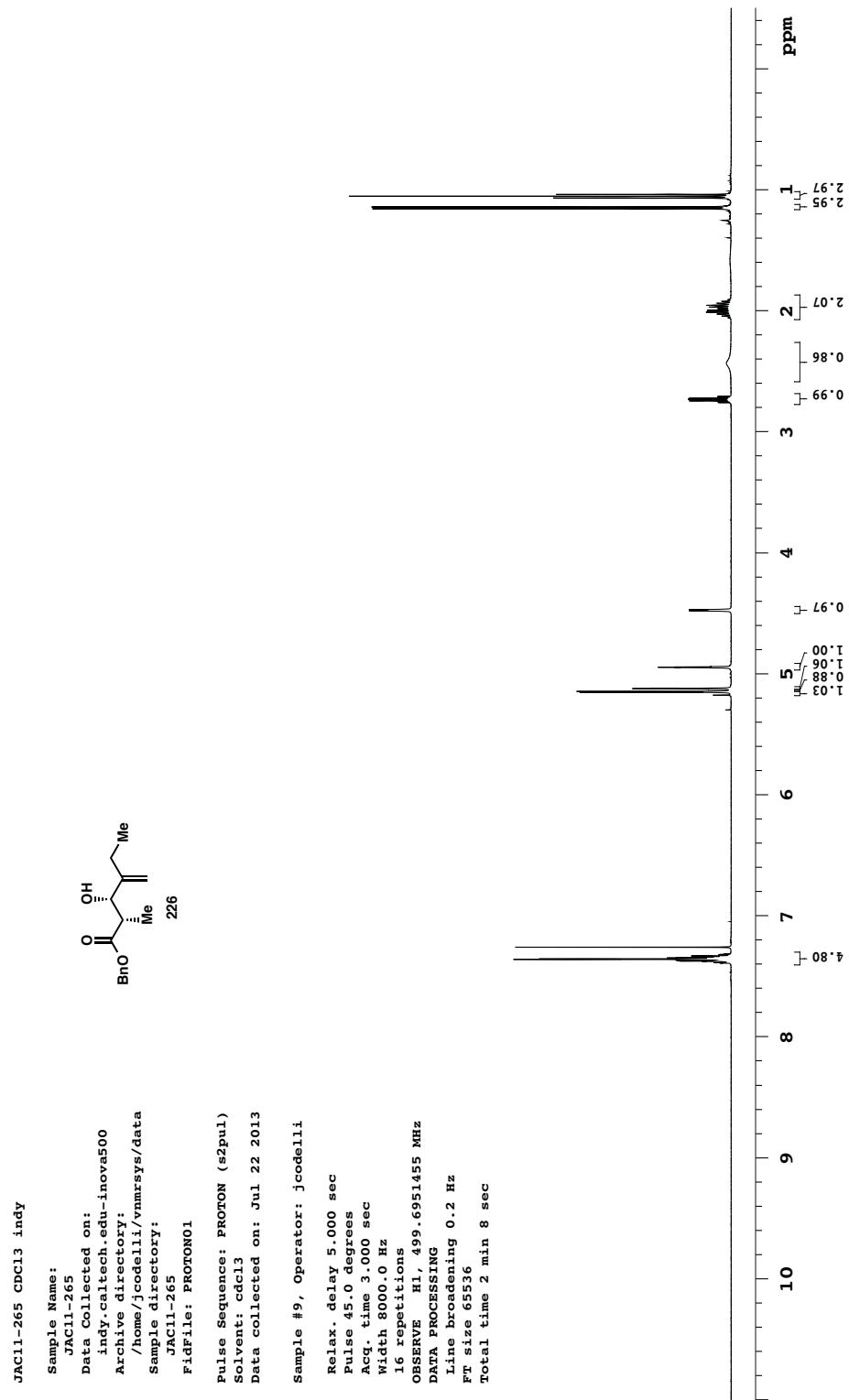


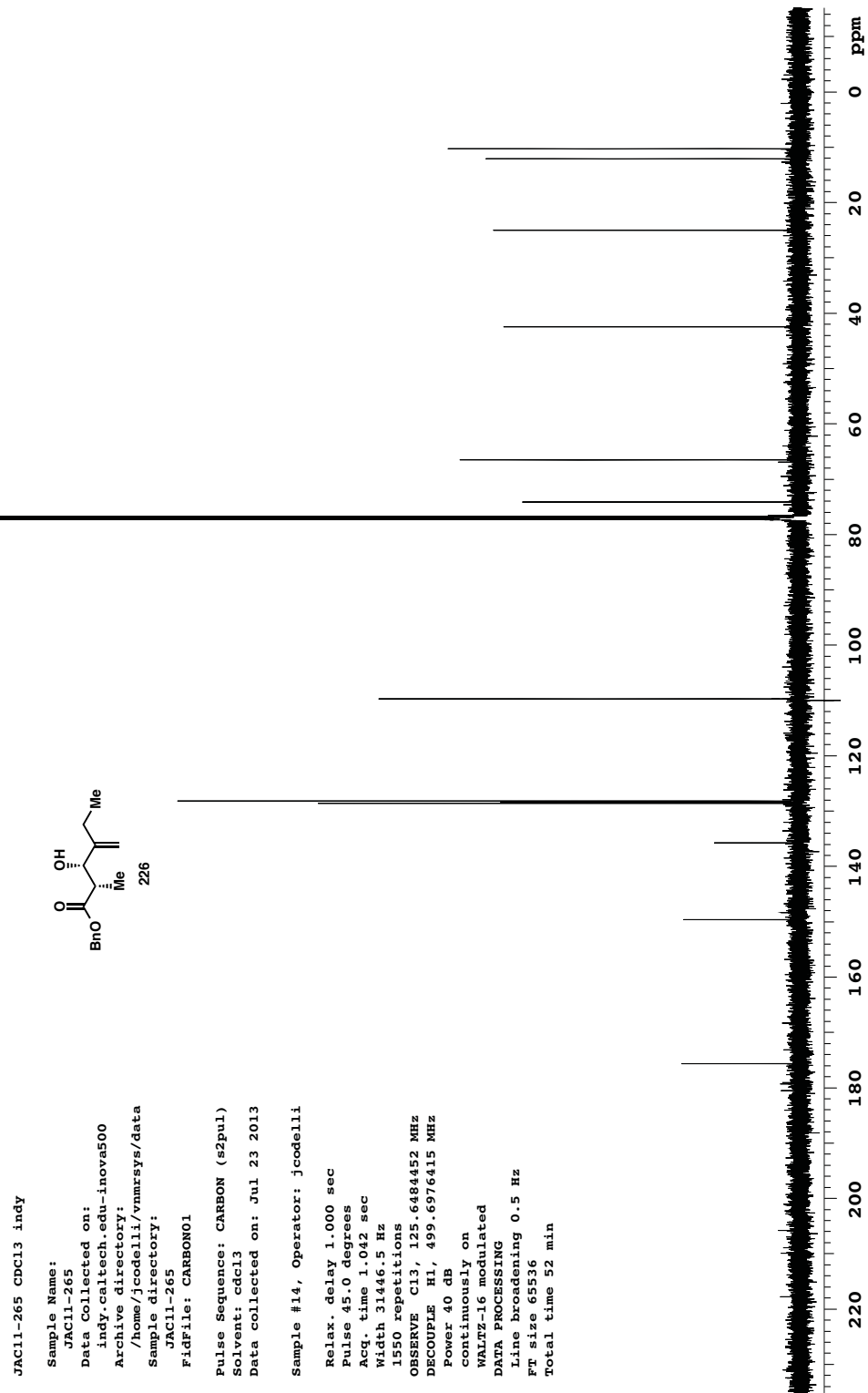


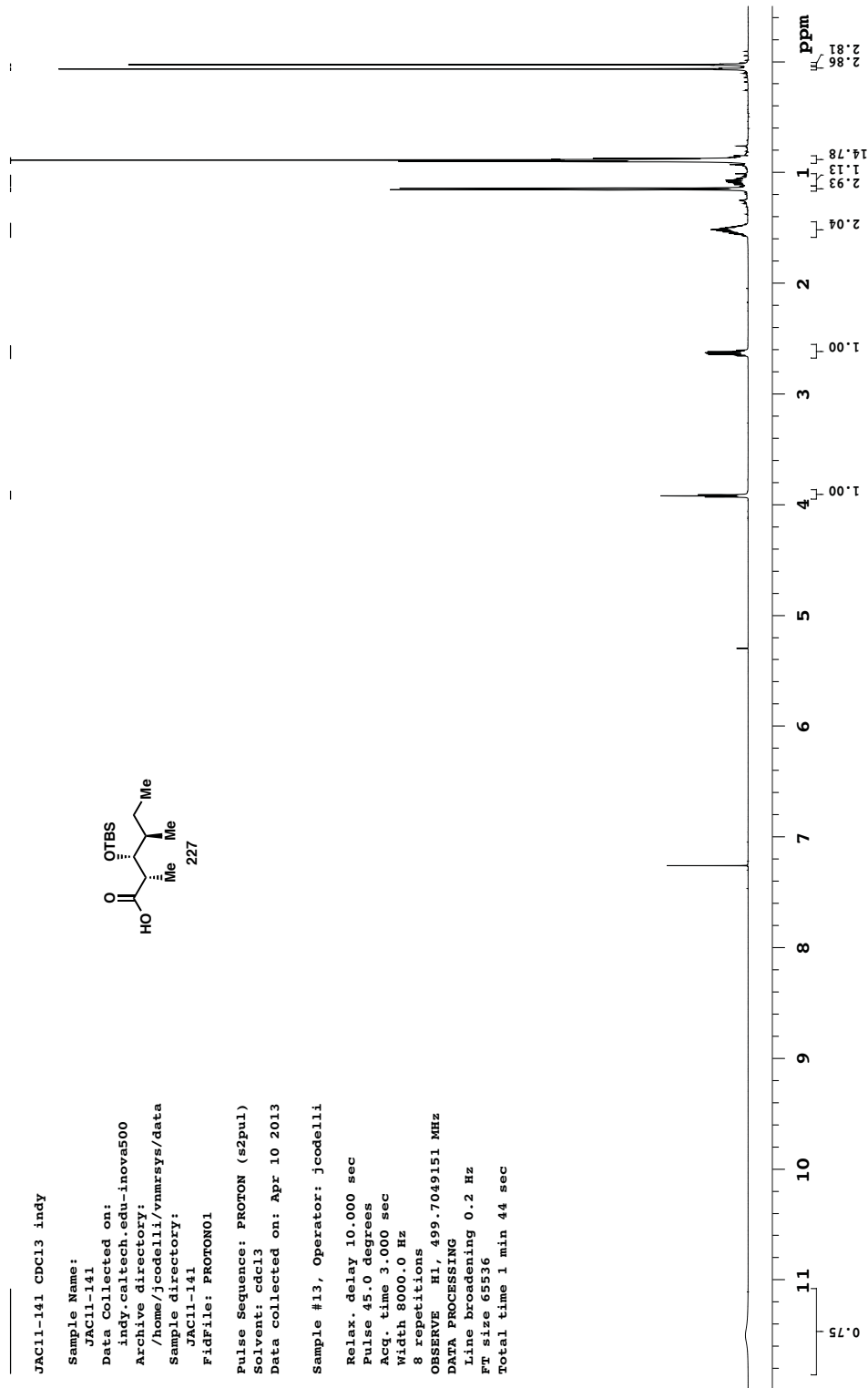


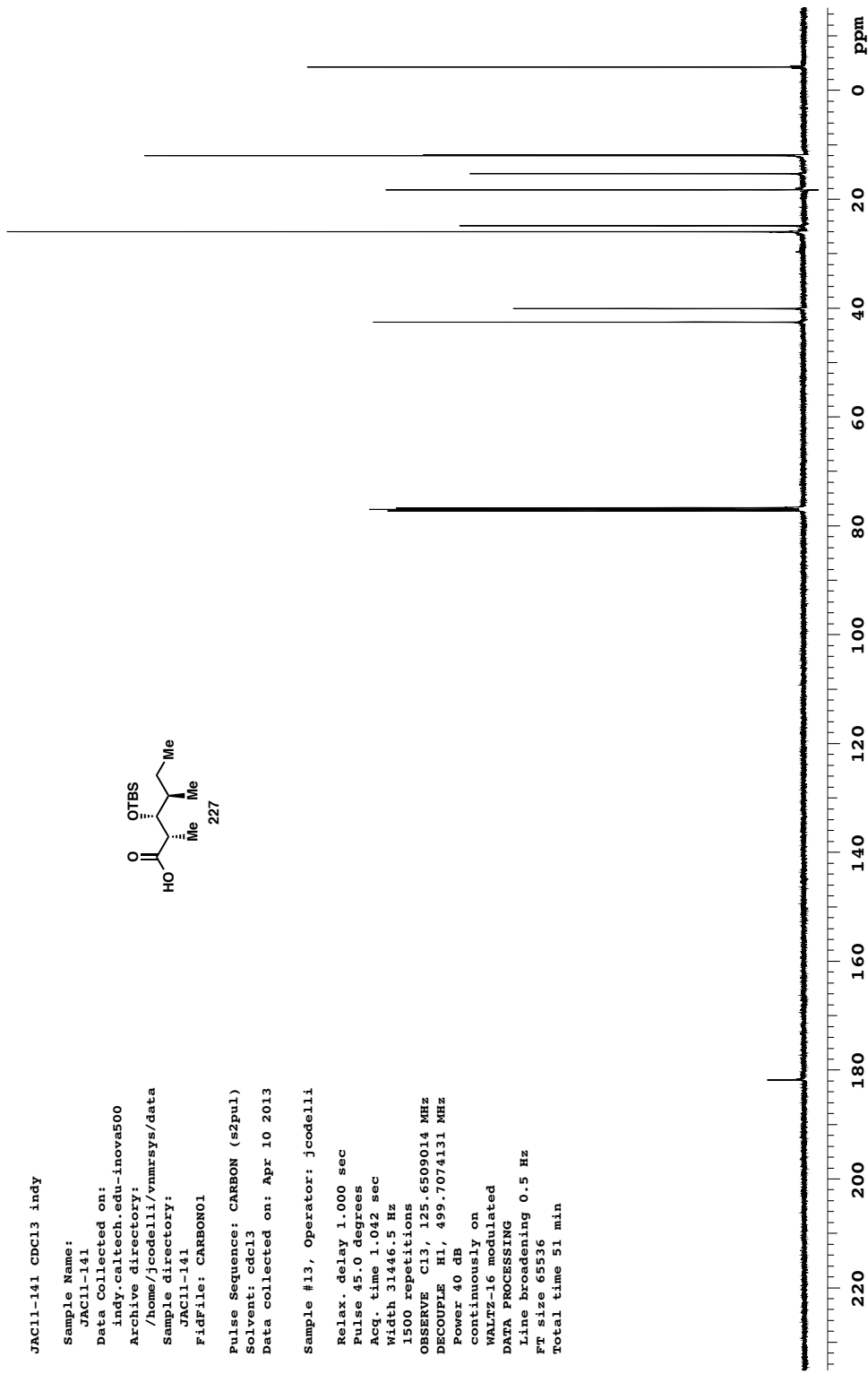


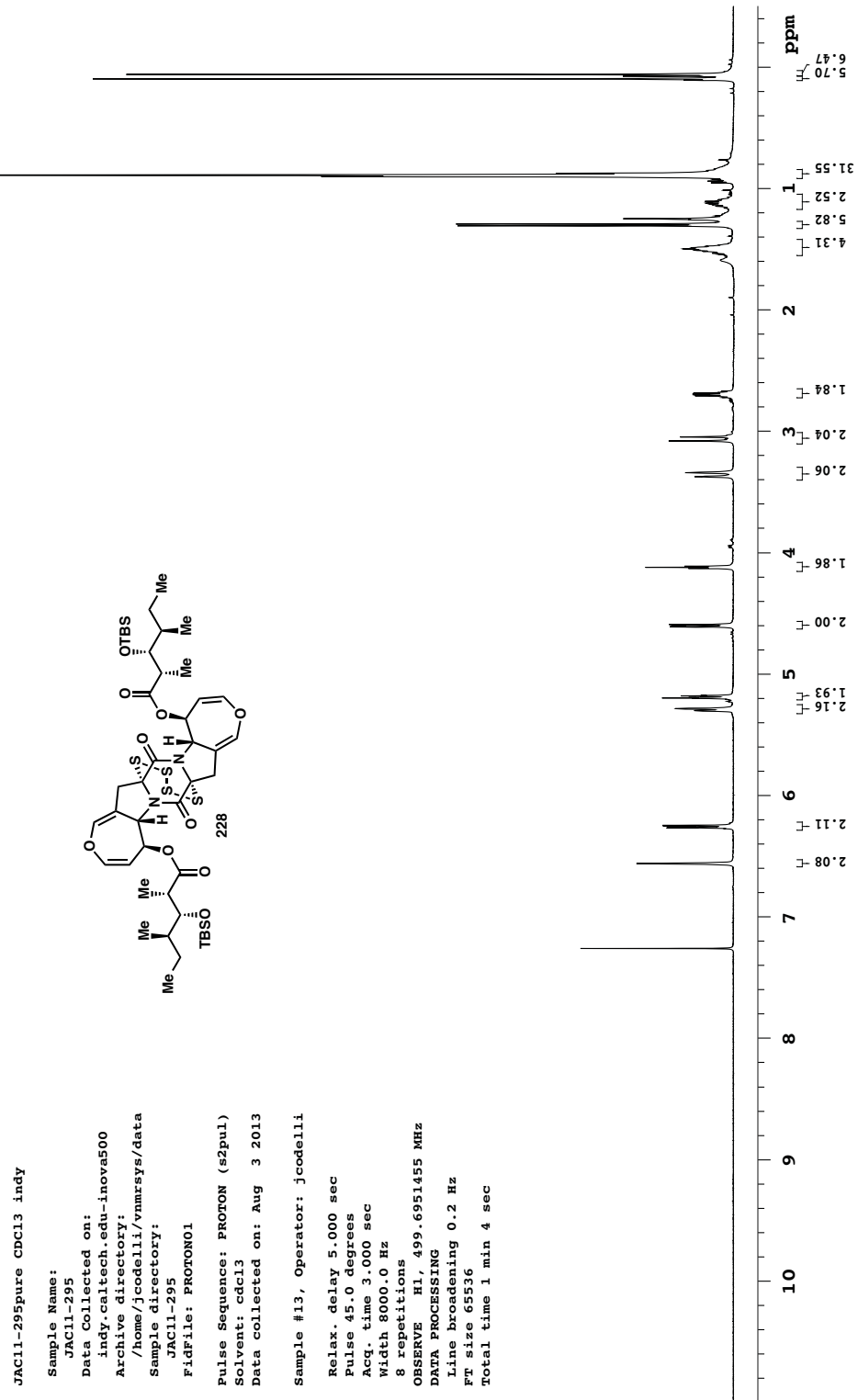


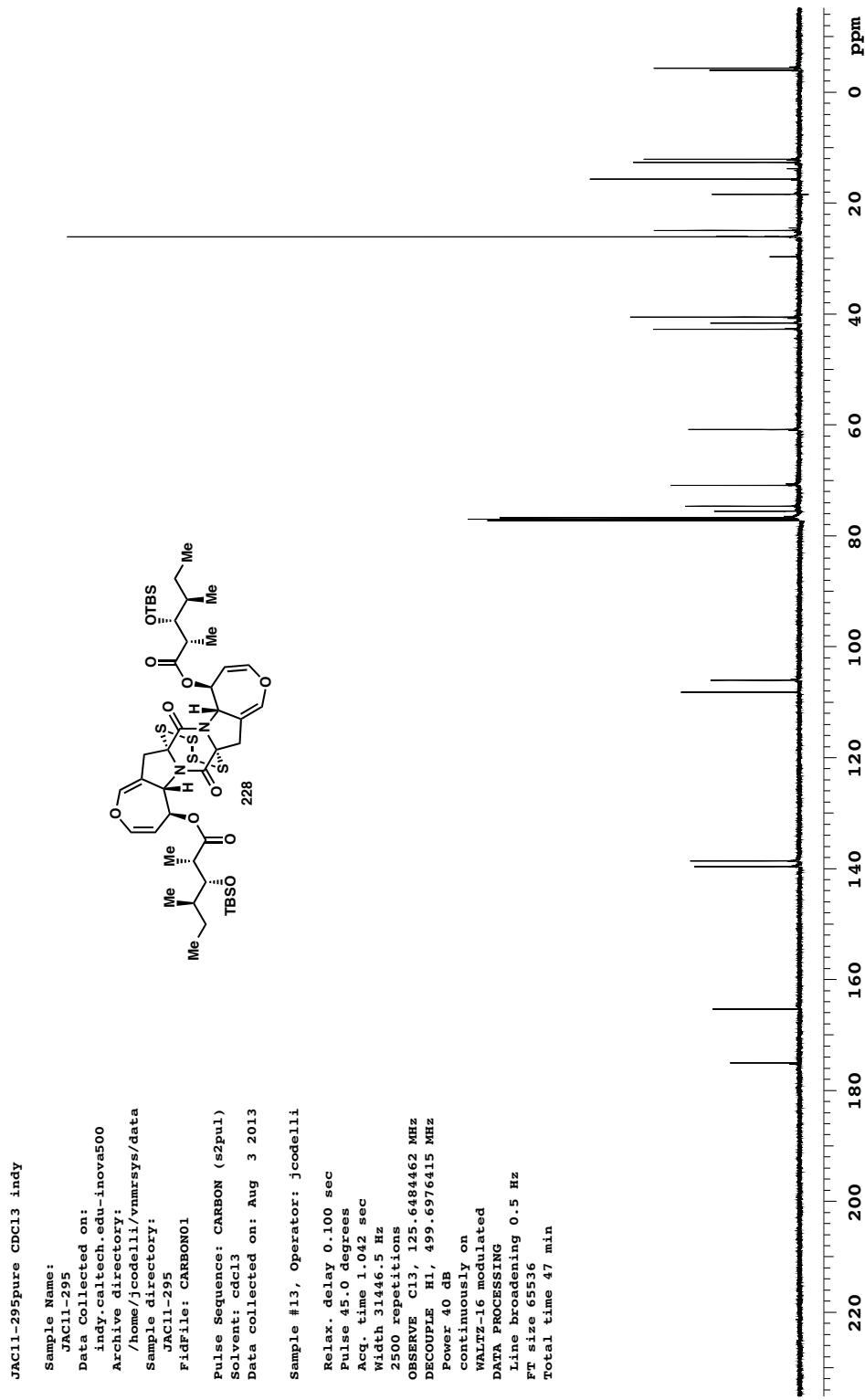


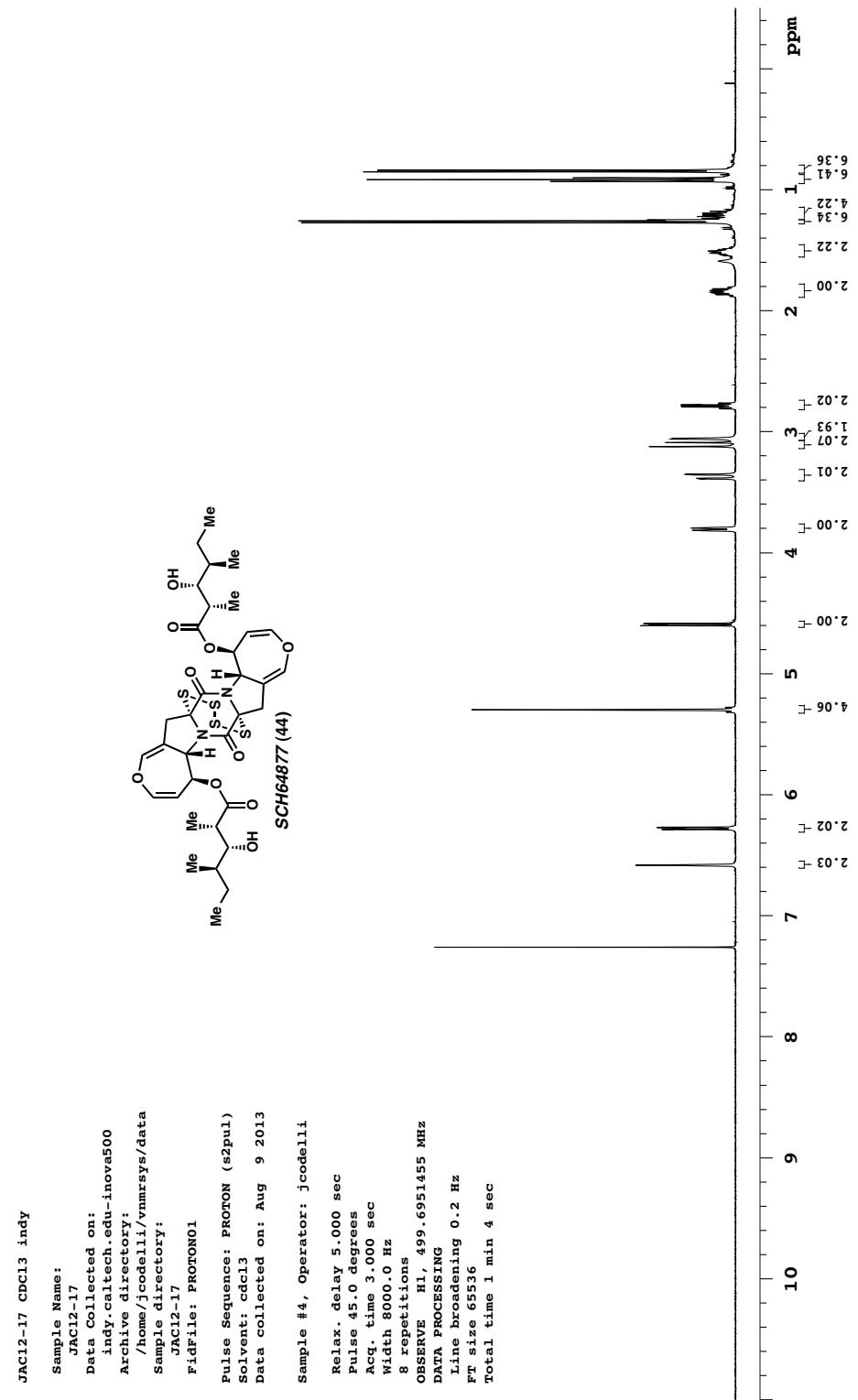


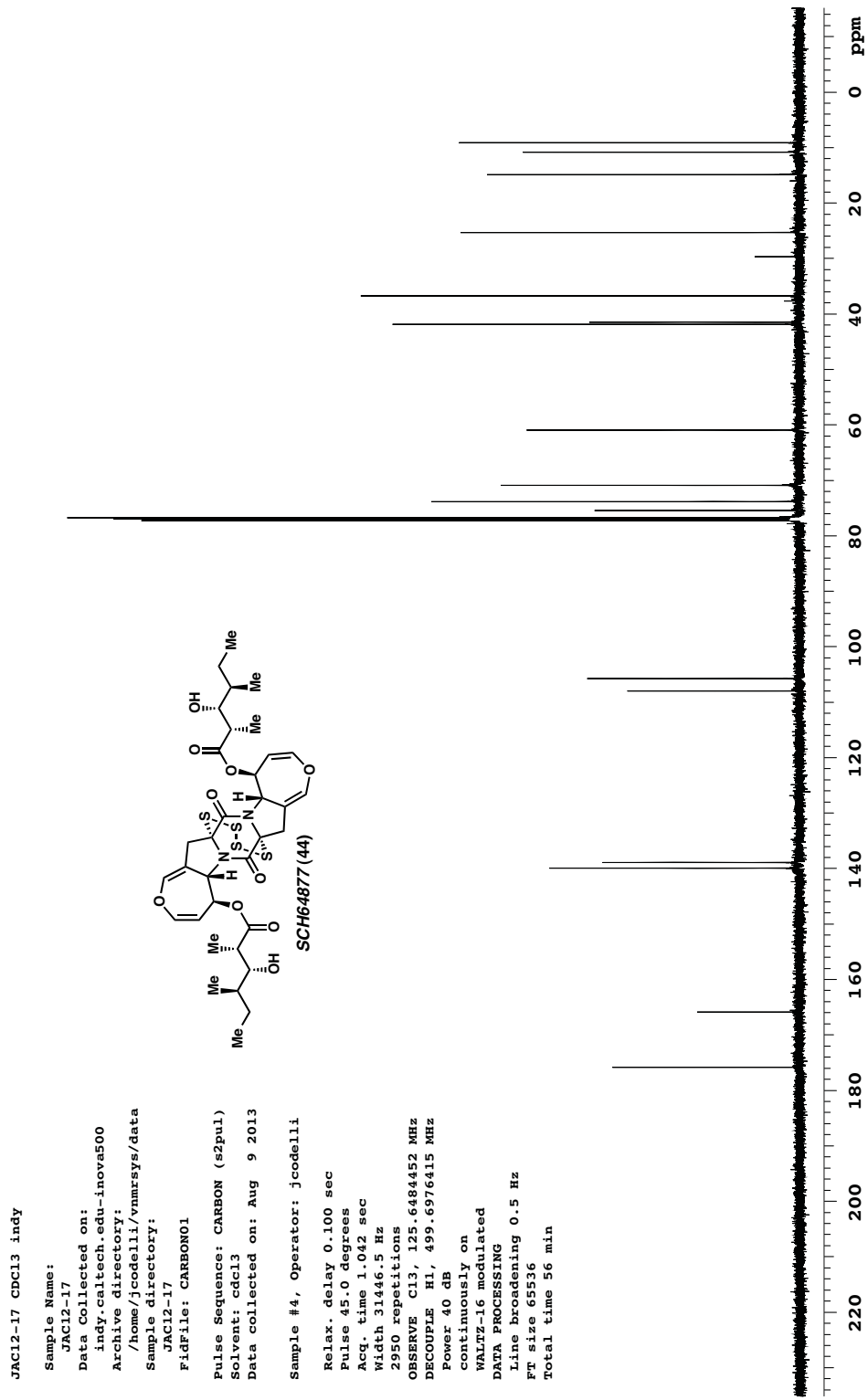


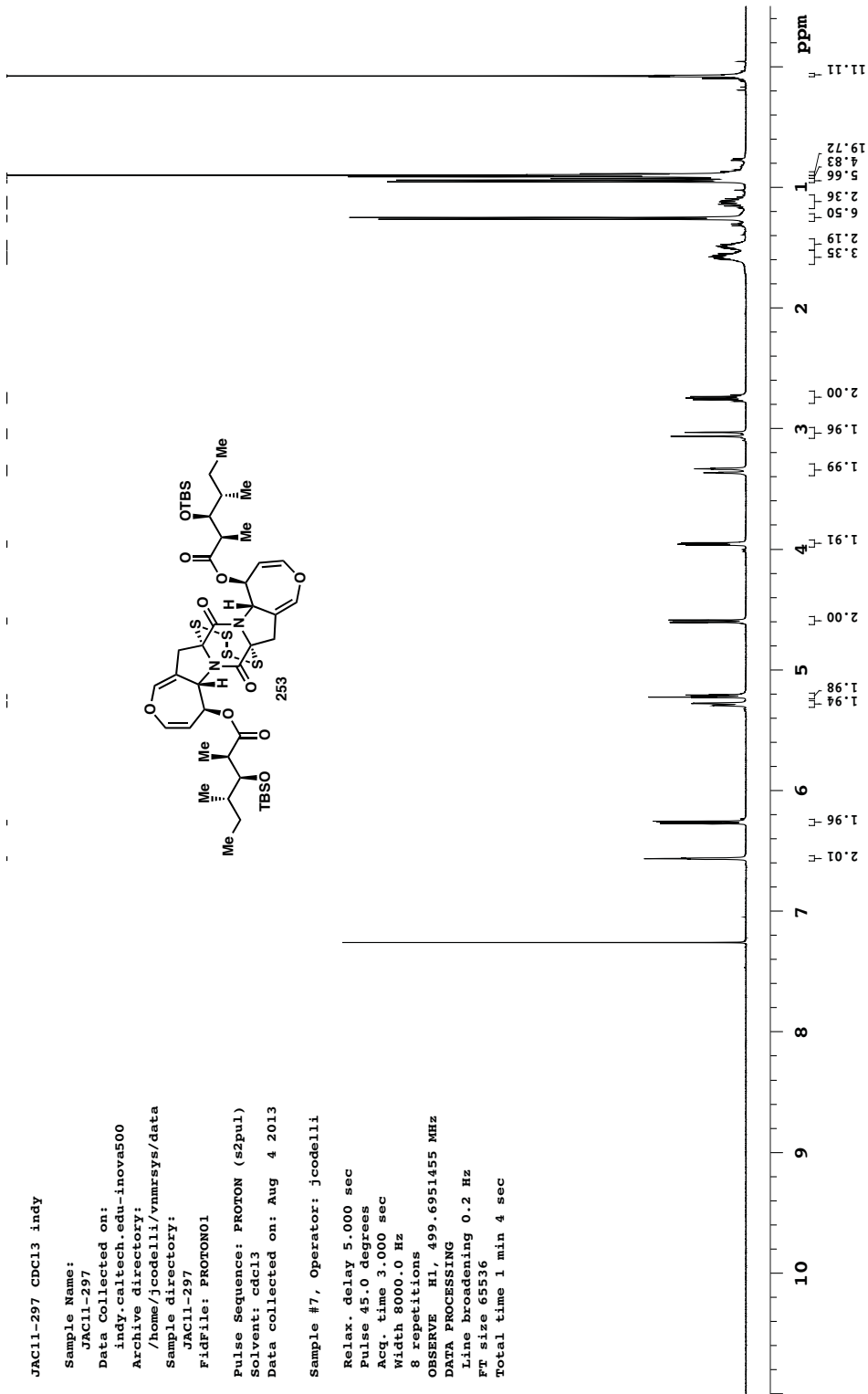


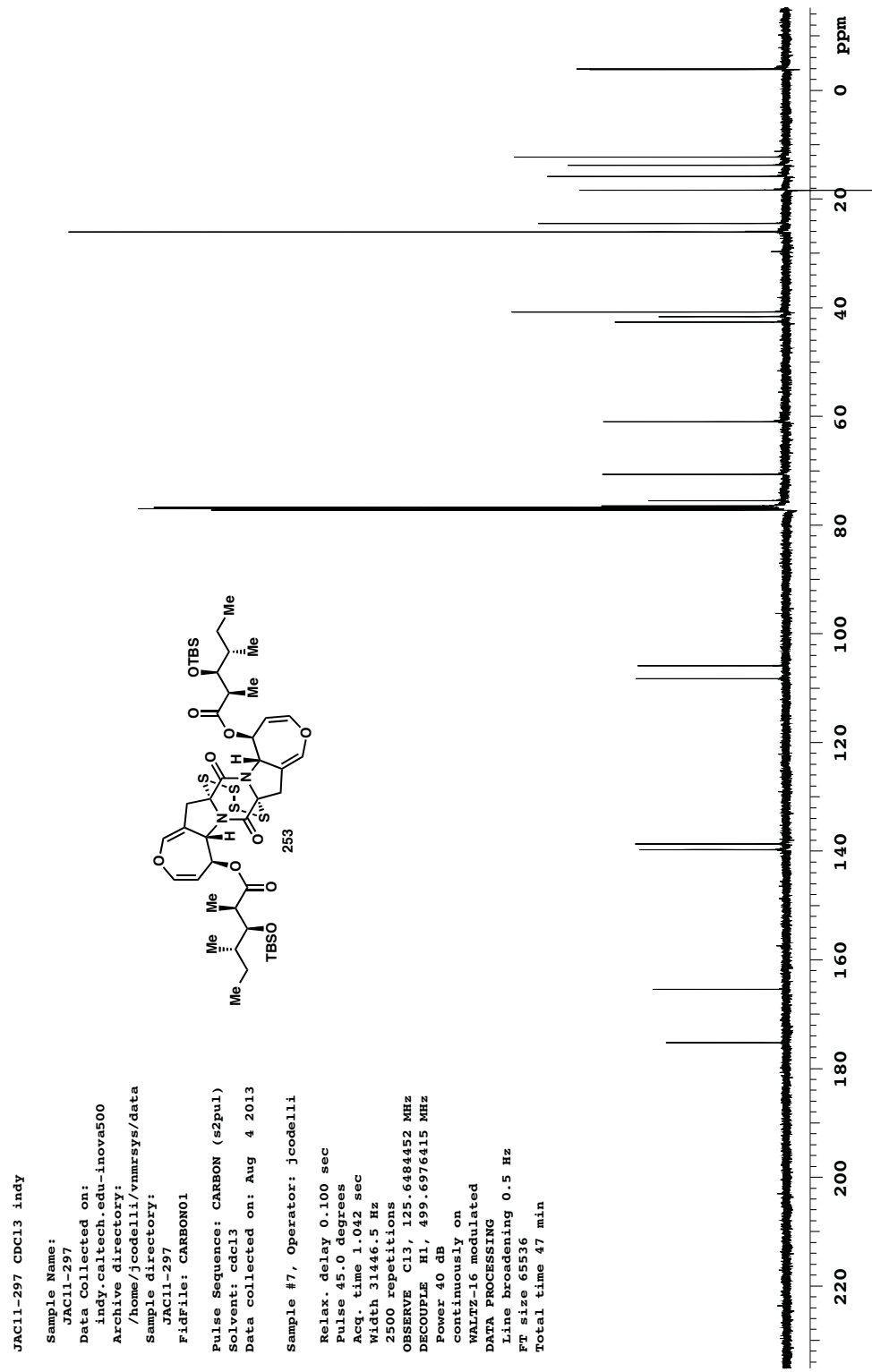


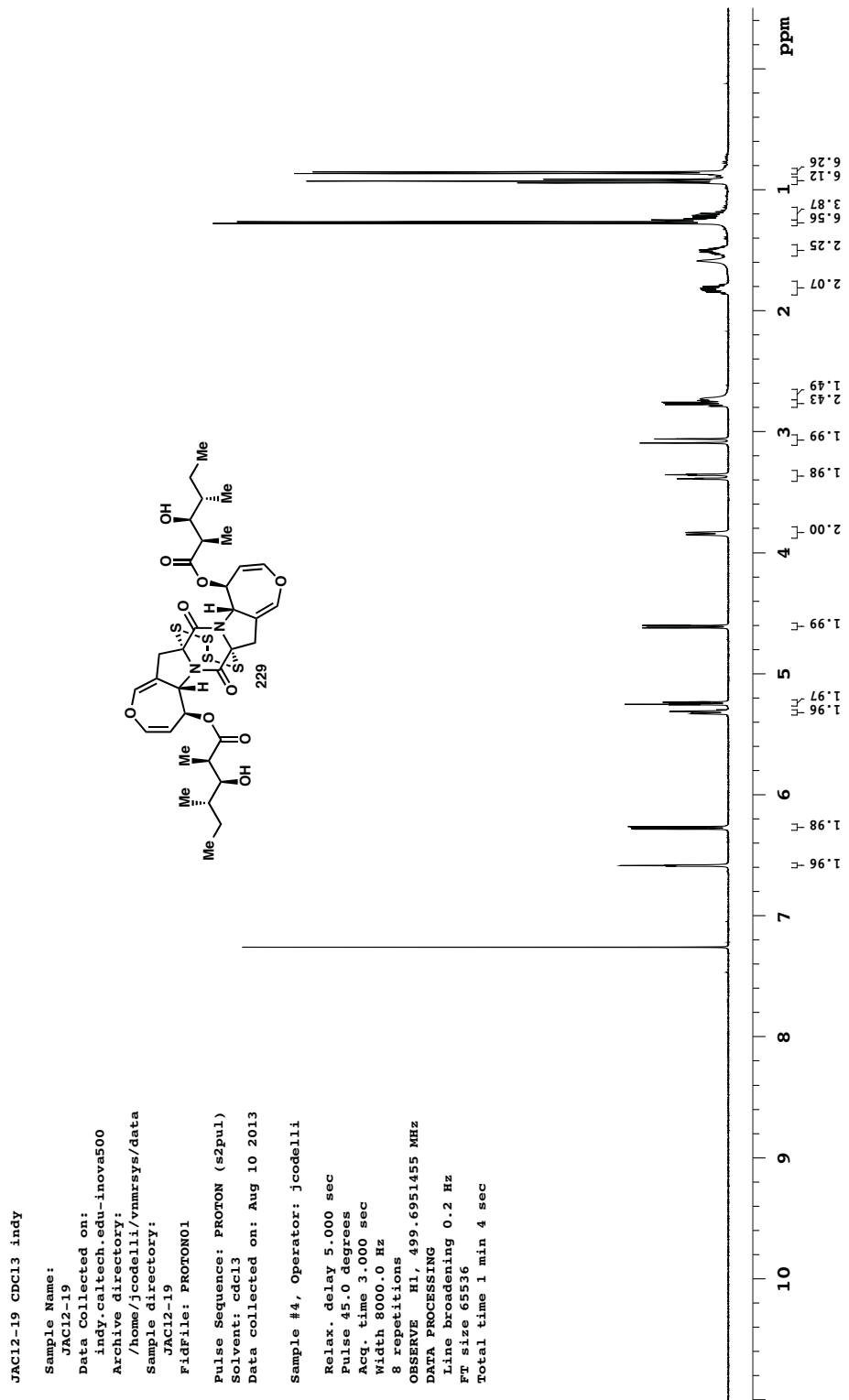


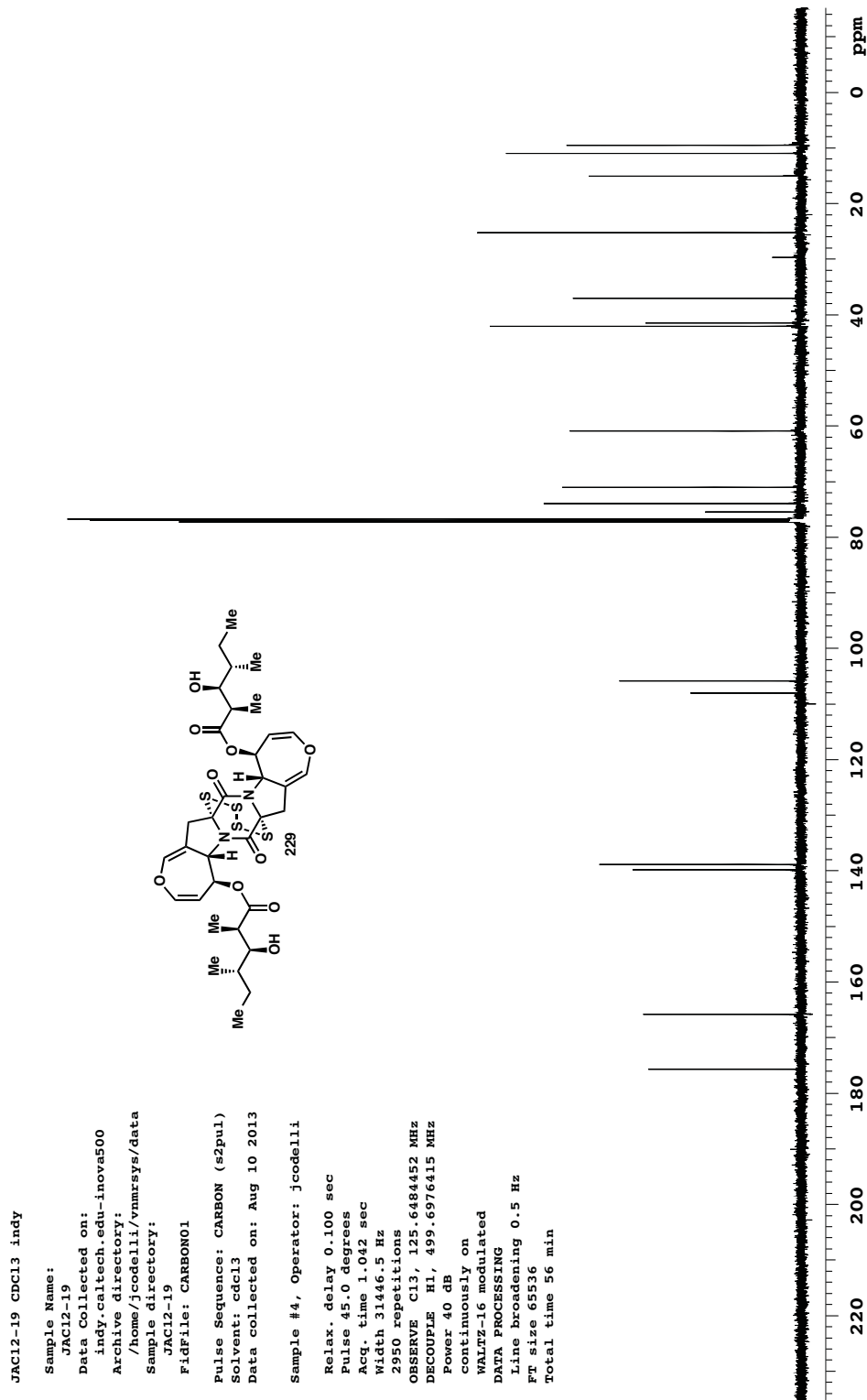


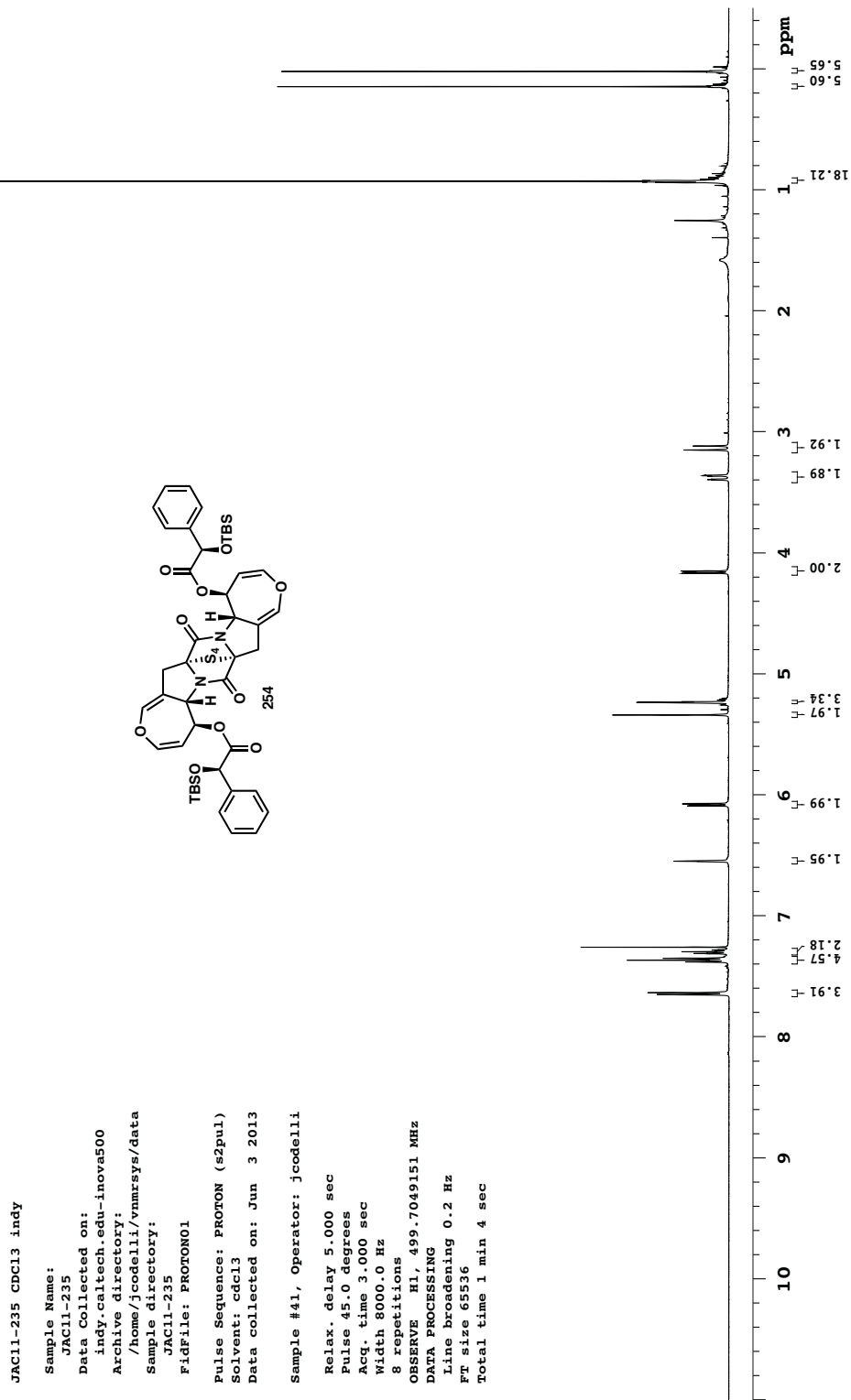


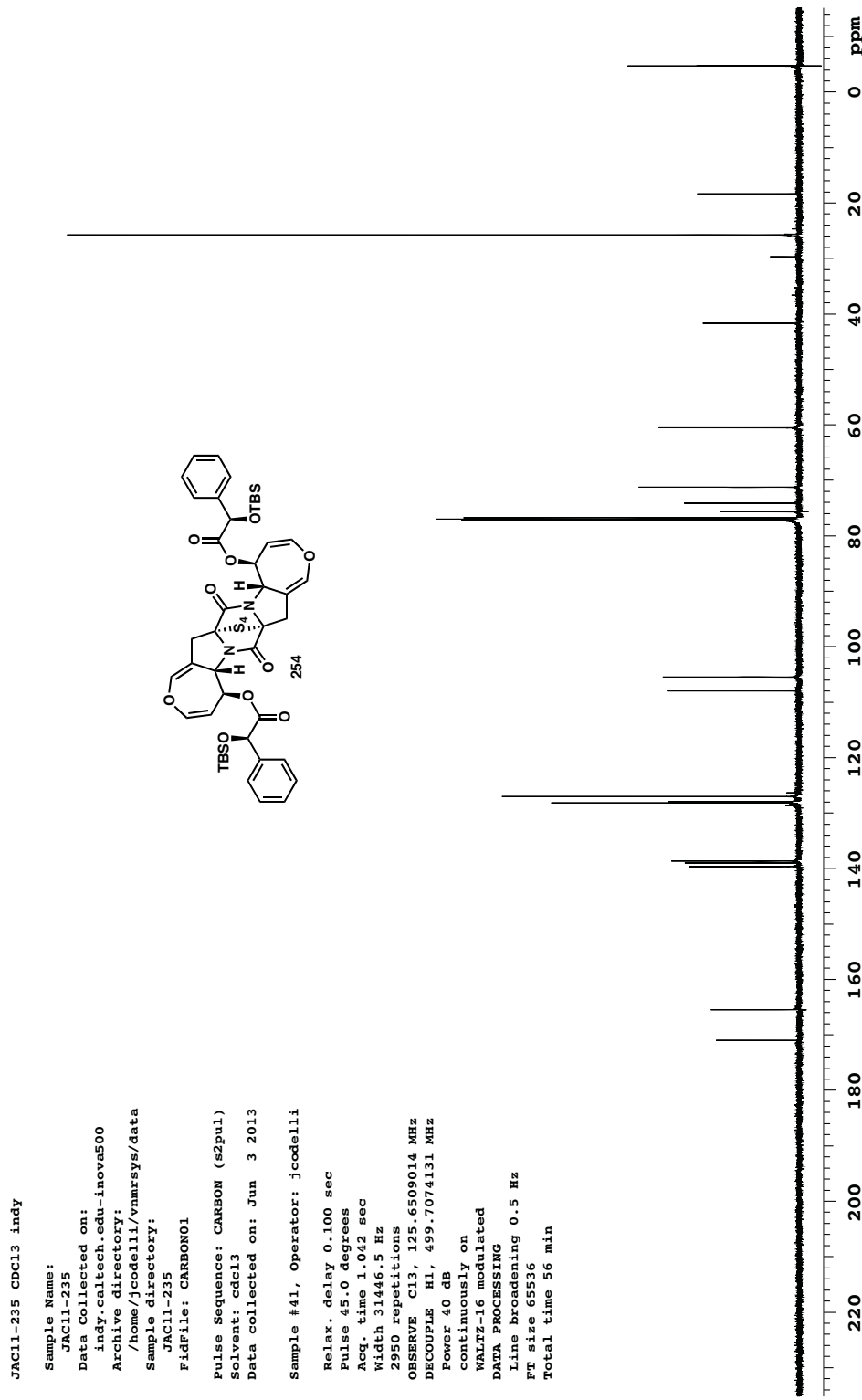


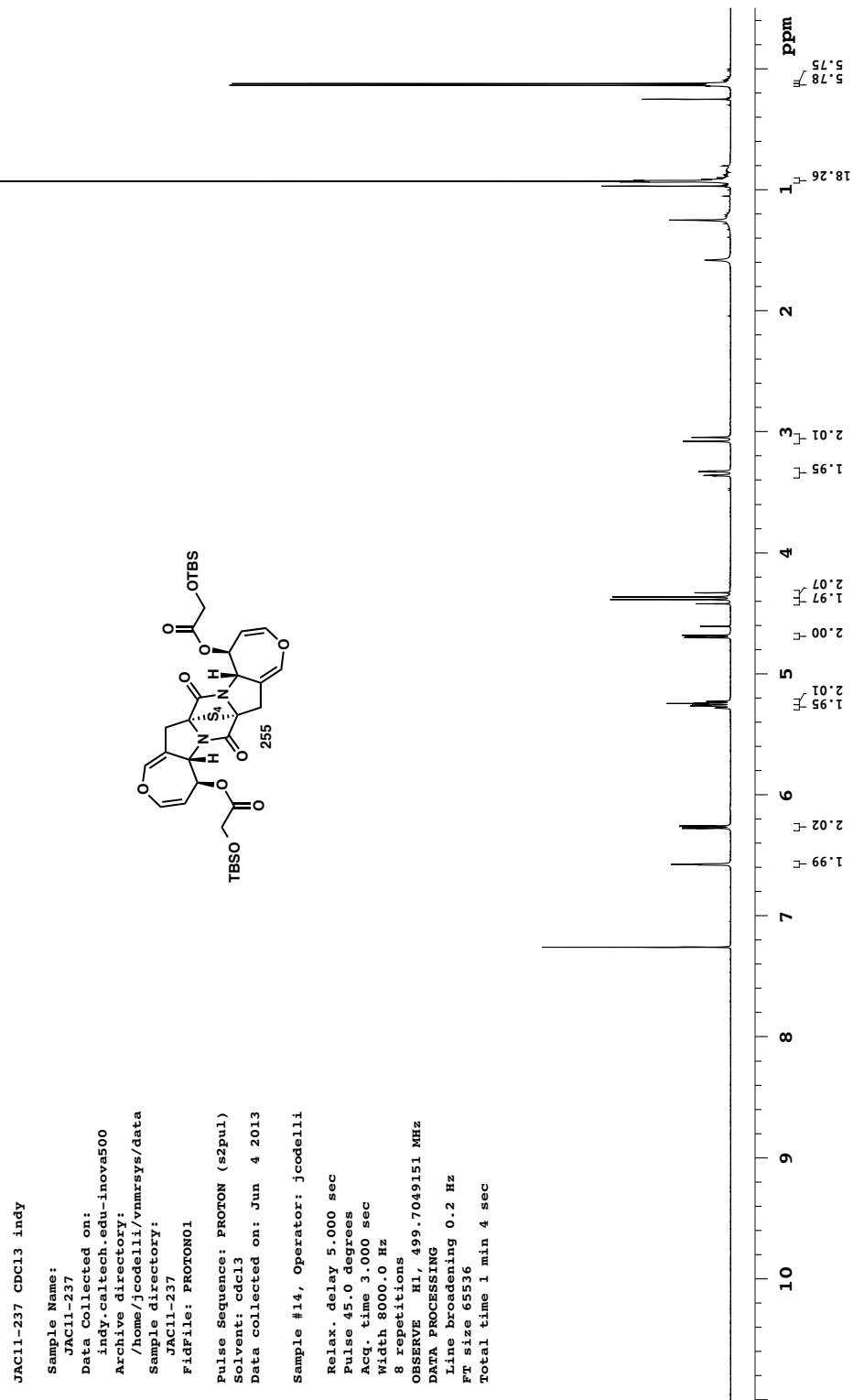


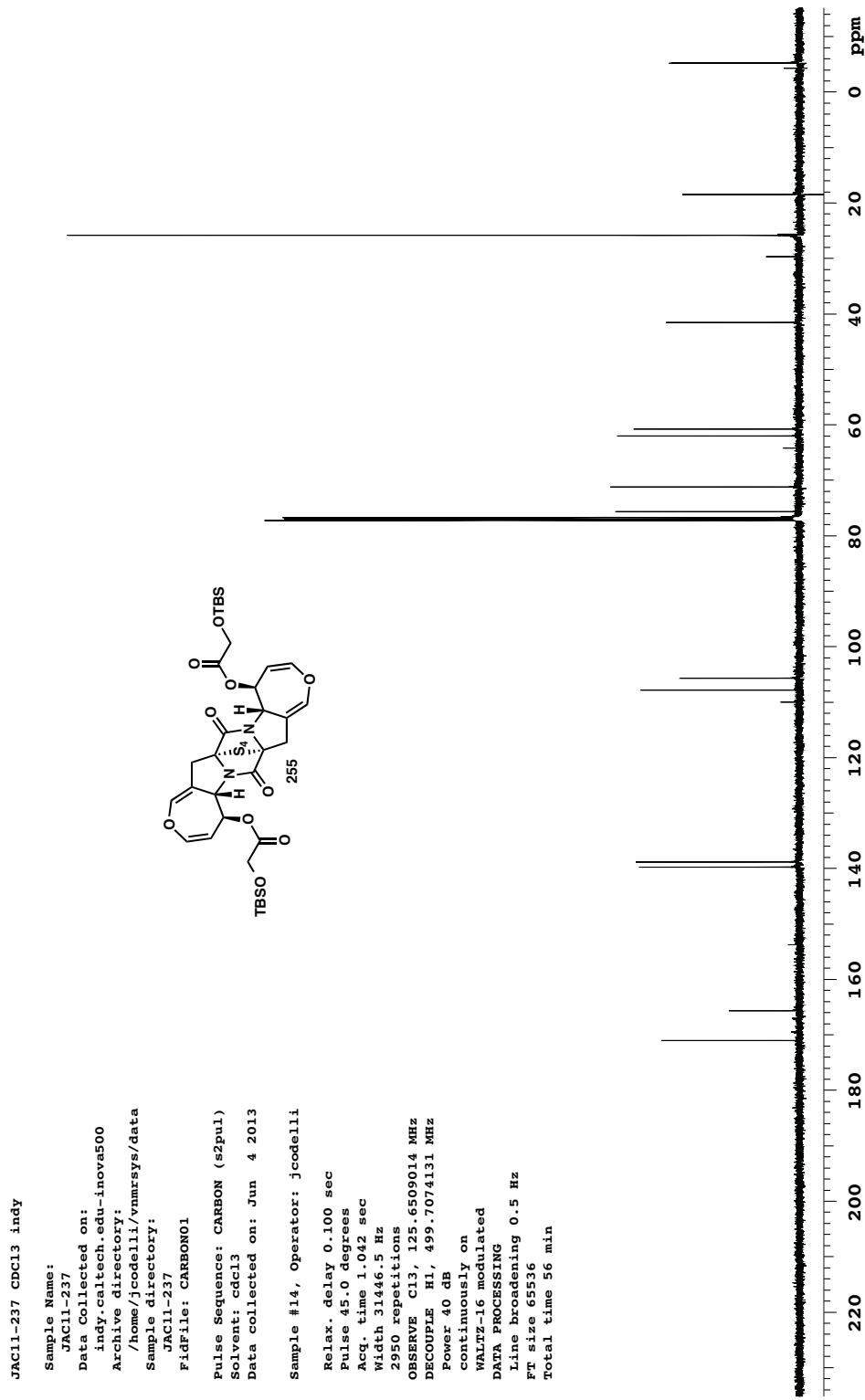


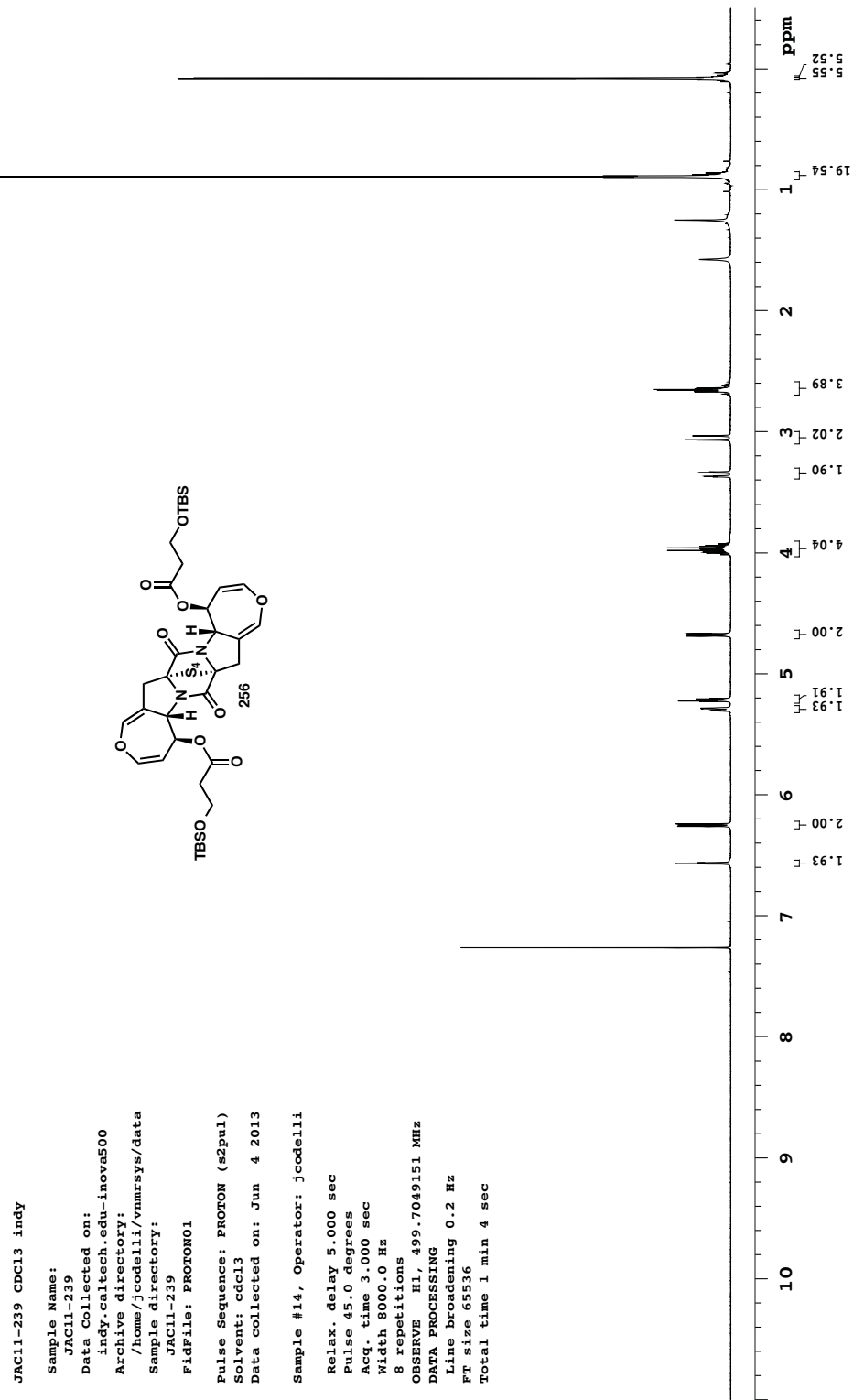


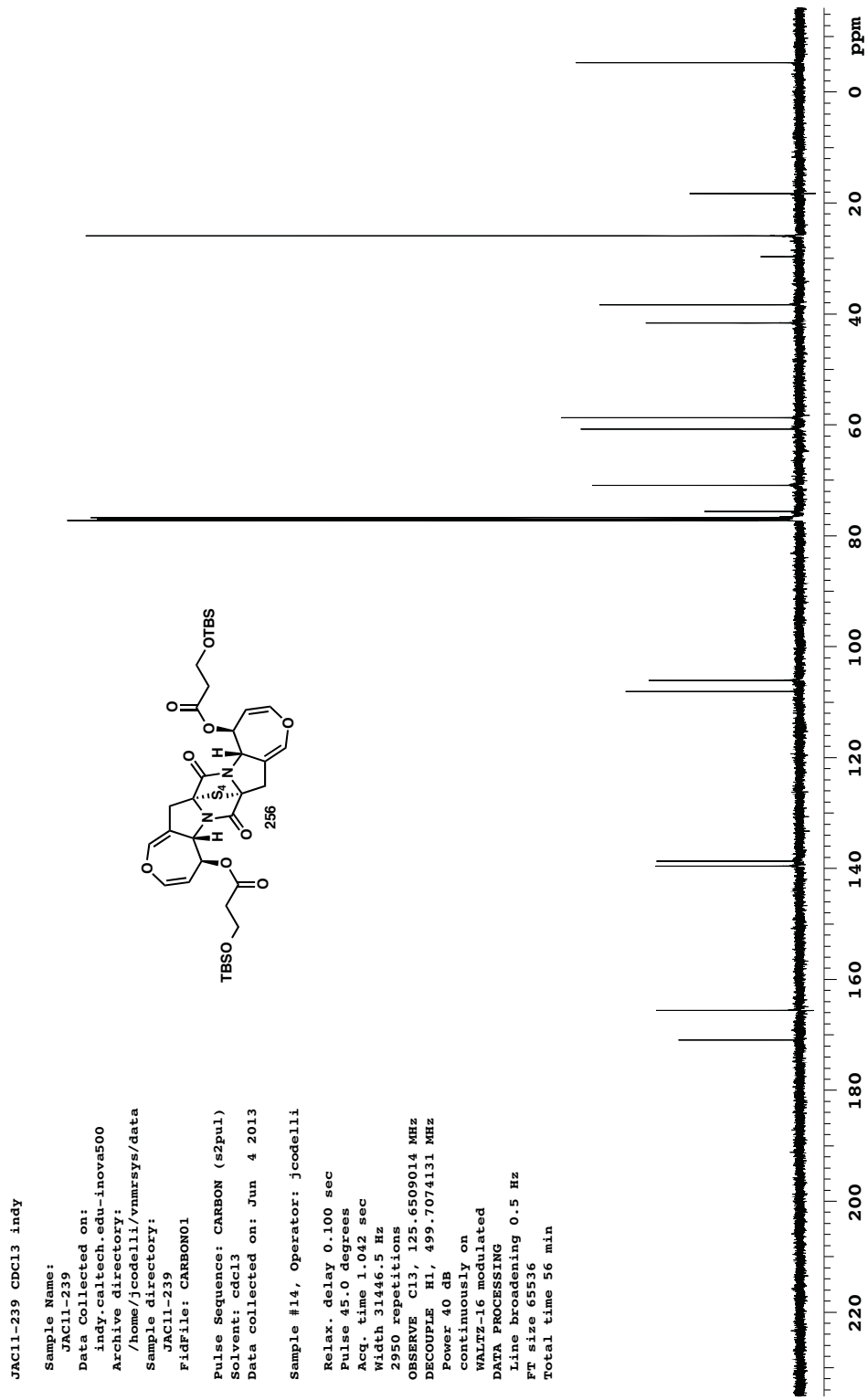


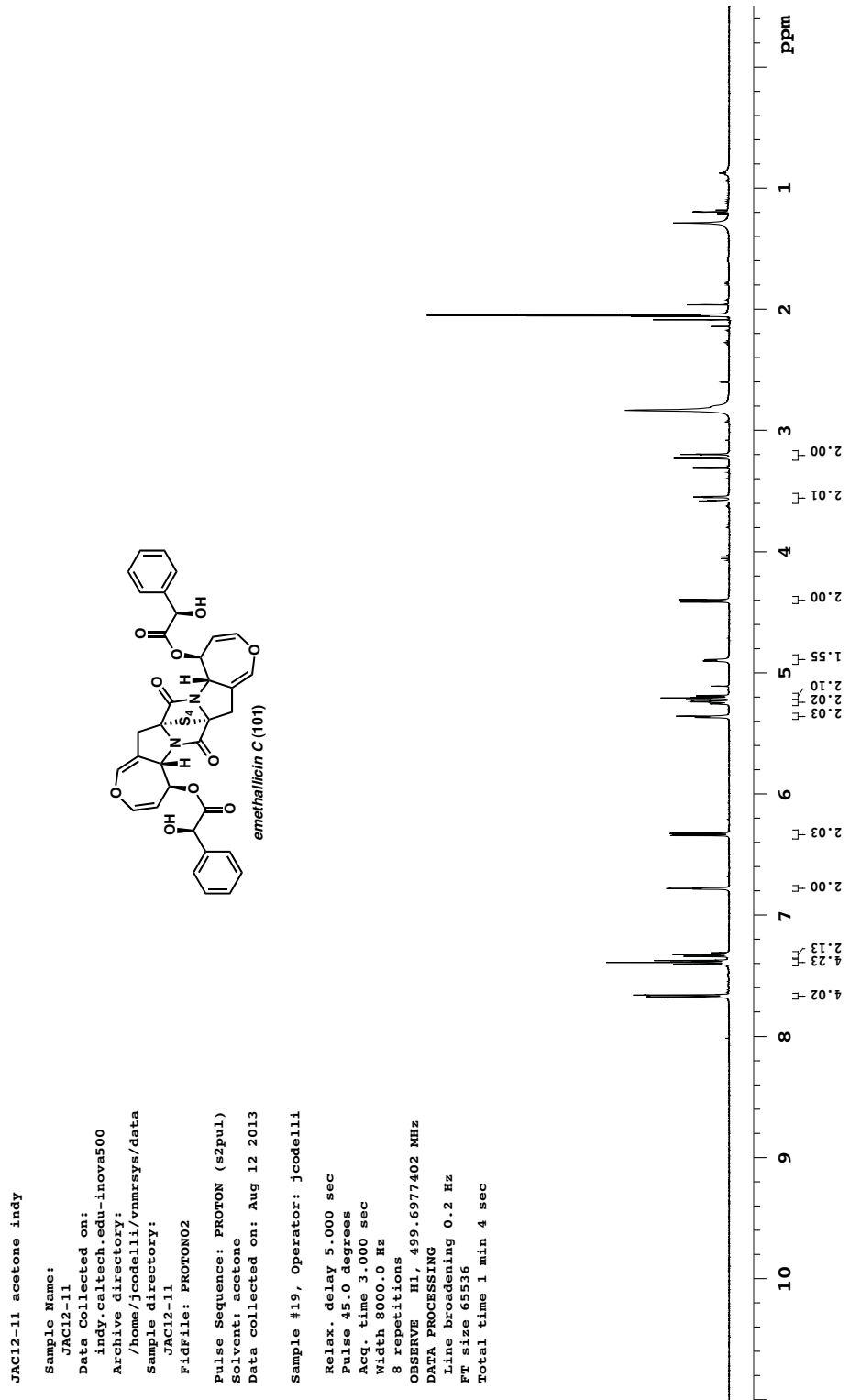


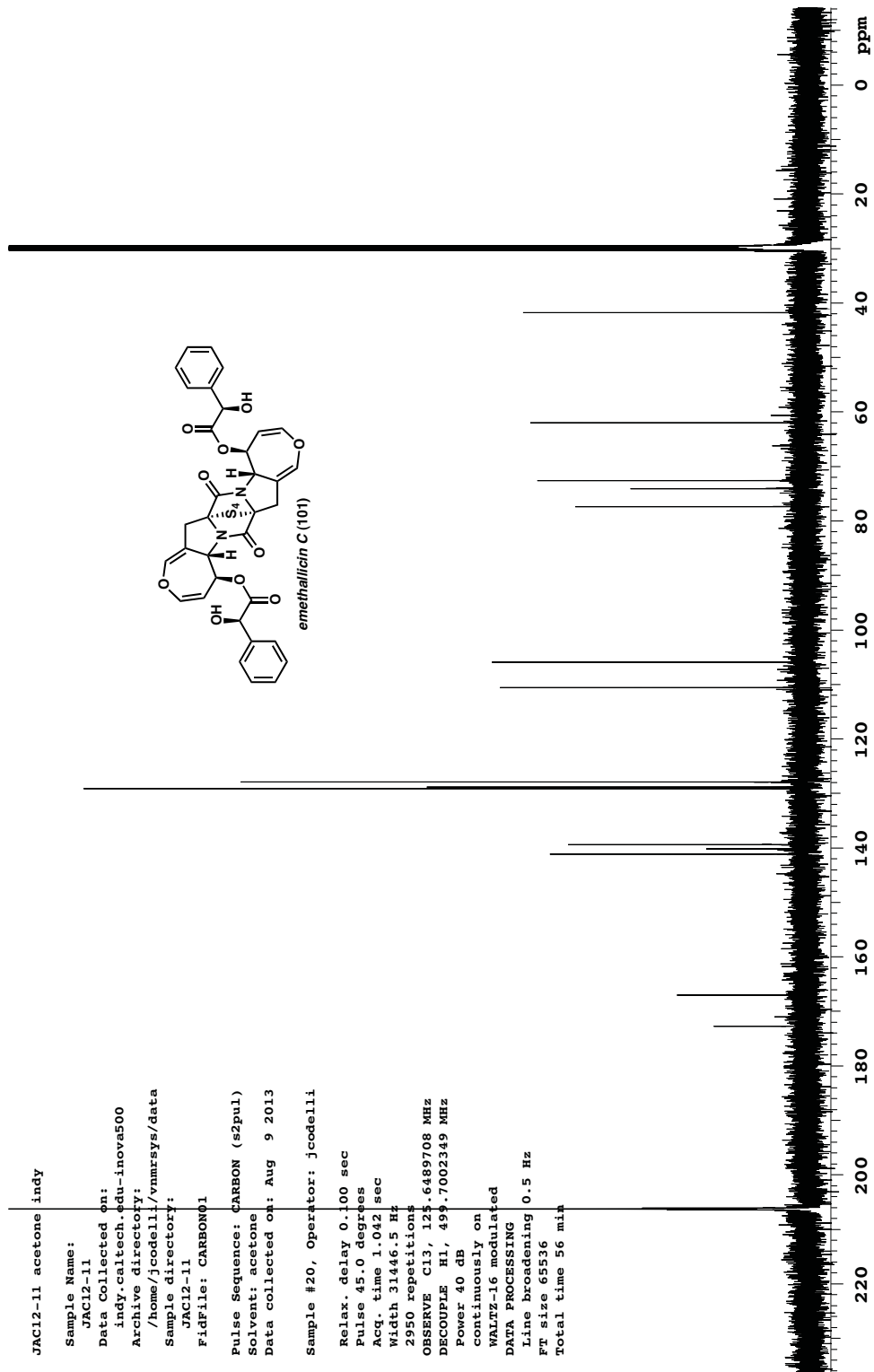


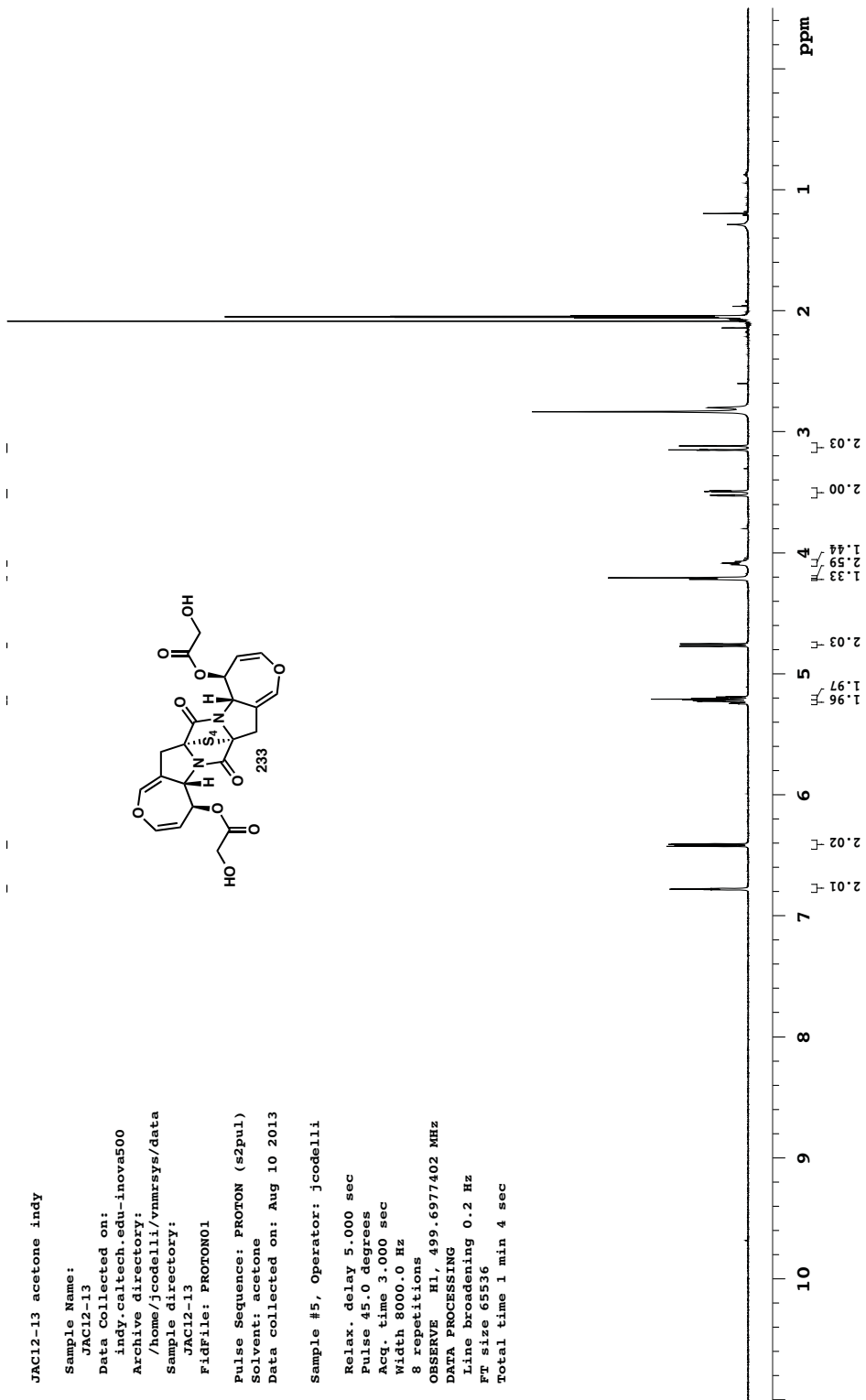


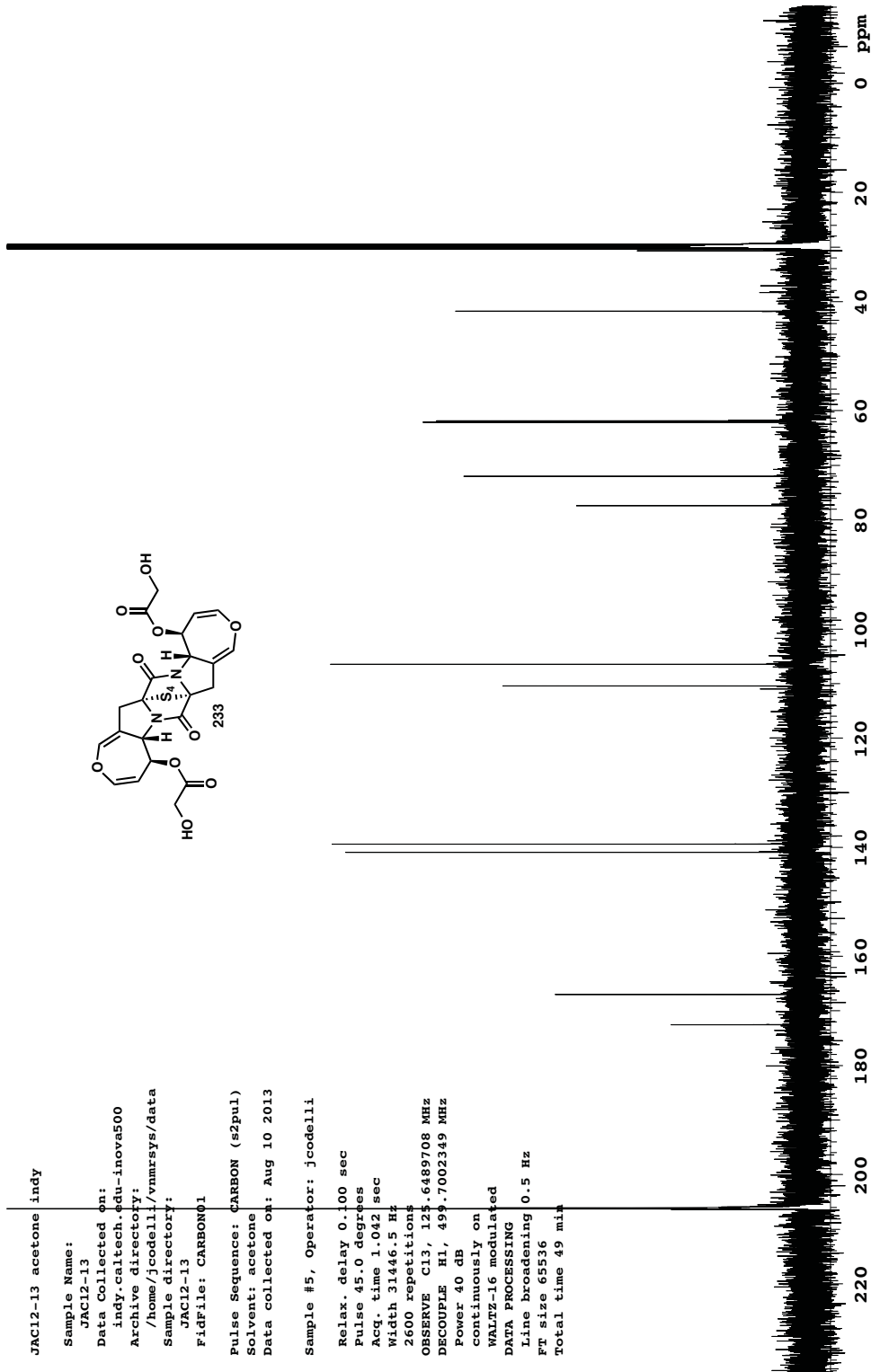


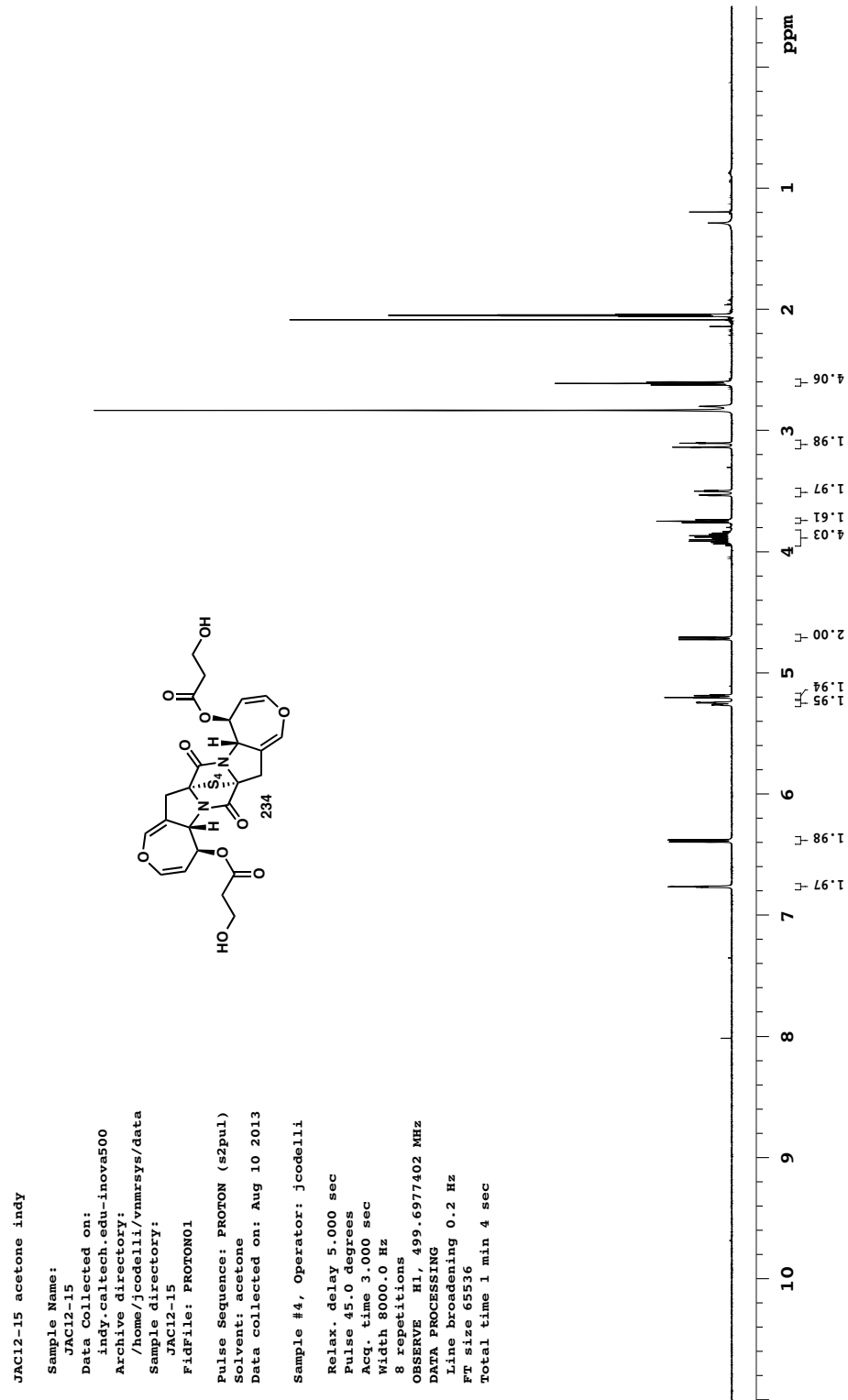


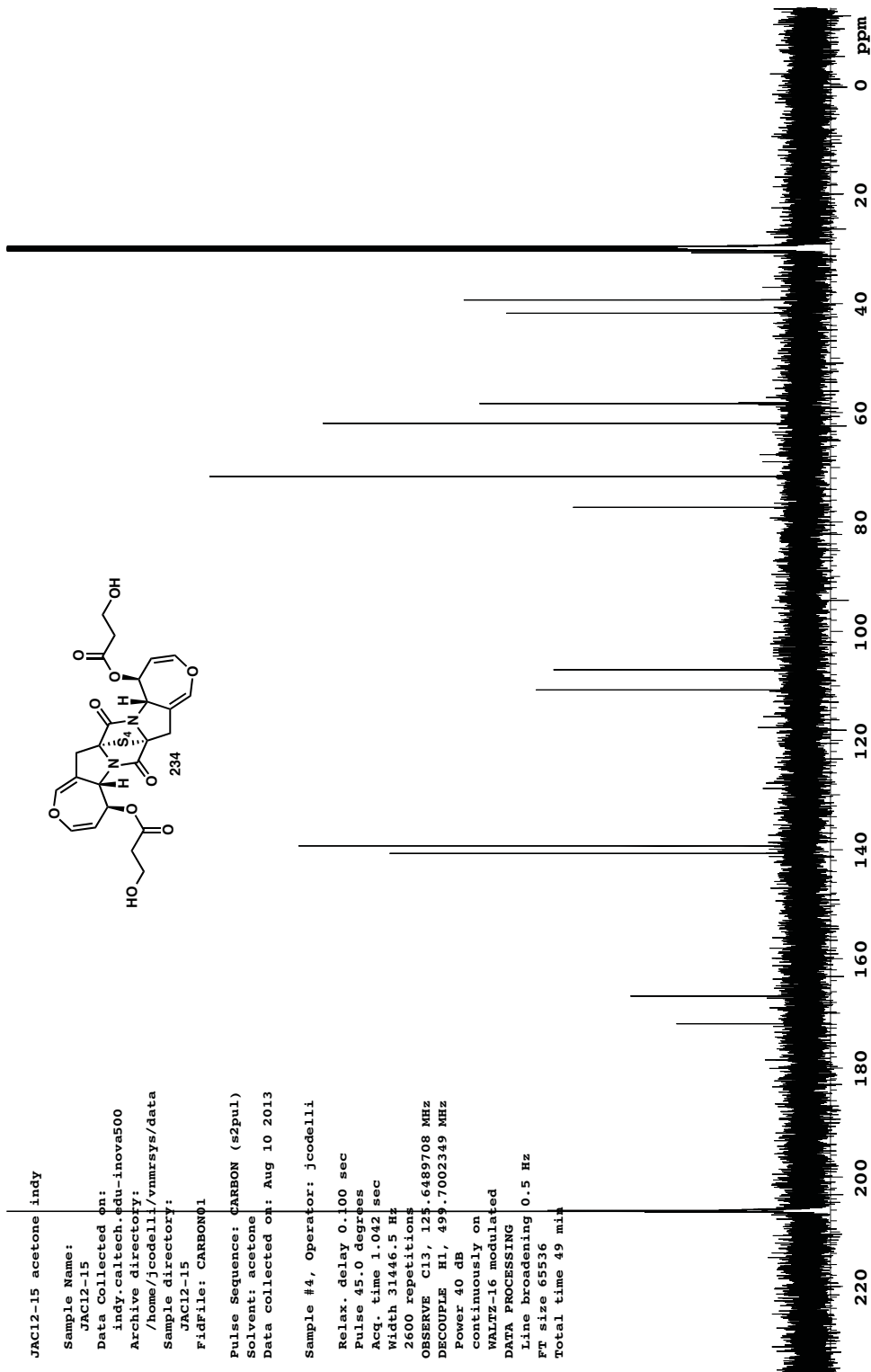


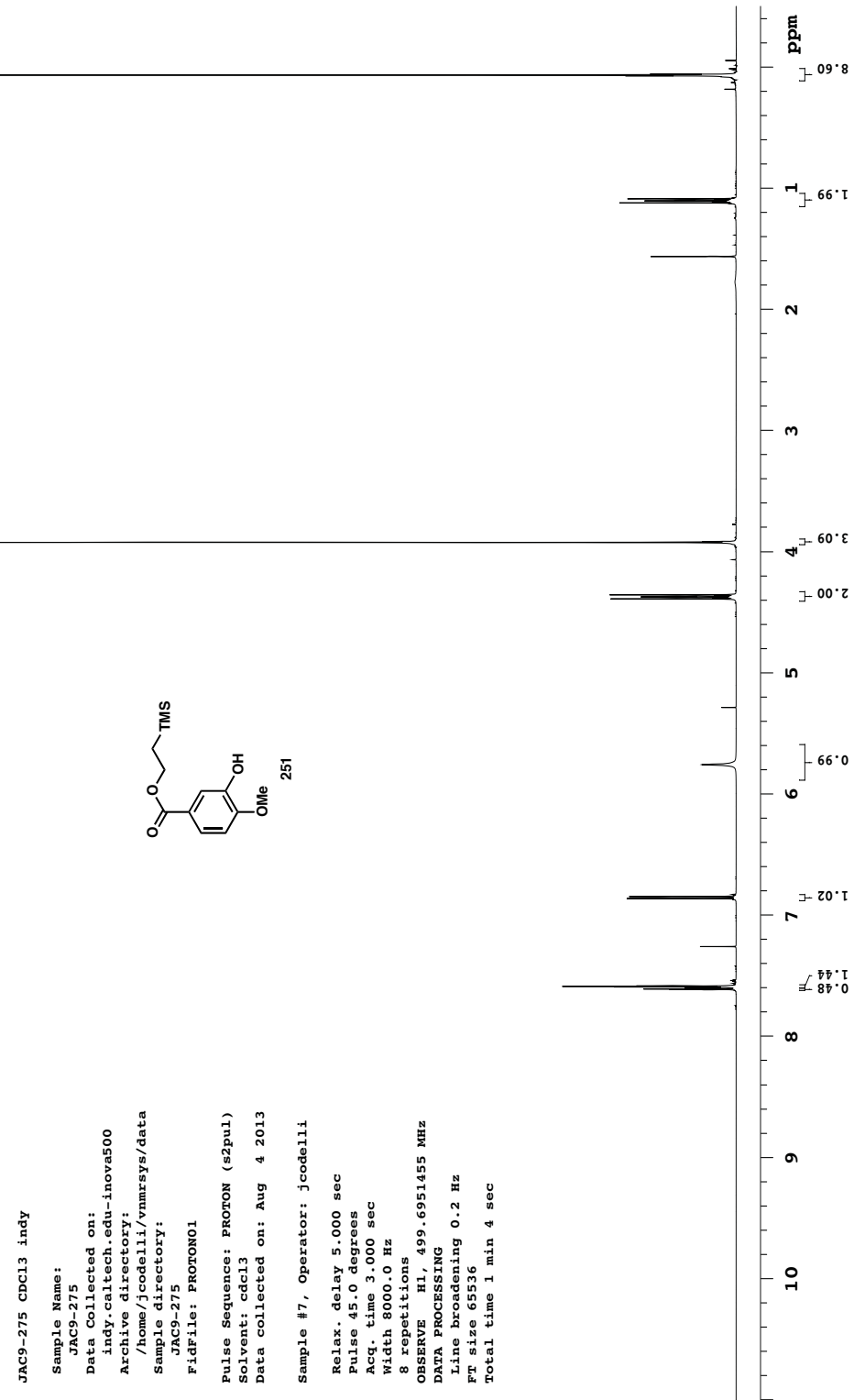


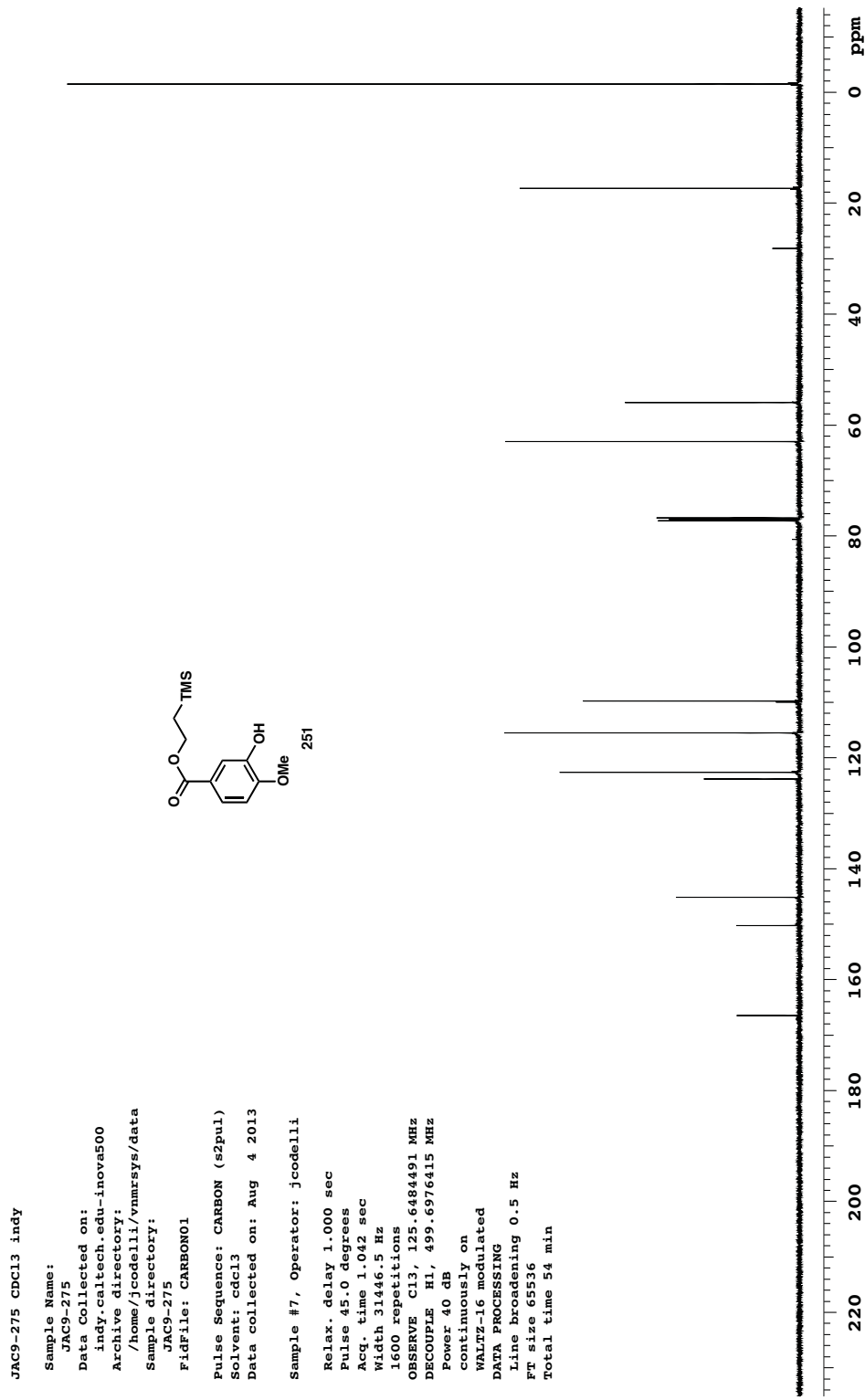


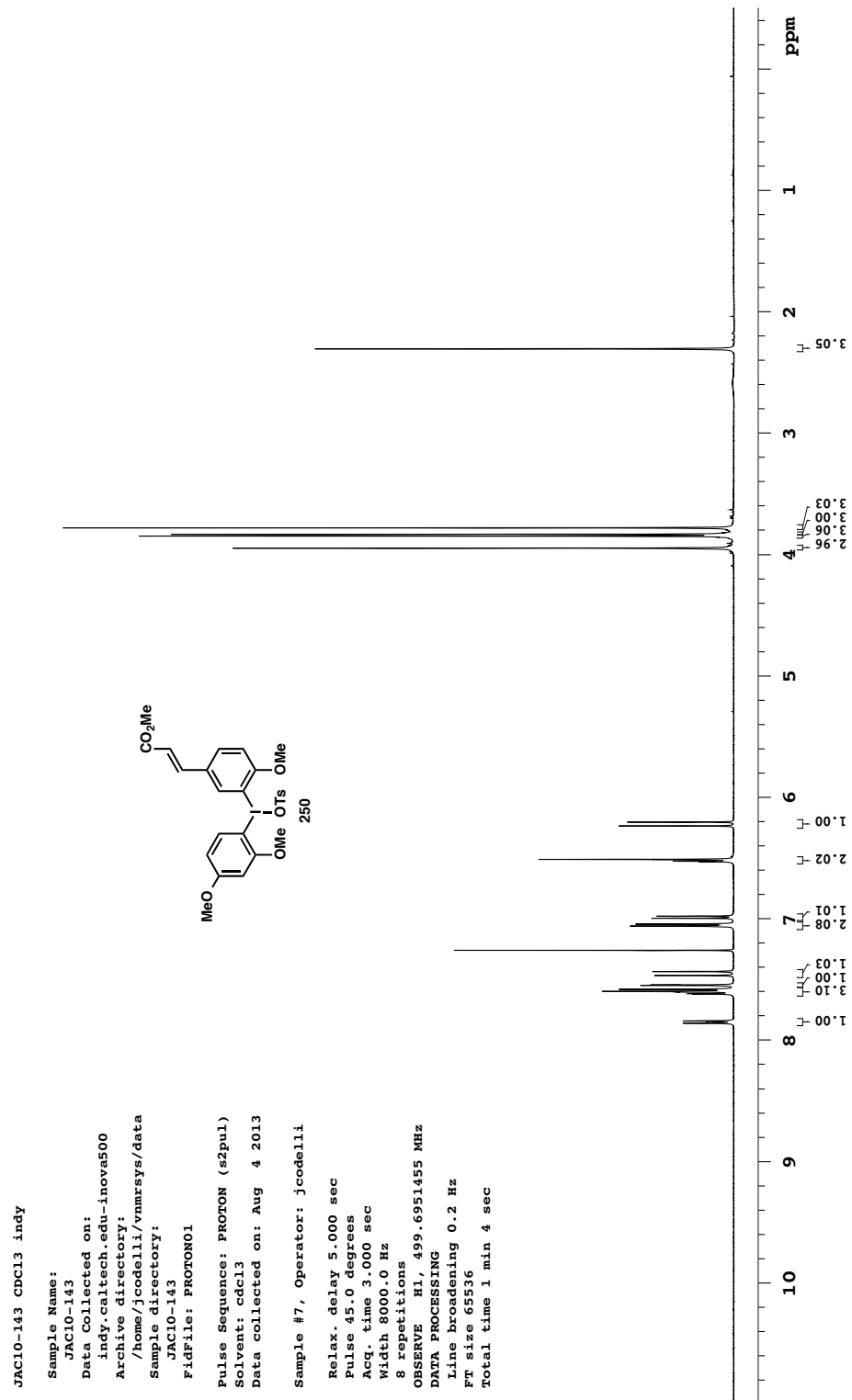


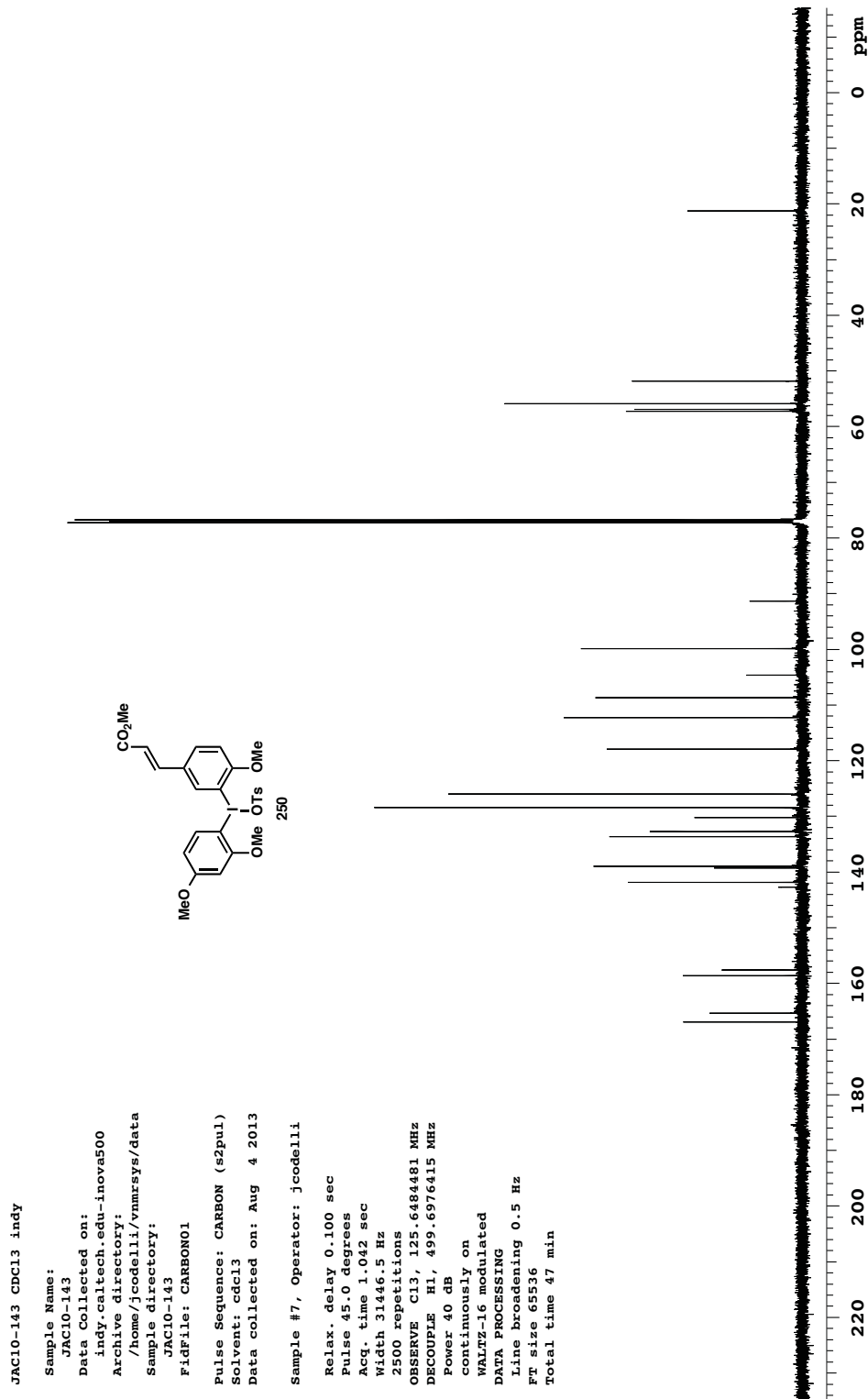


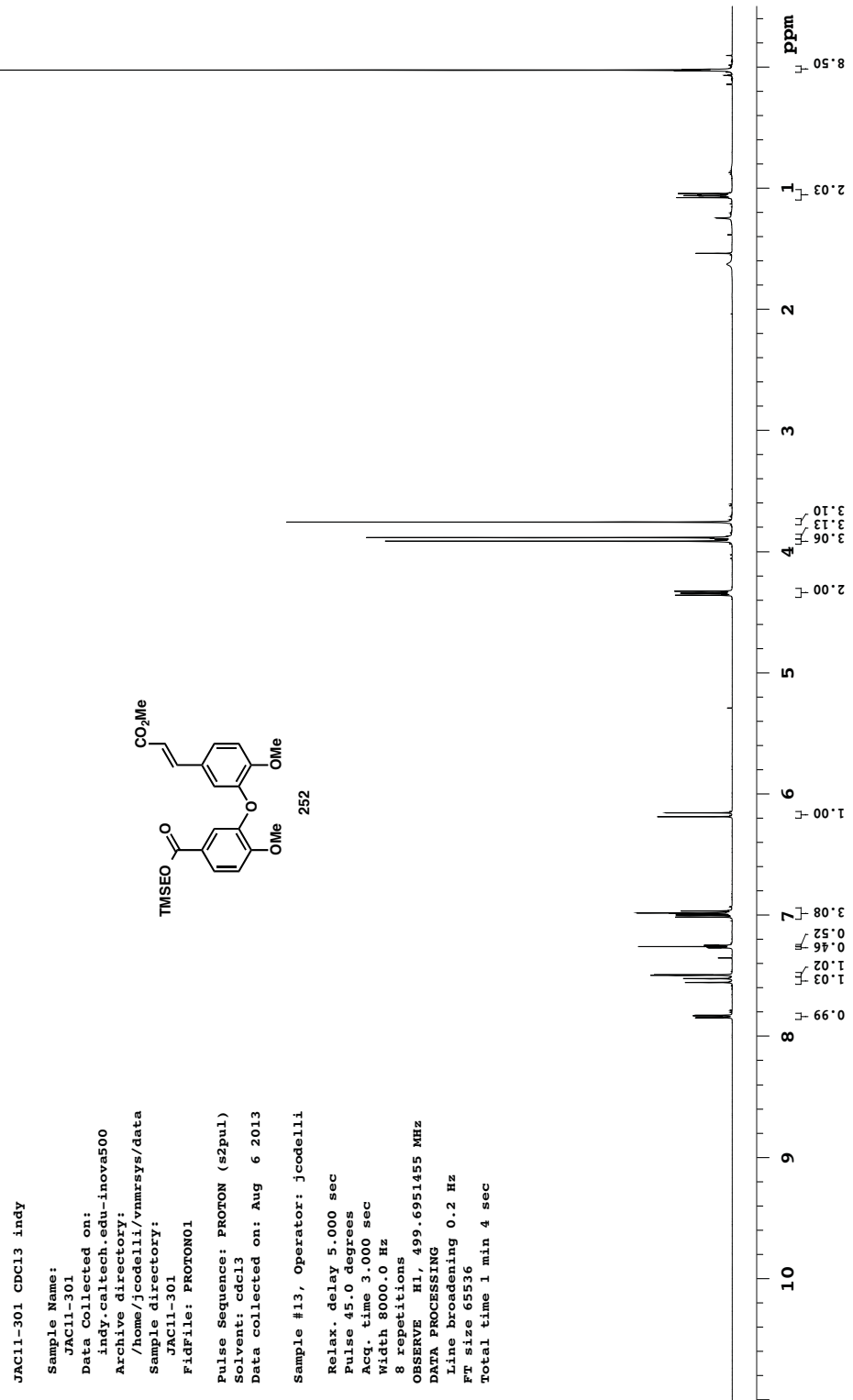


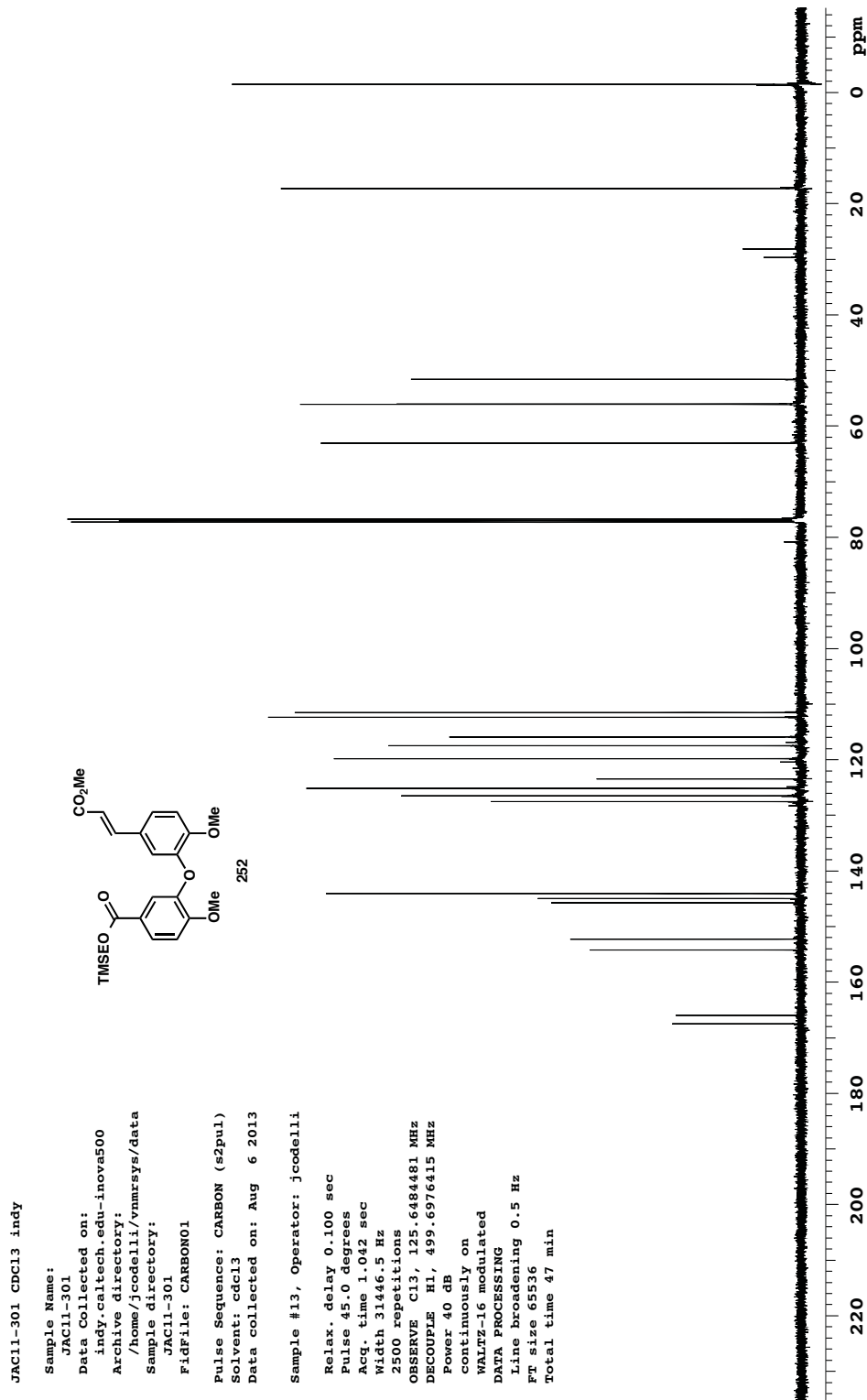












Chapter 4

Further Investigation of Side Reactions[†]

4.1 INTRODUCTION

One of the goals of any total synthesis research program is the discovery and development of new chemical reactions. This can occur either via the design of a novel transformation with a particular structural target in mind, *or* via the serendipitous observation of unintended yet interesting reactivity. Our synthetic studies toward acetylaranotin (**11**) required the development of several key transformations, such as the chlorohydrin cycloisomerization/elimination sequence for constructing the dihydrooxepine ring (see Chapter 2).¹ Furthermore, we observed several notable side reactions over the course of our efforts; in addition to the fluoride-promoted C–H oxidation mentioned in Chapter 2, we also observed a cascade cycloaddition process during our optimization of the enantioselective (1,3)-dipolar cycloaddition (1,3-DCA)

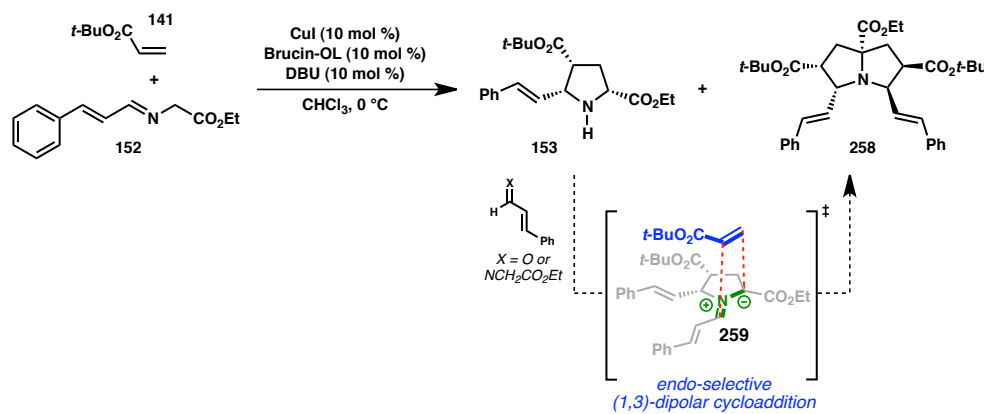
[†] Part of this chapter was published as the following communication: Lim, A. D.; Codelli, J. A.; Reisman, S. E. *Chem. Sci.* **2013**, 4, 650. The research discussed in this chapter was completed in collaboration with Andrew D. Lim, a graduate student in the Reisman Lab.

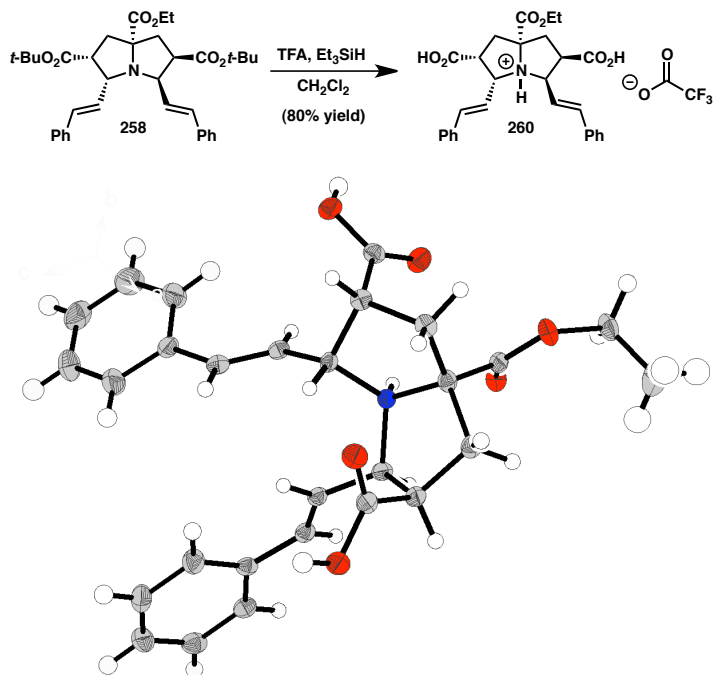
that initiates our synthetic route. Though these reactions were not productive with respect to our total synthesis efforts, our curiosity prompted the further investigation of their scope and mechanism.

4.2 AN ENANTIOSELECTIVE CASCADE CYCLOADDITION PROCESS TO FORM HIGHLY SUBSTITUTED PYRROLIZIDINES

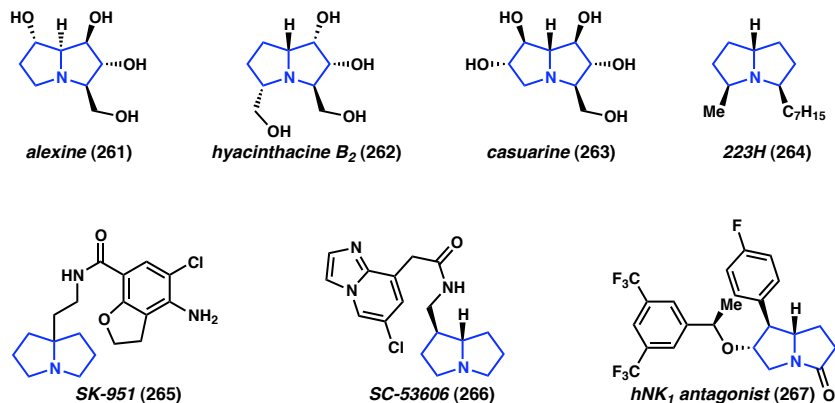
During studies aimed at optimizing the (1,3)-dipolar cycloaddition reaction utilized to prepare pyrrolidine **153** for the synthesis of acetylaranotin, we observed that under sub-optimal conditions the reaction stalls and a significant amount of pyrrolizidine **258** is isolated (Scheme 4.1). The structure of **258** was confirmed by single-crystal X-ray diffraction analysis of the corresponding TFA salt **260** (Scheme 4.2). We hypothesized that this product was being formed via a second (1,3)-dipolar cycloaddition, in which the initial pyrrolidine product **153** condenses with an equivalent of cinnamaldehyde or cinnamaldimine **152** to give ylide **259**, which then undergoes further reaction with *tert*-butyl acrylate to produce the final product (**258**).^{2,3}

Scheme 4.1. Observed formation of pyrrolizidine **258** during optimization of the Cu-catalyzed 1,3-dipolar cycloaddition

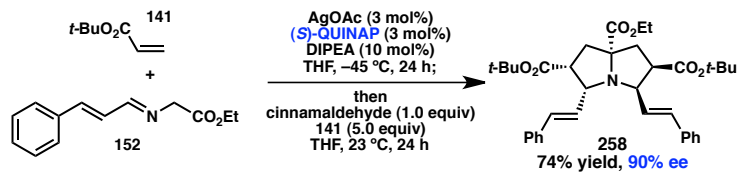


Scheme 4.2. Formation and X-ray crystal structure of TFA salt **260**

Given the presence of the pyrrolizidine ring system in a variety of bioactive natural products and pharmaceutical agents (see Figure 4.1),⁴ as well as the general lack of methods for the rapid enantioselective preparation of highly substituted pyrrolizidine derivatives,⁵ we sought to further develop this reaction, investigate its scope, and explore the subsequent reactivity of the resulting products.

Figure 4.1. Pyrrolizidine-containing natural products and pharmaceutical agents

In our initial survey of conditions for the enantioselective (1,3)-dipolar cycloaddition reaction to produce pyrrolidine **153**,^{6,7} we had identified the CuI/Brucin-OL catalyst system⁸ as optimal for the scalable preparation of **153**. On the other hand, the operational simplicity of the AgOAc/(S)-QUINAP catalyst conditions⁹ prompted us to use this system for investigations of pyrrolizidine formation.¹⁰ Following preliminary experimentation, we were pleased to find that treatment of a mixture of cinnamaldehyde-derived α -imino ester **152**, AgOAc (3 mol %), QUINAP (3 mol %) and DIPEA (10 mol %) with *tert*-butyl acrylate (**141**, 1.5 equiv) in THF at $-45\text{ }^\circ\text{C}$ for 24 h, followed by addition of cinnamaldehyde (1.0 equiv) and additional **141** (5.0 equiv) with warming to $23\text{ }^\circ\text{C}$ provided pyrrolizidine **258** in 74% yield and 90% *ee* (Scheme 4.3).^{11,12} Notably, warmer temperatures are required for the second (1,3)-DCA, which proceeds very slowly at $-45\text{ }^\circ\text{C}$. It is important that imine **152** is consumed before the reagents are added for the second cycloaddition; if **152** remains, it reacts rapidly and less selectively with *tert*-butyl acrylate upon warming to give **153**,¹³ which can lead to the isolation of pyrrolizidine **258** in reduced *ee*.

Scheme 4.3. Optimized conditions for preparation of pyrrolizidine **258**

With conditions in hand to prepare pyrrolizidine **258** in good yield and high *ee*, attention turned to evaluating the substrate scope of the reaction (Table 4.1). A variety of substituted aryl aldehyde-derived α -imino esters **268** furnished the corresponding pyrrolizidines **269** in good yields with high enantioselectivity. Substitution at the *ortho*-, *meta*-, and *para*-positions of the arene with both electron-donating and electron-withdrawing substituents is well-tolerated. In particular, α -imino esters bearing electron-withdrawing aryl substituents provide the pyrrolizidine products with uniformly high levels of enantioselectivity (Table 4.1, **269f–j**, **269m–o**). Notably, the α -imino ester derived from pyridine 3-carboxaldehyde is a suitable substrate, providing pyridyl-substituted pyrrolizidine **269r** in good yield and good *ee* (Entry 18). Alternatively, the 2-pyridyl α -imino ester provided pyrrolizidine **269s** in low yield and modest *ee* (Entry 19). It is possible that the proximal nitrogen results in an alternative binding mode between the azomethine ylide and the catalyst, decreasing the enantioselectivity during the first (1,3)-DCA.¹⁴ In addition, the pyrrolidine intermediate or the pyrrolizidine product (**269s**) might bind to and inhibit the silver catalyst.

Table 4.1. Substrate scope for catalytic asymmetric synthesis of highly substituted pyrrolizidines: α -imino ester

entry **---R** **yield^a ee^b (%) (%)** **entry** **---R** **yield^a ee^b (%) (%)** **entry** **---R** **yield^a ee^b (%) (%)**

1	269a		90	91	7	269g		91	95	14	269n		89	93
2	269b		91	91	8	269h		89	92	15	269o		82	92
3 ^c	269c		83	88	9	269i		70	96	16 ^d	269p		76	92
4 ^c	269d		82	92	10	269j		80	96	17 ^c	269q		84	93
5 ^c	269e		78	88	11 ^d	269k		86	90	18	269r		90	90
6	269f		87	93	12	269l		72	90	19	269s		33	44
					13	269m		87	94					

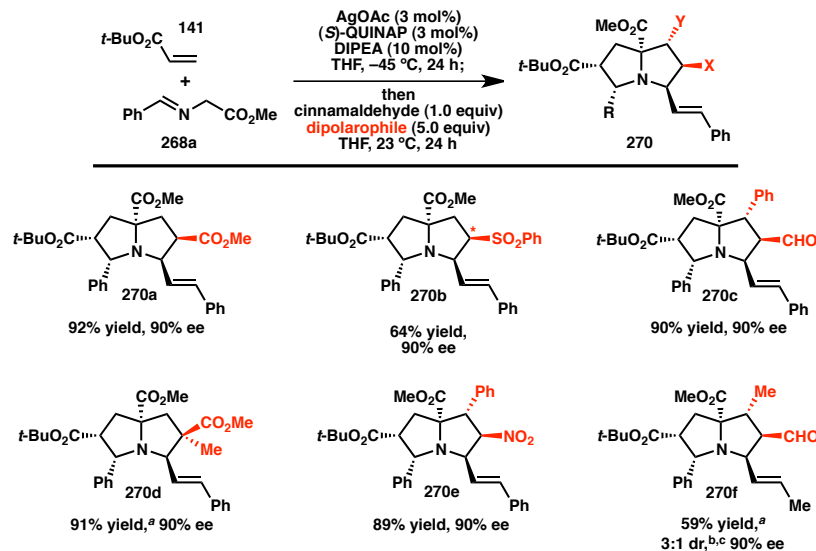
^a Isolated yield. ^b Determined by SFC using chiral stationary phase. ^c 6 mol % each AgOAc and (S)-QUINAP were employed.^d 6 mol % each AgOAc and (S)-QUINAP were employed at 0.1 M reaction concentration.

In some cases, the pyrrolizidine products were obtained in lower *ee* using our standard reaction conditions (e.g. compounds **269c–e**, **269q**).¹⁵ It was determined that for these α -iminoesters, the first (1,3)-DCA proceeds slowly relative to the more electron-poor substrates; we reasoned that the remaining imine reacts with lower enantioselectivity upon warming, which ultimately results in the formation of the pyrrolizidine with reduced *ee*. We hypothesized that increasing the catalyst loading should ensure complete consumption of the α -imino ester prior to warming the reaction for the second (1,3)-DCA. This hypothesis proved to be true; using 6 mol % each of AgOAc and (S)-QUINAP, pyrrolizidines **269c–e** and **269q** were obtained in good yields and high *ee* (Table 4.1, Entries 3, 5, 11 and 17). Alternatively, the solubility of *p*-

methoxy and 2-naphthyl α -iminoesters **268k** and **268p** was poor under our standard conditions; for these substrates the best results were obtained by lowering the overall reaction concentration (to 0.1 M versus 0.3 M) and increasing the catalyst loading to 6 mol %.

A variety of dipolarophiles can be used for the second (1,3)-DCA (Table 4.2). For example, use of *E*-1-nitro-2-phenylethylene as the second dipolarophile provides pyrrolizidine **270e** in 89% yield and 90% *ee*. This compound contains six stereogenic centers and is isolated as a *single* diastereomer. Use of methyl methacrylate provides pyrrolizidine **270d**, which contains an all-carbon quaternary center, in 91% yield and 90% *ee*.

Table 4.2. Substrate scope for catalytic asymmetric synthesis of highly substituted pyrrolizidines: second dipolarophile



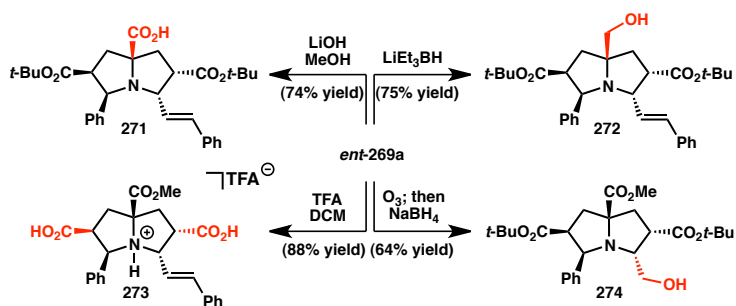
^a 10.0 equivs of dipolarophile were used. ^b For this reaction, crotonaldehyde was used instead of cinnamaldehyde. ^c Refers to *endo/exo* selectivity of the second (1,3)-DCA reaction.

Interestingly, α,β -unsaturated aldehydes appear to be uniquely well suited for generating the pyrrolidine-derived azomethine ylide for the second (1,3)-DCA. Attempts

to employ aryl aldehydes (e.g. benzaldehyde) or alkyl aldehydes (e.g. 2-ethylbutyraldehyde) for the second (1,3)-DCA failed to provide the pyrrolizidine products in synthetically useful yields (see Experimental Section). We believe this unique reactivity of α,β -unsaturated aldehydes explains why standard catalytic, asymmetric (1,3)-DCAs are not plagued by unwanted pyrrolizidine formation, since α -imino esters derived from enals are rarely employed in methods development.

Using benzaldehyde-derived α -imino ester **268a**, the catalytic asymmetric (1,3)-DCA cascade reaction has been conducted on gram-scale, providing pyrrolizidine *ent*-**269a**¹⁶ in 89% yield and slightly diminished *ee* (87%).¹⁷ Importantly, this compound can be selectively modified to give several intermediates capable of further derivitazation (Scheme 4.4). For example, the more reactive and accessible methyl ester of *ent*-**269a** can be selectively saponified using LiOH or reduced using LiEt₃BH to give carboxylic acid **271** or alcohol **272**, respectively. Alternatively, the *tert*-butyl esters can be cleaved upon treatment with trifluoroacetic acid (TFA) to give dicarboxylic acid **273**. Finally, the styrene of *ent*-**269a** can be ozonolytically cleaved and reduced *in situ* to provide amino alcohol **274** in 64% yield. Thus, each of the functional groups of *ent*-**269a** can be chemoselectively modified.

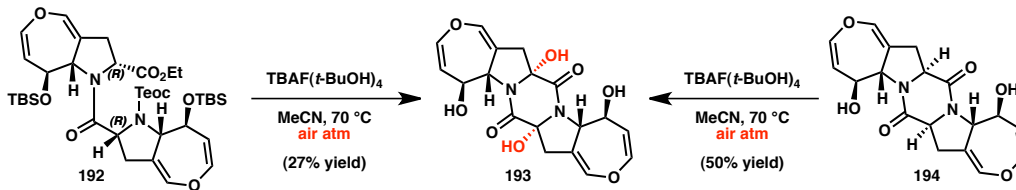
Scheme 4.4. Selective derivatization of pyrrolizidine *ent*-**269a**



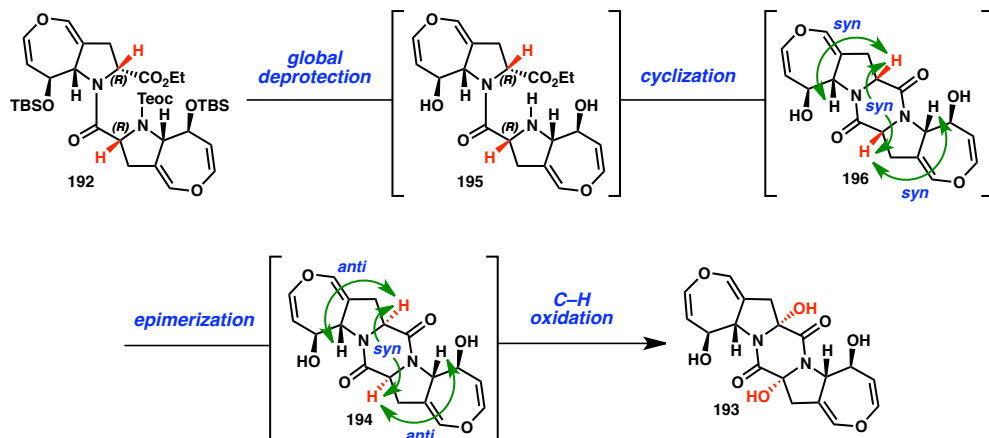
4.3 DIKETOPIPERAZINE OXIDATION AND STEREOCHEMISTRY

During studies aimed at the preparation of diketopiperazine **194** for the synthesis of acetylalaranotin (**11**), we observed the formation of tetraol **193** when dipeptide **192** was treated with $\text{TBAF}\bullet(t\text{-BuOH})_4$ in MeCN at 70 °C under an *air* atmosphere (see Scheme 4.5, also see Chapter 2).¹⁸ Furthermore, isolation of diketopiperazine **194** and resubjection to the above aerobic conditions provided the same oxidation product **193**. Based on these results, we tentatively proposed the mechanistic hypothesis shown in Scheme 4.6. First, fluoride-promoted global desilylation of **192** provides deprotected dipeptide **195**, which cyclizes to give the expected *syn,syn,syn* diketopiperazine **196**. Subsequent epimerization to the *anti,syn,anti* configuration affords the observed diketopiperazine **194**. Finally, *stereoretentive* aerobic oxidation of **194** then furnishes the tetraol **193**.

Scheme 4.5. Formation of dihydroxylated diketopiperazine **193**



Scheme 4.6. Proposed $\text{TBAF}\bullet(t\text{-BuOH})_4$ -promoted diketopiperazine formation/oxidation sequence

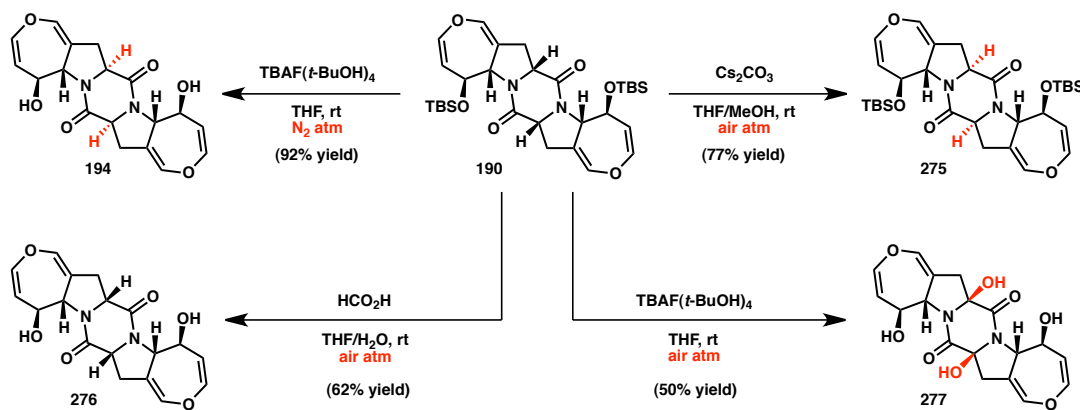


Such O₂-mediated α -oxidations are typically carried out using very strong, ionic bases (e.g. KOt-Bu or NaHMDS),^{19,20,21} although a recent report from Buckley and coworkers supports the hypothesis that the fluoride ion may play some role in the oxidizing capability of our system.²² Furthermore, the fact that no hydroperoxide intermediates or *anti,anti,syn* products are observed suggests that each oxygen atom on a single diketopiperazine ring may originate from a single molecule of O₂, via a sequence involving initial intermolecular oxidation of the first C–H bond by O₂ followed by intramolecular oxidation of the second C–H bond by the resulting peroxide radical.

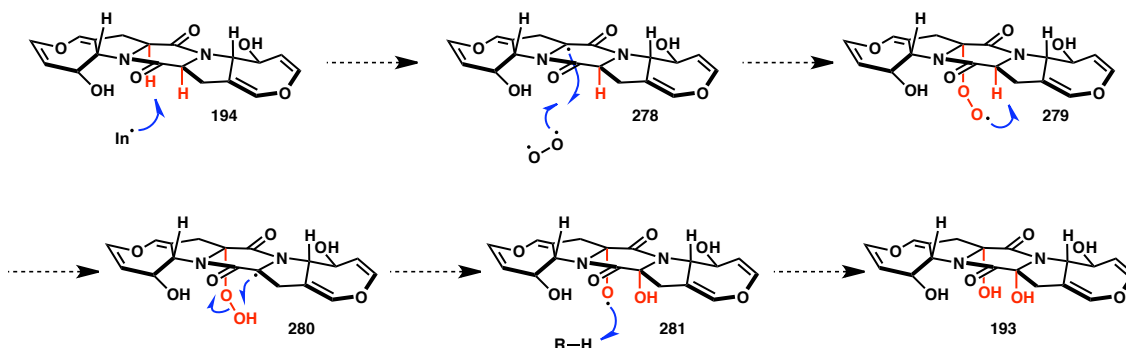
In an effort to further elucidate the nature of this oxidation process and better-understand its stereochemical outcome, control experiments were carried out using TBS-protected *syn,syn,syn* diketopiperazine **190** (see Scheme 4.7). Diketopiperazine **190** could be epimerized *with* or *without* concomitant cleavage of the TBS ethers, by treatment with TB⁺AF•(t-BuOH)₄ in THF under an inert atmosphere at ambient temperature or Cs₂CO₃ in THF/MeOH at ambient temperature to furnish diketopiperazines **194** or **275**, respectively. This suggests that for both the bis-TBS-protected and unprotected diketopiperazine, the thermodynamic preference is for the *anti,syn,anti* configuration. However, we were surprised to find that in the presence of ambient air atmosphere, diketopiperazine **190** undergoes TB⁺AF•(t-BuOH)₄-promoted deprotection with concomitant *stereoretentive* C–H oxidation to afford *syn,syn,syn* oxidation product **277**! This suggests that the TB⁺AF•(t-BuOH)₄-promoted oxidation is stereospecific, and unlikely to involve enol intermediates, given that no epimerization occurs prior to oxidation. Finally, it was observed that the unepimerized, unprotected diketopiperazine **276** could be obtained by subjection of **190**

to HCO_2H in THF/ H_2O , and future control experiments will seek to determine the stereochemical outcome of dihydroxylation or sulfenylation of this substrate.

Scheme 4.7. Manipulation of diketopiperazine oxidation and stereochemistry



Taken together, the above observations suggest the mechanism for oxidation of diketopiperazine **194** could be as shown in Scheme 4.8. Intermolecular hydrogen radical abstraction from **194** occurs to afford radical species **278**, which reacts with triplet O_2 to provide peroxide radical **279**. Subsequent intramolecular hydrogen radical abstraction affords diketopiperazine radical **280**, which undergoes intramolecular $\text{S}_{\text{H}}2$ -type displacement to afford alkoxy radical **281**. Final intermolecular hydrogen radical abstraction from another molecule of **194** or some propagating (or terminating) species R–H furnishes the oxidized product (**193**). Unfortunately, preliminary efforts aimed at applying these conditions to simpler diketopiperazines as a general method for C–H oxidation have proven unfruitful.

Scheme 4.8. Proposed mechanism for aerobic oxidation of diketopiperazine **194**

4.4 CONCLUDING REMARKS

In conclusion, a catalytic asymmetric double (1,3)-dipolar cycloaddition reaction has been developed, as part of our efforts to further explore interesting side reactions observed during synthetic studies toward acetylalarotin (**11**). This reaction provides access to highly substituted, enantioenriched pyrrolizidines from inexpensive, commercially available starting materials. Depending on which of the second dipolarophiles are employed, pyrrolizidines containing as many as six stereogenic centers have been prepared with high levels of enantio- and diastereoselectivity. We expect that this reaction could be of use for the preparation of natural product analogues of new lead compounds for pharmaceutical studies.

Likewise, a series of control experiments allowed us to probe the mechanism of the aerobic oxidation of diketopiperazine **194**. Though we were unable to develop this transformation into a general reaction methodology, future studies of related complex diketopiperazines may allow for the identification of structural parameters required for oxidation to occur.

4.5 EXPERIMENTAL SECTION

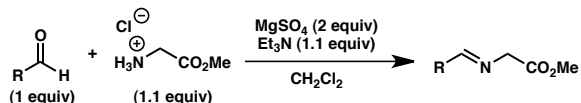
4.5.1 Materials and Methods

Unless otherwise stated, reactions were performed under a nitrogen atmosphere using freshly dried solvents. Tetrahydrofuran (THF), methylene chloride (CH_2Cl_2), acetonitrile (MeCN), dimethylformamide (DMF), and toluene (PhMe) were dried by passing through activated alumina columns. Triethylamine (Et_3N) and N,N -diisopropylethylamine (DIPEA) were distilled over calcium hydride prior to use. Unless otherwise stated, chemicals and reagents were used as received. All reactions were monitored by thin-layer chromatography using EMD/Merck silica gel 60 F254 pre-coated plates (0.25 mm) and were visualized by UV, *p*-anisaldehyde, or KMnO_4 staining. Flash column chromatography was performed either as described by Still et al.²³ using silica gel (particle size 0.032-0.063) purchased from Silicycle or using pre-packaged RediSep[®]Rf columns on a CombiFlash Rf system (Teledyne ISCO Inc.). Optical rotations were measured on a Jasco P-2000 polarimeter using a 100 mm path-length cell at 589 nm. ^1H and ^{13}C NMR spectra were recorded on a Varian 400 MR (at 400 MHz and 101 MHz, respectively), a Varian Inova 500 (at 500 MHz and 126 MHz, respectively), or a Varian Inova 600 (at 600 MHz and 150 MHz, respectively), and are reported relative to internal CHCl_3 (^1H , δ = 7.26), MeCN-*d*₂ (^1H , δ = 1.94), or acetone-*d*₅ (^1H , δ = 2.05), and CDCl_3 (^{13}C , δ = 77.0), CD_3CN (^{13}C , δ = 118.26), DMSO-*d*₆ (^{13}C , δ = 39.52). Data for ^1H NMR spectra are reported as follows: chemical shift (δ ppm) (multiplicity, coupling constant (Hz), integration). Multiplicity and qualifier abbreviations are as follows: s = singlet, d = doublet, t = triplet, q = quartet, m = multiplet, br = broad, app = apparent. IR spectra were recorded on a Perkin Elmer Paragon 1000 spectrometer and are reported in frequency of

absorption (cm^{-1}). HRMS were acquired using an Agilent 6200 Series TOF with an Agilent G1978A Multimode source in electrospray ionization (ESI), atmospheric pressure chemical ionization (APCI), or mixed (MM) ionization mode. Analytical SFC was performed with a Mettler SFC supercritical CO₂ analytical chromatography system with Chiralcel AD-H, OD-H, AS-H, OB-H, and OJ-H columns (4.6 mm x 25 cm) with visualization at 254 nm. Analytical chiral HPLC was performed with an Agilent 1100 Series HPLC utilizing a Chiraldak AD column (4.6 mm x 25 cm) obtained from Daicel Chemical Industries, Ltd. with visualization at 254 nm. Melting points were determined using a Büchi B-545 capillary melting point apparatus and the values reported are uncorrected.

4.5.2 Preparative Procedures and Spectroscopic Data

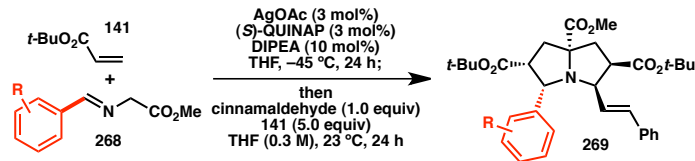
General procedure 1 for the synthesis of α -iminoesters 152, 268a-s



The α -iminoesters were prepared according to the procedure reported by Longmire et al.²⁴ To a suspension of the glycine methyl (or ethyl) ester hydrochloride (1.1 equiv) and magnesium sulfate (2.0 equiv) in methylene chloride was added triethylamine (1.1 equiv). This solution was stirred at room temperature for 1 h before the aldehyde (1.0 equiv) was added. After stirring at room temperature overnight, magnesium sulfate was filtered off and washed with methylene chloride. The filtrate was washed with distilled water (5x) and then with brine, dried over magnesium sulfate, filtered, and concentrated to afford the α -iminoesters. The crude iminoesters could be used directly for the cycloaddition reactions. The reactions reported above were performed on the scale of

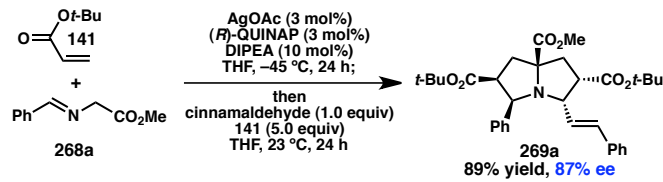
1.0–4.0 g of aldehydes at 0.5 M concentration. **NOTE:** Formation of α -iminoester **152** was allowed to proceed for 1.5 h rather than overnight in order to avoid decomposition.

General procedure 2 for the synthesis of pyrrolizidines **269a-s**



Silver(I) acetate (1.0 equiv) and (*S*)-QUINAP (1.0 equiv) were added to a vial. Tetrahydrofuran was then introduced, and this solution was stirred at room temperature for 1 h to make a stock solution of 0.009 M silver(I)/(*S*)-QUINAP catalyst. Silver(I) acetate/(*S*)-QUINAP catalyst solution (0.03 equiv) followed by the dipolarophile (*t*-Bu Acrylate; 1.5 equiv) and Hünig's base (0.1 equiv) were added to the α -iminoester (1.0 equiv) at -45 °C in the glovebox. The final concentration of the α -iminoester was 0.3 M. After stirring for 24 hours, the reaction was allowed to warm to room temperature and taken out of the glovebox. Dipolarophile (5 equiv) and then cinnamaldehyde (1 equiv) were added. After stirring for 24 hours, the reaction was quenched with a tetrahydrofuran solution of acetic acid (1.1 equiv) and concentrated directly. The reactions were performed on a scale of 20–80 mg of the iminoester.

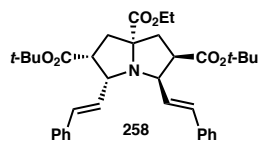
Gram-scale procedure for the preparation of pyrrolizidine *ent*-**269a**



18.8 mg silver (I) acetate (0.113 mmol) and 49.4 mg (*R*)-QUINAP (0.112 mmol) were added to a vial. Tetrahydrofuran (12.5 mL) was then introduced, and this solution

was stirred at room temperature for 1 h to make a stock solution of 0.009 M silver(I)/(*R*)-QUINAP catalyst. Silver(I) acetate/(*R*)-QUINAP catalyst solution (10 mL, 0.09 mmol) followed by the 0.66 ml *t*-butyl acrylate (4.5 mmol) and 52 μ L Hünig's base (0.30 mmol) were added to 532 mg of α -iminoester **268a** (3.00 mmol) at -45 °C. The final concentration of the α -iminoester was 0.3 M. After stirring for 24 hours, the reaction was allowed to warm to room temperature. 2.2 mL *t*-butyl acrylate (15 mmol) and then 380 μ L cinnamaldehyde (3.0 mmol) were added. After stirring for 24 hours, the reaction was quenched with 2 mL of a tetrahydrofuran solution of acetic acid (10:1 v/v) and concentrated directly. The crude reaction mixture was purified by silica gel column chromatography (5→20% ethyl acetate in hexanes) to obtain 1.46 g pyrrolizidine **269a** in 89% yield and 87% ee.

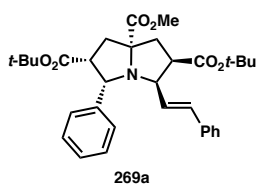
(2*R*,3*R*,5*R*,6*R*)-2,6-di-*tert*-butyl-7*a*-ethyl-3,5-di((*E*)-styryl)hexahydro-1*H*-pyrrolizine-2,6,7*a*-tricarboxylate (258)



According to the general procedure pyrrolizidine **258** was obtained as a light yellow foam after silica gel column chromatography (5→20% ethyl acetate in hexanes) in 73% yield and 90% ee. The enantiomeric excess was determined by chiral SFC analysis (OJ-H, 2.5 mL/min, 4% IPA in CO₂, λ = 254 nm): t_R (major) = 5.2 min, t_R (minor) = 6.6 min. $[\alpha]_D^{25} = -109.5^\circ$ ($c = 1.01$, CHCl₃); ¹H NMR (CDCl₃, 500 MHz) δ 7.40 – 7.36 (m, 2H), 7.35 – 7.23 (m, 7H), 7.19 – 7.15 (m, 1H), 6.63 (d, J = 15.5 Hz, 1H), 6.53 (d, J = 15.5 Hz, 1H), 6.20 (dd, J = 15.6, 7.7 Hz, 1H), 6.06 (dd, J = 15.5, 10.6 Hz, 1H), 4.30 (dd, J = 10.6, 7.6 Hz, 1H), 4.27 – 4.16 (m, 3H), 3.45 (ddd, J = 13.3, 7.6, 6.0 Hz, 1H), 3.08 (dt, J = 10.3, 7.7 Hz, 1H), 2.78 (dd, J = 13.5, 10.3 Hz, 1H), 2.49 (dd, J = 13.1, 6.0 Hz, 1H), 2.17 (dd, J = 13.5, 7.8 Hz, 1H), 2.11 (t, J = 13.0 Hz, 1H),

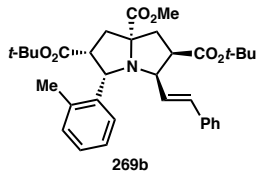
1.31 (t, $J = 7.1$ Hz, 3H), 1.30 (s, 9H), 1.28 (s, 9H); ^{13}C NMR (CDCl_3 , 126 MHz) δ 176.2, 170.5, 170.1, 137.1, 136.4, 136.2, 131.2, 128.6, 128.3, 128.2, 127.9, 127.1, 126.7, 126.4, 125.2, 80.8, 80.8, 75.5, 67.1, 64.4, 61.2, 50.8, 49.6, 37.4, 36.6, 28.1, 28.0, 14.3; FTIR (NaCl, thin film) 2978, 2932, 1727, 1495, 1477, 1449, 1392, 1367, 1257, 1152, 1029, 968, 848, 754 cm^{-1} ; HRMS (MM) calc'd for $[\text{M}+\text{H}]^+$ 588.3320, found 588.3284.

(2*R*,3*S*,5*R*,6*R*,7*aR*)-2,6-di-*tert*-butyl-7*a*-methyl-3-phenyl-5-((*E*)-styryl)hexahydro-1*H*-pyrrolizine-2,6,7*a*-tricarboxylate (269a)



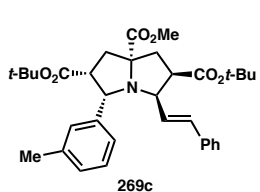
According to the general procedure pyrrolizidine **269a** was obtained as a white foam after silica gel column chromatography (5→20% ethyl acetate in hexanes) in 90% yield and 91% ee. The enantiomeric excess was determined by chiral SFC analysis (OD, 2.5 mL/min, 10% IPA in CO_2 , $\lambda = 254$ nm): t_{R} (major) = 6.1 min, t_{R} (minor) = 7.2 min. $[\alpha]_D^{25} = -103.3^\circ$ ($c = 0.74$, CHCl_3); ^1H NMR (CDCl_3 , 500 MHz) δ 7.39 (d, $J = 7.3$ Hz, 2H), 7.30 – 7.24 (m, 6H), 7.21–7.10 (m, 2H), 6.30 (d, $J = 15.6$ Hz, 1H), 6.02 (dd, $J = 15.6, 10.3$ Hz, 1H), 4.78 (d, $J = 8.3$ Hz, 1H), 4.19 (dd, $J = 10.3, 7.7$ Hz, 1H), 3.79 (s, 3H), 3.61 (ddd, $J = 12.1, 7.5, 6.5$ Hz, 1H), 3.39 (td, $J = 7.9, 3.8$ Hz, 1H), 2.99 (dd, $J = 13.2, 3.8$ Hz, 1H), 2.37 (dd, $J = 13.1, 6.5$ Hz, 1H), 2.29 (dd, $J = 19.1, 6.4$ Hz, 1H), 2.12 (dd, $J = 13.3, 7.7$ Hz, 1H), 1.26 (s, 9H), 0.96 (s, 9H); ^{13}C NMR (CDCl_3 , 126 MHz) δ 177.1, 171.0, 170.9, 141.1, 136.4, 135.3, 128.5, 127.9, 127.8, 127.7, 126.7, 126.5, 126.3, 80.7, 80.2, 76.8, 65.2, 65.0, 52.9, 52.2, 51.3, 39.1, 39.0, 28.0, 27.4; FTIR (NaCl, thin film) 2977, 1726, 1493, 1453, 1391, 1367, 1293, 1255, 1204, 1151, 1094, 968, 845, 746 cm^{-1} ; HRMS (MM) calc'd for $[\text{M}+\text{H}]^+$ 548.3007, found 548.3040.

(2*R*,3*R*,5*S*,6*R*,7*aR*)-2,6-di-*tert*-butyl-7*a*-methyl-3-((*E*)-styryl)-5-(*o*-tolyl)hexahydro-1*H*-pyrrolizine-2,6,7*a*-tricarboxylate (269b)



According to the general procedure pyrrolizidine **269b** was obtained as a white foam after silica gel column chromatography (5→20% ethyl acetate in hexanes) in 91% yield and 89% ee. The enantiomeric excess was determined by chiral SFC analysis (OD, 2.5 mL/min, 7% IPA in CO₂, $\lambda = 254$ nm): t_R (major) = 10.0 min, t_R (minor) = 11.5 min. $[\alpha]_D^{25} = -84.443^\circ$ ($c = 0.95$, CHCl₃); ¹H NMR (CDCl₃, 500 MHz) δ 8.03 (d, $J = 7.7$ Hz, 1H), 7.32 – 7.15 (m, 6H), 7.10 (t, $J = 7.4$ Hz, 1H), 7.01 (d, $J = 7.4$ Hz, 1H), 6.22 (d, $J = 15.6$ Hz, 1H), 5.99 (dd, $J = 15.6$, 10.4 Hz, 1H), 4.93 (d, $J = 8.2$ Hz, 1H), 4.10 (dd, $J = 10.2$, 7.6 Hz, 1H), 3.82 (s, 3H), 3.65 (ddd, $J = 13.5$, 7.4, 0.8 Hz, 1H), 3.50 (t, $J = 8.0$ Hz, 1H), 3.05 (d, $J = 13.1$ Hz, 1H), 2.40 (dd, $J = 13.5$, 6.0 Hz, 1H), 2.35 (t, $J = 12.8$ Hz, 1H), 2.09 (dd, $J = 13.1$, 7.7 Hz, 1H), 1.28 (s, 9H), 0.90 (s, 9H); ¹³C NMR (CDCl₃, 126 MHz) δ 177.37, 171.20, 170.72, 138.66, 136.50, 135.55, 135.03, 129.21, 128.41, 127.58, 126.78, 126.48, 126.35, 125.89, 80.61, 79.95, 77.25, 77.00, 76.75, 76.22, 64.01, 61.95, 52.14, 51.32, 50.98, 39.80, 39.23, 27.99, 27.47, 27.21, 19.14; FTIR (NaCl, thin film) 2976, 1727, 1479, 1458, 1392, 1367, 1294, 1256, 1199, 1151, 1097, 1034, 967, 844, 749 cm⁻¹; HRMS (MM) calc'd for [M+H]⁺ 562.3163, found 574.3159.

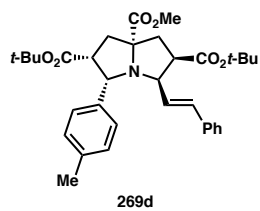
(2*R*,3*R*,5*S*,6*R*,7*aR*)-2,6-di-*tert*-butyl-7*a*-methyl-3-((*E*)-styryl)-5-(*m*-tolyl)hexahydro-1*H*-pyrrolizine-2,6,7*a*-tricarboxylate (269c)



According to the general procedure using 6 mol% AgOAc/QUINAP, pyrrolizidine **269c** was obtained as a white foam

after silica gel column chromatography (5→20% ethyl acetate in hexanes) in 76% yield and 88% ee. The enantiomeric excess was determined by chiral SFC analysis (OD, 2.5 mL/min, 7% IPA in CO₂, $\lambda = 254$ nm): t_R (major) = 9.8 min, t_R (minor) = 11.4 min. $[\alpha]_D^{25} = -236.413^\circ$ ($c = 0.93$, CHCl₃); ¹H NMR (CDCl₃, 500 MHz) δ 7.34 – 7.09 (m, 7H), 6.98 (d, $J = 7.4$ Hz, 2H), 6.35 (d, $J = 15.6$ Hz, 1H), 6.05 (dd, $J = 15.6, 10.3$ Hz, 1H), 4.76 (d, $J = 8.3$ Hz, 1H), 4.22 (dd, $J = 10.3, 7.7$ Hz, 1H), 3.81 (s, 3H), 3.61 (ddd, $J = 12.2, 7.5, 6.5$ Hz, 1H), 3.38 (td, $J = 7.9, 4.3$ Hz, 1H), 3.00 (dd, $J = 13.3, 4.3$ Hz, 1H), 2.39 (dd, $J = 13.1, 6.4$ Hz, 1H), 2.30 (s, 3H), 2.14 (dd, $J = 13.3, 7.8$ Hz, 1H), 1.29 (s, 9H), 0.99 (s, 9H); ¹³C NMR (CDCl₃, 126 MHz) δ 177.1, 171.0, 170.9, 141.0, 137.0, 136.5, 135.3, 128.6, 128.5, 127.8, 127.7, 127.4, 126.5, 126.3, 125.0, 80.7, 80.1, 76.6, 65.2, 65.2, 52.8, 52.2, 51.1, 39.0, 38.9, 28.0, 27.4, 21.5; FTIR (NaCl, thin film) 2978, 2930, 1732, 1606, 1456, 1367, 1256, 1152, 1099, 1038, 969, 846, 740 cm⁻¹; HRMS (MM) calc'd for [M+H]⁺ 562.3163, found 562.3163.

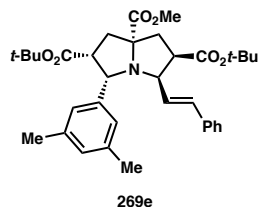
(2*R*,3*R*,5*S*,6*R*,7*aR*)-2,6-di-*tert*-butyl-7*a*-methyl-3-((*E*)-styryl)-5-(*p*-tolyl)hexahydro-1*H*-pyrrolizine-2,6,7*a*-tricarboxylate (269d)



According to the general procedure using 6 mol% AgOAc/QUINAP, pyrrolizidine **269d** was obtained as a white foam after silica gel column chromatography (5→20% ethyl acetate in hexanes) in 92% yield and 90% ee. The enantiomeric excess was determined by chiral SFC analysis (AD, 2.5 mL/min, 7% IPA in CO₂, $\lambda = 254$ nm): t_R (minor) = 10.2 min, t_R (major) = 11.3 min. $[\alpha]_D^{25} = -178.7^\circ$ ($c = 0.85$, CHCl₃); ¹H NMR (CDCl₃, 500 MHz) δ 7.34 – 7.19 (m, 7H), 7.05 (d, $J = 7.8$ Hz, 2H), 6.35 (d, $J = 15.6$ Hz, 1H), 6.04 (dd, $J = 15.6, 10.3$ Hz, 1H), 4.21 (dd, $J = 10.2, 7.7$ Hz, 1H), 3.81 (d, $J = 0.7$ Hz, 1H), 3.62 (dt, $J =$

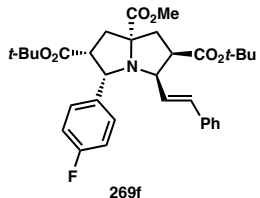
13.2, 6.9 Hz, 1H), 3.38 (td, $J = 8.1, 4.0$ Hz, 1H), 3.00 (dd, $J = 13.3, 4.0$ Hz, 1H), 2.38 (dd, $J = 13.2, 6.4$ Hz, 1H), 2.30 (s, 1H), 2.13 (dd, $J = 13.3, 7.6$ Hz, 1H), 1.28 (s, 1H), 1.00 (s, 1H); ^{13}C NMR (CDCl_3 , 126 MHz) δ 177.1, 171.0, 170.9, 138.0, 136.5, 136.1, 135.2, 128.4, 128.4, 127.8, 127.7, 126.5, 126.4, 80.7, 80.1, 76.6, 65.1, 64.9, 52.9, 52.2, 51.2, 39.0, 28.0, 27.4, 21.0; FTIR (NaCl, thin film) 2977, 1727, 1512, 1495, 1477, 1457, 1367, 1151, 968, 848, 748 cm^{-1} ; HRMS (MM) calc'd for $[\text{M}+\text{H}]^+$ 562.3163, found 562.3170.

(2*R*,3*S*,5*R*,6*R*,7*aR*)-2,6-di-*tert*-butyl-7*a*-methyl-3-(3,5-dimethylphenyl)-5-((*E*)-styryl)hexahydro-1*H*-pyrrolizine-2,6,7*a*-tricarboxylate (269e)**



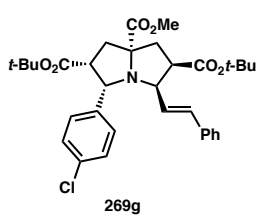
According to the general procedure using 6 mol% AgOAc/QUINAP, pyrrolizidine **269e** was obtained as a white foam after silica gel column chromatography (5→20% ethyl acetate in hexanes) in 78% yield and 88% ee. The enantiomeric excess was determined by chiral SFC analysis (AD, 2.5 mL/min, 5% IPA in CO_2 , $\lambda = 254$ nm): t_{R} (minor) = 9.0 min, t_{R} (major) = 10.5 min. $[\alpha]_D^{25} = -120.032^\circ$ ($c = 0.86$, CHCl_3); ^1H NMR (CDCl_3 , 500 MHz) δ 7.33 – 7.22 (m, 6H), 6.97 (s, 1H), 6.80 (s, 1H), 6.38 (d, $J = 15.6$ Hz, 1H), 6.06 (dd, $J = 15.6, 10.3$ Hz, 1H), 4.72 (d, $J = 8.3$ Hz, 1H), 4.22 (dd, $J = 10.3, 7.7$ Hz, 1H), 3.82 (s, 1H), 3.61 (ddd, $J = 12.3, 7.5, 6.5$ Hz, 1H), 3.35 (td, $J = 7.9, 4.8$ Hz, 1H), 2.99 (dd, $J = 13.3, 4.8$ Hz, 1H), 2.39 (dd, $J = 13.1, 6.4$ Hz, 1H), 2.33 – 2.26 (m, 1H), 2.26 (s, 1H), 2.13 (dd, $J = 13.3, 7.8$ Hz, 1H), 1.29 (s, 9H), 1.00 (s, 9H); ^{13}C NMR (CDCl_3 , 126 MHz) δ 177.09, 170.91, 170.86, 140.95, 136.89, 136.49, 135.28, 128.44, 128.29, 127.65, 126.53, 126.30, 125.68, 80.68, 80.02, 76.62, 65.34, 65.28, 52.66, 52.16, 51.04, 38.98, 38.69, 28.03, 27.38, 21.35; FTIR (NaCl, thin film) 2977, 1728, 1603, 1456, 1391, 1366, 1152, 968, 847, 747 cm^{-1} ; HRMS (MM) calc'd for $[\text{M}+\text{H}]^+$ 576.3320, found 576.3318.

(2*R*,3*S*,5*R*,6*R*,7*aR*)-2,6-di-*tert*-butyl-7*a*-methyl-3-(4-fluorophenyl)-5-((*E*)-styryl)hexahydro-1*H*-pyrrolizine-2,6,7*a*-tricarboxylate (269f)



According to the general procedure pyrrolizidine **269f** was obtained as a white foam after silica gel column chromatography (5→20% ethyl acetate in hexanes) in 87% yield and 93% ee. The enantiomeric excess was determined by chiral SFC analysis (OJ, 2.5 mL/min, 4% IPA in CO₂, $\lambda = 254$ nm): t_R (minor) = 7.8 min, t_R (major) = 9.7 min. $[\alpha]_D^{25} = -40.596^\circ$ ($c = 0.79$, CHCl₃); ¹H NMR (CDCl₃, 500 MHz) δ 7.41 – 7.36 (m, 2H), 7.30 – 7.26 (m, 2H), 7.24 – 7.20 (m, 3H), 6.93 (t, $J = 8.8$ Hz, 2H), 6.29 (d, $J = 15.6$ Hz, 1H), 6.00 (dd, $J = 15.6$, 10.4 Hz, 1H), 4.76 (d, $J = 8.2$ Hz, 1H), 4.15 (dd, $J = 10.3$, 7.7 Hz, 1H), 3.79 (s, 3H), 3.59 (ddd, $J = 12.2$, 7.5, 6.5 Hz, 1H), 3.36 (td, $J = 7.8$, 3.4 Hz, 1H), 2.36 (dd, $J = 13.1$, 6.5 Hz, 1H), 2.32 – 2.25 (m, 1H), 2.11 (dd, $J = 13.3$, 7.7 Hz, 1H), 1.27 (s, 9H), 0.99 (s, 9H); ¹³C NMR (CDCl₃, 126 MHz) δ 177.0, 170.9, 170.8, 162.9, 160.9, 136.7, 136.7, 136.3, 135.3, 129.5, 129.4, 128.5, 127.8, 126.5, 126.1, 114.6, 114.4, 80.7, 80.3, 76.6, 64.7, 64.4, 53.0, 52.2, 51.3, 39.2, 39.0, 28.0, 27.5; FTIR (NaCl, thin film) 3435, 2978, 2931, 1726, 1603, 1507, 1457, 1392, 1367, 1153, 846, 754 cm⁻¹; HRMS (MM) calc'd for [M+H]⁺ 566.2912, found 566.2909.

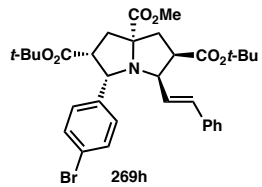
(2*R*,3*S*,5*R*,6*R*,7*aR*)-2,6-di-*tert*-butyl-7*a*-methyl-3-(4-chlorophenyl)-5-((*E*)-styryl)hexahydro-1*H*-pyrrolizine-2,6,7*a*-tricarboxylate (269g)



According to the general procedure pyrrolizidine **269g** was obtained as a yellow oil after silica gel column chromatography (5→20% ethyl acetate in hexanes) in 91% yield and 95% ee. The enantiomeric excess was determined by chiral SFC analysis (OJ, 2.5 mL/min, 2% IPA in

CO_2 , $\lambda = 254 \text{ nm}$): t_{R} (major) = 6.2 min, t_{R} (minor) = 8.1 min. $[\alpha]_D^{25} = -476.013^\circ$ ($c = 0.98$, CHCl_3); ^1H NMR (CDCl_3 , 500 MHz) δ 7.39 (d, $J = 8.4 \text{ Hz}$, 2H), 7.30 – 7.17 (m, 7H), 6.30 (d, $J = 15.6 \text{ Hz}$, 1H), 6.01 (dd, $J = 15.6, 10.4 \text{ Hz}$, 1H), 4.77 (d, $J = 8.2 \text{ Hz}$, 1H), 4.16 (dd, $J = 10.2, 7.7 \text{ Hz}$, 1H), 3.78 (s, 3H), 3.62 (dt, $J = 12.3, 6.9 \text{ Hz}$, 1H), 3.38 (td, $J = 7.9, 2.9 \text{ Hz}$, 1H), 2.99 (dd, $J = 13.2, 2.7 \text{ Hz}$, 1H), 2.40 – 2.26 (m, 1H), 2.12 (dd, $J = 13.3, 7.7 \text{ Hz}$, 1H), 1.27 (s, 9H), 1.00 (s, 9H); ^{13}C NMR (CDCl_3 , 126 MHz) δ 176.8, 170.7, 170.5, 139.5, 136.1, 135.2, 132.2, 129.2, 128.4, 127.7, 127.7, 126.3, 126.0, 80.6, 80.2, 76.5, 64.5, 64.3, 52.9, 52.1, 51.2, 39.2, 38.9, 27.9, 27.3; FTIR (NaCl, thin film) 3431, 2977, 2932, 1727, 1489, 1456, 1292, 1151, 1088, 1014, 847, 750 cm^{-1} ; HRMS (MM) calc'd for $[\text{M}+\text{H}]^+$ 582.2617, found 582.2611.

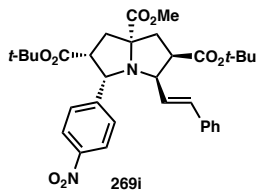
(2*R*,3*S*,5*R*,6*R*,7*aR*)-2,6-di-*tert*-butyl-7*a*-methyl-3-(4-bromophenyl)-5-((*E*)-styryl)hexahydro-1*H*-pyrrolizine-2,6,7*a*-tricarboxylate (269h)**



According to the general procedure pyrrolizidine **269h** was obtained as a white foam after silica gel column chromatography (5→20% ethyl acetate in hexanes) in 89% yield and 92% ee. The enantiomeric excess was determined by chiral SFC analysis (OJ, 2.5 mL/min, 3% IPA in CO_2 , $\lambda = 254 \text{ nm}$): t_{R} (major) = 6.1 min, t_{R} (minor) = 8.0 min. $[\alpha]_D^{25} = -59.159^\circ$ ($c = 0.70$, CHCl_3); ^1H NMR (CDCl_3 , 500 MHz) δ 7.41 – 7.36 (m, 2H), 7.35 – 7.27 (m, 4H), 7.27 – 7.22 (m, 3H), 6.31 (d, $J = 15.6 \text{ Hz}$, 1H), 6.00 (dd, $J = 15.6, 10.4 \text{ Hz}$, 1H), 4.75 (d, $J = 8.2 \text{ Hz}$, 1H), 4.16 (dd, $J = 10.4, 7.6 \text{ Hz}$, 1H), 3.80 (s, 3H), 3.62 (ddd, $J = 12.3, 7.4, 6.5 \text{ Hz}$, 1H), 3.38 (td, $J = 7.8, 3.1 \text{ Hz}$, 1H), 2.99 (dd, $J = 13.2, 3.1 \text{ Hz}$, 1H), 2.38 (dd, $J = 13.2, 6.4 \text{ Hz}$, 1H), 2.35 – 2.25 (m, 1H), 2.11 (dd, $J = 13.3, 7.7 \text{ Hz}$, 1H), 1.28 (s, 9H), 1.01 (s, 9H); ^{13}C NMR (CDCl_3 , 126 MHz) 177.0, 170.9, 170.7, 140.2, 136.2, 135.4, 130.8, 129.8,

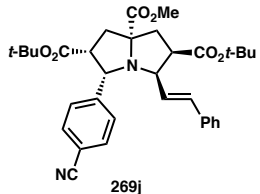
128.5, 127.8, 126.5, 126.1, 120.4, 80.8, 80.4, 76.6, 64.7, 64.5, 53.0, 52.2, 51.3, 39.4, 39.0, 28.0, 27.4; FTIR (NaCl, thin film) 3447, 2978, 2932, 1728, 1586, 1456, 1393, 1368, 1257, 1151, 1011, 845, 739 cm⁻¹; HRMS (MM) calc'd for [M+H]⁺ 626.2112, found 626.2096.

(2*R*,3*S*,5*R*,6*R*,7*aR*)-2,6-di-*tert*-butyl-7*a*-methyl-3-(4-nitrophenyl)-5-((*E*)-styryl)hexahydro-1*H*-pyrrolizine-2,6,7*a*-tricarboxylate (269i)



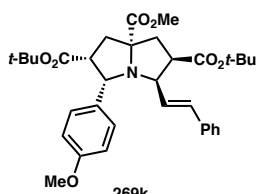
According to the general procedure pyrrolizidine **269i** was obtained as a yellow foam after silica gel column chromatography (5→20% ethyl acetate in hexanes) in 70% yield and 96% ee. The enantiomeric excess was determined by chiral SFC analysis (OJ, 2.5 mL/min, 2% IPA in CO₂, $\lambda = 254$ nm): t_R (major) = 3.8 min, t_R (minor) = 5.2 min. $[\alpha]_D^{25} = -101.586^\circ$ ($c = 0.77$, CHCl₃); ¹H NMR (CDCl₃, 500 MHz) δ 8.13 (d, $J = 8.8$ Hz, 2H), 7.66 (d, $J = 8.6$ Hz, 2H), 7.31 – 7.19 (m, 5H), 6.27 (d, $J = 15.6$ Hz, 1H), 6.00 (dd, $J = 15.6$, 10.4 Hz, 1H), 4.88 (d, $J = 8.2$ Hz, 1H), 4.16 (dd, $J = 10.4$, 7.6 Hz, 1H), 3.81 (s, 3H), 3.65 (ddd, $J = 12.2$, 7.4, 6.8 Hz, 1H), 3.47 (td, $J = 7.9$, 2.6 Hz, 1H), 3.03 (dd, $J = 13.2$, 2.6 Hz, 1H), 2.38 (dd, $J = 14.5$, 8.0 Hz, 1H), 2.37 – 2.29 (m, 1H), 2.16 (dd, $J = 13.3$, 7.7 Hz, 1H), 1.28 (s, 9H), 0.98 (s, 9H); ¹³C NMR (CDCl₃, 126 MHz) δ 176.7, 170.5, 170.5, 149.2, 146.9, 135.9, 135.7, 128.8, 128.5, 128.0, 126.4, 125.6, 123.0, 80.9, 80.7, 76.7, 64.6, 64.4, 53.1, 52.3, 51.3, 39.6, 39.0, 28.0, 27.4; FTIR (NaCl, thin film) 2978, 1727, 1598, 1522, 1457, 1392, 1367, 1346, 1294, 1249, 1199, 1151, 850, 745 cm⁻¹; HRMS (MM) calc'd for [M+H]⁺ 593.2857, found 593.2854.

(2*R*,3*S*,5*R*,6*R*,7*aR*)-2,6-di-*tert*-butyl-7*a*-methyl-3-(4-cyanophenyl)-5-((*E*)-styryl)hexahydro-1*H*-pyrrolizine-2,6,7*a*-tricarboxylate (269j)



According to the general procedure pyrrolizidine **269j** was obtained as a yellow foam after silica gel column chromatography ($5 \rightarrow 20\%$ ethyl acetate in hexanes) in 80% yield and 96% ee. The enantiomeric excess was determined by chiral SFC analysis (OJ, 2.5 mL/min, 4% IPA in CO₂, $\lambda = 254$ nm): t_R (major) = 5.7 min, t_R (minor) = 7.1 min. $[\alpha]_D^{25} = -57.101^\circ$ ($c = 0.70$, CHCl₃); ¹H NMR (CDCl₃, 500 MHz) δ 7.62 – 7.53 (m, 4H), 7.31 – 7.19 (m, 5H), 6.27 (d, $J = 15.6$ Hz, 1H), 5.99 (dd, $J = 15.6, 10.4$ Hz, 1H), 4.84 (d, $J = 8.2$ Hz, 1H), 4.14 (dt, $J = 7.1, 5.9$ Hz, 1H), 3.79 (s, 3H), 3.67 – 3.57 (m, 1H), 3.44 (td, $J = 7.9, 2.7$ Hz, 1H), 3.01 (dd, $J = 13.2, 2.6$ Hz, 1H), 2.38 (dd, $J = 13.2, 6.6$ Hz, 1H), 2.35 ? 2.28 (m, 1H), 2.14 (dd, $J = 13.3, 7.8$ Hz, 1H), 1.28 (s, 9H), 0.97 (s, 9H); ¹³C NMR (CDCl₃, 126 MHz) δ 176.8, 170.6, 170.6, 147.2, 136.0, 135.7, 131.7, 128.8, 128.6, 128.0, 126.5, 125.8, 119.2, 110.4, 80.9, 80.9, 80.6, 76.8, 64.7, 64.6, 53.0, 52.3, 51.4, 39.6, 39.1, 28.0, 27.5; FTIR (NaCl, thin film) 3453, 2978, 2931, 1732, 1608, 1456, 1393, 1368, 1257, 1151, 844, 738 cm⁻¹; HRMS (MM) calc'd for [M+H]⁺ 573.2959, found 573.2924.

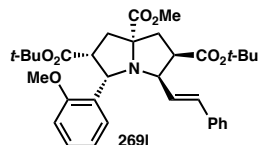
(2*R*,3*S*,5*R*,6*R*,7*aR*)-2,6-di-*tert*-butyl-7*a*-methyl-3-(4-methoxyphenyl)-5-((*E*)-styryl)hexahydro-1*H*-pyrrolizine-2,6,7*a*-tricarboxylate (269k)



According to the general procedure using 6 mol% AgOAc/QUINAP in 0.1M THF, pyrrolizidine **269k** was obtained as a yellow foam after silica gel column chromatography ($5 \rightarrow 20\%$ ethyl acetate in hexanes) in 86% yield and 90% ee. The enantiomeric excess was determined by chiral SFC analysis (AD, 2.5 mL/min, 7% IPA in CO₂, $\lambda = 254$ nm): t_R

(minor) = 9.8 min, t_R (major) = 10.5 min. $[\alpha]_D^{25} = -201.710^\circ$ ($c = 0.94$, CHCl_3); ^1H NMR (CDCl_3 , 500 MHz) δ 7.36 – 7.20 (m, 7H), 6.80 (d, $J = 8.7$ Hz, 2H), 6.34 (d, $J = 15.6$ Hz, 1H), 6.04 (dd, $J = 15.6, 10.3$ Hz, 1H), 4.75 (d, $J = 8.3$ Hz, 1H), 4.19 (dd, $J = 10.3, 7.7$ Hz, 1H), 3.80 (s, 3H), 3.77 (s, 3H), 3.65 – 3.56 (m, 1H), 3.36 (td, $J = 7.9, 4.0$ Hz, 1H), 2.99 (dd, $J = 13.3, 4.0$ Hz, 1H), 2.38 (dd, $J = 13.1, 6.4$ Hz, 1H), 2.34 – 2.26 (m, 1H), 2.13 (dd, $J = 13.3, 7.8$ Hz, 1H), 1.28 (s, 9H), 1.01 (s, 9H); ^{13}C NMR (CDCl_3 , 126 MHz) δ 177.1, 171.0, 170.9, 158.5, 136.4, 135.1, 133.2, 128.9, 128.4, 127.7, 126.5, 126.3, 113.2, 80.6, 80.1, 76.5, 65.0, 64.6, 55.3, 52.9, 52.2, 51.2, 38.9, 38.9, 28.0, 27.5; FTIR (NaCl, thin film) 2977, 1726, 1603, 1511, 1367, 1248, 1151, 1034, 845, 752 cm^{-1} ; HRMS (MM) calc'd for $[\text{M}+\text{H}]^+$ 578.3112, found 578.3119.

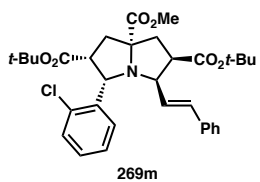
(2*R*,3*R*,5*S*,6*R*,7*aR*)-2,6-di-*tert*-butyl-7*a*-methoxy-3-((*E*)-styryl)-5-(*o*-tolyl)hexahydro-1*H*-pyrrolizine-2,6,7*a*-tricarboxylate (269l)



According to the general procedure pyrrolizidine **269l** was obtained as a white foam after silica gel column chromatography (5 → 20% ethyl acetate in hexanes) in 72% yield and 90% ee. The enantiomeric excess was determined by chiral SFC analysis (OD, 2.5 mL/min, 15% IPA in CO_2 , $\lambda = 254$ nm): t_R (major) = 4.0 min, t_R (minor) = 4.6 min. $[\alpha]_D^{25} = -188.252^\circ$ ($c = 1.0$, CHCl_3); ^1H NMR (CDCl_3 , 500 MHz) δ 7.89 (dd, $J = 7.5, 1.2$ Hz, 1H), 7.30 – 7.23 (m, 3H), 7.23 – 7.12 (m, 3H), 6.95 (t, $J = 7.3$ Hz, 1H), 6.71 (d, $J = 8.0$ Hz, 1H), 6.23 (d, $J = 15.6$ Hz, 1H), 6.02 (dd, $J = 15.6, 10.4$ Hz, 1H), 5.01 (d, $J = 7.8$ Hz, 1H), 4.14 (dd, $J = 10.3, 7.6$ Hz, 1H), 3.79 (s, 3H), 3.63 (s, 3H), 3.55 (td, $J = 7.7, 1.5$ Hz, 1H), 3.01 (d, $J = 12.8$ Hz, 1H), 2.35 (dd, $J = 9.4, 4.0$ Hz, 2H), 2.10 (dd, $J = 13.1, 7.7$ Hz, 1H), 1.28 (s, 9H), 0.93 (s, 9H); ^{13}C NMR (CDCl_3 , 126 MHz) δ 177.5, 171.8, 170.7, 157.0, 136.7, 134.8,

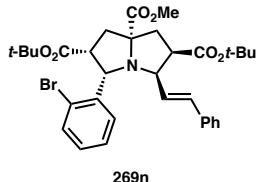
129.2, 129.0, 128.3, 127.4, 127.4, 127.0, 126.5, 120.3, 109.3, 80.6, 79.6, 76.2, 64.4, 59.6, 55.0, 52.1, 51.5, 51.3, 39.7, 39.3, 36.6, 28.0, 27.3, 24.6; FTIR (NaCl, thin film) 2977, 2949, 1723, 1600, 1489, 1458, 1437, 1391, 1367, 1294, 1242, 1152, 1106, 1031, 968, 848, 756 cm⁻¹; HRMS (MM) calc'd for [M+H]⁺ 578.3112, found 578.3137.

(2*R*,3*S*,5*R*,6*R*,7*aR*)-2,6-di-*tert*-butyl-7*a*-methyl-3-(2-chlorophenyl)-5-((*E*)-styryl)hexahydro-1*H*-pyrrolizine-2,6,7*a*-tricarboxylate (269m)



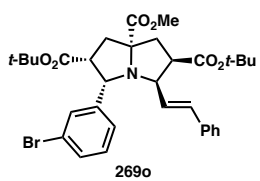
According to the general procedure pyrrolizidine **269m** was obtained as a white foam after silica gel column chromatography (5→20% ethyl acetate in hexanes) in 87% yield and 94% ee. The enantiomeric excess was determined by chiral SFC analysis (OJ, 2.5 mL/min, 2% IPA in CO₂, $\lambda = 254$ nm): t_{R} (minor) = 5.3 min, t_{R} (minor) = 6.2 min. $[\alpha]_D^{25} = -76.881^\circ$ ($c = 0.75$, CHCl₃); ¹H NMR (CDCl₃, 500 MHz) δ 8.08 (dd, $J = 7.7, 1.6$ Hz, 1H), 7.29 – 7.18 (m, 7H), 7.14 (td, $J = 7.6, 1.7$ Hz, 1H), 6.23 (d, $J = 15.6$ Hz, 1H), 5.99 (dd, $J = 15.6, 10.4$ Hz, 1H), 5.11 (d, $J = 8.1$ Hz, 1H), 4.09 (dd, $J = 10.6, 7.8$ Hz, 1H), 3.80 (s, 3H), 3.67 (td, $J = 7.8, 1.5$ Hz, 1H), 3.62 (dt, $J = 11.8, 7.1$ Hz, 1H), 3.04 (d, $J = 13.0$ Hz, 1H), 2.40 (dd, $J = 13.0, 6.7$ Hz, 1H), 2.38 – 2.32 (m, 1H), 2.12 (dd, $J = 13.2, 7.7$ Hz, 1H), 1.29 (s, 9H), 0.94 (s, 9H); ¹³C NMR (CDCl₃, 126 MHz) 177.2, 171.2, 170.6, 138.4, 136.5, 135.4, 133.5, 130.5, 128.4, 128.3, 127.9, 127.6, 126.6, 126.5, 126.2, 80.7, 80.0, 76.4, 64.1, 62.3, 52.2, 51.4, 50.8, 39.7, 39.1, 28.0, 27.3; FTIR (NaCl, thin film) 3444, 2978, 1728, 1456, 1393, 1367, 1256, 1205, 1152, 1034, 969, 844, 752 cm⁻¹; HRMS (MM) calc'd for [M+H]⁺ 582.2617, found 582.2617.

(2*R*,3*S*,5*R*,6*R*,7*aR*)-2,6-di-*tert*-butyl-7*a*-methyl-3-(2-bromophenyl)-5-((*E*)-styryl)hexahydro-1*H*-pyrrolizine-2,6,7*a*-tricarboxylate (269n)



According to the general procedure pyrrolizidine **269n** was obtained as a white foam after silica gel column chromatography (5→20% ethyl acetate in hexanes) in 89% yield and 93% ee. The enantiomeric excess was determined by chiral SFC analysis (OJ, 2.5 mL/min, 3% IPA in CO₂, $\lambda = 254$ nm): t_R (minor) = 4.4 min, t_R (major) = 5.0 min. $[\alpha]_D^{25} = -85.978^\circ$ ($c = 0.88$, CHCl₃); ¹H NMR (CDCl₃, 500 MHz) δ 8.09 (dd, $J = 7.7, 1.6$ Hz, 1H), 7.41 (dd, $J = 7.9, 1.0$ Hz, 1H), 7.35 – 7.15 (m, 6H), 7.07 (td, $J = 7.6, 1.7$ Hz, 1H), 6.23 (d, $J = 15.6$ Hz, 1H), 5.98 (dd, $J = 15.6, 10.4$ Hz, 1H), 5.07 (d, $J = 8.1$ Hz, 1H), 4.08 (dd, $J = 10.3, 7.5$ Hz, 1H), 3.81 (s, 3H), 3.70 (td, $J = 7.9, 1.2$ Hz, 1H), 3.61 (dt, $J = 11.7, 7.2$ Hz, 1H), 3.04 (d, $J = 13.1$ Hz, 1H), 2.42 – 2.32 (m, 2H), 2.12 (dd, $J = 13.2, 7.7$ Hz, 1H), 1.29 (s, 9H), 0.94 (s, 9H); ¹³C NMR (CDCl₃, 126 MHz) δ 177.2, 171.2, 170.6, 139.9, 136.5, 135.5, 131.7, 130.9, 128.3, 128.3, 127.6, 127.3, 126.5, 126.2, 123.9, 80.7, 80.0, 76.5, 64.7, 64.0, 52.2, 51.4, 50.7, 39.7, 39.2, 28.0, 27.3; FTIR (NaCl, thin film) 2977, 1727, 1457, 1392, 1367, 1293, 1257, 1203, 1151, 1094, 1022, 968, 843, 751 cm⁻¹; HRMS (MM) calc'd for [M+H]⁺ 626.2112, found 628.2134.

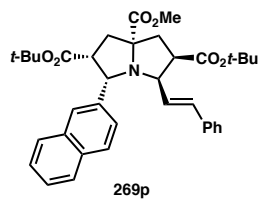
(2*R*,3*S*,5*R*,6*R*,7*aR*)-2,6-di-*tert*-butyl-7*a*-methyl-3-(3-bromophenyl)-5-((*E*)-styryl)hexahydro-1*H*-pyrrolizine-2,6,7*a*-tricarboxylate (269o)



According to the general procedure pyrrolizidine **269o** was obtained as a white foam after silica gel column chromatography (5→20% ethyl acetate in hexanes) in 82% yield and 92% ee. The enantiomeric excess was determined by chiral SFC analysis (OJ, 2.5 mL/min, 2% IPA in

CO_2 , $\lambda = 254 \text{ nm}$): t_{R} (minor) = 6.9 min, t_{R} (major) = 8.0 min. $[\alpha]_D^{25} = -102.419^\circ$ ($c = 0.67, \text{CHCl}_3$); ^1H NMR (CDCl_3 , 500 MHz) δ 7.63 (s, 1H), 7.38 – 7.20 (m, 6H), 7.13 (t, $J = 7.8 \text{ Hz}$, 2H), 6.33 (d, $J = 15.6 \text{ Hz}$, 1H), 6.01 (dd, $J = 15.6, 10.4 \text{ Hz}$, 1H), 4.77 (d, $J = 8.3 \text{ Hz}$, 1H), 4.18 (dd, $J = 10.3, 7.7 \text{ Hz}$, 1H), 3.82 (s, 3H), 3.61 (ddd, $J = 12.4, 7.4, 6.6 \text{ Hz}$, 1H), 3.40 (td, $J = 7.9, 3.3 \text{ Hz}$, 1H), 2.99 (dd, $J = 13.2, 3.3 \text{ Hz}$, 1H), 2.40 (dd, $J = 13.1, 6.4 \text{ Hz}$, 1H), 2.31 (t, $J = 12.8 \text{ Hz}$, 1H), 2.12 (dd, $J = 13.3, 7.7 \text{ Hz}$, 1H), 1.29 (s, 9H), 1.02 (s, 9H); ^{13}C NMR (CDCl_3 , 126 MHz) δ 176.9, 170.7, 170.6, 143.8, 136.2, 135.5, 131.0, 129.8, 129.5, 128.5, 127.8, 126.5, 125.9, 122.1, 80.8, 80.5, 76.7, 64.7, 64.5, 53.0, 52.2, 51.2, 39.3, 39.0, 28.0, 27.4; FTIR (NaCl, thin film) 2978, 1728, 1594, 1569, 1456, 1393, 1367, 1293, 1257, 1204, 1151, 969, 845, 746 cm^{-1} ; HRMS (MM) calc'd for $[\text{M}+\text{H}]^+$ 626.2112, found 626.2127.

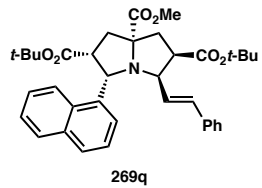
(*2R,3S,5R,6R,7aR*)-2,6-di-*tert*-butyl-7a-methyl-3-(naphthalen-2-yl)-5-((*E*)-styryl)hexahydro-1*H*-pyrrolizine-2,6,7a-tricarboxylate (269p)



According to the general procedure using 6 mol% AgOAc/QUINAP in 0.1M THF, pyrrolizidine **269p** was obtained as a yellow foam after silica gel column chromatography (5 → 20% ethyl acetate in hexanes) in 93% yield and 92% ee. The enantiomeric excess was determined by chiral SFC analysis (AD, 2.5 mL/min, 7% IPA in CO_2 , $\lambda = 254 \text{ nm}$): t_{R} (major) = 6.0 min, t_{R} (minor) = 9.8 min. $[\alpha]_D^{25} = -387.655^\circ$ ($c = 0.93, \text{CHCl}_3$); ^1H NMR (CDCl_3 , 500 MHz) δ 7.97 (s, 1H), 7.85 – 7.77 (m, 2H), 7.74 (d, $J = 8.5 \text{ Hz}$, 1H), 7.52 (dd, $J = 8.5, 1.6 \text{ Hz}$, 1H), 7.47 – 7.40 (m, 2H), 7.30 – 7.19 (m, 4H), 6.29 (d, $J = 15.6 \text{ Hz}$, 1H), 6.09 (dd, $J = 15.6, 10.3 \text{ Hz}$, 1H), 4.99 (d, $J = 8.2 \text{ Hz}$, 1H), 4.27 (dd, $J = 10.3, 7.6 \text{ Hz}$, 1H), 3.86 (s, 3H), 3.74 – 3.65 (m, 1H), 3.50 (td, $J = 7.8, 3.4 \text{ Hz}$, 1H), 3.08 (dd, $J = 13.2, 3.3 \text{ Hz}$, 1H).

Hz, 1H), 2.45 (dd, $J = 13.1, 6.4$ Hz, 1H), 2.38 (t, $J = 12.7$ Hz, 1H), 2.19 (dd, $J = 13.2, 7.7$ Hz, 1H), 1.30 (s, 9H), 0.82 (s, 9H); ^{13}C NMR (CDCl_3 , 126 MHz) δ 177.11, 170.96, 170.71, 138.60, 136.30, 135.25, 133.30, 132.77, 128.40, 127.91, 127.66, 127.39, 127.18, 126.46, 126.41, 126.25, 125.47, 125.11, 80.68, 80.12, 76.64, 65.26, 64.83, 53.11, 52.19, 51.25, 39.26, 39.05, 27.99, 27.22; FTIR (NaCl, thin film) 2977, 1727, 1457, 1391, 1368, 1256, 1199, 1151, 845, 751 cm^{-1} ; HRMS (MM) calc'd for $[\text{M}+\text{H}]^+$ 598.3163, found 598.3155.

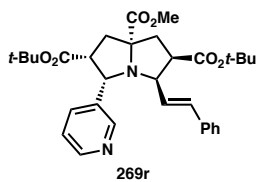
(2*R*,3*S*,5*R*,6*R*)-di-*tert*-butyl-3-(naphthalen-1-yl)-5-((*E*)-styryl)hexahydro-1*H*-pyrrolizine-2,6-dicarboxylate (269q)



According to the general procedure using 6 mol% AgOAc/QUINAP, pyrrolizidine **269q** was obtained as a white foam after silica gel column chromatography (5→20% ethyl acetate in hexanes) in 84% yield and 93% ee. The enantiomeric excess was determined by chiral SFC analysis (AD, 2.5 mL/min, 7% IPA in CO_2 , $\lambda = 254$ nm): t_{R} (minor) = 8.4 min, t_{R} (major) = 9.8 min. $[\alpha]_D^{25} = -188.706^\circ$ ($c = 0.82$, CHCl_3); ^1H NMR (CDCl_3 , 500 MHz) δ 8.30 (d, $J = 7.1$ Hz, 1H), 7.88 (d, $J = 8.3$ Hz, 1H), 7.83 (dd, $J = 8.1, 1.2$ Hz, 1H), 7.72 (d, $J = 8.1$ Hz, 1H), 7.54 – 7.47 (m, 1H), 7.38 (dd, $J = 22.6, 8.2, 6.8, 1.3$ Hz, 2H), 7.20 – 7.13 (m, 3H), 7.01 – 6.98 (m, 2H), 6.17 (d, $J = 15.6$ Hz, 1H), 6.00 (dd, $J = 15.6, 10.3$ Hz, 1H), 5.56 (d, $J = 8.4$ Hz, 1H), 4.19 (dd, $J = 10.2, 7.5$ Hz, 1H), 3.84 (s, 3H), 3.77 (td, $J = 8.0, 1.8$ Hz, 1H), 3.70 (dt, $J = 11.2, 7.4$ Hz, 1H), 3.11 (dd, $J = 13.0, 1.5$ Hz, 1H), 2.45 (dd, $J = 9.3, 3.3$ Hz, 2H), 2.19 (dd, $J = 13.1, 7.7$ Hz, 1H), 1.28 (s, 9H), 0.53 (s, 9H); ^{13}C NMR (CDCl_3 , 126 MHz) δ 177.3, 171.1, 170.9, 136.4, 136.3, 135.3, 133.4, 131.7, 128.3, 128.3, 127.5, 127.2, 126.6, 126.4, 125.9, 125.3, 124.8, 123.3, 80.7, 79.6, 76.3, 64.4, 61.5, 52.3,

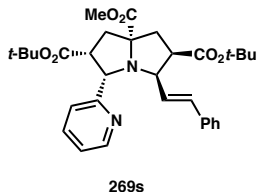
52.2, 51.5, 40.0, 39.2, 28.0, 26.9; FTIR (NaCl, thin film) 2977, 1727, 1596, 1457, 1391, 1367, 1152, 968, 775, 752 cm⁻¹; HRMS (MM) calc'd for [M+H]⁺ 598.3163, found 598.3156.

(2*R*,3*S*,5*R*,6*R*,7*aR*)-2,6-di-*tert*-butyl-7*a*-methyl-3-(pyridin-3-yl)-5-((*E*)-styryl)hexahydro-1*H*-pyrrolizine-2,6,7*a*-tricarboxylate (269r)



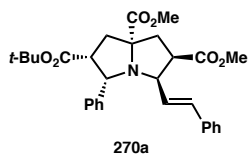
According to the general procedure pyrrolizidine **269r** was obtained as a yellow foam after silica gel column chromatography (5→20% ethyl acetate in hexanes) in 90% yield and 90% ee. The enantiomeric excess was determined by chiral SFC analysis (OJ, 2.5 mL/min, 20% IPA in CO₂, $\lambda = 254$ nm): t_R (major) = 2.7 min, t_R (minor) = 3.7 min. $[\alpha]_D^{25} = -218.400^\circ$ ($c = 0.79$, CHCl₃); ¹H NMR (CDCl₃, 500 MHz) δ 8.53 (s, 1H), 8.43 (d, $J = 4.7$ Hz, 1H), 7.92 (d, $J = 7.8$ Hz, 1H), 7.32 – 7.18 (m, 6H), 6.31 (d, $J = 15.6$ Hz, 1H), 6.01 (dd, $J = 15.6$, 10.4 Hz, 1H), 4.83 (d, $J = 8.3$ Hz, 1H), 4.15 (dd, $J = 10.2$, 7.7 Hz, 1H), 3.80 (s, 3H), 3.59 (dt, $J = 12.1$, 7.0 Hz, 1H), 3.44 (td, $J = 8.0$, 3.4 Hz, 1H), 3.01 (dd, $J = 13.2$, 3.4 Hz, 1H), 2.40 (dd, $J = 13.2$, 6.5 Hz, 1H), 2.31 (t, $J = 12.7$ Hz, 1H), 2.15 (dd, $J = 13.3$, 7.7 Hz, 1H), 1.27 (s, 9H), 0.98 (s, 9H); ¹³C NMR (CDCl₃, 126 MHz) δ 176.78, 170.62, 149.35, 147.87, 136.89, 136.00, 135.63, 128.50, 127.89, 126.46, 125.69, 123.19, 80.83, 80.61, 76.63, 64.78, 62.65, 52.75, 52.28, 51.26, 39.26, 38.90, 27.98, 27.40; FTIR (NaCl, thin film) 2978, 1730, 1586, 1457, 1420, 1369, 1256, 1152, 1026, 844, 737 cm⁻¹; HRMS (MM) calc'd for [M+H]⁺ 549.2954, found 549.2954.

(2*R*,3*S*,5*R*,6*R*,7*aR*)-2,6-di-*tert*-butyl-7*a*-methyl-3-(pyridin-2-yl)-5-((*E*)-styryl)hexahydro-1*H*-pyrrolizine-2,6,7*a*-tricarboxylate (269s)



According to the general procedure pyrrolizidine **269s** was obtained as a white foam after silica gel column chromatography (5→20% ethyl acetate in hexanes) in 33% yield and 44% ee. The enantiomeric excess was determined by chiral SFC analysis (AD, 2.5 mL/min, 20% IPA in CO₂, $\lambda = 254$ nm): t_R (major) = 2.2 min, t_R (minor) = 3.9 min. $[\alpha]_D^{25} = -68.157^\circ$ ($c = 0.92$, CHCl₃); ¹H NMR (500 MHz, CDCl₃) δ 8.41 (d, $J = 4.1$ Hz, 1H), 7.72 (d, $J = 7.8$ Hz, 2H), 7.67 – 7.55 (m, 2H), 7.26 – 7.19 (m, 2H), 7.08 (dd, $J = 6.5, 5.1$ Hz, 2H), 6.45 (dd, $J = 22.7, 15.6$ Hz, 1H), 6.04 (dt, $J = 28.1, 14.0$ Hz, 1H), 4.83 (d, $J = 7.9$ Hz, 1H), 4.26 (dt, $J = 22.8, 11.4$ Hz, 1H), 3.75 (d, $J = 8.7$ Hz, 2H), 3.68 – 3.59 (m, 1H), 3.51 (td, $J = 8.0, 5.5$ Hz, 1H), 3.08 (dd, $J = 13.3, 5.4$ Hz, 1H), 2.38 – 2.35 (m, 1H), 2.34 (d, $J = 3.1$ Hz, 1H), 2.22 (dt, $J = 15.5, 7.8$ Hz, 1H), 1.31 – 1.20 (m, 8H), 1.06 (s, 7H); ¹³C NMR (126 MHz, CDCl₃) δ 177.04, 170.94, 170.47, 161.47, 136.22, 135.97, 128.47, 127.85, 126.66, 125.49, 122.60, 121.63, 80.80, 80.20, 76.64, 66.44, 66.06, 52.27, 52.18, 50.80, 39.08, 38.87, 28.06, 27.54; FTIR (NaCl, thin film) 2976, 1726, 1589, 1457, 1434, 1366, 1256, 1151, 968, 847, 751 cm⁻¹; HRMS (MM) calc'd for [M+H]⁺ 549.2959, found 549.2908.

(2*R*,3*S*,5*R*,6*R*,7*aR*)-2-*tert*-butyl-6,7*a*-dimethyl-3-phenyl-5-((*E*)-styryl)hexahydro-1*H*-pyrrolizine-2,6,7*a*-tricarboxylate (270a)

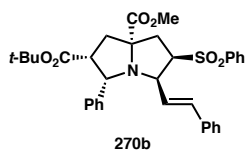


According to the general procedure using 1.1 equivalents of *t*-Bu acrylate in the first (1,3)-dipolar cycloaddition and methyl acrylate as the dipolarophile in the second (1,3)-dipolar cycloaddition, pyrrolizidine **270a** was obtained as a white foam after silica gel column chromatography

(5→20% ethyl acetate in hexanes) in 92% yield and 90% ee. The enantiomeric excess was determined by chiral SFC analysis (AD, 2.5 mL/min, 10% IPA in CO₂, $\lambda = 254$ nm):

t_R (major) = 7.6 min, t_R (minor) = 9.4 min. $[\alpha]_D^{25} = -96.513^\circ$ ($c = 0.94$, CHCl₃); ¹H NMR (CDCl₃, 500 MHz) δ 7.42 – 7.38 (m, 2H), 7.32 – 7.21 (m, 6H), 7.19 – 7.15 (m, 2H), 6.34 (d, $J = 15.6$ Hz, 1H), 6.03 (dd, $J = 15.6, 10.3$ Hz, 1H), 4.83 (d, $J = 8.4$ Hz, 1H), 4.28 (dd, $J = 10.2, 7.8$ Hz, 1H), 3.82 (s, 3H), 3.70 (ddd, $J = 11.9, 7.7, 6.8$ Hz, 1H), 3.56 (s, 3H), 3.44 (td, $J = 7.8, 4.5$ Hz, 1H), 3.03 (dd, $J = 13.3, 4.5$ Hz, 1H), 2.45 (dd, $J = 13.2, 6.6$ Hz, 1H), 2.37 (dd, $J = 13.2, 11.9$ Hz, 1H), 2.19 (dd, $J = 13.3, 7.8$ Hz, 1H), 0.98 (s, 9H); ¹³C NMR (CDCl₃, 126 MHz) δ 176.8, 172.4, 170.8, 140.9, 136.4, 135.3, 128.5, 127.9, 127.8, 127.8, 126.8, 126.6, 125.8, 80.3, 76.8, 65.3, 52.6, 52.3, 51.8, 50.5, 39.1, 38.7, 27.4; FTIR (NaCl, thin film) 3450, 2978, 1730, 1493, 1451, 1367, 1152, 970, 844, 747 cm⁻¹; HRMS (MM) calc'd for [M+H]⁺ 506.2537, found 506.2523.

(2*R*,3*S*,5*R*,6*R*,7*aS*)-2-*tert*-butyl-7*a*-methyl-3-phenyl-6-(phenylsulfonyl)-5-((*E*)-styryl)hexahydro-1*H*-pyrrolizine-2,7*a*-dicarboxylate (270b)



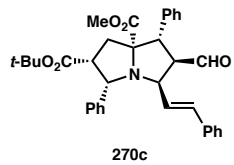
According to the general procedure using 1.1 equivalents of *t*-Bu acrylate in the first (1,3)-dipolar cycloaddition and vinyl sulphone as the dipolarophile in the second (1,3)-dipolar cycloaddition, pyrrolizidine **270b** was obtained as a white foam after silica gel column chromatography (5→20% ethyl acetate in hexanes) in 64% yield and 90% ee. The enantiomeric excess was determined by chiral SFC analysis (AD, 2.5 mL/min, 10% IPA in CO₂, $\lambda = 254$ nm):

t_R (minor) = 3.9 min, t_R (major) = 4.6 min; $[\alpha]_D^{25} = -10.465^\circ$ ($c = 0.87$, CHCl₃); ¹H NMR (CDCl₃, 500 MHz) δ 7.77 (dd, $J = 8.3, 1.1$ Hz, 2H), 7.55 (t, $J = 7.5$ Hz, 2H), 7.42 – 7.10 (m, 11H), 6.28 (dd, $J = 15.6, 10.6$ Hz, 1H), 5.96 (d, $J = 15.6$ Hz, 1H), 4.87 (d, $J = 8.6$ Hz,

1H), 4.41 – 4.29 (m, 1H), 3.98 (dd, $J = 10.5, 7.0$ Hz, 1H), 3.80 (s, 3H), 3.43 (ddd, $J = 16.7, 10.2, 6.2$ Hz, 1H), 3.07 (dd, $J = 13.2, 3.8$ Hz, 1H), 2.69 (dd, $J = 13.0, 6.4$ Hz, 1H), 2.56 (t, $J = 12.5$ Hz, 1H), 2.14 (dd, $J = 13.3, 7.8$ Hz, 1H), 0.95 (s, 9H); ^{13}C NMR (CDCl_3 , 126 MHz) δ 175.8, 170.8, 140.4, 138.9, 136.1, 135.6, 133.6, 128.8, 128.4, 128.4, 127.8, 127.8, 126.8, 126.7, 124.0, 80.3, 75.8, 68.0, 64.6, 64.0, 52.4, 52.1, 38.9, 36.9, 27.3, 27.3; FTIR (NaCl, thin film) 2979, 1726, 1446, 1367, 1305, 1248, 1148, 1085, 749, 722 cm^{-1} ; HRMS (MM) calc'd for $[\text{M}+\text{H}]^+$ 588.2414, found 588.2407.

(2*R*,3*S*,5*R*,6*R*,7*S*,7*aS*)-2-*tert*-butyl-7*a*-methyl-6-formyl-3,7-diphenyl-5-((*E*)-

styryl)hexahydro-1*H*-pyrrolizine-2,7*a*-dicarboxylate (270c)

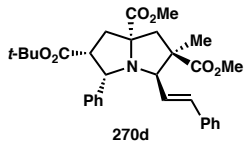


According to the general procedure using 1.1 equivalents of *t*-Bu acrylate in the first (1,3)-dipolar cycloaddition and cinnamaldehyde as the dipolarophile in the second (1,3)-dipolar cycloaddition, pyrrolizidine **270c** was obtained as a white foam after silica gel column chromatography (5–20% ethyl acetate in hexanes) in 90% yield and 90% ee. The enantiomeric excess was determined by chiral SFC analysis (OB-H, 2.5 mL/min, 10% IPA in CO₂, $\lambda = 254$ nm): t_{R} (minor) = 3.7 min, t_{R} (major) = 4.9 min; $[\alpha]_{\text{D}}^{25} = -39.981^\circ$ ($c = 0.96$, CHCl_3); ^1H NMR (CDCl_3 , 500 MHz) δ 9.64 (d, $J = 1.8$ Hz, 1H), 7.37 – 7.11 (m, 14H), 6.44 (d, $J = 15.5$ Hz, 1H), 6.14 (dd, $J = 15.5, 10.7$ Hz, 1H), 4.87 (d, $J = 7.9$ Hz, 1H), 4.79 (dd, $J = 10.7, 8.1$ Hz, 1H), 4.55 (ddd, $J = 12.0, 8.1, 1.7$ Hz, 1H), 3.86 (d, $J = 12.1$ Hz, 1H), 3.47 (td, $J = 7.9, 4.5$ Hz, 1H), 3.30 (s, 3H), 3.04 (dd, $J = 13.5, 4.6$ Hz, 1H), 2.40 (dd, $J = 13.6, 7.9$ Hz, 1H), 1.33 – 1.23 (m, 1H), 1.01 (s, 9H); ^{13}C NMR (CDCl_3 , 126 MHz) δ 199.9, 174.1, 170.5, 140.4, 136.1, 136.0, 135.9, 128.5, 128.5, 128.1, 127.9, 127.6, 127.4, 126.8, 126.7, 125.8, 81.8, 80.4, 64.6, 63.1, 60.1, 54.2, 52.7, 51.4, 37.3, 27.4; FTIR (NaCl, thin

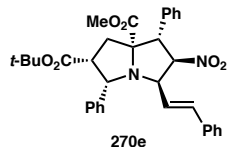
film) 2978, 1728, 1495, 1452, 1391, 1367, 1204, 1152, 1073, 747 cm⁻¹; HRMS (MM) calc'd for [M+H]⁺ 552.2744, found 552.2712.

(2*R*,3*R*,5*S*,6*R*,7*aS*)-6-*tert*-butyl-2,7*a*-dimethyl-2-methyl-5-phenyl-3-((*E*)-styryl)hexahydro-1*H*-pyrrolizine-2,6,7*a*-tricarboxylate (270d)

According to the general procedure using 1.1 equivalents of *t*-Bu acrylate in the first (1,3)-dipolar cycloaddition and methyl methacrylate as the dipolarophile in the second (1,3)-dipolar cycloaddition, pyrrolizidine **270d** was obtained as a white foam after silica gel column chromatography (5→20% ethyl acetate in hexanes) in 91% yield and 90% ee. The enantiomeric excess was determined by chiral SFC analysis (OB-H, 2.5 mL/min, 10% IPA in CO₂, $\lambda = 254$ nm): t_R (major) = 2.8 min, t_R (minor) = 3.3 min; $[\alpha]_D^{25} = -67.966^\circ$ ($c = 0.97$, CHCl₃); ¹H NMR (CDCl₃, 500 MHz) δ 7.45 (dd, $J = 8.1, 1.0$ Hz, 1H), 7.26 – 7.17 (m, 6H), 7.13 – 7.07 (m, 3H), 6.39 (d, $J = 15.6$ Hz, 1H), 5.99 (dd, $J = 15.6, 9.7$ Hz, 1H), 5.02 (d, $J = 9.0$ Hz, 1H), 3.90 (d, $J = 9.3$ Hz, 1H), 3.84 (s, 3H), 3.64 (s, 3H), 3.56 (ddd, $J = 9.0, 7.8, 6.3$ Hz, 1H), 3.02 (dd, $J = 13.2, 6.3$ Hz, 1H), 2.78 (d, $J = 13.8$ Hz, 1H), 2.36 – 2.28 (m, 2H), 1.38 (s, 3H), 0.99 (s, 9H); ¹³C NMR (CDCl₃, 126 MHz) δ 176.8, 176.8, 170.9, 142.1, 136.7, 134.6, 128.3, 128.2, 127.7, 127.5, 126.7, 126.4, 125.1, 80.2, 76.9, 75.0, 65.4, 56.1, 56.1, 52.3, 51.9, 50.4, 48.0, 39.0, 27.4, 23.1; FTIR (NaCl, thin film) 2950, 1727, 1493, 1433, 1450, 1367, 1253, 1152, 1121, 969, 746 cm⁻¹; HRMS (MM) calc'd for [M+H]⁺ 520.2694, found 520.2644.

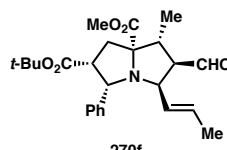


(2*R*,3*S*,5*R*,6*R*,7*R*,7*aS*)-2-*tert*-butyl-7*a*-methyl-6-nitro-3,7-diphenyl-5-((*E*)-styryl)hexahydro-1*H*-pyrrolizine-2,7*a*-dicarboxylate (270e)



According to the general procedure using 1.1 equivalents of *t*-Bu acrylate in the first (1,3)-dipolar cycloaddition and crotonaldehyde as the dipolarophile in the second (1,3)-dipolar cycloaddition, pyrrolizidine **270e** was obtained as a yellow foam after silica gel column chromatography (5–20% ethyl acetate in hexanes) in 89% yield and 90% ee. The enantiomeric excess was determined by chiral SFC analysis (OJ, 2.5 mL/min, 10% IPA in CO₂, $\lambda = 254$ nm): t_R (minor) = 6.0 min, t_R (major) = 7.4 min; $[\alpha]_D^{25} = -27.059^\circ$ ($c = 0.98$, CHCl₃); ¹H NMR (CDCl₃, 500 MHz) δ 7.40 – 7.15 (m, 15H), 6.48 (d, $J = 15.5$ Hz, 1H), 6.22 – 6.11 (m, 1H), 5.05 (d, $J = 8.1$ Hz, 1H), 4.94 (dd, $J = 10.1, 8.0$ Hz, 1H), 4.23 (d, $J = 11.1$ Hz, 1H), 3.59 (td, $J = 7.9, 4.9$ Hz, 1H), 3.38 (s, 3H), 3.12 (dd, $J = 13.6, 4.9$ Hz, 1H), 2.48 (dd, $J = 13.7, 7.9$ Hz, 1H), 1.02 (s, 9H); ¹³C NMR (CDCl₃, 126 MHz) δ 173.2, 170.2, 139.9, 138.2, 135.6, 133.7, 128.8, 128.4, 128.3, 128.3, 127.9, 127.5, 127.1, 127.0, 126.8, 122.0, 92.1, 80.6, 80.5, 65.3, 64.8, 57.2, 51.6, 51.5, 37.1, 27.4; FTIR (NaCl, thin film) 2949, 1730, 1550, 1452, 1205, 1152, 1074, 911, 734 cm⁻¹; HRMS (MM) calc'd for [M+H]⁺ 569.2646, found 569.2632.

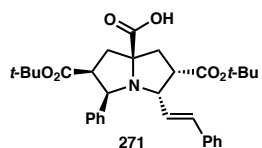
(2*R*,3*S*,5*R*,6*R*,7*R*,7*aS*)-2-*tert*-butyl-7*a*-methyl-6-formyl-7-methyl-3-phenyl-5-((*E*)-styryl)hexahydro-1*H*-pyrrolizine-2,7*a*-dicarboxylate (270f)



According to the general procedure using 1.1 equivalents of *t*-Bu acrylate in the first (1,3)-dipolar cycloaddition and crotonaldehyde as the dipolarophile in the second (1,3)-dipolar cycloaddition, pyrrolizidine **270f** was obtained as a white foam after silica gel column chromatography

(5→20% ethyl acetate in hexanes) in 59% yield (3:1 mixture of diastereomers) and 90% ee. The enantiomeric excess was determined by chiral SFC analysis (AD, 2.5 mL/min, 5% IPA in CO₂, $\lambda = 254$ nm): t_R (major) = 5.9 min, t_R (minor) = 6.7 min; $[\alpha]_D^{25} = -39.981^\circ$ ($c = 0.96$, CHCl₃); ¹H NMR (CDCl₃, 500 MHz) δ 9.56 (d, $J = 1.6$ Hz, 1H), 7.30 – 7.20 (m, 5H), 5.50 (dq, $J = 14.8, 6.5$ Hz, 1H), 5.27 (ddd, $J = 15.0, 10.9, 1.6$ Hz, 1H), 4.70 (d, $J = 7.9$ Hz, 1H), 4.36 (dd, $J = 10.8, 8.2$ Hz, 1H), 3.78 (s, 3H), 3.48 (ddd, $J = 11.7, 8.2, 1.5$ Hz, 1H), 3.33 – 3.26 (m, 1H), 3.00 (dd, $J = 13.6, 5.3$ Hz, 1H), 2.44 (tt, $J = 13.6, 6.8$ Hz, 1H), 2.04 (dd, $J = 13.6, 7.9$ Hz, 1H), 1.61 (dd, $J = 6.5, 1.5$ Hz, 3H), 1.03 (s, 9H); ¹³C NMR (CDCl₃, 126 MHz) δ 201.2, 175.3, 170.6, 141.0, 132.6, 128.3, 127.8, 127.6, 127.6, 127.4, 126.7, 80.3, 80.3, 77.3, 77.0, 76.8, 64.4, 63.3, 62.3, 52.6, 51.7, 43.3, 36.8, 27.5, 17.7, 13.7; FTIR (NaCl, thin film) 2976, 2932, 1732, 1453, 1367, 1367, 974, 745 cm⁻¹; HRMS (MM) calc'd for [M+H]⁺ 428.2431, found 428.2431.

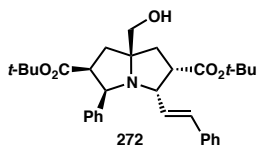
(2*S*,3*R*,5*S*,6*S*,7*aS*)-2,6-bis(*tert*-butoxycarbonyl)-3-phenyl-5-((*E*)-styryl)hexahydro-1*H*-pyrrolizine-7*a*-carboxylic acid (271)



20 mg of pyrrolizidine **ent-269a** was dissolved in 0.4 ml THF. 4.4 mg of LiOH was dissolved in 0.4 ml of H₂O and then transferred to the organic solution. The reaction was allowed to stir for 14 h and then quenched with 1 ml of 10% NaH₂PO₄ and extracted with 1 ml DCM three times. The organic solution was then dried with MgSO₄, filtered, and concentrated. The crude mixture was then purified (5→20% ethyl acetate in hexanes) to afford 14 mg of **271** in 74% yield. ¹H NMR (500 MHz, CDCl₃) δ 7.32 – 7.22 (m, 6H), 7.12 (dd, $J = 7.6, 1.7$ Hz, 4H), 6.32 (d, $J = 15.5$ Hz, 1H), 5.98 (dd, $J = 15.5, 10.5$ Hz, 1H), 4.87 (d, $J = 7.7$ Hz, 1H), 4.29 (dd, $J = 10.4, 7.8$ Hz, 1H), 3.45 (tdd, $J = 7.6, 6.0, 3.9$ Hz, 2H), 2.88 (dd, $J =$

13.9, 2.5 Hz, 1H), 2.74 (dd, $J = 13.3, 6.5$ Hz, 1H), 2.47 – 2.33 (m, 2H), 1.28 (s, 9H), 1.04 (s, 9H); ^{13}C NMR (126 MHz, CDCl_3) δ 176.83, 171.33, 169.92, 138.32, 136.48, 135.82, 128.54, 128.37, 128.18, 127.54, 127.21, 126.56, 123.56, 81.67, 81.41, 78.12, 77.28, 77.02, 76.77, 66.20, 65.71, 53.40, 51.37, 38.80, 38.53, 27.99, 27.42; FTIR (NaCl, thin film) 2977, 2928, 1725, 1495, 1454, 1367, 1250, 1151, 1030, 970, 845, 744 cm^{-1} ; HRMS (MM) calc'd for $[\text{M}+\text{H}]^+$ 534.2832, found 534.285.

(2*R*,3*S*,5*R*,6*R*,7*aR*)-di-*tert*-butyl-7*a*-(*hydroxymethyl*)-3-phenyl-5-((*E*)-styryl)hexahydro-1*H*-pyrrolizine-2,6-dicarboxylate (272)

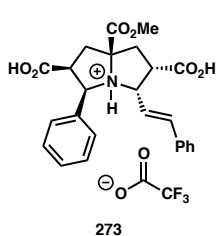


20 mg of pyrrolizidine **ent-269a** was dissolved in 0.73 ml THF and put to 0 °C. 0.11 ml of 1 M LiEt_3BH in THF was added drop-wise.

The reaction was then quenched with 1 ml of saturated aqueous NH_4Cl and extracted with 1 ml DCM three times. The organic solution was then dried with MgSO_4 , filtered, and concentrated. The crude mixture was then purified (5 → 20% ethyl acetate in hexanes) to afford 14 mg of **272** in 74% yield. ^1H NMR (500 MHz, CDCl_3) δ 7.26 (dd, $J = 8.1, 1.0$ Hz, 2H), 7.15 – 7.06 (m, 4H), 7.06 – 6.99 (m, 2H), 6.94 – 6.91 (m, 2H), 6.29 (d, $J = 15.6$ Hz, 1H), 5.90 (dd, $J = 15.6, 9.8$ Hz, 1H), 4.89 (d, $J = 9.4$ Hz, 1H), 4.15 – 4.05 (m, 1H), 3.48 (s, 2H), 3.47 – 3.42 (m, 1H), 3.18 (dd, $J = 17.4, 8.7$ Hz, 1H), 2.62 (dd, $J = 13.5, 6.5$ Hz, 1H), 2.17 (dd, $J = 13.4, 9.1$ Hz, 1H), 2.03 (dd, $J = 13.5, 8.9$ Hz, 1H), 1.95 (dd, $J = 13.4, 8.4$ Hz, 1H), 1.22 (s, 9H), 0.90 (s, 9H); ^{13}C NMR (126 MHz, CDCl_3) δ 173.15, 172.26, 141.97, 136.59, 134.14, 128.32, 128.23, 127.92, 127.51, 126.87, 126.31, 126.09, 80.87, 80.41, 77.28, 77.02, 76.77, 75.48, 66.18, 65.77, 65.54, 51.63, 50.12, 38.22, 36.07, 29.72, 28.01, 27.40; FTIR (NaCl, thin film) 2975,

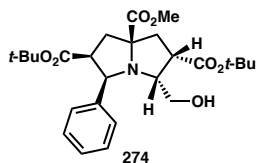
2928, 1722, 1493, 1452, 1367, 1249, 1151, 1030, 970, 846, 743 cm^{-1} ; HRMS (MM) calc'd for $[\text{M}+\text{H}]^+$ 520.3012, found 520.3012.

(2*S*,3*R*,5*S*,6*S*,7*aS*)-2,6-dicarboxy-7*a*-(methoxycarbonyl)-3-phenyl-5-((*E*)-styryl)octahydropyrrolizin-4-i um 2,2,2-trifluoroacetate (273)



To a stirring solution of triester **ent-269a** (204 mg, 0.372 mmol) in 2.6 mL of CH_2Cl_2 was added triethylsilane (0.29 mL, 1.8 mmol), followed by 1.0 mL of trifluoroacetic acid. The resulting solution was stirred for 20 h, and subsequently concentrated *in vacuo*. The crude residue was dissolved in 4 mL of Et_2O , and added dropwise to 30 mL of vigorously stirring hexanes, resulting in precipitation of a white solid (the reaction vessel was rinsed twice with 2 mL of Et_2O , and the rinsates added to the hexanes mixture). The solids were isolated by filtration to afford 180 mg (88% yield) of trifluoroacetate salt **273** as a white amorphous solid. $[\alpha]_{\text{D}}^{25} = +171.4^\circ$ ($c = 1.04$, MeOH); ^1H NMR (CDCl_3 , 500 MHz) δ 9.89 (s, 3H), 7.36 – 7.26 (m, 10H), 6.52 (d, $J = 15.5$ Hz, 1H), 6.23 (dd, $J = 15.5, 10.5$ Hz, 1H), 5.16 (d, $J = 7.4$ Hz, 1H), 4.68 (dd, $J = 10.5, 7.6$ Hz, 1H), 3.84 (s, 3H), 3.67 – 3.60 (m, 1H), 2.97 (dd, $J = 13.9, 3.4$ Hz, 1H), 2.69 – 2.55 (m, 3H); ^{13}C NMR (CDCl_3 , 126 MHz) δ 173.8, 173.6, 171.5, 160.7 (q, $J_{\text{C}-\text{F}} = 36.5$ Hz), 140.9, 136.1, 134.8, 129.9, 129.7, 129.6, 129.5, 128.4, 127.9, 120.0, 117.2 (q, $J_{\text{C}-\text{F}} = 290.8$ Hz), 81.1, 69.5, 68.8, 54.5, 52.3, 50.3, 38.8, 38.1; FTIR (NaCl, thin film) 2960, 2530, 1955, 1907, 1732, 1652, 1495, 1454, 1439, 1409, 1318, 1263, 1193, 1141, 976, 797, 750 cm^{-1} ; HRMS (MM) calc'd for $[\text{M}-\text{C}_2\text{F}_3\text{O}_2]^+$ 436.1760, found 436.1779.

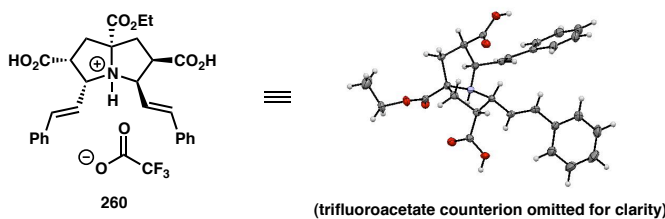
(3a*R*,5*R*,6*S*,7a*R*,8a*S*)-7a-(methoxycarbonyl)-1-oxo-5-phenyloctahydro-1*H*-furo[3,4-*b*]pyrrolizine-6-carboxylic acid (274)



A solution of styrene **ent-269a** (150 mg, 0.274 mmol) and *p*-toluenesulfonic acid hydrate (261 mg, 1.37 mmol) in 2.8 mL of EtOAc was cooled to -78 °C with stirring. Ozone was bubbled through the solution until it became a pale blue suspension. The suspension was then sparged with oxygen (until the blue color no longer persisted), warmed to 0 °C in an ice bath, and diluted with 2.8 mL of saturated aqueous NaHCO₃. Sodium borohydride (104 mg, 2.75 mmol) was added portionwise, and the resulting mixture was stirred vigorously at 0 °C for 1 h. An additional portion of sodium borohydride (104 mg, 2.75 mmol) was added, and vigorous stirring continued at 0 °C for 1 h. A final portion of sodium borohydride (52 mg, 1.37 mmol) was added, and vigorous stirring continued at 0 °C for 1 h. The reaction mixture was then further diluted with saturated aqueous NaHCO₃ and extracted with EtOAc (5 x 5 mL) (**NOTE:** effervescence was allowed to subside prior to extraction), and the combined organic layers were dried over Na₂SO₄, filtered, and concentrated *in vacuo*. The resulting residue was subjected to silica gel column chromatography (50:1→10:1 CH₂Cl₂–Et₂O), to afford 83 mg (64% yield) of **274** as a white foam. [α]_D²⁵ = +346.27 (c = 0.98, CHCl₃); ¹H NMR (CDCl₃, 500 MHz) δ 7.48 – 7.42 (m, 2H), 7.29 – 7.24 (m, 2H), 7.21 – 7.17 (m, 1H), 4.83 (d, *J* = 8.9 Hz, 1H), 3.79 (s, 3H), 3.68 – 3.60 (m, 2H), 3.57 – 3.48 (m, 2H), 3.28 (dd, *J* = 16.7, 8.2 Hz, 1H), 2.95 (dd, *J* = 13.0, 5.8 Hz, 1H), 2.41 (dd, *J* = 13.1, 7.9 Hz, 1H), 2.32 – 2.23 (m, 2H), 2.20 (dd, *J* = 8.7, 5.0 Hz, 1H), 1.49 (s, 9H), 0.96 (s, 9H); ¹³C NMR (CDCl₃, 126 MHz) δ 176.56, 174.21, 170.85, 141.72, 128.11, 127.91, 127.17, 81.90, 80.16, 77.26, 77.00, 76.75, 64.83,

64.01, 60.67, 52.25, 51.25, 49.13, 39.75, 37.40, 27.98, 27.38; FTIR (NaCl, thin film) 3502, 2977, 2929, 1729, 1478, 1456, 1392, 1367, 1303, 1252, 1209, 1152, 1094, 1042, 919, 845, 735 cm⁻¹; HRMS (MM) calc'd for [M+H]⁺ 476.2643, found 476.2644.

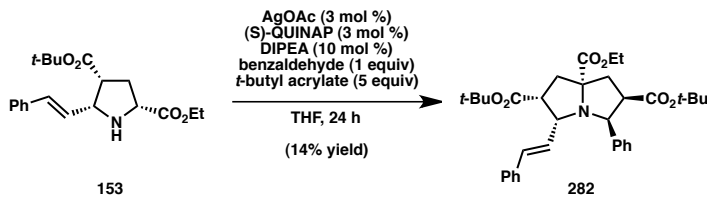
(2*R*,3*R*,5*R*,6*R*)-2,6-dicarboxy-7*a*-(ethoxycarbonyl)-3,5-di((*E*)-styryl)octahydropyrrolizin-4-i um 2,2,2-trifluoroacetate (260)



To a stirring solution of triester **258** (racemic, 191 mg, 0.325 mmol) in 2.3 mL of CH₂Cl₂ was added triethylsilane (0.26 mL, 1.6 mmol), followed by 0.93 mL of trifluoroacetic acid. The resulting solution was stirred for 24 h, and subsequently concentrated *in vacuo*. The crude residue was suspended in 3 mL of EtOAc, and added dropwise to 35 mL of vigorously stirring hexanes, resulting in precipitation of a white solid (the reaction vessel was rinsed twice with 2 mL of EtOAc, and the rinsates added to the hexanes mixture). The solids were isolated by filtration to afford 153 mg (80% yield) of trifluoroacetate salt **260** as a white amorphous solid. Crystals suitable for X-ray diffraction analysis (XRD) were obtained by vapor diffusion of pentane into a saturated solution of **260** in acetone. ¹H NMR (acetone-*d*₆, 500 MHz) δ 9.88 (s, 3H), 7.54 – 7.50 (m, 2H), 7.38 – 7.26 (m, 7H), 7.25 – 7.20 (m, 1H), 6.85 (d, *J* = 15.5 Hz, 1H), 6.74 (dd, *J* = 15.7, 1.1 Hz, 1H), 6.50 (dd, *J* = 15.5, 10.6 Hz, 1H), 6.34 (dd, *J* = 15.7, 7.6 Hz, 1H), 4.72 (dd, *J* = 10.6, 7.5 Hz, 1H), 4.63 (td, *J* = 7.4, 1.3 Hz, 1H), 4.27 (q, *J* = 7.1 Hz, 2H), 3.69 (ddd, *J* = 11.7, 7.6, 6.8 Hz, 1H), 3.57 (dt, *J* = 9.0, 7.6 Hz, 1H), 2.93 (dd, *J* = 13.7, 9.0 Hz, 1H), 2.65 – 2.54 (m, 1H),

2.49 (dd, $J = 13.7, 7.7$ Hz, 1H), 1.32 (t, $J = 7.1$ Hz, 3H); ^{13}C NMR (DMSO- d_6 , 126 MHz) δ 173.8 (br), 171.8, 171.2, 158.5 (q, $J_{C-F} = 36.1$ Hz), 137.5 (br), 136.4, 135.9, 132.5 (br), 128.7, 128.4, 127.9, 127.1, 126.4, 125.7 (br), 122.6 (br), 115.8 (q, $J_{C-F} = 291.8$ Hz), 76.5, 68.0, 64.8, 61.7, 49.3, 48.5, 36.8, 35.4, 14.0; FTIR (NaCl, thin film) 3029, 2528, 1718, 1653, 1452, 1405, 1375, 1263, 1191, 1139, 971, 797, 749, 720 cm $^{-1}$; HRMS (MM) calc'd for [M–C₂F₃O₂]⁺ 476.2068, found 476.2068.

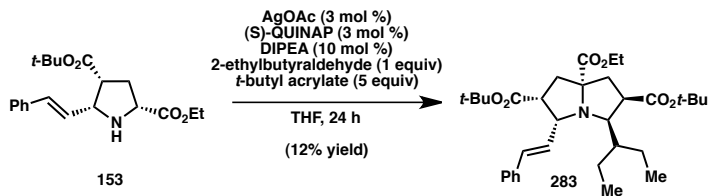
(2*R*,3*S*,5*R*,6*R*,7*aS*)-2,6-di-*tert*-butyl 7*a*-ethyl 3-phenyl-5-((*E*)-styryl)hexahydro-1*H*-pyrrolizine-2,6,7*a*-tricarboxylate (282)**



3 mol % catalyst solution in THF was pre-stirred for 30 minutes and then added to 52 mg of pyrrolidine **153**. 15 μl of benzaldehyde was added followed by 11 μl of *t*-Bu Acrylate and 3 μl of DIPEA. After 24 h the reaction mixture was concentrated and purified by silica gel column chromatography (5→20% ethyl acetate in hexanes) to afford **282** in 14% yield. The enantiomeric excess was determined by chiral SFC analysis (OD, 2.5 mL/min, 7% IPA in CO₂, $\lambda = 254$ nm): t_R (major) = 10.6 min, t_R (minor) = 11.5 min. $[\alpha]_D^{25} = -66.858^\circ$ ($c = 0.95$, CHCl₃); ^1H NMR (500 MHz, CDCl₃) δ 7.36 – 7.23 (m, 5H), 7.23 – 7.13 (m, 5H), 6.33 (dd, $J = 15.7, 0.8$ Hz, 1H), 6.07 (dd, $J = 15.7, 7.1$ Hz, 1H), 4.79 (d, $J = 9.0$ Hz, 1H), 4.25 (tdd, $J = 10.7, 7.1, 3.6$ Hz, 2H), 3.84 – 3.73 (m, 1H), 3.69 (t, $J = 7.2$ Hz, 1H), 3.11 (dd, $J = 14.9, 8.0$ Hz, 1H), 2.88 (dd, $J = 13.4, 6.9$ Hz, 1H), 2.51 (dd, $J = 13.1, 6.8$ Hz, 1H), 2.37 (t, $J = 13.2$ Hz, 1H), 2.20 (dd, $J = 13.4, 8.1$ Hz, 1H), 1.33 (dd, $J = 23.0, 12.8$ Hz, 1H), 1.26 (s, 9H), 0.98 (s, 9H); ^{13}C NMR (126 MHz, CDCl₃) δ 176.81,

170.86, 170.59, 138.21, 137.26, 130.50, 129.44, 128.97, 128.32, 128.24, 127.95, 127.00, 126.37, 80.56, 80.38, 76.04, 67.07, 63.22, 61.05, 51.89, 50.88, 39.01, 37.18, 28.07, 27.98, 27.35, 14.35; FTIR (NaCl, thin film) 2977, 2930, 1728, 1599, 1494, 1477, 1458, 1367, 1247, 1152, 1096, 1029, 969, 848, 744 cm⁻¹; HRMS (MM) calc'd for [M+H]⁺ 562.3169, found 562.3148.

(2*R*,3*R*,5*R*,6*R*,7*aR*)-2,6-di-*tert*-butyl 7*a*-methyl 3-(pentan-3-yl)-5-((*E*)-styryl)hexahydro-1*H*-pyrrolizine-2,6,7*a*-tricarboxylate (283)



3 mol % catalyst solution in THF was pre-stirred for 30 minutes and then added to 52 mg of pyrrolidine **153**. 18 μ l of 2-ethyl butyraldehyde was added followed by 11 μ l of *t*-Bu Acrylate and 3 μ l of DIPEA. After 24 h the reaction mixture was concentrated and purified by silica gel column chromatography (5 \rightarrow 20% ethyl acetate in hexanes) to afford **283** in 12% yield and 96% ee. The enantiomeric excess was determined by chiral SFC analysis (AD, 2.5 mL/min, 5% IPA in CO₂, λ = 254 nm): t_R (minor) = 3.4 min, t_R (major) = 5.3 min. $[\alpha]_D^{25} = -70.072^\circ$ ($c = 0.89$, CHCl₃); ¹H NMR (500 MHz, CDCl₃) δ 7.38 (s, 1H), 7.35 – 7.26 (m, 2H), 7.23 – 7.17 (m, 2H), 6.74 (d, J = 15.6 Hz, 1H), 6.16 (dd, J = 15.7, 6.7 Hz, 1H), 4.46 – 4.38 (m, 1H), 4.26 – 4.14 (m, 2H), 3.60 (ddd, J = 13.0, 8.8, 6.3 Hz, 1H), 3.35 (dd, J = 11.7, 6.7 Hz, 1H), 2.91 (ddd, J = 10.3, 6.8, 3.7 Hz, 1H), 2.74 (dd, J = 14.3, 10.2 Hz, 1H), 2.66 (t, J = 13.0 Hz, 1H), 2.09 (dd, J = 12.8, 6.2 Hz, 1H), 1.89 (dd, J = 14.3, 3.7 Hz, 1H), 1.54 (s, 9H), 1.38 (s, 9H), 1.32 (t, J = 7.1 Hz, 1H), 0.87 (t, J = 7.4 Hz, 3H), 0.76 (t, J = 7.4 Hz, 3H); ¹³C NMR (126 MHz, CDCl₃) δ 175.57,

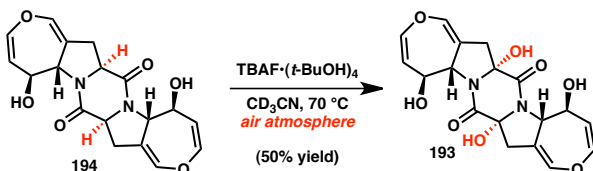
174.77, 170.79, 137.62, 131.09, 130.48, 128.37, 126.91, 126.46, 80.95, 80.55, 75.83, 69.39, 60.89, 60.41, 48.34, 47.21, 41.04, 38.19, 35.98, 28.15, 28.15, 21.78, 20.75, 14.31, 10.48, 7.55; FTIR (NaCl, thin film) 2974, 1718, 1559, 1457, 1366, 1247, 1146, 847 cm^{-1} ; HRMS (MM) calc'd for $[\text{M}+\text{H}]^+$ 556.3638, found 556.3625.

Table 4.3. Relevant ^1H NMR data for stereochemical assignment of pyrrolizidines 270a-f

X, Y	J_{XY} (Hz)	X, Y	J_{XY} (Hz)	X, Y	J_{XY} (Hz)
H _A , H _B	7.5, 7.7	H _A , H _B	7.6	H _A , H _B	7.5, 7.8
X, Y	J_{XY} (Hz)	X, Y	J_{XY} (Hz)	X, Y	J_{XY} (Hz)
H _A , H _B	7.8	H _A , H _B	6.6, 7.0	H _A , H _B	8.1
H _B , H _C	13.2	H _B , H _C	12.0, 12.1	H _B , H _C	12.0
H _B , H _D	6.6	H _B , H _D	6.6, 7.0	H _B , H _J	1.8
nOe interactions					
H _A -H _B	H _B -H _D	H _A -H _B	H _B -H _D	H _A -H _B	H _I -H _H
H _C -H _E	H _I -H _H	H _C -H _E	H _I -H _H	H _C -H _E	H _I -H _C
H _E -H _G	H _I -H _C	H _E -H _G	H _I -H _C	H _E -H _G	no H _I -H _B
H _G -H _H	no H _I -H _B	H _G -H _H	no H _I -H _B	H _G -H _H	—
X, Y	J_{XY} (Hz)	X, Y	J_{XY} (Hz)	X, Y	J_{XY} (Hz)
—	—	H _A , H _B	8.0	H _A , H _B	8.2
—	—	H _B , H _C	11.1	H _B , H _C	11.8

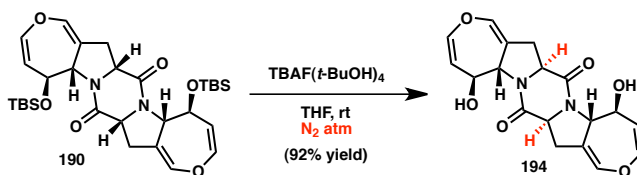
—		—		H _B , H _J	1.6
nOe interactions				nOe interactions	
H _A –H _L	H _G –H _H	H _A –H _B	H _I –H _H	H _A –H _B	H _I –H _H
H _D –H _L	H _I –H _H	H _C –H _E	H _I –H _C	H _C –H _E	H _K –H _C
H _E –H _C	—	H _E –H _G	H _H –H _C	H _E –H _G	H _I –H _C
H _E –H _G	—	H _G –H _H	H _H –H _E	H _G –H _H	no H _I –H _B

Oxidation of diketopiperazine 194 to tetraol 193



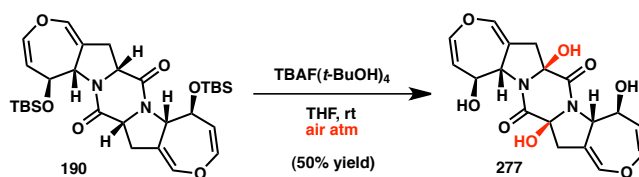
Diketopiperazine **194** (2.0 mg, 5.6 μ mol) and mesitylene (\sim 1 μ L) were dissolved in CD₃CN (600 μ L) and transferred to an NMR tube. An initial ¹H NMR spectrum was acquired in order to determine the exact ratio of starting material to internal standard. The solution was then transferred to a 1-dram vial equipped with a stir bar, and TBAF(*t*-BuOH)₄ (43 mg, 77 μ mol) was added. The vial (open to ambient air until now) was sealed with a Teflon screw cap and was then heated to 70 °C with vigorous stirring. After 4 h, the orange-brown solution was cooled to room temperature and transferred to an NMR tube. A final ¹H NMR spectrum was acquired, and it was determined that tetraol **193** had been formed in 50% yield (based on the mesitylene internal standard) and was the predominant dihydroooxepine-containing species.

Preparation of diol **194** from bis(*tert*-butyldimethylsilyl) ether **190**



A solution of bis(*tert*-butyldimethylsilyl) ether **190** (105 mg, 0.179 mmol) in 9 mL THF and a separate solution of TBAF•(t-BuOH)₄ (1.20 g, 2.15 mmol) in 9 mL THF were each sparged with N₂ for 1 h. The solution of TBAF•(t-BuOH)₄ was then added to the solution of **190**, and the resulting mixture was stirred under N₂ for 52 h. The reaction mixture was then diluted with sat. *aq.* Na₂SO₄ and extracted with EtOAc (3x). The combined organics were then washed with sat. *aq.* Na₂SO₄ and filtered through a plug of SiO₂. The resulting aqueous wash was back-extracted with EtOAc, and the resulting organic layer again passed through the SiO₂ plug, which was finally rinsed with excess EtOAc. The resulting filtrate was then concentrated *in vacuo*, and purification via flash chromatography (gradient elution, 1→5% MeOH in 1:1 CH₂Cl₂/EtOAc) to afford diol **194** (59.2 mg, 92% yield) as an off-white amorphous solid.

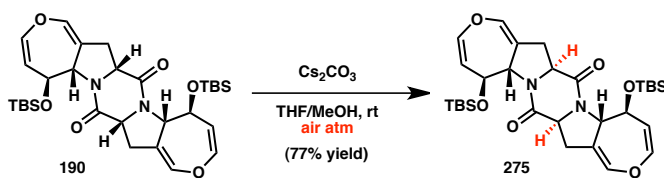
Preparation of tetraol 277 from bis(*tert*-butyldimethylsilyl) ether 190



A solution of bis(*tert*-butyldimethylsilyl) ether **190** (11 mg, 0.017 mmol) in 1.7 mL of THF under an air atmosphere was treated with TBAF•(*t*-BuOH)₄ (114 mg, 0.204 mmol), and the resulting solution was stirred for 46 h. The mixture was then diluted with sat. *aq.* Na₂SO₄ and extracted with EtOAc (3x). The combined organics were then washed with sat. *aq.* Na₂SO₄ and filtered through a plug of SiO₂. The resulting aqueous wash was back-extracted with EtOAc, and the resulting organic layer again passed through the SiO₂ plug, which was finally rinsed with excess EtOAc. The resulting filtrate was then concentrated *in vacuo*, and purification via flash chromatography (gradient

elution, 1:1→1:2 hexanes–EtOAc followed by 100% EtOAc) to afford tetraol **277** (3.3 mg, 50% yield) as a white amorphous solid. $[\alpha]_D^{25.0} = -188^\circ$ ($c = 0.17$, CH_2Cl_2); ^1H NMR (500 MHz, CD_3CN) δ 6.65 – 6.62 (m, 2H), 6.32 (dd, $J = 8.4, 1.9$ Hz, 2H), 5.93 (d, $J = 1.6$ Hz, 2H), 5.69 (d, $J = 0.9$ Hz, 2H), 4.79 (ddd, $J = 8.1, 2.4, 2.4$ Hz, 2H), 4.66 (dd, $J = 8.4, 1.8$ Hz, 2H), 4.29 (dddd, $J = 7.9, 1.7, 1.7, 1.7$ Hz, 2H), 3.02 – 2.94 (m, 2H), 2.84 (ddd, $J = 16.4, 1.1, 0.6$ Hz, 2H); ^{13}C NMR (126 MHz, CD_3CN) δ 170.2, 140.9, 140.1, 115.6, 109.5, 91.9, 69.1, 67.7, 38.5; IR (NaCl/thin film): 3305, 2922, 2851, 1672, 1400, 1323, 1284, 1199, 1132, 1063, 1034, 978, 917, 869, 796, 767, 735 cm^{-1} ; LRMS (ESI/APCI) calc'd for $\text{C}_{18}\text{H}_{17}\text{N}_2\text{O}_8$ [M–H] $^-$ 389.1, found 389.1.

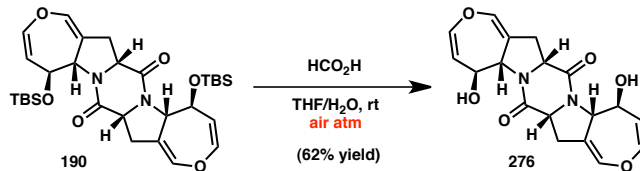
Preparation of **275** from bis(*tert*-butyldimethylsilyl) ether **190**



A solution of diketopiperazine **190** (10.0 mg, 0.0170 mmol) in 2.5 mL THF/MeOH (1:1) was treated with Cs_2CO_3 (222 mg, 0.680 mmol), and the resulting mixture was stirred under an air atmosphere overnight. The mixture was then diluted with H_2O and extracted with CH_2Cl_2 (3x). The combined organic layers were then washed with sat. *aq.* NH_4Cl , dried over Na_2SO_4 , filtered, and concentrated *in vacuo*. Purification by flash chromatography (isocratic elution, 3:1 hexanes–EtOAc) afforded diketopiperazine **275** (7.7 mg, 77% yield) as a white, amorphous solid. $[\alpha]_D^{25.0} = -323^\circ$ ($c = 0.39$, CHCl_3); ^1H NMR (500 MHz, CDCl_3) δ 6.48 (ddd, $J = 2.5, 2.5, 1.0$ Hz, 2H), 6.14 (dd, $J = 8.2, 2.2$ Hz, 2H), 5.09 (dddd, $J = 8.0, 1.6, 1.6, 1.6$ Hz, 2H), 4.75 (dd, $J = 8.2, 1.8$ Hz, 2H), 4.25 – 4.20 (m, 4H), 3.00 (dddd, $J = 14.9, 6.4, 1.2, 1.2$ Hz, 2H), 2.74 (dddd, $J =$

14.7, 11.7, 2.1, 2.1 Hz, 2H), 0.90 (s, 18H), 0.08 (s, 6H), 0.03 (s, 6H); ^{13}C NMR (126 MHz, CDCl_3) δ 163.4, 138.6, 137.0, 112.4, 110.1, 69.2, 62.8, 58.1, 35.4, 25.7, 18.0, -4.6, -4.7; IR (NaCl/thin film): 2948, 2924, 2884, 2853, 1670, 1418, 1335, 1288, 1282, 1257, 1243, 1198, 1183, 1162, 1128, 1101, 1072, 1059, 1018, 996, 939, 904, 889, 871, 834, 806, 774, 723 cm^{-1} ; HRMS (ESI) calc'd for $\text{C}_{24}\text{H}_{31}\text{N}_2\text{O}_5\text{Si}$ [M– $\text{C}_6\text{H}_{15}\text{OSi}$] $^+$ 455.1997, found 455.2008 (detected fragment has undergone loss of *tert*-butyldimethylsilanolate anion).

Preparation of diol **276** from bis(*tert*-butyldimethylsilyl) ether **190**



To a solution of bis(*tert*-butyldimethylsilyl) ether **190** (8.9 mg, 0.015 mmol) in 1.05 mL THF/ H_2O (6:1) was added 0.45 mL HCO_2H with stirring. After 2.5 h, the mixture was quenched with sat. *aq.* NaHCO_3 and extracted with EtOAc (3x). The combined organics were then washed with sat. *aq.* NaHCO_3 (back-extracting the aqueous with EtOAc), dried over Na_2SO_4 , filtered, and concentrated *in vacuo*. Purification by flash chromatography (gradient elution, 1:1→2:3 hexanes–EtOAc) afforded diol **276** (3.4 mg, 62% yield). $[\alpha]_D^{25.0} = -264^\circ$ ($c = 0.17$, CHCl_3); ^1H NMR (500 MHz, CDCl_3) δ 6.57 (ddd, $J = 2.1, 2.1, 2.1$ Hz, 2H), 6.27 (dd, $J = 8.3, 1.9$ Hz, 2H), 6.12 (d, $J = 2.2$ Hz, 2H), 4.78 (dd, $J = 8.3, 1.8$ Hz, 2H), 4.70 (ddd, $J = 8.1, 2.2, 2.2$ Hz, 2H), 4.44 (dd, $J = 10.3, 8.0$ Hz, 2H), 4.30 (dd, $J = 8.0, 2.0, 2.0, 2.0$ Hz, 2H), 2.98 – 2.86 (m, 4H); ^{13}C NMR (101 MHz, CDCl_3) δ 170.3, 140.2, 139.1, 114.4, 108.7, 69.2, 66.9, 62.1, 29.5; IR (NaCl/thin film): 3583, 3305, 2916, 2848, 1663, 1419, 1351, 1319, 1294, 1206, 1174, 1129, 1079,

1035, 905, 884, 808, 750 cm^{-1} ; HRMS (ESI) calc'd for $\text{C}_{18}\text{H}_{15}\text{N}_2\text{O}_4$ [$\text{M}-\text{H}_2\text{O}-\text{HO}$] $^+$ 323.1026, found 323.1050 (detected fragment has undergone loss of H_2O and OH^-).

4.6 NOTES AND REFERENCES

-
- (1) Codelli, J. A.; Puchlopek, A. L. A.; Reisman, S. E. *J. Am. Chem. Soc.* **2012**, *134*, 1930.
 - (2) Decarboxylative (1,3)-dipolar cycloaddition between proline and cinnamaldehyde to give the racemic pyrrolizidine: (a) Kang, T.-R.; Cheng, Y.; He, L.; Ye, J.; Liu, Q.-Z. *Tetrahedron Lett.* **2012**, *53*, 2552. (b) Hong, B.-C.; Liu, K.-L.; Tsai, C.-W.; Liao, J.-H. *Tetrahedron Lett.* **2008**, *49*, 5480.
 - (3) A single, non-enantioselective example of a related double (1,3)-DCA has been reported: Cui, P.; Xu, L.; Shi, Z.; Gan, L. *J. Org. Chem.* **2011**, *76*, 4210.
 - (4) (a) Hartmann, T.; Witte, L., in *Alkaloids: Chemical and Biological Perspectives*, ed. S.W. Pelletier, Pergamon, Oxford, **1995**, 155. (b) Nash, R. J.; Fellows, L. E.; Dring, J. V.; Fleet, G. W. J.; Derome, A. E.; Hamor, T. A.; Scofield, A. M.; Watkin, D. J. *Tetrahedron Lett.* **1988**, *29*, 2487. (c) Asano, N.; Kuroi, H.; Ikeda, K.; Kizu, H.; Kameda, Y.; Kato, A.; Adachi, I.; Watson, A. A.; Nash, R. J.; Gleet, G. W. J. *Tetrahedron: Asymmetry* **2000**, *11*, 1. (d) Nash, R. J.; Thomas, P. I.; Waigh, R. D.; Fleet, G. W. J.; Wormald, M. R.; Lilley, P. M. D.; Watkin, D. J. *Tetrahedron Lett.* **1994**, *35*, 7849. (e) Asano, N.; Nash, R. J.; Molyneux, R. J.; Fleet, G. W. J. *Tetrahedron: Asymmetry* **2000**, *11*, 1645. (f) Daly, J. W. *J. Nat. Prod.* **1998**, *61*, 162. (g) Garraffo, H. M.; Spande, T. F.; Daly, J. W.; Baldessari, A.; Gros, E. G. *J. Nat. Prod.* **1993**, *56*, 357. (g) Takeda, M.; Tsukamoto, K.; Mizutani, Y.; Suzuki, T.; Taniyama, K. *Jpn. J. Pharmacol.* **1999**, *203*. (h) Becker, D. P.; Flynn, D. L.; Moormann, A. E.; Nosal, R.; Villamil, C. I.; Loeffler, R.;

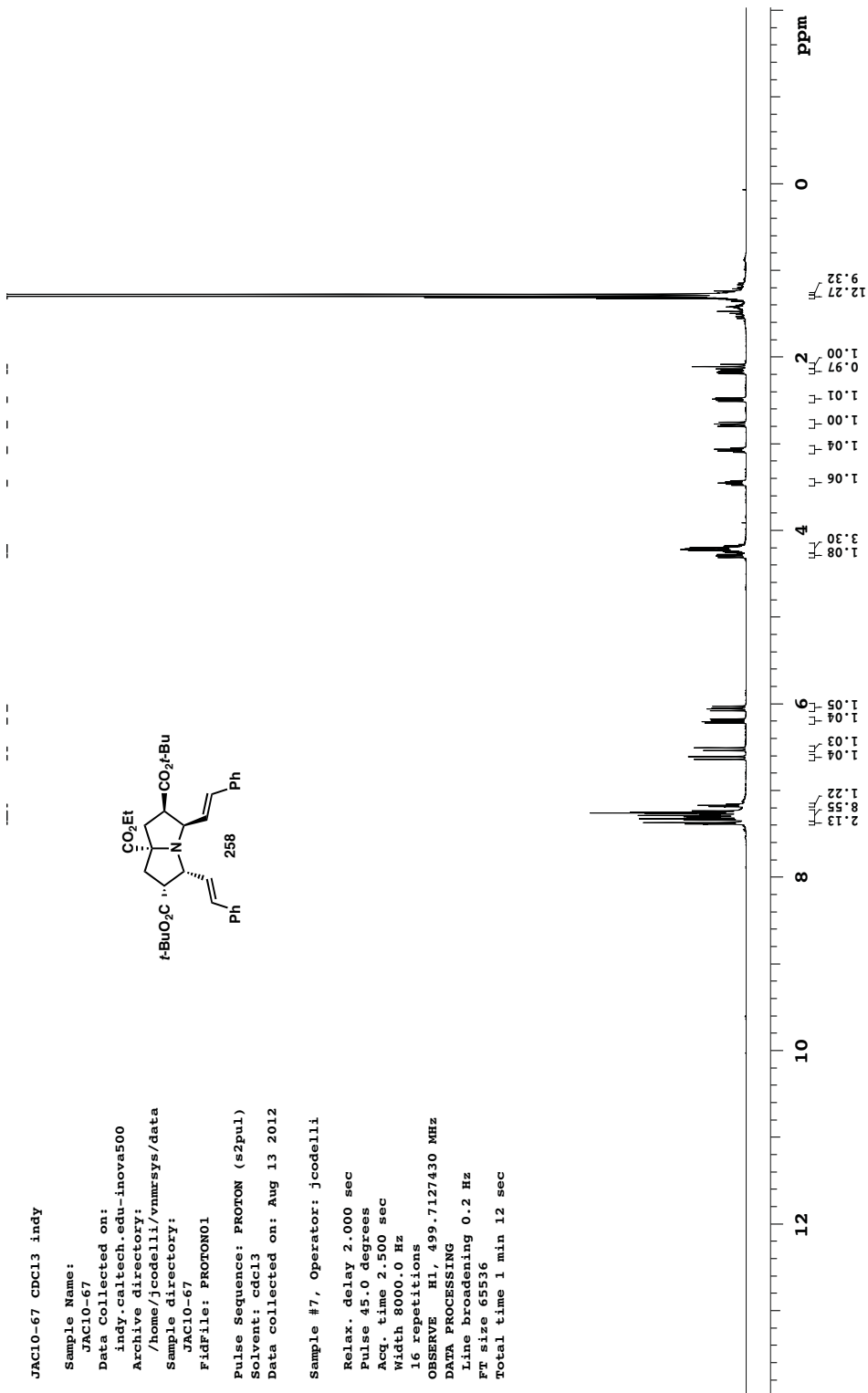
-
- Gullikson, G. W.; Moummi, C.; Yang, D.-C. *J. Med. Chem.* **2006**, *49*, 1125. (i)
- Morriello, J.; DeVita, R. J.; Mills, S. G.; Young, J. R.; Lin, P.; Doss, G.; Chicchi, G. G.; DeMartino, J.; Kurtz, M. M.; Tsao, K.-L. C.; Carlson, E.; Townson, K.; Wheeldon, A.; Boyce, S.; Collinson, N.; Rupniak, N.; Moore, S. *Bioorg. Med. Chem.* **2008**, *16*, 2156.
- (5) (a) Broggini, G.; Zecchi, G. *Synthesis* **1999**, 905. (b) Brandi, A.; Cardona, F.; Cicchi, S.; Cordero, F. M.; Goti, A. *Chem.—Eur. J.* **2009**, *15*, 7808.
- (6) The first highly enantioselective catalytic (1,3)-dipolar cycloadditions of azomethine ylides: (a) Gothelf, A. S.; Gothelf, K. V.; Hazell, R. G.; Jørgensen, K. A. *Angew. Chem., Int. Ed.* **2002**, *41*, 4236. (b) Longmire, J. M.; Wang, B.; Zhang, X. M. *J. Am. Chem. Soc.* **2002**, *124*, 13400.
- (7) Selected examples of metal-catalyzed enantioselective 1,3-DCAs between *unsubstituted* acrylates and azomethine ylides derived from a-(arylideneamino)esters: (a) Yamashita, Y.; Imaizumi, T.; Kobayashi, S. *Angew. Chem., Int. Ed.* **2011**, *50*, 4893. (b) Shimizu, K.; Ogata, K.; Fukuzawa, S.-I. *Tetrahedron Lett.* **2010**, *51*, 5068. (c) Wang, C.-J.; Liang, G.; Xue, Z.-Y.; Gao, F. *J. Am. Chem. Soc.* **2008**, *130*, 17250. (d) Najera, C.; Retamosa, M. D.; Sansano, J. M. *Angew. Chem., Int. Ed.* **2008**, *47*, 6055. (e) Zeng, W.; Zhou, Y.-G. *Org. Lett.* **2005**, *7*, 5055. (f) Gao, W.; Zhang, X.; Raghunath, M. *Org. Lett.* **2005**, *7*, 4241.
- (8) Kim, H. Y.; Shih, H.-J.; Knabe, W. E.; Oh, K. *Angew. Chem., Int. Ed.* **2009**, *48*, 7420.
- (9) Chen, C.; Li, X. D.; Schreiber, S. L. *J. Am. Chem. Soc.* **2003**, *125*, 10174.

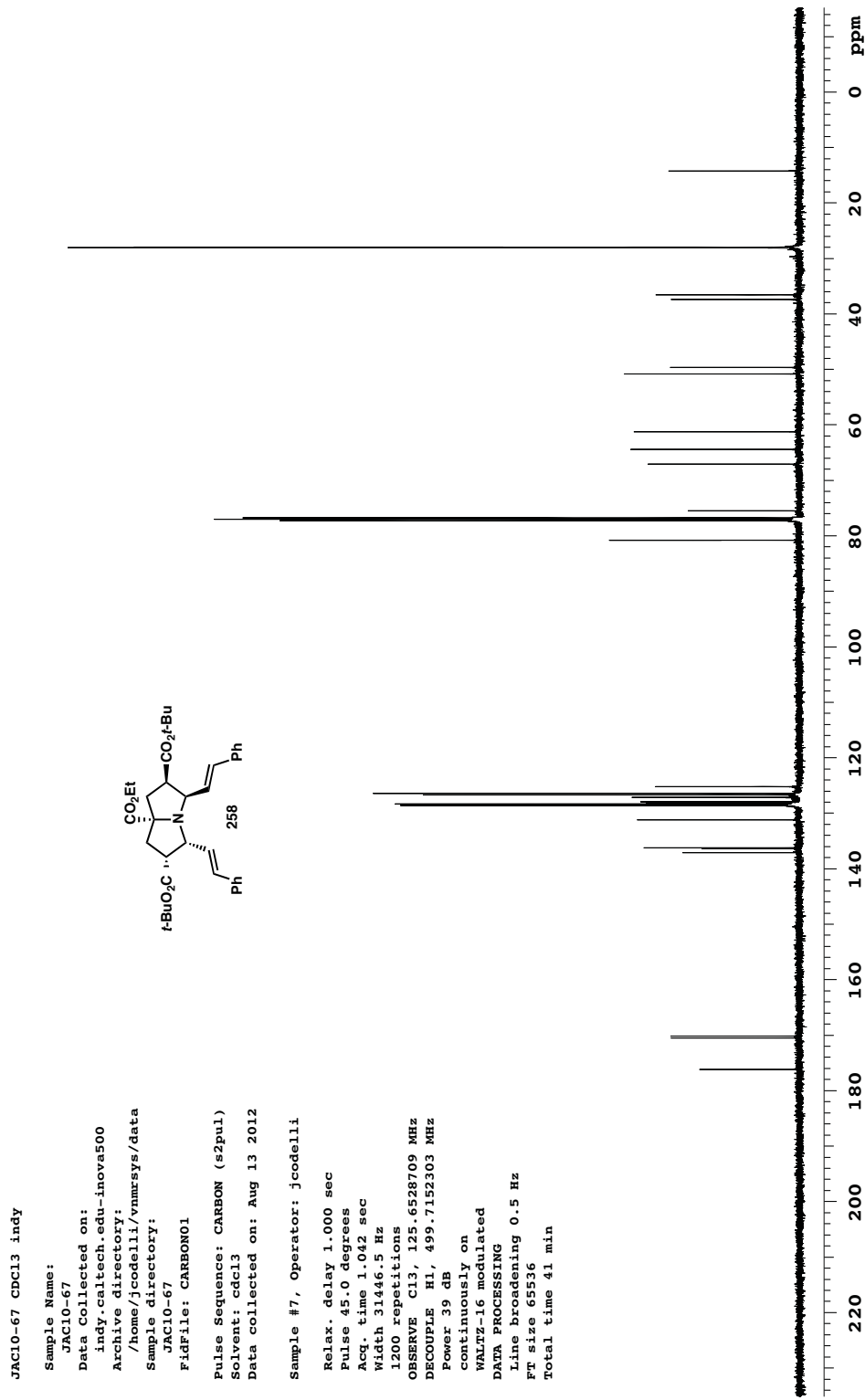
-
- (10) Specifically, the AgOAc/(S)-QUINAP conditions require a substantially shorter prestir for catalyst generation. The resulting catalyst solution is homogeneous and could be used as a stock solution, facilitating our methodological studies.
 - (11) We have consistently found that pyrrolizidine **258** can be isolated in higher yields than the corresponding pyrrolidine **153**. We attribute this to challenges in isolating and purifying the free N–H pyrrolidine.
 - (12) Although the studies reported herein utilized co-catalytic quantities of DIPEA, we have determined that cycloadditions can also be carried out in the absence of DIPEA, with equal or slightly reduced yields.
 - (13) The AgOAc/QUINAP-catalyzed 1,3-DCA between **141** and **152** at 23 °C furnishes pyrrolidine **153** in 77% ee.
 - (14) *N*-(2-Pyridylmethyl)imines have been shown to participate in Cu-catalyzed asymmetric (1,3)-DCA reactions: Padilla, S.; Tejero, R.; Adrio, J.; Carretero, J. C. *Org. Lett.* **2012**, *12*, 5608.
 - (15) Ee values obtained using standard conditions: **269c** (80%), **269d** (83%), **269e** (73%), **269q** (84%), **269k** (84%), **269p** (82%).
 - (16) (*R*)-QUINAP was used.
 - (17) On 0.15 mmol scale, **269a** could be prepared in 88% yield and 90% ee using 1 mol% catalyst in conjunction with a 48 h reaction period for the first (1,3)-DCA. Use of 1 mol% catalyst under standard conditions provided **269a** in 64% yield and 86% ee.
 - (18) Kim, D.-W.; Jeong, H.-J.; Lim, S.-T.; Sohn, M.-H. *Angew. Chem., Int. Ed.* **2008**, *47*, 8404.

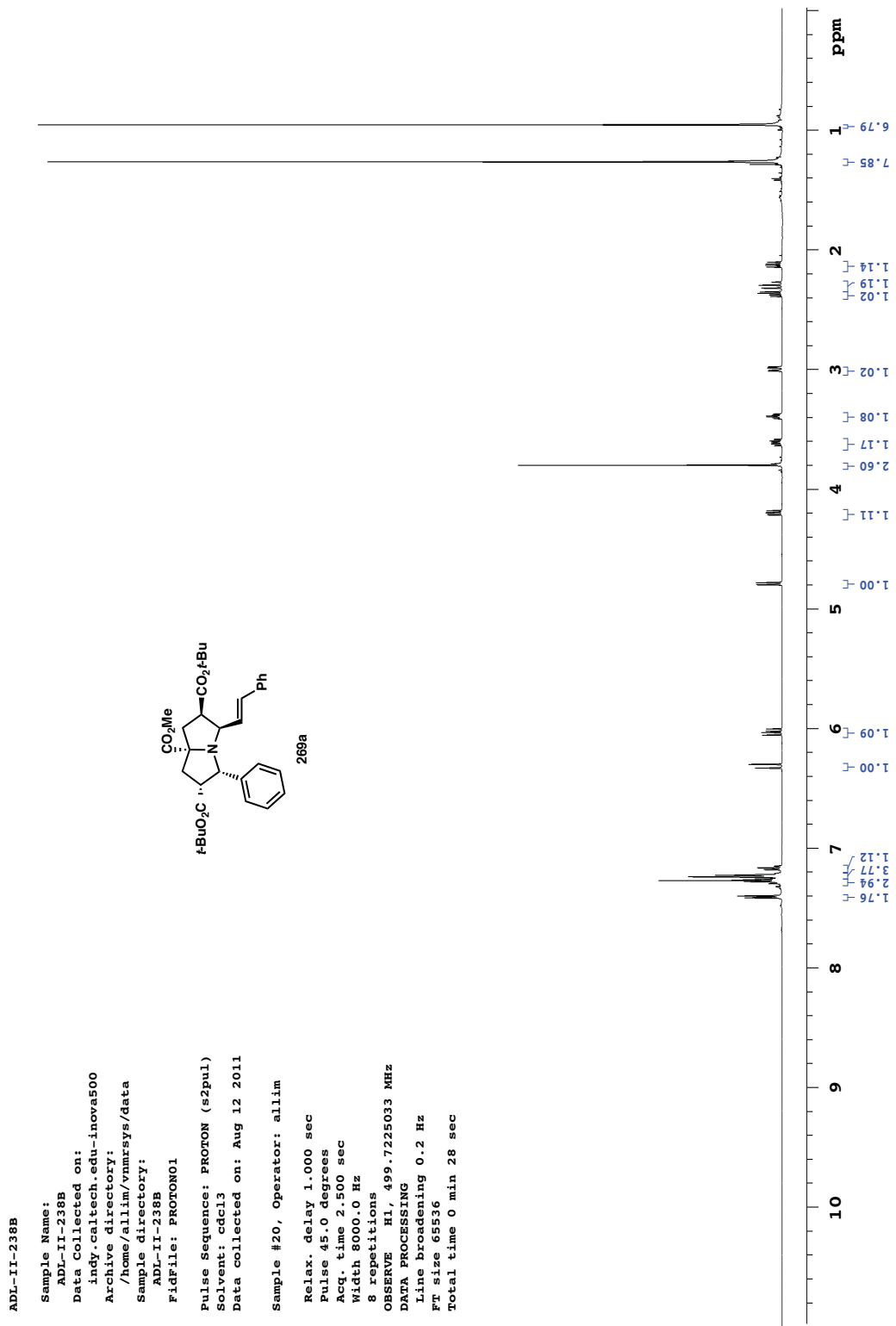
-
- (19) Review: Jones, A. B. in *Comprehensive Organic Synthesis*, Vol. 7: *Oxidation*, ed. Trost, B. M.; Fleming, I.; Ley, S. V., Pergamon, Oxford, **1991**, 151.
 - (20) Bailey, E. J.; Barton, D. H. R.; Elks, J.; Templeton, J. F. *J. Chem. Soc.* **1962**, 1578.
 - (21) Quasdorf, K. W.; Huters, A. D.; Lodewyk, M. W.; Tantillo, D. J.; Garg, N. K. *J. Am. Chem. Soc.* **2012**, 134, 1396.
 - (22) Buckley, B. R.; Fernández, D.-R. *Tetrahedron Lett.* **2013**, 54, 843.
 - (23) Still, W. C., Kahn, M. & Mitra, A. *J. Org. Chem.* **1978**, 43, 2923.
 - (24) Longmire, J. M.; Wang, B.; Zhang, X. *J. Am. Chem. Soc.* **2002**, 124, 13400.

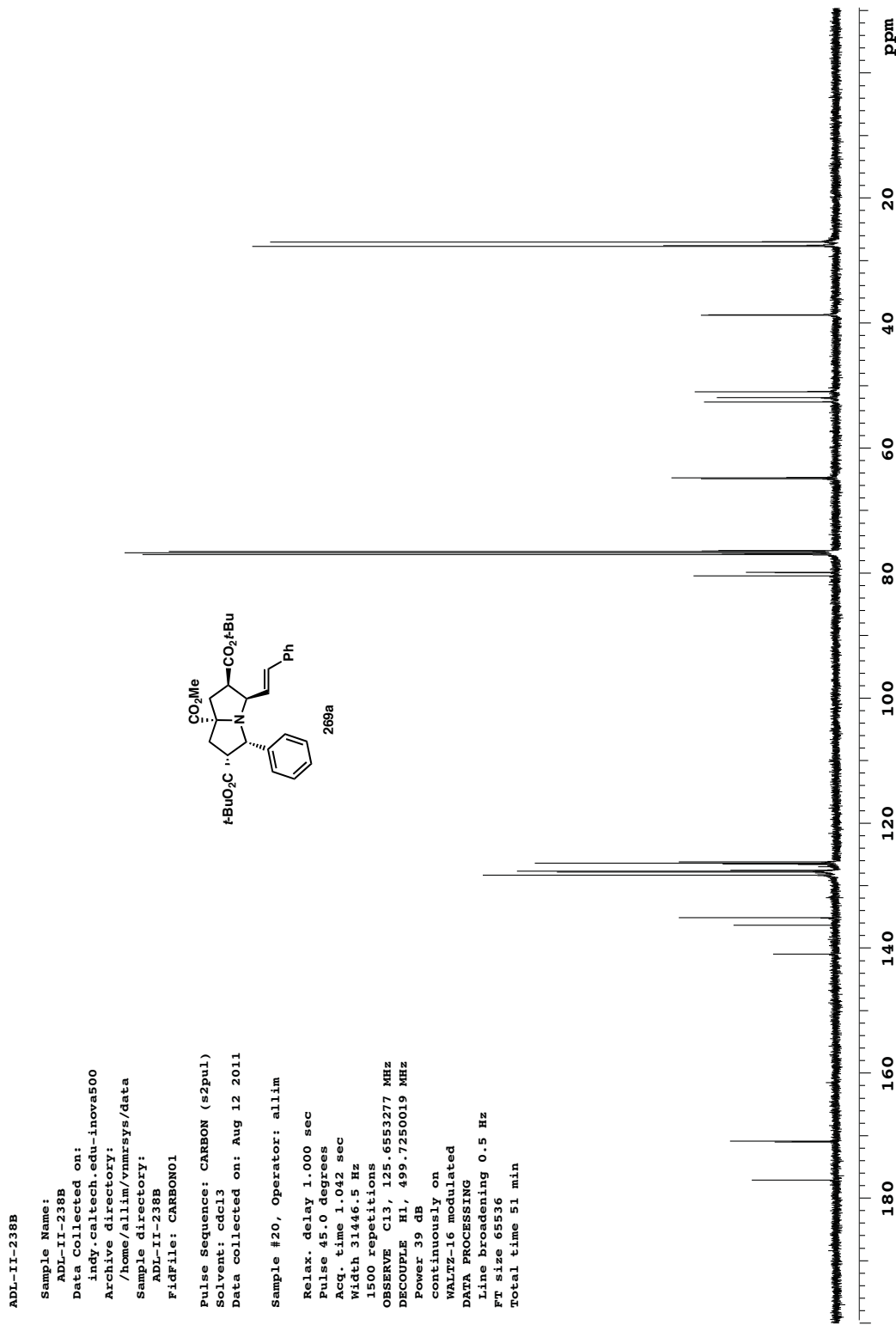
Appendix 4

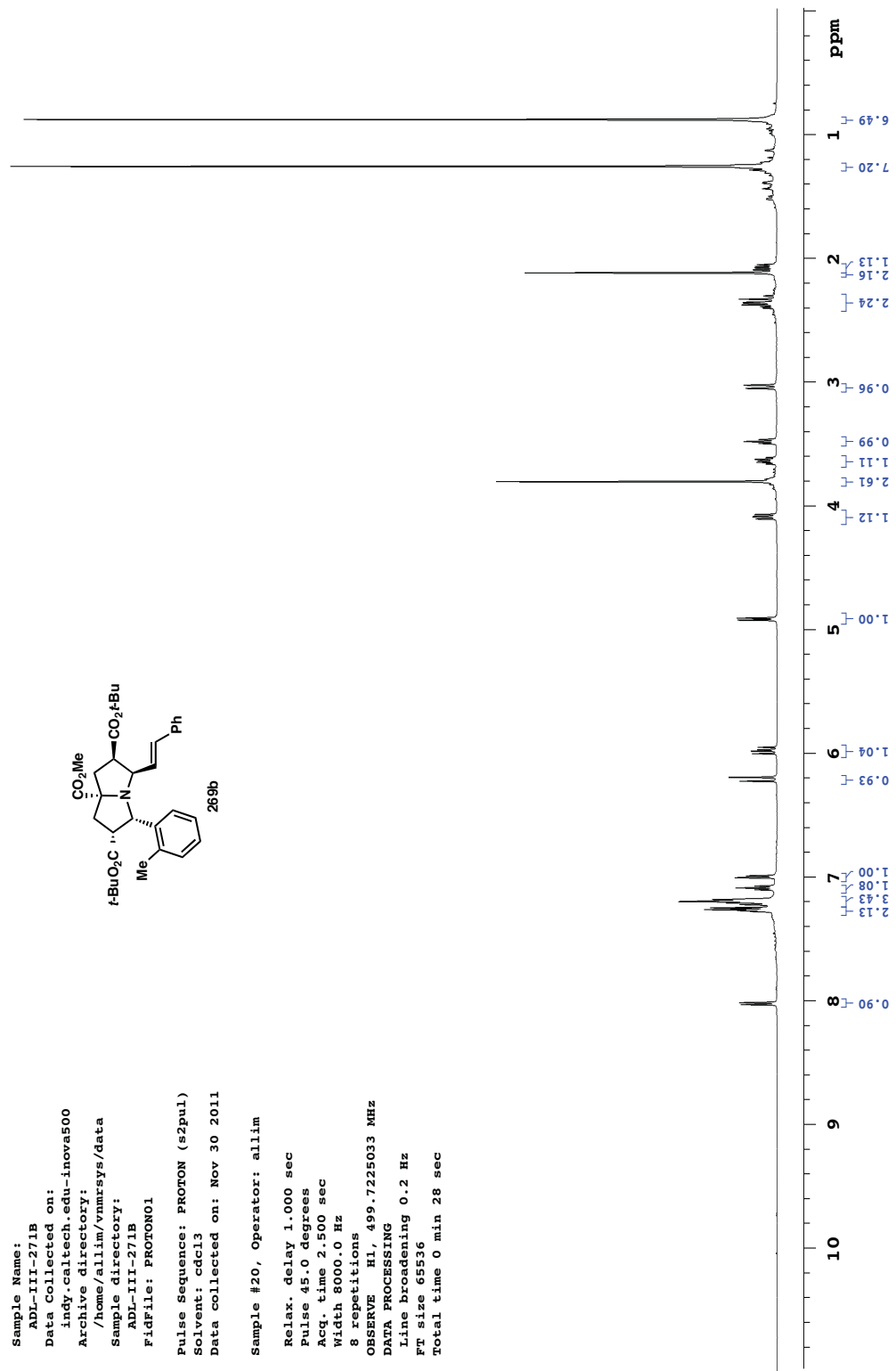
*Spectra Relevant to Chapter 4:
Further Investigation of Side Reactions*

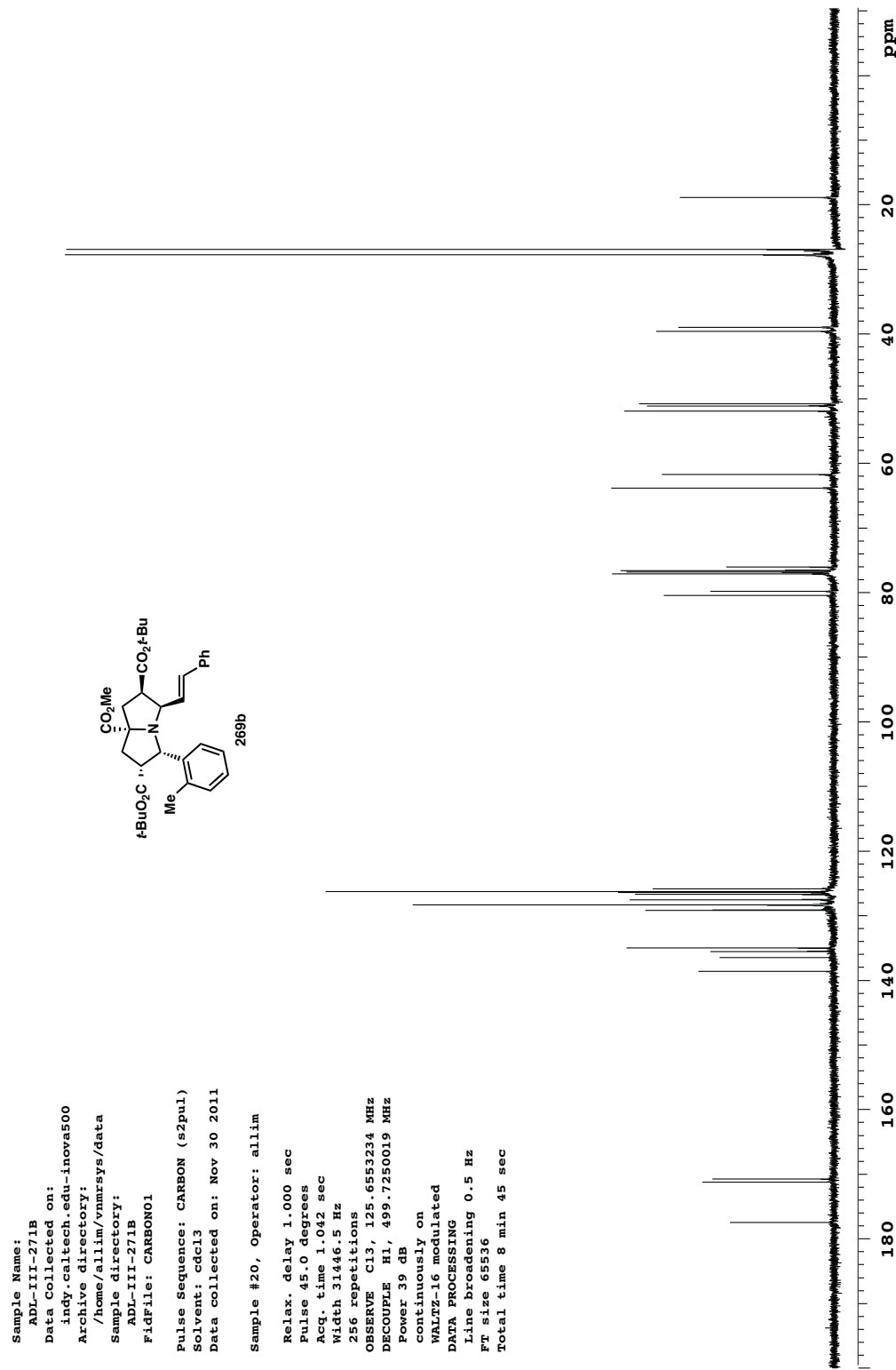


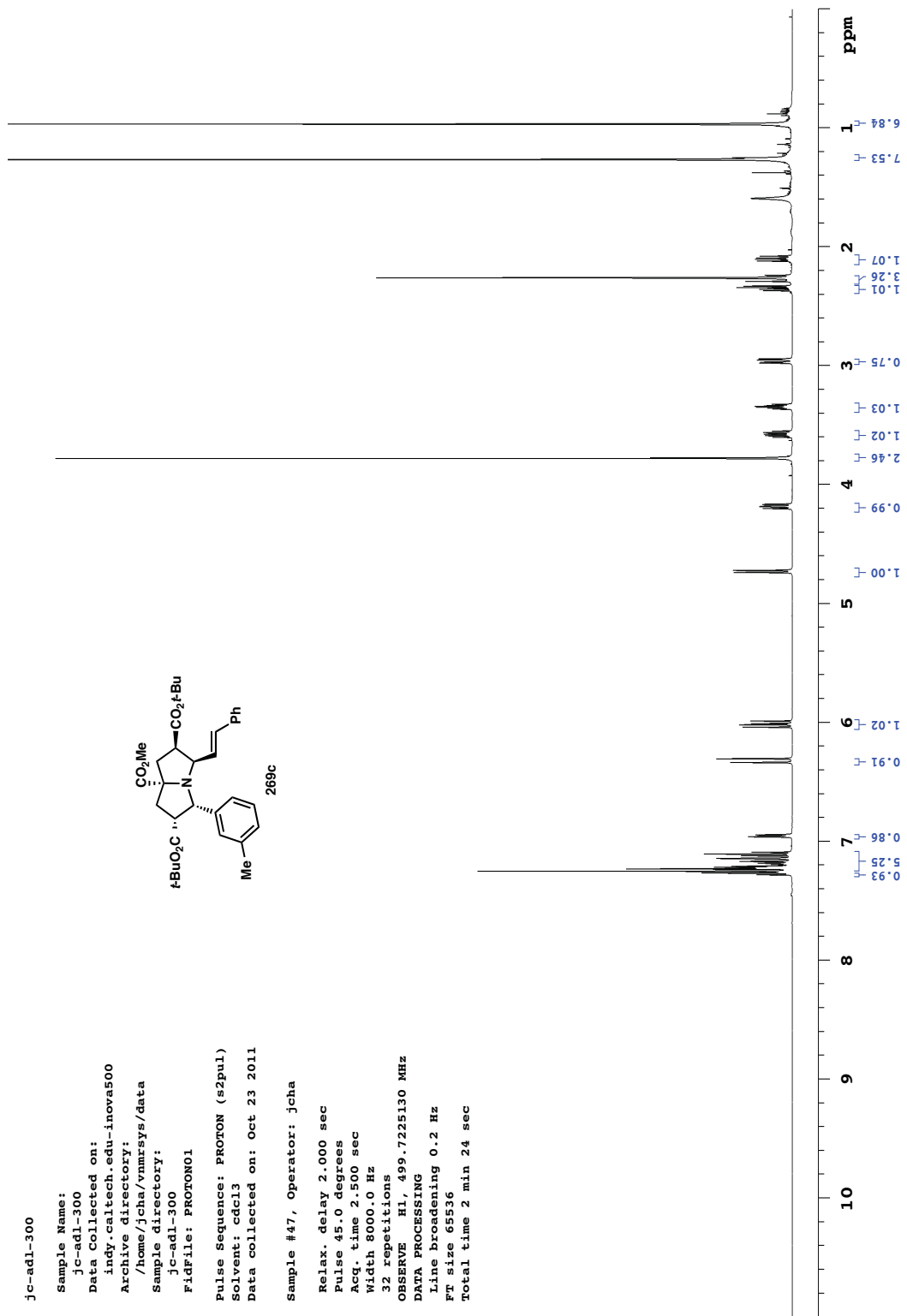


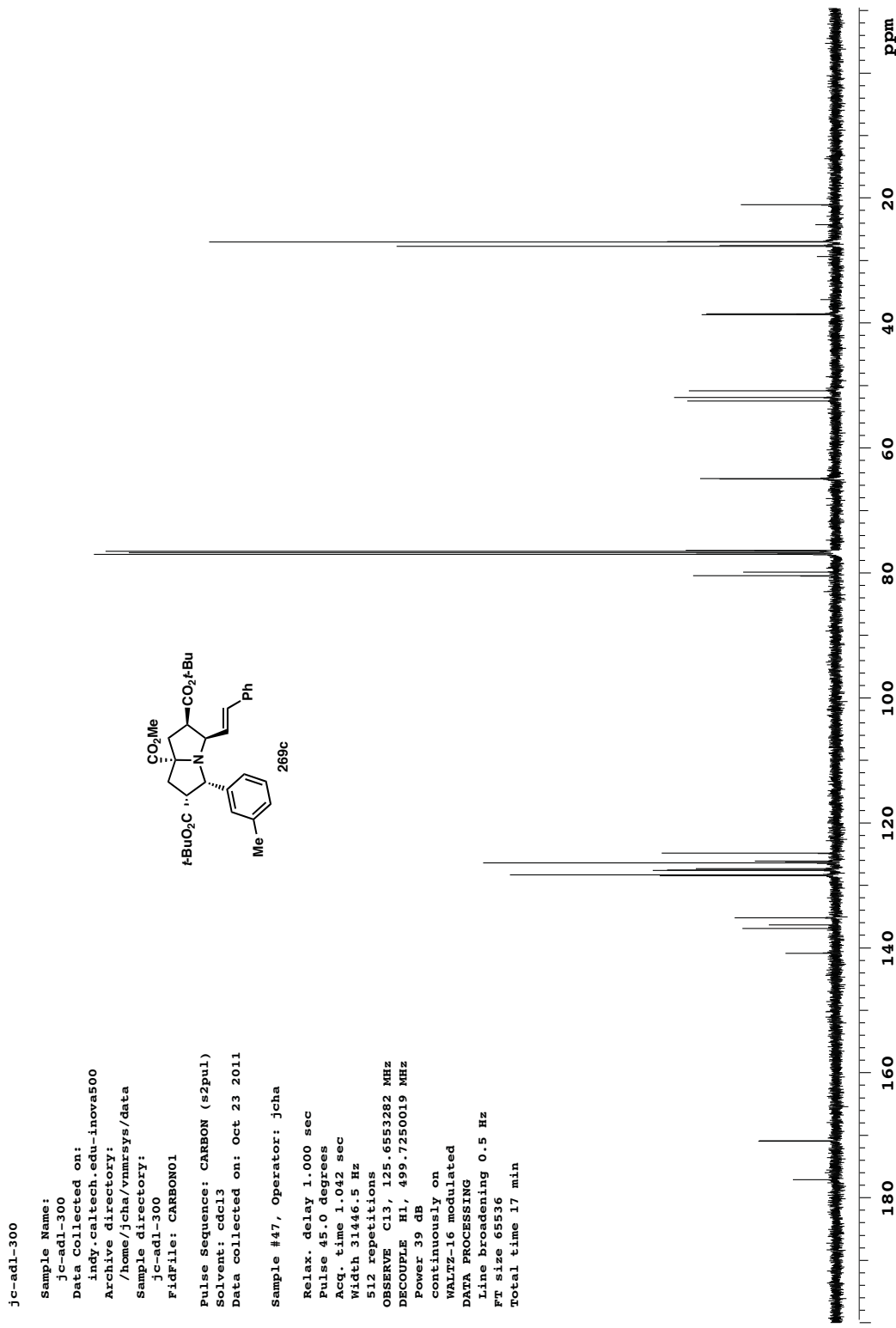


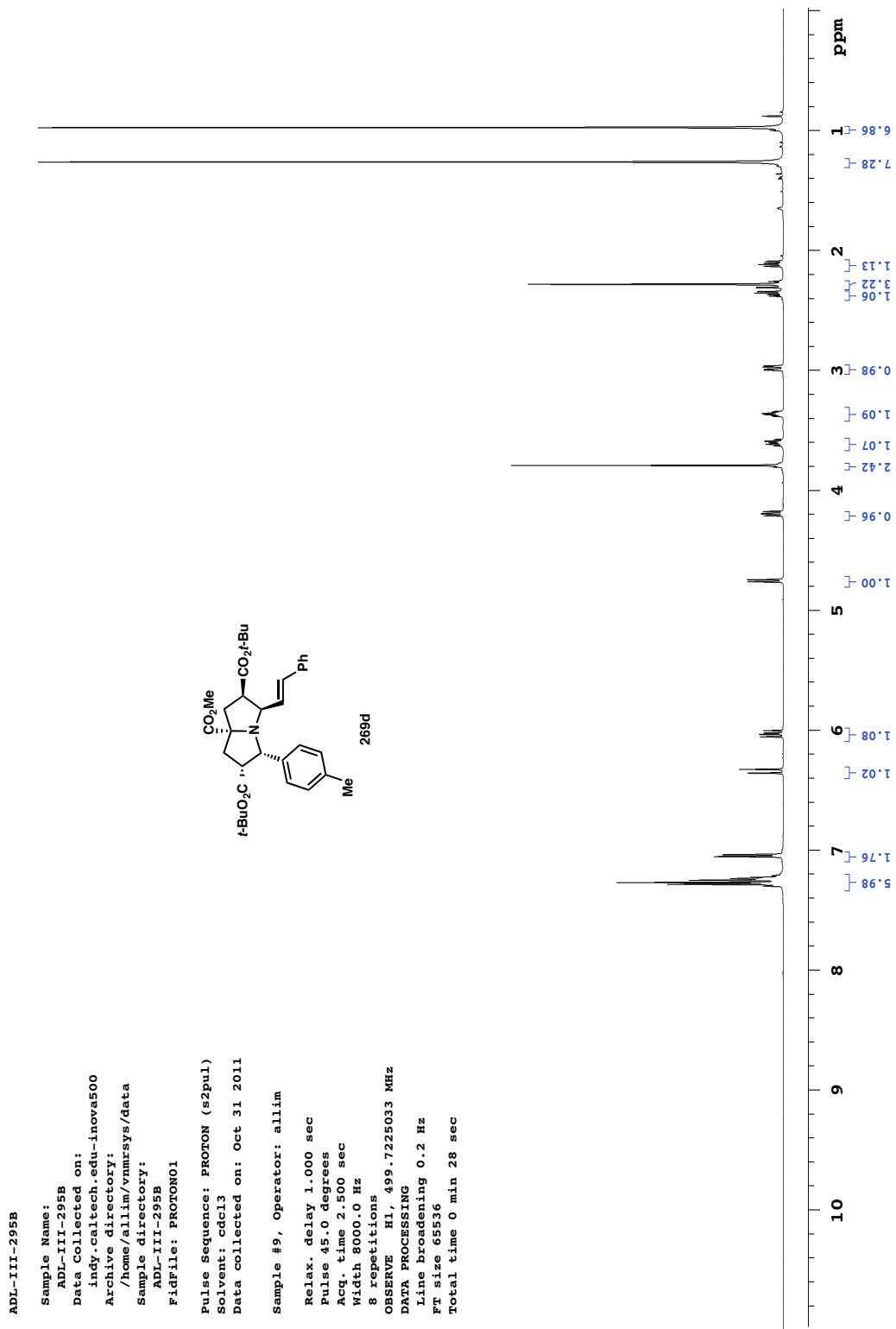


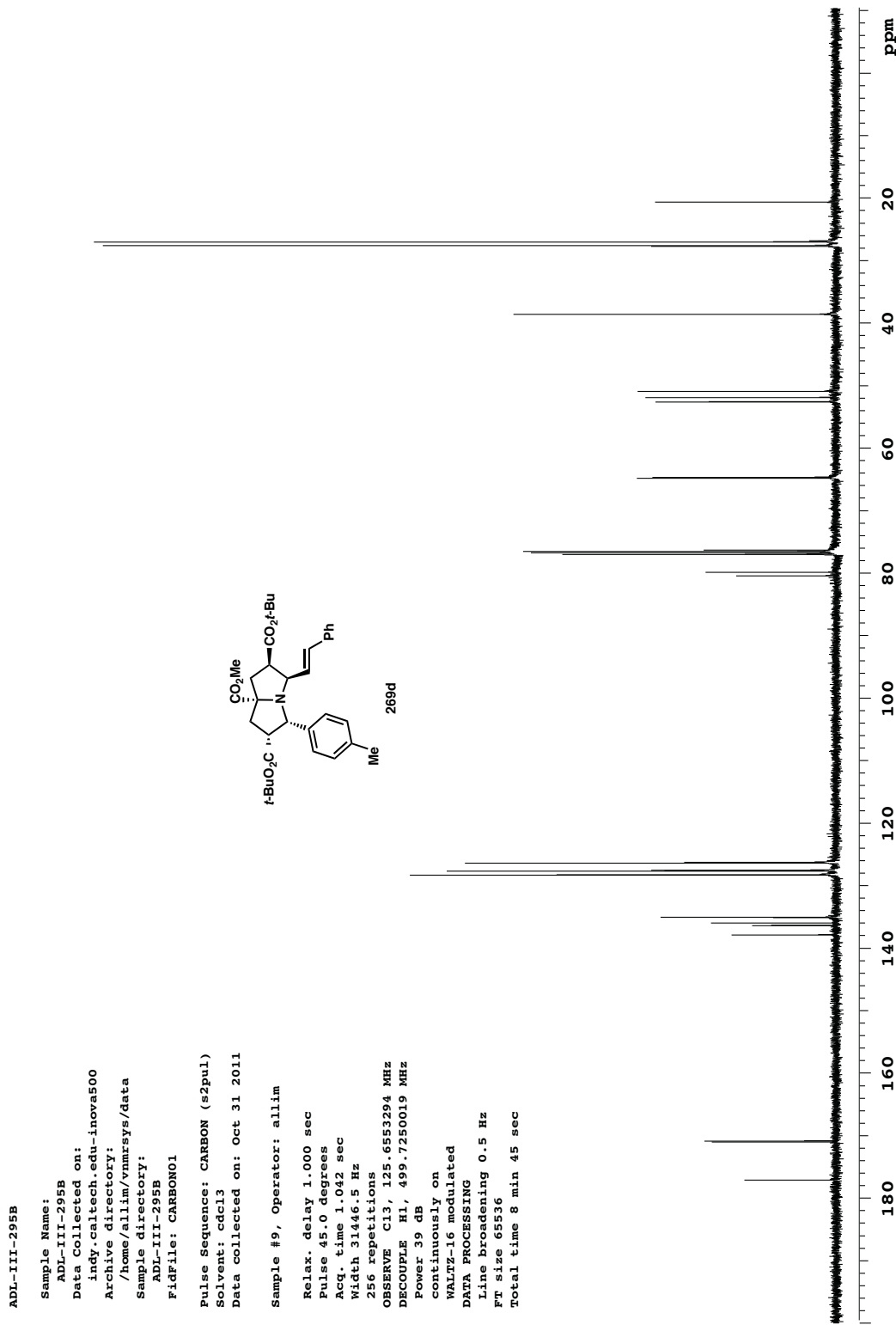


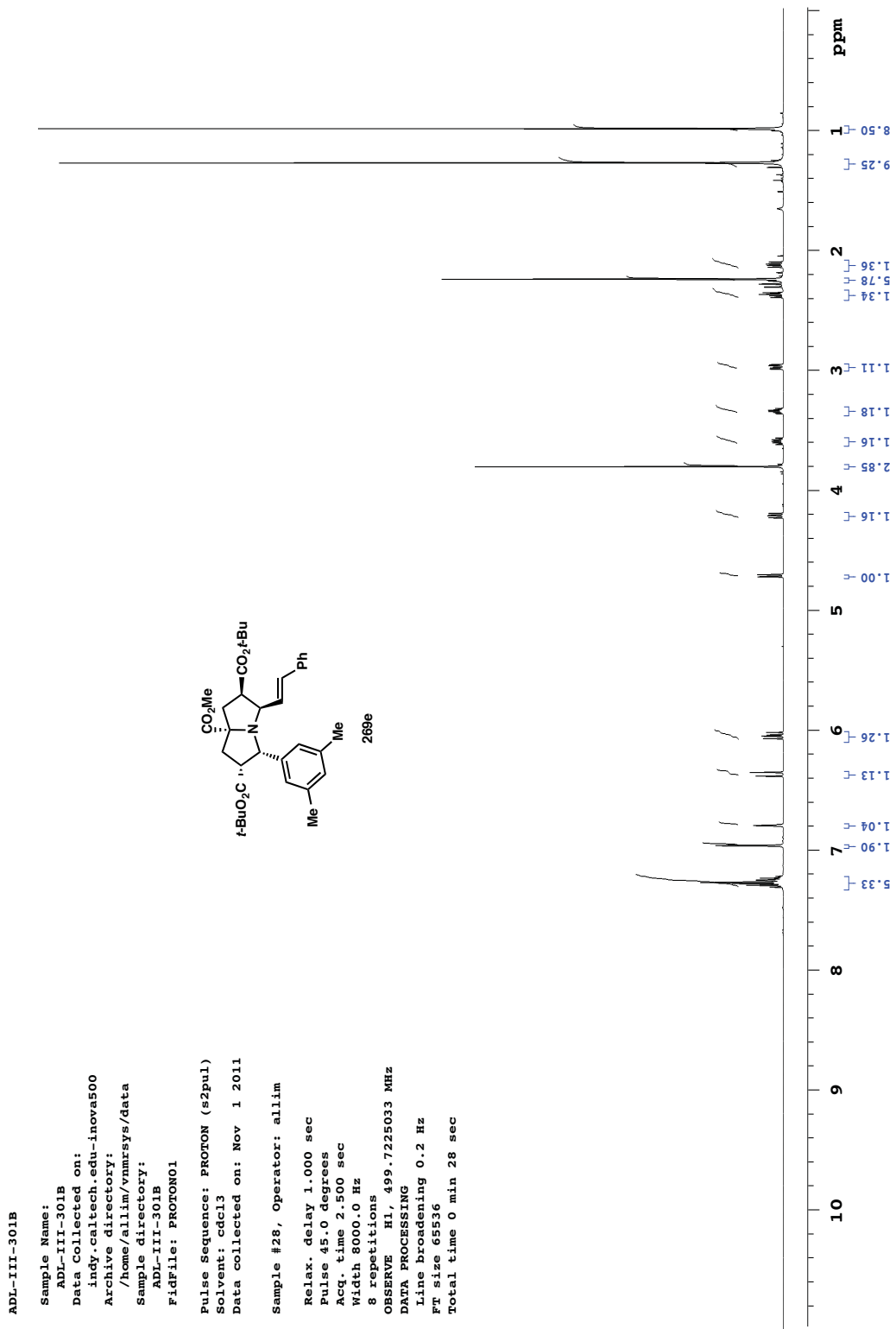


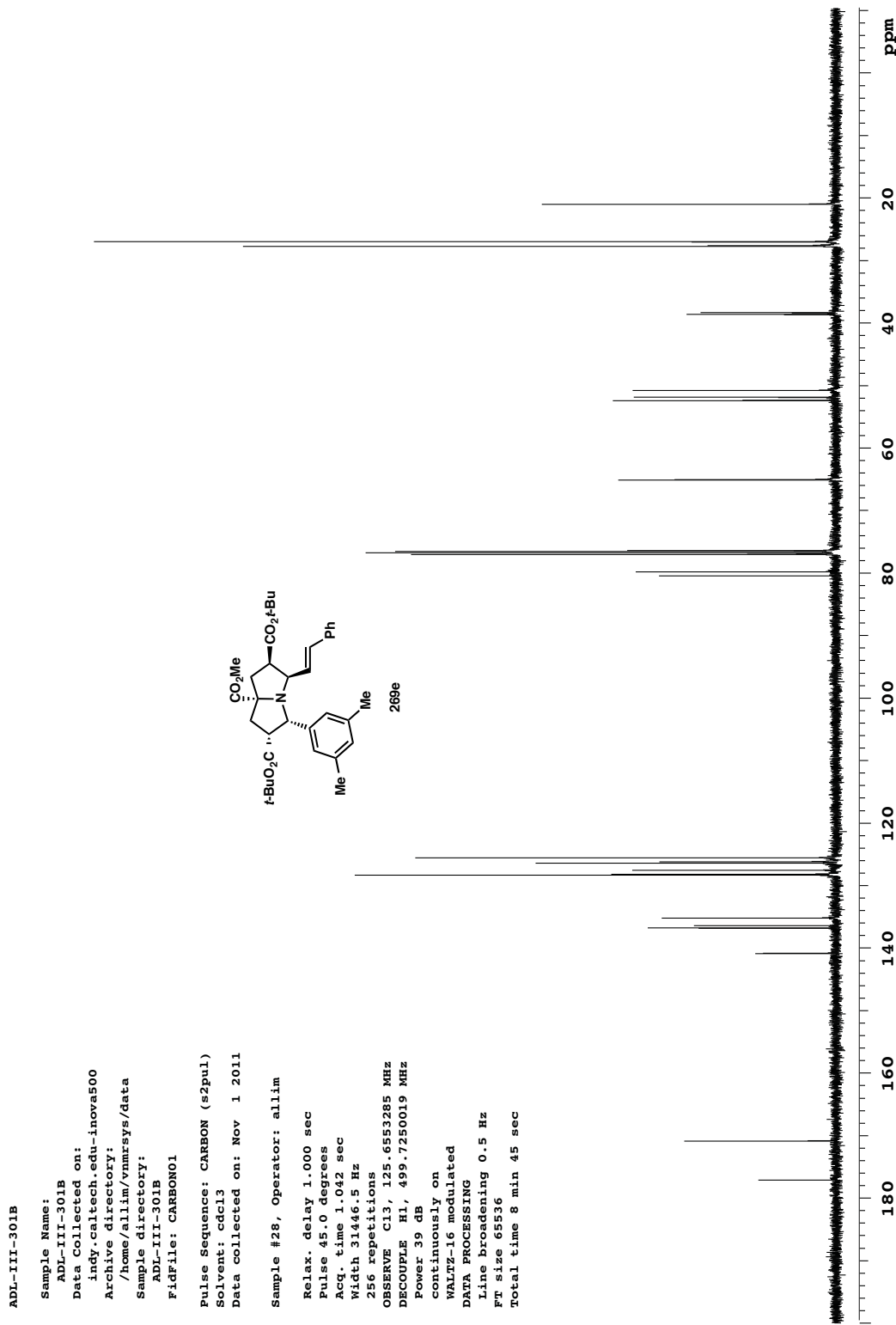


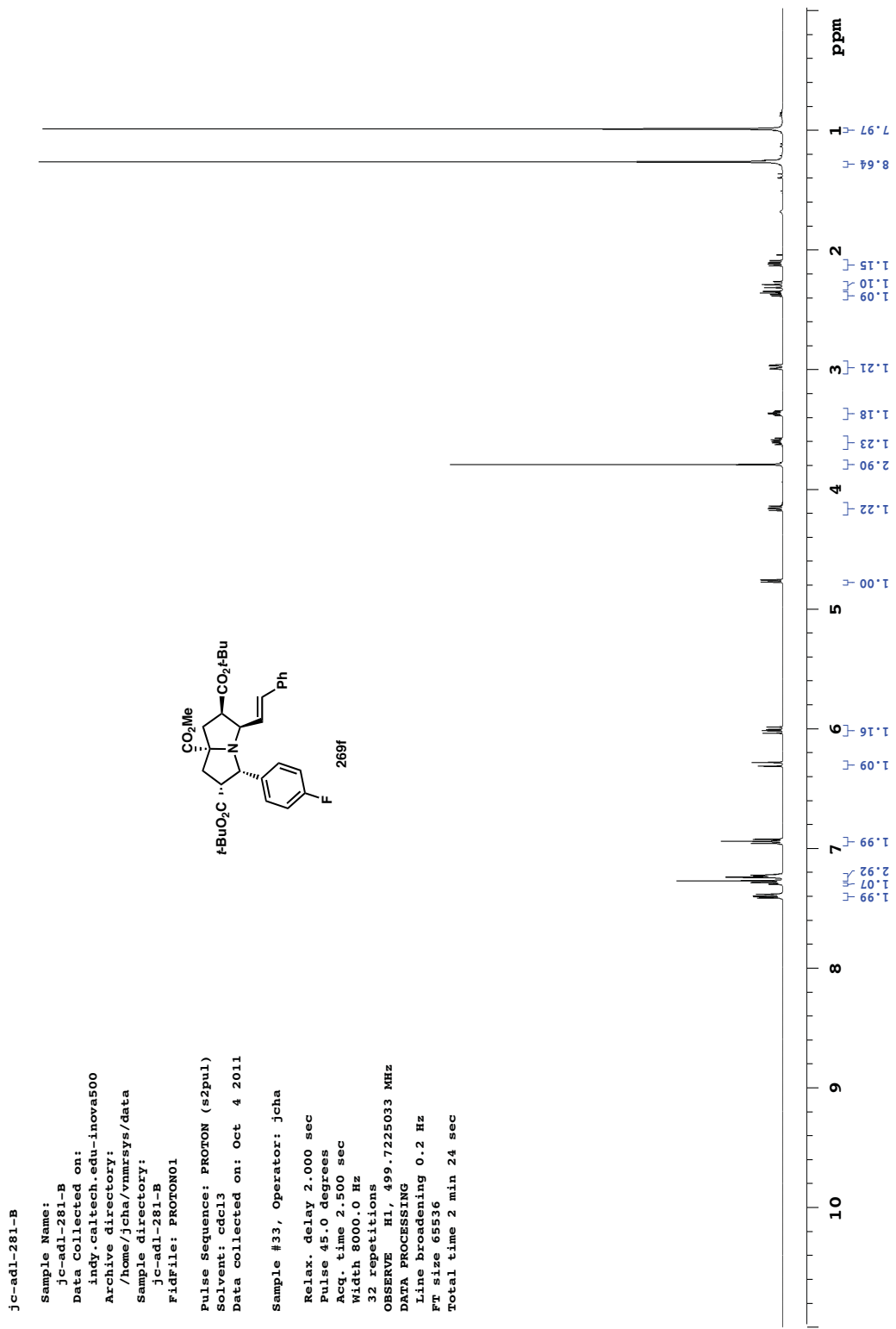


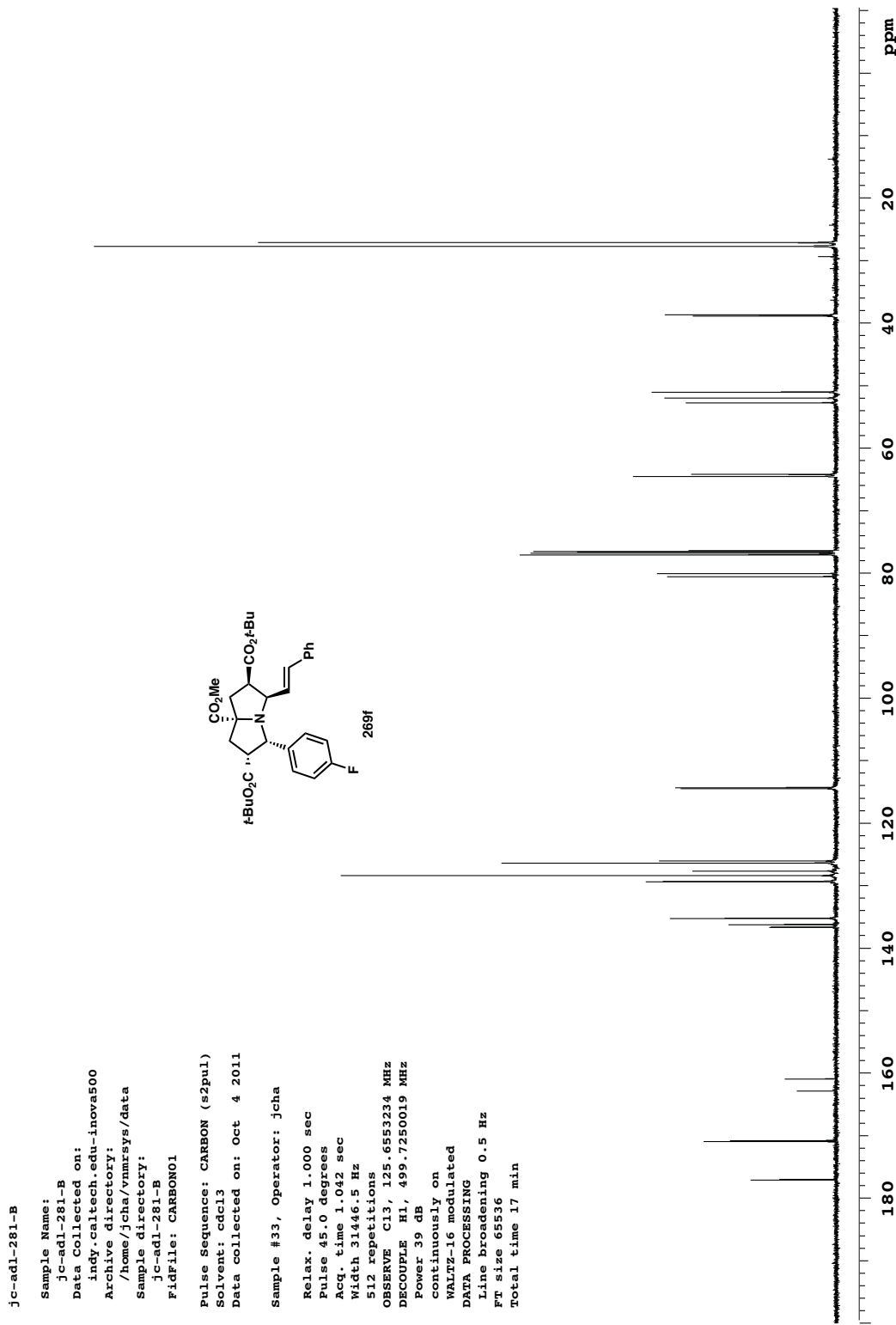


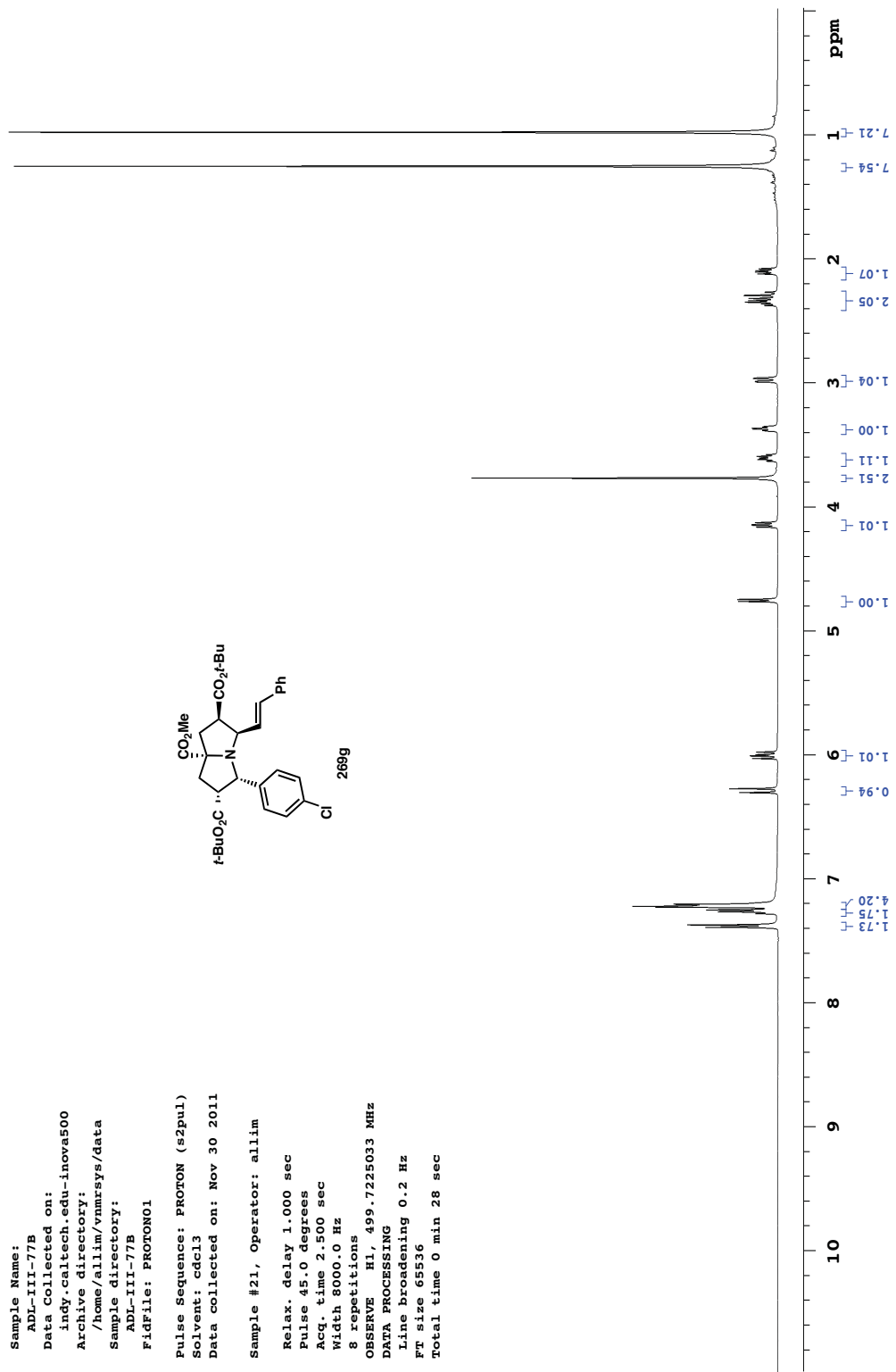


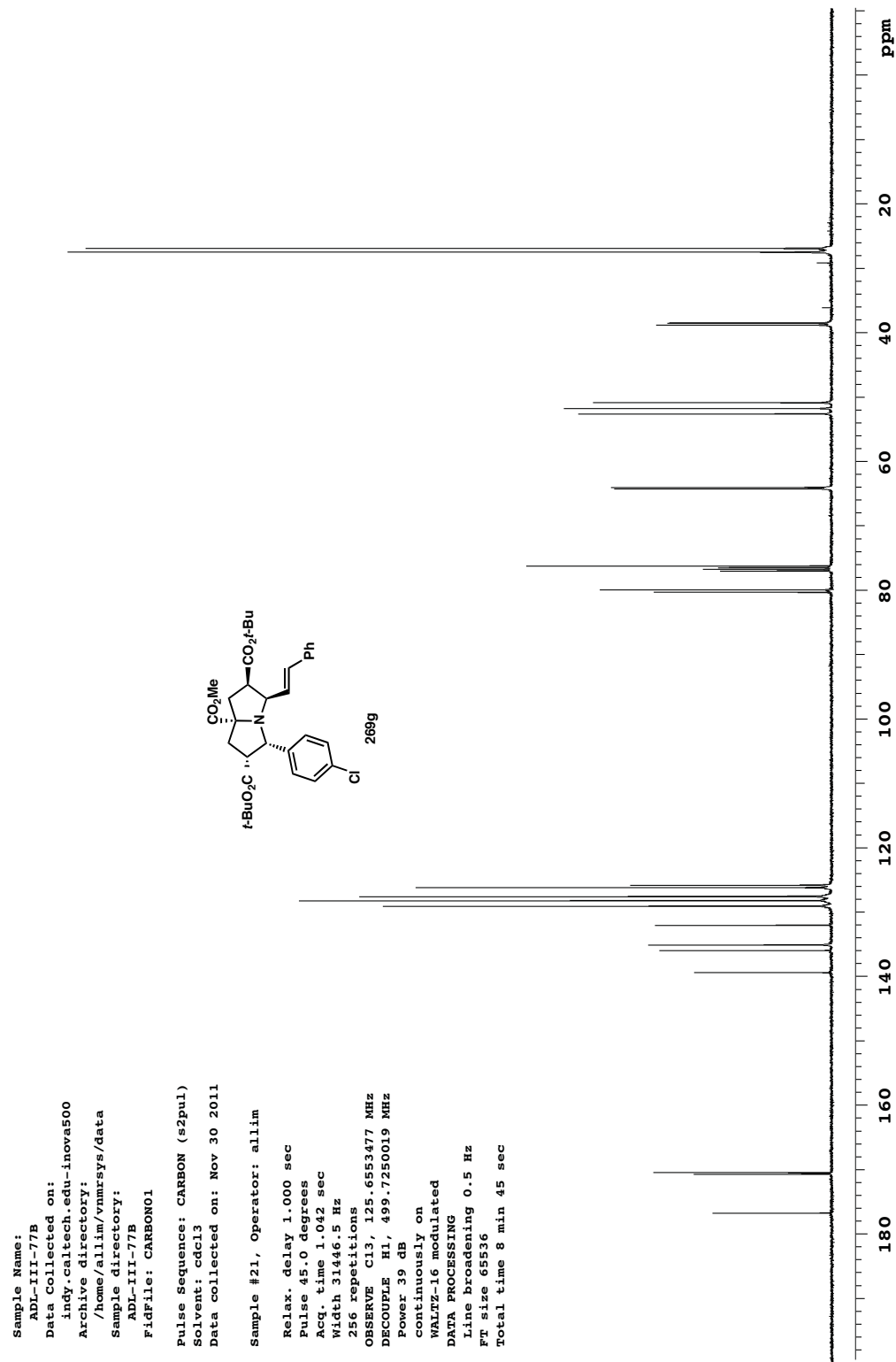


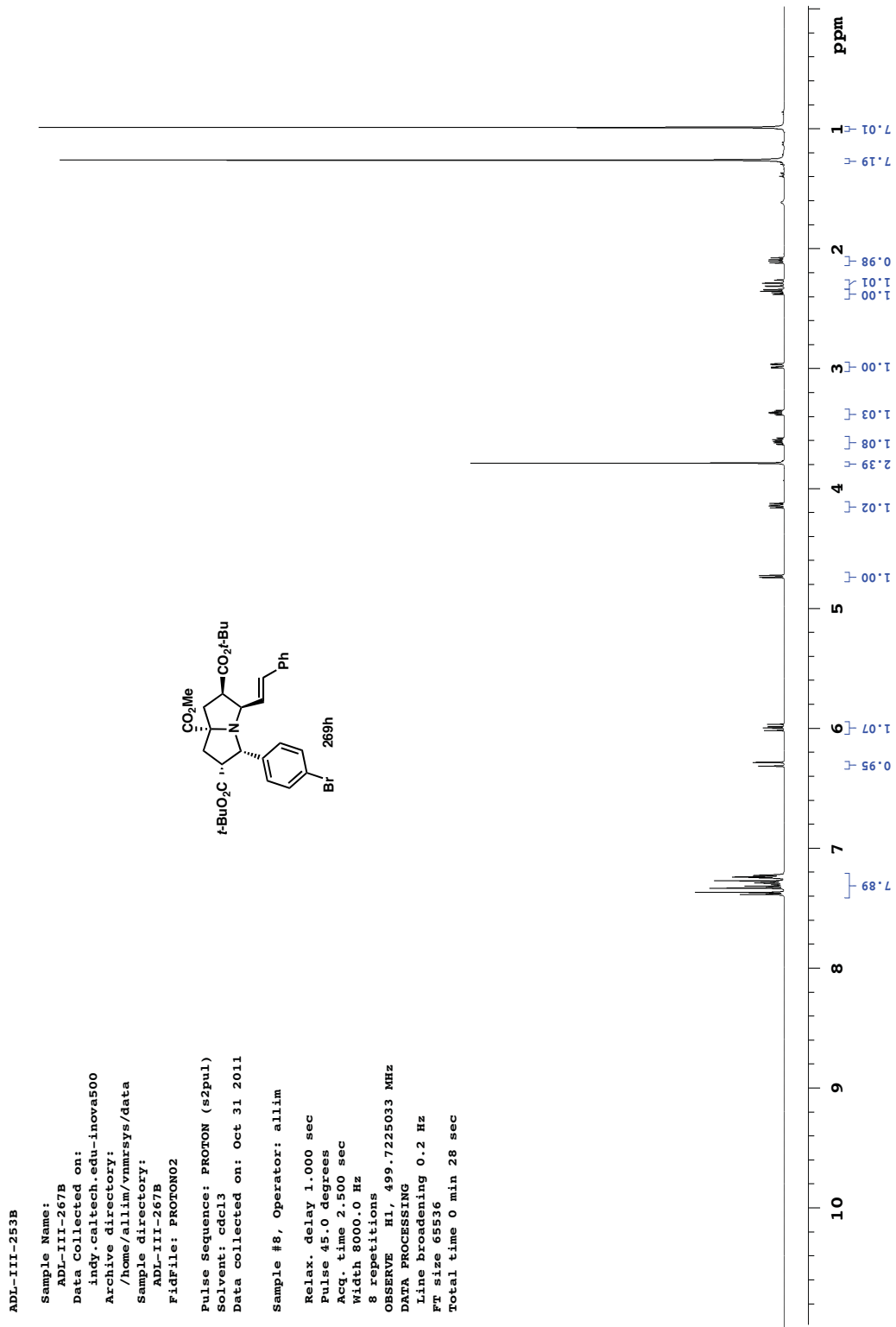


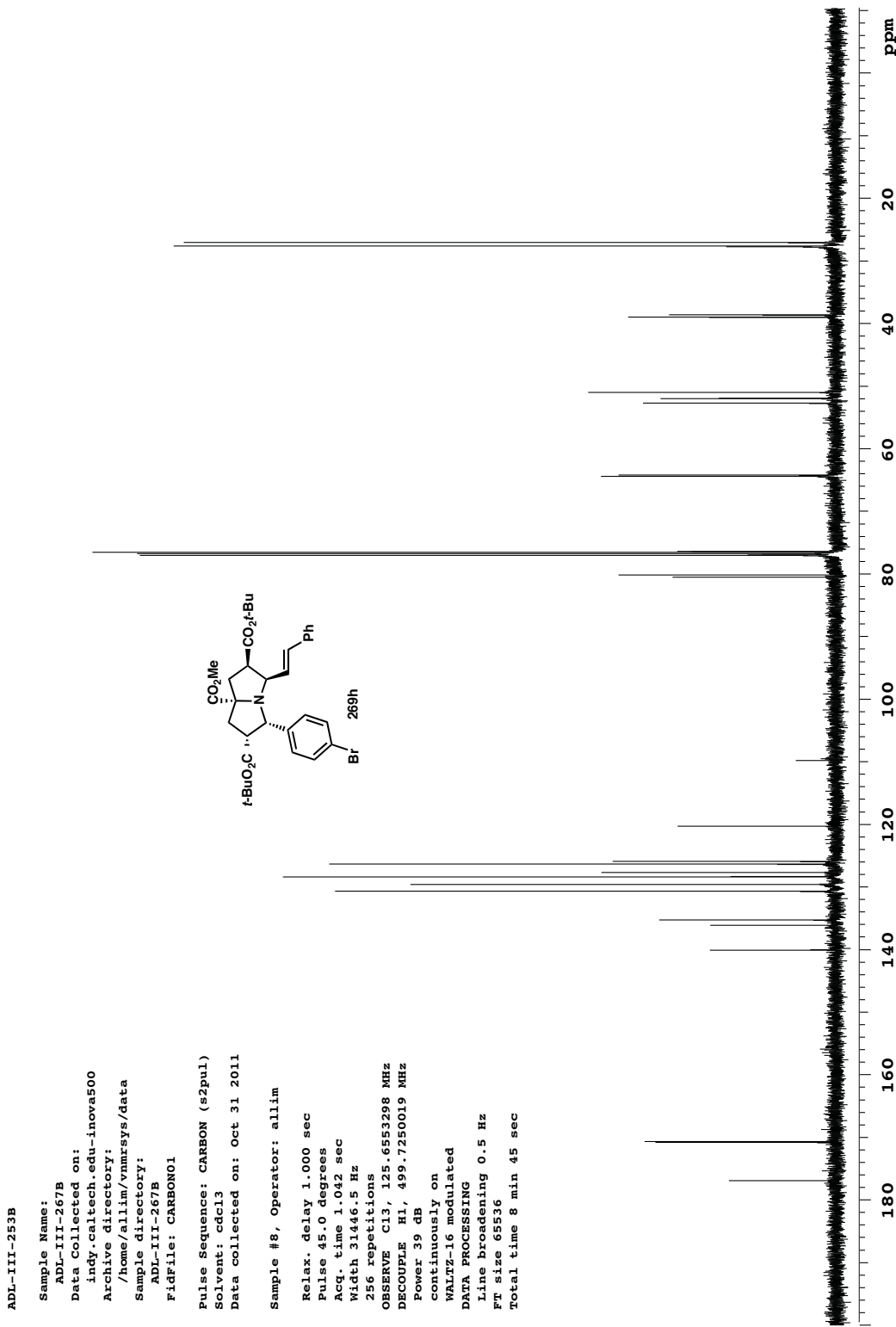


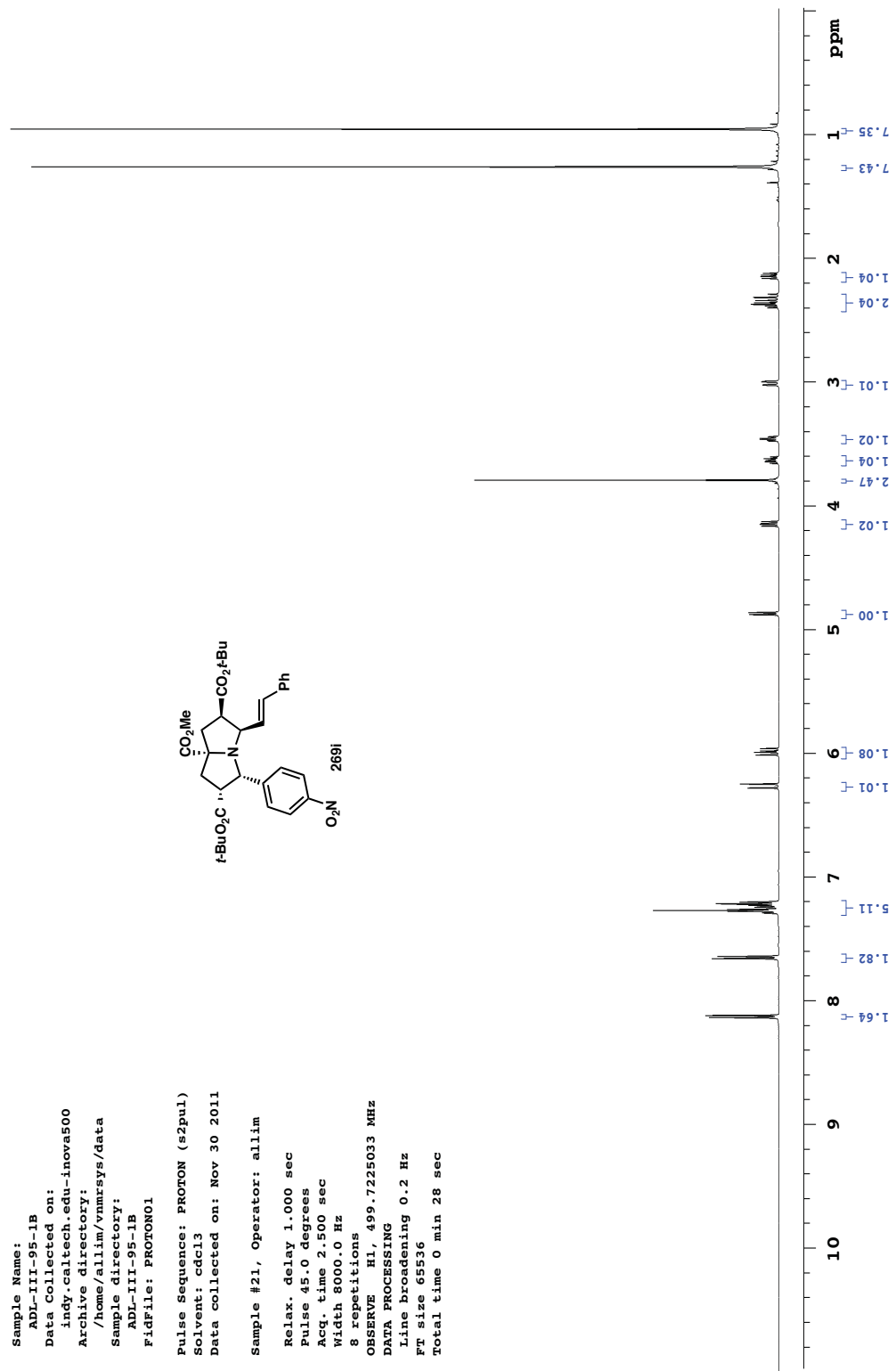


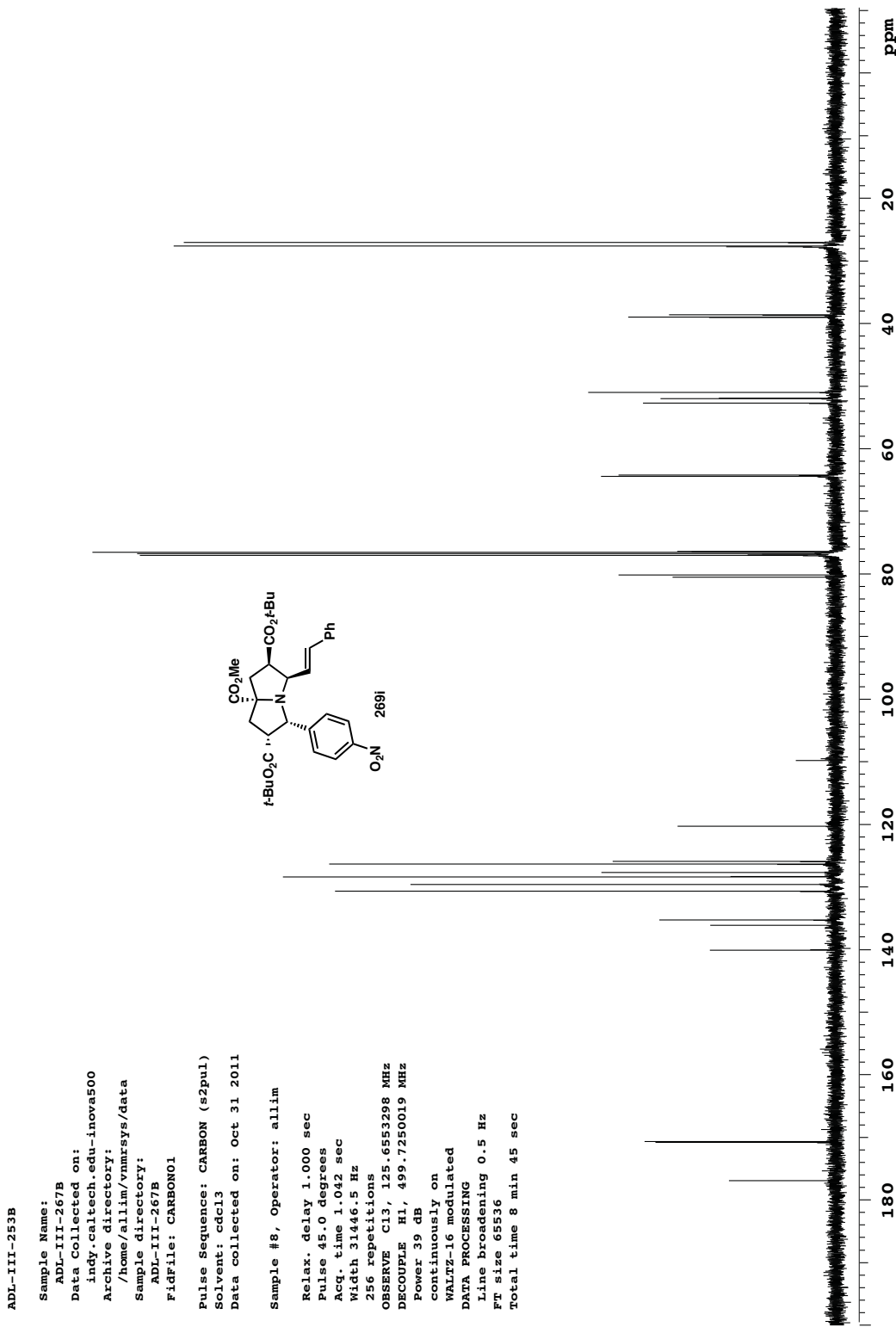


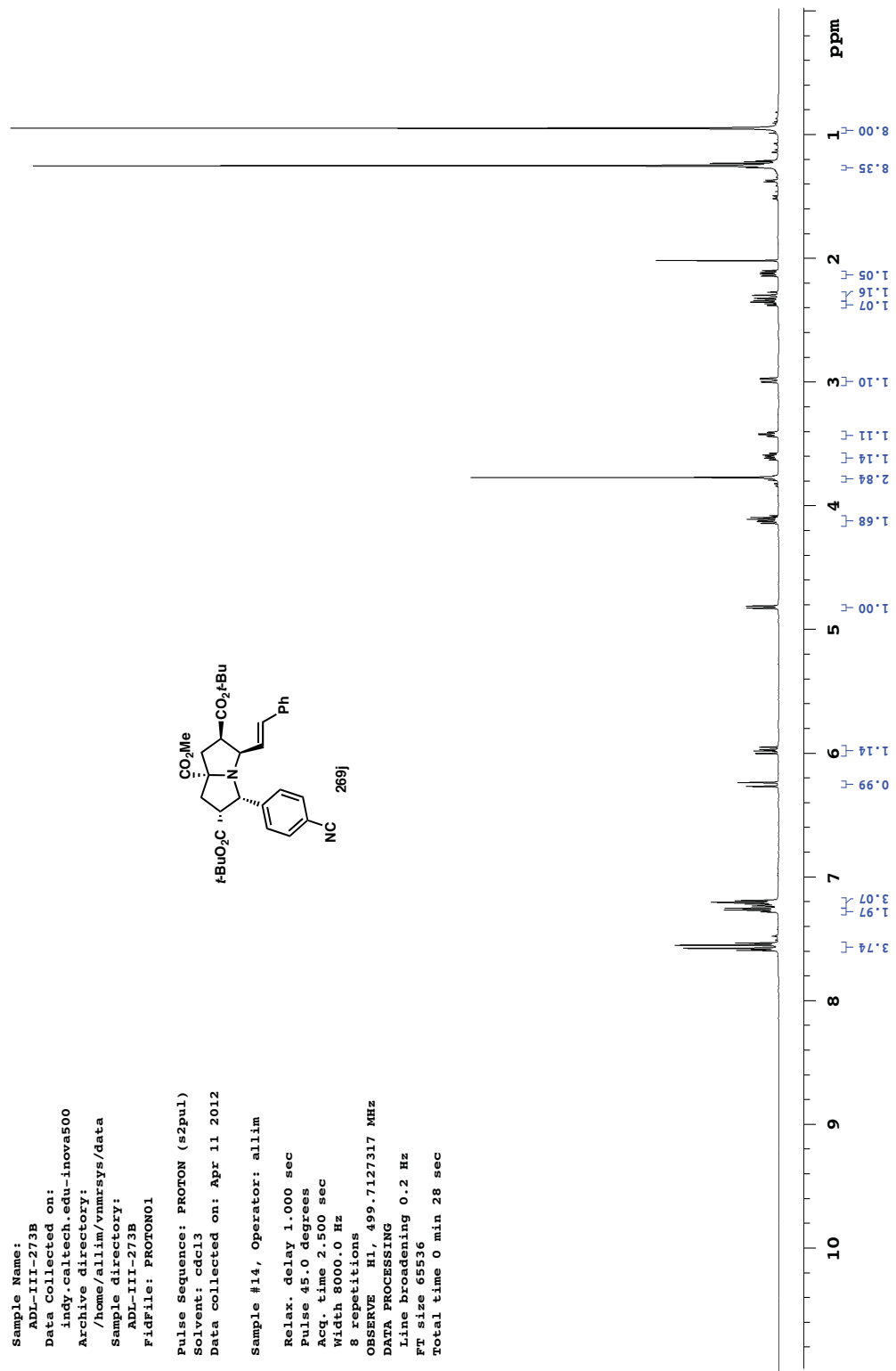


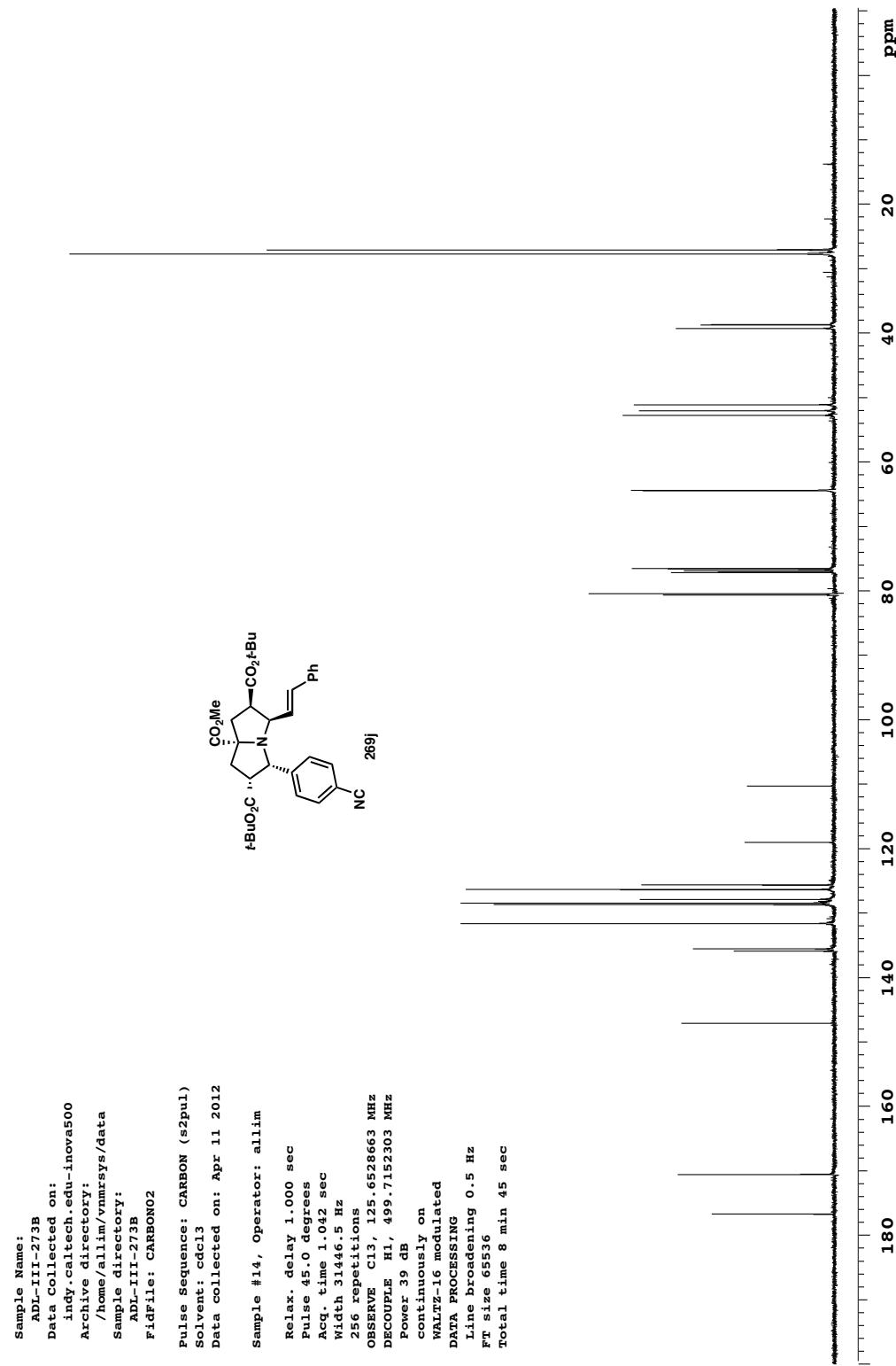


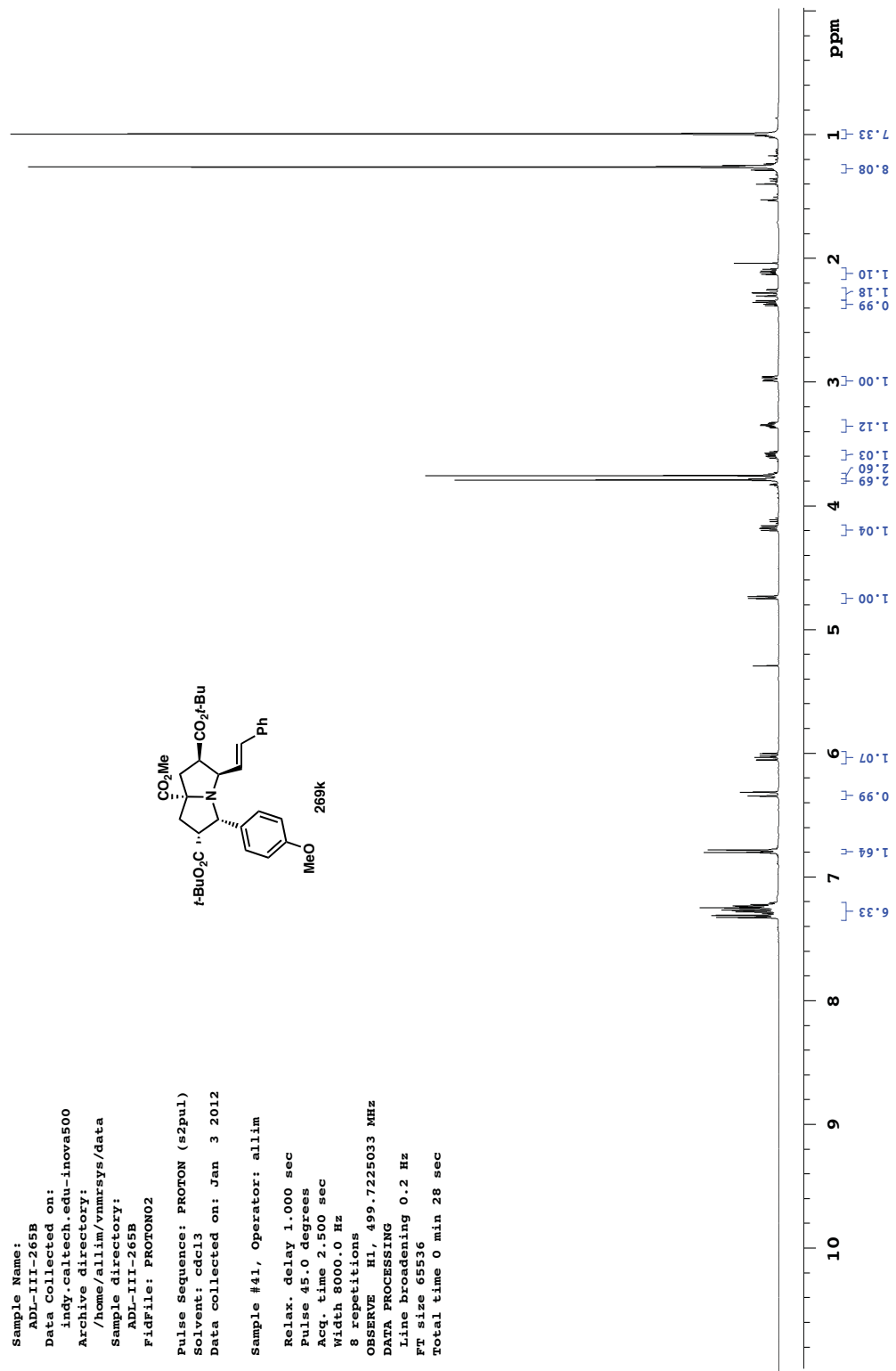


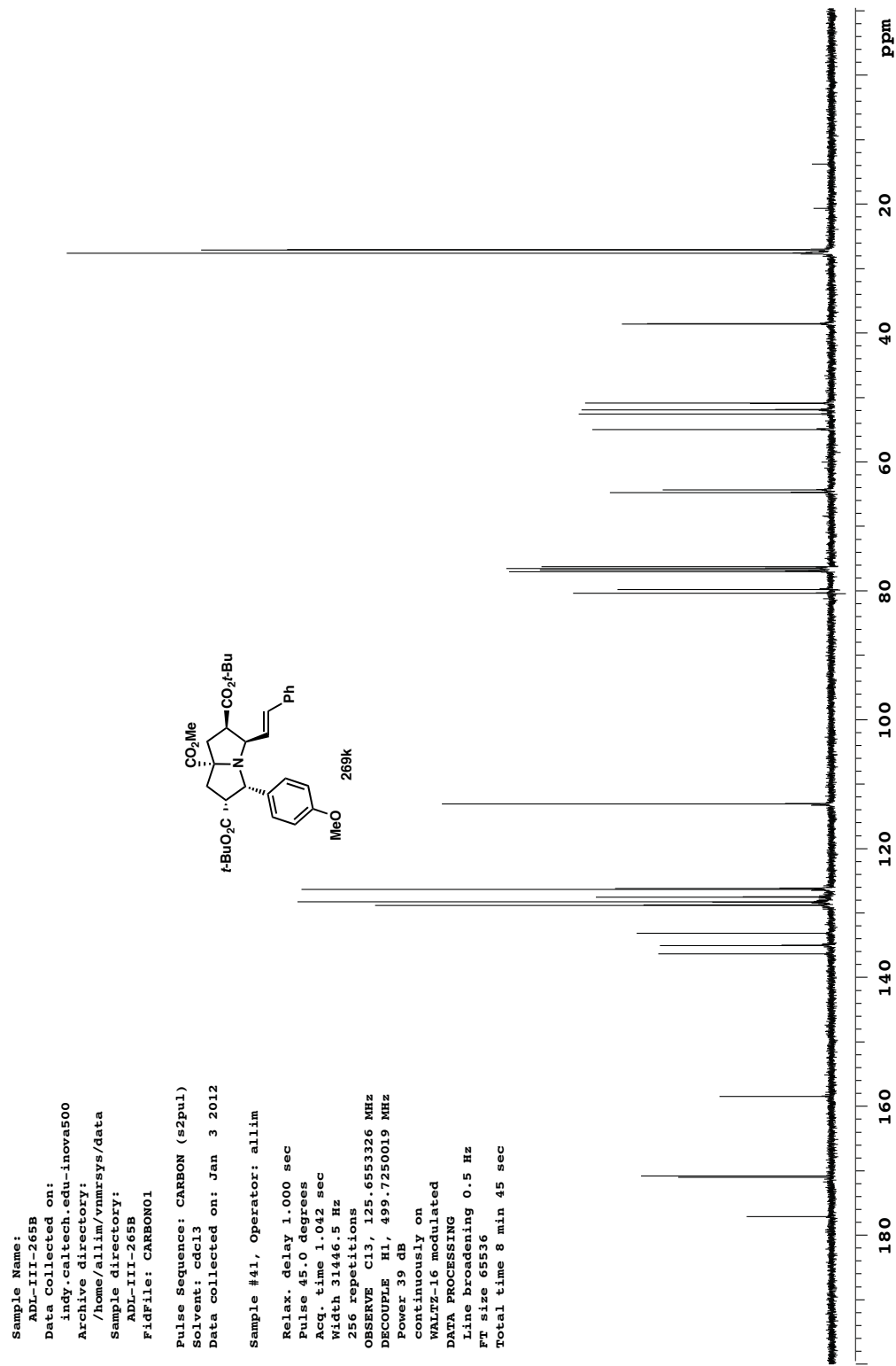


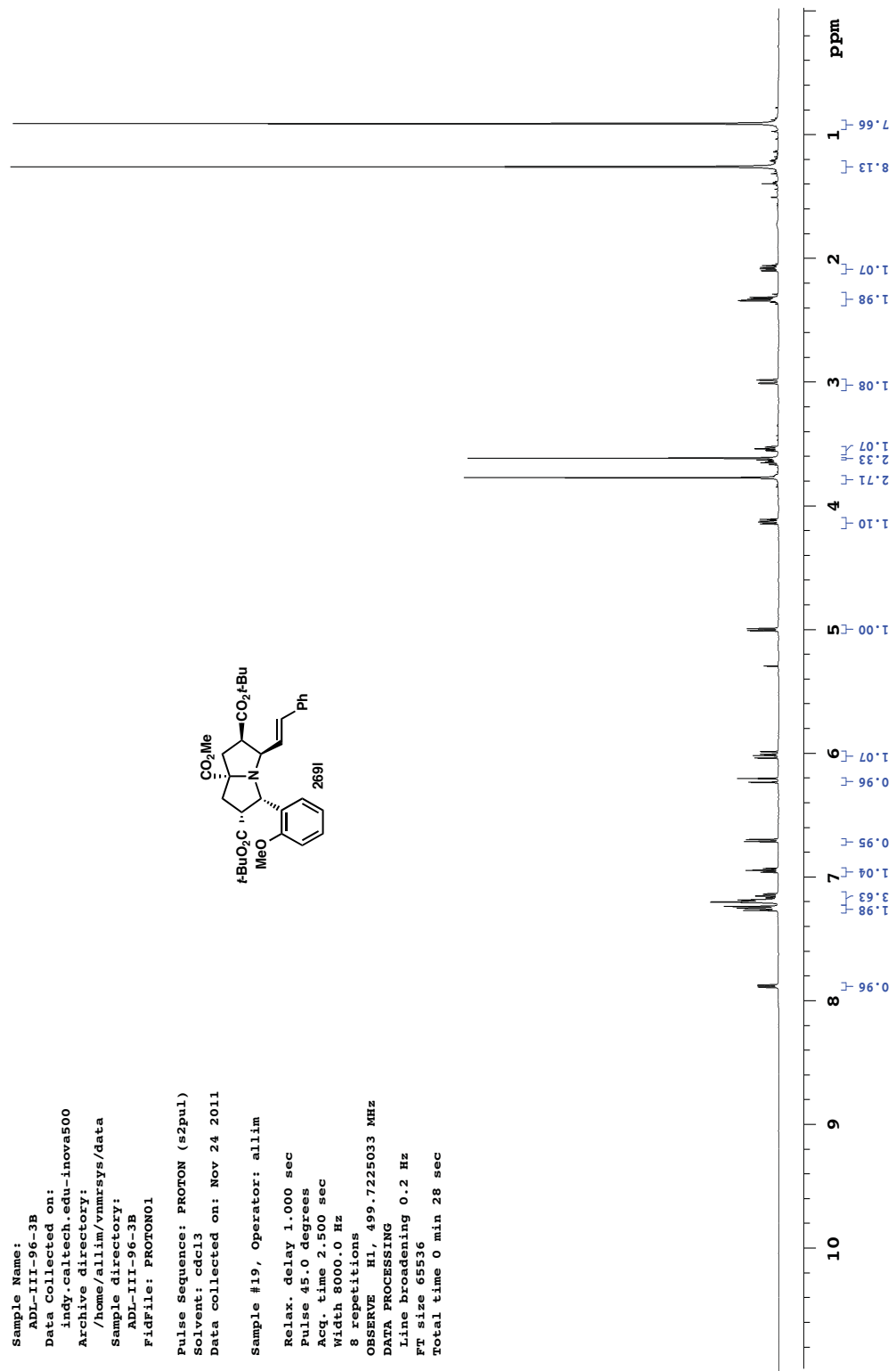


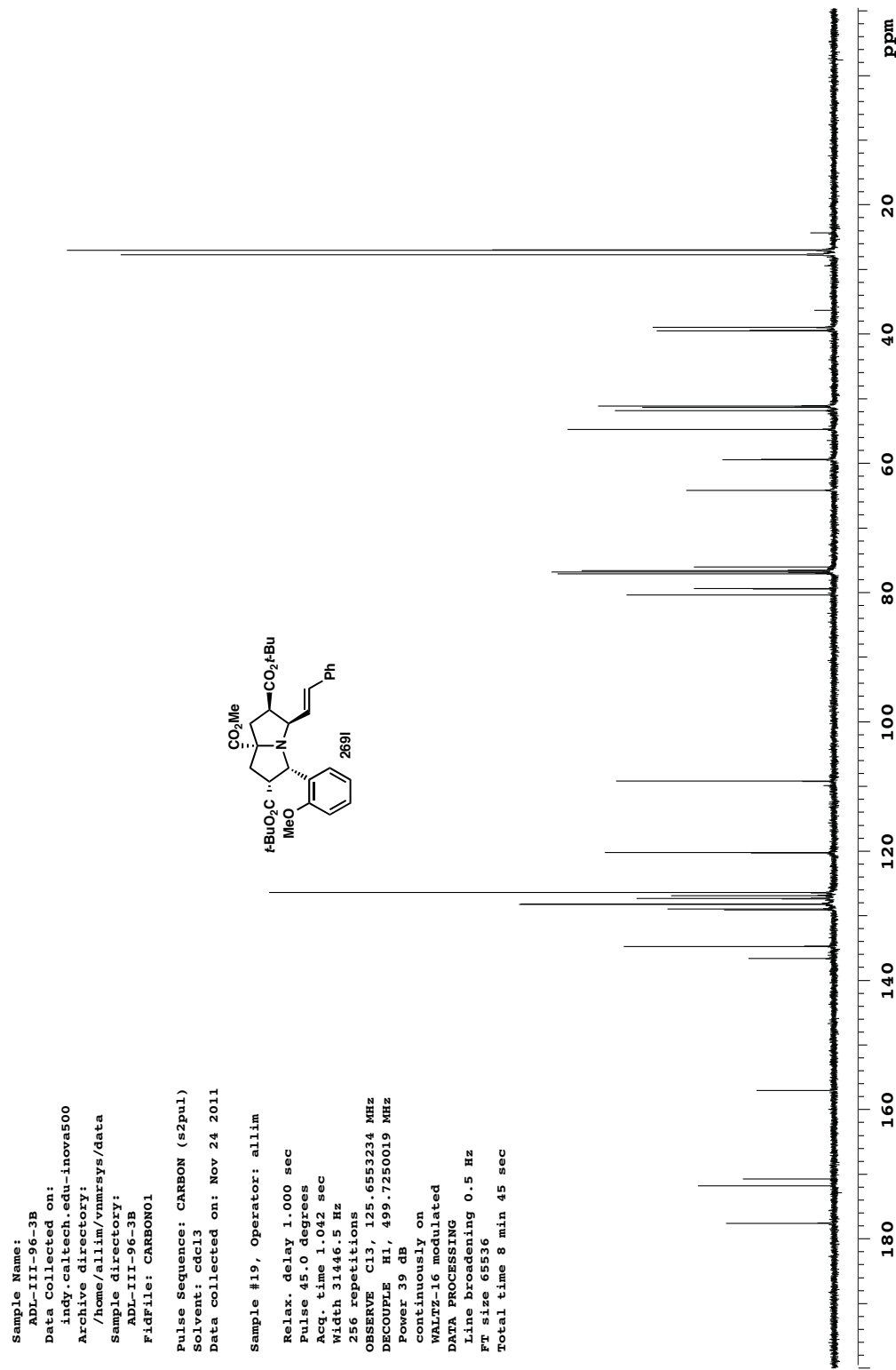


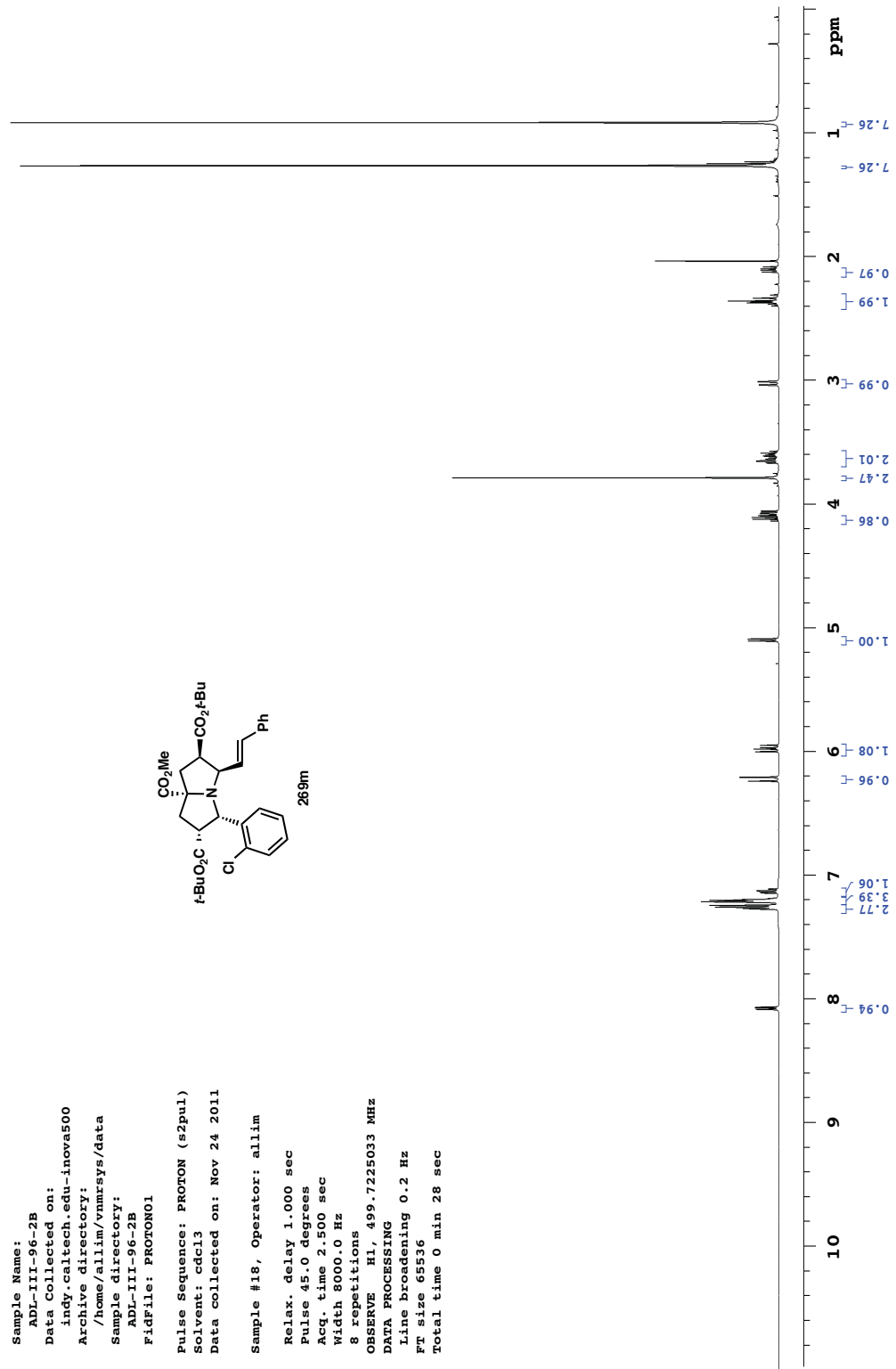


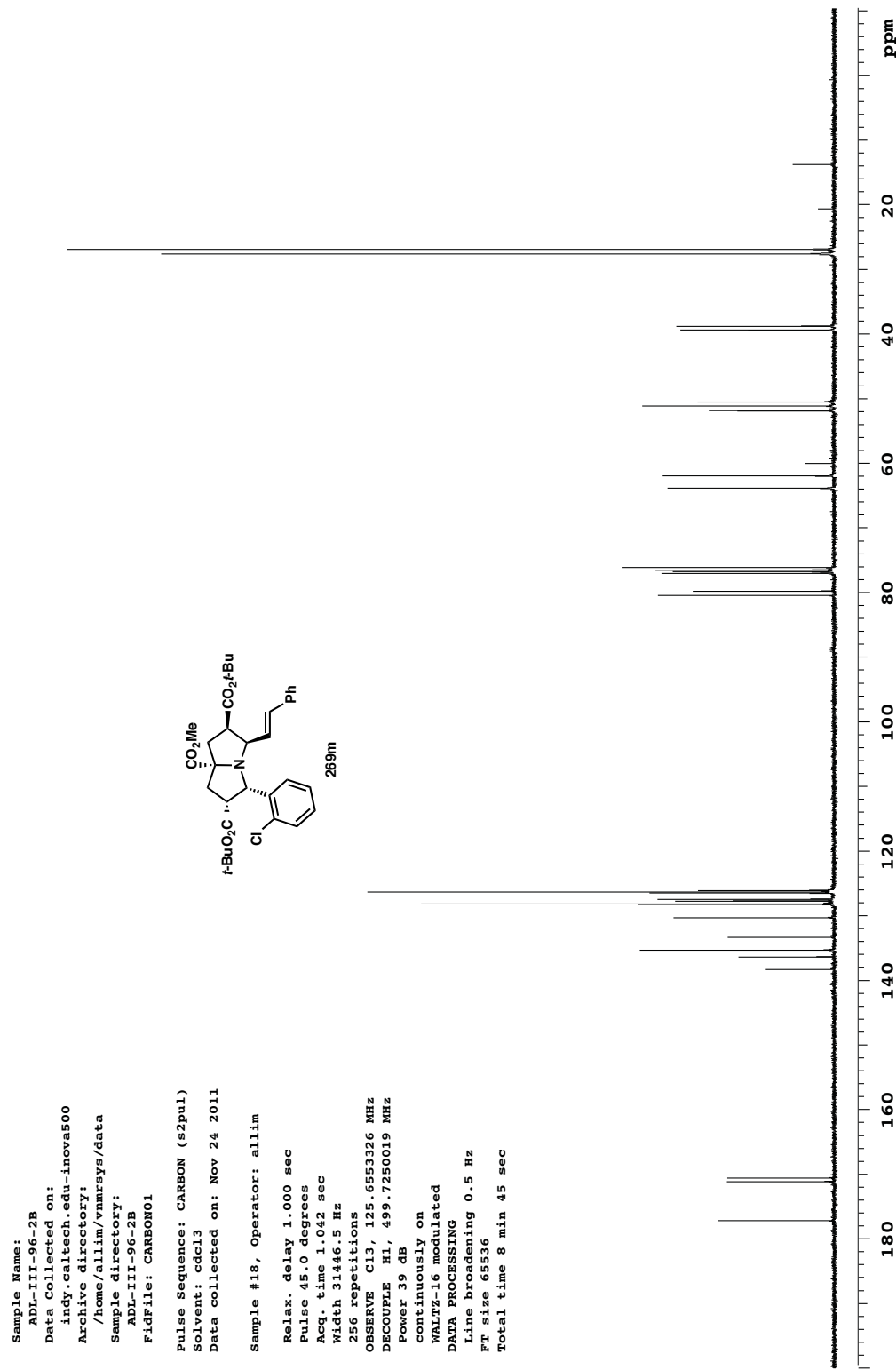


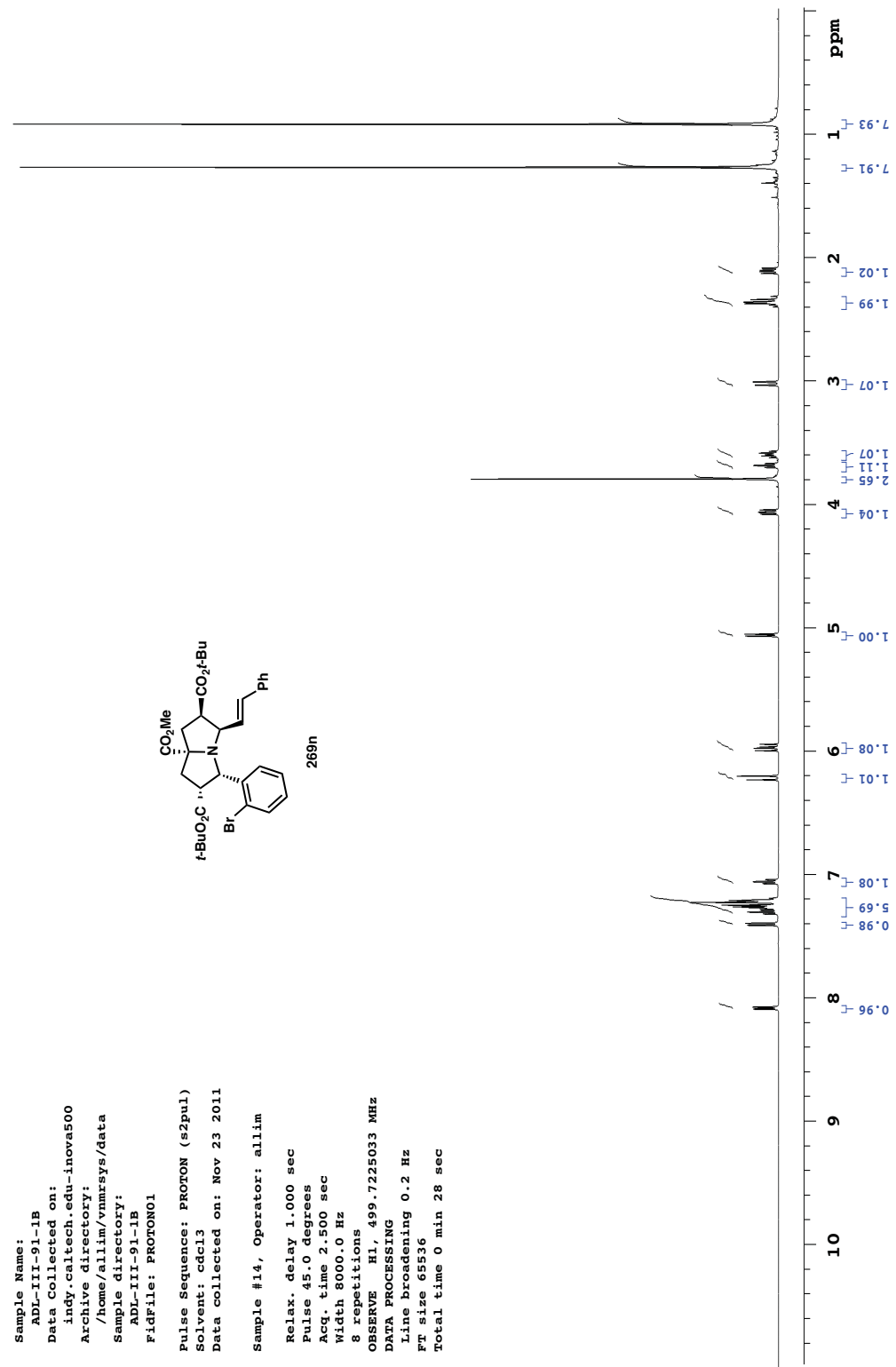


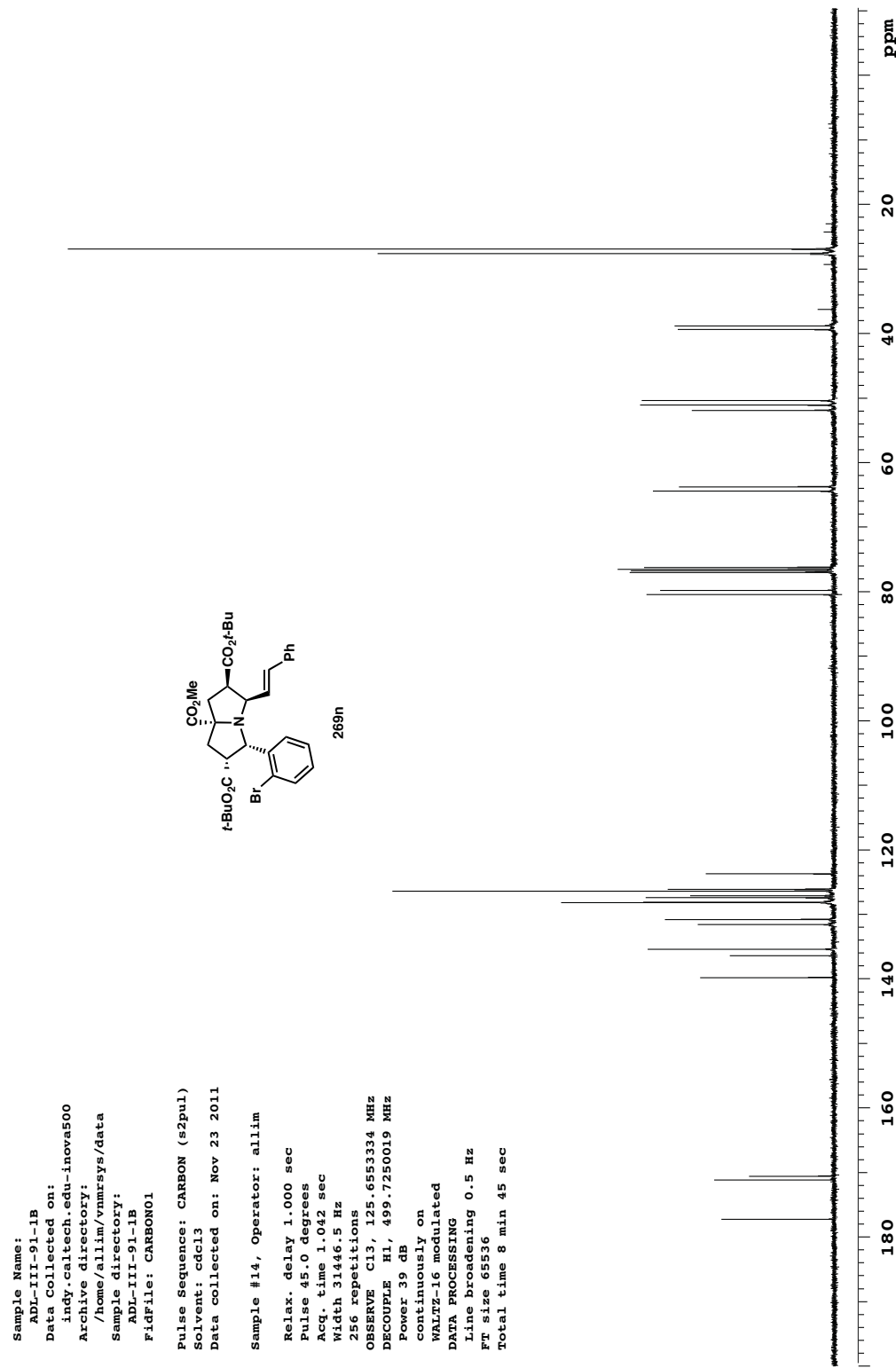


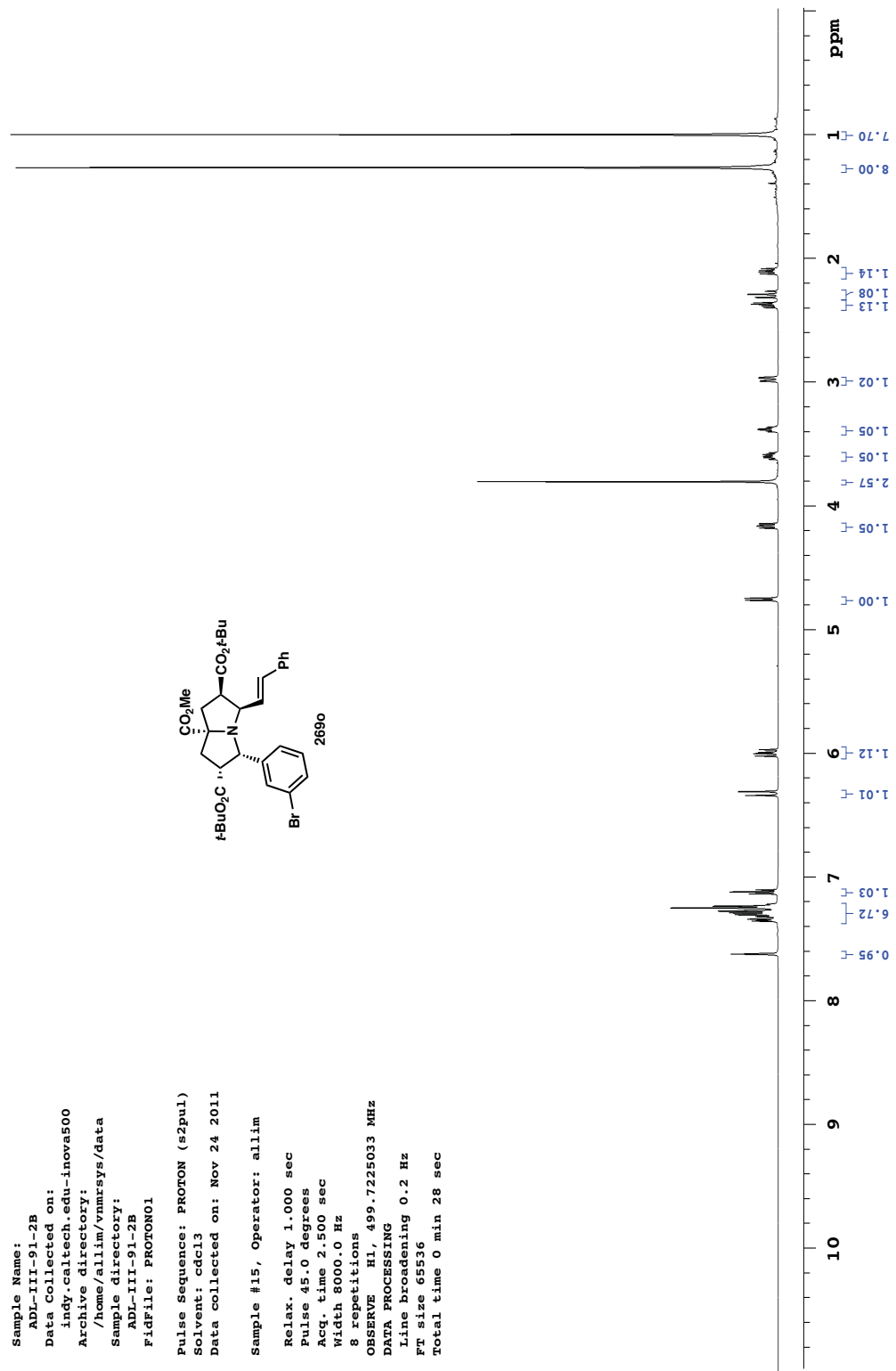


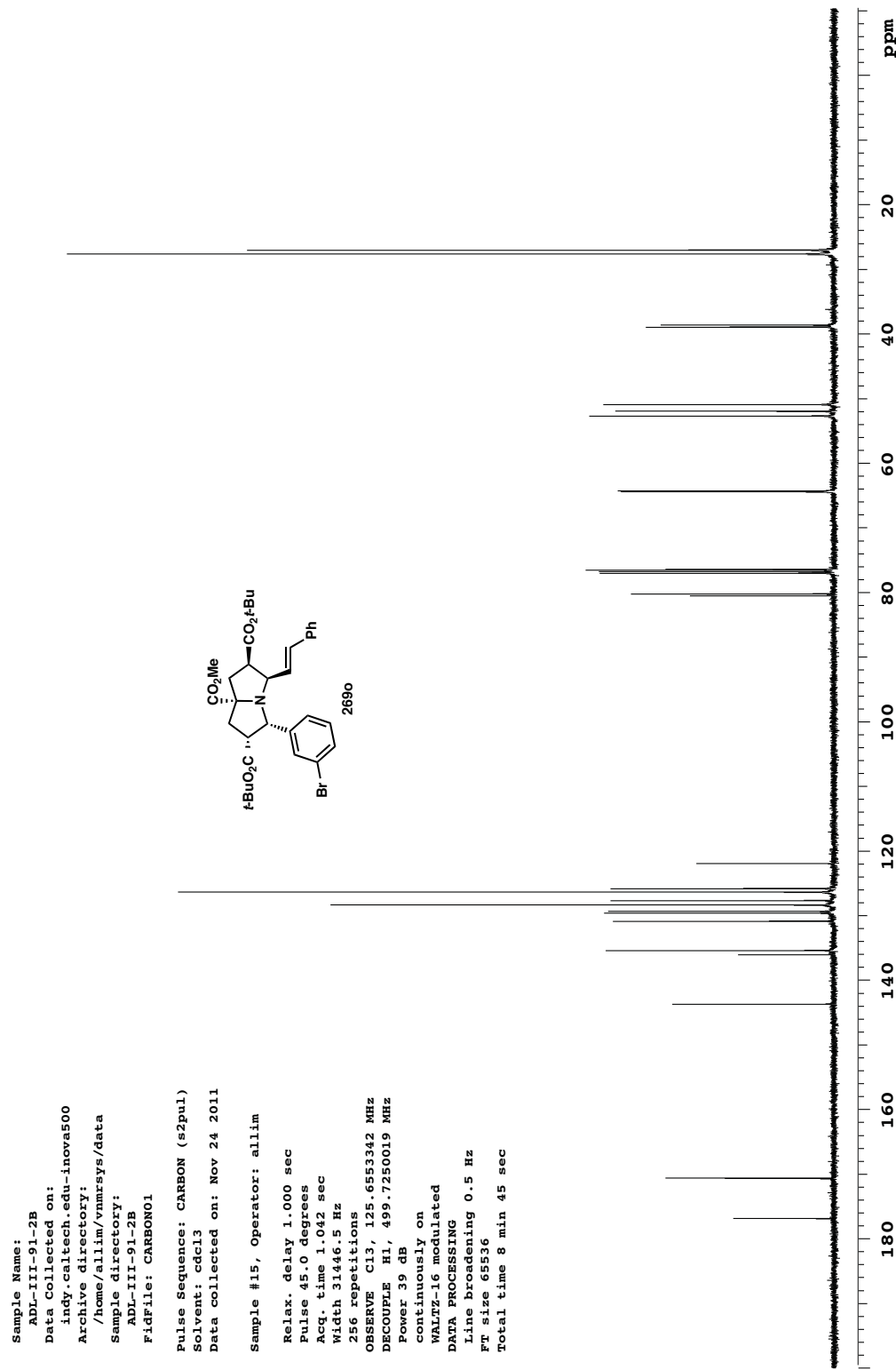


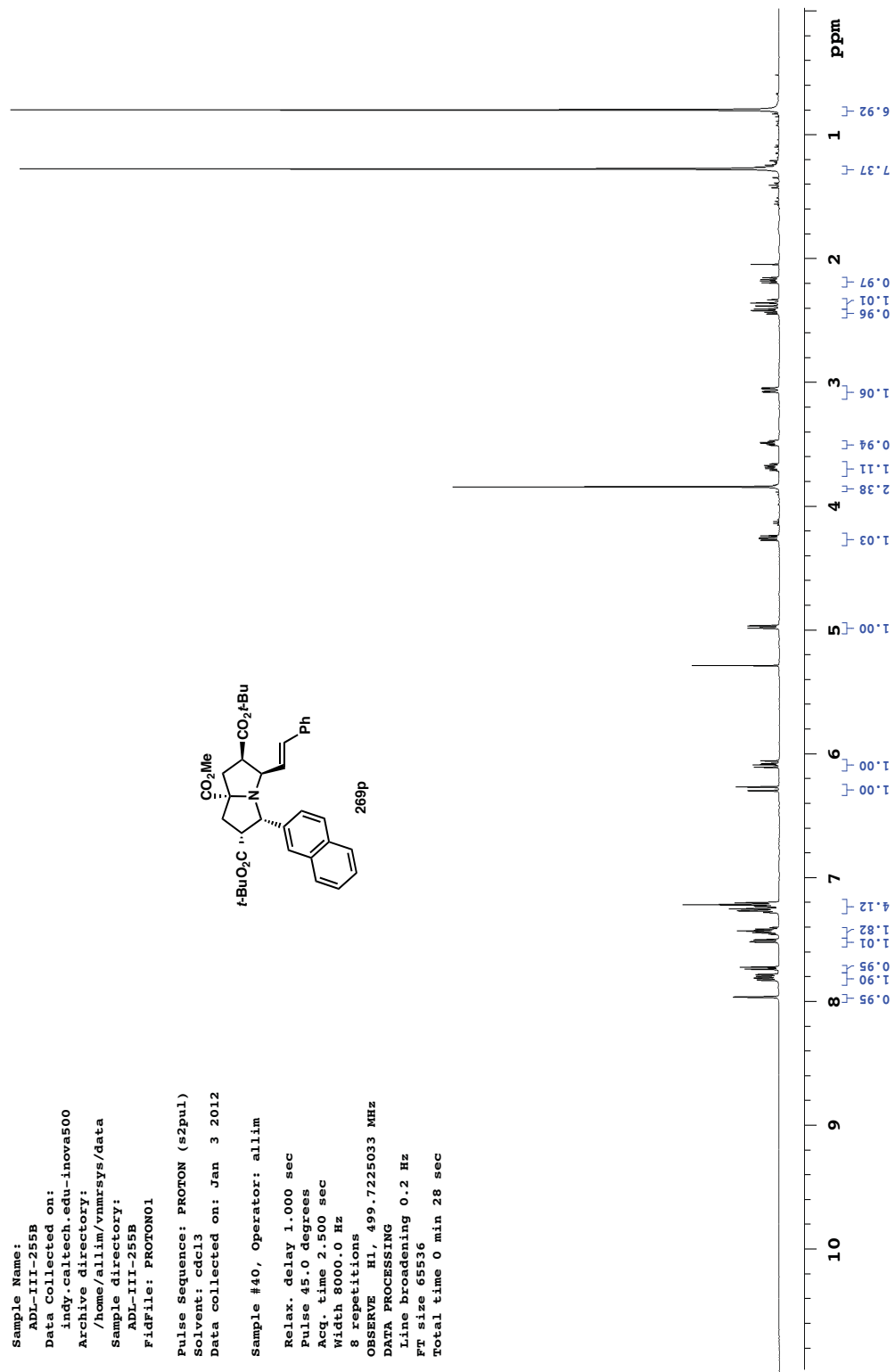


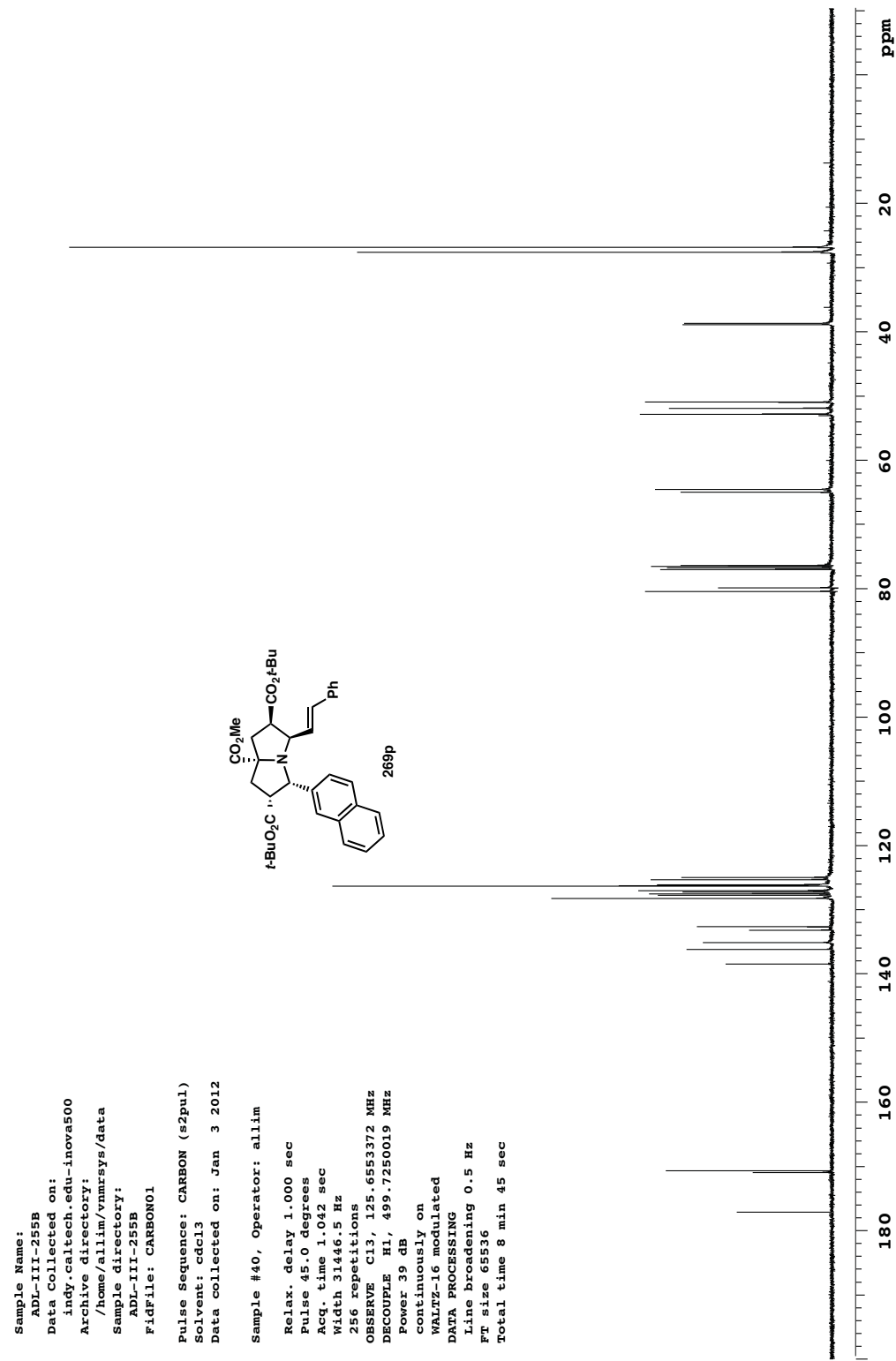


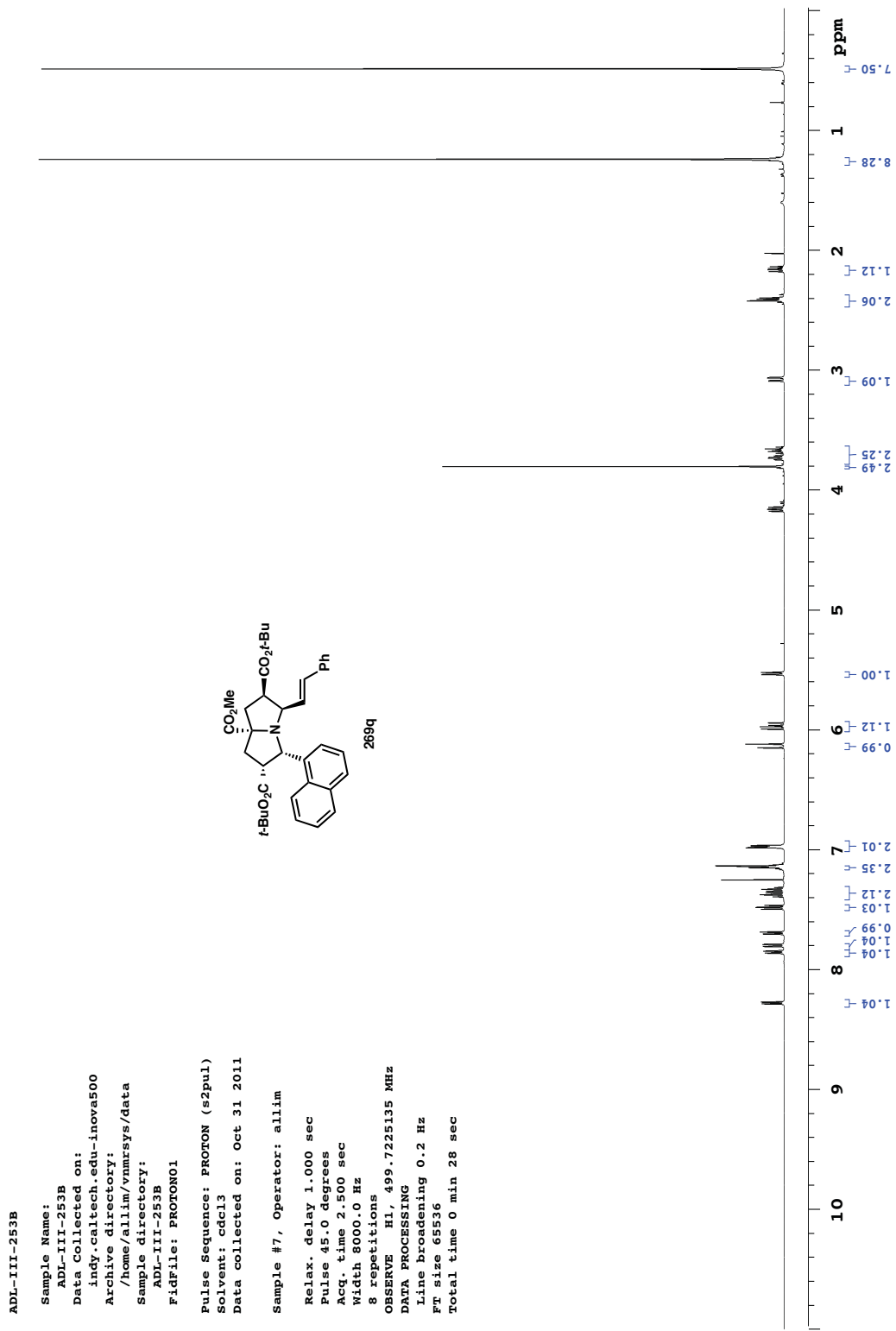


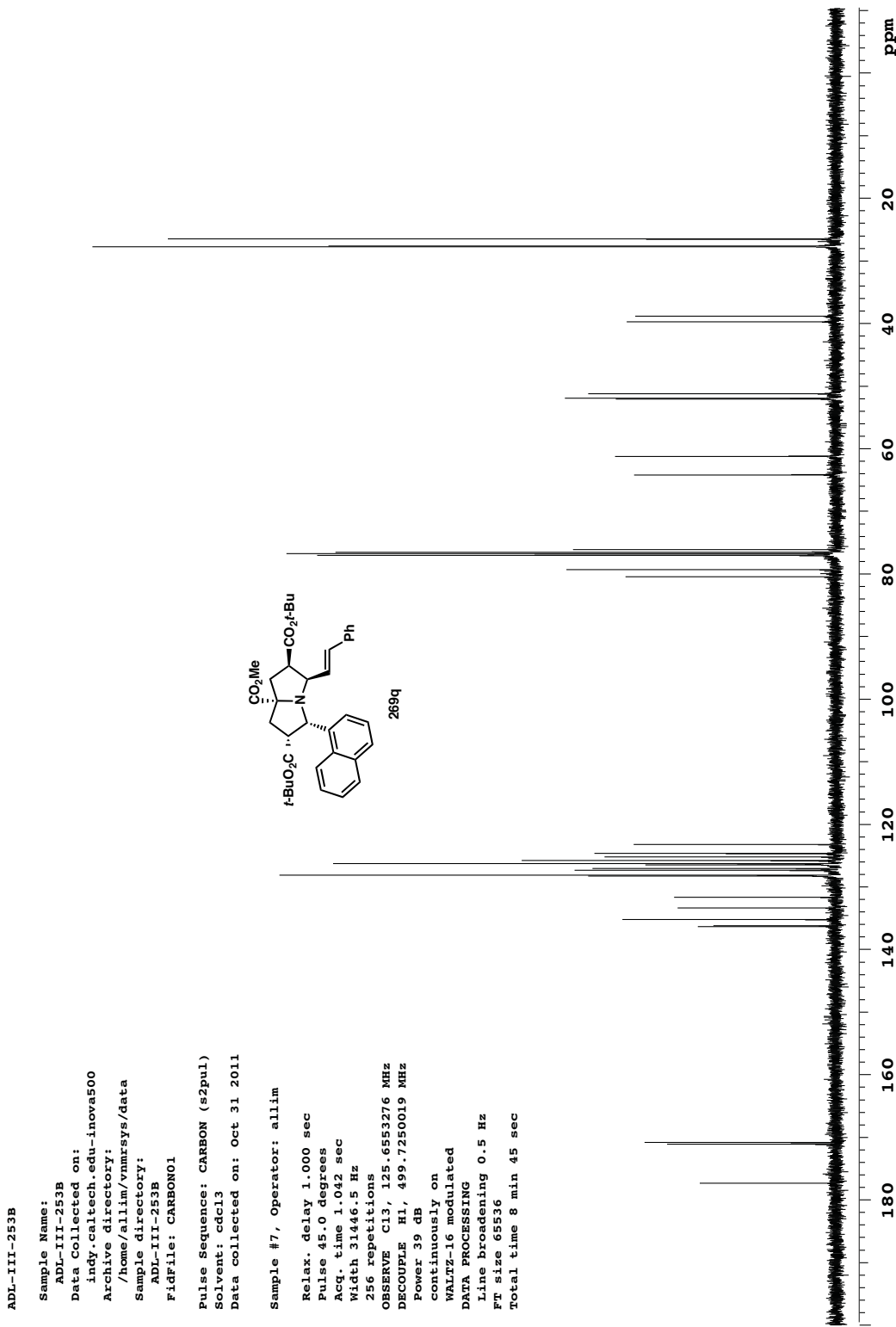


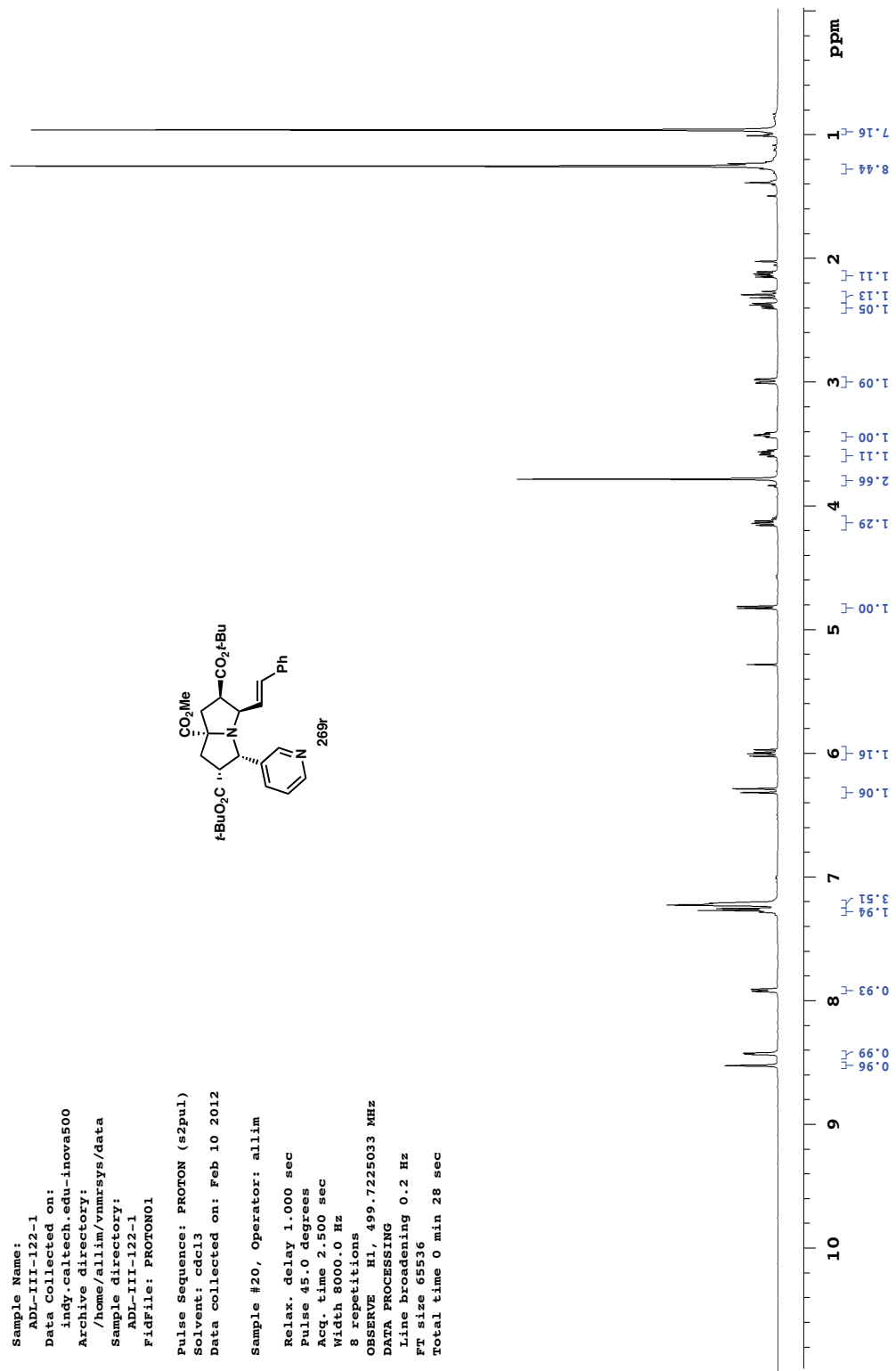


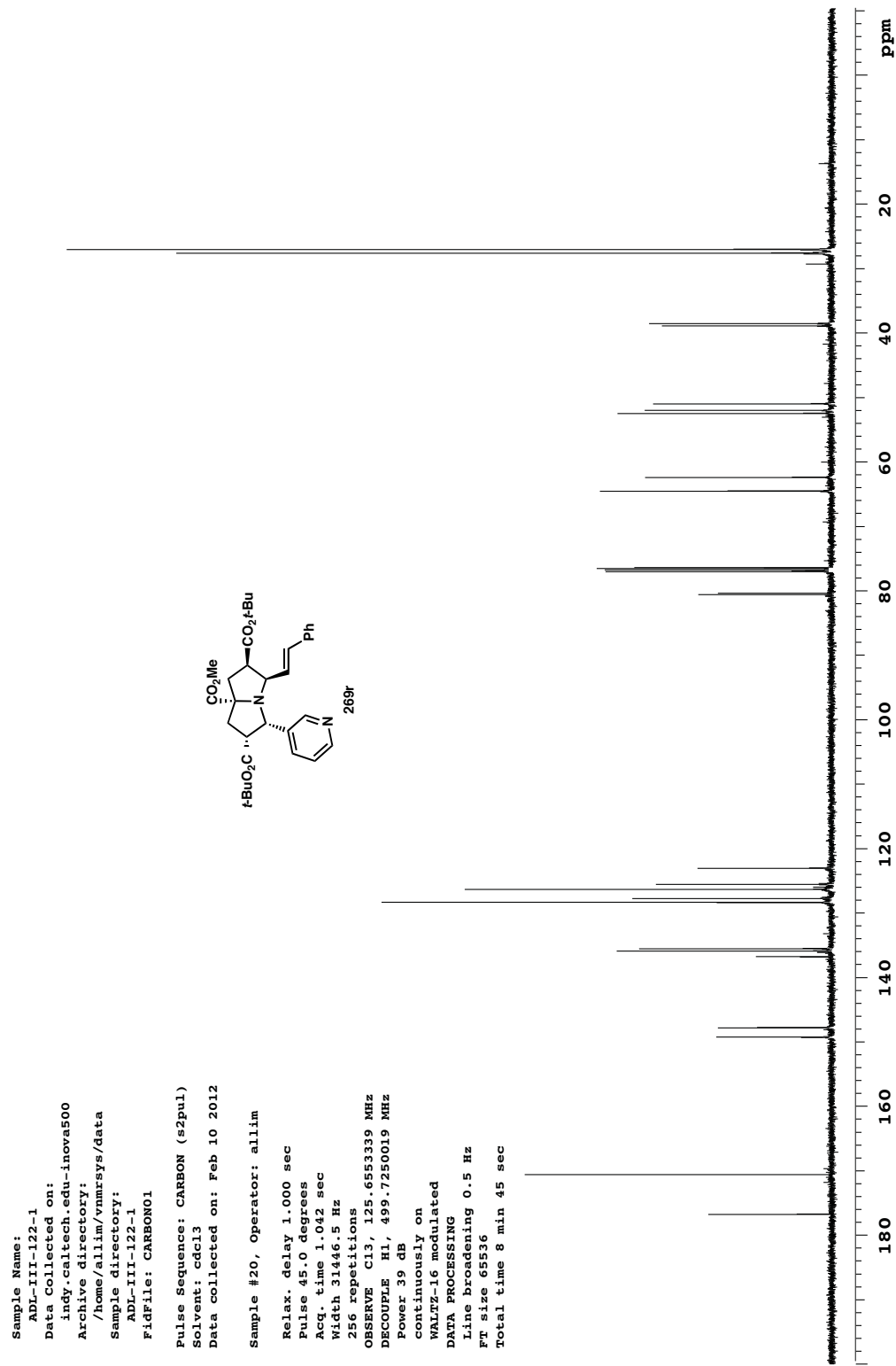


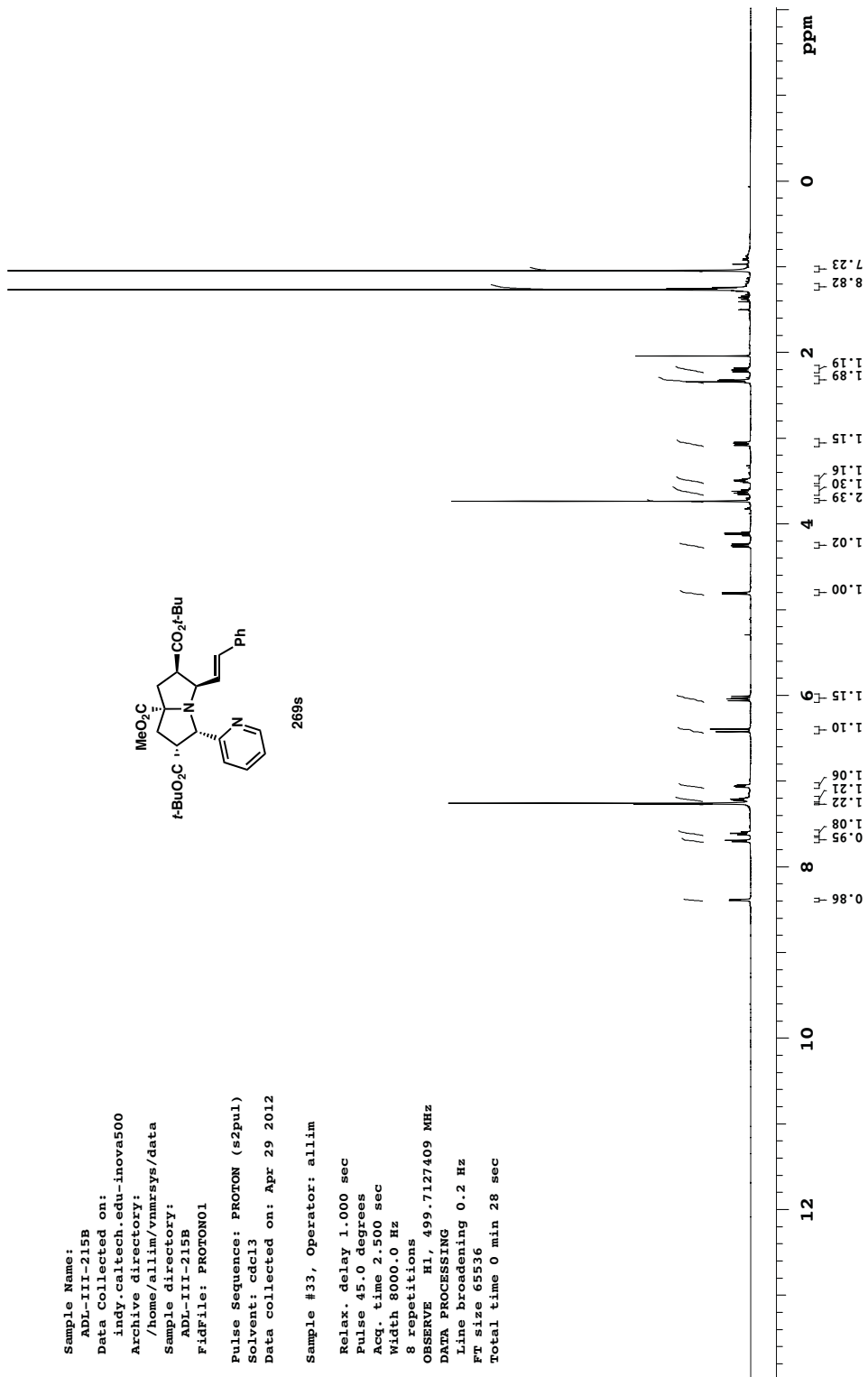


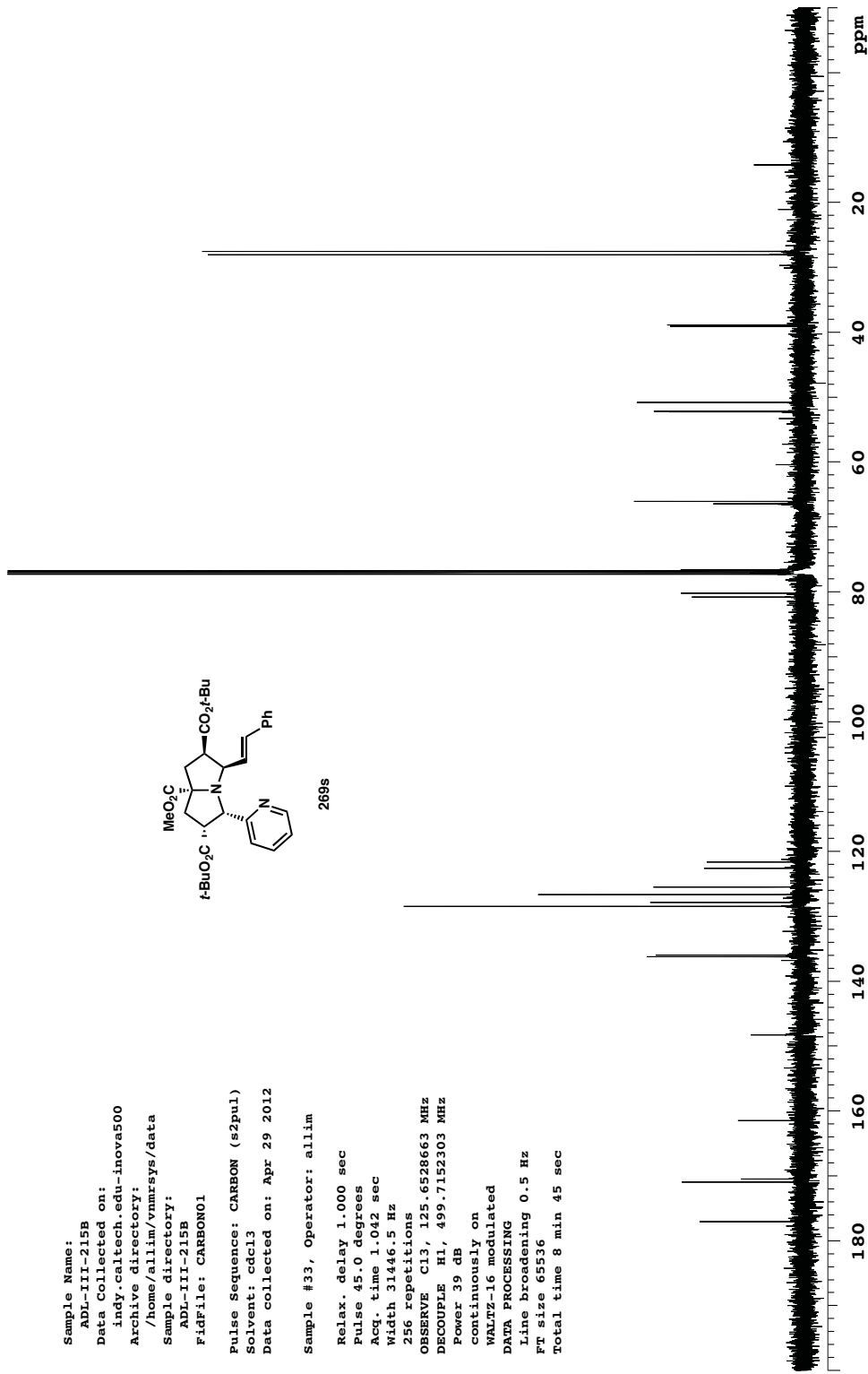


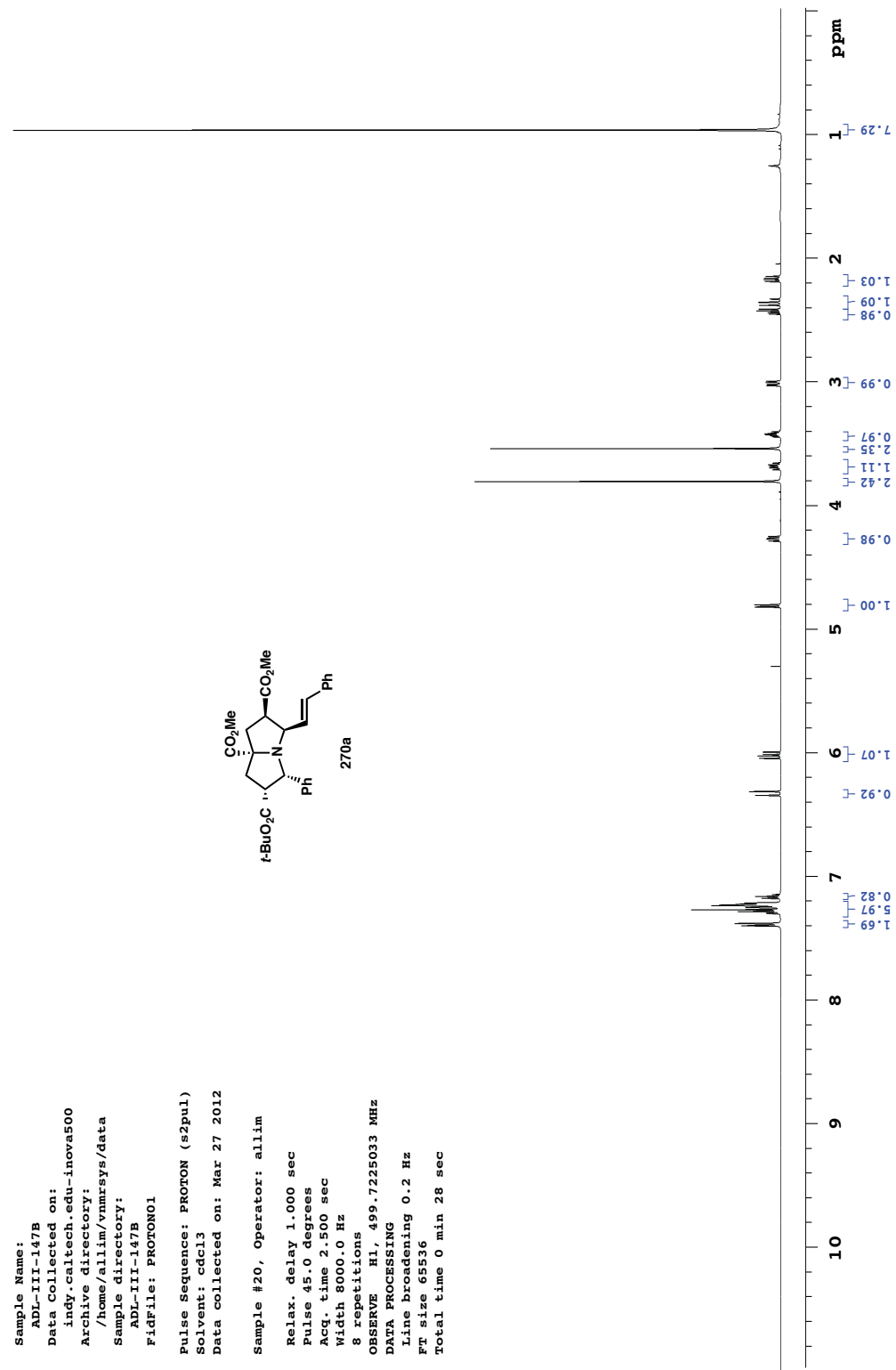


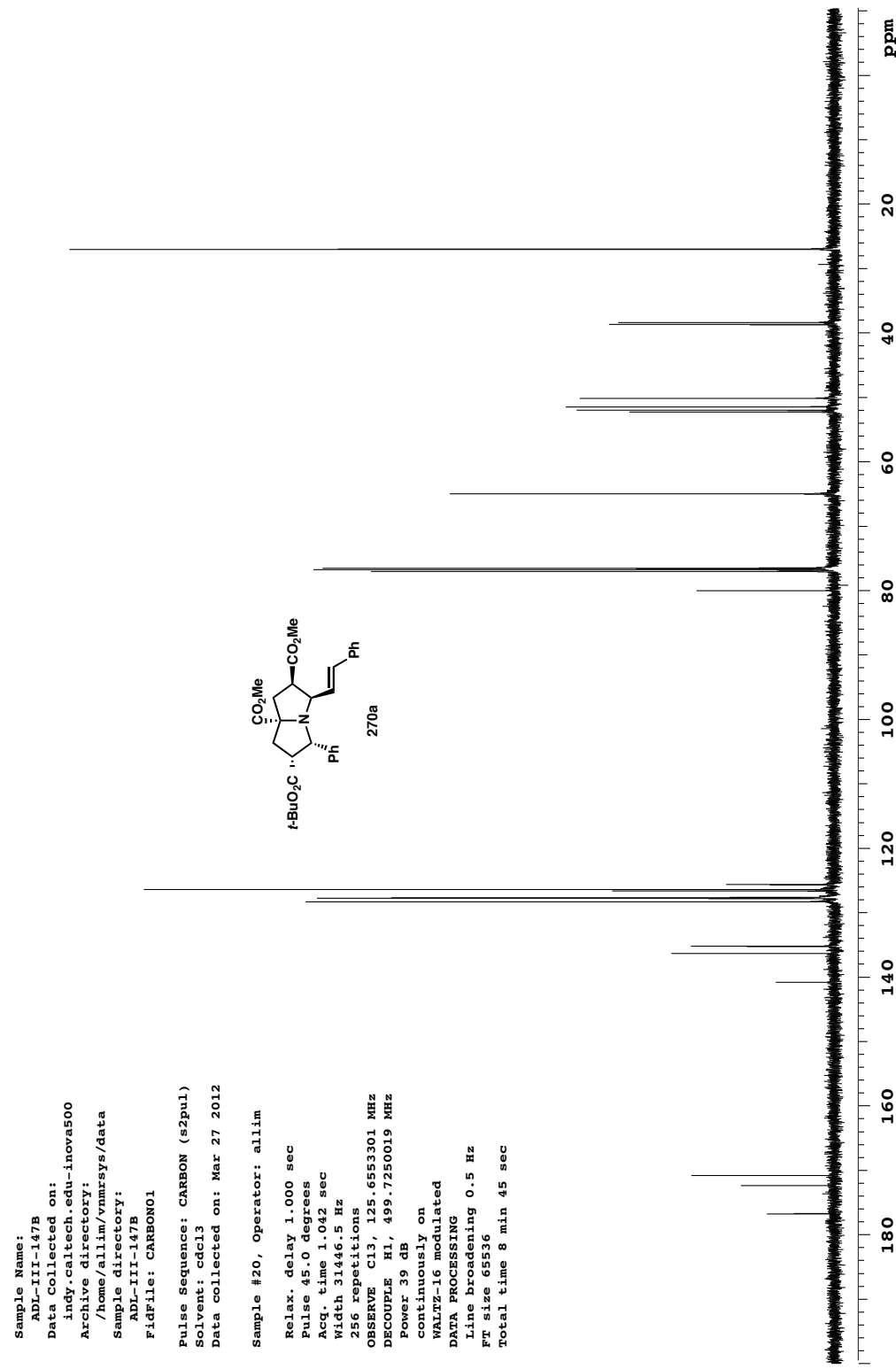


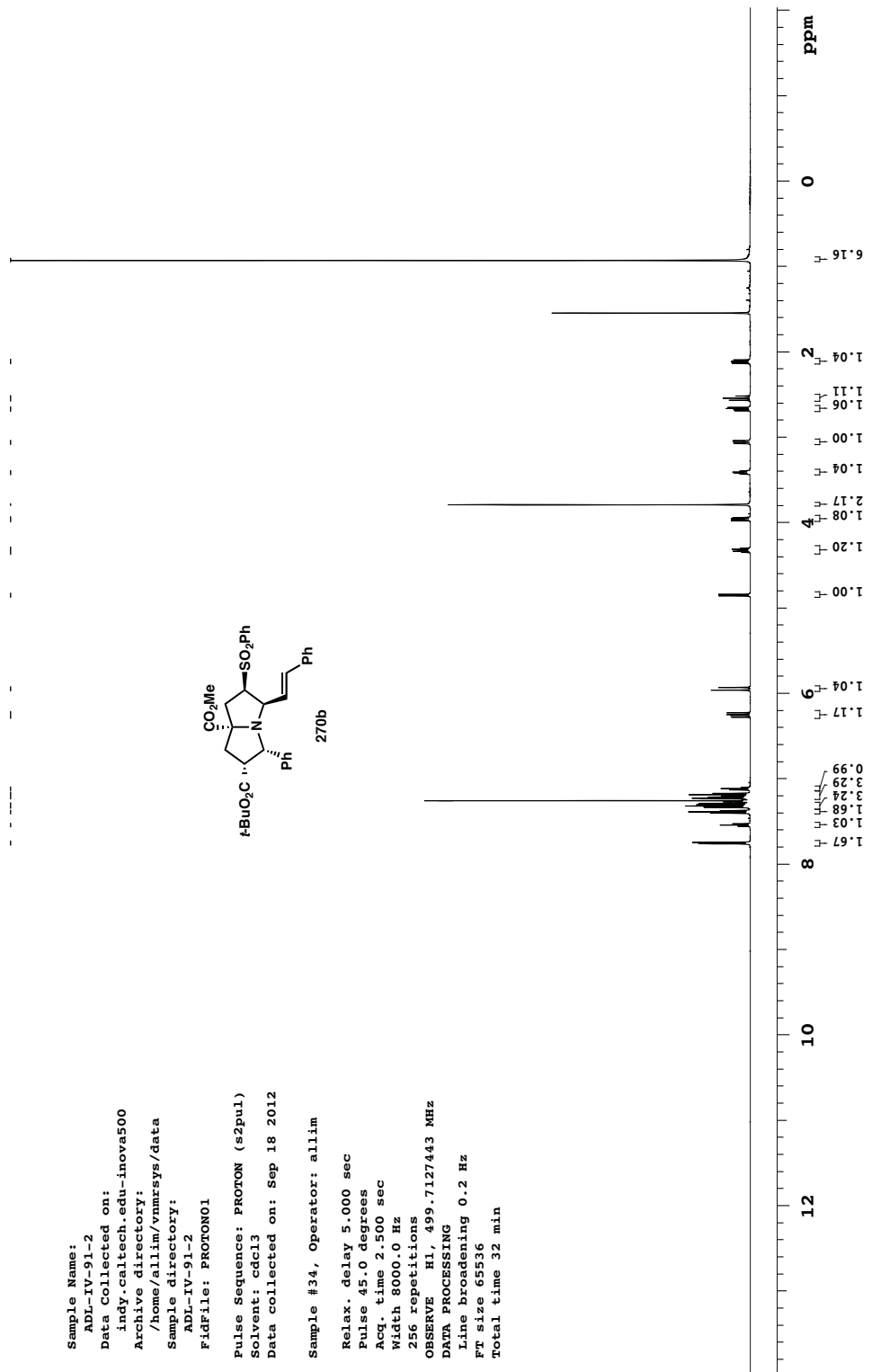


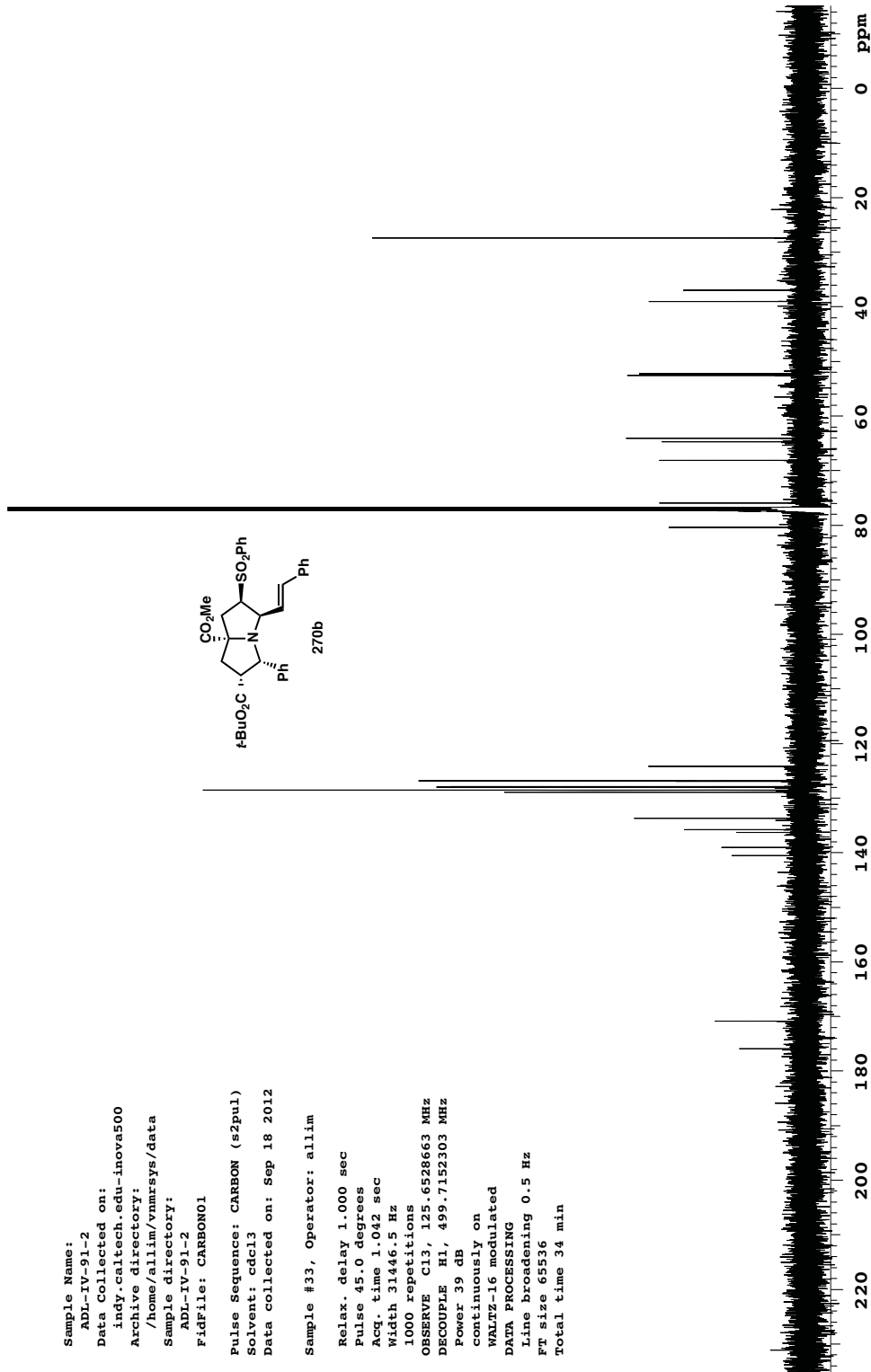


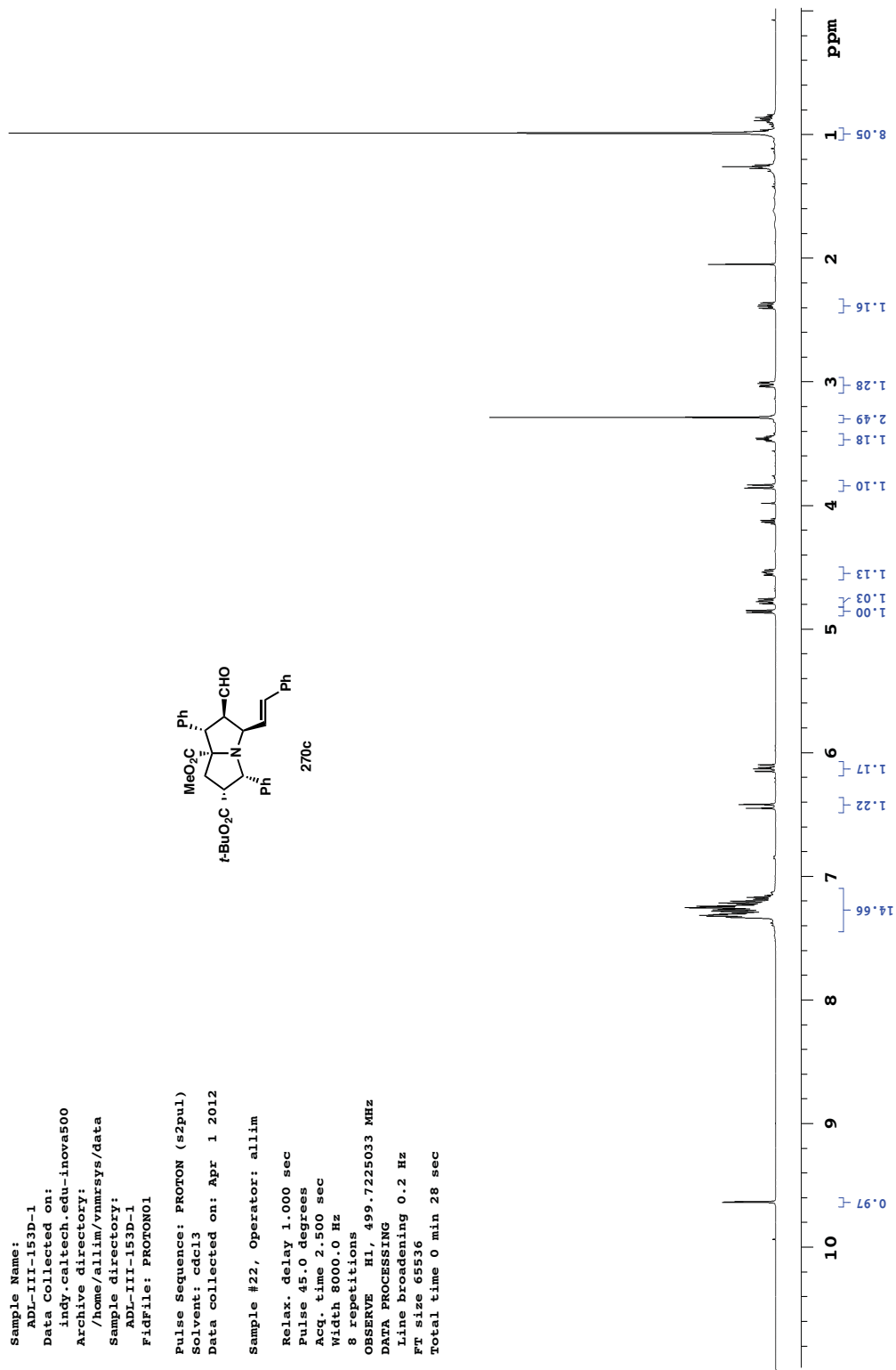


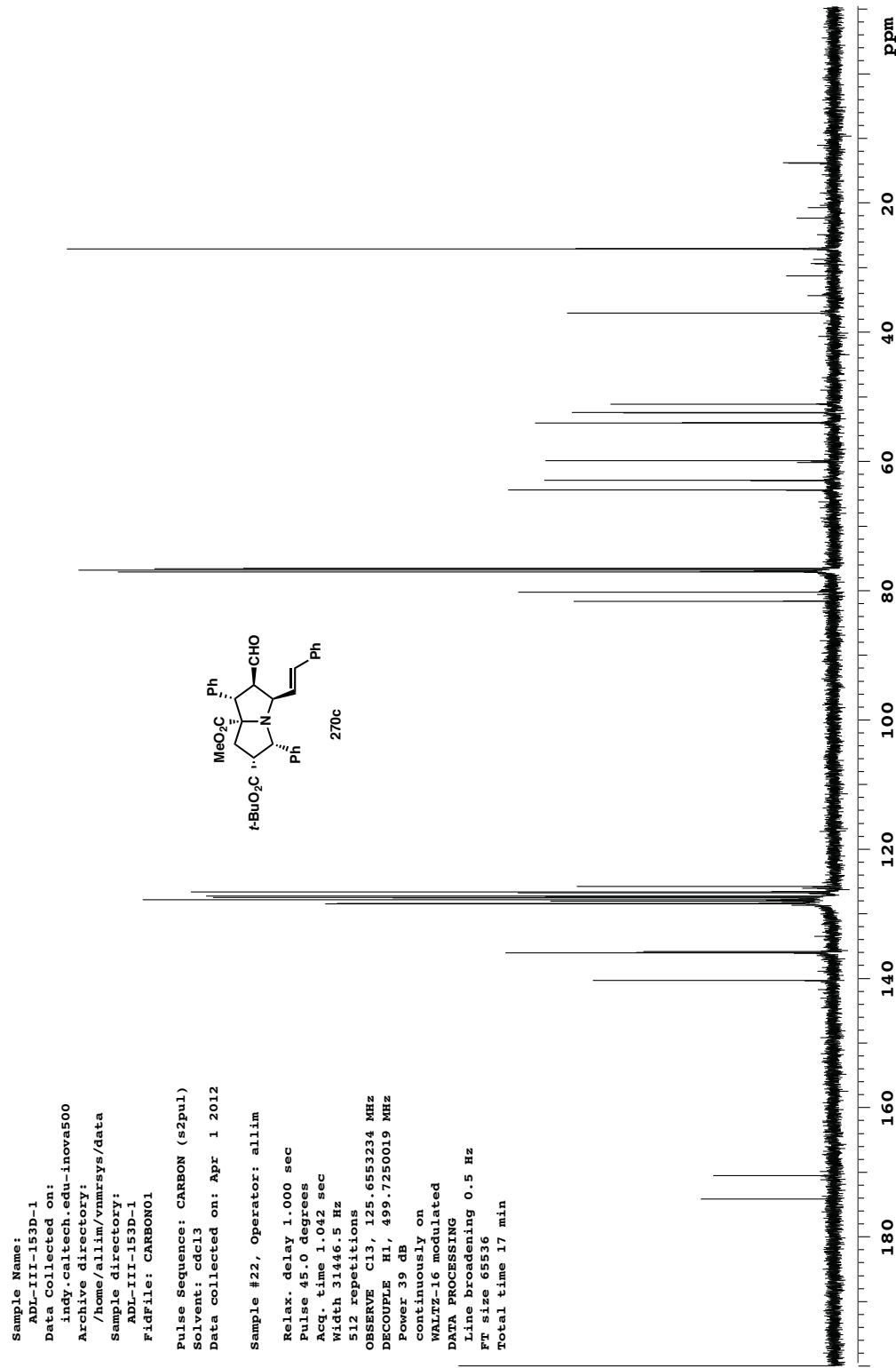


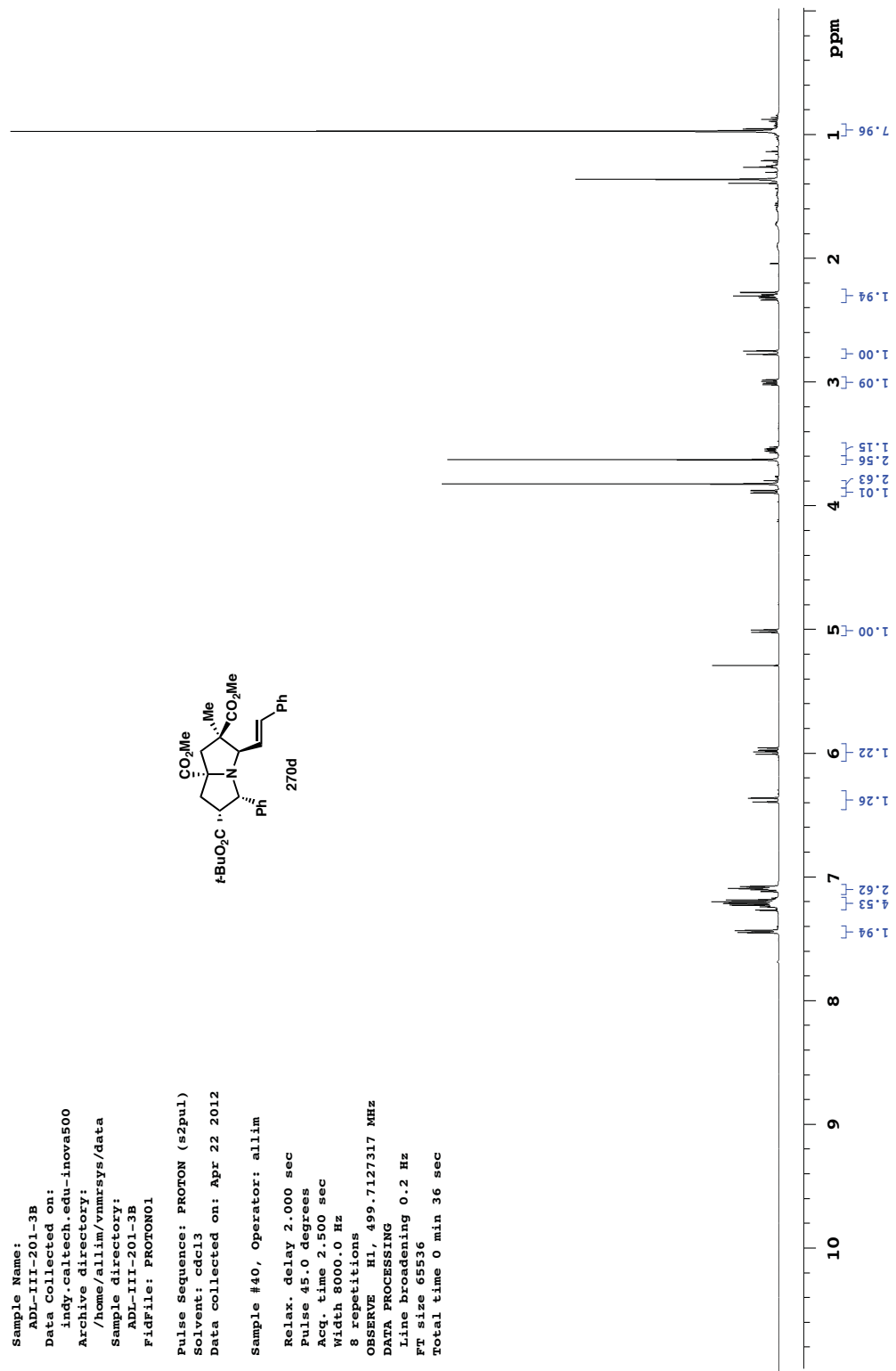


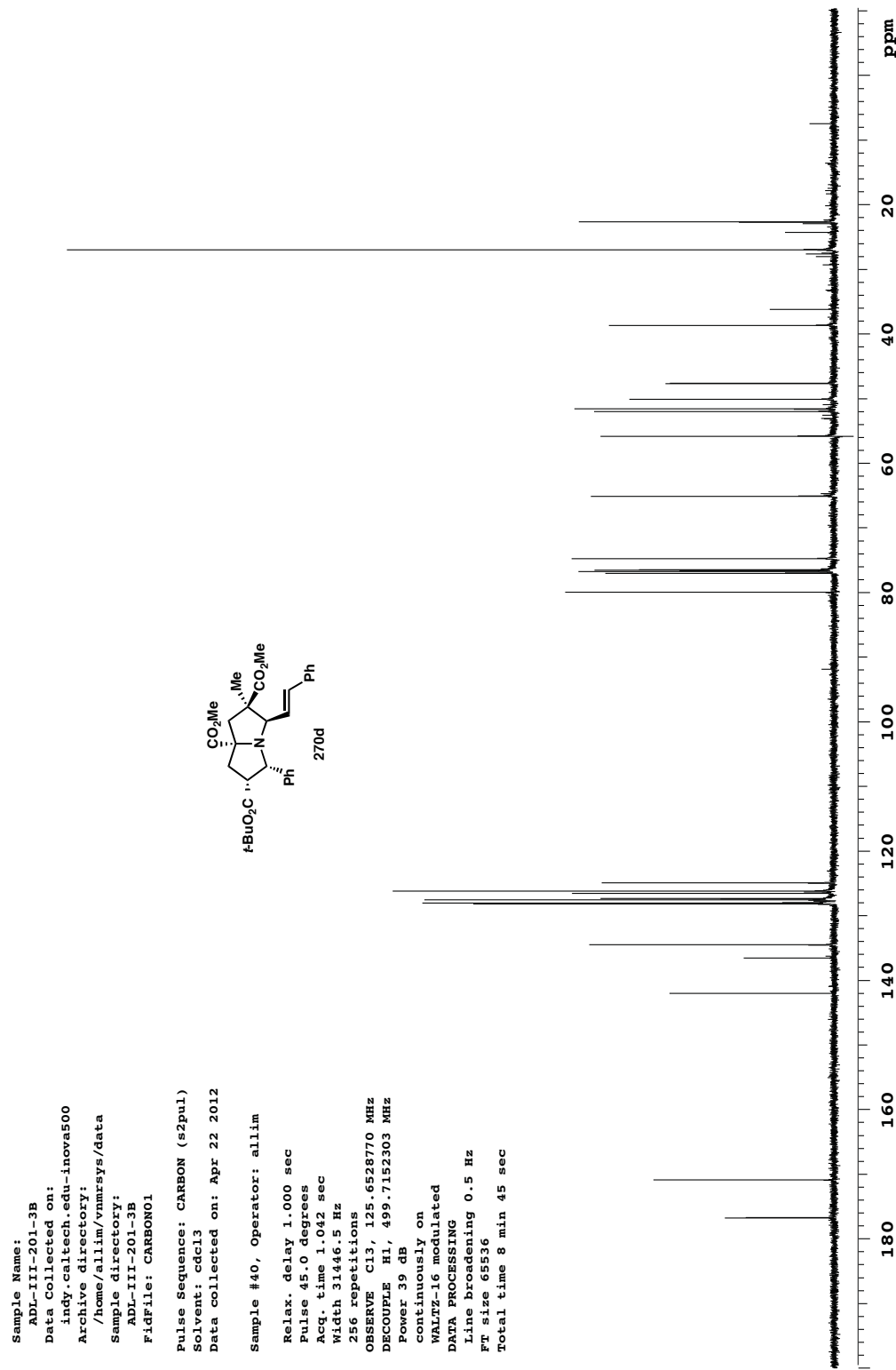


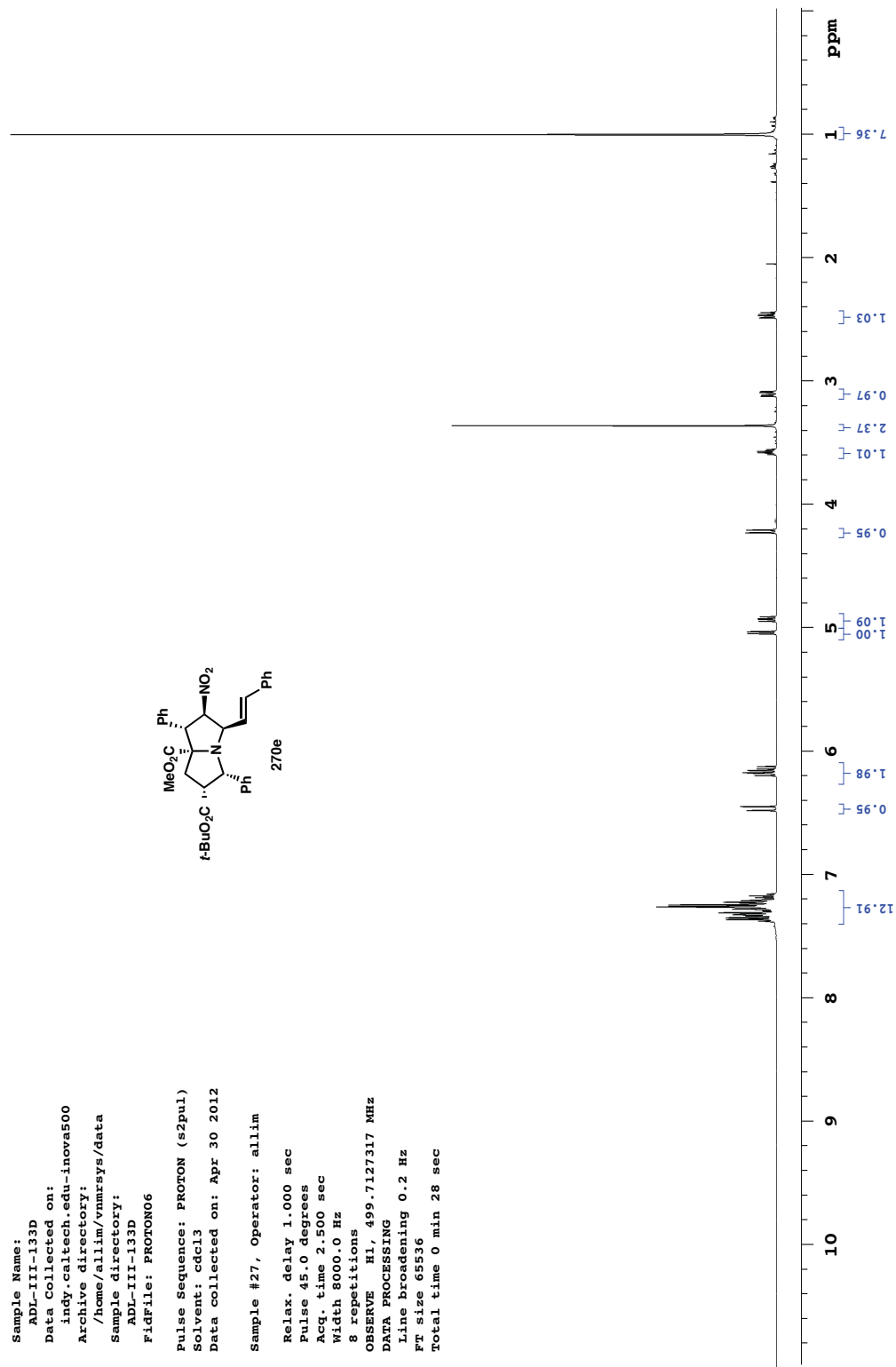


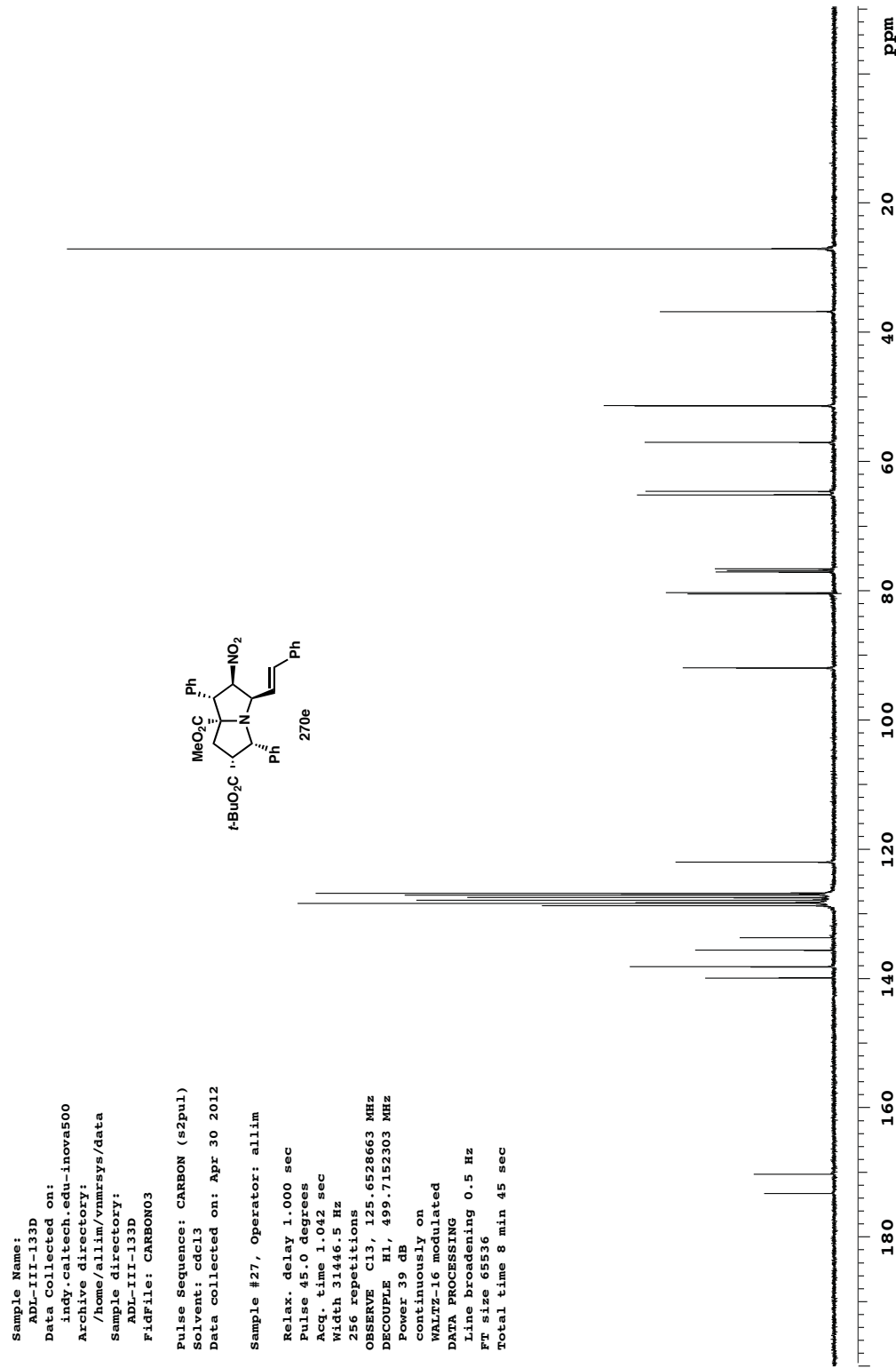


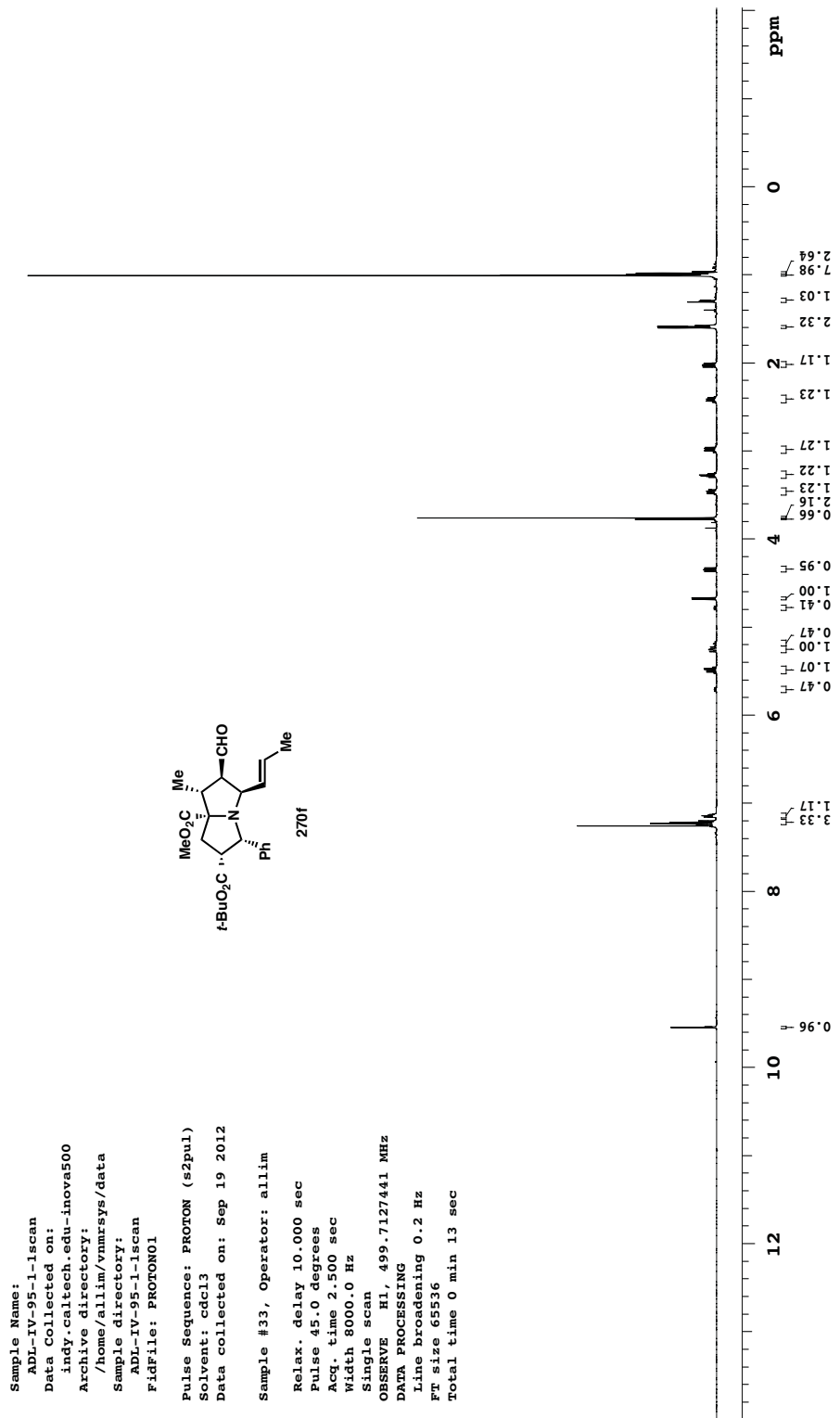


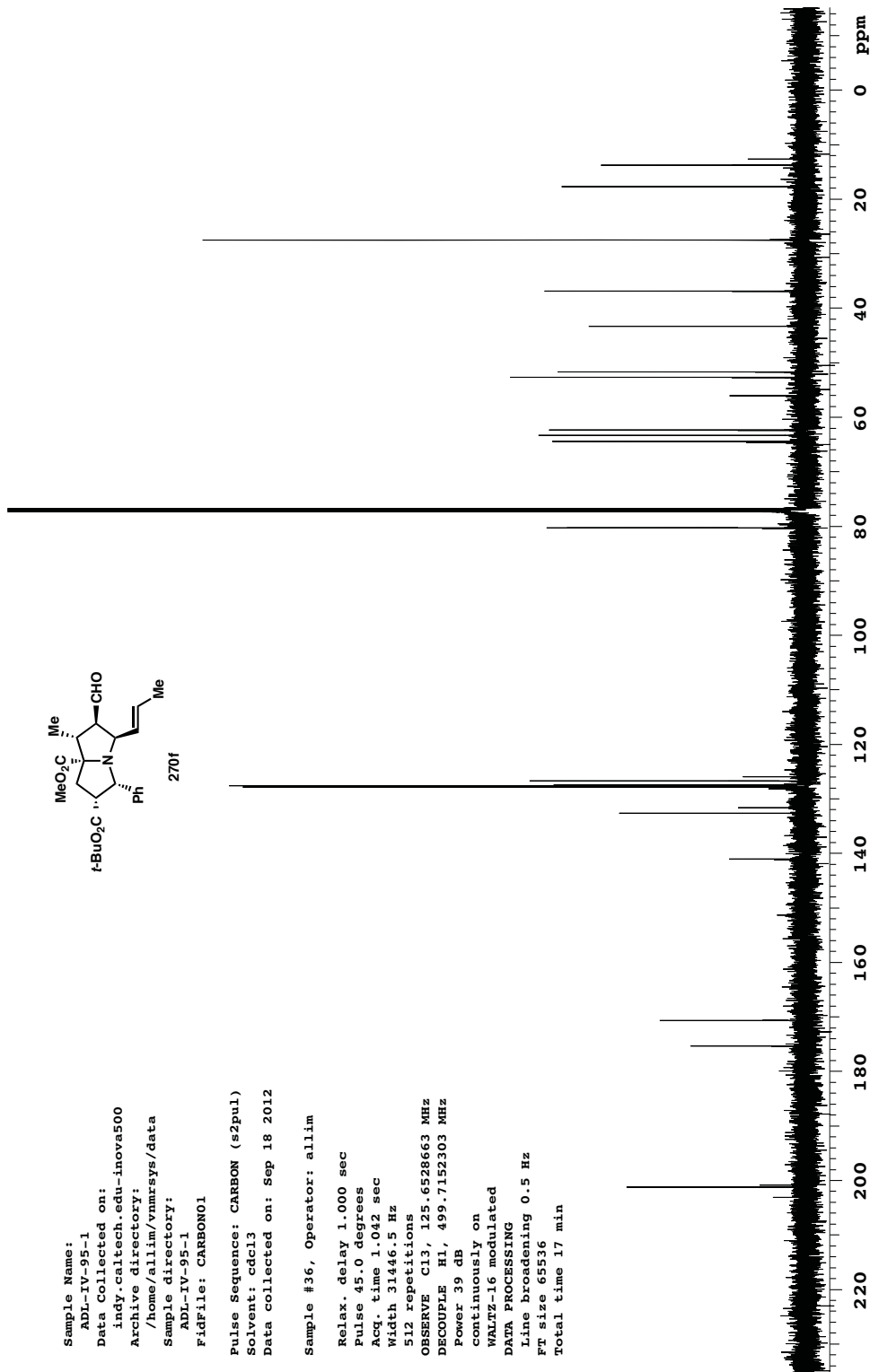


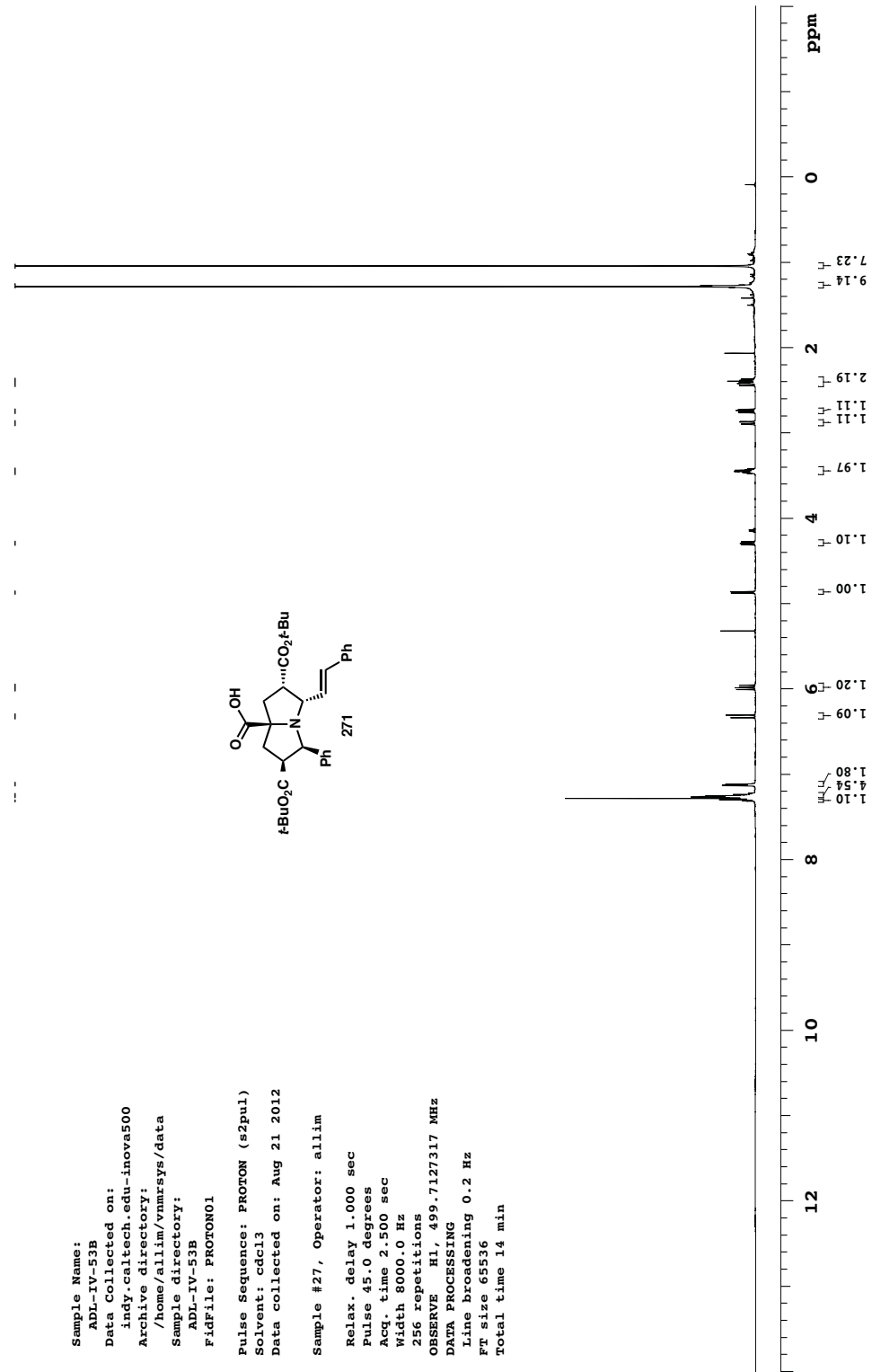


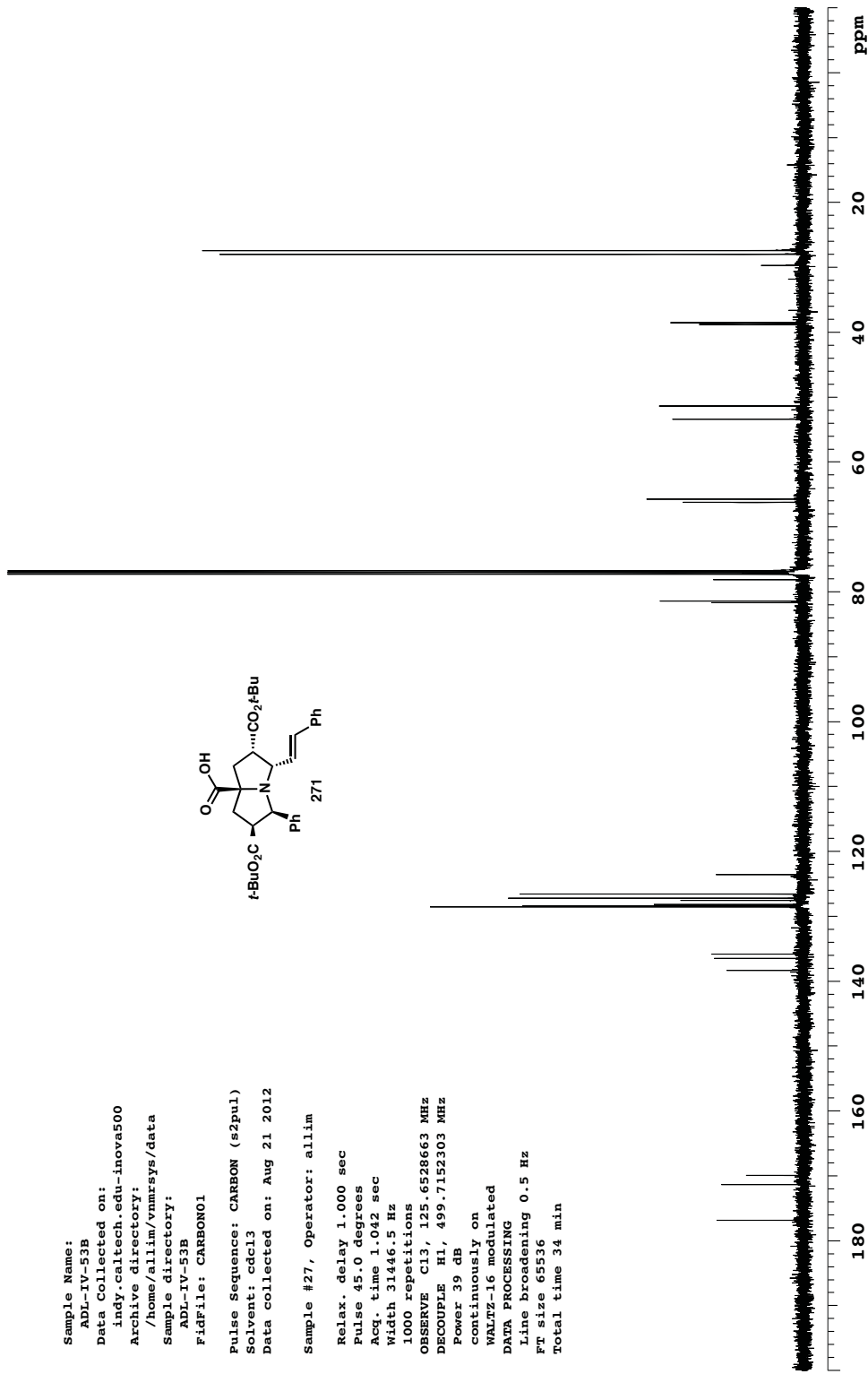


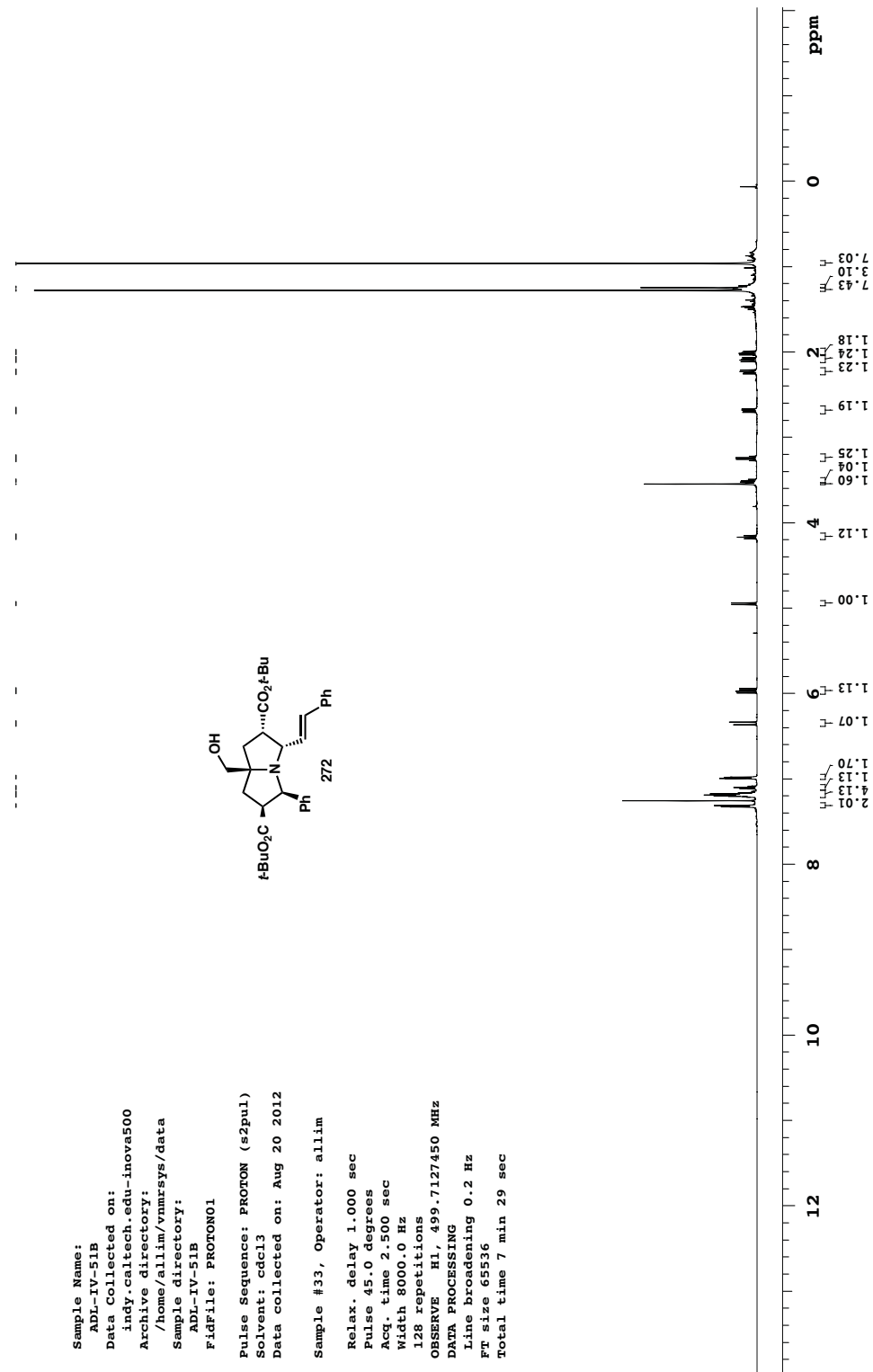


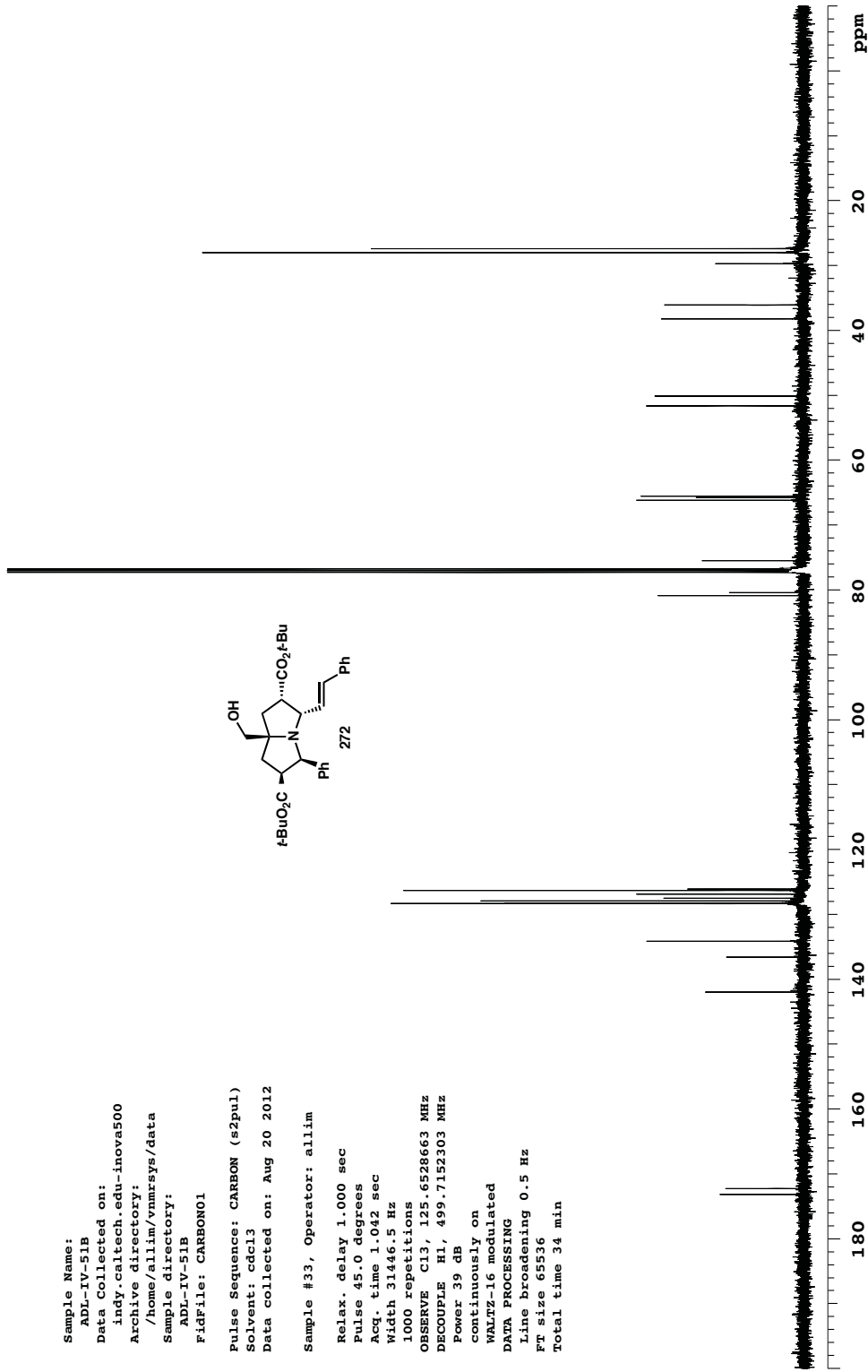


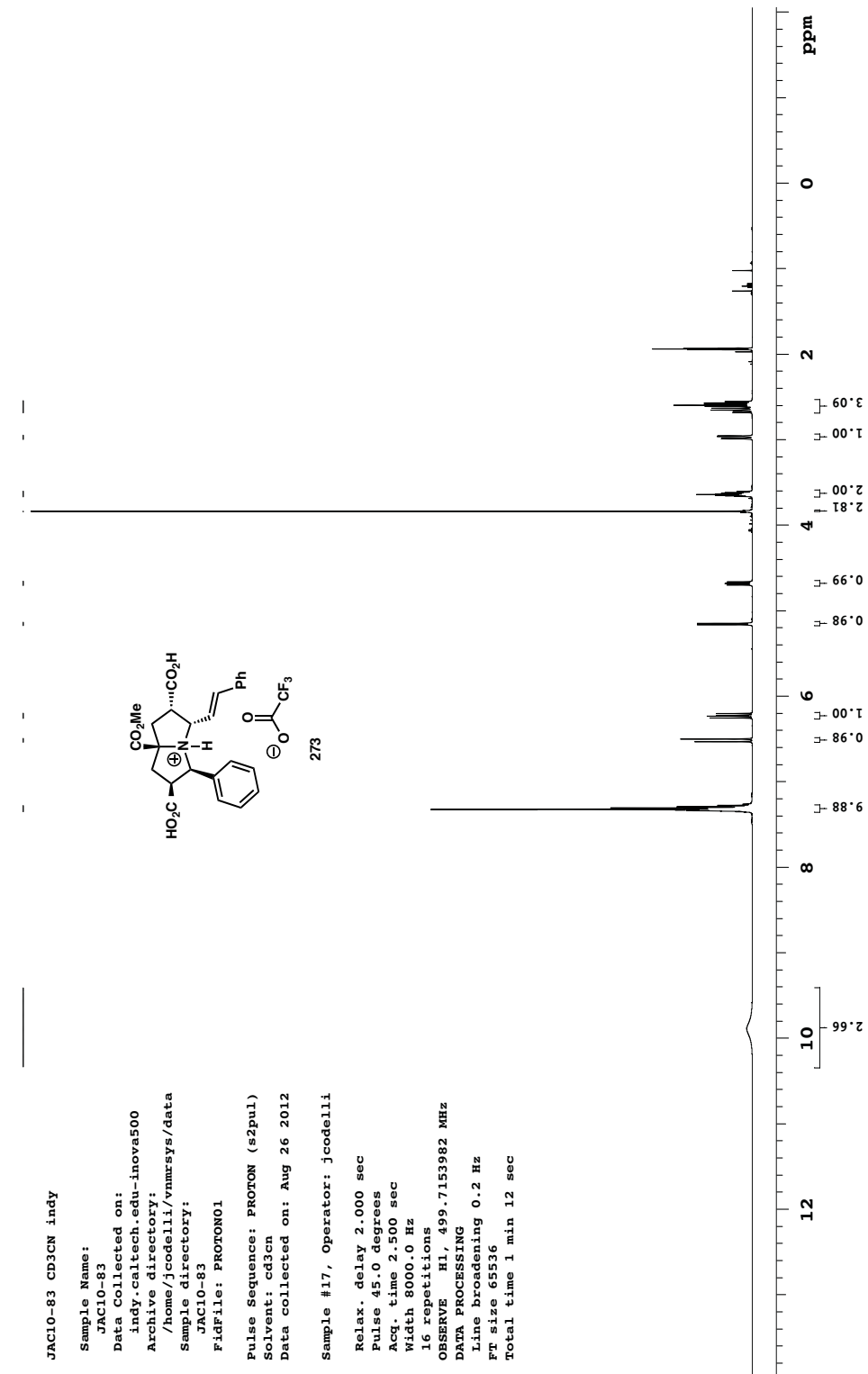


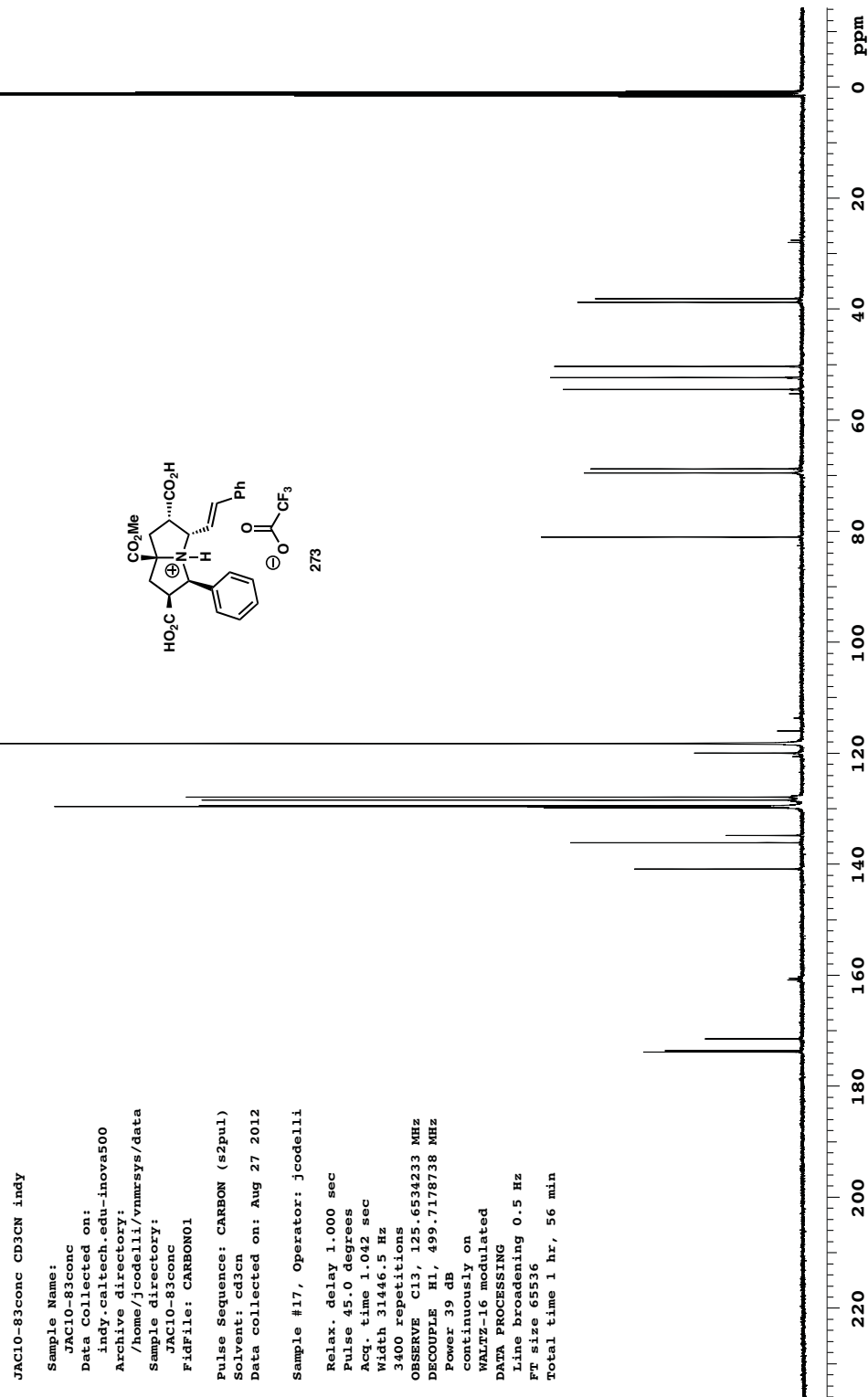


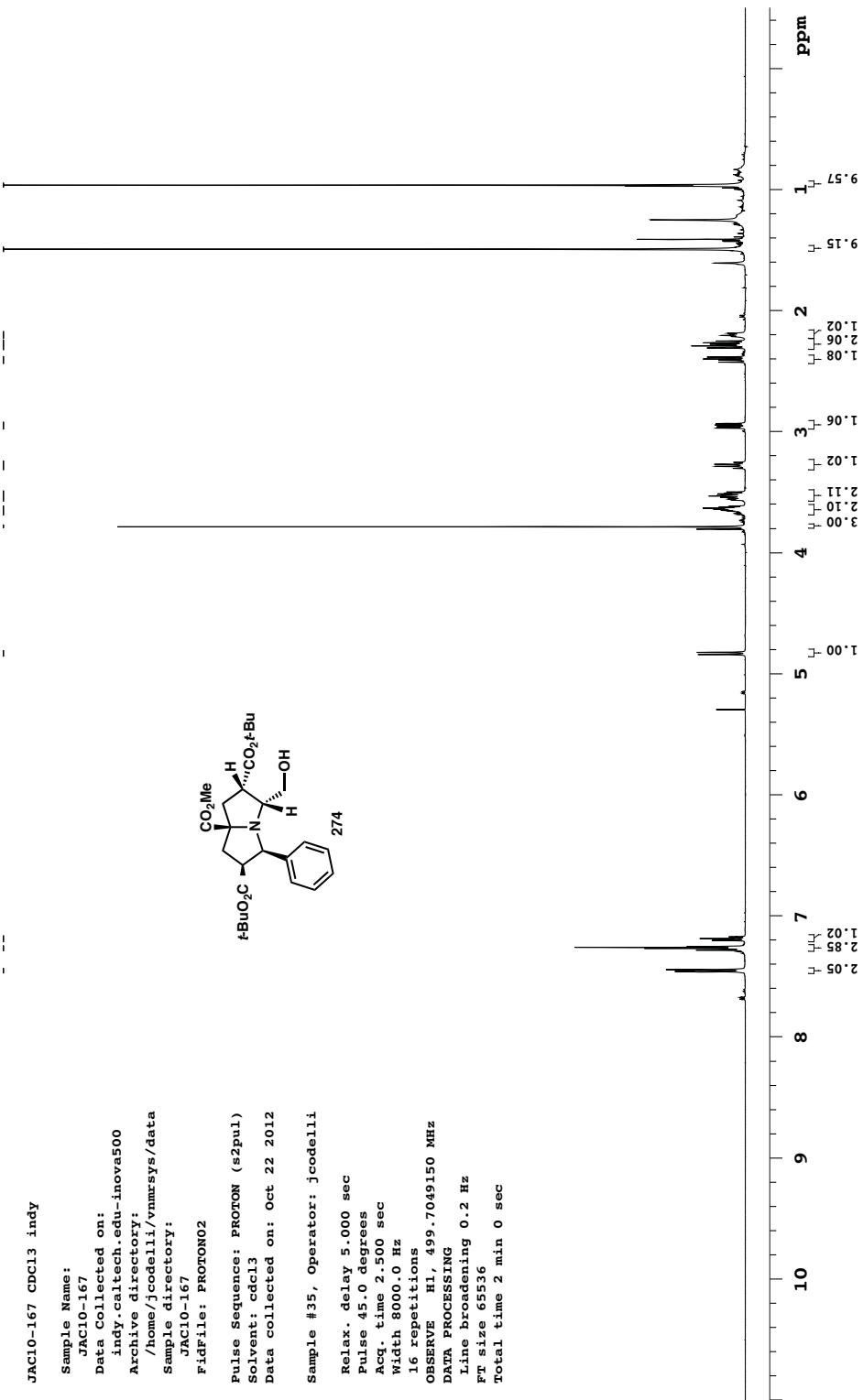


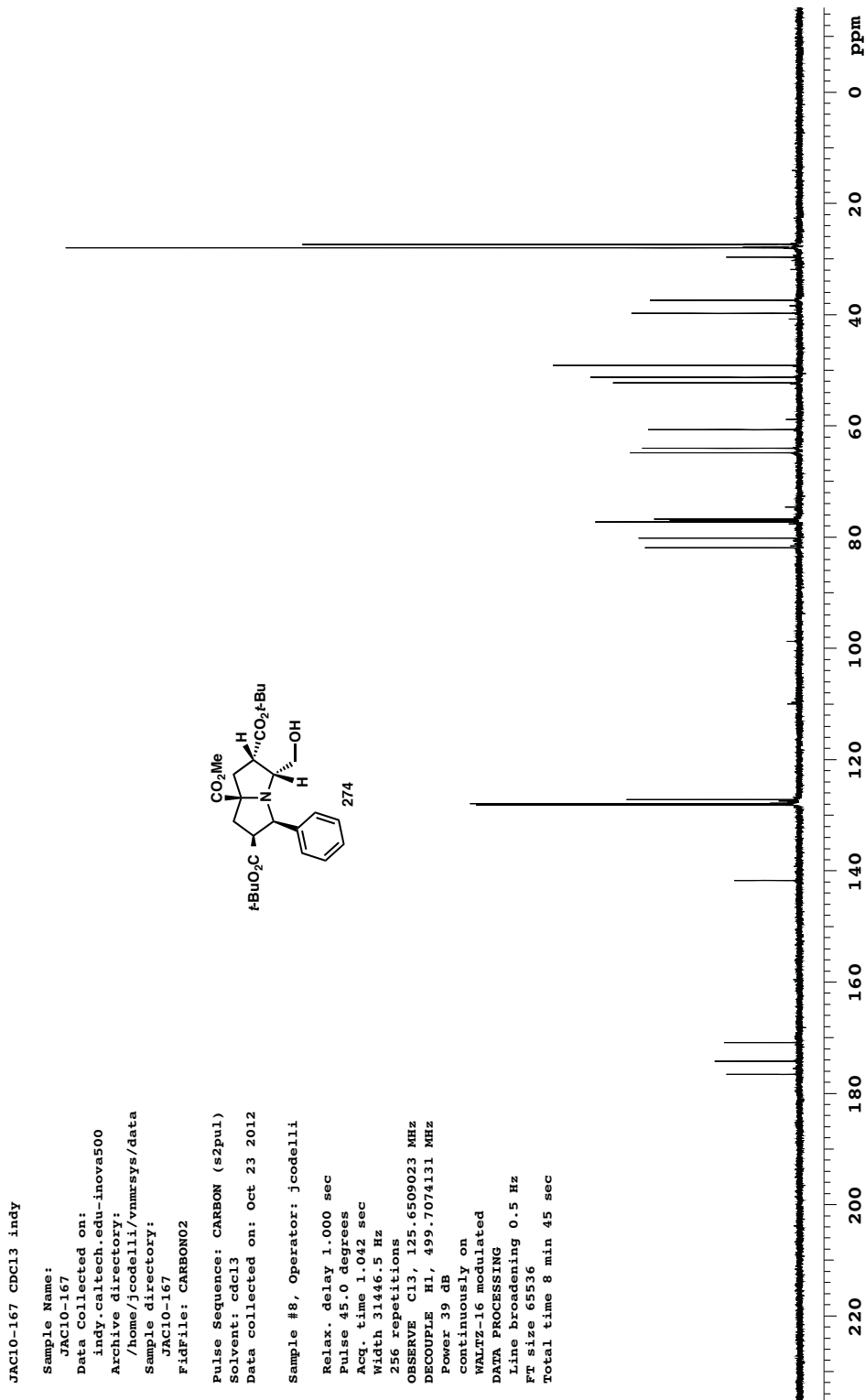


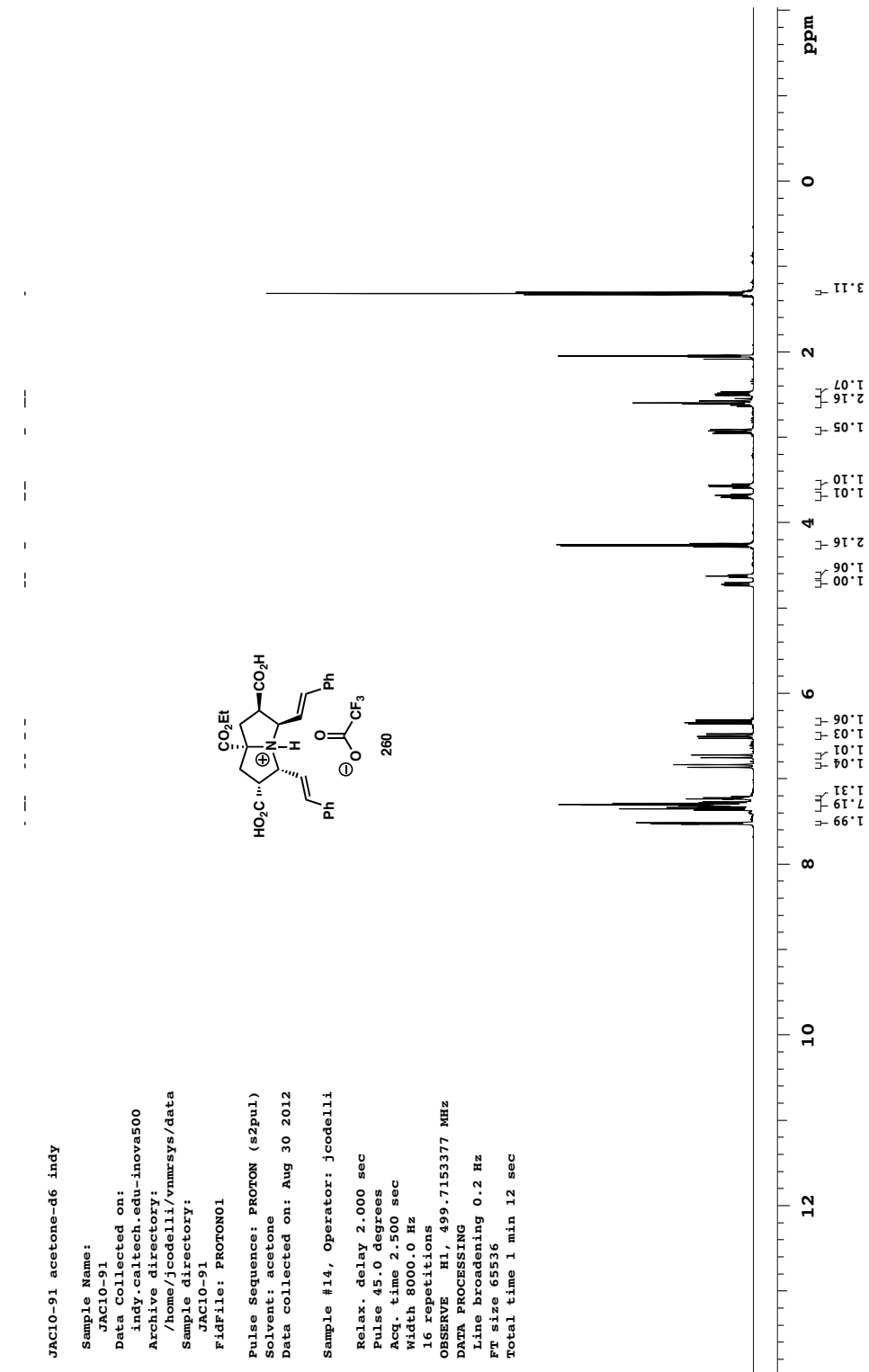


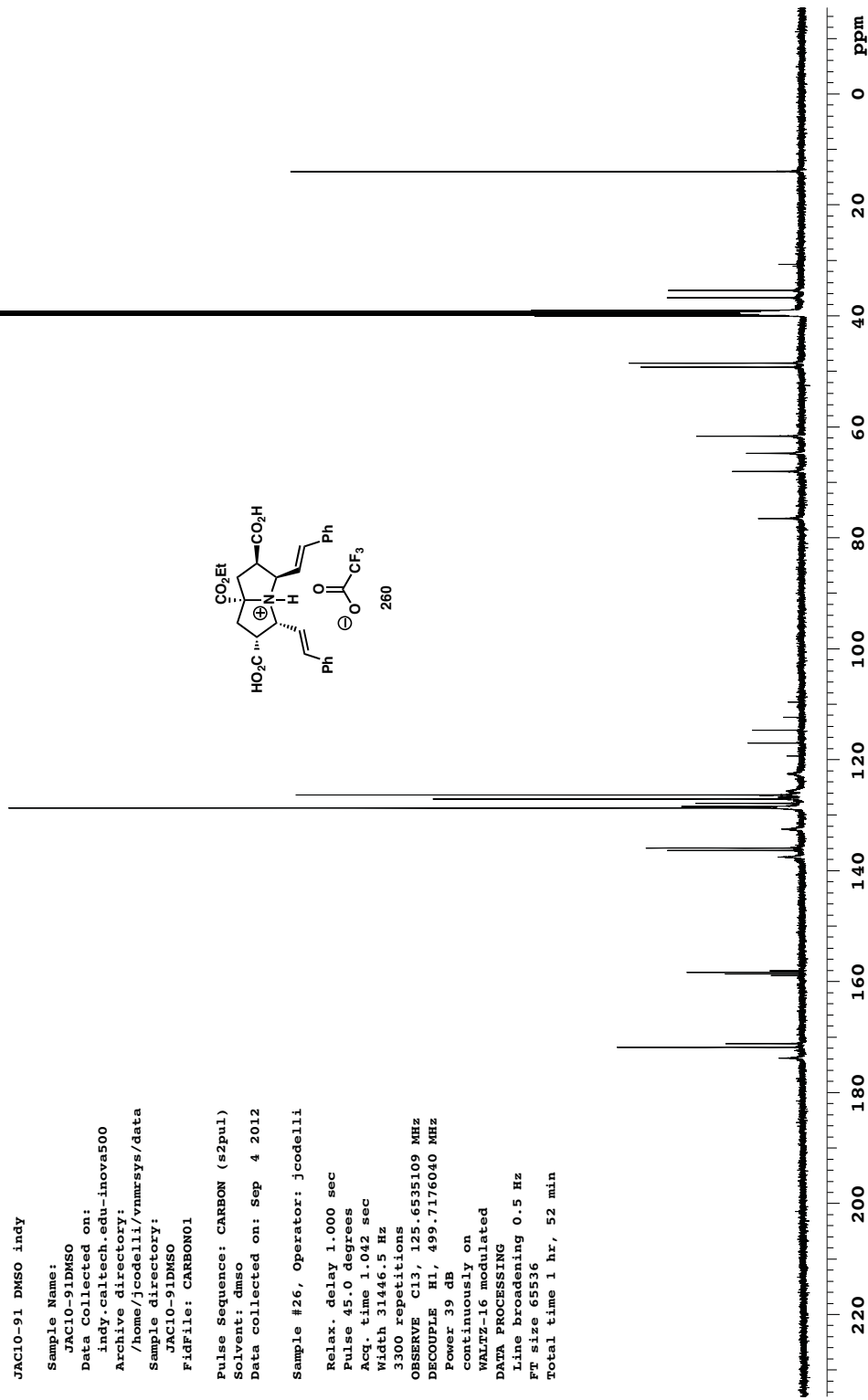


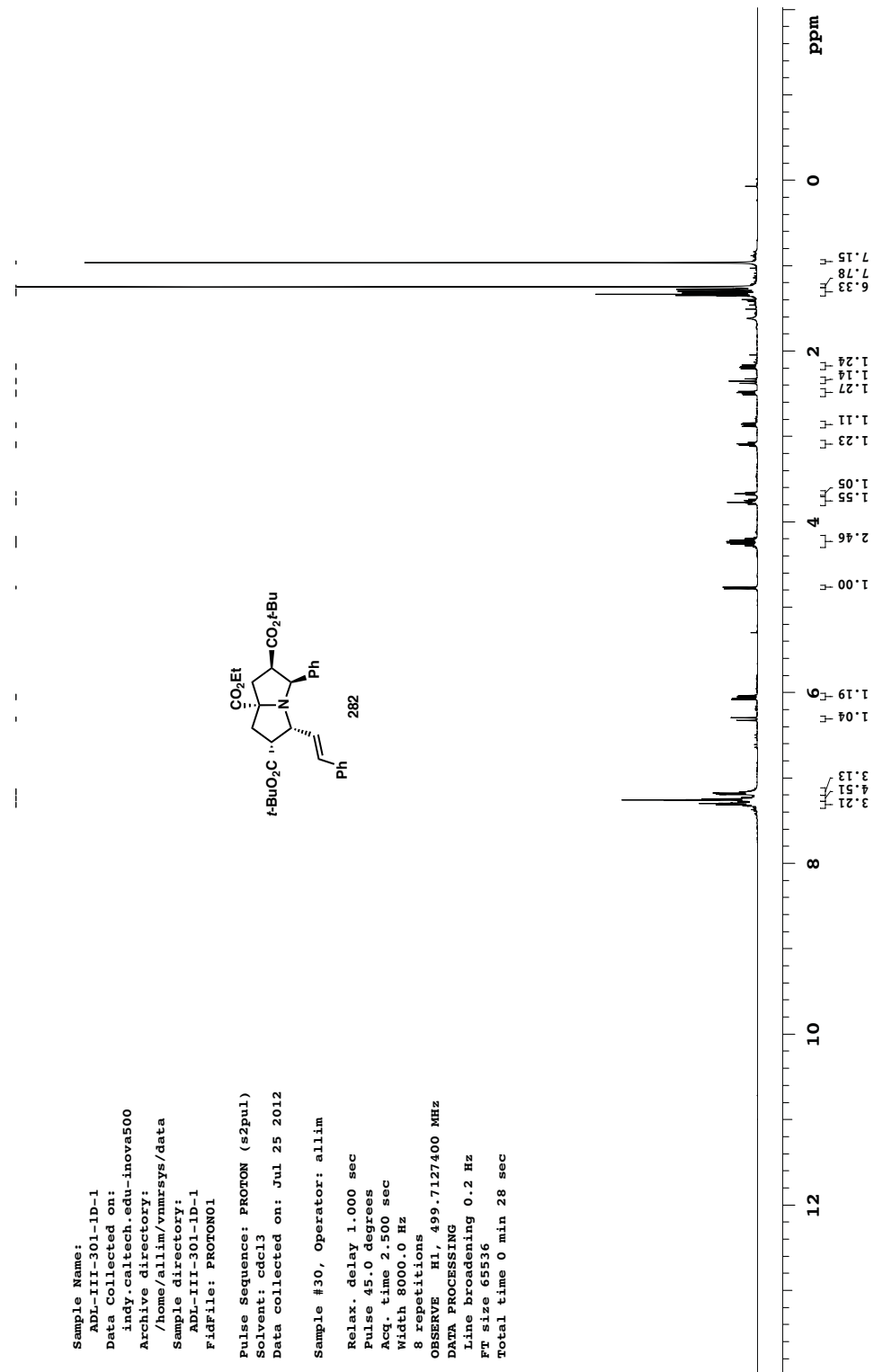


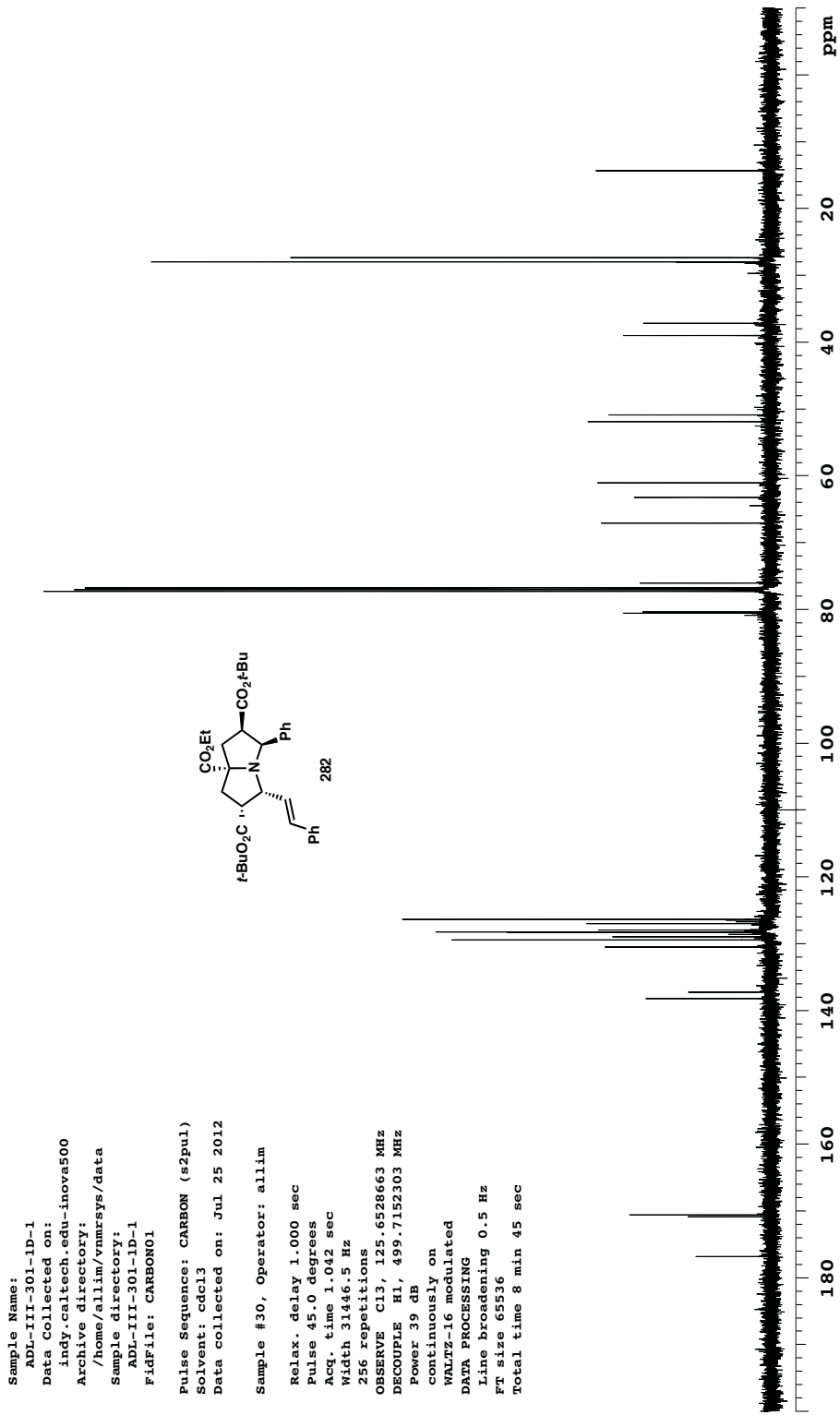


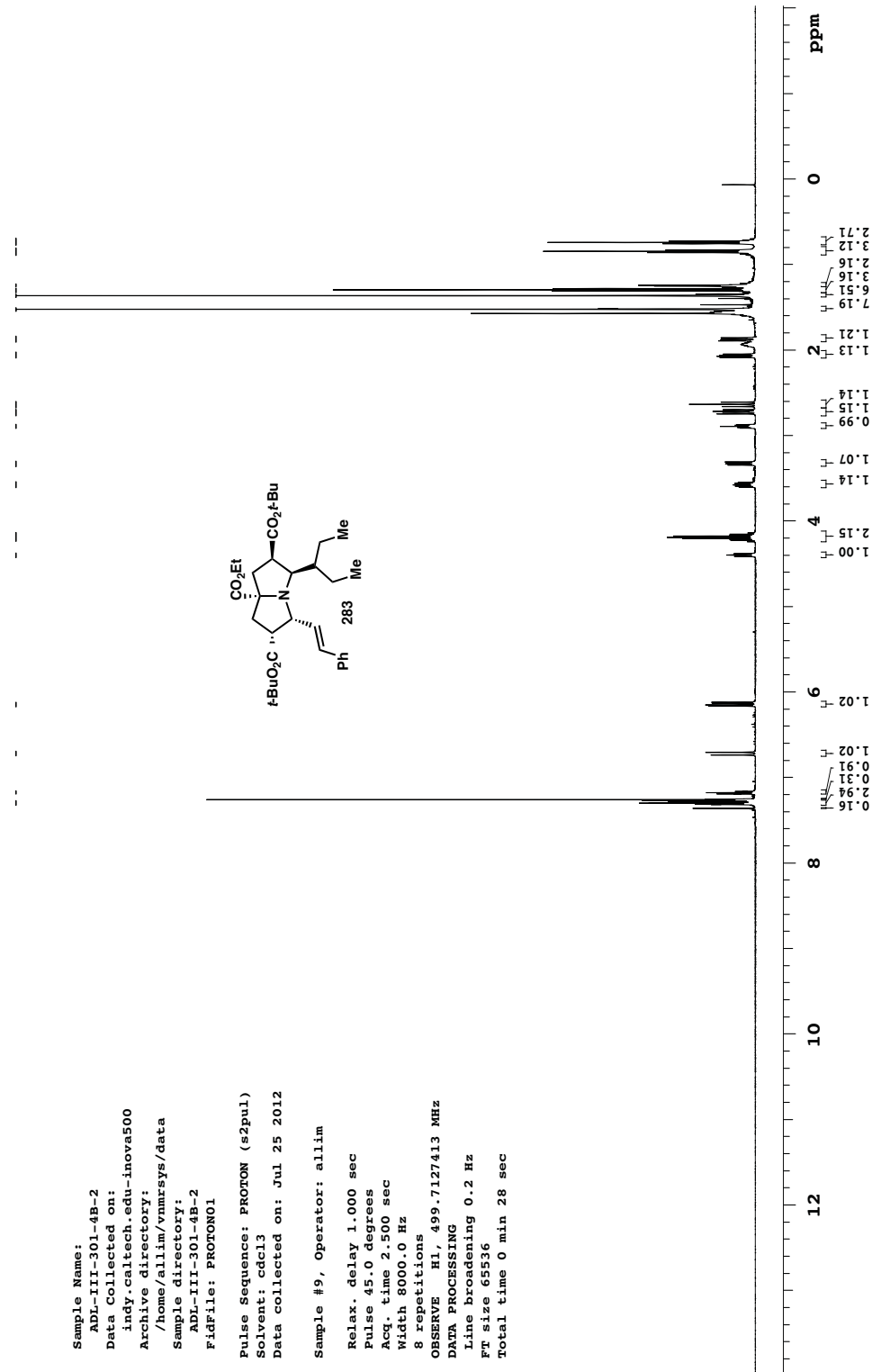


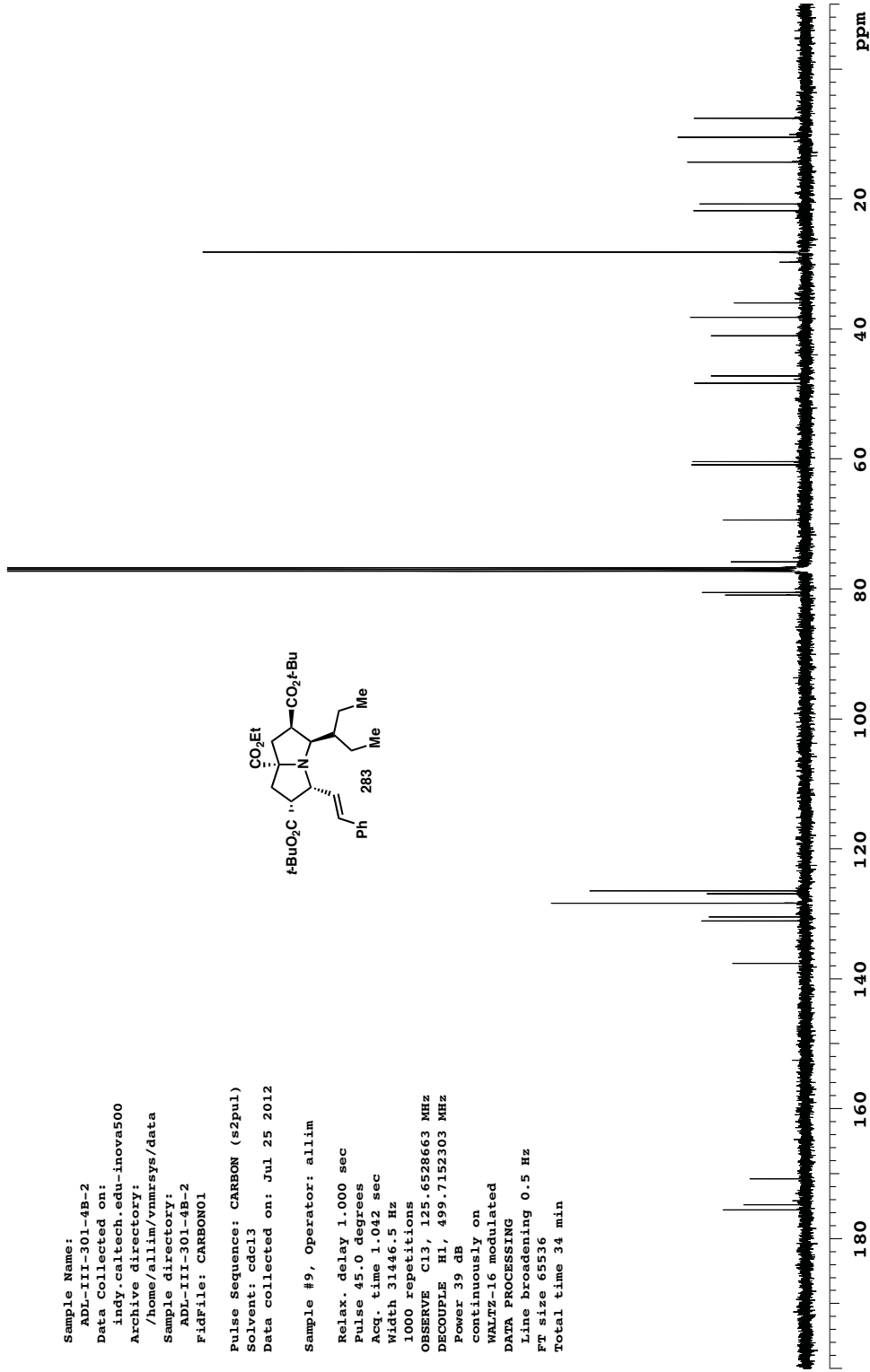


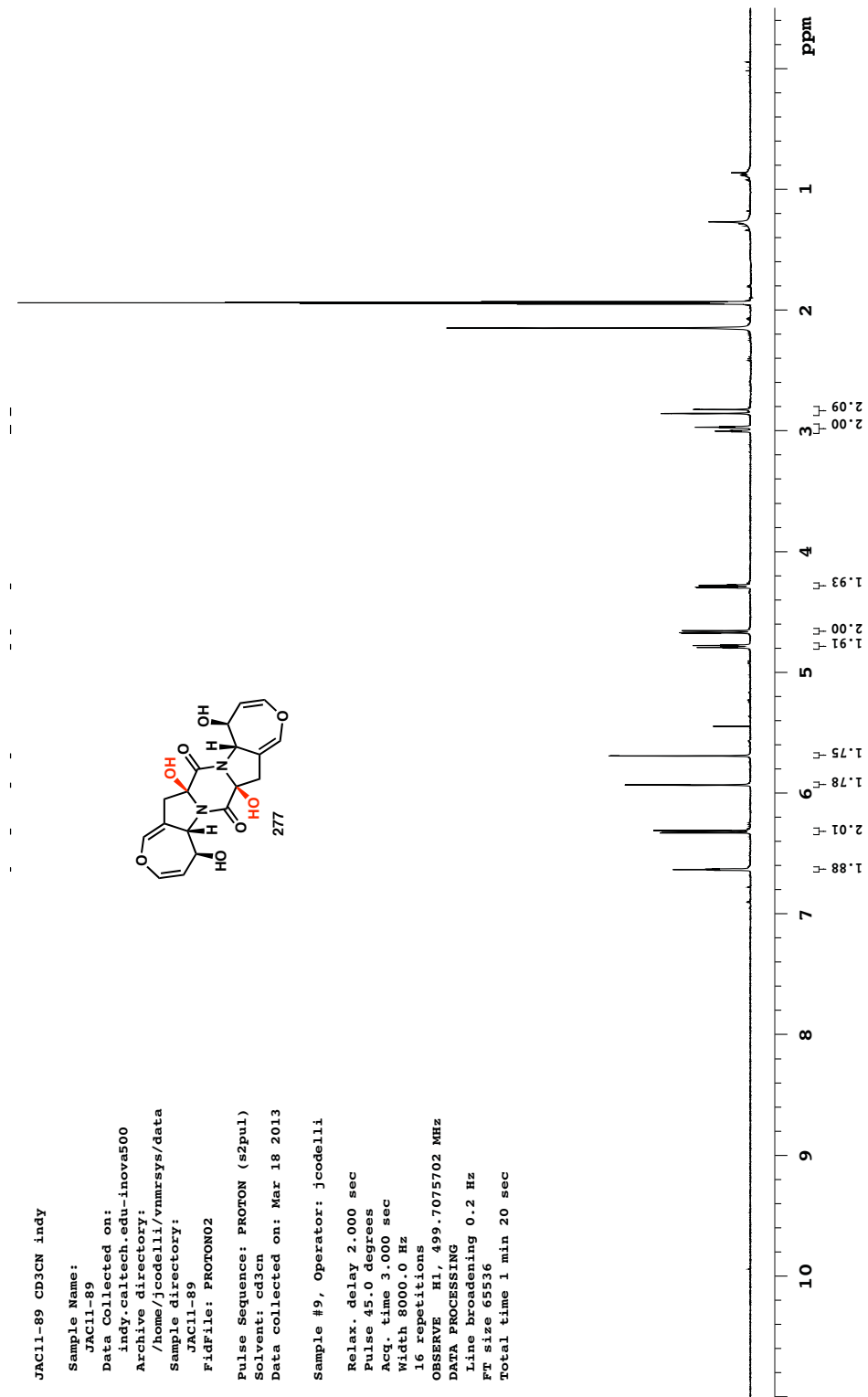


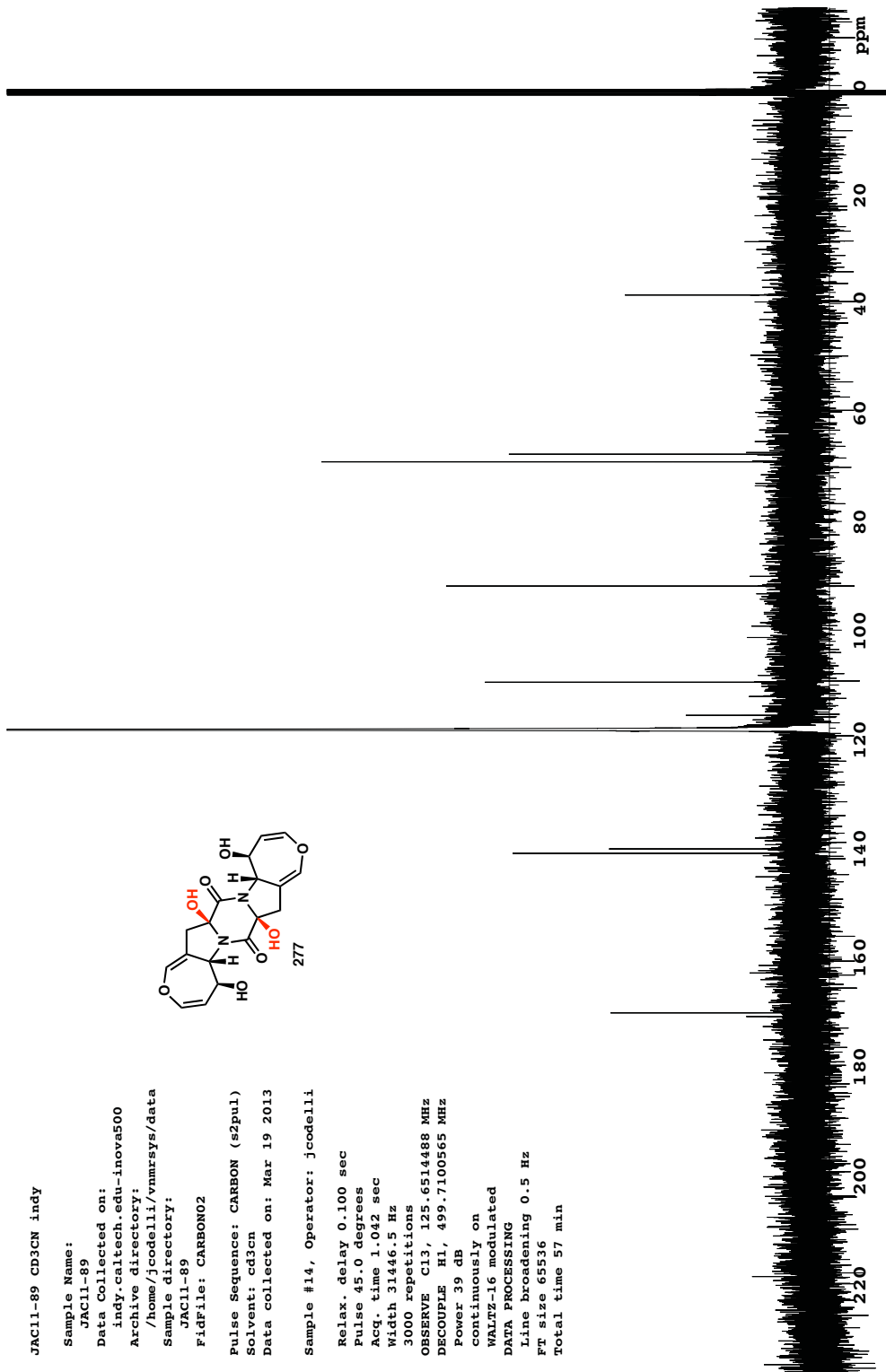


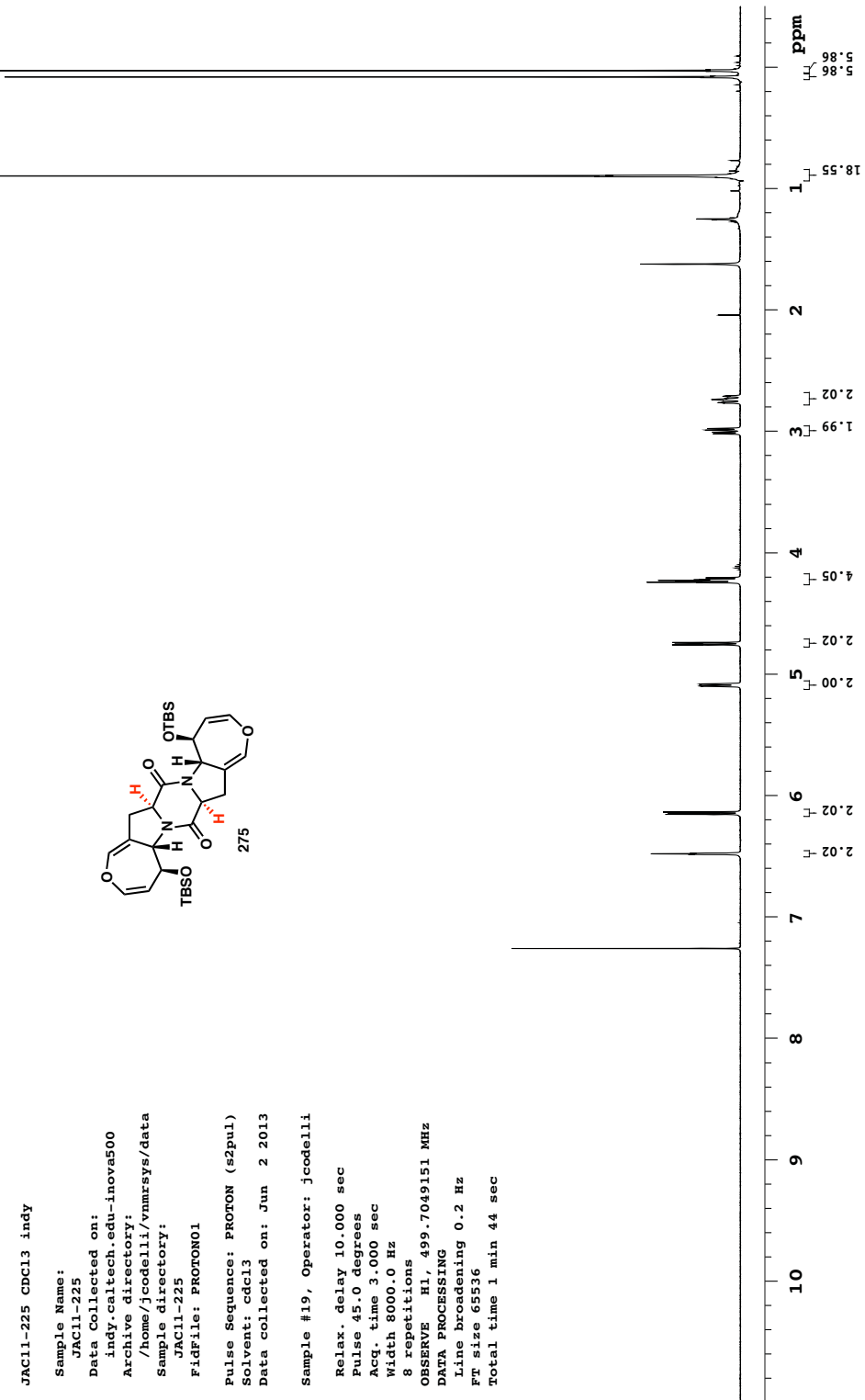


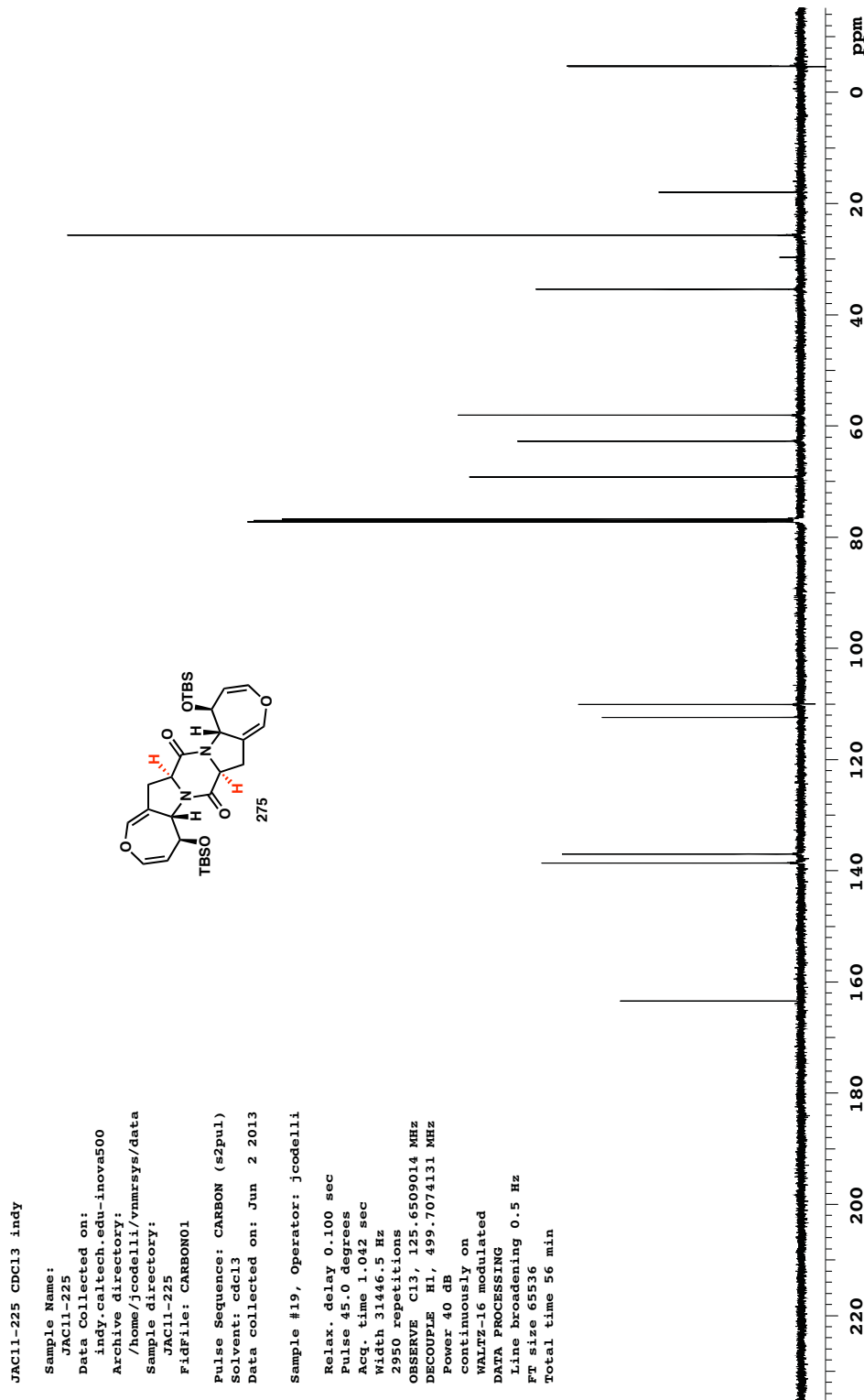












```

jaa11-217 cdc13 daytona

Sample Name:          jac11-217
Data Collected on:   data collected on: daytona.caltech.edu-ino
Archive directory:   Sample directory: /jaa11-217-proton

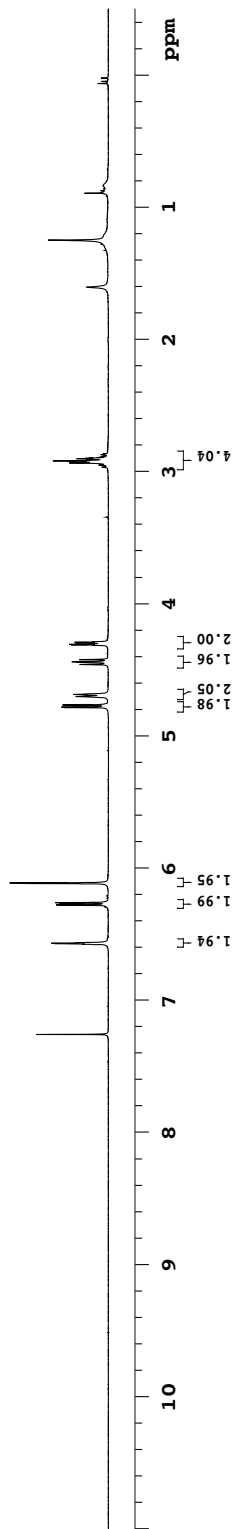
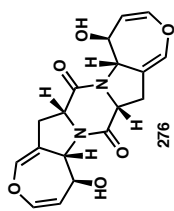
File: jac11-217-proton

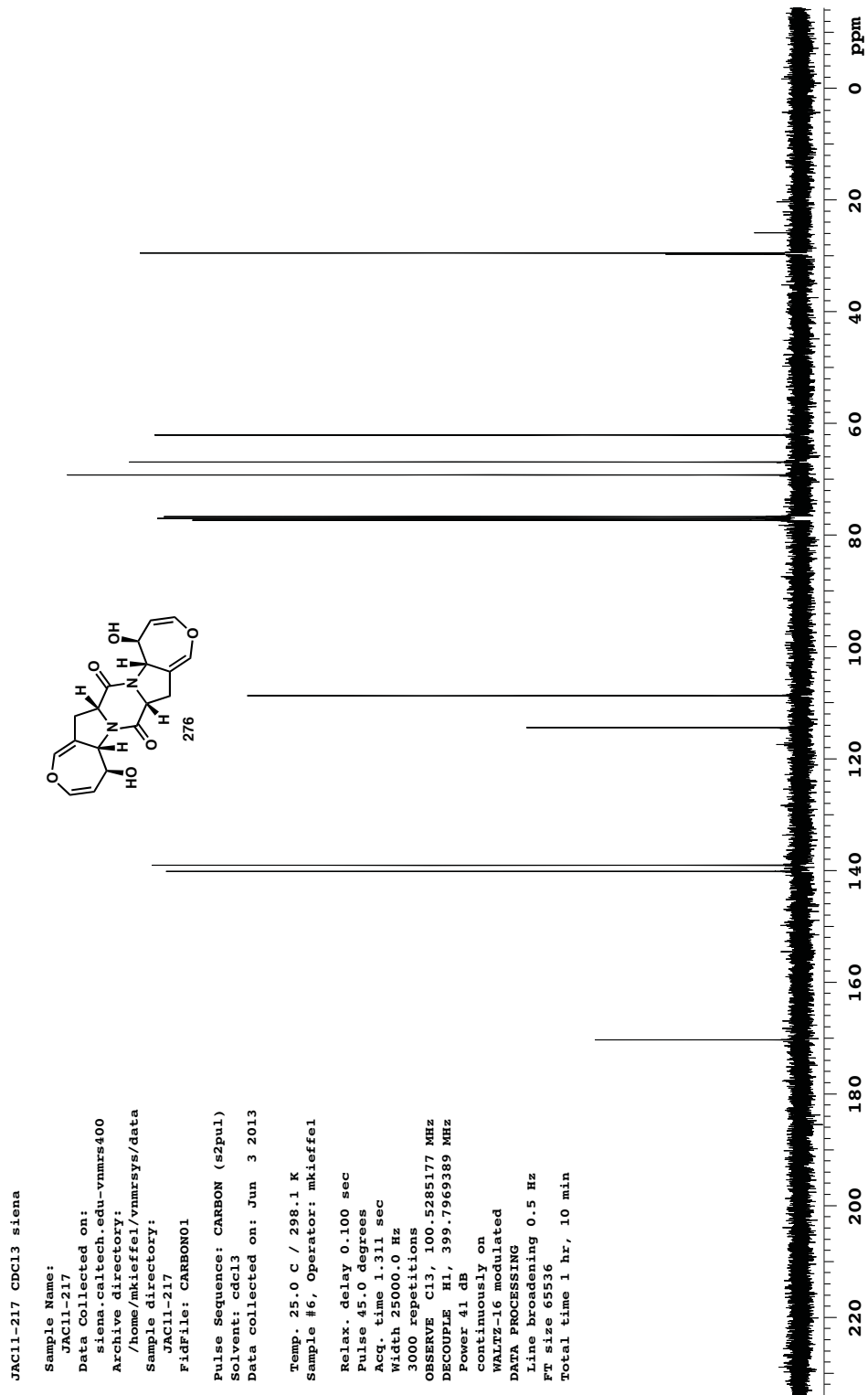
Pulse Sequence: PROTON (s2)
Sovent: cdc13
Data collected on: Jun  2

Temp. 25.0 C / 298.1 K
operator: yeomanjo

Relax. delay 5.000 sec
Pulse 45.0 degrees
Acq. time 2.048 sec
Width 8000.0 Hz
8 repetitions
OBSERVE H1, 499.8488915
DATA PROCESSING
FT size 32768
Total time 0 min 56 sec

```





Appendix 5

X-Ray Crystallography Reports Relevant to Chapter 4: Further Investigation of Side Reactions[†]

[†] The work disclosed in this appendix for the X-ray crystallographic analysis of **260** was completed entirely by Larry Henling and Dr. Michael Day in the Caltech X-ray crystallography lab.

A5.1. CRYSTAL STRUCTURE ANALYSIS OF PYRROLIZIDINE 260

Figure A5.1. Pyrrolizidine **260** (trifluoroacetate counterion omitted). Crystallographic data have been deposited at the CCDC, 12 Union Road, Cambridge CB2 1EZ, UK and copies can be obtained on request, free of charge, by quoting the publication citation and the deposition number 831402.

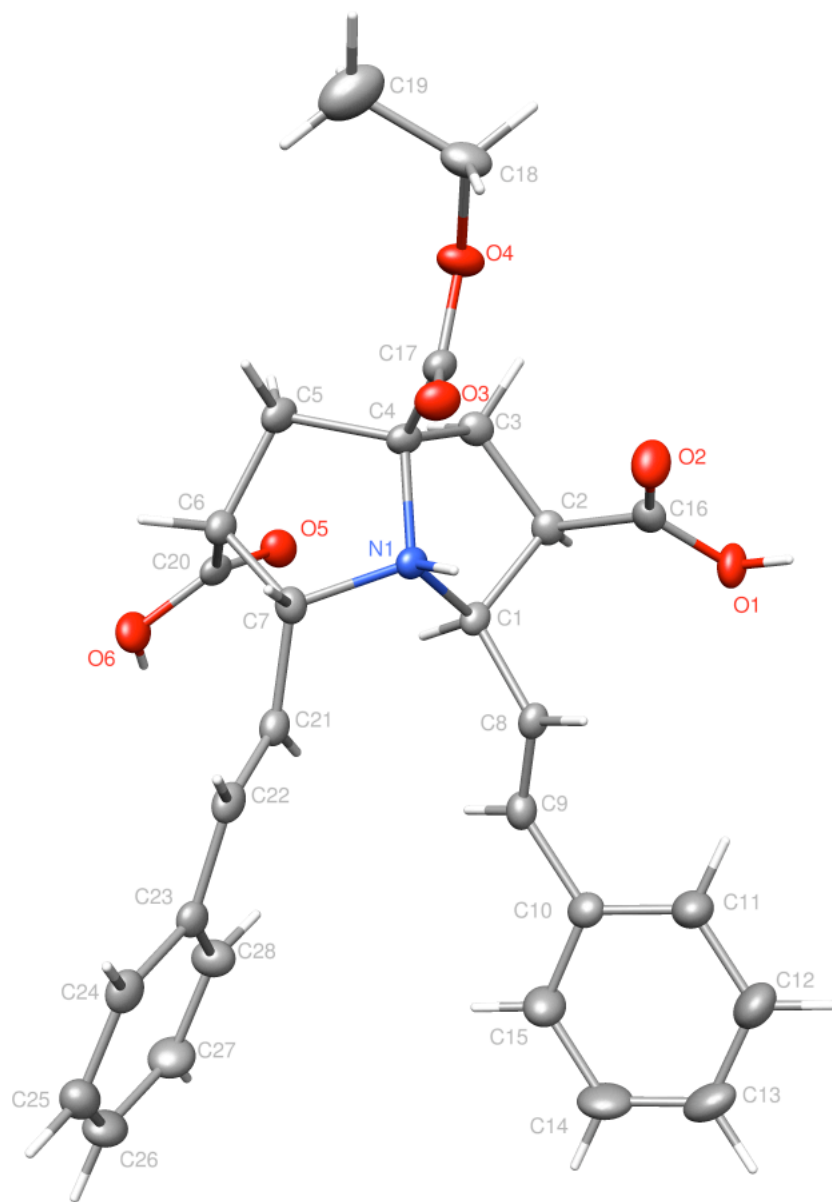


Table A5.1. Crystal data and structure refinement for pyrrolizidine **260** (CCDC 831402).

Empirical formula	$[C_{28}H_{30}NO_6]^+ [C_2F_3O_2]^-$
Formula weight	589.55
Crystallization Solvent	Acetone/pentanes
Crystal Habit	Plate
Crystal size	0.36 x 0.33 x 0.11 mm ³
Crystal color	Colorless

Data Collection

Type of diffractometer	Bruker SMART 1000
Wavelength	0.71073 Å MoKα
Data Collection Temperature	100(2) K
θ range for 9978 reflections used in lattice determination	2.39 to 27.12°
Unit cell dimensions	a = 16.1696(19) Å b = 9.6337(11) Å c = 18.988(2) Å
	α = 90° β = 106.742(2)° γ = 90°
Volume	2832.4(6) Å ³
Z	4
Crystal system	Monoclinic
Space group	P 2 ₁ /n
Density (calculated)	1.383 Mg/m ³
F(000)	1232
θ range for data collection	1.96 to 27.61°
Completeness to θ = 27.61°	99.5 %
Index ranges	-20 ≤ h ≤ 20, -12 ≤ k ≤ 12, -24 ≤ l ≤ 24
Data collection scan type	ω scans; 6 settings
Reflections collected	42760
Independent reflections	6554 [R _{int} = 0.0503]
Absorption coefficient	0.113 mm ⁻¹
Absorption correction	Semi-empirical from equivalents
Max. and min. transmission	0.7456 and 0.6474

Table A5.1 (cont.)**Structure Solution and Refinement**

Structure solution program	SHELXS-97 (Sheldrick, 2008)
Primary solution method	Direct methods
Secondary solution method	Difference Fourier map
Hydrogen placement	Geometric positions
Structure refinement program	SHELXL-97 (Sheldrick, 2008)
Refinement method	Full matrix least-squares on F^2
Data / restraints / parameters	6554 / 0 / 410
Treatment of hydrogen atoms	Riding
Goodness-of-fit on F^2	2.325
Final R indices [$I > 2\sigma(I)$, 4759 reflections]	$R = 0.0492$, $wR = 0.0710$
R indices (all data)	$R = 0.0733$, $wR = 0.0735$
Type of weighting scheme used	Sigma
Weighting scheme used	$w = 1/\sigma^2(Fo^2)$
Max shift/error	0.013
Average shift/error	0.001
Largest diff. peak and hole	0.281 and -0.312 e. \AA^{-3}

Special Refinement Details

Crystals were mounted on a glass fiber using Paratone oil then placed on the diffractometer under a nitrogen stream at 100K.

Refinement of F^2 against ALL reflections. The weighted R-factor (wR) and goodness of fit (S) are based on F^2 , conventional R-factors (R) are based on F, with F set to zero for negative F^2 . The threshold expression of $F^2 > 2\sigma(F^2)$ is used only for calculating R-factors(gt) etc. and is not relevant to the choice of reflections for refinement. R-factors based on F^2 are statistically about twice as large as those based on F, and R-factors based on ALL data will be even larger.

All esds (except the esd in the dihedral angle between two l.s. planes) are estimated using the full covariance matrix. The cell esds are taken into account individually in the estimation of esds in distances, angles and torsion angles; correlations between esds in cell parameters are only used when they are defined by crystal symmetry. An approximate (isotropic) treatment of cell esds is used for estimating esds involving l.s. planes.

Table A5.2. Atomic coordinates ($\times 10^4$) and equivalent isotropic displacement parameters ($\text{\AA}^2 \times 10^3$) for pyrrolizidine **260** (CCDC 831402). $U(\text{eq})$ is defined as the trace of the orthogonalized U^{ij} tensor.

	x	y	z	U_{eq}	Occ
N(1)	548(1)	1210(1)	1090(1)	16(1)	1
O(1)	-1579(1)	3781(1)	489(1)	25(1)	1
O(2)	-759(1)	2797(1)	-147(1)	28(1)	1
O(3)	670(1)	806(1)	-294(1)	23(1)	1
O(4)	1170(1)	2975(1)	-361(1)	25(1)	1
O(5)	1918(1)	2777(1)	2575(1)	25(1)	1
O(6)	2539(1)	788(1)	3074(1)	26(1)	1
C(1)	36(1)	2023(2)	1518(1)	17(1)	1
C(2)	-108(1)	3419(2)	1109(1)	18(1)	1
C(3)	755(1)	3679(2)	952(1)	20(1)	1
C(4)	1065(1)	2252(2)	780(1)	18(1)	1
C(5)	2030(1)	1918(2)	1165(1)	21(1)	1
C(6)	2048(1)	890(2)	1782(1)	20(1)	1
C(7)	1179(1)	104(2)	1512(1)	19(1)	1
C(8)	-768(1)	1304(2)	1551(1)	18(1)	1
C(9)	-963(1)	1085(2)	2172(1)	22(1)	1
C(10)	-1790(1)	540(2)	2231(1)	24(1)	1
C(11)	-2548(1)	711(2)	1668(1)	36(1)	1
C(12)	-3319(1)	204(2)	1732(1)	44(1)	1
C(13)	-3350(1)	-471(2)	2361(1)	42(1)	1
C(14)	-2610(1)	-639(2)	2924(1)	44(1)	1
C(15)	-1831(1)	-126(2)	2865(1)	35(1)	1
C(16)	-848(1)	3306(2)	410(1)	20(1)	1
C(17)	911(1)	1927(2)	-29(1)	20(1)	1
C(18)	1308(1)	2725(2)	-1082(1)	28(1)	1
C(19)	2251(1)	2581(2)	-975(1)	50(1)	1
C(20)	2157(1)	1604(2)	2514(1)	21(1)	1
C(21)	906(1)	-619(2)	2099(1)	19(1)	1
C(22)	837(1)	-1988(2)	2127(1)	20(1)	1
C(23)	717(1)	-2773(2)	2753(1)	19(1)	1
C(24)	790(1)	-4211(2)	2759(1)	23(1)	1
C(25)	753(1)	-4984(2)	3366(1)	29(1)	1
C(26)	644(1)	-4326(2)	3973(1)	32(1)	1
C(27)	553(1)	-2897(2)	3971(1)	32(1)	1
C(28)	588(1)	-2134(2)	3370(1)	27(1)	1
C(31)	1037(1)	1596(3)	4807(1)	40(1)	1
C(32)	1369(1)	1469(2)	4134(1)	23(1)	1
F(1)	1353(4)	2727(5)	5180(2)	88(2)	0.751(12)
F(2)	205(3)	1790(11)	4627(3)	115(2)	0.751(12)
F(3)	1266(4)	589(4)	5255(3)	93(2)	0.751(12)
F(1B)	967(17)	2814(10)	5038(10)	101(6)	0.249(12)
F(2B)	292(10)	975(19)	4709(9)	91(6)	0.249(12)
F(3B)	1501(11)	980(30)	5382(9)	158(9)	0.249(12)
O(7)	2184(1)	1448(1)	4281(1)	30(1)	1

O(8)	829(1)	1394(1)	3536(1)	27(1)	1
------	--------	---------	---------	-------	---

Table A5.3. Bond lengths [\AA] and angles [$^\circ$] for pyrrolizidine **260** (CCDC 831402).

N(1)-C(4)	1.5278(18)	C(7)-N(1)-C(1)	117.25(11)
N(1)-C(7)	1.5317(17)	C(17)-O(4)-C(18)	118.26(12)
N(1)-C(1)	1.5326(17)	C(8)-C(1)-N(1)	113.34(12)
O(1)-C(16)	1.3149(17)	C(8)-C(1)-C(2)	114.91(12)
O(2)-C(16)	1.2127(18)	N(1)-C(1)-C(2)	101.87(11)
O(3)-C(17)	1.2078(17)	C(16)-C(2)-C(3)	112.08(13)
O(4)-C(17)	1.3201(17)	C(16)-C(2)-C(1)	110.27(12)
O(4)-C(18)	1.4692(17)	C(3)-C(2)-C(1)	103.20(12)
O(5)-C(20)	1.2102(18)	C(2)-C(3)-C(4)	105.50(12)
O(6)-C(20)	1.3228(17)	C(17)-C(4)-N(1)	107.80(12)
C(1)-C(8)	1.4903(19)	C(17)-C(4)-C(3)	115.61(13)
C(1)-C(2)	1.537(2)	N(1)-C(4)-C(3)	105.10(11)
C(2)-C(16)	1.513(2)	C(17)-C(4)-C(5)	106.40(12)
C(2)-C(3)	1.5296(19)	N(1)-C(4)-C(5)	105.64(11)
C(3)-C(4)	1.530(2)	C(3)-C(4)-C(5)	115.61(12)
C(4)-C(17)	1.518(2)	C(6)-C(5)-C(4)	106.80(12)
C(4)-C(5)	1.554(2)	C(20)-C(6)-C(5)	112.38(13)
C(5)-C(6)	1.529(2)	C(20)-C(6)-C(7)	112.28(12)
C(6)-C(20)	1.516(2)	C(5)-C(6)-C(7)	104.38(12)
C(6)-C(7)	1.548(2)	C(21)-C(7)-N(1)	114.94(12)
C(7)-C(21)	1.484(2)	C(21)-C(7)-C(6)	114.82(12)
C(8)-C(9)	1.323(2)	N(1)-C(7)-C(6)	103.75(11)
C(9)-C(10)	1.471(2)	C(9)-C(8)-C(1)	123.07(14)
C(10)-C(15)	1.382(2)	C(8)-C(9)-C(10)	125.41(15)
C(10)-C(11)	1.385(2)	C(15)-C(10)-C(11)	118.25(15)
C(11)-C(12)	1.377(2)	C(15)-C(10)-C(9)	120.36(15)
C(12)-C(13)	1.373(2)	C(11)-C(10)-C(9)	121.36(15)
C(13)-C(14)	1.366(2)	C(12)-C(11)-C(10)	120.75(17)
C(14)-C(15)	1.387(2)	C(13)-C(12)-C(11)	120.44(18)
C(18)-C(19)	1.487(2)	C(14)-C(13)-C(12)	119.58(17)
C(21)-C(22)	1.326(2)	C(13)-C(14)-C(15)	120.34(18)
C(22)-C(23)	1.468(2)	C(10)-C(15)-C(14)	120.62(17)
C(23)-C(24)	1.390(2)	O(2)-C(16)-O(1)	125.22(15)
C(23)-C(28)	1.392(2)	O(2)-C(16)-C(2)	122.11(14)
C(24)-C(25)	1.387(2)	O(1)-C(16)-C(2)	112.65(14)
C(25)-C(26)	1.371(2)	O(3)-C(17)-O(4)	126.43(15)
C(26)-C(27)	1.384(2)	O(3)-C(17)-C(4)	123.05(14)
C(27)-C(28)	1.371(2)	O(4)-C(17)-C(4)	110.09(13)
C(31)-F(1B)	1.269(11)	O(4)-C(18)-C(19)	108.20(14)
C(31)-F(3)	1.272(4)	O(5)-C(20)-O(6)	124.48(15)
C(31)-F(3B)	1.280(13)	O(5)-C(20)-C(6)	123.76(14)
C(31)-F(2)	1.303(4)	O(6)-C(20)-C(6)	111.76(14)
C(31)-F(2B)	1.311(10)	C(22)-C(21)-C(7)	122.94(15)
C(31)-F(1)	1.319(4)	C(21)-C(22)-C(23)	125.23(15)
C(31)-C(32)	1.527(2)	C(24)-C(23)-C(28)	117.80(15)
C(32)-O(8)	1.2193(17)	C(24)-C(23)-C(22)	119.29(15)
C(32)-O(7)	1.2666(18)	C(28)-C(23)-C(22)	122.78(15)
		C(25)-C(24)-C(23)	121.22(16)
C(4)-N(1)-C(7)	107.65(11)	C(26)-C(25)-C(24)	119.78(17)
C(4)-N(1)-C(1)	107.88(11)	C(25)-C(26)-C(27)	119.74(17)

C(28)-C(27)-C(26)	120.42(17)	F(3B)-C(31)-F(1)	83.5(13)
C(27)-C(28)-C(23)	121.00(17)	F(2)-C(31)-F(1)	103.5(4)
F(1B)-C(31)-F(3)	120.8(7)	F(2B)-C(31)-F(1)	130.6(7)
F(1B)-C(31)-F(3B)	103.1(10)	F(1B)-C(31)-C(32)	116.8(5)
F(3)-C(31)-F(3B)	24.3(14)	F(3)-C(31)-C(32)	113.2(3)
F(1B)-C(31)-F(2)	76.7(9)	F(3B)-C(31)-C(32)	114.6(6)
F(3)-C(31)-F(2)	111.4(4)	F(2)-C(31)-C(32)	112.1(3)
F(3B)-C(31)-F(2)	126.7(6)	F(2B)-C(31)-C(32)	112.1(7)
F(1B)-C(31)-F(2B)	107.5(9)	F(1)-C(31)-C(32)	109.9(2)
F(3)-C(31)-F(2B)	79.9(9)	O(8)-C(32)-O(7)	128.74(16)
F(3B)-C(31)-F(2B)	101.4(10)	O(8)-C(32)-C(31)	117.03(15)
F(2)-C(31)-F(2B)	35.9(7)	O(7)-C(32)-C(31)	114.23(15)
F(1B)-C(31)-F(1)	27.2(11)		
F(3)-C(31)-F(1)	106.2(3)		

Table A5.4. Anisotropic displacement parameters ($\text{\AA}^2 \times 10^4$) for pyrrolizidine **260** (CCDC 831402). The anisotropic displacement factor exponent takes the form: -
 $2p^2[h^2a^*{}^2U^{11} + \dots + 2hka^*b^*U^{12}]$

	U ¹¹	U ²²	U ³³	U ²³	U ¹³	U ¹²
N(1)	139(7)	204(8)	146(7)	2(6)	30(5)	-10(6)
O(1)	174(6)	362(7)	190(6)	-20(6)	-1(5)	51(6)
O(2)	246(6)	397(8)	197(7)	-54(6)	45(5)	41(6)
O(3)	244(6)	239(7)	217(6)	-34(5)	81(5)	-48(5)
O(4)	306(7)	284(7)	190(6)	22(5)	99(5)	-62(5)
O(5)	236(6)	257(7)	229(7)	-9(5)	40(5)	-12(5)
O(6)	233(6)	350(7)	187(6)	16(6)	37(5)	45(5)
C(1)	148(8)	228(9)	144(9)	-14(7)	43(7)	10(7)
C(2)	185(8)	172(9)	184(9)	-26(7)	40(7)	-7(7)
C(3)	211(9)	199(9)	183(9)	-10(7)	45(7)	-25(7)
C(4)	160(8)	221(9)	171(9)	5(7)	48(7)	-42(7)
C(5)	142(8)	303(10)	190(9)	-6(8)	36(7)	-30(7)
C(6)	150(8)	266(10)	193(9)	22(7)	44(7)	16(7)
C(7)	174(8)	200(9)	186(9)	9(7)	42(7)	33(7)
C(8)	136(8)	187(9)	202(9)	-15(7)	26(7)	2(7)
C(9)	177(9)	235(10)	226(10)	17(8)	34(7)	31(7)
C(10)	210(9)	230(10)	291(10)	25(8)	114(8)	27(8)
C(11)	255(10)	446(13)	398(12)	148(10)	121(9)	1(9)
C(12)	215(10)	558(14)	557(14)	139(11)	102(10)	-18(10)
C(13)	294(11)	388(12)	648(15)	47(11)	256(11)	-49(10)
C(14)	458(13)	496(14)	461(13)	138(11)	288(11)	-27(11)
C(15)	302(10)	456(12)	321(11)	95(9)	125(9)	16(9)
C(16)	195(9)	182(9)	222(10)	37(8)	48(7)	-3(7)
C(17)	145(8)	252(10)	204(9)	34(8)	57(7)	-4(7)
C(18)	375(11)	319(11)	179(10)	26(8)	133(8)	-9(9)
C(19)	403(12)	682(16)	480(14)	-132(11)	243(11)	-74(11)
C(20)	112(8)	296(10)	213(9)	40(8)	27(7)	-35(8)
C(21)	145(8)	231(10)	176(9)	-5(7)	33(7)	28(7)
C(22)	147(8)	268(10)	181(9)	-22(8)	29(7)	11(7)
C(23)	131(8)	206(9)	225(10)	17(8)	17(7)	-10(7)
C(24)	174(9)	247(10)	261(10)	-22(8)	37(7)	-10(7)
C(25)	238(10)	240(10)	392(12)	83(9)	79(9)	2(8)
C(26)	310(10)	355(12)	337(11)	128(9)	138(9)	6(9)
C(27)	353(11)	366(12)	303(11)	18(9)	184(9)	16(9)
C(28)	309(10)	236(10)	308(11)	16(8)	143(8)	1(8)
C(31)	250(11)	614(17)	306(13)	-81(12)	47(9)	18(11)
C(32)	237(10)	207(9)	220(10)	-7(8)	40(8)	-13(8)
F(1)	950(30)	1110(30)	551(17)	-580(20)	176(17)	22(18)
F(2)	289(18)	2770(70)	387(15)	-300(30)	109(13)	250(30)
F(3)	1370(50)	920(30)	700(30)	484(17)	620(30)	210(20)
F(1B)	2050(170)	330(50)	1220(100)	370(60)	1380(110)	390(70)
F(2B)	590(90)	1560(110)	740(80)	-540(80)	470(80)	-890(90)
F(3B)	540(60)	4000(300)	320(50)	820(100)	330(50)	1040(100)
O(7)	178(6)	507(8)	195(6)	-11(6)	15(5)	-11(6)

O(8)	228(6)	307(7)	224(7)	-24(5)	2(5)	-14(5)
------	--------	--------	--------	--------	------	--------

Table A5.5. Hydrogen bonds for pyrrolizidine **260** (CCDC 831402) [\AA and $^\circ$].

D-H...A	d(D-H)	d(H...A)	d(D...A)	\angle (DHA)
N(1)-H(1)...O(3)#1	0.93	2.02	2.8670(16)	149.8
O(1)-H(1A)...O(7)#2	0.84	1.74	2.5814(14)	176.1
O(6)-H(6)...O(7)	0.84	1.77	2.5979(15)	168.4

Symmetry transformations used to generate equivalent atoms:

#1 -x,-y,-z

#2 x-1/2,-y+1/2,z-1/2

ABOUT THE AUTHOR

Julian Andrew Codelli was born on January 8th, 1986 in Atlanta, Georgia to Chris H. and Carol W. Codelli. He grew up in Livermore, California, and attended Livermore High School, where he played football and basketball. Though he had always enjoyed learning about science, he recalls becoming particularly interested in biology as a junior in high school, shortly following his diagnosis with Type 1 Diabetes.

Though Julian began his undergraduate studies at the University of California, Berkeley with the intention of majoring in molecular and cell biology, he quickly discovered a love for organic chemistry, and ultimately chose to pursue a degree in chemical biology. After a brief summer research experience with Dr. Monique Cosman at the Lawrence Livermore National Lab, where he studied the stereochemistry of DNA-arene oxide adducts as it relates to the fidelity of nucleotide excision repair, he joined Prof. Carolyn Bertozzi's laboratory. Julian's work in the Bertozzi lab focused on the design and preparation of synthetically tractable difluorocyclooctyne reagents for use in copper-free azide-alkyne cycloaddition reactions.

Following completion of his undergraduate studies, Julian made the short journey to Pasadena, CA, where in July of 2008 he began his doctoral research under the guidance of Prof. Sarah E. Reisman at the California Institute of Technology. His work has focused on the development of a synthetic strategy toward dihydrooxepine-containing epipolythiodiketopiperazine natural products, such as acetylaranotin, SCH64877, and MPC1001B. On May 18th, 2013, he married his high school sweetheart, Megan, and in September 2013, they will move to Seattle, Washington, where Julian will join the medicinal chemistry department at Gilead Sciences.